MEASUREMENT UNCERTAINTY IN GEAR METROLOGY

By

R. C. Frazer, BSc (Hons)

This thesis is submitted in fulfilment of the requirements for the

Degree of Doctor of Philosophy

School of Mechanical and Systems Engineering

Newcastle University

UK

May 2007

Abstract

Gears play an important role in mechanical power transmission systems. They enable the prime mover characteristic (a gas turbine for example) to be matched to the characteristic of the driven load (say, a slow speed propeller), thus reducing the cost of both manufacturing and operating the system. The customer requirements for higher power density and lower noise demands more accurate gears. This imposes more stringent requirements on the measuring equipment that controls the quality of the manufacturing machines. Many gears have flank form and tooth spacing tolerances that are less then 10μm, and according to the so called 'Golden rule', measuring equipment on the shop floor should have a measurement uncertainty of between 1 to 2μm. These are stringent requirements that demand the highest standards of metrology. Thus the need to accurately quantify the measurement uncertainty of inspection machines is of paramount importance if costly mistakes are to be avoided.

The work reported in this thesis was completed as part of the activities undertaken by the author in his role as head of the UK National Gear Metrology Laboratory (NGML). The laboratory is accredited by the United Kingdom Accreditation Service (UKAS) for gear measurement and on-site calibration of gear measuring machines. The work is mainly experimental in nature. In fact, much of what is reported is centred on work undertaken with two artefact sets: one set consisting of 100mm diameter lead and profile artefacts and a second set of 200mm diameter artefacts. These gear artefacts are probably the most valuable in the world because of the volume and quality of the calibration data associated with them.

The work undertaken has included:

- A review of gear measurement methods, identifying sources of error in the measurement process and quantifying their effect on the gear measurands of profile and helix (total, slope and form error parameters) and also adjacent and cumulative pitch errors.

- An evaluation and re-interpretation of an industrial measurement capability survey, quantifying achievable performance, typical instrument capability and identifying the cause of some of the excessive instrument errors. The analysis also revealed some limitations in the testing method employed.

- Research into the international compatibility of gear measurement by National Measurement Institutes (NMIs) from the UK, Germany and USA. The analysis showed 'generally' good compatibility between NMIs, well within their claimed measurement uncertainty. In the case where differences were considered significant, clear causes were identified. However, the work concluded that uncertainty estimates from the NMIs are probably pessimistic.

- An implementation of the classical measurement uncertainty methods defined by the ISO 'Guide to the expression of uncertainty in measurement'. Uncertainty budgets for all gear parameters defined in ISO 1328-1, 1995, have been developed. Limitations of this procedure are discussed.

- An evaluation of standard comparator methods of estimating measurement uncertainty defined in ISO 18653 and the British Gear Association (BGA) 'Codes of practice'. Limitations with these processes are quantified by comparison with the uncertainty budget method and recommendations are made to revise and in some cases, withdraw the documents.

- A limitation that has been identified during this programme of work is that current methods of estimating measurement uncertainty are based on evaluated parameters, including form and total errors parameters. These parameters are insensitive to the position of errors and thus may induce an apparent overestimate of uncertainty when using the comparator method. A programme of work to develop a data point by data point comparison on an error curve was implemented following work undertaken with a Japanese Double Ball Artefact.

- The point by point calibration method was developed further by evaluating data supplied by the Physikalisch Technisch Bundesanstalt (PTB), Germany in a preliminary study to establish traceability using this method. The initial work indicated this is a viable method and it was further developed with the aid of a Monte Carlo Simulation to model the measurement process.

- A series of conclusions and recommendations complete the work programme.

Like all research programmes, the work poses more questions than answers.

Acknowledgments

Much of the core research work was completed during projects funded by the UK Department of Trade and Industry (DTI) National Measurement System (NMS) over a number of years. It provides a stable, robust measurement infrastructure and ensures that centres of excellence are available for the benefit of both manufactures and users alike. Long may it continue.

Special thanks must go to Dr. R. Bicker, my supervisor, whose advice and patient and persistent encouragement have culminated in the delivery of this thesis. I am indebted to Mr E.J. Myers who has inspired and supported both myself and my colleagues through many enjoyable technical discussions over the years. I also indebted to Prof. D.A. Hofmann, OBE, Director, Design Unit, whose enthusiasm and engineering expertise never ceases to astound me.

I gratefully acknowledge the support of Dr F. Härtig, Head of the Gear Calibration Laboratory at PTB, Germany for whom I have the greatest respect and admiration.

Finally, on a personal note, I would like to thank my wife, Linda and our boys, Matt and Will for their support and understanding. Words are simply not enough so I dedicate this thesis to you.

Linda, Matt & Will.

Abbreviations

AIST	National Institute of Advanced Industrial Science and Technology, Japan.
A2LA	American Association of Laboratory Accreditation.
BGA	British Gear Association.
CMM	Coordinate Measuring Machine.
CNC	Computer Numerical Control.
DUGATES	Design Unit Gear Analysis and Transmission Error Software.
DTI	Department of Trade and Industry, UK.
FFT	Fast Fourier Transform.
ISO	International Standard Organisation.
KCRV	Key Comparison Reference Values.
MCS	Monte Carlo Simulation.
NGML	National Gear Metrology Laboratory, UK.
NIST	National Institute of Science and Technology, USA.
NMI	National Measurement Institute.
NMS	National Measurement System, DTI, UK.
NPL	National Physical Laboratory, UK.
PTB	Physikalisch Technisch Bundesanstalt, Braunschweig, Germany.
TCA	Tooth Contact Analysis.
TE	Transmission Error.
TCE	Total Composite Error.
UKAS	United Kingdom Accreditation Service.
VDI	Institute of Mechanical Engineers, Germany.
VIM	Vocabulary in Metrology.
Y12	Oakridge Metrology Centre, LLXT LLC, Y12, USA

Contents

Chapter 1

INTRODUCTION

Gears are important elements that are an integral part of most mechanical power transmission systems. Their primary purpose is to maximise the efficiency of the overall power transmission system by converting speed and torque into more usable quantities, depending on the requirements of the system. They are thus important parts in any modern power transmission system where minimising operating costs and reducing environmental impact are important requirements. Initially, gears were little more than simple wooden pegs attached to a wheel and transferred low power. An early widespread application of geared transmission systems were in water mills. In the Domesday book (of 1086), there were recorded 5624 water driven mills using oak wheels and elm pinions [Lacey]. It was a classical gearing application: high-speed millstones are required for the efficient milling of wheat and barley, whereas the water wheels that provide the power operate most efficiently at low speed. The transmission systems that were developed allowed the low speed water wheel to transmit rotation through a speed increasing gear drive thus permitting the millstones to rotate at their most efficient speed. An additional benefit in this arrangement was that the milling stones could now be located adjacent to the river thus improving the ease of delivery of wheat and barley and the subsequent retrieval of the flour.

Modern transmission systems have the same basic elements as the early gear applications. The driven system may be a generator, conveyer, pump or propeller that will have its own operating characteristic with an optimum operating condition for maximum efficiency and minimum cost. The driving system, or prime mover, such as gas or steam turbine, electric motor, wind turbine, or combustion engine will also have its own operating characteristics and have an optimum operating condition that works most efficiently. The purpose of the gearbox is to match the characteristics of the driving system with the characteristic of the

driven system and thus optimise the efficiency and reduce the cost of the overall system. For example, a Wind Turbine driving a 1MW generator rotating at 20rev/min is prohibitively large and expensive, but a 1MW generator rotating at 1500rev/min or 3000rev/min is smaller, lighter and more economical to manufacture and maintain.

After a gear is designed, specified on a drawing and manufactured, it is necessary to measure its geometrical accuracy. Standard measurement processes are applied and the results from the analytical measurement process are analysed to verify the component complies with its accuracy specification. Geometry errors influence the load capacity, life expectancy and noise levels of a gear set during service so it is important that they conform to the designer specification. During this analysis process, an experienced metrologist should question the validity of the measurements results. Have any mistakes been made? Are the results accurate? How accurate is the measurement process? Has the accuracy of the measuring instrument been tested? How confident are we in the results obtained from this measurement process?

Compliance with an accuracy specification is an important issue for any gear manufacturer. The financial risks to the manufacturer are significant if customers have no confidence in the ability to measure and thus control the quality of the manufacturing process. However, a gear measurement result provided without a traceable statement of its 'measurement uncertainty' is incomplete and it not possible to make reliable decisions regarding fitness for purpose. Manufacturers risk losing credibility and income if their components are outside specification. Whilst there has been much theoretical work undertaken on the statistical nature of measurement uncertainty estimation processes, little of it has been applied to the unique application of gear measurement. This apparent shortcoming has inspired the author to undertake a programme of work to develop an appropriate and robust procedure to address the needs of gear manufacturing industry.

1.1 Scope of the research

Accordingly, the following research hypothesis directed this programme of work:

Is it possible to develop a systematic and quantifiable measurement uncertainty procedure applicable to the gear measurement process?

Gear measurement involves scanning the surfaces of high accuracy and geometrically complex components, at relatively high speed in a shop floor environment. Thus, they provide very difficult challenges for a metrologist. The specific objectives of this research are to:

- Undertake an in-depth review of existing and accepted measurement uncertainty procedures applied to the gear measurement process.

- Design and apply systematic measurement uncertainty evaluation procedures to gear measurement.

- Test the procedures on a range of instruments including shop floor installations and those found in national laboratories.

- Carry out a detailed analysis of the results to recommend:

    - suitable statistical procedure for estimating gear measurement uncertainty.
    - appropriate methodology for gear artefact design.
    - revision to ISO and other internationally accepted documentation, where appropriate.
    - the direction of future research into gear measurement necessary to provide support for the ongoing needs of both gear manufacturers and gear users in the UK.

1.2 Layout of Thesis

The research work presented in this thesis was completed over a number of years by the author as part of his role as Head of the UK National Gear Metrology Laboratory. This has afforded a unique opportunity to review and apply statistical measurement uncertainty procedures to a wide range of instruments in an equally wide range of environments.

Chapter 2 provides some background describing the purpose of gears in transmission systems and introduces the common gear measurement processes. It explains why the involute gear shape is the most common form of gear used. A discussion on the influence

of gear accuracy on performance, quantified using standard stress analysis procedures in accordance with ISO 6336. The reduction in contact stress has been quantified further using a FE mesh model and tooth contact analysis (TCA). It describes the parameters measured (and evaluated) on gears with specific reference to ISO 1328. It introduces the principle of measurement traceability and the UK traceability structure.

Chapter 3 reviews the development of gear measuring instruments from the earliest instruments in the 1920s through to present day. A discussion of the benefits and limitations of different measuring instruments is included. It defines good measurement practice and reviews the sources of measurement error (measurement uncertainty) with the guidelines in ISO TS 14253-2.

Chapter 4 discusses some of the standard measurement uncertainty models used in dimensional metrology applications. The review contains reference to some of the key texts that provide the foundation for uncertainty evaluation methods for classical (frequency based) statistical methods, the so-called 'robust methods', Bayesian approaches and Monte Carlo Simulation methods. A description of different methods of establishing traceability is included.

Chapter 5 applies the simple comparator method for evaluating measurement uncertainty in a survey of industrial instruments in the UK. It describes a method of determining a reference value using the weighted mean from the survey results (using a similar method to those applied to Key Comparison Reference Values). Comparisons of reference data from National Measurement Institutes (NMIs) are reviewed. Some of the differences identify flaws in the survey procedure and stability problems with some of the artefacts used for the survey.

Chapter 6 describes the results from the first international comparisons of gear measurement capability of helix and profile errors arranged by the author and presents some results of a pitch measurement comparison arranged by the USA. Differences between NMIs demonstrate excellent compatibility but this may simply indicate that the uncertainty estimates provided by the laboratories are pessimistic.

Chapter 7 describes the application of the classical uncertainty evaluation methods in accordance with the ISO guidelines and provides uncertainty estimates for all the evaluated measurement parameters defined in ISO 1328. Although this method is probably flawed, it is the reference method for evaluating the procedures described in

ISO 18653 and the BGA codes of practice for gear measurement. It recommends changes to these documents and limitations on their application. However, it observes that because these processes appear to over-estimate measurement uncertainty, all the methods described may be considered validated by these test results.

Chapter 8 identifies some flaws in the so called 'parameter based' method of evaluation and describes a series of tests performed on a range of artefacts using individual data points from helix and profile measurement data to quantify errors in the measurement process. It describes a development to include an initial comparison with PTB, Germany to establish traceability. A Monte Carlo Simulation of the measurement process further explores the benefits of this approach for establishing traceability.

Chapter 9 discuses the work undertaken, summarises the conclusions reached and makes recommendations for further research work.

Chapter 2

GEARS AND GEAR MEASUREMENT

There are two of different types of geared systems that are in regular use in power transmission systems:

- Parallel axis or cylindrical gears. These are generally spur or helical involute gears as illustrated in figure 2.1 and are the most commonly used gear form, and arguably the most developed and researched.

- Cross axis gears. These can be straight or spiral bevel gears, worm gears, hypoid gears, spiroidal gear types. They differ from cylindrical involute gears mainly because the geometry of the gear depends on the manufacturing method and supplier of manufacturing equipment. For this reason, standard analytical measurement techniques are not as developed as cylindrical involute gears.

The work in this thesis is primarily concerned with involute spur and helical gears, although many of the principles can be applied to other gear types.

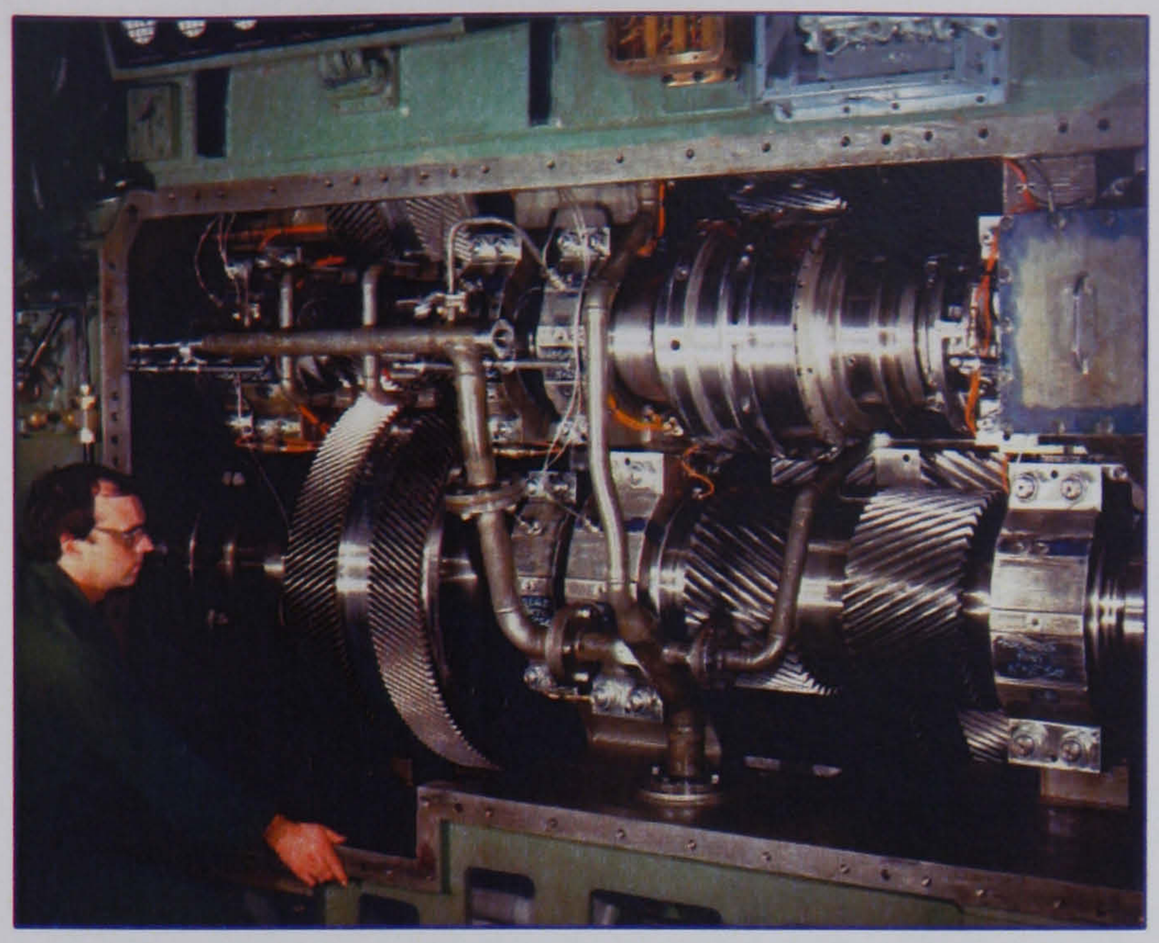

Figure 2.1 Involute helical gears in a marine propulsion drive.

2.1 The involute gear form

Involute gears are named after the involute curve that forms the active part of the tooth flank form and is illustrated in figure 2.2 (the involute is the shape of a curve formed by unwrapping a cord from a circle). They were developed in the early 1900 but became widely utilised because of a number of important properties:

- They were easy to manufacture. A single involute cutter can 'generate' gears with any number of teeth. Other tooth forms also use the generation process but they require a specific cutter for a particular number of teeth which significantly increases tooling costs and delivery times.

- Involute gears are insensitive to changes in shaft centre distance; so mounting and assembly is easier than for other tooth forms, however they must still be aligned parallel for good load distribution.

- Involute gears can be made to suit varying centre distance by applying an 'addendum modification' or 'rack shift' to the basic geometry.

- Involute gears are relatively easy to measure. The first measuring instruments were available for the accurate measurement of involute gears in the 1920s [Rolt]. Bevel gears and worm wheels could not be measured using analytical methods until the

early 1980s after the development of the Co-ordinate Measuring Machines (CMMs) and Computer Numerical Control (CNC) dedicated gear measuring machines.

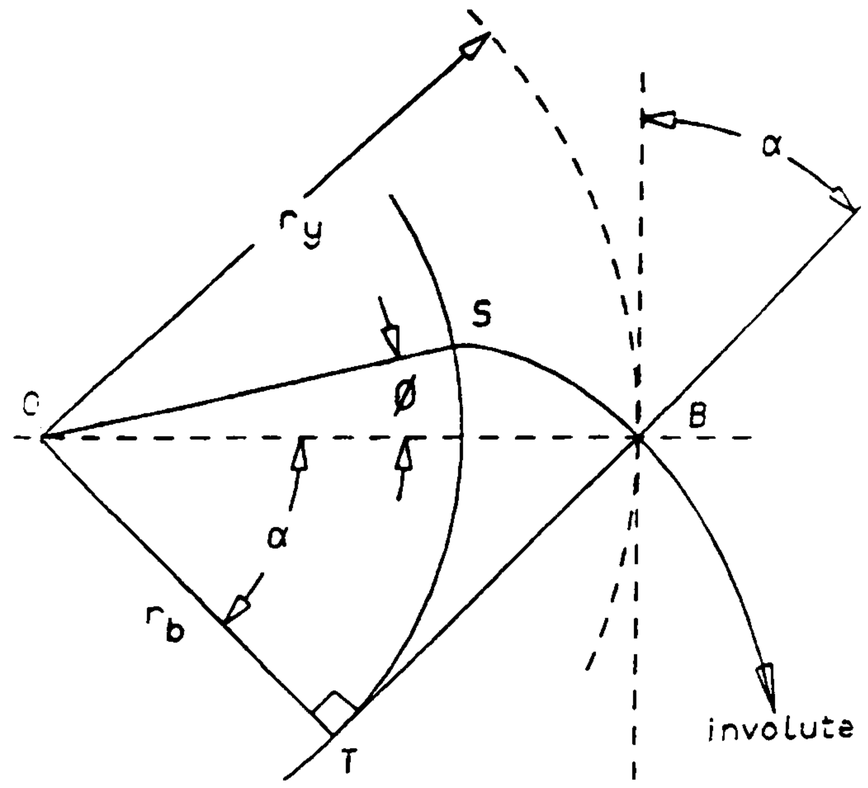

Figure 2.2 Involute curve [Kohler, 1989]

2.2 Involute gear measurement

There are two methods of measuring involute gears:

- Composite methods that measure the composite effect of tooth flank form and spacing errors, and
- Individual methods that measure individual parameters on selected gear teeth of lead (helix) or tooth alignment, profile or involute form and pitch or tooth spacing errors.

The limitations and benefits for these are discussed in more detail in the following sections.

2.2.1 Dual flank composite measurement

Dual flank or roll testing of gears involves rotating a product gear with a master gear in tight mesh (under a light spring force) and measuring the resulting change in centre distance as the gears are rotated (see figure 2.3).

Geometrically perfect gears, mounted concentrically to the datum axis, will rotate without any effective change in centre distance. Errors in tooth thickness, involute form, tooth alignment (sometimes known as helix error) and pitch (spacing) errors will increase the effective tooth thickness and thus increase the close mesh centre distance. The change in centre distance is recorded and plotted as a deviation from a straight line, as shown in

figure 2.4. The benefits and limitations of the composite measurement process are summarised in Table 2.1.

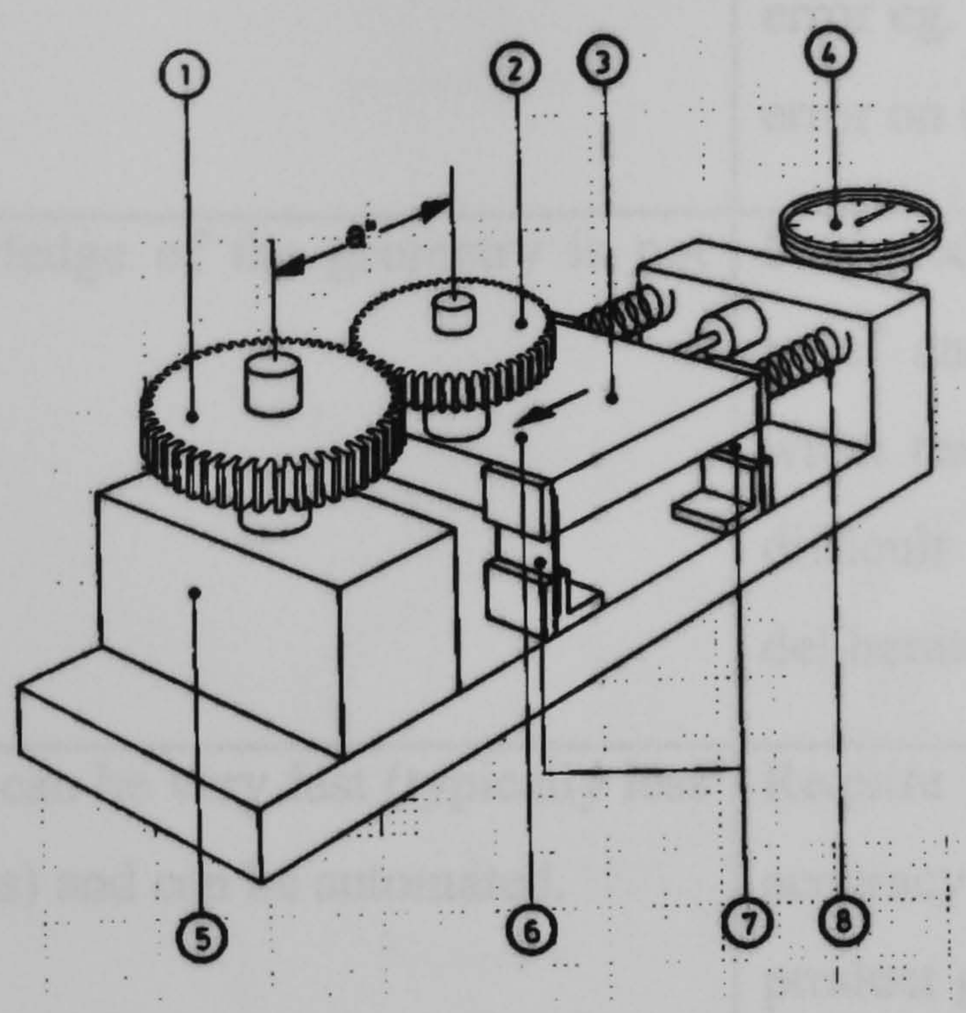

1. Master Gear
2. Product gear
3. Moving Platen
4. Indicator or LVDT to measure change in centre distance.
5. Fixed platen
6. Measurement direction
7. Flexure
8. Pre-load spring

Figure 2.3 Dual flank measurement principles

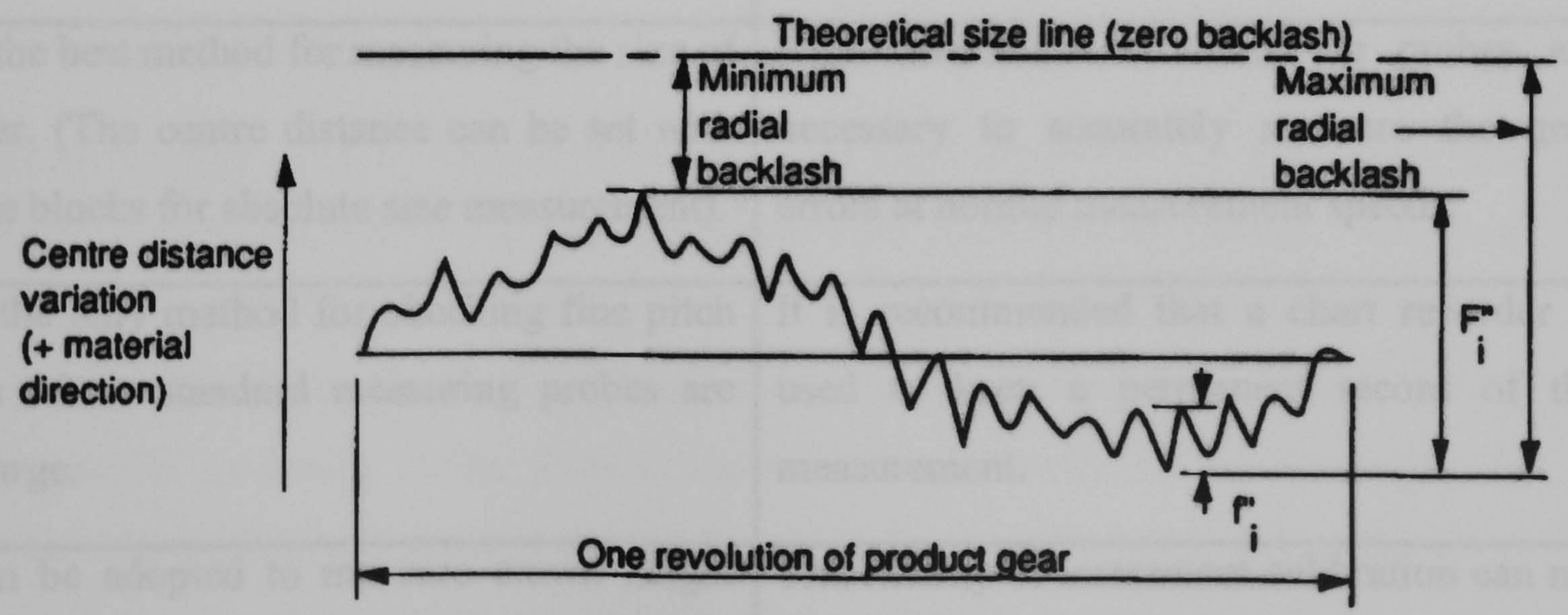

Figure 2.4 Dual flank measurement result format illustrating the evaluated parameters [Munro, 1989]

Table 2.1 Benefits and limitations of the dual flank composite method

Benefits	**Limitations**
The total active flank is checked on all the teeth .	Can be difficult to identify the cause of an error eg. lead and profile errors give the same error on the trace.
Detailed knowledge of the geometry is not required.	Designed departures from the involute eg tip relief and lead correction, cause deviations when tested under very low load. It is then difficult to identify true errors from the deliberate deviations.
The technique can be very fast (typically less than 15 seconds) and can be automated.	Require a master gear which is at least 3 accuracy grades better than the measured product gear, thus limiting most applications to product gears of ISO accuracy grade 6 .
It is excellent for detecting damage to teeth because the whole tooth surface is tested.	It is not a functional check - indexing errors on gear can not be measured with this technique.
It is the best method for measuring the size of a gear. (The centre distance can be set with gauge blocks for absolute size measurement).	High discrimination clocks or probes are necessary to accurately measure the gear errors at normal measurement speeds.
It is the only method for checking fine pitch gears where standard measuring probes are too large.	It is recommended that a chart recorder is used to keep a permanent record of the measurement.
It can be adopted to measure crown height and lead errors on specially adapted automatic machines.	Traceability of instrument calibration can not be established by the simple comparator method.
The equipment is much cheaper than lead, profile and pitch measuring instruments.	

2.2.2 Single flank composite measurement

Single flank measurement or transmission error measurement is a functional test of the kinematic accuracy of a pair of gears or, if required, a complete gearbox assembly. This is shown in figure 2.5.

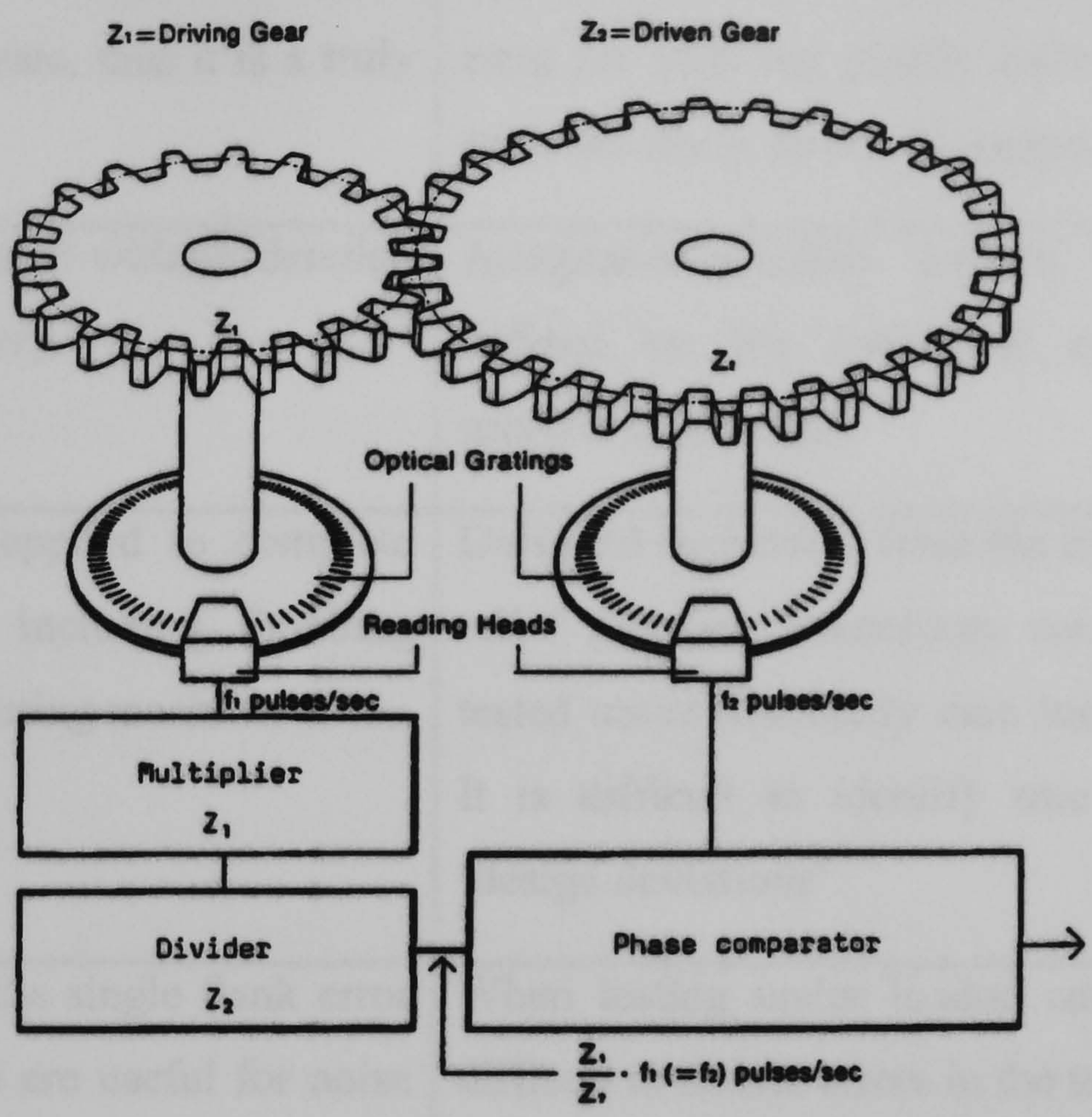

Figure. 2.5 The principle of Single Flank Measurement [Munro 1989]

Transmission error (TE) is defined as the error in angular position of the driven gear compared to its theoretical position if the gears were geometrically perfect. A typical error trace is similar to the dual flank trace in figure 2.4 except that the suffix (″) is replaced by suffix (′) to denote the difference in the error terms. This method is often used when the geometry of the gears is too complex for analytical measurement, the kinematic accuracy of the gears is critical (eg. an indexing table) or if kinematic errors from the manufacturing process are present. Some advocate its use for predicting noise but the results are only valid for torque applied during the test [Smith, Munro].

A typical Single Flank error trace and Fast Fourier Transform (FFT) analysis is shown in figures 2.6 and 2.7 respectively. The method is invaluable for identifying errors in the

manufacturing process that can cause excessive noise and vibration levels The benefits and limitations of the process are described in Table 2.2.

Table 2.2. Benefits and limitations of the single flank measurement method

Benefits	**Limitations**
Checks all the teeth in the same manner in which the gear will operate, thus it is a truly functional test.	Can be difficult to identify the cause of an error i.e. lead and profile errors produce the same deviation on the TE graph.
It allows gears to be tested without detailed knowledge of the geometry.	Acceptance/rejection criteria is normally defined by the individual company and specific application.
The technique can be applied to complete transmission systems including hobbing machines and gear measuring machines.	Designed departures from the involute eg. tip relief and lead correction, cause TE when tested under nominally zero load conditions. It is difficult to identify true errors from 'design deviations'.
Subsequent analysis of the single flank error trace by FFT techniques are useful for noise investigation and identifying the causes of production errors.	When testing under loaded conditions it is difficult to isolate errors in the test instrument from errors in the test gears A variable speed drive is necessary for this to eliminate resonances.
The technique is fast when used to check product gears.	Although the quasi-static single flank measurement technique is very powerful, there have been very few developments in equipment or use of the technique during recent years.
It is excellent for picking up damage to teeth as the whole tooth surface is tested.	
It can be used to identify phantom tones produced by machine elements in the gear manufacturing machines.	

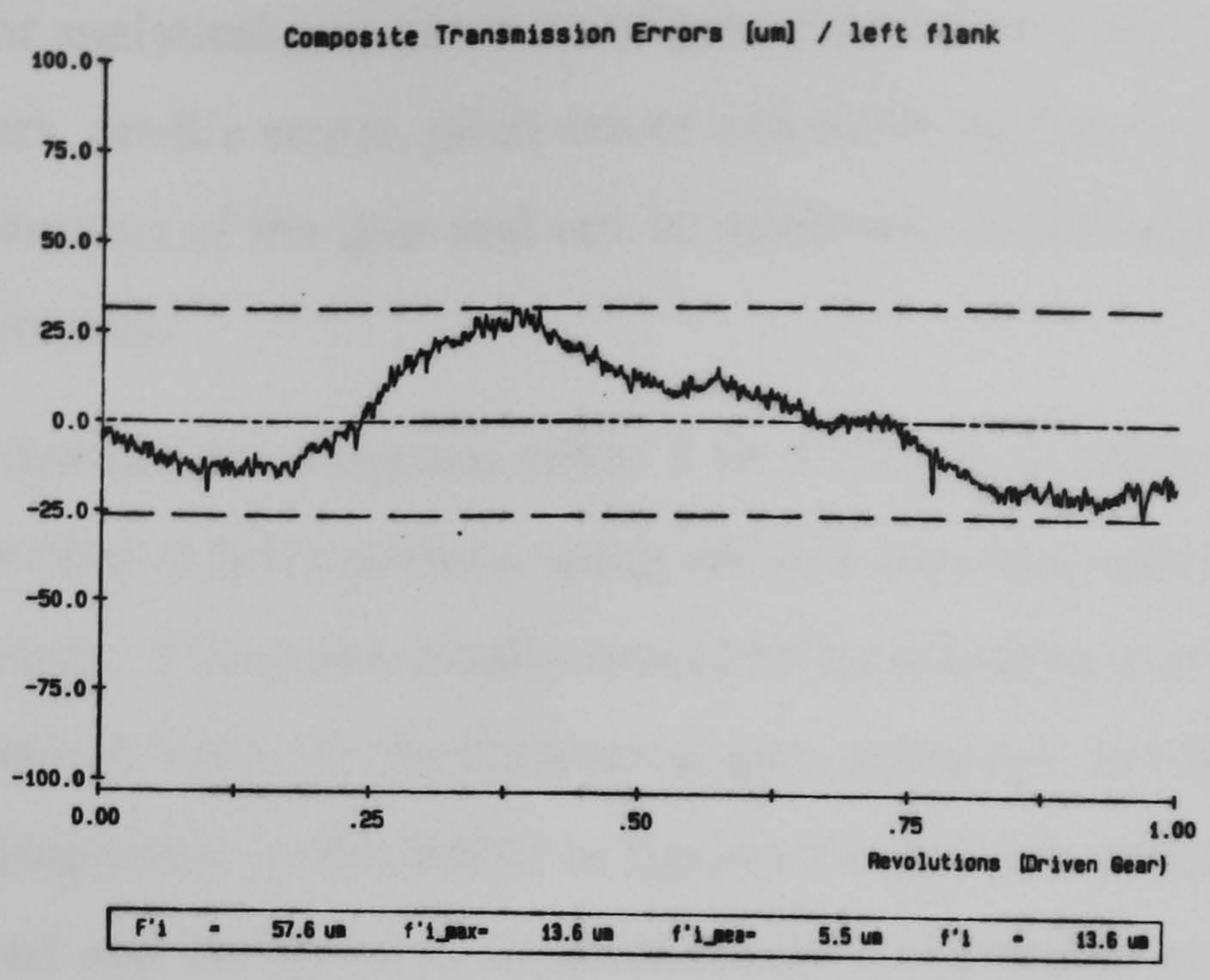

Figure 2.6 Example of a single flank error trace showing the composite single flank error for a 30 to 79 tooth gear mesh. (The graph shows deviations over 1 revolution of the 79 tooth wheel).

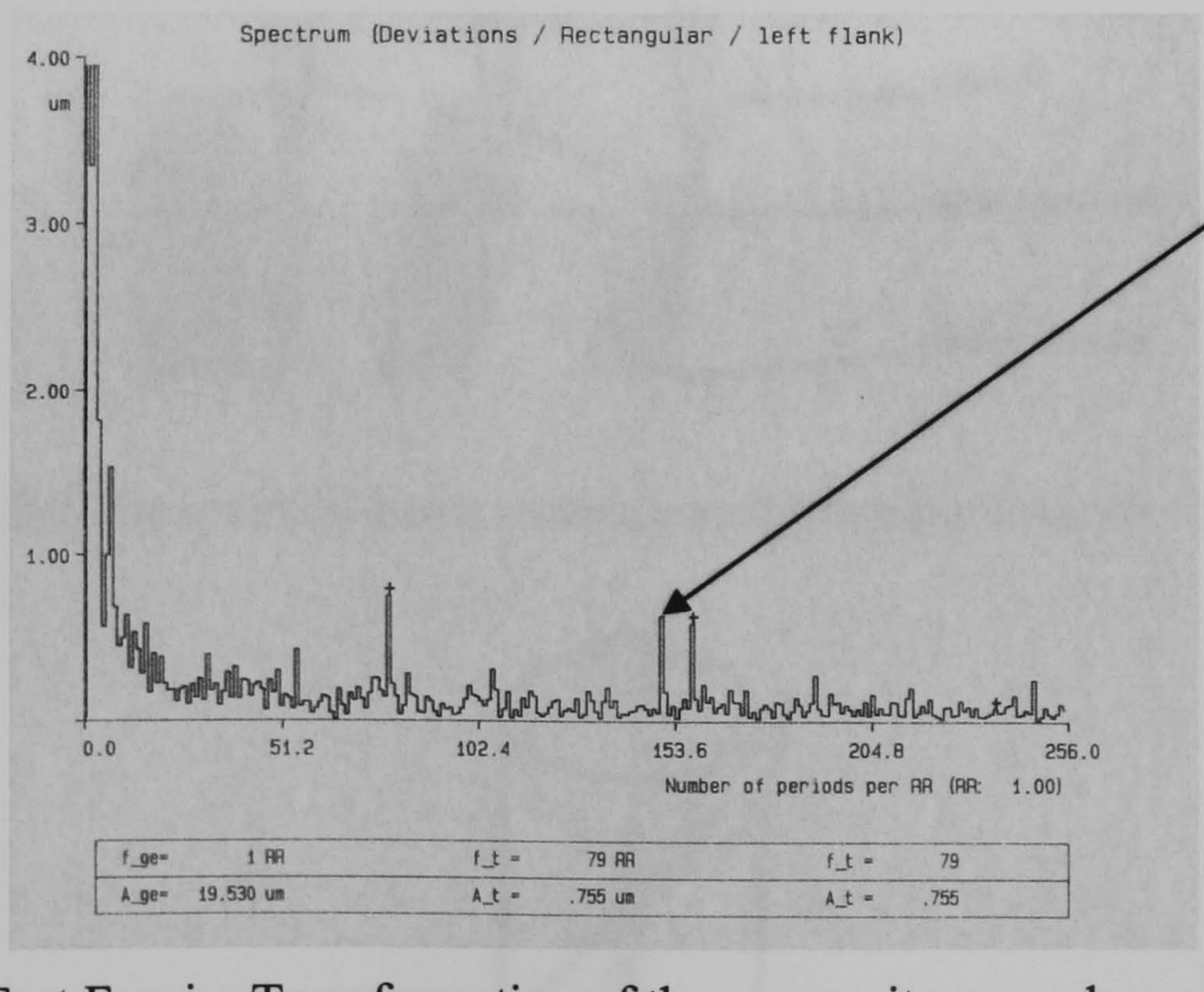

Figure 2.7 The Fast Fourier Transformation of the composite error shown in figure 2.6 is more revealing. The tooth passing frequency at 79RR and its 2nd harmonic at 158RR are shown clearly. A Phantom Tone at 150RR is shown which is from the grinding machine 150 tooth rotary table worm wheel.

2.2.3 Measurement of individual error parameters

The individual or analytical measurement of gear parameters involves the measurement of helix (lead) errors, profile errors, pitch errors and tooth thickness. These are parameters that affect the function of the gear and can be analysed, controlled or adjusted during the manufacturing process.

The measuring instrument comprises either 3 or 4 axes to position a measuring probe at the theoretical profile or helix position using either a base-disc and mechanical slides or a CNC control system. The probe usually measures by scanning over the flank surface and records the difference between the theoretical gear geometry and the actual geometry of the flank being inspected, as illustrated in figures 2.8 and 2.9, respectively. In figure 2.8 the gear is rotated and the stylus is simultaneously translated across the gear flank from root to tip (shown at 3 positions for the tooth flank inspected). Deviations from a true involute curve deflect the stylus producing plus or minus metal deviations. The measurement method is identical for spur or helical gears.

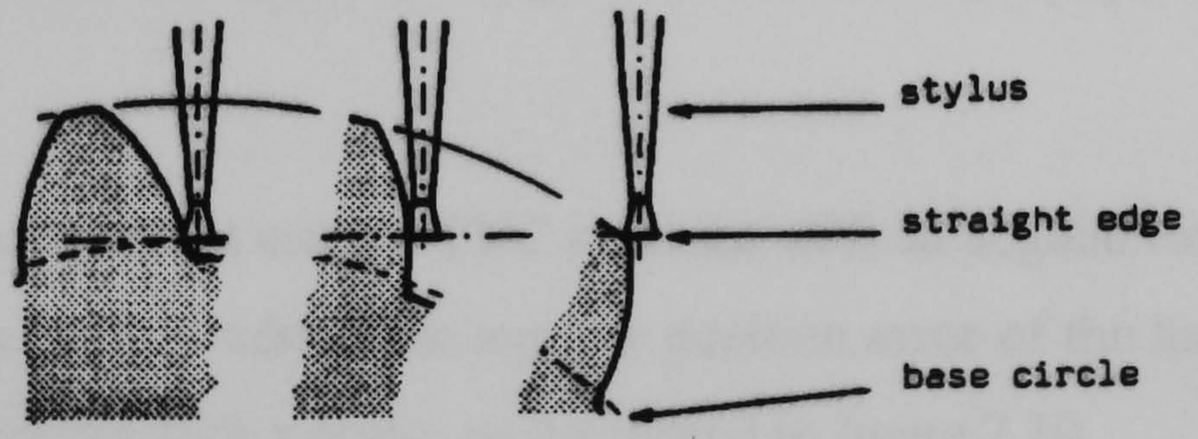

Figure 2.8 The involute curve measurement principle [Munro, 1989].

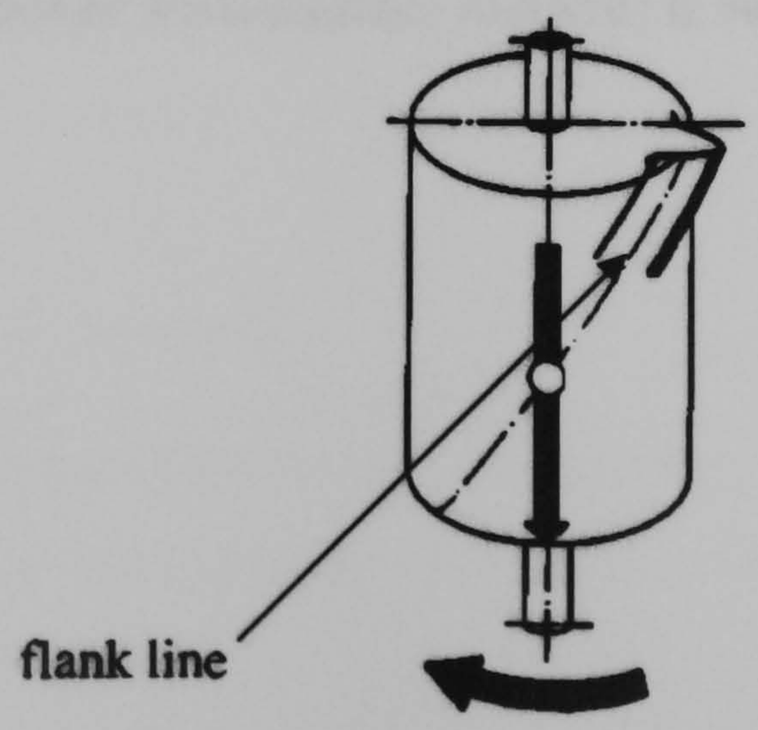

Figure 2.9 The lead or helix measurement principle [Klingelnberg].

Figure 2.9 illustrates the measurement of helix or lead error. The stylus is moved down vertically as shown and the rotary table (on which the gear is mounted concentrically) is simultaneously rotated to generate the theoretical helix. Deviations between the theoretical helix and actual helix deflect the stylus resulting in plus or minus metal deviations from the theoretical helix angle

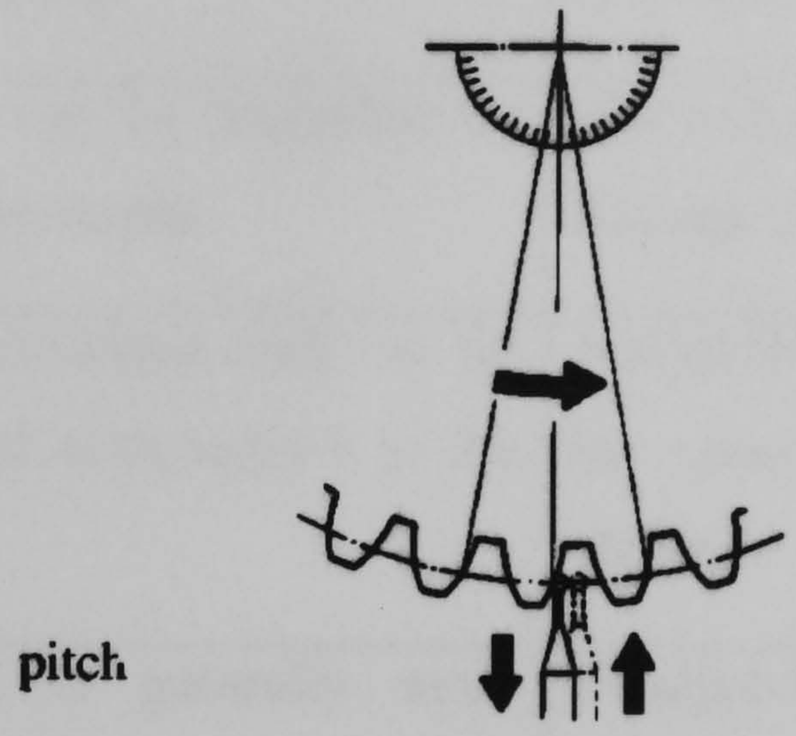

Figure. 2.10 Pitch measurement using an angular encoder as a datum measures the deviation between theoretical flank spacing and actual flank spacing [Klinglenberg].

Pitch measurement is carried out using a CNC machine with an angular reference, such as an angular encoder on a rotary table. The angular position error of the teeth is measured relative to the angle encoder with a probe, as illustrated in figure 2.10.

The benefits and limitations of the analytical or individual measurement method (in comparison to the composite measurement method) is summarised in Table 2.3.

Table 2.3. Benefits and limitations of the analytical error measurement method

Benefits	Limitations
The errors can be easily analysed, although it is a skilled job if not carried out automatically by a computer.	The measurement method is quite slow for one off measurement (much data is necessary to measure the gear correctly).
The causes of errors can be identified by carefully interpreting the results.	The complete tooth surface is not checked - damage, nicks or burrs may go unnoticed.
The departures from involutes such as tip relief can be quantified with respect to the design profile.	Not all the teeth are checked, and if they are, the process is slow and interpretation difficult.
Measuring equipment is generally more accurate than the composite methods of measurement so more informed and accurate decisions can be made with this method.	Detailed knowledge of the gear geometry is required.
High accuracy gears may be inspected with acceptable measurement accuracy.	It can be difficult to check fine pitch gears (i.e. <0.5mm module).
Once the data is programmed on a CNC machine, the measurement process is quite fast (4 to 10 minutes on a CNC machine or 10 to 30 minutes in a manual machine).	In high volume environments it is too slow to check every gear manufactured.

Analytical measurement method

Analytical gear measuring instruments are usually dedicated CNC 'gear checkers', manual gear checkers or general purpose CMMs with gear measurement and analysis software. The instruments measure the geometry of a gear with respect to the theoretical reference gear geometry. Deviations from the reference gear geometry are errors in the gear.

It is not practical to check the whole tooth flank surface of all the teeth in a gear for geometric accuracy because it would be too time consuming. Instead, only a sample are measured as described in the BGA (British Gear Association) codes of practice for inspecting gears. The recommended procedure is to measure:

- 4 teeth, spaced at approximately 90° intervals , on both left and right flanks for alignment (helix) accuracy.
- The same 4 teeth for profile accuracy at the mid face width.
- Spacing errors of all teeth, including adjacent pitch error (the error in spacing between consecutive flanks of teeth) and cumulative pitch error (the error in spacing between any teeth in the gear). Cumulative pitch is calculated by summing the adjacent pitch errors. These are measured at the mid-face and at mid tooth depth.
- Radial runout of the tooth space is the equivalent of the variation in radial position that a ball takes when placed in a tooth space and is often computed from the pitch results.
- Tooth thickness measurement on CNC or CMMs with gear inspection software.

The measurements are analysed and compared with an accuracy specification which should be unambiguously defined on the gear drawing. If any single error is outside its tolerance, the gear has failed its accuracy specification. Most accuracy standards use manufacturing machine capability as basis for defining the parameter rather than influence on load distribution or transmission error, for example. The parameters evaluated for each measured feature are described below.

Profile parameters

An example of a profile measurement result for a single tooth flank is shown in figure 2.11. The complex involute curve measurement has been plotted such that deviations from a straight, horizontal line are errors in the involute form.

ISO 1328-1, 1995 analyses the graphical profile result using the following parameters :

Total Profile error F_α or F_f (this parameter is mandatory)

Profile least squares fit slope $f_{H\alpha}$ (this parameter is optional)

Profile form error $f_{f\alpha}$ or f_f (this parameter is optional)

The value for each of these parameters is analysed for every measured profile. The largest value measured is used to determine the accuracy grade of the gear. Deviations are usually measured in μm.

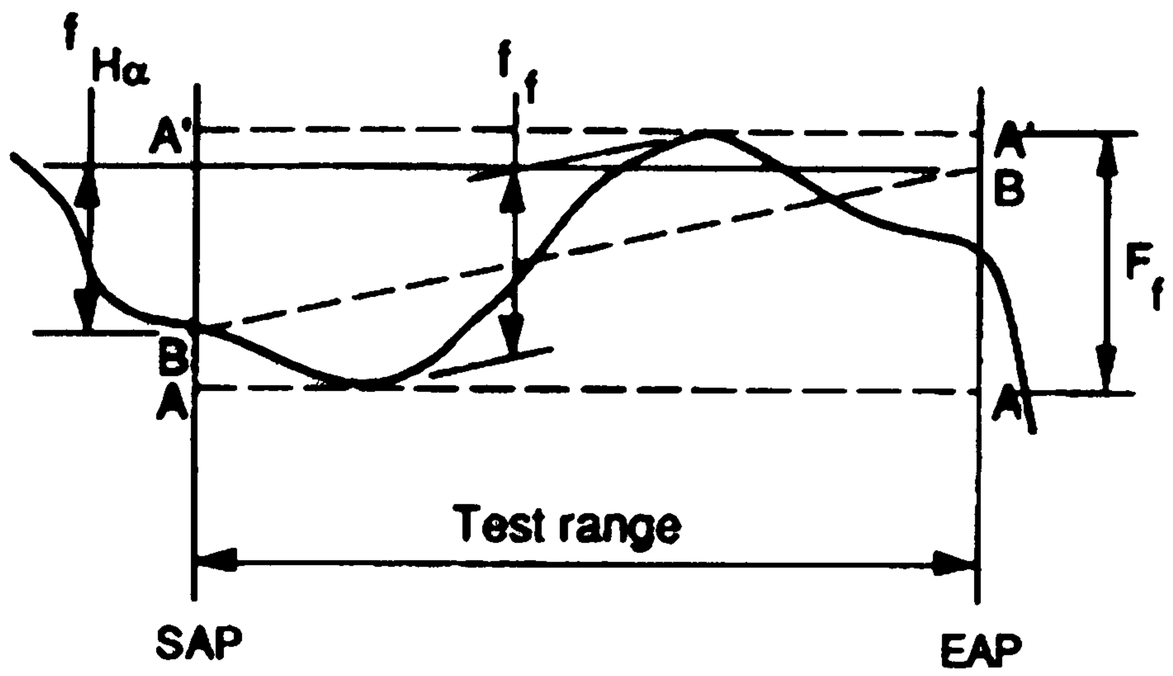

Figure 2.11 Profile parameters evaluated in accordance with ISO 1328-1, 1995.

Lead (helix) measurement

An example of lead (helix) measurement results from a single tooth flank is shown in figure 2.12. The deviations from a straight horizontal line are errors in the lead (helix). ISO 1328-1,1995 analyses the graphical result using the following parameters :

Total helix or alignment error F_β (this parameter is mandatory)

Helix or alignment least squares fit slope $f_{H\beta}$ (this parameter is optional)

Helix or alignment form error $f_{f\beta}$ (this parameter is optional)

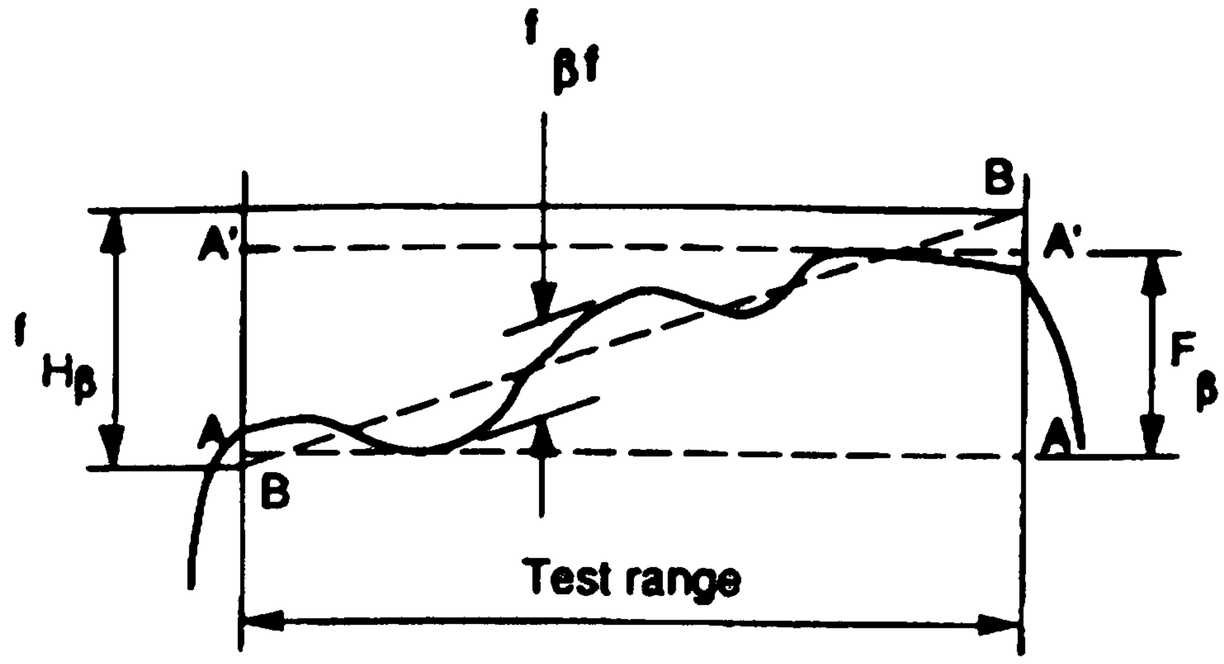

Figure 2.12 Lead (helix) parameters evaluated in accordance with ISO1328-1, 1995

The value for each of these parameters is analysed for every measured flank. The largest value measured is used to determine the accuracy grade of the gear. Deviations are usually in measured in μm and the parameter symbols are the same as profile parameters accept the (α) for profile is replaced by a (β) for helix.

Pitch error parameters

Figure 2.13 illustrates the adjacent pitch, cumulative pitch and radial runout errors for all the teeth, on both left and right flanks. The parameters evaluated are :

adjacent pitch f_p : the deviation in pitch or spacing between successive adjacent flanks (the largest value on the left flank and right flank is tabulated)

cumulative pitch F_p : the summation of adjacent pitch errors and the highest to lowest point on the cumulative pitch chart for left and right flank is evaluated

radial runout of the tooth space F_r : usually calculated from pitch measurement results rather than measured directly and the highest to lowest point of the radial runout error trace is evaluated.

Deviations are measured in μm at the measurement diameter. The largest value measured on the flanks is used to determine the accuracy grade for each parameter measured. The accuracy grade of the gear is determined by the lowest (least accurate) grade evaluated. The upper part of figure 2.13 illustrates adjacent pitch errors which are the spacing errors between successive adjacent pairs of teeth. The lower part of figure 2.13 illustrates the

cumulative pitch error chart which is formed by 'accumulating' the adjacent pitch errors and measuring the range of the resulting chart (highest point to the lowest point).

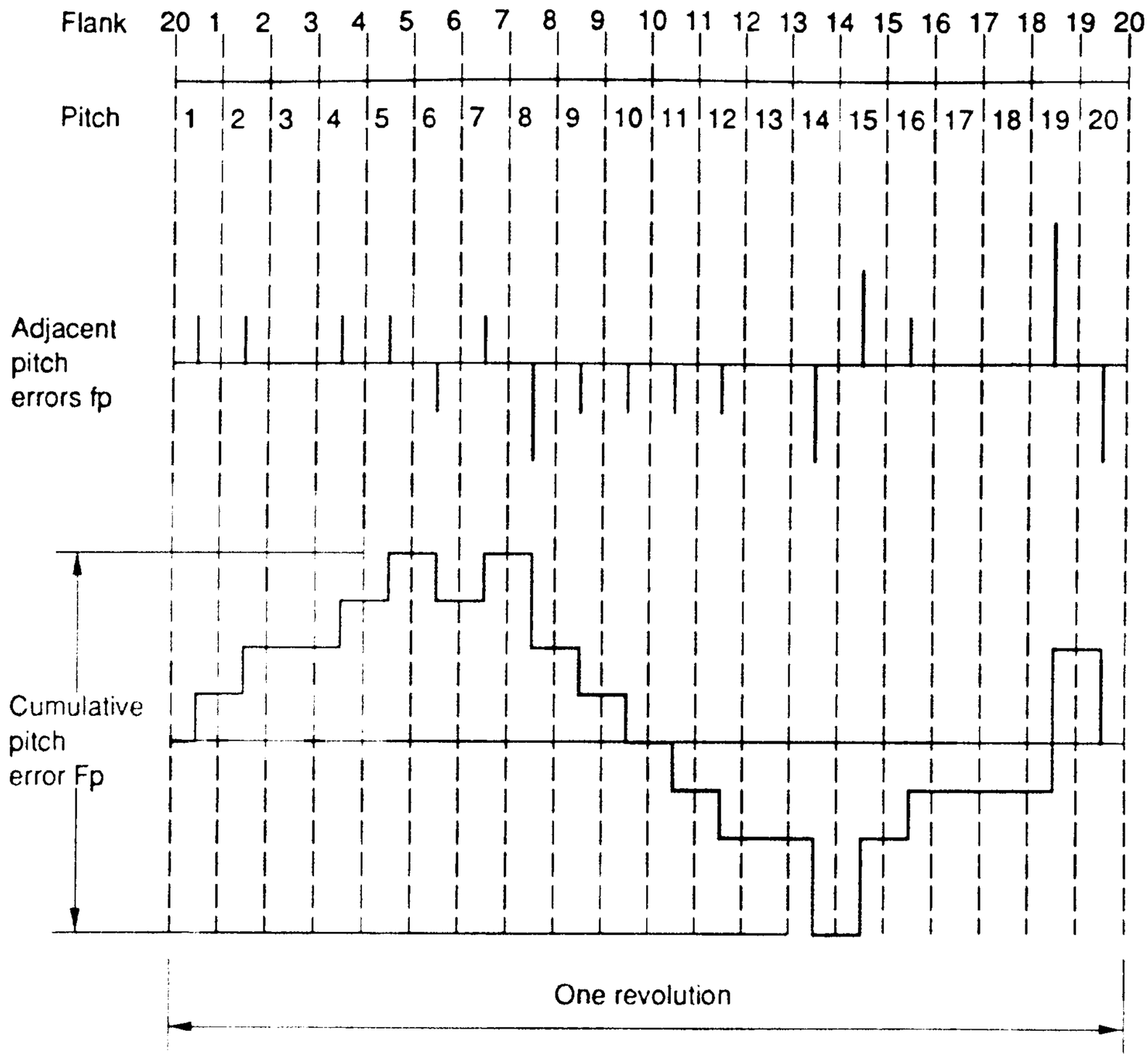

Figure 2.13 Adjacent pitch and cumulative pitch parameters measured at a designated diameter in a transverse circular plane.[Munro,1989]

Tooth thickness

Normal circular tooth thickness cannot easily be measured directly when a gear is in the process of manufacture so alternative indirect method are used such as the, dimension over rollers (or balls) or span over a number of teeth. Tolerance values should be specified on the drawing and limits can be applied in the evaluation software.

Definition of left and right flanks

Figure 2.14 defines the left and right flanks in accordance with ISO notation specified in ISO/TR 10064.

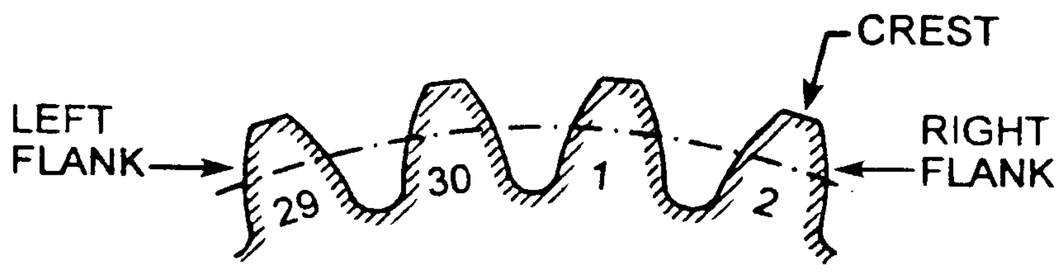

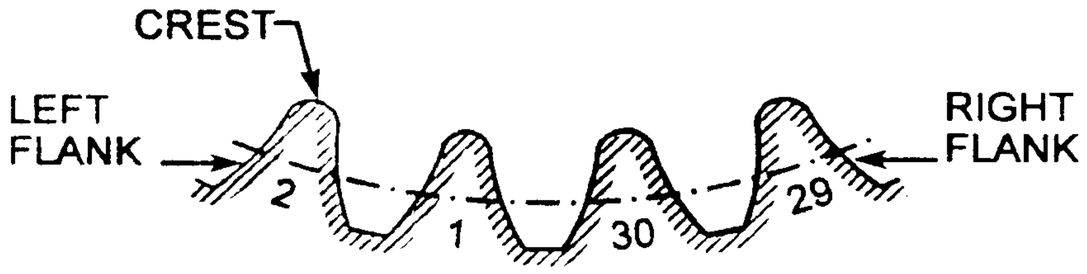

Figure 2.14 The definition of left and right flanks in accordance with ISO/TR 10064-1

2.3 Gear accuracy standards

There are several standards that specify allowable tolerances for parameters defined in the previous section. The standards have much in common and although there are many obsolete standards in daily use, many Standards authorities are using International Standards Organisation (ISO) standards as the foundation for national standards and for this reason only the ISO accuracy standards [ISO 1328-1:1995 & ISO 1328-2, 1997] will be used in this thesis.

The ISO 1328 accuracy standards define a consistent set of helix, profile and pitch tolerances for a range of accuracy grades. They are guidance documents only and the individual designer may select different tolerances if appropriate. Accuracy grades are numbered from 1 (for very accurate gears) to 12 (lowest accuracy gears). The tolerances for lead, profile and pitch parameters are defined in the Standard for a grade 5 gear. The tolerances for each successive grade are calculated by multiplying (or dividing) the tolerance formula by $\sqrt{2}$. The tolerance formula are defined in ISO 1328 parts 1 & 2.

Unlike its predecessors, ISO 1328-1 allows for the deliberate departures in profile and helix shape from the nominal involute shape that is required to allow for elastic deflection of workpieces under normal operating torque and random geometrical errors caused by manufacturing and assembly tolerances. This feature is welcome from the designers view

point but produces additional complications in interpreting results, as will be discussed in later chapters.

2.4 The influence of gear accuracy on gear performance

The geometrical accuracy of a gear has a direct influence on both the load carrying capacity and the noise levels generated during operation. A high accuracy gear can transmit higher loads because the load distribution across the face width is improved and vibration is generally reduced if appropriate corrections are applied. For a given load torque, the volume of the gear can be reduced and thus the power density increased. As a first approximation, the volume of the gearbox is proportional to manufacturing costs, thus for a given manufacturing strategy, high accuracy gears reduce the cost of the gearbox manufacture and improve competitiveness.

Effect of gear accuracy on gear failure modes

The common ways in which gears fail are:

- Bending stress failure, where a fatigue crack propagates from near the root of the gear tooth eventually leading to breakage of the tooth.
- Pitting failure due to excessive contact force. The failure occurs on the active flank in the form of pits, of size 0.2 to 5mm or greater, that appear to initiate from the surface, propagate parallel to the surface of the flank before they turn and head back to the flank surface leaving a crater or pit.
- Spalling, in case hardened gears, in which the sub surface fatigue crack is initiated and travels along the case-core interface and un-noticed until a large area of the flank breaks away.
- Scuffing failure occurs by excessive contact pressure causing the lubricant film to break down and allowing the gear teeth surface asperities to contact and instantaneously weld together, before being torn apart as the gears continue to rotate. This type of failure mode is very difficult to predict but is definitely influenced by gear geometry errors.
- Micro-pitting or 'grey staining' is a more recently identified failure mode that at present is not easy to predict. It is a type of pitting failure in which the pits are

typically 0.005mm deep. The causes have been attributed to a change in the base oil used to lubricate gears and improvements in steel composition and. Sometimes the pits stop propagating and the effect is self arresting but in other situations further pits are developed that produce a wear type of mechanism. This can lead to surface initiated bending type failures. It is the opinion of the author that this is not fully understood but it is known that geometry errors, surface finish will influence how it initiates and develops.

Methods of predicting pitting or bending failure modes are well established and published in the ISO 6336 series of standards. A quantitative relationship between the occurrence of scuffing and micro-pitting failures has yet to be developed and published in ISO standards.

ISO 6336 parts 2 and 3 contains calculation procedures to predict the likelihood of failure of a defined gear pair for pitting or bending failure modes. This is expressed as a Safety Factor, SH, for contact stress and SF for bending stress. A SH of 1.0 is considered acceptable for contact stress and a SF of 1.4 for bending stress.

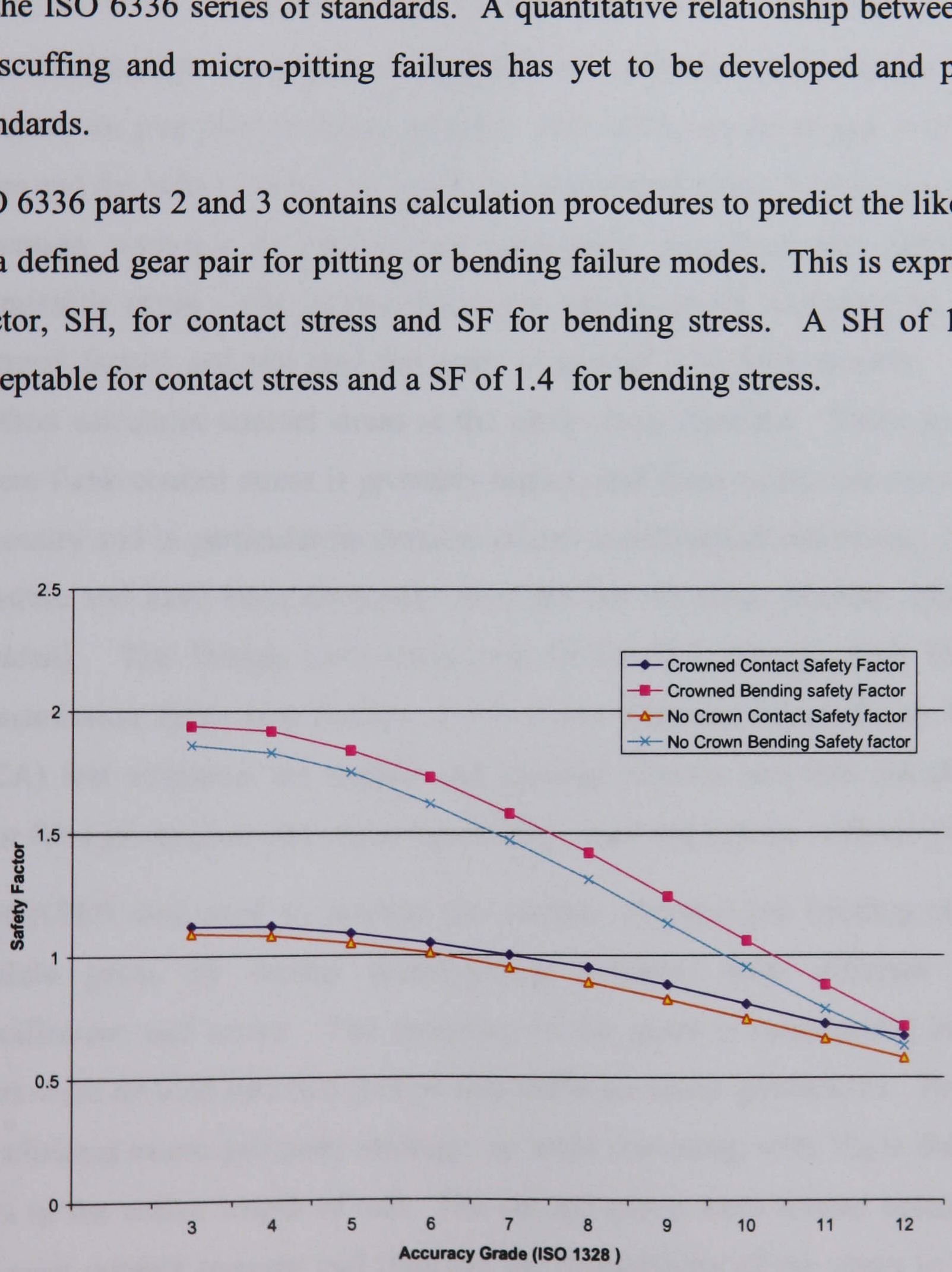

Figure 2.15 The relationship between bending and contact stress safety factor and accuracy grade using the ISO 6336 procedure on a 20 tooth pinion.

The relationship between contact and bending stress Safety Factor is illustrated in figure 2.15. This shows that as accuracy is reduced the safety factor also reduces with an approximate linear relationship for grade 6 gears and below. The safety factor is difficult to define quantitatively [Myers, 2001]. It does not imply that gears with a contact stress safety factor, SH, of 1 or greater will not fail during the defined life for the application. It merely states that for many applications an SH of 1 is found to be acceptable. Some particular applications may show that they require a lower or higher SH to achieve acceptable performance. Specific applications still require the user to define the requirements when particularly arduous applications are encountered.

The relationships illustrated in figure 2.16 probably underestimate the influence of accuracy on gear load carrying capacity. ISO 6336 was developed over a period of forty years and the safety factors are based on a calculated stress, which uses gear accuracy and mounting accuracy as part of the calculation procedure and estimate an assumed permissible stress. The permissible stress values are set according to geometry factors, material factors and test data for gears of around 3 to 5mm module. For example, the method calculates contact stress at the pitch circle diameter. There are many instances where flank contact stress is probably higher, and these values are more sensitive to gear geometry and in particular its detailed micro- specification and errors. Other analysis are possible and have been developed over the last 40 years [Kohler, 1959, Munro, 1962, Haddad]. The Design Unit developed DUGATES (Design Unit Gear Analysis for Transmission Error and Stress), a 3D Finite Element based Tooth Contact Analysis (TCA) that estimates the contact and bending stresses and also calculates transmission error for a given geometry, micro-geometry , load and system stiffness [Hofmann].

DUGATES was used to analyse the contact stresses and bending stresses in 4.5mm module gears for testing micro-pitting initiation with different micro geometry specification and errors. The geometry of the gears is summarised in Table 2.4. The gears were divided into two groups with different micro geometries. The first group used a traditional micro geometry strategy: no helix crowning, with 70μm linear tip relief over 20% of the active length of roll. The second group were further optimised to minimise the peak contact stresses and improve the insensitivity of the gears to alignment errors. The resulting micro geometry was, 20μm of helix crowning, 70μm parabolic tip relief extending over 27.8% of the active profile length.

Table 2.4 Macro test gear geometry.

Parameter	Symbol	Driver	Driven
Teeth	z	33	34
Module	M_n	4.5mm	4.5mm
Pressure Angle	α_n	20.0°	20.0°
Helix Angle	ß	19.578°	19.578°
Profile Shift	x	0.0	0.0
Face Width	b	44.0mm	44.0mm
Tip Diameter	da	166.61mm	171.39mm
Centre Distance	a	160.0mm	160.0mm
Contact Ratio	ε_α	1.545	1.545
Overlap Ratio	$\varepsilon_ß$	1.043	1.043
Tip Sliding Factor	K_{ga}	0.270	0.271

The results from the DUGATES analysis are summarised in Table 2.5 which shows the maximum contact stress and transmission error (TE) for the two groups for 0 and ±15µm alignment error.

Table 2.5 Maximum contact stress variation and TE with alignment error and relief strategy.

Strategy	Crown [µm]	Alignment error [µm]	TE [µm]	Contact Stress [N/mm^2]
Standard	0	0	1.4	1967
		-15	2.0	2022
		+15	1.7	2054
Optimised	15	0	1.3	1730
		-15	2.0	1754
		+15	1.2	1758

Table 2.5 shows that although there is no significant change in TE between the two design strategies, there is a significant reduction in predicted contact stress by an average of 13% (from 2014 N/mm^2 to 1747 N/mm^2). This is a significant reduction in stress (or potential improvement in load carrying capacity) and can be achieved at no additional manufacturing cost. Furthermore the optimised design is less sensitive to alignment errors with a variation in maximum stress of 28 N/mm^2 compared to the standard design strategy with a variation of 87 N/mm^2. This is shown graphically with contact stress plots

taken along three lines of contact (at the start of involute action, end of involute action and through the pitch diameter at the centre of the facewidth) in figure 2.16 for the standard gears and figure 2.17 for the optimised gears. This illustrates how susceptible most designs are to alignment errors caused by gear manufacturing or assembly errors and also how these can these can be minimised by careful design optimisation and analysis.

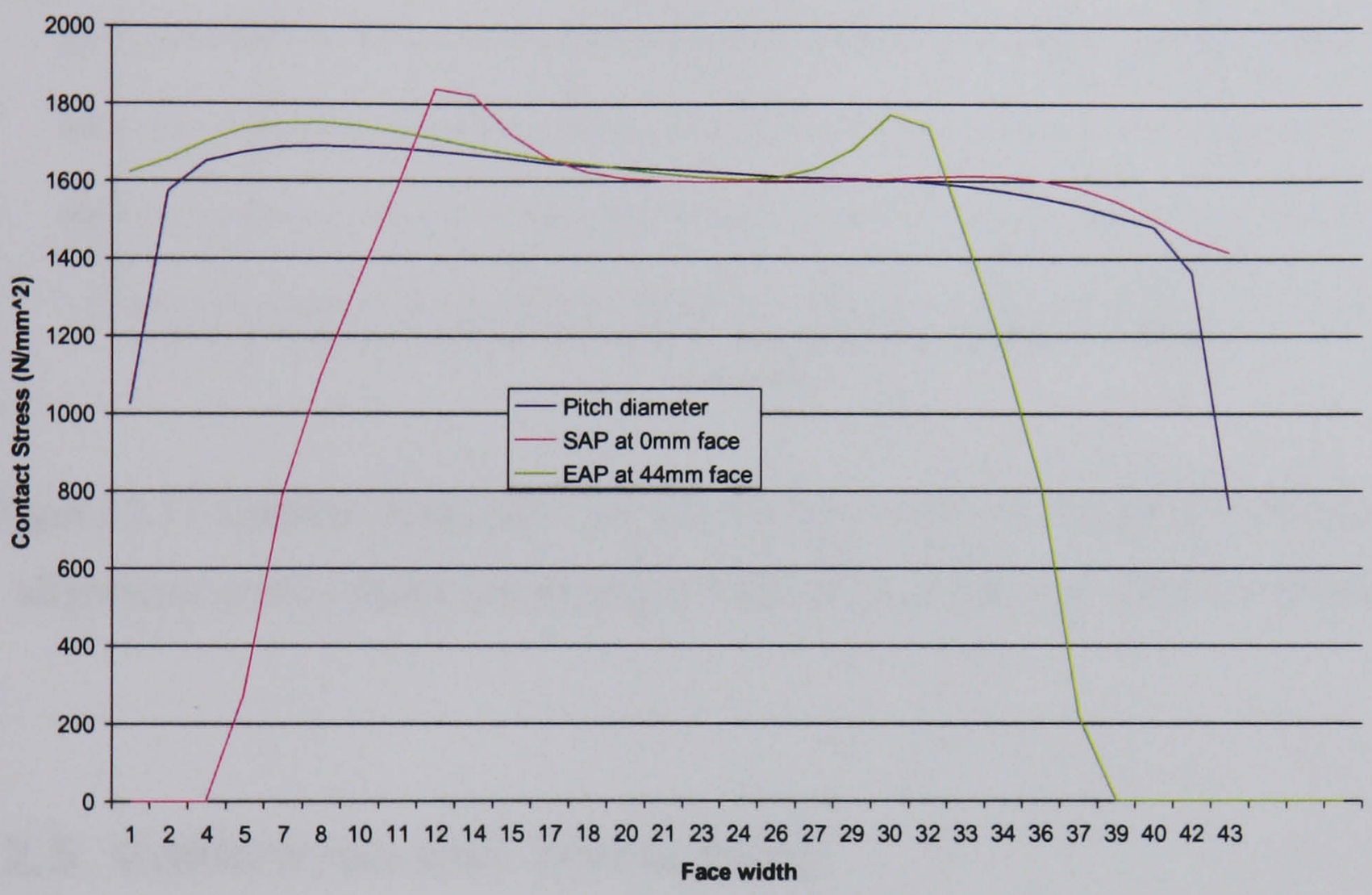

Figure 2.16 Contact stress plots across the face width of the standard design with 15µm alignment error. (These are example lines only and do not show the maximum stress).

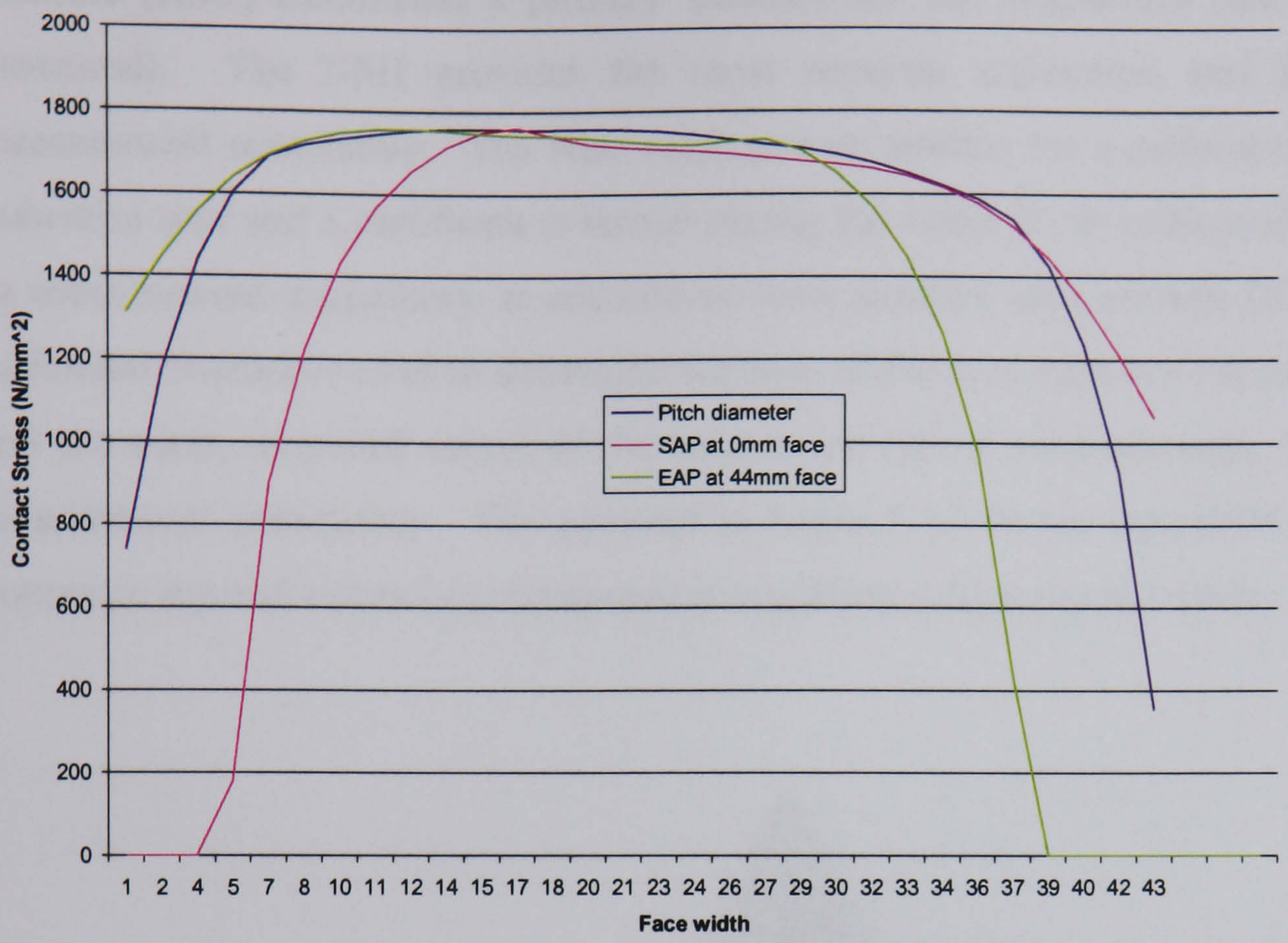

Figure 2.17 Contact stress plots across the face width of the optimised design with 15μm alignment error. (These are example lines only and do not show the maximum stress).

2.5 Calibration and Traceability

Within the UK there is an established structure called the National Measurement System (NMS) that is supported by the Department of Trade and Industry (DTI). The purpose of the NMS is to establish and then disseminate, through a network of accredited calibration laboratories, a structure of traceable measurements where by an unbroken chain of measurements link a shop floor measurement back to the primary standards established by the National Laboratory.

Figure 2.18 shows how the traceability structure works in practice. A National Metrology Institute (NMI) establishes a primary standard for the *measurand* (the quantity to be measured). The NMI provides the most accurate calibration and has the lowest measurement uncertainty. The NMI calibrates an artefact for a calibration laboratory or industrial user and a certificate is issued stating the value of the calibrated parameter and its measurement uncertainty, in accordance with standard requirements [ISO17025]. The calibrated artefact is used to determine the bias (difference between the calibration value and the users measured value) of the instrument and, if used correctly, to estimate the measurement uncertainty. The pyramid in figure 2.18 shows traceability running from bottom to top and increasing measurement uncertainty from top to bottom.

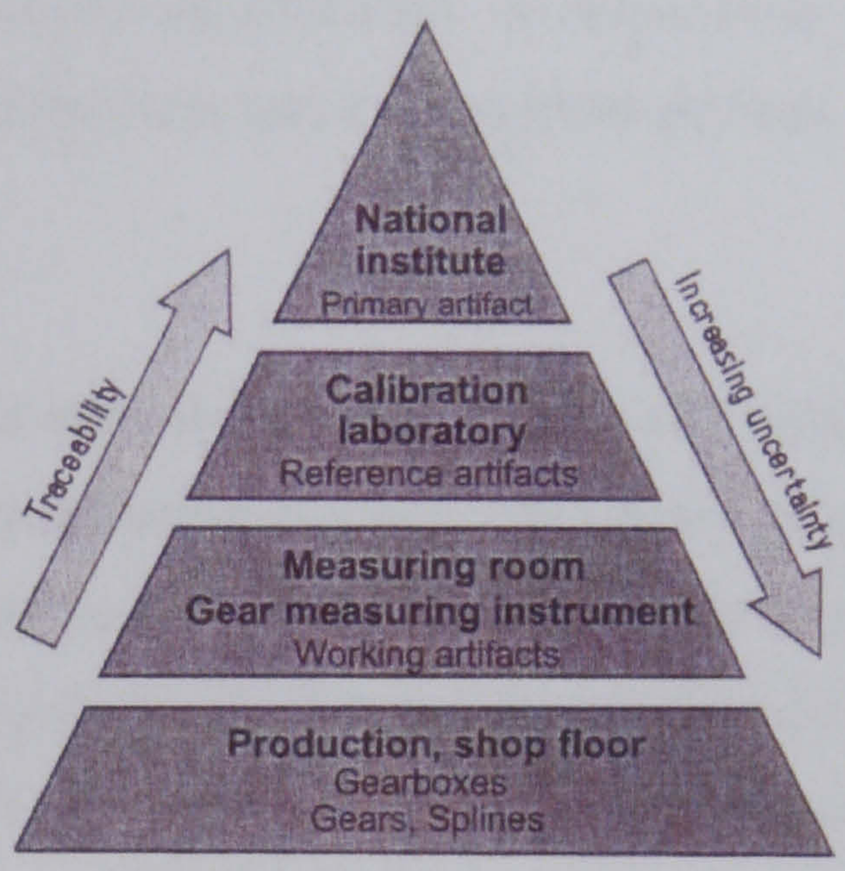

Figure 2.18 Establishment of traceability for measurement on the shop floor.

Definitions

Definitions of common terms are taken from British Standard Institute document, [PD 6461]. However, in the opinion of the author, these explanations are not clear so additional text has been added for clarity.

(a) *Calibration* is defined as a set of operations that establish, under specified conditions, the relationship between values of quantities indicated by a measuring instrument or system, or values represented by material measure or a reference material, and the corresponding values realised by standards.

(b) *Measurement uncertainty* is the parameter associated with the result of a measurement which characterises the dispersion of the values that could reasonably be attributed to the measurand. It is usual in metrology to define measurement uncertainty as a statistical dispersion quoted with a confidence interval, usually a 95% confidence interval (U_{95}). It defines limits which cover the prediction that there is a 95% chance that the actual or *true* measurement result lies within a ± error range defined by the value. Of course, there is a 5% chance that the actual result lies outside this region. Other confidence intervals may be used where deemed appropriate provided they are reported as such.

(c) *Traceability* of a measurement is the property whereby it can be related to stated references, usually national or international standards, through an unbroken chain of comparisons all having stated uncertainties. In dimensional metrology this is usually established by calibrated artefacts and a comparison process.

UK Accreditation Service

To ensure that calibration is carried out correctly, the laboratory, process and staff must be accredited. The UK Accreditation Service (UKAS) are responsible for verifying the suitability of laboratories and staff for completing agreed calibrations. UKAS accredit a laboratory as being compliant with the requirements defined in ISO 17025, 2005. The UKs National Gear Metrology Laboratory (NGML), operated by the Design Unit at Newcastle University, and is accredited by UKAS for disseminating gear parameter traceability throughout the UK. However the NGML is not a primary laboratory.

A EUROMET agreement with the Physikalisch Technisch Bundesanstalt (PTB), the German National Laboratory establishes PTB as the UKs Primary Gear Laboratory. Traceability to PTB is established by calibrated gear artefacts sent from NGML. Users of the services of NGML are thus traceable to the primary laboratory at PTB.

National Laboratories

There are few national laboratories that have calibrated facilities to measure gears. Those who do include:

(a) Physikalisch Technisch Bundesanstalt (PTB), Germany. (Primary facility)

(b) Oakridge Metrology Centre LLXT, Y12 , USA (Primary facility)

(c) National Institute of Standards and Technology (NIST), USA (Primary facility)

(d) Japanese National Laboratory, National Institute of Advanced Industrial Science and Technology(AIST), Tsukuba, Germany (primary facility)

(e) UK National Gear Metrology Laboratory (NGML), (secondary facility)

Comparisons are carried out between national laboratories on a voluntary basis to verify both the measurement compatibility and measurement uncertainty.

2.6 General co-ordinate measurement uncertainty.

A gear measurement result provided without a statement of its measurement uncertainty is incomplete and it not possible to make reliable decisions regarding fitness for purpose. Manufacturers risk losing credibility and income if their components are subsequently found to be outside specification. The following section reviews the relevant research and publications that relate to gear measurement uncertainty.

Measurement uncertainty

There is much published information on the statistical methods that may be applied to measurement uncertainty. Generic methods that are most readily applied when large volumes of statistical data are available from the process industries, in which the problem is to condense large volumes of 'data' into meaningful 'information' [Mandel,1964]. These methods generally model the dispersion in results with Gaussian, Rectangular or Poisson's distributions. For many applications in dimensional metrology large volumes of data are not available to define the distribution. The issues relating to this are to some extent addressed in documents published from 1990 onwards by Standards Institutes or consortia, who serve industry and calibration laboratories [WECC-19, NIST, 1994, PD 6461,1995, UKAS, 1997, ASME, 1998, EA-4/02, 1999, Adams, 2002]. The documents provide procedures for the user to follow but give little insight to the underlying theory. In the metrology field the work by [Dietrich] provides a robust platform for applying these methods. In particular, Dietrich addresses methods to accommodate low data volumes or even single measurements are discussed and simple approximate distributions and rectangular distribution example analyses are provided.

References for applications to complex measurement processes such as CMMs or gear measuring instruments in which there are large number of uncertainty sources are

addressed by the comparator method [ISO 15530] that recommends the use of calibrated artefacts for 'Task Specific' calibration of measurement processes. These are essentially the guidelines that are applied to gear measuring instruments, although the recommendations, drafted by the author, for gear measuring instruments pre-date the CMM material by 8 years [BGA, 1994].

An alternative approach is the application of the Virtual CMM in which a mathematical model of the measurement process and data obtained from appropriate measurement methods [Cox, 2002]. In the authors opinion. this requires very stable measurement processes and is only suitable for instruments situated in closely controlled environments because the data used to generate the virtual measurement process must be appropriate to the current measuring conditions for accurate estimates of measurement uncertainty. The virtual CMM requires a Monte Carlo Simulation (MCS) of the measurement process to generate the virtual measurements.

A further very important limitation is that none of the published work on these classical approaches to measurement uncertainty provide the user with methods to account for bias or systematic errors that remain uncorrected. Methods have been suggested in the flow calibration field [ISO TR5168] but these are not backed by published rigorous testing or published theory, although they are likely to be sound and based on many years of practical experience.

There are other limitations of the classical measurement uncertainty estimation methods, for example they cannot accommodate single sided or asymmetric distributions. This is important when values are near zero or for example when an uncertainty contribution term is biased; a common example is a cosine error that always reduces the magnitude of the measurand.

These issues may be avoided by estimating measurement uncertainty using a Monte Carlo Simulation (MCS) method which has been developed over recent years at most of the leading calibration institutes, including the National Physical Laboratory (NPL) in the UK [Cox, 2001]. Current thinking is that this will be established as the reference method for estimating measurement uncertainty and that over the next few years, applications using MCS method will be compared to results from the 'classical' approach. Applications that yield the same results will prove that the classical methods are acceptable, however when a divergence occurs it will be assumed this is due to limitations in the classical methods.

The MCS method differs from the classical methods by actually simulating a series of virtual measurements rather than simply combining probability distributions. The model allows each input variable to be assigned a probability distribution and then the measurement is simulated by using a random number generator to generate results from each of the input variables. The results are summed linearly and the simulated measurement result is the output, according to the mathematical model. The process is repeated many times, typically between 1000 and 100000 times depending on the complexity, with a random number generator producing different 'virtual' results each time. The distribution of the output values can then be analysed and the 95% confidence interval values established for the actual distribution. This method has been successfully applied to many applications [Cox,2001] but in the authors opinion although it has many advantages, it has some significant limitations:

- the inputs or sources of uncertainty distributions must be accurately measured and validated to ensure the validity of the virtual measurement results, and
- the bias or systematic errors cannot be included unless they are compensated or added linearly.

However the method has developed for use in a gear measurement application in Chapter 7 and yields some very promising results.

All these methods have a further anomaly that is difficult to quantify; the more work that is carried out in measurement uncertainty assessment, the larger the estimate of measurement uncertainty. This can be easily demonstrated by considering a measurement process that has its measurement uncertainty established with a single calibration item. The uncertainty estimate can be validated by a second calibrated test item and found to be acceptable by a comparison with the calibration data. If the measurement uncertainty is further validated by a series of tests on a range of calibrated items, eventually a U_{95} that is greater than the original estimate derived from a single artefact is estimated. Thus the additional work provides us with a larger uncertainty but greater confidence, while few tests give us lower uncertainty without the perceived reduction in confidence by the user. This encourages less testing and calibration, not more, and is clearly counter intuitive.

A Bayesian statistical approach, avoids some of these issues. It is applied to measurement applications where the historical data is used to improve the estimate of a measurement process and reduce measurement uncertainty [Weise]. It has been adopted

for limited applications for Key Comparison Reference Values (KCRV) evaluation and may be suitable for other comparator type assessment work (eg. gear measurement) but has yet to be implemented [Cox, 2001].

The methods are discussed in more detail in Chapter 4.

Establishing traceability

There are a number of methods of establishing traceability or calibrating a measurement process that are largely independent of the statistical model used to estimate measurement uncertainty. The methods are directly applicable to CMMs or CNC controlled gear measuring instruments and most mechanical (older) gear measuring instruments.

- **Comparator method**

The comparator method uses a calibrated artefact to estimate measurement uncertainty, where the artefact has similar geometry to the workpiece inspected. For involute gears, this means an involute form artefact with similar dimensional size and mounting arrangement to the workpieces. Each parameter that is measured and evaluated should be calibrated on the artefact with a nominal value and measurement uncertainty stated.

The comparator method is the easiest to apply on the shop floor and provides the user with a relatively simple but robust estimate of the measurement process uncertainty. Furthermore, it is a functional check on the total measurement system performance. The disadvantages of the process are that it has limited scope and only checks the performance at a specific geometry. Also it provides no information on the cause of any excessive differences between calibration certificate values and measured values. This method is researched and applied extensively in Chapters 5, 6 and 7.

- **Surrogate artefact method**

This method is similar to the comparator method but there is a lack of similarity between the calibration artefact and workpieces. Often this is because the calibrated artefact is designed with features that reduce the uncertainty of calibration. For example the involute profile may be replaced by the surface of the sphere because it has lower form errors. However because the geometry is different there remains the question of whether the measurement on the surrogate artefact is more or less accurate than those obtained on a workpiece. This method is researched in Chapter 8.

- **Decomposition method**

The decomposition method is more complex than either of the two previous methods and is only applied in national or primary calibration facilities. The method involves using very basic but easily calibrated artefacts such as gauge blocks or step gauges to estimate the uncertainty of the measurement of the measuring volume used for calibration purposes. In the authors experience it has only been used on 3-axis CMMs [Harary,1994] without a rotary table and is not practical for shop floor instruments.

- **Virtual co-ordinate measuring machines (VCMMs)**

This technique is currently being developed by NIST in the USA and by NPL and PTB in Europe with industrial support [Härtig, 1997]. The method uses a MCS method to estimate random uncertainty combined with a parametric error map to estimate systematic errors in the measuring volume. At present the method has been developed for 3 axis linear CMMs without a rotary table, but it is proposed that PTB and an industrial collaborator will implement a model of the rotary table to allow the method to be extended to gear measurement [Härtig, 2004]. This method requires an accurate parametric error map that has a sufficiently fine grid so that important high frequency form errors are included in the compensation. A parametric error map involves measuring each of the 6 possible sources of error on each axis. This is time consuming and very difficult to perform with sufficient accuracy to ensure reliable results are obtained.

A summary of CMM and gear measuring instrument calibration procedures

CMM uncertainty evaluation procedures were traditionally used to define single axis and volumetric length measurement uncertainty. However, the latest revisions to ISO 10360 include the measurement of probe scanning performance and rotary table accuracy. The documents prescribe a series of tests that allow the user to compare the performance of different measurement solutions and verify the stability and reproducibility of the instrument, however they do not recommend acceptance limits or provide procedures to estimate measurement uncertainty. Furthermore, the documents do not allow the user to estimate the uncertainty of performing measurement tasks on reference artefacts or workpieces. Guidance on this if found in other ISO documents [ISO 14253-1].

The German Institute of Mechanical Engineers (VDI) publish a series of guidelines [VDI/VDE 2617 Parts 1 to 6] that provide recommendations for checking CMMs and gear measuring instruments. These include how to check CMMs and include guidance on checking straightness, length measurement uncertainty, squareness, angular errors and probing errors. The documents are based on machine tool testing practices but again they fail to provide the information necessary to estimate measurement uncertainty.

The VDI also provide recommendations for gear measuring instruments. These documents are more helpful and provide acceptance limits for pitch measurement [VDI/VDE 2613], profile measurement [VDI/VDE 2612-1] and lead (helix) measurement [VDI/VDE 2612-2]. The documents include acceptance limits and define a measurement uncertainty U_{95} when measuring calibrated gear artefacts and master gears and they also recommend the calibration requirements of gear artefacts and the basic instrument alignments required for achieving the stated uncertainty. It is evident that although these documents were written in the early 1980's they are more specific, and hence more useful than those prepared for general purpose CMMs in the late 1990's.

To rectify this a new series of documents was prepared in the UK and published by the British Gear Association (BGA) [BGA, 1994]. These 'codes of practice' defined uncertainty requirements, a measurement procedure and evaluation procedure that included a method of combining random and systematic errors in common with, but developed independent to the Flow Calibration document [ISO/TR 5168]. However in the authors opinion the estimates of uncertainty are still inflated for typical shop floor instruments but, as discussed in Chapter 7, they tend to underestimate uncertainty values when applied to processes with low bias and repeatability.

Finally, a guidance document [ISO 18653] was prepared by ISO TC60/WG2, with participation from the author (as the UK expert) on evaluating gear measuring instrument performance. This document was obliged to use a statistical evaluation procedure outlined in ISO 14253-1, which in the authors opinion produces results that are even more pessimistic than those of the earlier BGA 'Codes of practice'.

Chapter 3

SOURCES OF MEASUREMENT ERROR

The history of gear measuring equipment is reviewed and methods to minimise errors in the measurement process are discussed in this chapter. A comprehensive review of sources of error in the measurement process is also included.

3.1 Measuring equipment

Early Instruments

The ease with which involute gears could be measured was one of the key reasons the involute form was readily adopted by manufacturers. Measuring instruments from Sykes, Wickman, Maag, Zeiss, Lewis, Orcutt, Illinios Tool Works, were developed in the 1920's [Rolt]. Figure 3.1 illustrates an instrument developed by Tomlinson at NPL which was designed to measure cumulative pitch error and profile errors. The early versions of the instrument measured profile deviation by a micrometer screw drive on a calliper but this was replaced by a Pantograph mechanism (shown in figure 3.2) that was used as a comparator with a x10 template [Tomlinson, 1923] .

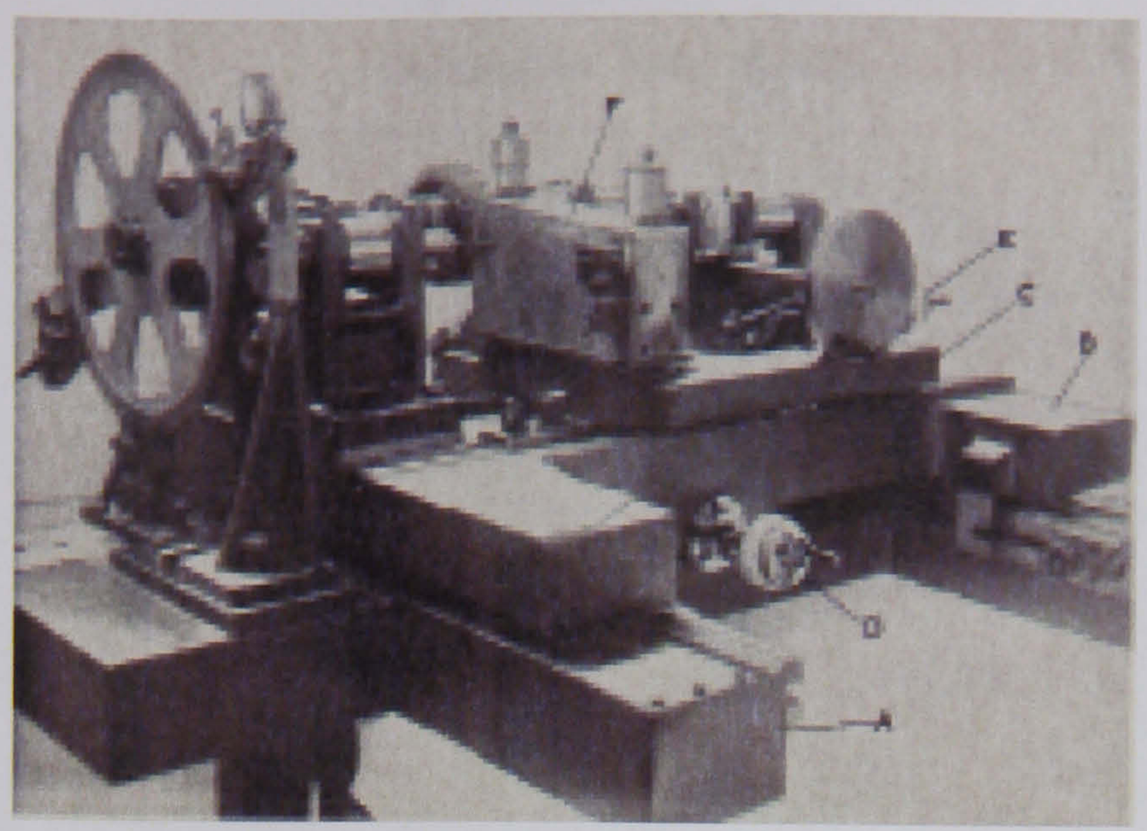

Figure 3.1 Tomlinson gear measuring machine (circa 1923) [Rolt].

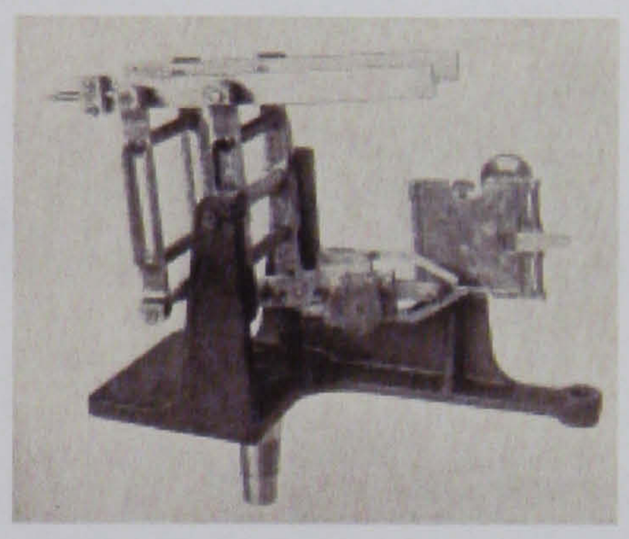

Figure 3.2 Tomlinson pantograph profile measurement with a x10 template [Rolt].

It was reported that a magnification of x10 was used for profile charts and instruments had 0.0001" discrimination for pitch error. Furthermore, users clearly understood how the results could be analysed to identify the cause of the errors [Rolt]. Figure 3.3 shows the cumulative pitch error plot from a gear and figure 3.4 show the sine bar indexing system used to measure them. Provided that this type of indexing mechanism is repeatable, the pitch measurement method is accurate within the reproducibility of the system because setting errors can be compensated by a closing error calculation. This calculation method was used on a number of later instruments, including several modern CNC measuring instruments.

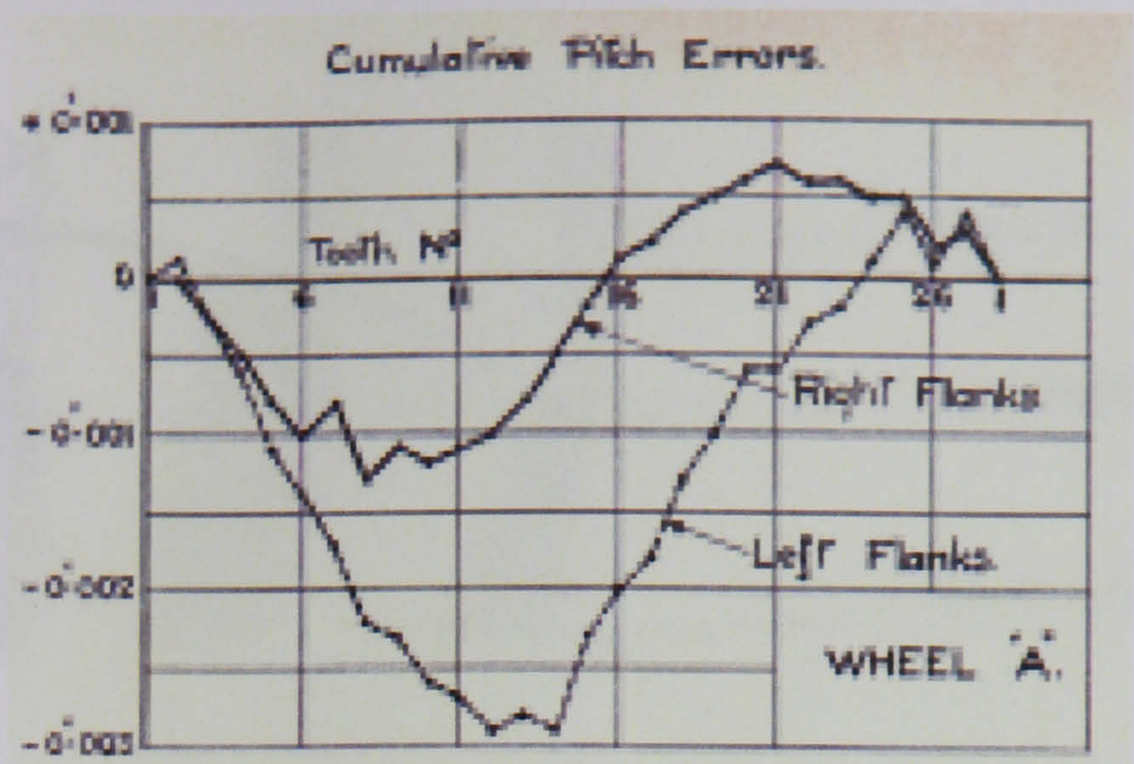

Figure 3.3 Cumulative pitch plot [Rolt].

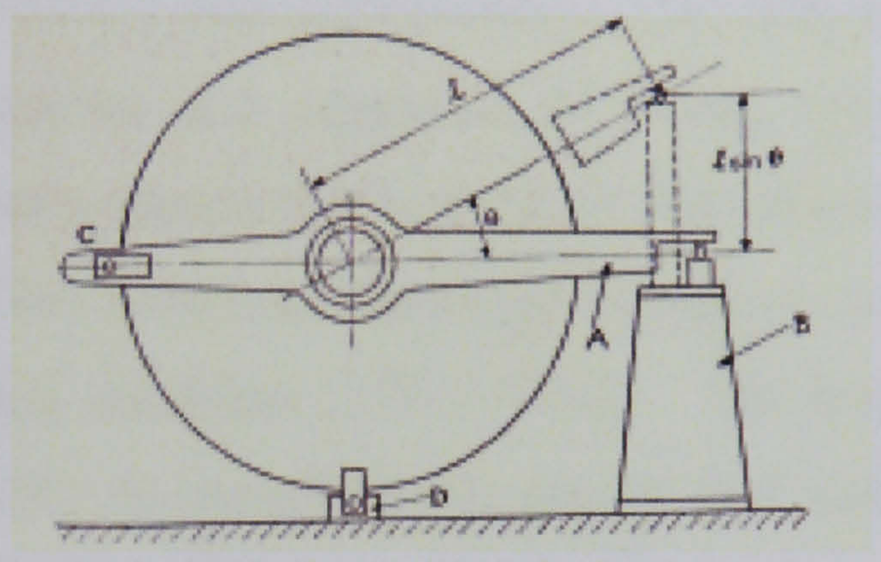

Figure 3.4 Cumulative pitch sine bar indexing system [Rolt].

The next generation machines were base disc involute measuring instruments that have been in use through to the present day. The principle of measurement is illustrated in figure 3.5. The base disc generates the theoretical involute shape by rolling a disc of the same diameter as the base diameter of the gear to be measured. As the disc rotates along a straight edge the translation of the centre of the disc drives a chart recorder that enables the deviations from the true involute to be described as a deviation from a straight line. Analysing the departure from a straight line is very simple compared to evaluating the deviations from a complex involute curve. Thus in the early 1930s involute gears were measured with mechanical scanning machines with acceptable accuracy to control gear quality. The machine layout is illustrated in figure 3.6 and an example of a machine is shown in figure 3.7.

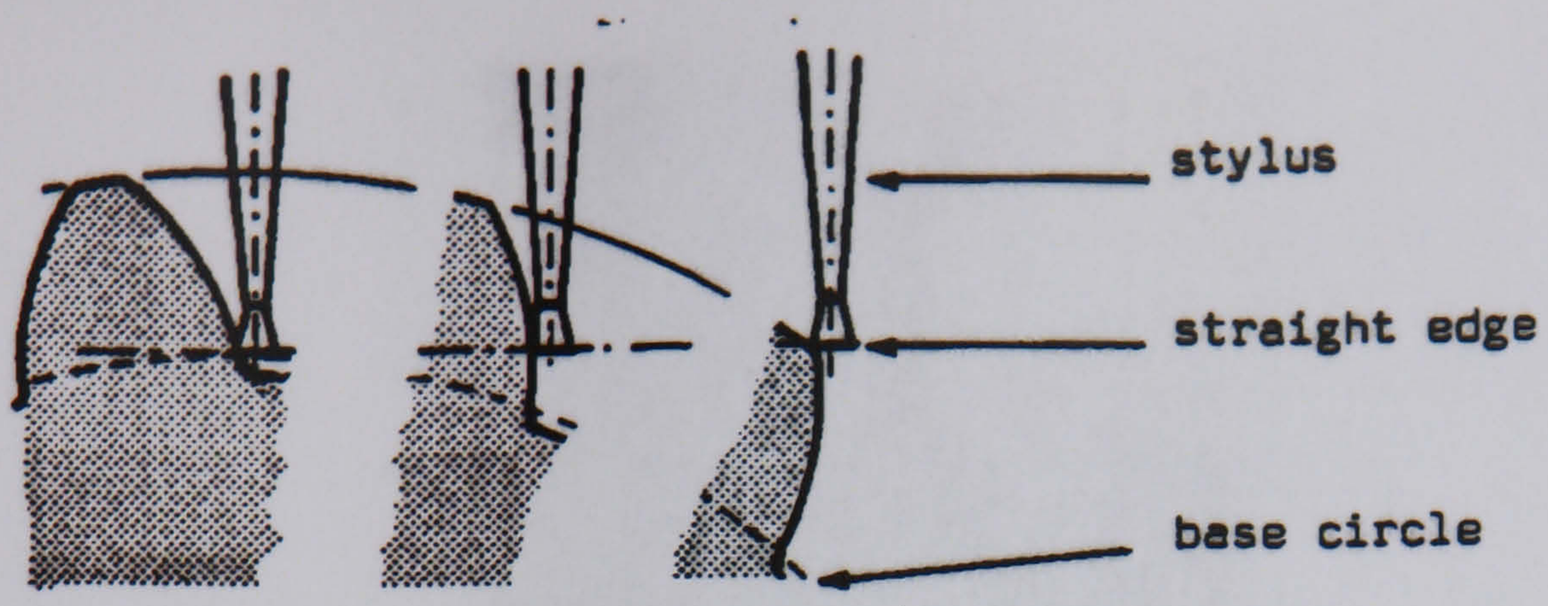

Figure 3.5 Involute gear measurement using a rolling base disc [Munro]

Instruments of this design were developed by Maag, David Brown, Frenco and others during the last 50 years to improve their performance. The main focus for improvements were better measurement probes and improved recording systems for measurement records [Timms]. Early systems used a line scribed on smoked glass plate, then used pen and ink on paper (early 1950s), electrical discharge etching on conductive paper (1950-60) followed by X-Y plotting machines (1970-1980s). The final development was to interface instruments to a PC to automatically record and evaluate the results to a recognised accuracy standard [Frenco].

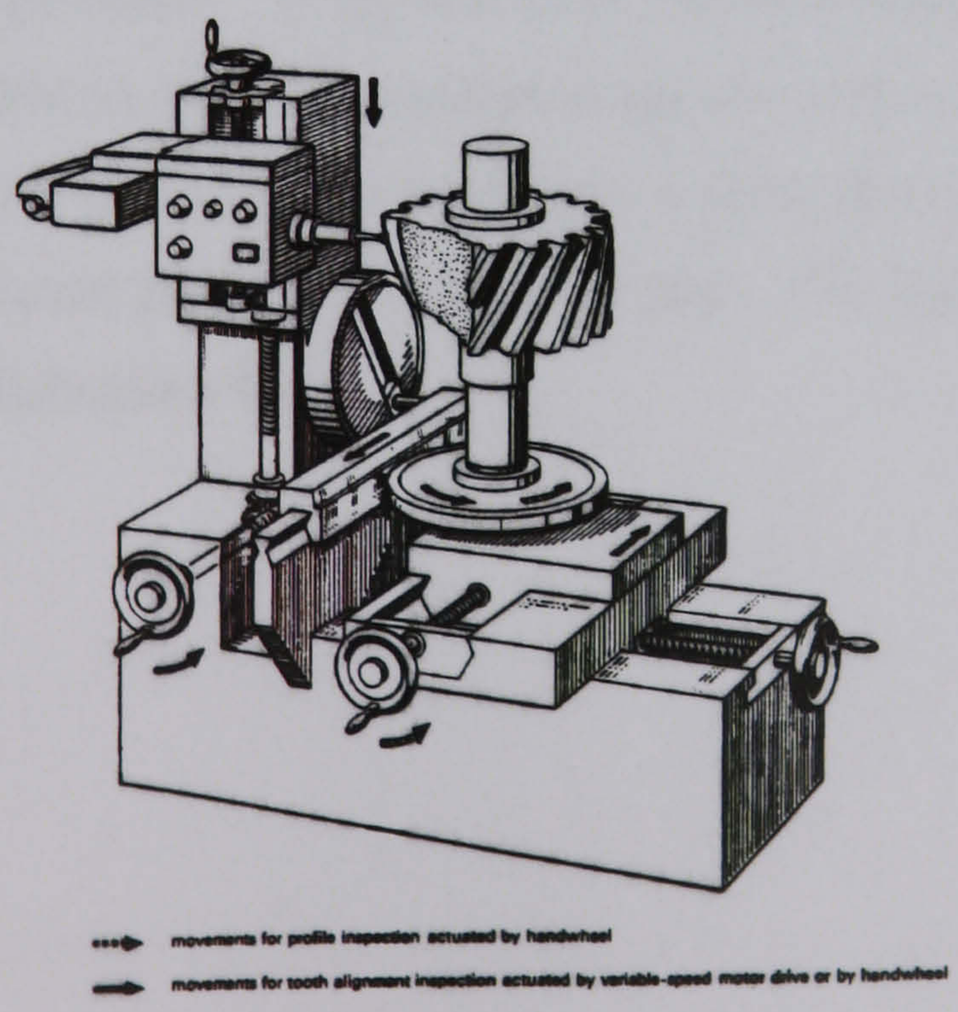

Figure 3.6 A simple lead and profile measuring machine with rolling base disc [Munro,1989].

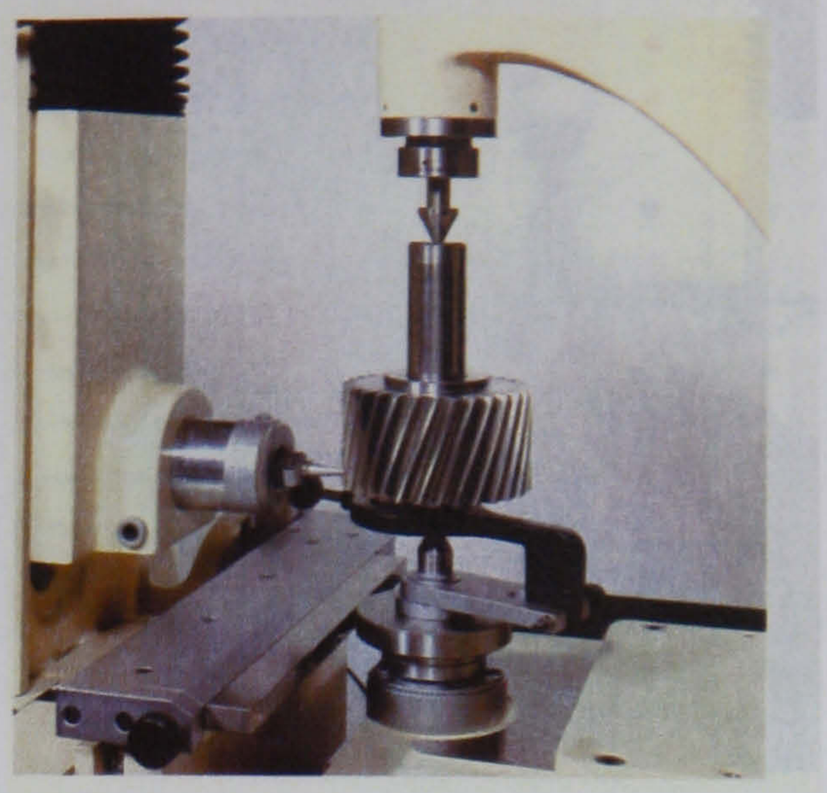

Figure 3.7 Mechanical base disc lead and profile measuring instrument [Frenco].

The same profile measurement principle, that of rotating the gear and translating a probe in the base tangent plane was employed in the early CNC measuring machines [Lawson] and is still used in present day measuring instruments.

One of the disadvantages of these relatively robust and simple mechanical instruments is that they can not measure pitch errors. Additional attachments or instruments were needed to measure pitch errors. A typical pitch measurement attachment is shown in figure 3.8. The portable instrument requires a spindle with a constant speed drive to allow the control system to drive the probes into a tooth space in order to measure the difference between adjacent pitches on each tooth pair. The instrument can also be used on gear cutting and grinding machines.

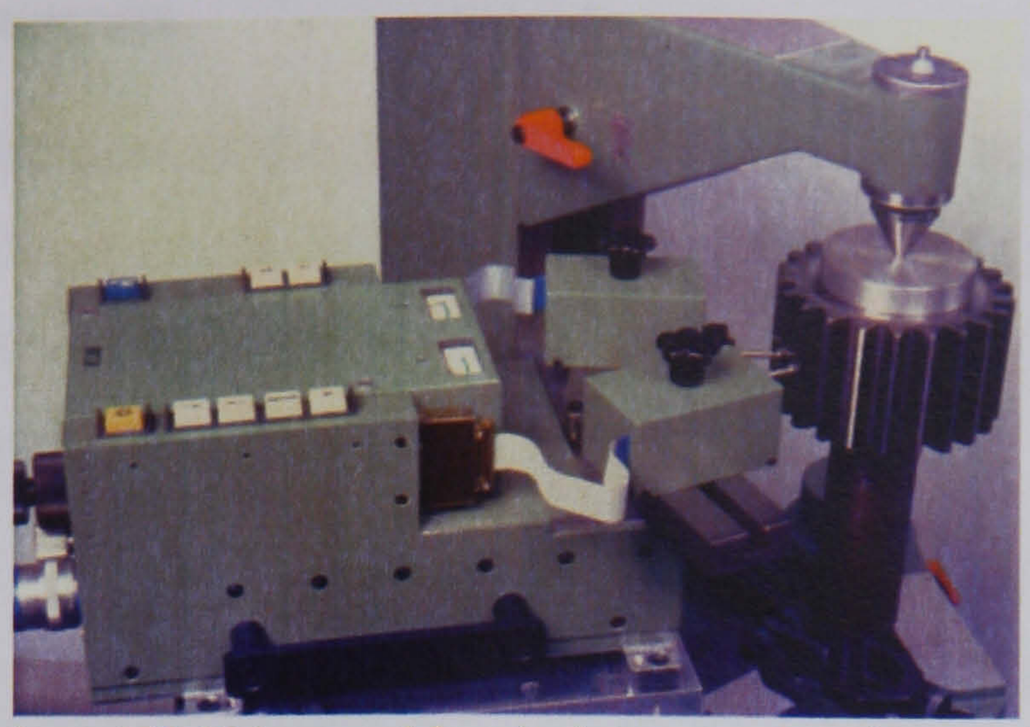

Figure 3.8 Maag ES401 portable pitch measuring instrument.

The operating principle of the portable pitch measuring attachments is illustrated in figure 3.9. Two probes are used. One probe is either a solid probe or is a measuring probe that has a trigger point to define when the deflection has reached a predetermined value. The second is a measurement probe which detects the error. The difference between the probe values is thus the adjacent pitch value. This is repeated on all the teeth and the measured error values are determined by subtracting the mean value of all the teeth from the measured value. The results are then plotted out manually on the early instruments or automatically on the later instruments. Early instruments required manual closing error analysis whilst later instruments also had the benefit of automatic evaluation that reduced operator errors and also speeded up the measurement process.

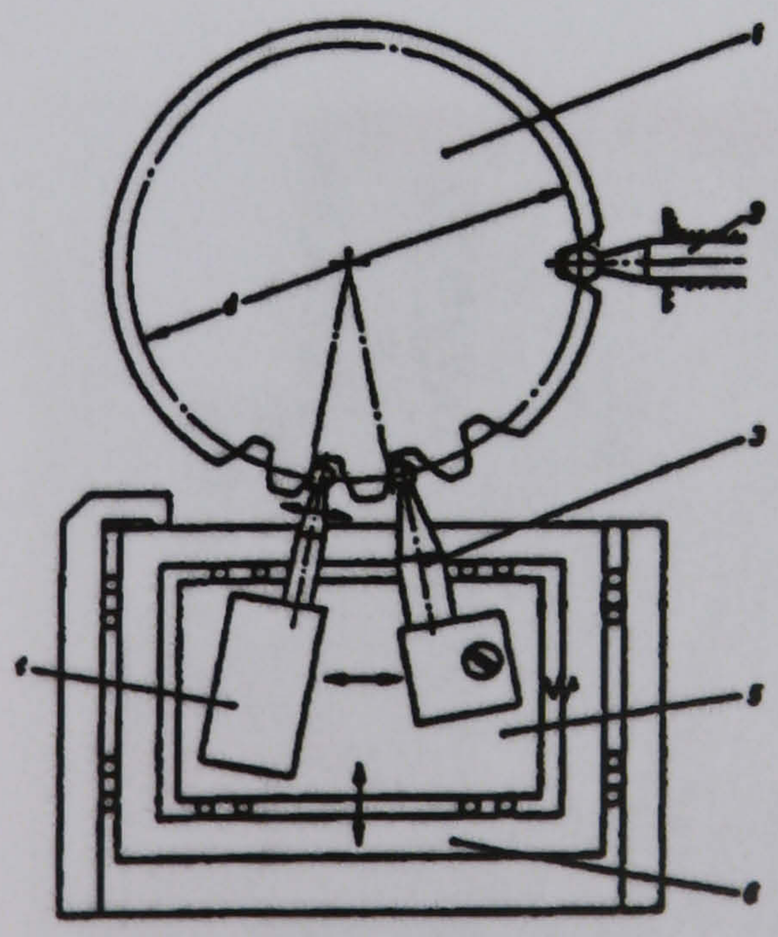

Figure 3.9 Principle of operation of portable pitch measuring instruments

(1- gear, 2-locating probe, 3- reference probe, 4-measuring probe, 5-horizontal carriage, 6- radial carriage).

Modern measuring instruments

The development and refinement of the dedicated CNC gear checking machine over the last 30 years has had a crucial role in improving gear manufacturing capability [Munro, 1997]. High accuracy CMMs equipped with rotary tables and scanning probes are also very capable of measuring high quality gears.

There are many designs of CNC gear measuring machine available. They fall into 2 main types: 4-axis and 3-axis CNC machines, as illustrated in figures 3.10 and 3.11 respectively [Frazer, 1996].

4-axis dedicated CNC gear measuring instruments

4-axis CNC gear measuring instruments comprise 3 linear axes (vertical, radial and tangential axes) and 1 rotary axis, measure involute profile using the same principles developed for the simple base disc mechanical machines. The mechanical linkages of the sine bar for lead measurement and base circle disc for involute measurement are replaced by a CNC controller that is usually configured in a master-slave mode. The single axis mechanical probe is usually replaced by a single axis LVDT, such as the Tesa GT31 bi-directional probe or a full 3 axis LVDT scanning probe. In many earlier instruments a clamping system was used to lock the probe axes that are not used during gear measurement.

Figure 3.10 A 4-axis Sigma 7 from M&M in the USA is equipped with a 3-axis LVDT probe, linear motor drives and a direct drive rotary table.

Linear axes are constructed with ground guides and rolling element bearings and the drive system usually comprises a ballscrew driven by a servo motor with Heidenhain type linear optical encoder used for position feedback. The rotary tables use an angular encoder with a multi-stage friction or belt reduction drive and the rotary axis are usually of the rolling element type bearing. A key factor on performance of the instruments is the resolution of the encoder that provide feedback for CNC position control. The higher the resolution the smoother and more accurate the resulting position control. Work at the NGML [Maillio] shows that most control systems require approximately 10-12 counts following error as the best that is practically achievable. Early CNC instruments had a linear encoder resolution of 0.1μm [Höfler] but later instruments achieve 0.008μm [Klingelnberg] providing better control and higher repeatability.

Recent designs of instrument use linear motors to simplify and improve the performance of the linear axes and the complicated and somewhat unreliable multi-stage rotary table drives have been replaced by direct drive torque motors. This has improved repeatability for lead, profile and pitch measurement parameters to around 0.1μm but the new designs are susceptible to thermal problems during operation [Mancasola, 2003].

Table 3.1 contains a summary of the benefits and limitations of dedicated CNC measuring instruments.

Table 3.1 Benefits and limitations of CNC gear measuring instruments

Benefits	Limitations
1. Fast - they measure lead, profile and pitch errors in one setting and will evaluate the results and compare them to the relevant standards or accuracy requirements specified on the gear drawing. They can also take multiple measurements across the face-width to allow for further analytical work for controlling quality.	1. Expensive.
2. Do not need skilled personnel to evaluate the results- only partly true but certainly less evaluation is required.	2. Require a reasonable environment if they are to work accurately.
3. Are inherently more accurate because the slide design are more simple, reliable and stiffer.	3. When they do go wrong, only qualified personnel can fix them - the standard of after sales support can be of paramount importance.
4. Other features may be measured as well as gear parameters eg journal runout.	4. Despite all the modern developments, they still only check a few teeth at a few positions on the flank, so it is still possible to miss tooth damage or the largest error on the gear.
5. Mounting errors may be corrected so gear errors may be measured directly with reference to the functional datum surfaces.	5. Can not guarantee accuracy just because the results are tabulated to 0.1μm. The accuracy of the machine will depend on the skill of the operator, the environment and the how the accuracy of the machine is verified..
6. Statistical records may be kept and records linked to other computer programs.	
7. More complex components may be measured with the same equipment, eg cutters- hobs, shaving tools, shaping tools, worms, bevel gears and prismatic parts.	
8. More clients expect to see records from a CNC machine.	

3-axis dedicated CNC gear measuring instruments

3-axis machines dedicated to gear measurement use 2 linear axes (Z, vertical axis & Y, radial axis) and a rotary (φ axis) to measure the gear as illustrated in figure 3.11. The main difference in operation between these and dedicated 4-axis machines is how they measure profile.

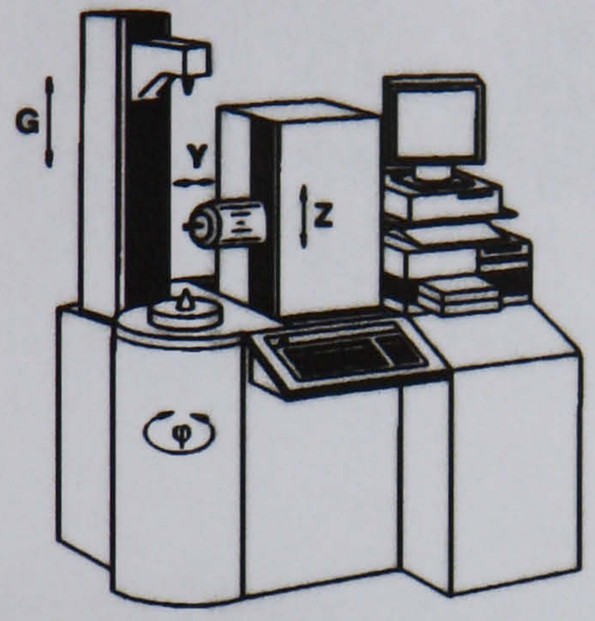

Figure 3.11 An example of a 3-axis CNC gear measuring machine [Klingelnberg]

The benefit a 4-axis machine is that the involute generation process ensures that the measurement axis always coincides with the line of action of the involute gear. Thus errors that are not in this line of action plane have only a second order effect on the involute measurement accuracy. For example, probe datum errors and stylus geometry errors have little influence on the involute measurement accuracy. In 3-axis measurement this is not the case. The instrument generates the involute as an absolute curve in space. Because the probe contact position changes as it moves over the involute curve, all errors including the probe geometry become important. Thus to obtain accurate involute measurements on a 3-axis machine requires an accurately and frequently calibrated probe stylus.

Three-axis instruments, for example the Klingelnberg PNC33 pictured in figure 3.12 have some benefits; they are more simple and cheaper because they require fewer parts and do not require the additional servo control and expensive drive components that is needed by a 4-axis machine. However they are no longer manufactured because drive components in general are becoming cheaper and the need for optimum measurement accuracy is increasingly demanding.

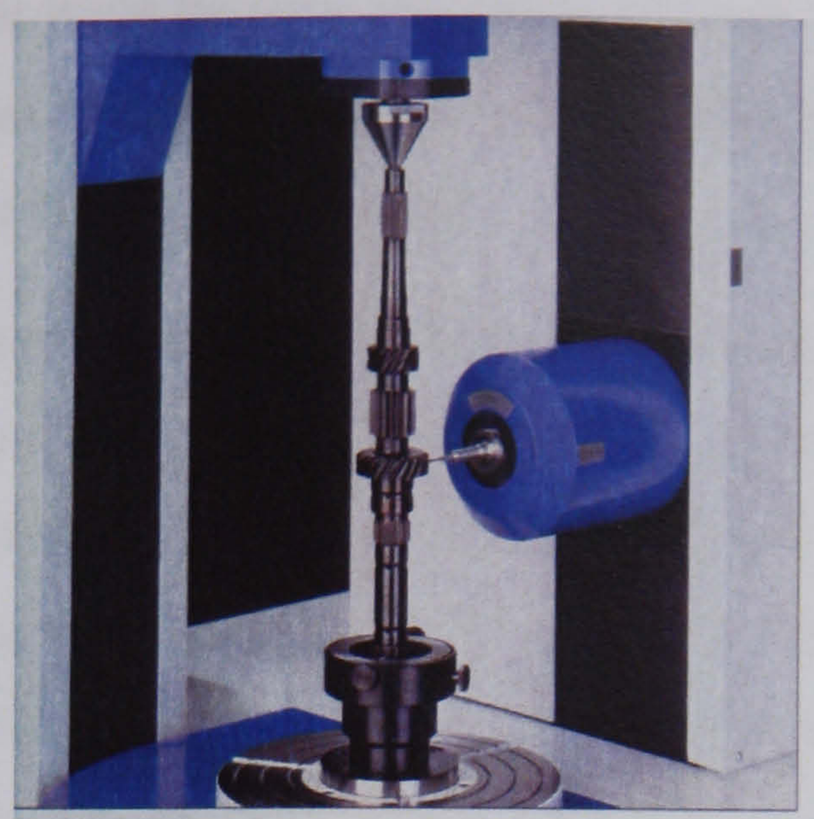

Figure 3.12 An example of a 3-axis dedicated CNC gear measuring instrument (Klingelnberg PNC 33)

Coordinate measuring machines (CMMs)

The limitations of 3-axis machines apply to the performance of 3-axis CMMs with gear software (both with and without a rotary table). These are compounded on CMMs however because the lack of a rotary table requires either a star type of probe arrangement or a Renishaw indexing head such as the PH10M.

For significantly less than the cost of a gear measuring machine, it is possible to buy a CMM with software which will facilitate the measurement of gears. While this may appear to be cost effective, there are a number of points which must be noted :

- Most gears are manufactured to a high accuracy and will require measurement using a very accurate CMM (which is expensive).
- Some lower quality gears with larger tolerances (eg ISO 1328 grade 8 and lower) may be measured with appropriate accuracy on average CMMs with touch trigger type probes. They generally require a scanning type probe if sufficient data is to be obtained in a time which is comparable with a dedicated CNC gear measuring machine.
- Gears are complex shapes and will usually require a rotary table to index the gear to the correct orientation for the probe to access the flanks. (alternatively they will need 8 accurately calibrated probes to execute a standard measurement on a gear or a motorised probe such as a Renishaw PH10M).

- The datum axis of the gear must be very accurately defined if the measurements are valid, which may be a time consuming process on a CMM, and there are sometimes practical issues with access for probing journals.

An example of a high accuracy Zeiss UPMC CMM is shown in figure 3.13. It has a portable rotary table (RT05) and is being used to measure an automotive lay-shaft. The rotary table reduces the number of styli that are required to complete a standard gear measurement. The measurement procedure also involves determining the position and axis direction of the rotary table , prior to determining the mounting position of the gear on the rotary table. Few CMMs use a tailstock, although the Zeiss ZMC550 is the exception, which was designed as a dedicated gear measuring instrument with in-built rotary table.

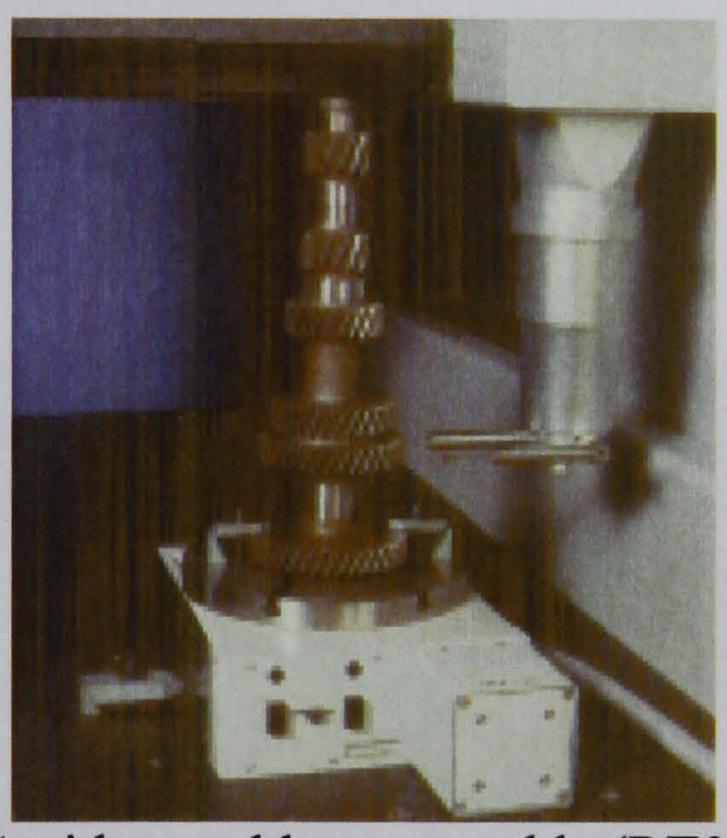

Figure 3.13 A Zeiss UPMC with portable rotary table (RT05) used to measure an automotive lay-shaft

A Mitutoyo CMM equipped with a Renishaw SP25M scanning probe mounted on a PH10M indexing head is a more common shop floor instrument and is shown in figure 3.14. This is the more usual arrangement for a CMM used to measure gears only occasionally. The calibration of the position of the probe stylus centre is critical for accurate pitch measurement. The process of calibrating the PH10M indexing positions for gear measurement takes approximately 45 minutes. Gear measurement takes approximately 15 to 25 minutes depending on the data density, which is considerably longer than a dedicated CNC gear measuring instrument. Figure 3.15 shows how a CMM can be used to measure large batches of gears without operator intervention.

Figure 3.14 Mitutoyo CMM equipped with a Renishaw SP25M scanning probe mounted on a PH10M indexing head.

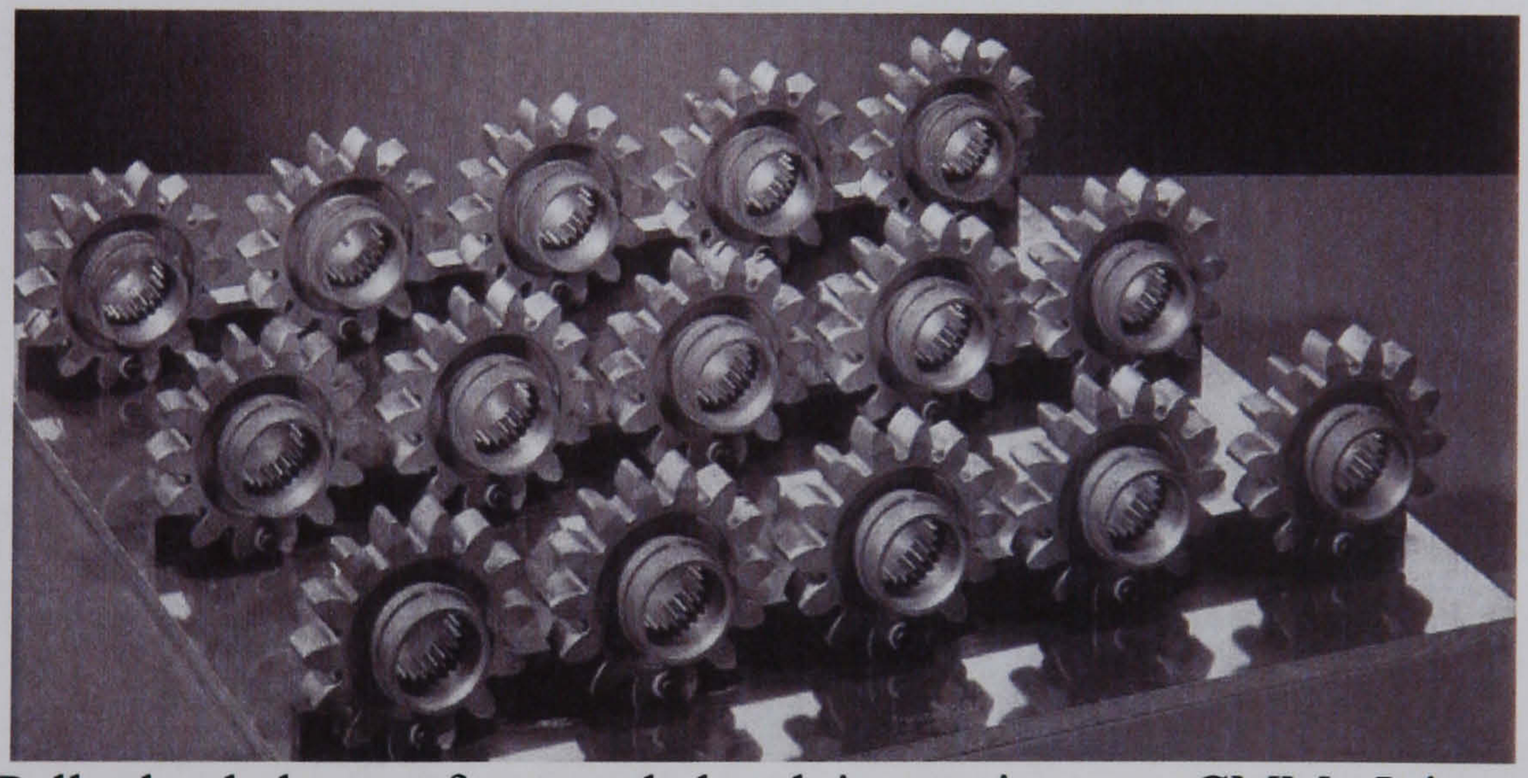

Figure 3.15 Pallet loaded gears for sample batch inspection on a CMM. It is very difficult to replicate this measurement strategy on a dedicated gear measuring instrument.

The benefits and limitation of the CMM method is summarised in Table 3.2.

Table 3.2. Benefits and limitations of using CMMs for gear measurement

Benefits	Limitations
1. Very flexible.	1. Require a good quality CMM, which can be expensive.
2. By definition are able to check any feature on the gear, not just the gear parameters	2. Tend to be slow compared to dedicated gear measuring instruments.
3. Can measure pallet loads of gears without operator intervention.	3. Often require a rotary table that will add to the cost of the machine.
4.Useful if you only check gears occasionally.	4. Need a high accuracy probe if they are to achieve the accuracy required for top quality gears.
	5. many do not measure profile using the generating method of measurement used by simple base disc machines. This makes the process more sensitive to errors in the probe system and temperature effects.

3.2 Measurement procedures

There are no national or internationally agreed procedures for measuring gears. Standards such as ISO 1328 specify the accuracy grades and related tolerances, but do not specify the detailed methods or procedures which should be used, what should be checked and where and what equipment should be used and how accurate it should be. Some additional information is provided in the supporting Technical Report [ISO/TR10064-1] but the guidance falls short of a prescriptive step by step procedure. The British Gear Association codes of practice [BGA, 1994] are an attempt to address these short-comings in the standards.

DUCOP.03 Involute Gear Measurement, defines a measurement method for involute gear measurement. It addresses:

- the accuracy requirements of gear measuring machines, related to gear accuracy grade
- permissible gear mounting errors
- recommended environmental conditions

- gear parameters to be checked
- measuring position
- the number of teeth to be measured
- tooth numbering
- how to evaluate the results
- interpretation of results and the resulting actions (if any) that should be taken
- inspection records required for valid measurement results
- expected differences in results between measurement processes
- certificates of conformity

Mounting errors create errors in the gear parameters measured and may result from mounting errors during the manufacturing process or from measurement process. Without the accurate measurement and definition of the reference surfaces on the machine we may introduce excessive errors into the measurement process.

The CNC instrument probe can also measure the runout of the journal surface as part of the measurement process. Measured errors are used to define the gear axis and thus correct mounting errors. There are two methods that may be applied, either

- correcting the path the probe describes to account for the mounting errors as the gear is measured (which is the preferred method) or
- by measuring the part and then correcting the measurement results for the known mounting errors (which may lead to residual secondary errors).

DUCOP03 Measurement procedure:

The recommended procedure for the inspection of gears is.

1. verify the instrument is calibrated (once per week minimum)
2. select and calibrate the correct probe size
3. clean the gear flanks and the datum surfaces and check to see all the teeth have been cleaned up in the final grinding process and the gear is free from nicks, burrs and damage

4. verify the gear data fully specifies the design requirements

5. mount the gear on the machine and verify that it runs true (5μm or less for most applications) and record the mounting error on the record sheet. See figures 3.16 and 3.17 for examples of mounting methods.

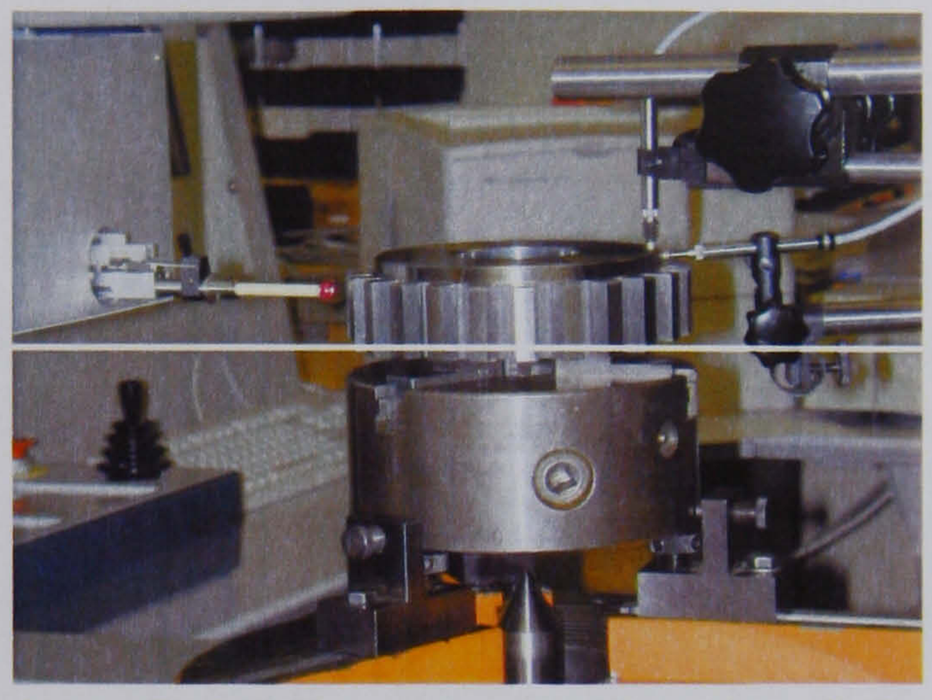

Figure 3.16 Use of Feinpruf LVDT probes to measure radial and axial runout on a gear mounted directly on the rotary table.

Figure 3.17 A large gear mounted on the measuring machine where the instrument stylus measures the runout of the journal surface as part of the measurement process.

6. measure 4 teeth, left and right flanks, at approximately 90 degree intervals for helix (lead) and profile error. (Note if there is a significant variation in the lead results or profile results re-check additional teeth between the original ones)

7. measure all teeth, left and right flanks, for cumulative pitch, adjacent pitch and radial runout error

8. check the results to establish if any are outside the tolerance. If so the gear has failed its accuracy specification (record this on the record sheet)

Note :

a. always ensure the gear is removed from any manufacturing fixture before inspection to avoid errors

b. if in doubt, take the time to repeat the inspection; it is always cheaper than finding out later in service that a mistake has been made.

The above procedure, even if correctly implemented, will introduce errors into the measurement process. The following section addresses the most common error sources in the gear measurement process and provides some approximate calculation procedures to demonstrate the effect on involute profile, lead or tooth alignment and pitch measurement results.

3.3 Sources of error in the gear measurement process.

Errors in the measurement processes and their influence on the measurands need to be carefully considered. Sources of error fall into a number of easily defined categories and are summarised in ISO TS 14253-2 as illustrated in figure 3.18. Each of the 10 categories may have a number of individual sources of error and the influence from each will depend upon how sensitive the measurand is to the effect of the error source. This sensitivity is defined as the sensitivity coefficient in M3003 [UKAS, 1995].

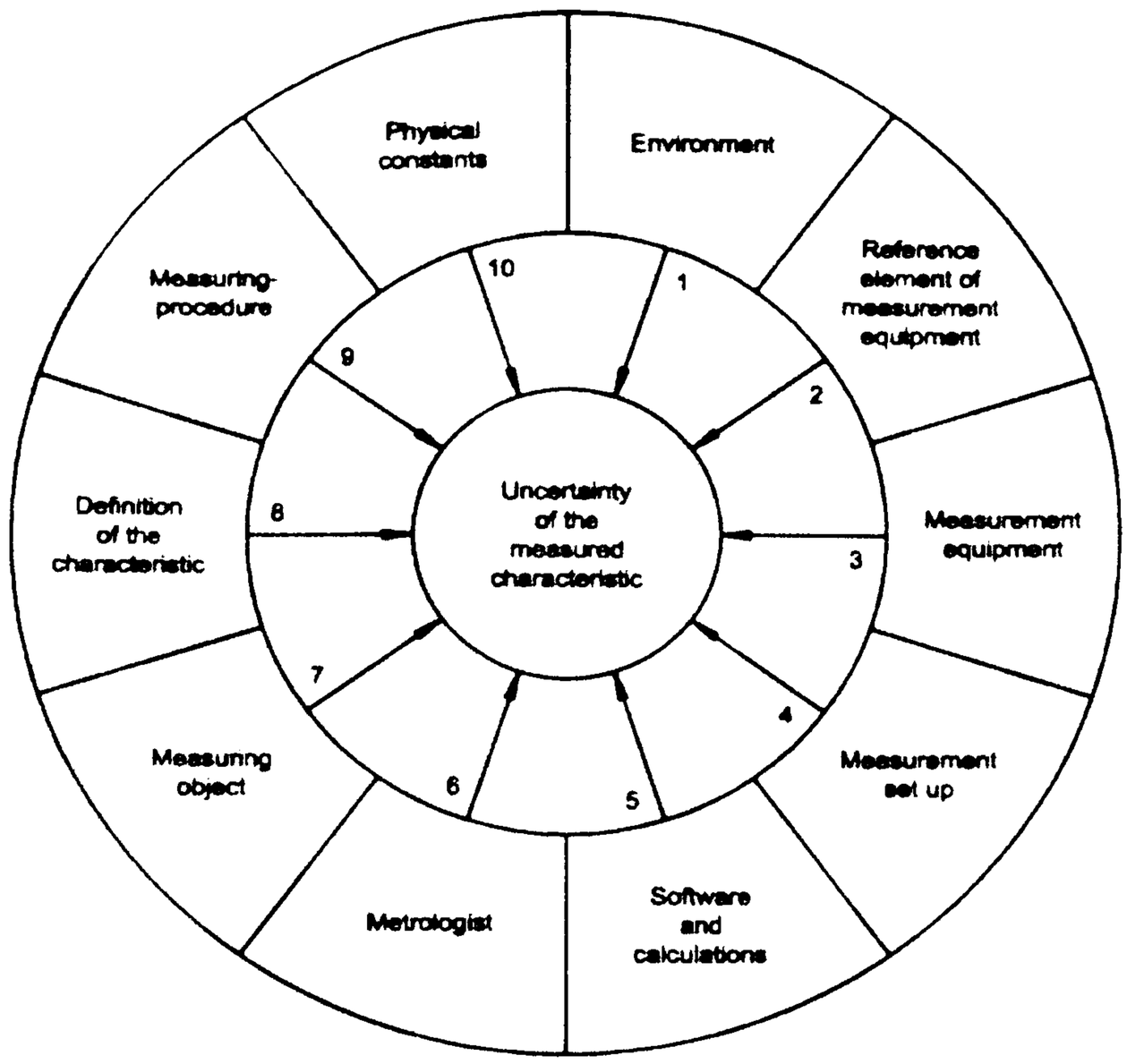

Figure 3.18 A general summary of the sources of error in the measurement process from ISO TS 14253-2.

This sensitivity coefficient may be considered as a simple mathematical model quantifying how the error affects the result of the measurement process. It requires knowledge of the measurement process and the geometry of the measured workpiece. The following sections discuss some example sensitivity coefficients.

3.3.1 Profile measurement

The measurement of profile error is illustrated in figure 3.6, and is based on the measurement of the gear length of roll. Thus it is similar to any length measurement process and subject to the same sources of error. Taking each of the potential sources of error in turn and using ISO TS 14253-2 as a guide:

Environment.

The most critical environmental effect on length measurement is temperature. The reference temperature used for all dimensional measurements is 20°C. Any deviation from this temperature will change the length of the measurement. There are two significant 1st order temperature effects: the nominal core material temperature of the

measured gear and temperature of the measuring instrument scales used as a datum scale. It is very difficult to measure the core temperature of the gear material unless it has been stabilised in the measuring instrument environment for a minimum of 24 hours and provided that this environment is itself stable [UKAS, 1998]. Experience with measuring temperature effects in lead measurement [Brentnall] has shown that it is usually more accurate to measure core temperature by placing a surface mounted temperature probe underneath the gear. Convection and buoyancy effects are thus minimised. Master gear manufacturers design master gears and gauges with a 2mm diameter hole that allows the core temperature to be measured with more accuracy with a temperature measuring probe [Frenco, 1992].

Change in length of roll depends upon the expansion coefficient of the workpiece. For steel this is usually between 10.6 to 12.6×10^{-6} (1/°C/mm), such that

$$\Delta F_a = (T-20).\ \alpha_t.\ L_a \qquad (3.1)$$

Where

ΔF_a change in length of roll [mm]

T actual temperature [°C]

α_t. Expansion coefficient (for the work piece or instrument scale as applicable) [1/°C/mm]

L_a Length of roll at 20°C [mm].

The same equation may also be applied to errors in instrument reference scale temperature. In this case the coefficient of linear expansion of the measurement scale would be used. Most scales are made of either glass or steel with a range of expansion coefficient of between 8.0 to 12.8×10^{-6}(1/°C/mm), however it is difficult to measure the temperature of the scales correctly. Local heat sources such as motors or temperature gradients across the instrument will change the scale temperature depending on measurement location. With 4-axis CNC gear measuring instruments, temperature effects of the rotary table encoder will also produce a similar effect. Again, equation (3.1) will apply to error in scale temperature.

Temperature variations on the other axes of a 4-axis CNC measuring instrument do not significantly affect profile measurement. This is one of the reasons involute gears can be accurately measured.

The traditional base disc profile measuring instruments are also affected by temperature. The base disc diameter on these instruments provides the reference for the measurement so changes in size due to temperature also affect the results. Equation 3.1 may be used directly with the expansion coefficient for the base disc used.

3-axis CMMs (with 3 linear axes) or 3-axis dedicated gear measuring instruments (2 linear axis and a rotary table) used for measuring gears are more sensitive to temperature variation. The effect of the temperature of the workpiece is the same but the effect of temperature errors in the scales depends on the orientation of the gear with respect to the linear axes and varies as the direction of involute normal varies across the tooth from root to tip. An analysis of these effects has not been conducted here.

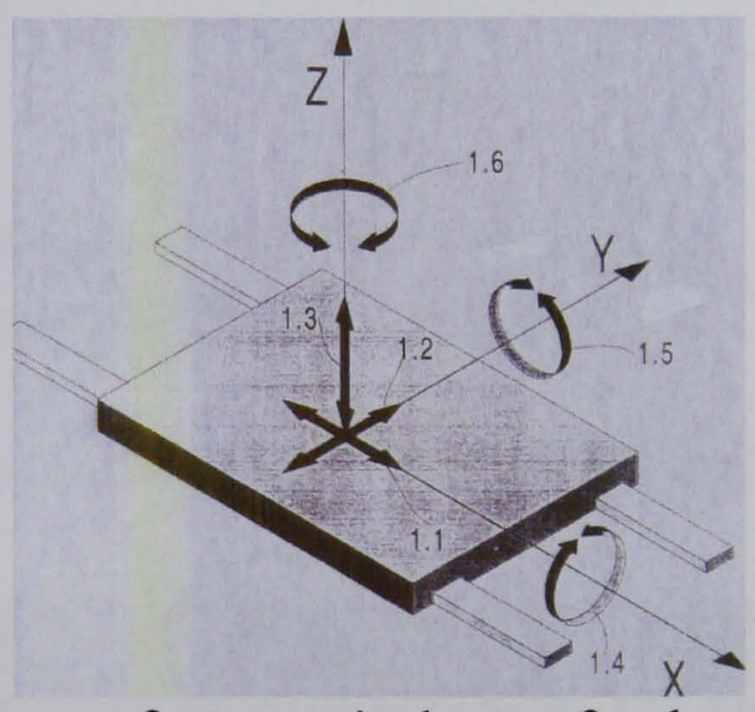

Figure 3.19 Six sources of geometrical error for the axis designated 'X'.

There are other temperature effects that may have 1st order effects on measurement results. One temperature effect is to change the geometry of an axis guide. Figure 3.19 shows a typical guide with six sources of error defined as; 1.1 position error, 1.2 straightness in Y direction, 1.3 straightness in Z direction, 1.4, roll angle error about X axis, 1.5 pitch angle error about Y axis, 1.6 Yaw angle error about Z axis. Each linear axis has these error sources plus the squareness error for each angle between the 3 linear axes. If temperature gradients exist across the machine base the geometry of the slide will change which will in turn, affect the path the probe stylus takes. The size of this error depends on the Abbé offset, defined as the distance between the reference scale and the measurement probe as shown in figure 3.20. The larger this distance the larger the

sensitivity to angular errors and change in angular errors on the measurement result. It is not possible to design a conventional measuring instrument working in a three dimensional volume without an Abbé offset. The objective is thus to minimise it and to ensure that it is either a fixed distance (and can be compensated) or that it minimises the effect of the measurand. The most preferred layout for a dedicated gear measuring machine is the Hőfler EMZ 632 illustrated in figure 3.21. It has a fixed Abbé offset for profile and lead measurement and so is optimised for gear measurement. This slide arrangement does have some limitations, namely the capacity of gears that can be measured by the generating method of measurement due to limited size of the X-axis

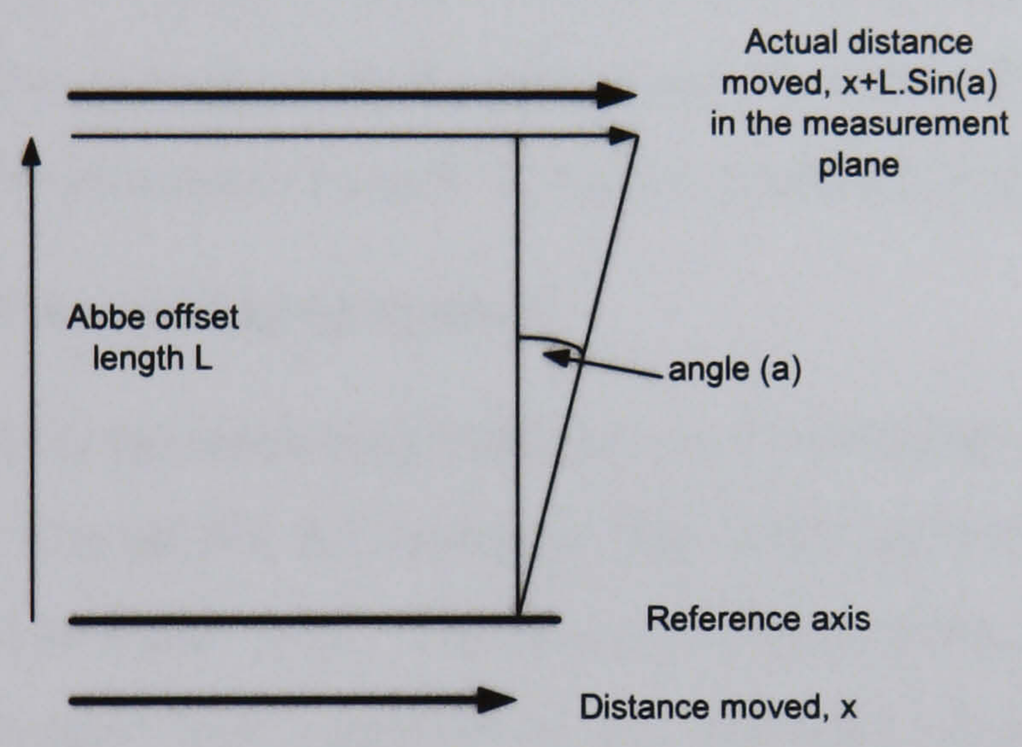

Figure 3.20 Definition of Abbé offset error.

Figure 3.21 Hofler EMZ 632 CNC gear measuring machine manufactured 1990

(no longer available)

A further issue with thermal effects is the time period of the temperature fluctuation compared to the time constant for the instrument. Fluctuation with a frequency 30

minutes or longer will affect the measuring instrument [ISO TR10065-5]. The errors from thermal effects can be significant in shop floor environments where the instrument temperature is changing at a critical rate and also that of the workpiece temperature after it has been removed from the manufacturing or cleaning machine. In a calibration laboratory where temperature variations do not normally exceed 1°C thermal effects are not a significant source of error. This is demonstrated with the uncertainty model in Chapter 6.

A further environmental effect on the measurement process is vibration. It is not possible to accurately quantify the effect vibration will have on measurement results. The only guidance available is that frequencies above 50Hz are not a problem and are naturally damped by the cast iron or granite instrument, the 13-50Hz region requires attenuation with compliant vibration mounting on the instrument base but vibration between 0-13Hz is critical and cannot be attenuated by anti vibration mounts [Klingelnberg].

Reference element of measuring equipment

The reference element on the measuring machine can be interpreted as the element(s) that establish traceability. For profile measurement this is the calibrated profile master, such as the example shown in figure 3.22. The source of error in the profile master includes the error in the calibration data supplied by the calibration laboratory, the mounting accuracy, the effect of uncertainty of temperature errors and differences between calibration data from the calibration laboratory and the measured data on the measuring machine used.

Figure 3.22. An example of an involute profile master mounted on a Klingelnberg P65 Gear Measuring Centre, used to establish the reference or traceability of the profile measurement accuracy.

Measurement equipment

It is evident that gear measuring instruments are complex and have many sources of measurement error. These include

- measuring system resolution and performance. This is the smallest bit size (in units of the measured error) that may be used in the measurement process. This value may be attributed to the probe system, rotary table or linear guide-way encoder (or electronic interpolation) or more likely is the resolution of the output results.
- Instrument discrimination. This is the smallest change that the instrument measuring and evaluation system may detect. For example hysteresis in the probe head, mechanical or electronic filtering or the resolution of input parameters that define the system discrimination. Discrimination is usually greater than or identical to the system resolution.
- Internal vibration caused by axis drives can create errors in the measurement process. Other effects such as the 'cogging' of linear motors can produce ripples during profile scanning.

- Uncorrected errors that are not detected by the calibrated profile artefact because of differences between the part geometry change in Abbé offset will cause measurement errors. Geometrical errors on each linear slide (defined in figure 3.19) can cause measurement errors, which depend on the instrument kinematic design and the geometry of the workpiece. The sensitivity coefficients are therefore different for each error source, and can only be established with a simple kinematic model of the measuring instrument and the workpiece. This is complex and involves significant work, and explains why parametric calibration is avoided by calibration laboratories whenever possible. The alignment of the instrument axes with respect to the rotary table axis (defined as the reference axis) provides an additional source of error.

- The repeatability and reproducibility of the measurement process can be significant and is defined as a standard deviation of a series of tests. Standard deviation values of between 2.0 and 0.5μm are common in CNC measuring instruments, depending on their condition and operating environment.

Measurement setup (CNC machines only)

The alignment of the workpiece on the instrument and runout of the workpiece datum, cause errors in the parameters measured.

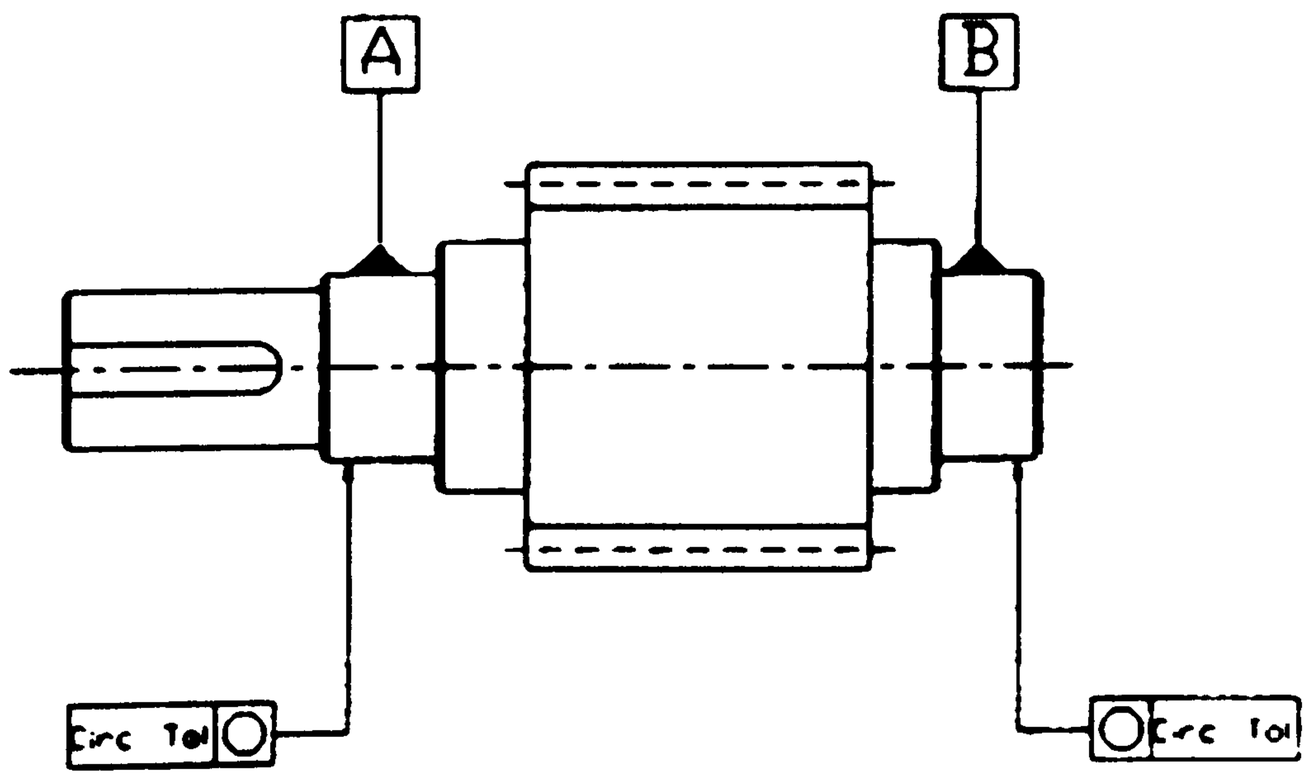

Figure 3.23 Datum surfaces and errors in mounting the gear on a rotary table.

The effect of gear mounting errors on profile measurement is estimated in the approximation below:

$$\Delta F_\alpha \approx 0.5 e_r Sin\left(\frac{2L_\alpha}{dCos(\alpha_t)}\right) \qquad (3.2)$$

Where:

ΔF_a change in profile error [mm]

e_r radial runout [mm] Total Indicator Reading

L_a profile length of roll [mm]

d reference diameter [mm]

α_t transverse pressure angle [°]

This assumes that the runout is in the plane of profile measurement but in practice it is not (as illustrated in figure 3.23). To account for this out of plane measurement and the fact that there are two sources of runout error, it is normal practice to add the two runout values in quadrature as the square root of the sum of the squares. This approach estimates the most likely effect from errors in a different axial measuring plane and the phase angle between the high points of the two runout measurements. In practice we do not know the phase angle between the high point of the resultant eccentricity relative to the four teeth selected for measurement.

A more precise analysis of the effect that mounting error has on runout is illustrated in figure 3.24 and in equation 3.3 below. Radial and axial runout errors introduce a first order effect.

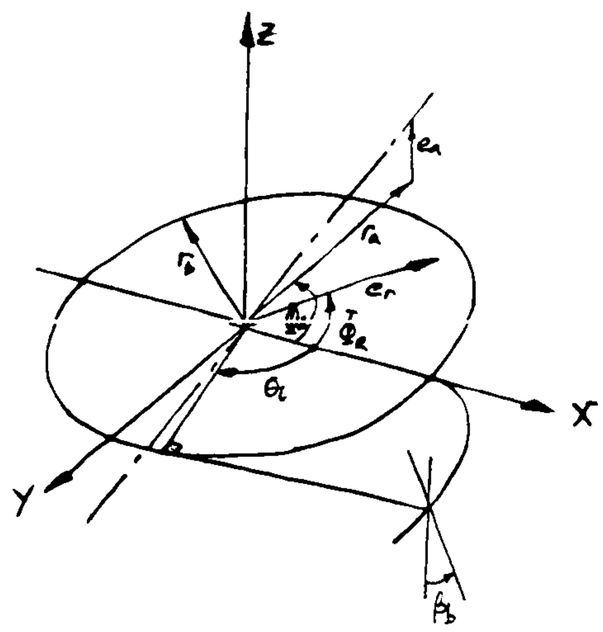

Figure 3.24. Effect of eccentricity on profile error measurement

$$\Delta F_{\alpha i} = e_r Sin(\theta_i + \Phi_r) + \left(\frac{e_a}{r_a}\right) z_p Sin(\theta_i + \Phi_a) + \left(\frac{e_a}{r_a}\right) r_y Tan\beta_b Cos(\theta_i + \Phi_a) \qquad (3.3)$$

Where:

$\Delta F_{\alpha i}$ instantaneous profile error due eccentricity [mm] at angle θi

e_r radial runout amplitude[mm]

e_a axial runout amplitude[mm]

θ_i instantaneous roll angle[°]

Φ_r angle to maximum radial runout vector[°] e_r

Φ_a angle to maximum axial runout vector[°] e_a

r_a radius used to determine axial runout[mm]

r_y radius to contact point [mm]

z_p profile measuring axial height above radial runout datum[mm]

A further source of uncertainty is the alignment of the axis defined by the centres. With a spur gear (with 0° helix) the effect is second order and only dependent on the gear form errors. With a helical gear there is an effect from a change in the axial contact position of the measurement position on the gear caused by a squareness error between the gear axis and the profile measurement axis. This relationship is given by:

$$\Delta F_a \approx \Delta a \frac{L_\alpha}{L} Tan(\beta_b) \tag{3.4}$$

Where:

Δa alignment error of gear axis with profile measurement X-axis[mm]

ΔF_α change in total profile error [mm]

L_α length of profile [mm]

L length between the datum surfaces [mm] A and B in figure 3.23

β_b base helix angle [°]

Apart from the direct errors when mounting a gear between the rotary table centre and tailstock centre, other errors are introduced; for example the resulting elastic deflection of the tailstock or workpiece under the measurement force (typically 0.2N).

A second measurement setup is illustrated in figure 3.25. The gear is mounted on the rotary table without the tailstock so the determination of workpiece alignment is easier.

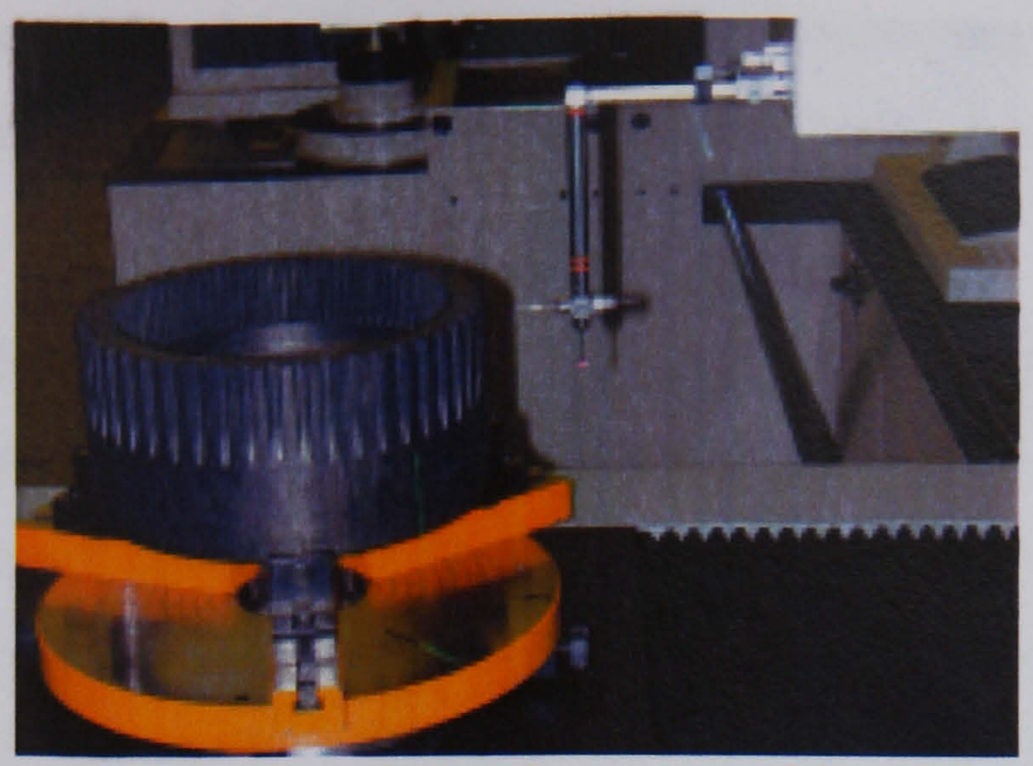

Figure 3.25 Mounting the gear directly on the rotary table minimises error sources but is only suitable for relatively short gears due excessive elastic deflection (L/b<3).

Long, shaft mounted, gears cannot be securely mounted and deflect excessively (between 10-20μm) under probe contact forces. This is particularly the case when measuring runout of datum surfaces to define the gear axis. Furthermore, when a thin walled gear is clamped it may deflect excessively due to clamping loads.

Software and calculations

Errors in this category emanate from two sources:

- the 'firmware' used by the CNC controller to move the machine, gather measurement data, and perform error and gear axis compensation moves and
- high level analysis software used to evaluate parameters defined by the Standards. This included features such as lead crown height, conformance to a tolerance requirement, measurement data input calculation to convert geometry data into a format acceptable by the controller etc.

Software is very difficult to evaluate independently of the rest of the measurement system although NPL [Cox, 2001] have developed very robust data generation algorithms that generate data points which produce known solutions. The data points generated for testing the target software can be varied by increasing the standard deviation and can thus quantify the robustness of the software and define when it fails to deliver a reliable result. PTB [Härtig, 2004] have (independently) produced reliable algorithms to verify the involute evaluation software in a collaborative project with instrument manufacturers and will certify involute measurement software capability defining acceptable errors as less than 0.1μm compared to the reference software. In the authors opinion it is appropriate that accuracy standards define robust algorithms for

evaluating parameters defined in the standards. At present they do not, which is not a satisfactory situation and algorithms remain untested apart from the use of calibrated artefacts.

Firmware also evades independent testing. Some studies at NGML [Frazer, 2001] to verify the performance of the CNC 'electronic gearbox' using the Transmission Error method produced some success. Using a rotary table with external encoder and a Renishaw Laser interferometer, allowed independent verification of the nominal performance of the CNC control. The tests excluded the performance of the correction software that compensates probe readings for known errors in the CNC control system. Also error mapping and compensation software can not be verified without the use of calibrated artefacts.

Metrologist

Errors or mistakes from the metrologist are difficult to quantify and can be avoided by adopting best practice procedures and independent checking of measurement results and procedures adopted.

Measuring object

The measuring object or workpiece can be a significant source of errors. Its stiffness during probing, the temperature, temperature distribution and thermal expansion coefficient can cause errors. A very precise component is easy to measure accurately but poor quality components with large form errors, poor datum surfaces and poor surface texture are invariably difficult to measure. Some workpiece designs are more difficult to measure than others. Workpiece datum surface locations that are inappropriately defined, non-functional or provide a poor geometrical definition of the axes can cause additional errors.

Definition of the characteristic

Defining profile error parameters (as illustrated in figure 2.11) in accordance with ISO 1328-1:1995 is not sufficient to fully define the requirements. The data density, mechanical, electrical and digital filter characteristic will affect the accuracy and validity of the measurement result when scanning a surface. Gear measurement results do not define these on the measurement record sheet and differences of 2.0μm on some workpieces have been noted [Wilson, 2004]. Thus omissions in the definition of the

measured and evaluated parameters defined in the ISO 1328 can lead to significant measurement errors.

Measuring procedure

Measuring involute profile involves scanning across a single line in the transverse plane of the gear, ie a single line across a single tooth flank and is thus only a sample of the involute flank profile error. Different measurement positions on the tooth flank will produce different measurement results. ISO 1328-1 recommends a minimum of 3 teeth are measured at approximately equally spaced intervals on both left and right flanks. Traditionally profile is measured at mid face width position. The profile measurements from a gear are thus a sample and may not fully represent the errors in the gear. When gears fail, generally the largest geometry error will cause the greatest stress and therefore the likely failure initiation point in the gear. There is no guarantee that the teeth measured have the largest error so care and attention is required in interpreting the results to ensure sound decisions are taken. These decisions require a detailed understanding of errors in the manufacturing and measurement process.

For example, the form grinding process that can produce different profile errors across the face width if lead or helix crowning is applied to a helical gear. Measuring the gear in the centre of the face will give satisfactory results but at each end of the face width a 3.0μm difference in results is typical, but larger differences (up to 30μm) have been measured [Frazer, 2005]. Grinding machine manufacturers know about this potential error but users often fail to take appropriate measurements to verify the error compensation process has been correctly implemented.

Definition of datum surface runout is probably the most common source of error in both measurement and manufacture. If adequate care is not taken to ensure the gear is mounted properly on the rotary table or the axis definition is not correctly established the profile results will be in error. The measurement procedure should include provision for evaluation of variation in profile results that result from mounting errors [BGA DUCOP06]. An example of variation in profile errors caused by datum runout is shown in figure 3.26.

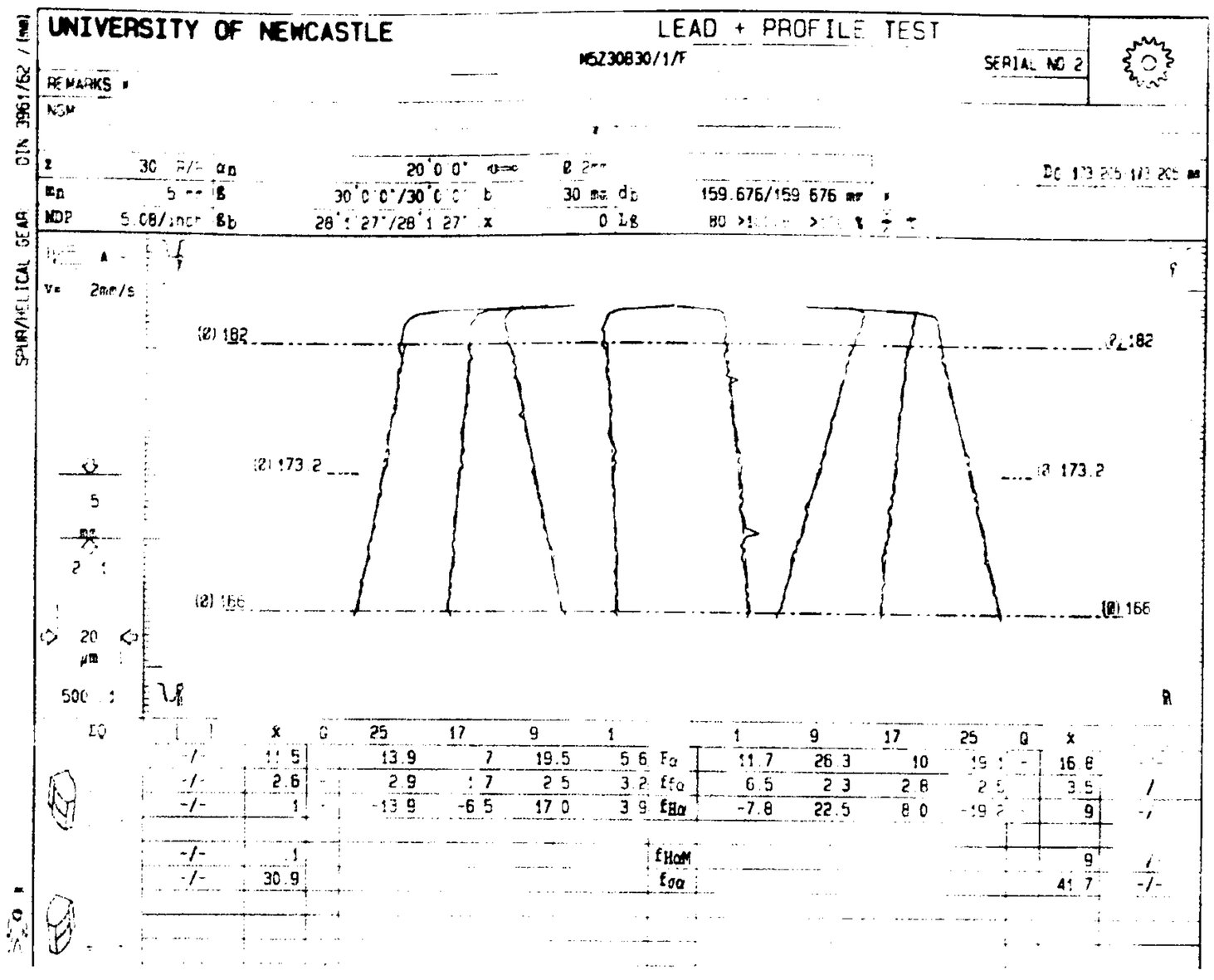

Figure 3.26 Variation in profile slope error ($f_{H\alpha}$) caused by datum surface runout

Physical constants

The errors in physical constants such as coefficient of linear thermal expansion and Young's modulus are sources of error in gear measurement although not so significant. Coefficient of linear expansion is the most sensitive error and it is usual practice to assume a maximum error of 10% of the expansion coefficient due to material composition variations. Since this effect is dependent on temperature differences between the reference temperature (20°C) and actual temperature, the error is not a significant contribution to the overall process uncertainty.

3.3.2 Lead measurement

Many of the error sources cited with profile measurement are equally valid for lead measurement. Because we are measuring and evaluating a different parameter which is measured in a different direction the sensitivity coefficients are different. The sensitivity coefficients for lead measurement are discussed below:

Environment

The general discussion on temperature affects for profile measurement also relate to lead measurement. The change in lead length depends upon the expansion coefficient of the workpiece:

$$\Delta f_{H\beta} = -(T-20)\alpha_t L_\beta \tan(\beta_b) \qquad (3.5)$$

Where

$\Delta f_{H\beta}$ change in lead error slope [mm]

T actual temperature [˚C]

α_t. Expansion coefficient (for the work piece or instrument scale as applicable)

L_β evaluation length of face width [mm].

β_b base helix angle [˚]

The effect of temperature depends on the helix angle. In a spur gear there is no effect for a uniform temperature change, with the exception of a (usually) negligible effects on the position of the evaluation lines and the measurement position. The same equation may also be applied to errors in instrument reference scale temperature as discussed for profile measurement.

Reference element of measurement equipment

The reference element that establishes traceability is a calibrated gear artefact. The discussion for profile measurement is also applicable to lead measurement.

Measuring equipment

The same sources of error described for profile measurement apply to lead measurement.

Measurement setup

The alignment of the workpiece on the instrument and the mounting errors of the workpiece datum cause alignment errors and therefore errors in the parameters measured. The effect of mounting errors on lead measurement is given in the following approximation:

$$\Delta f_{H\beta} \approx 0.5 e_r Sin\left(\frac{L_\beta Tan(\beta_b)}{r_b}\right) \tag{3.6}$$

Where:

e_r radial runout (Total Indicator Reading) [mm]

L_β Lead evaluation length [mm]

r_b base circle radius[mm]

β_b base helix angle [°]

This assumes that the runout is in the plane of measurement. By modelling the affect of the runout a *sine* function assumes a worst case scenario. In practice it is not, and is similar to the example illustrated in figure 3.23. Similar to the profile measurement discussion, it is accepted practice to add the two runout values in quadrature as the square root of the sum of the squares. This compensates for the different measuring plane and includes the effect that the phase between the high point of the two runout positions is likely to be different.

A more precise analysis of the effect that mounting error has on runout is given in equation 3.7.

$$\Delta F_{\beta i} = e_r Sin(\theta_i + \Phi_r) + \frac{e_a}{r_a} z_i Sin(\theta_i + \Phi_a) \tag{3.7}$$

Where:

$\Delta F_{\beta i}$ instantaneous profile error due eccentricity at angle θ_I

e_r radial runout amplitude [mm].

e_a axial runout amplitude[mm]

θ_β roll angle for lead measurement diameter[°]

Φ_{ri} angle to maximum radial runout vector e_r at axial position z_i

Φ_{ai} angle to maximum axial runout vector e_a at axial position z_i

r_a radius used to determine axial runout [mm]

z_i axial height above radial runout datum[mm].

A further source of error is the effect of alignment of the workpiece axis, either between centres or the spindle axis. This effect is approximated using:

$$\Delta F_\beta \approx \Delta a \frac{L_\beta}{L} \tag{3.8}$$

Where

Δa alignment error of gear axis in the base tangent plane length L [mm]

ΔF_β change in total lead error [mm]

L_β Length of lead evaluation [mm]

L Length over which alignment is measured [mm]

The discussion of elastic deflection of the workpiece in the previous section also applies to helix measurement Lead measurement is more sensitive to these errors than profile measurement and this is reflected in the sensitivity coefficients for each uncertainty source.

Software and calculations

The same sources of error described for profile measurement apply to lead measurement.

Metrologist

The same sources of error described for profile measurement apply to lead measurement.

Measuring object

The same sources of error described for profile measurement apply to lead measurement.

Definition of the characteristic

The same sources of error described for profile measurement apply to lead measurement but the issue of data density is often more critical because the lead path length is usually longer than profile length of roll. Form errors in lead measurement can be more significant effect because of lower data density.

Measuring procedure

The same sources of error described for profile measurement apply to lead measurement. With lead measurement the selection of teeth measured is just as critical as for profile measurement but the measurement is more sensitive to axial runout or swash error than radial runout, and is also dependent on helix angle. The relationship between runout and lead error is shown in equation 3.6.

Physical constants

The same sources of error described for profile measurement apply to lead measurement.

3.3.3 Pitch measurement

Pitch measurement differs from lead and profile measurement in a number of ways:

- The definition of pitch error is a length [mm] but it is an expression of a residual error of angle at a defined radius.
- Because pitch error is the difference between the average pitch length and an individual pitch length (illustrated in figure 3.30) it is insensitive to uniform temperature difference.
- The process can be self calibrating using a closure technique that allows the errors in the pitch artefact to be separated from errors in the machine. This is a standard metrology procedure as used by M&M [Dama] for assessing rotary table errors.
- Pitch is insensitive to environmental errors.
- Although pitch measurement does not require a reference artefact, it is good practice to use a calibrated artefact with defined pitch errors associated with each tooth number.

Measurement equipment

The measurement equipment used for pitch measurement usually requires a rotary table to optimise measurement speed and accuracy. The linear slide errors are usually considered negligible provided the repeatability is acceptably low. The rotary table errors are most conveniently considered in polar co-ordinate form. Radial and axial runout and position errors can be measured directly with probes but position errors can only be measured by a closure technique or with a calibrated rotary encoder. The errors in angle position

linearly effect the pitch measurement so the artefact reference circle radius is the sensitivity coefficient.

Measurement set-up

The set-up of the gear on the instruments is critical for accurate pitch measurement. The relationship of runout of the journal datum surface to the cumulative pitch error for the left and right flanks is given in the equation (3.7 & 3.8) below:

$$F_{pr} = \frac{e_r Sin(\varphi + \alpha_t)}{Cos(\alpha_t)} \tag{3.7}$$

$$F_{pl} = \frac{e_r Sin(\varphi - \alpha_t)}{Cos(\alpha_t)} \tag{3.8}$$

Where:

e_r radial runout in the measurement plane [mm]

α_t transverse pressure angle [°]

φ nominal angle position of the tooth flank [°]

Thus the transverse pressure angle is relevant to radial runout and the maximum and minimum values of F_p for left and right flanks are shifted by an angle of twice the transverse pressure angle. This is illustrated in figure 3.27.

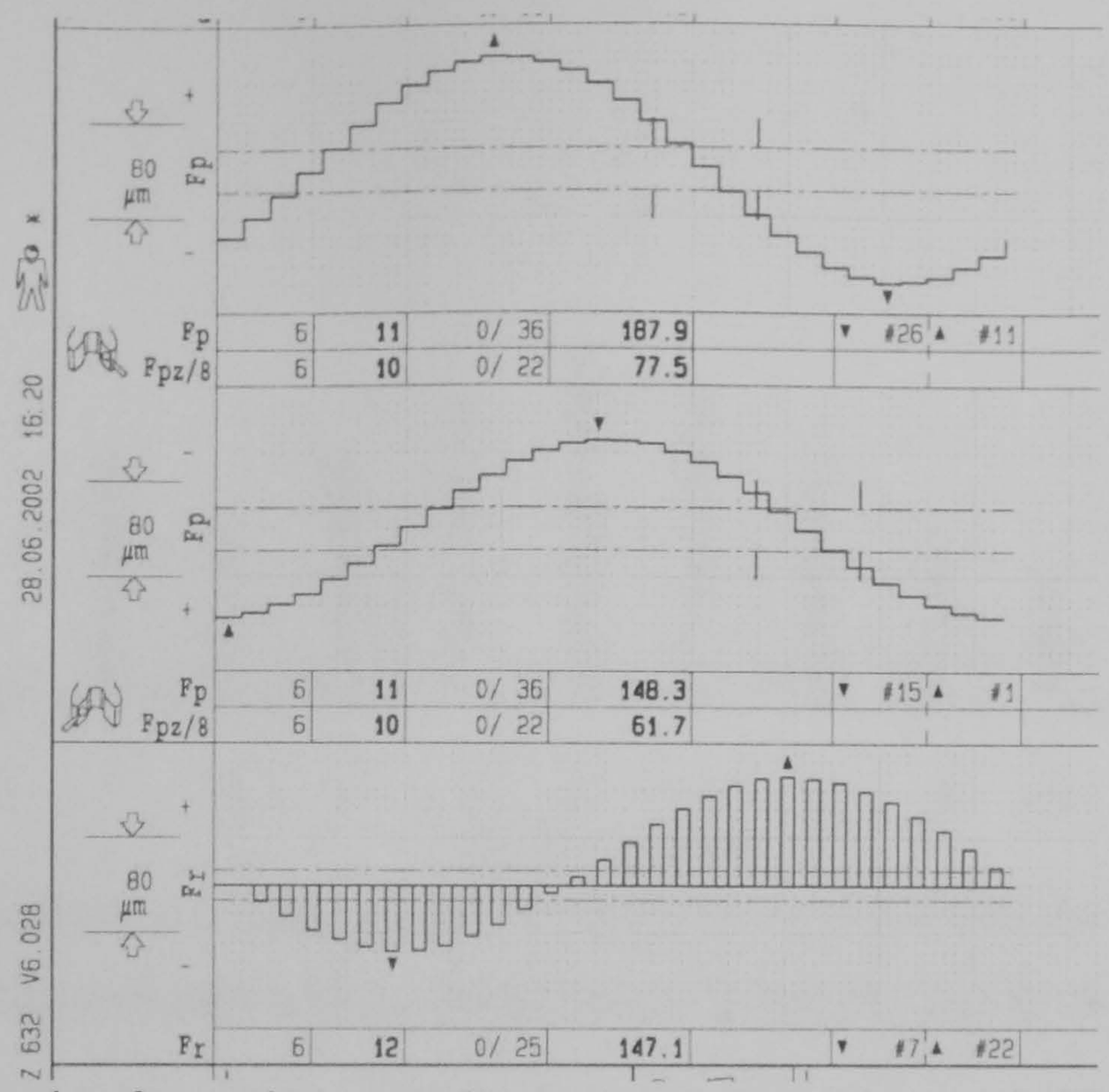

Figure 3.27 An example of cumulative pitch error caused predominantly by radial runout of the gear blank clearly illustrating the change in phase of the maximum pitch deviation between Left and Right flanks.

Software and calculations

The software and calculations can be significant to pitch evaluation accuracy if a closing error calculation is not performed. Closing error is calculated by measuring all the teeth on a gear and finally repeating the measurement on the first tooth at the end of the test. With a repeatable instrument there should be no change in the measured value for the first tooth, ie. you should come back to the same point on the tooth.

Rounding errors or mechanical setting errors may mean that the table is incremented with a constant error for each pitch. These accumulate with each successive tooth until the first tooth is re-measured at the end. The difference in reading of the first tooth is *(z*indexing error),* so the closing error calculation increases the pitch measurement accuracy. An example of closing error calculation is illustrated graphically figure 3.28.

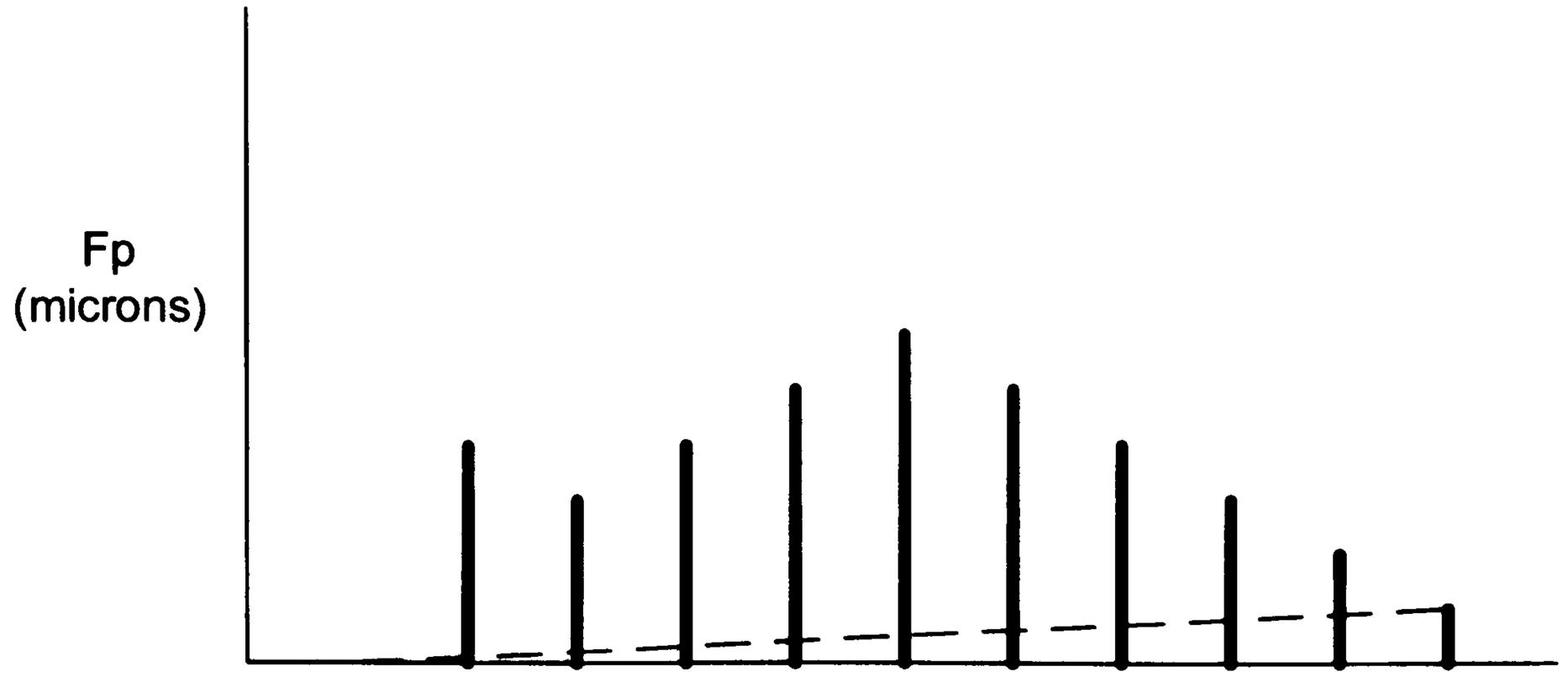

Figure 3.28 An illustration of a closing error calculation to compensate for errors in table index. (The reference line for the pitch test is thus the dashed line).

Metrologist

As previous comments.

Measuring object

The quality of the workpiece form errors influence the repeatability of the measurement process and the likely difference between the results from different measurement processes. The accuracy of the datum surface runout and its definition is very critical for accurate pitch measurement, because unlike lead and profile measurement the measurement is nominally a single point reading.

Definition of the characteristic

The definition of adjacent pitch error is shown if figure 2.13 and 3.29. This shows a single point definition with an error measured as an arc length on a circle. Most measuring instruments measure a series of pitch points (typically 10) and take an average value as a single pitch value. Thus pitch is often measured over a small surface, not a single point as defined by the standard. This is not in accordance with the standards but provides a more robust and realistic result.

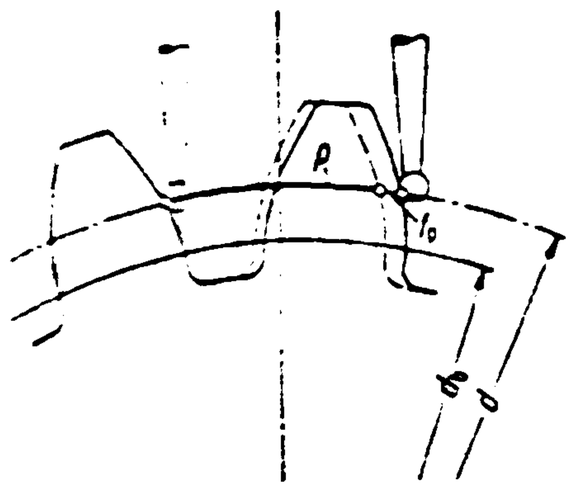

Figure 3.29 Definition of adjacent pitch error as a linear arc length along a defined circle.

Measuring procedure

There are two common measuring procedures used in modern CNC machines. A single probe system that measures absolute pitch error relative to an angular grating or two probe system that measures the difference between two successive pitches. The most significant effect of the measurement process is that a two probe method is difficult to set up so that both probes contact at the same diameter on successive teeth. The effect is to include profile form error effects into the pitch measurement results thus producing different results. Figure 3.7 illustrates a typical two probe measuring instrument.

The definition of the first pitch and measurement direction is often different for different measuring instruments. The Technical Report [ISO/TR10064-1] defines the ISO method unambiguously and also includes internal gear definitions.

Physical constants

Pitch is not sensitive to thermal effects or stiffness issues because at all times the error difference is measured, not the absolute error. The only requirement is that errors are measured at nominally constant measurement force.

3.4 Summary

Gear measurement is essentially a combined length and form measurement and the relationship of errors in the measurement process to the parameters measured is simple geometry. This chapter has reviewed the error sources and quantified the effect that the errors will have on the measurands. A difficulty arises because of the large number of these error sources and the fact that measurements are taken dynamically by scanning the flank surfaces. Methods for reliably detecting these errors in the same conditions as they

occur when inspecting gears is difficult. Thus the measurement procedures discussed in Section 3.2 are defined in order to minimise the critical errors that can occur during a product gear measurement process thus ensuring that measurements results are reliable.

Chapter 4

UNCERTAINTY MODELS

This chapter reviews several models that are frequently used in the dimensional metrology field to estimate process measurement uncertainty. Most use statistical models at the core of the evaluation process to model the variation in input variable and predict the effect on the output or measurand. The chapter also reviews the assumptions and discusses their application to the gear measurement process. Appropriate references are made to fundamental work where the theories are fully derived in detail.

4.1 Introduction

Anyone working in metrology will have observed that results from a measurement process will vary if they are repeated in what would normally be considered identical conditions. Occasionally the metrologist may obtain an unusual result, that is obviously wrong and this may be recorded but ignored in any subsequent analysis. Over a longer period of time, the result from this measurement process may tend to drift or change. Furthermore if results from different measurement processes are compared, differences will be observed because no matter how much care is taken when making measurements, the final result contains errors. In fact the only 'certainty' is that a measurement result is wrong. Thus to make a sensible interpretation of the validity of a measurement process we estimate the expected or predicted range of output values, in order to estimate its measurement uncertainty.

Simply estimating the range of the output value is one solution. This is the basis of a draft document, ISO/TS 15530-2, that describes the methodology of this process [Duncan, 2002]. This approach may be acceptable but it has only limited application because the cause of the measurement uncertainty is not understood and it is therefore

difficult to quantify how the process may be improved. Alternative methods are widely implemented that quantify the range of values of input factors can reasonably be expected to take, then calculate the effect on the output result, thus predicting the range of variation in the output result.

When trying to predict the likely errors in the measurement process it is important to define the range and likely distribution of the contributing variables and thus, the mathematics of statistics and probability can reasonably be applied to estimating measurement uncertainty.

An obvious technique is to combine the limits of errors or uncertainty distributions by simply summing their limiting values [UKAS, M3003]. While this appears acceptable, it leads to significantly higher values of measurement uncertainty than is encountered during testing. This is primarily because the probability that all errors occur at their maximum limits at the same time and with the same sign is very small, and thus rarely occurs. Simple arithmetical summation of uncertainties is thus very pessimistic.

The uncertainty model should produce realistic estimates of measurement uncertainty [VIM, 1995]. Safe or conservative estimates of measurement uncertainty initially appears to be a sensible approach but they unnecessarily increase costs to manufacturers who have to reduce manufacturing tolerances as a necessary effect of this approach [ISO 14253-1]. A further effect if applied to national laboratories is that overly pessimistic with measurement uncertainty statements cascades to second tier laboratories, and instrument manufacturers who then have no tangible benefit to improve their calibration performance. Any benefit of developing new processes is lost because of the large uncertainty from the NMI.

4.2 General uncertainty evaluation procedure

All uncertainty modelling processes involve the following generic procedure, although some stages may be omitted:

- Definition of the mathematical model that represents the contributing variaables and the output quantity or measurand.

- Definition of the relationship between each input quantity and its effect on the output quantity. These are called the sensitivity coefficients or the partial derivative of the output function with respect to the input quantity.

- Determine any correlation between the input quantities. If there is any correlation, define the correlation coefficient that links the two distributions.

- Assign a probability density function (pdf) to define the shape of the distribution of the input quantity. Typical distributions in dimensional measurement are Gaussian (normal), rectangular or triangular distributions as discussed in section 4.3.

- Define the limits for each input quantity as a standard uncertainty, ie one standard deviation known as the Standard Error (SE).

- Use the uncertainty model to estimate the output standard uncertainty.

- Determine the confidence interval and limits for the output uncertainty statement, usually with a 95% probability requirement.

4.3 Common statistical distributions

Gaussian distribution

The Gaussian distribution, illustrated in figure 4.1 is the most commonly used when modelling random errors and because of the central limit theorem, is usually reasonably accurately applied for dimensional metrology.

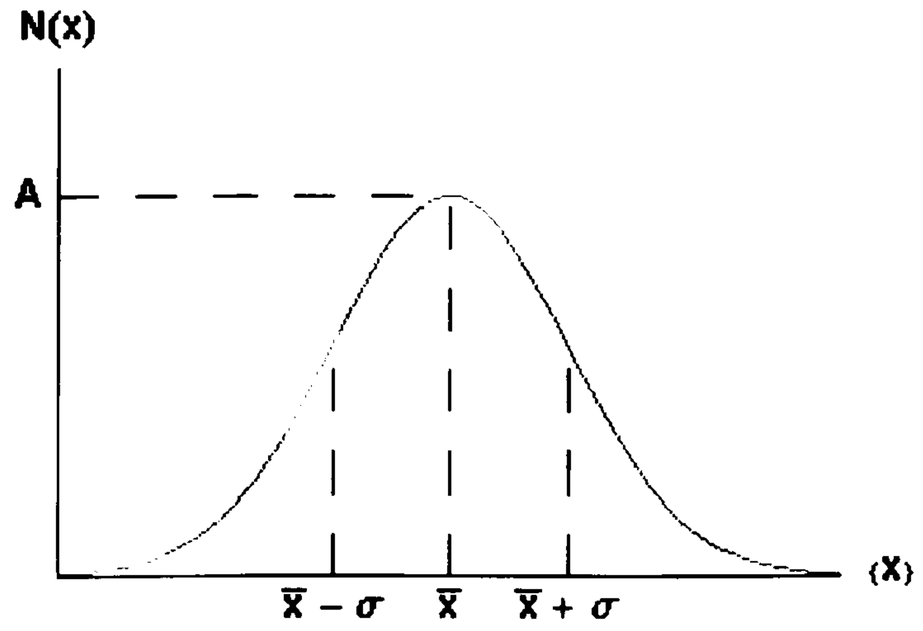

Figure 4.1 Gaussian or Normal Distribution

The key issues that give the Gaussian distribution its properties are [Dietrich]

- The function p is continuous and differentiable over its whole range

- The single greatest function of p occurs at a maximum of $f(x)$
- The square of the sum of quantities $f(x)^2$ is a minimum, called the principle of least squares, a feature that is important for probability estimation.

The mean is given by

$$\bar{x} = \frac{1}{n}\sum_{i=1}^{n}(x_i) \tag{4.1}$$

the variance is estimated by

$$\sigma_{n-1}{}^2 = \frac{1}{n-1}\sum_{i=1}^{n}(x_i - \bar{x})^2 \text{ for small sample sizes (n<200)} \tag{4.2}$$

the standard deviation of the distribution is estimated by σ_{n-1}

$$\sigma_{n-1} = \sqrt{\frac{1}{n-1}\sum_{i=1}^{n}(x_i - \bar{x})^2} \tag{4.3}$$

Rectangular Distribution

The uniform or rectangular distribution is used where the probability of obtaining any value within the limits is equal. It is applied only when the upper and lower bound of the error is known for example, or if the resolution of the measurement system is a discrete value, where the actual value will lie with equal probability within the least significant bit of the quantity. For example, the digital resolution of a measuring system.

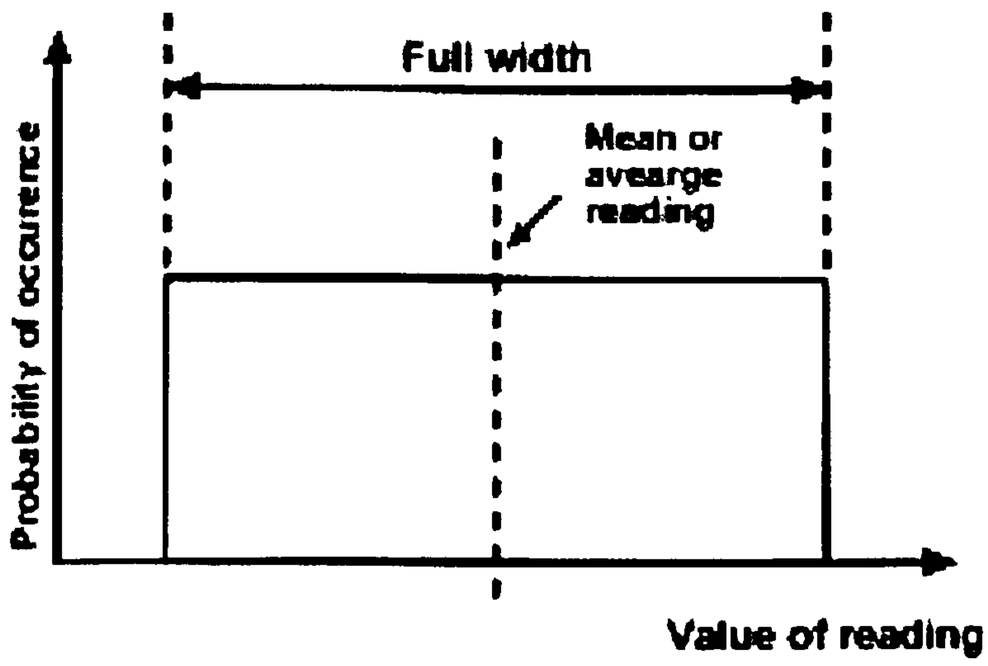

Figure 4.2 Rectangular distribution

In figure 4.2 we can define the full width of the distribution as 2a long, then the height of the probability distribution is 1/2a, because the area of the probability distribution is 1. The variance and hence standard deviation of the distribution is given by

$$\sigma^2 = \sum_{i=1}^{n} x^2 p \tag{4.4}$$

$$\sigma^2 = \frac{a^2}{3} \tag{4.4a}$$

$$\sigma = \frac{a}{\sqrt{3}} \tag{4.5}$$

Occasionally the instrument manufacturer states a 'tolerance limit' with a confidence interval of 3 standard deviation (σ) of the manufacturer's production probability distribution, then the SE may be approximated as below [UKAS, M3003]

$$\sigma = \frac{Tolerance}{3} \tag{4.6}$$

A feature of the rectangular distribution compared to the Gaussian distribution is that for given limits, the rectangular distribution gives a more pessimistic interpretation of standard deviation and is therefore considered a safe option if there is insufficient data to define the probability distribution. This is particularly the case when using students t-distribution (see the following section) which can generate unreasonably large uncertainty values for small sample sizes.

Triangular distribution

If two rectangular distributions with different limits are convoluted, the result is a trapezoidal distribution. However if they have the same limits, the result is a triangular distribution [Deitrich]. The standards deviation for a triangular distribution is given by

$$\sigma = \frac{a}{\sqrt{6}} \tag{4.7}$$

If greater than 3 rectangular distributions with the same limits are convoluted, the Gaussian distribution yields a better approximation [VIM, 1995].

4.4 Coverage factors

After establishing the standard deviation (spread) of a distribution or the standard error (SE) of the mean of series of tests, it is necessary to define a confidence interval. The enclosed percentage of a distribution that is enclosed by ±1 standard deviation is dependent on the pdf, for a Gaussian distribution ±1 standard deviation from the mean covers 68.26% of the probability distribution. Different distributions have different confidence intervals. The confidence interval states the expected probability that a result will lie within the defined interval. In metrology it is traditional to use a confidence interval for 95% coverage of the distribution. Thus for a Gaussian distribution a coverage factor (k) would be $1.96*\sigma_{n-1}$ for a 95% confidence interval,

$$U_{95} = k_{95} * \sigma_{n-1} \tag{4.8}$$

In many instances k_{95} is rounded from 1.96 to 2 to define the confidence interval for 95% coverage of a Gaussian distribution [UKAS,M3003]. Often this is done regardless of the number of degrees of freedom of the process because errors are often less than 10% of the calculated interval and therefore not worth the additional calculation time for a small benefit. NMIs however usually use the appropriate value for the effective degrees of freedom [Cross, 2002].

4.5 Students t-distribution

The coverage factor discussed previously is used to determine the confidence interval required for a specific probability statement. In this case it is assumed that the standard deviation of the process is known. In general the mean and standard deviation of a process or trial are unknown and may vary from trial to trial so we need to account for the confidence we have in assigning the mean and standard deviation of a distribution.

Students t-distribution is a series of distributions that relate the degrees of freedom, $\upsilon = n - 1$, with the confidence interval coverage factor by [Mandel]

$$\left| \frac{\bar{x} - \mu}{\sigma \sqrt{n}} \right| \leq t \tag{4.9}$$

As the number of degrees of freedom $\upsilon \to \infty$, the confidence intervals for the t-distribution approaches that of the Gaussian distribution.

The t-distribution works well but sometimes it is better to use a rectangular distribution if applied to small sample sizes with limits defined by trials. Experiments should be performed on each application to determine when this should be adopted.

4.6 Effective degrees of freedom

A limitation of the t-distribution is that the degrees of freedom must be determined for a single distribution. When distributions are convoluted, we must estimate the equivalent combined degrees of freedom for the process.

The Welch-Satterthwaite formula (equ. 4.10) is used with acceptable accuracy [UKAS, M3003] to approximate the effective degrees of freedom, ν_{eff}. It should be used to determine the approximate coverage factor from the appropriate t-distribution confidence interval

$$\nu_{eff} = \frac{u_c^4(y)}{\sum_{i=1}^{n} \frac{u_i^4}{\nu_i}} \tag{4.10}$$

where $u_c^2(y) = \sum_{i=1}^{n} u_i^2(y)$ (4.11)

and $\nu_{eff} \leq \sum_{i=1}^{n} \nu_i$ (4.12)

Note that the units of $u_i(y)$ must be identical.

Particular applications of the effective selection of the degrees of freedom and the use of the t-distribution are rendered obsolete by some standards [ISO 18653] by choosing a coverage factor k=2 because the difference between values using k=2 and the correct coverage factor is less than 10% of the final uncertainty value.

In gear measurement this can be justified because the most significant uncertainty source is usually the value from the calibrated artefact. This has infinite degrees of freedom and thus dominates the estimate of uncertainty. Standards [VIM, 1995] recommend the following approximation for estimating the degrees of freedom for such circumstances, as shown below.

$$v = \frac{1}{2}\left[\frac{\Delta u(x_i)}{u(x_i)}\right]^{-2} \tag{4.13}$$

The quantity in large brackets is the relative uncertainty of the estimate and is a subjective quantity that may be estimated based on professional expertise. This approach is not approved by UKAS in gear measurement uncertainty estimates [Cubis, 2002]. A 'professional' is defined by ISO [Duncan] as an approved signatory for an ISO 17025 accredited laboratory.

4.7 Central Limit Theorem

The central limit theorem states that as the number of random inputs with similar distributions are convoluted or combined, the resulting probability density function tends to a Gaussian distribution as the number of input variables increases. Also, the more Gaussian the distributions, or the smaller the spread of the limits of the distributions, the fewer the number of distributions required to be accurately represented by a Gaussian distribution [VIM, 1995]. The practical benefit of this is that all convoluted distributions have probabilities that are greater than that of a Gaussian distribution for the same limits. Thus convoluting non-Gaussian distributions produce confidence intervals that are slightly pessimistic compared to a Gaussian distribution.

A rectangular distribution is an example of a significantly non-Gaussian distribution but as few as 3 rectangular distributions of equal width produces a good approximation of a Gaussian distribution. The 95% confidence intervals for the convoluted distribution is 1.9375σ while the Gaussian distribution is 1.960σ [VIM,1995].

We may thus conclude that convoluting various input variables encountered in gear measurement should be considered an acceptable way of estimating measurement uncertainty.

4.8 Random Uncertainties

When a process is repeated numerous times, the results from the process vary either due to variation in the artefact or the process itself. This variation is due to small changes in instrument measurement position, instrument alignments, temperature and environmental effects etc. (see Chapter 3).

If the measurement is repeated under the same nominal conditions, by the same operator, in a short period of time, the random uncertainty is termed the system repeatability. If the time period is extended, it includes (possibly) different operators and greater environment

variation and instrument stability then the term is called the system reproducibility. The uncertainty or spread of results includes more random effects and is thus usually larger than the repeatability uncertainty, it provides an excellent way of combining many sources of uncertainty, some of which may well be correlated into a single variable. Most random processes have a Gaussian or near Gaussian distribution but they also take other forms. In dimensional metrology there is usually very little data available to establish the frequency distribution. In these cases it is recommended that a rectangular distribution is selected after suitable limits are established.

If a measurement process uses the mean of a series of measurements to establish the bias in results or reports the mean from the series as the result, we need to report the standard error or standard uncertainty of the mean from those results. The variance of the results is given by equation 4.14

$$\sigma_{n-1}(x_i)^2 = \frac{1}{n-1}\sum_{i=1}^{n}(x_i - \bar{x})^2 \qquad (4.14)$$

Note that *(n-1)* is used because there are only *(n-1)* independent observations in the x_i values; because the last observation can be determined from knowledge of the mean value. The variance of the mean is given by

$$\sigma_{n-1}(\bar{x})^2 = \frac{1}{n(n-1)}\sum_{i=1}^{n}(x_i - \bar{x})^2 \qquad (4.15)$$

Hence the standard deviation of the mean of a series of n tests is given by

$$\sigma(\bar{x}) = \frac{\sigma_x}{\sqrt{n}} \qquad (4.16)$$

and is commonly termed the Standard Error of the process (SE).

4.9 Systematic uncertainties and systematic errors (bias)

Systematic uncertainties may be considered as fixed uncertainties in a measurement process that cannot be influenced by modification, repetition or adjustments to the measurement process. Examples include uncertainty statements on calibration items used to establish traceability, discrimination of the measurement process or the effect of form error on the uncertainty of the measurand.

Modelling of the bias (or error) between the calibration data value and the actual measured value is problem in a statistical model. Statistical modelling processes can not easily cope with a 'known value' because the basis of the analysis is modelling unknown values with distributions. Thus most models assume any bias, established through a calibration process, is compensated. However in many processes bias is not corrected because the value may vary over time or only represent a single value that is possibly not relevant because of differences in geometry, weight or helix angle, for example. Some models simply add the bias to overall uncertainty estimate at the end of the process but in the authors opinion the method adopted by Dietrich and UKAS [M3003] and described below is the most reasonable approach.

Systematic uncertainties may also be applied to modelling the 'bias' or 'uncorrected errors' in a measurement process [Dietrich]. The bias is the difference between a reference value (x_{ref}) and the mean measured value ($\bar{x}$). This assumes that the so called 'true value' is unknown and hence irrelevant but we may represent this (singular) error value as a rectangular distribution. This may be justified because the bias is likely to change over a period of time so the actual bias that should be applied for correcting a specific set of measurement results is thus unknown.

The use of a rectangular distribution is relatively safe because the standard error (SE) of a rectangular distribution is greater than the normal distribution. Many standards, including ISO 18653, add bias linearly to the uncertainty assessment. This results in pessimistic estimates of measurement uncertainty, and is not consistent with the directive that uncertainty estimates should be realistic rather than safe. However with the method adopted by ISO 18653 and ISO 14253-1 is widely accepted so that much work is required to establish evidence that the approach used in these standards is wrong.

Alternative methods have been proposed that use the bias value to change the limits of uncertainty [Eberhard]. They were investigated to explore the relationship between random uncertainty and bias. The work shows that the method proposed in the BGA Code of practice significantly underestimates the uncertainty when the bias is greater than the SE. While this is statistically correct it highlights the anomaly of attempting to combine a known bias with an uncertainty distribution. In the authors opinion the approach of Dietrich to model bias with a rectangular distribution is the only one which is statistically defendable because it avoids the combination of 'known' error with

'unknown error' values. If the bias is known and significant with respect to the process measurement uncertainty (greater than the U_{95} value) it should be appropriately compensated.

4.10 Classical or 'mainstream GUM' uncertainty models

The classical or conventional methods of modelling measurement uncertainty are embodied in the procedures described in the Guide for the expression of uncertainty in measurement [VIM, 1995] known simply as 'GUM' in the metrology field. It has been successfully applied in every field of measurement and is described in many references including [Deitrich, VIM, 1995]. The following explanation, which is paraphrased by the author, is from GUM [VIM, 1995].

The output quantity, the measurand, $z = f(x_1, x_2, ..., x_n)$ depends on N input quantities $x_1, x_2 ..... x_n$. Each input x_n has a known describable probability distribution associated with the likely range of values the quantity can take. We can use the Taylor Series expansion, provided the function f(x) is real, continuous and differentiable, to describe the behaviour of z for small deviations in x_i about the expected mean value of x_i , namely μ_i . The use of a Taylor Series expansion is a sensible way for investigating the effects of changes in x_i on z.

$$z - \mu_z = \sum_{i=1}^{n} \frac{\partial f}{\partial x_i}(x_i - \mu_i) \tag{4.17}$$

Equation 4.17 assumes that relationships are linear and that higher order terms are negligible.

The square of the deviations z-μ_z gives

$$(z - \mu_z)^2 = \left[\sum_{i=1}^{n} \frac{\partial f}{\partial x_i}(x_i - \mu_i)\right]^2 \tag{4.18}$$

$$= \sum_{i=1}^{n}\left[\frac{\partial f}{\partial x_i}\right]^2 (x_i - \mu_i)^2 + 2\sum_{i=1}^{n-1}\sum_{j=i+1}^{n} \frac{\partial f}{\partial x_i}\frac{\partial f}{\partial x_j}(x_i - \mu_i)(x_j - \mu_j) \tag{4.19}$$

The variance of z is the expectations of $E[(z-\mu_z)^2]$ which is σ_z^2 , so from equation 4.19

$$\sigma_z^{\,2} = \sum_{i=1}^{n}\left[\frac{\partial f}{\partial x_i}\right]^2 \sigma_i^{\,2} + 2\sum_{i=1}^{n-1}\sum_{j=i+1}^{n}\frac{\partial f}{\partial x_i}\frac{\partial f}{\partial x_j}\sigma_i\sigma_j\rho_{ij} \qquad (4.20)$$

where $E[(x_i-\mu_i)\ (x_j-\mu_j)]] = v(x_i,x_j)$ is the covariance of x_i and x_j and ρ_{ij} is the correlation coefficient of x_i and x_j given by $\rho_{ij}= v(x_i,x_j)/(\sigma_i\ \sigma_j)$.

Equation 4.20 is not a simple substitution but is a more convenient form because it eliminates the covariance terms which may have non-standard units and the correlation coefficient simply becomes a number between ±1.

If the input quantities are independent then correlation coefficients become zero and the expression for measurement uncertainty simplifies to

$$\sigma_z^{\,2} = \sum_{i=1}^{n}\left[\frac{\partial f}{\partial x_i}\right]^2 \sigma_i^{\,2} \qquad (4.21)$$

In the dimensional field, a first order approximation is reasonable. Furthermore GUM, clause F1.2.4, [VIM,1995] shows that it is still possible to use equation 4.21 in the presence of correlated uncertainties by simply combining these is a single variable prior to implementing the equation. This is valid because of the Law of Propagation of Uncertainty that is the embodiment of equation 4.21. It shows that independent variables contribute equally to the uncertainty estimate and can thus be considered identical, irrespective of the uncertainty source. This includes so called systematic uncertainties from previous calibrations and calibration data.

The term $\left(\frac{\partial f}{\partial x_i}\right)$ is the partial derivative of the measurand with respect to a single input variable. This is termed the sensitivity coefficient in many documents [UKAS,M3003]. In some measurement fields this term is complex or difficult to differentiate and is seen as a significant limitation. Some further observations on using the method are outlined below:

- Equation 4.21 is independent of bias in the measurement results. Bias or errors are established by calibration and are normally compensated before reporting the measurement results. In many processes such as instrument calibration or gear measurement errors are minimised by correct instrument set-up but are ever present and not fully compensated. The method adopted by ISO 14253-1 is to add the bias

linearly to the uncertainty estimate and this technique was also adopted in ISO 18653. That this only represents a small increase in probability due to the long tails of a Gaussian distribution is statistically correct, it is nevertheless inconsistent with GUM, that uncertainty estimates should be 'realistic' rather than 'safe'.

- Some uncertainties are single sided or asymmetrical. For example a cosine error (alignment error) results in a value which is always smaller than the actual value when using a laser interferometer to measure length. Mainstream GUM or classical uncertainty methods are not capable of propagating this through to reliable estimates in measurand uncertainty. The effect of this is small because other sources are greater and therefore more dominant in the final analysis of gear measurement uncertainties.

- When some x_i values are small, the variance or expanded uncertainty may yield values that are not practical, for example form errors may not be less than zero but this may be implied by the expanded uncertainty. This can occur more often with evaluated parameters rather than directly measured values. Again mainstream GUM does not adequately account for these circumstances.

- If the σ_i input distributions are Gaussian, the output will also be Gaussian. If all are Gaussian distributions the confidence interval will also be appropriately transferred through equation 4.17. If they are not, the confidence interval will change for a given input variable confidence because the model cannot define the relationship between σ and the confidence interval.

4.11 Numerical uncertainty evaluation models

The classical methods of estimating measurement uncertainty described in the GUM [VIM,1995] have been widely applied but have some limitations as discussed in the previous section. Monte Carlo Simulation or MCS is a numerical method that has been widely applied to predict the behaviour of complex systems, including weather forecasting, traffic flow analysis, manufacturing process simulation etc. It is also becoming more commonly used in measurement uncertainty analysis to model more complex measurement processes or when the implementation of the mainstream GUM methods are not practical. Numerous research and application papers [Basil], [Cox, 1999], [Robert] and [Schwenke, 2000] have been published and discussed [Cox, 2001] and the implementation described in detail.

The implementation of the MCS process is described below [Cox, 2001]:

- Develop a statistical model of the process (similar with mainstream GUM). For example it may be modelled as a straight line fit to obtain the slope with the input variables appropriately incorporated.

- Input-output modelling. This is the development of the model in accordance with the GUM guide determining any relevant relationship and correlated uncertainties that require investigation.

- Assignment of probability density functions to the input quantities and determine their limits.

- Determine the probability density function (pdf) for the output quantity by running the MCS model.

- Establish the coverage interval for the output quantities, for example by 2.5 and 97.5 percentiles which may result in an asymmetric distribution of the confidence interval.

Running a MCS involves repeatedly sampling the values of the pdfs that define the input variables and using these discrete values to calculate an output value from the input-output model. This results in a series of simulated measurement results that can be used to estimate the range of likely output results expected.

The process involves:

- Selecting the number n of MC trials needed (generally by trial and error), depending on the degree of complexity and number of significant digits required but often between 20,000 and 100,000 trials.

- Generate the n samples using a random number generator and a pdf with limits defined by practical tests or an experienced metrologist for each input variable x_i .

- Use the x_i values to calculate or simulate the output value from the model using $f(x_i)$ for the output quantity.

- Calculate the mean $f(x_i)$, $s(x_i)$ and define the 2.5 and 97.5 percentiles for a 95% confidence interval for the mean output value.

The process is robust and may be used for any measurement process but it has not yet been applied to gear measurement uncertainty models. The primary reason for this is that

with the largest uncertainty source, that of the imported uncertainty from the calibration laboratory, no amount of simulation is likely to significantly improve the uncertainty estimate validity (see Chapter 7).

However if the method of establishing traceability with simple evaluated parameter comparison (f_p, F_r, $f_{H\alpha}$ etc) is changed to a comparison of actual measurement point data, then the MCS technique will be more appropriate.

The MCS approach can be implemented on commercially available software such as Matlab [Onakereru], provided that robust, validated random number generators are employed.

4.12 Robust statistical models

Established uncertainty estimation methods utilise classical statistical theory and in many applications are appropriate. However they are prone to errors, particularly when small samples sizes are used. Classical statistical techniques were developed initially as a method to reduce large quantities of data into meaningful information and as a method of predicting the characteristics of a large population of data based on a small sample size. In statistical calculations a small sample size is less than 200 [Mandel], however this is large compared to the sample sizes that are available in dimensional measurement, typically in the order of between 1 and 10 are more commonly found. When estimating the effective degrees of freedom using Students t-distribution (as shown in Chapter 7) excessive values for measurement uncertainty, compared to measurement results are obtained. This is primarily due to the susceptibility of the calculation of least squares to the presence of extreme data values and the resultant influence on mean and variance estimates generated by the classical methods. Simply screening data to eliminate outliers is possible and is sometimes practised but in many cases is not an effective solution because:

- Users do not always screen data effectively and it is often relies on the individual to decide whether to reject data or not.
- The simple decision to reject data is wasteful, particularly in circumstances where the data is sparse. Down-weighting data is a more effective method of handling dubious results without the simple yes/no decision, but the method employed can make significant differences to the analysis results.

- Rejecting outliers changes the distribution theory of random sampling and underestimates values from data analysis, eg variance is reduced.
- There is no agreed method of defining outliers, although arbitrarily 3σ is often used.

There is a wealth of statistical theory and applications based on so-called 'Robust Statistical Methods' from well respected researchers [Huber, Hampel et al]. But the methods have not been developed by National laboratories or their statistical research groups. Reviewing work by [NIST, 2001] and [NPL, 2003 and 2004] show little work has been undertaken in this field, to date. One reason for this is possibly that the methods are not particularly relevant to the NMIs themselves and there are few requests from industry to encourage such research.

4.12.1 Numerical example

The mean value of a sample may be replaced with the median value which is the middle value in a list of data ranked form highest to lowest value. For example, values of F_α (Total profile error) are [4.2, 4.8, 5.9, 5.2, 4.7] from the Höfler EMZ 632 CNC gear measuring instrument in NGML from which the mean value of 4.96μm is calculated. However, without the highest value, a marginal outlier of 5.9, the mean is reduced to 4.73μm. The median value is [4.2, 4.7, **4.8**, 4.2, 5.9] is 4.8, which is intolerant of the value of the extreme values and is closer to the mean value if the marginal outlier is ignored. The standard deviation is 0.64μm because of the 5.9μm value, and the expanded error of the mean (p=95%) is large because of the degrees of freedom for ν=4 with a 95% confidence interval is 4.18. (U_{95}=4.18*0.64=±2.68μm). A robust parameter such as 'average deviation' is less sensitive to the outlier values because the differences are not squared

$$\text{Average deviation} = \frac{1}{n}\sum_{i=1}^{n}\left|x_i - x_{med}\right| \qquad (4.22)$$

In the above example, the average deviation is 0.48μm.

It is of interest to note that if the data is 'normally distributed' there is a defined relationship between the average deviation and the standard deviation as given by

$$\text{Average deviation} = 0.8 \text{ .standard deviation} \quad \text{where } 0.8 = \sqrt{\frac{2}{\pi}} \text{ . [Mandel, 1964]}$$

In the above example the average deviation is 0.48μm so the resulting theoretical standard deviation should be 0.51μm. This is consistent with the premise that the 5.9 value is an outlier.

There are other parameters used commonly for linear regression, for example the 'Least mean squares' or LMS of residuals is sometimes limited to a defined percentile of say 90% of the squared quantities. However these require more computing power than conventional LS methods and the decision regarding the definition of the quartile limit is arbitrary.

The application of these robust statistical techniques to gear measurement offers some sensible solutions for estimating the effects of process uncertainty. However, whilst being similar to the MCS methods, the dominant uncertainty contribution is the uncertainty resulting from the reference artefacts which yields little benefit from the additional effort required to evaluate the data.

4.13 Bayesian uncertainty models

Classical statistical theory adopted by GUM is used throughout metrology fields to produce estimates of measurement uncertainty. A Bayesian statistical approach is being researched by NPL and others [NPL, 2004] with particular reference to interpreting key comparison data which are used to ensure compatibility of primary calibration facilities throughout the world and have been applied to comparison data [Weise, 1992] as a procedure for enhancing mainstream GUM methods. Bayesian methods have been also been developed for comparison purposes [Weise, 1994]. With this background, Bayesian methods may also be applicable to gear measurement that relies heavily on comparisons to establish traceability.

The Bayesian view recommends a pdf assignment to each input quantity based on whatever information is available. It provides a rigorous means of incorporating prior information into a measurement and is based on the mathematics of conditional probability. Classical statistical theory is solely concerned with counting and frequency distributions, without regard for the condition of the process. The Bayesian approach is the probability of an event occurring given that a further condition is fulfilled, i.e. in metrology, prior information from a process can be used to affect the likely result of a current process.

For example, consider the effect of testing a gear measuring instrument with two calibrated artefacts. In general, using the classical theory the more tests performed, the larger the uncertainty. If the two artefacts A and B have respective uncertainties of U_{calA} and $U_{cal\ B}$ most uncertainty processes would use the worst case bias, either $(\overline{x_a} - x_{calA})$ or $(\overline{x_b} - x_{calB})$ and worst repeatability to provide uncertainty estimates of the measurement process. Thus by performing two calibration processes the uncertainty estimate can be increased, despite the fact more tests are performed with an improved the estimate of measurement uncertainty.

An alternative approach to estimating uncertainty based on Bayesian statistics is described in the draft Technical Report TS 15530-5 'Techniques for determining the uncertainty of measurement using statistical measurement history' [ISO, 2002].

After reviewing the calibration procedures at the NGML (described in Chapter 7) the implementation of GUM or MCS method is appropriate, if the measurement history or historical data is not considered. The uncertainty budget methods described in Chapter 7 use data from 5 tests on a calibrated master to determine the bias and repeatability of the instrument. Data from previous measurements on calibrated artefacts of various sizes and types is available from previous calibration processes, but this is ignored. Other calibration techniques such as using gauge blocks or step gauges may be used to verify guide-ways. The information from these tests is also helping to improve confidence in the measurement results on the gear, but the tests do not reduce uncertainty in the final uncertainty assessment; on the contrary they may actually increase it if they are included all. The Bayesian statistical approach to assessing measurement uncertainty provides a method of including this data and reducing measurement uncertainty, thus showing tangible benefits for the effort involved in obtaining the data. The specific mechanism for implementing this in a complex dimensional measurement application and has yet to be completed at an NMI.

Bayesian inference provides a rigorous method of incorporating this historical or *a priori* information into a measurement process uncertainty, based on conditional probability. The result for Gaussian distributions is shown in equation 4.23 [ISO,2002]

$$y = y_m\left(\frac{\gamma}{1+\gamma^2}\right) + y_{pe}\left(\frac{1}{1+\gamma^2}\right) \tag{4.23}$$

$$\gamma = \frac{u_{pe}}{u_{cm}} \tag{4.24}$$

$$\frac{1}{u_c^2} = \frac{1}{u_{cm}^2} + \frac{1}{u_{pe}^2} \tag{4.25}$$

where:

y best estimate of the measurement result

y_m best estimate of the measurement result without prior information

y_{pe} prior evaluation ie. best estimate of the mean value based on prior (historical) information of the workpiece measurement result

u_c combined standard uncertainty

u_{cm} combined standard uncertainty with prior information included

u_{pe} standard uncertainty based on prior evaluation from historical data

Equation 4.24 is effectively the weighted average of the measurement result using *a priori* data. An obvious requirement is that the measurement process is 'stable', or the 'instability' is at least included in the historical information. Equation 4.25 shows that the combined uncertainty is always less than the uncertainty without including the historical information. In other words, we are rewarded by fully investigating and evaluating the measurement process, but the benefit depends on the relative uncertainties of the contributions. The implementation of Bayesian methods to evaluate processes that measure identical workpieces is established [Weiss] provided historical calibration data is available.

The implementation of Bayesian methods for a range of workpieces, or for when data from weakly related measurement tasks has yet to be established would be of significant benefit for complex measurement tasks such as gear measurement in which greater confidence in results from data measured from artefacts are used to establish traceability by the comparator method. Although intuitively, Bayesian statistics is the obvious candidate solution for gear measurement uncertainty, the benefit of this, like other methods is limited by the significant uncertainty from calibration data values used to establish traceability.

4.14 Summary

Classical uncertainty theory has been successfully applied to gear measurement for many years, using the comparator method, however robust statistical methods offer no significant benefit over the classical methods when a process is well established with few outliers.

MCS methods may have some benefit for estimating uncertainty of data point analysis, in particular the LS fit parameters for lead and profile measurement, and for pitch parameters.

Whilst the Bayesian statistical approach has not previously been applied to gear measurement it offers the most benefit when combined with MCS methods to data point analysis. In particular, it offers the ability to *use* historical data from calibration processes, including the benefit to be gained from non-gear calibration activities.

The work in this thesis concentrates on the application mainstream GUM and MCS methods but makes recommendations for the investigation of Bayesian methods in Chapter 9.

Chapter 5

SURVEY OF UK GEAR MEASUREMENT CAPABILITY

This chapter describes the first survey of gear measurement capability conducted in the UK and includes an estimate of gear measurement uncertainty using the comparator method. When the work was originally published there was no reliable reference data available so a weighted mean was used from the survey results to estimate the reference data. Additional comparisons with PTB data are presented and discussed.

5.1 Introduction

In 1988 when the NGML was established at Newcastle University it was appropriate to quantify the measurement capability of the industry supported. A survey of capability was thus undertaken using selected master gears from NGML with the following objectives:

- To quantify the attainable measurement uncertainty of modern gear measuring equipment used in industry.
- To assess the gear metrology needs, capabilities and practices of the gear industry.
- To develop a programme of support for the gear industry using the National Measurement System supported by the Department of Trade and Industry and accreditation bodies.

The work involved the author visiting companies with a selection of master gears and gear artefacts from the NGML to assess the measurement capability of industry. This was supported by personal interviews with Inspection and Quality Assurance personnel within each organisation by consultants, Prof. R. Munro and Mr. P. Smith.

Questionnaires were used to broaden the coverage of the survey and confirm the findings. The scope of the measurement work included:

- Involute profile measurement capability with a 200mm diameter profile artefact.
- Helix measurement capability with two helix artefacts of 100mm and 200mm diameter.
- Cumulative pitch measurement capability with a pitch artefact of 190mm diameter.

A procedure was developed to estimate the reference data value for the calibrated flanks and then to use this data to estimate the measurement uncertainty of the individual measuring instruments. Although the work predated more recent standardised methods [VIM,1995], the methodology is broadly consistent with the recommendations in this document. Individual participating companies were issued with a confidential report that included an uncertainty statement for the instrument and, where appropriate, comments on faults or excessive errors that were revealed. All results from the companies were coded for confidentiality and used to prepare both a confidential individual visit report and a summary report that allowed the organisation to benchmark their capability against other participating organisations.

The work programme was completed in December 1990 and reported to the DTI and participating companies [Frazer,1990]. Site visits were made to establish the measurement uncertainty on measuring instruments and to assess the QA system and capability. The work described in this chapter includes the detailed methodology and analysis of results that enabled the study to meet the first two objectives of the work programme. Since this work was completed there has been a similar survey of gear measurement capability undertaken by the American Gear Manufacturers Association (AGMA) for involute profile measurement [Smith]. The findings support the UK work, although the scope of the AGMA programme was more limited.

5.2 Research methodology

The gear artefacts used for the work have the geometry shown in Tables 5.1 to 5.4. and are illustrated in figures 5.1 to 5.4. These are very challenging artefacts to measure accurately. The helix artefacts comprise a series of different helix angles that enable the

diagnosis of the probable causes of any excessive errors measured and estimate measurement uncertainty.

Table 5.1 200mm Lead/Helix artefact basic gear geometry and evaluation range

Parameter	Helix angle (β)			
	0°	15° LH & RH	30° LH & RH	45° LH & RH
Teeth (z)	25	25	25	25
Normal module (m_n)	8.000 mm	7.72741 mm	6.92820 mm	5.65685 mm
Normal pressure angle (α_n)	20°0'0"	19°22'12"	17°29'43"	14°25'58"
Diameter (d)	200.000 mm	200.000 mm	200.00 mm	200.000 mm
Evaluation length (L_β)	100.0 mm	100.0 mm	100.0 mm	100.0 mm
Face width (b)	127.0 mm	127.0 mm	127.0 mm	127.0 mm

Note the 45˚ helix angles were not evaluated because few instruments could measure these over the full face width.

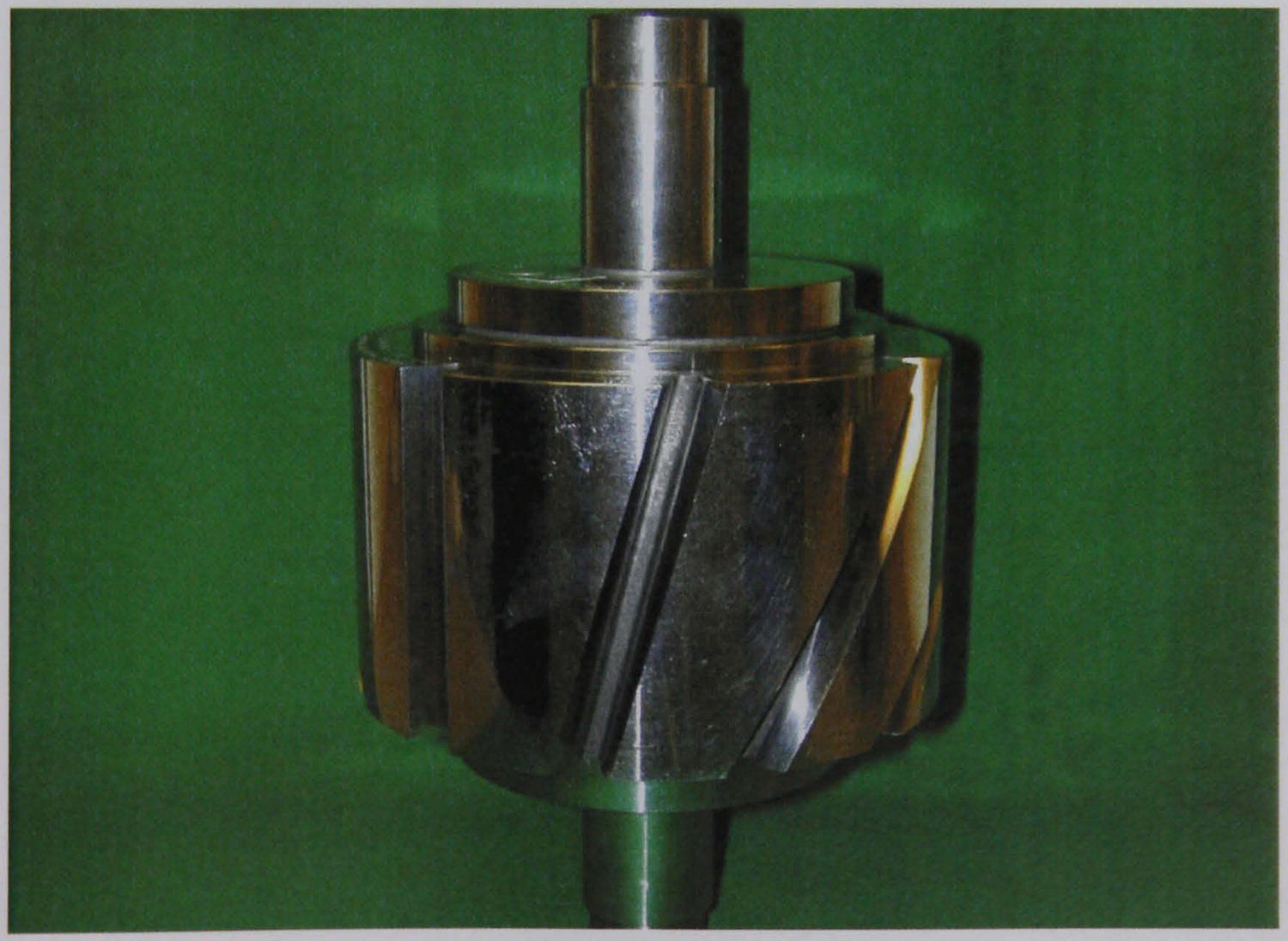

Figure 5.1 200mm diameter helix/lead artefact with 14 calibrated flanks with 0˚, 15˚LH. 15˚RH, 30˚LH, 30˚RH, 45˚LH & 45˚RH helix angles.

Table 5.2 100mm Lead/Helix artefact basic gear geometry and evaluation range

Parameter	Helix angle (β)		
	0°	15° LH & RH	30° LH & RH
Teeth (z)	20	20	20
Normal module (m_n)	5.00000 mm	4.82963 mm	4.33013 mm
Normal pressure angle (α_n)	20°0'0"	19°22'12"	17°29'43"
Diameter (d)	100.000 mm	100.000 mm	100.00 mm
Evaluation length (L_β)	100.0 mm	100.0 mm	100.0 mm
Face width (b)	125.0 mm	125.0 mm	125.0 mm

Figure 5.2 100mm Helix/lead artefact with 10 calibrated flanks and helix angles of 0°, 15°LH. 15°RH, 30°LH & 30°RH.

Table 5.3 200mm Profile artefact basic gear geometry and evaluation range

Parameter	
Teeth (z)	25
Helix angle (β)	0°
Normal module (m_n)	8.000 mm
Normal pressure angle (α_n)	20°0'0"
Diameter (d)	200.000 mm
Evaluation length (L_α)	38.0.0 mm
Face width (b)	6.0 mm

Figure 5.3 200mm profile master with left and right calibrated flanks.

Table 5.4 200mm Pitch artefact basic gear geometry and evaluation range

Parameter	
Teeth (z)	48
Helix angle (β)	0°
Normal module (m_n)	3.95833 mm
Normal pressure angle (α_n)	00°0'10"
Diameter (d)	190.000 mm
Face width (b)	8.6 mm

Figure 5.4 190mm diameter pitch master with 48 teeth

The research was divided into 2 parts, designated A and B. The decision to include a company in part A or B was made by NGML based on existing experience of a companies capability. A description of the two parts follows:

Part A. This was designed to provide information on the best capability of modern instruments in an industrial environment. The work was completed under direct supervision of NGML staff. A range of new or older well calibrated gear measuring

instruments were selected for this work that were known to be situated in a reasonable environment.

Part B. This was designed to provide information on the actual capabilities of industrial gear measurement in the UK. For this work the instrument operators were allowed to use their own standard procedures. Instruments involved include examples of the same type used in the part A survey. Because the artefacts were of different geometry to the standard gears measured on the instruments on a daily basis some instrument operators expressed concern about this or wanted additional checks to be carried out to verify the instrument was fit for purpose. Any detected error was subsequently used to correct the measurement data before the measurement results were analysed.

5.2.1 Part A procedure.

After making a record of the instrument visual condition, calibration status, location and the environment, the following tests were completed:

Initial tests

- *Runout* of top and lower centres was recorded over two complete revolutions using a 1μm discrimination indicator.

- *Tailstock centre alignment* was measured with a mandrel mounted between centres and with a 1μm discrimination indicator used to 'Trammel' the top centre. Results were recorded at 90° intervals of table rotation. The resulting error may be due to an alignment error of the axis that supports the tailstock or because the top centre is translated in the horizontal plane relative to the spindle axis. The error was measured at 350mm centre separation but additional measurements at different heights are needed to determine the cause of the error. Base disc type machines were tested whenever possible with the base disc rolling along the base tangent slide because the bias force of the base disc can cause serious alignment errors. Excessive errors were adjusted before use with prior agreement from the organisation.

- *Base helix angle* zero setting error was tested by placing an indicator on the base tangent slide and verifying the change is acceptably small (within 2μm) over the lead axis length on mechanical instruments only. Excessive errors were adjusted before gear artefact calibration.

- *Parallelism of the lead axis* and axis between centres was measured with a 350mm long mandrel mounted between centres. The runout of the mandrel was verified before use. Excessive errors were adjusted before measuring gear artefacts.

- *Magnification of the probe system* was checked before using the system to measure gear artefacts. Regrettably it was not possible to verify probe discrimination.

Artefact measurement procedure

- The artefact was mounted between centres and a suitable driver coupling fitted.

- The temperature of the artefact was measured and verified to be within ±2°C using a calibrated surface contact Mercury in Glass thermometer.

- Radial runout of the reference bands was measured and recorded at 90° intervals.

- The spur flute (gash) was aligned with a reference mark on the bottom spindle. Each flank was measured a minimum of 4 times with the gear artefact indexed by 90° intervals between each measurement. The variation in results was attributed to instrument repeatability, effects of centre runout and base disc runout at each position on the centres.

- Any excessive variation in measurement result is verified by measurement of the reference bands on the artefacts.

Note that on some instruments it was not practical to index the artefact. In these situations four straight repeat tests were recorded.

Parameters evaluated:

- The lead error slope parameter $f_{H\beta}$ was selected for evaluation purposes because it is robust, and has a clear definition of positive or negative errors. As such, it is the best parameter to estimate measurement uncertainty

- The profile error slope parameter $f_{H\alpha}$ was also selected for evaluation, again because it is robust, with a clear definition of positive or negative errors.

- The last parameter chosen for evaluation was cumulative pitch, F_p because it is easy to evaluate and indicates the maximum variation in F_p due to runout between centres.

Refer to Chapter 2 for definition of the parameters in accordance with ISO 1328 and ISO TR10064-1.

5.2.2 Part B procedure

The purpose of these tests was to determine the actual operating capability of the UK gear manufacturers using the same artefacts and parameters from the part A tests. Care was taken to ensure that the instrument operators understood that they should use their best practice but that the methods adopted should be typical of those that they use on a day to day basis. Instrument operators were allowed to complete checks on artefacts without calibrating the instrument in any way unless they initiated tests themselves.

After the artefact tests, the author completed the tests used to verify the instruments as described in Part A. Any findings were reported directly to the company in a confidential report.

5.3 Determination of reference data.

There was no reliable reference data available for the artefacts prior to the tests, primarily because the facilities at NGML were, at the time, newly established and the instrument performance was not fully validated, and also because the laboratory personnel did not have sufficient experience in the field of gear measurement to provide reliable data for the comparison. Data from PTB was available [PTB, 1982] but there was some concern over the validity of the data reported in the certificates following their recall and revision.

A decision was taken to use a weighted mean of the survey results, weighted inversely proportional to the variance of the measured data [Mandel], for helix errors and an un-weighted mean of results for involute profile and pitch errors. The difference in strategy was due to less data being available from the pitch and profile artefacts to produce a reliable variance. The procedure for estimating a weighted mean for the helix results is described below:

- An initial estimate of the actual errors on each calibrated flank a, b, c….. where a, b, c etc are separate flanks using the unbiased arithmetic mean.
- Calculate an initial deviation or error for each instrument measured error

$$e_{ai} = a_i - a \tag{5.1}$$

Similarly calculate e_{bi}, e_{ci} etc for each calibrated flank where 'i' is the instrument number

- By assuming that the measurement uncertainty is the same for each flank on a particular instrument then estimate the standard deviation (s_i) of the measurement process using:

$$s_i^2 = \left(e_{ai}^2 + e_{bi}^2 + e_{ci}^2 + e_{ni}^2\right)/(m-1) \tag{5.2}$$

Where m is the number of flanks checked.

- The weighted values of a_{iw}, b_{iw}, c_{ie}, etc can thus be calculated according to the variance s_i^2) using:

$$a_{iw} = a_i/\left(1 + ks_i^2\right) \tag{5.3}$$

This weighting method has several benefits over a standard weighting of $1/s_i^2$. The standard method was tested and it was found that the weighted value did not converge to the same a_{iw} if different initial estimates of a_i were used. Also if one instrument happened to have results similar to the un-weighted mean used for the initial estimate, the resulting variance would be very small and hence the result for that instrument would be very highly weighted. The expression in equation (5.3) is very stable and insensitive to initial conditions. A sensitivity coefficient k=0.08 was chosen with the result that the weighting varied by a factor six from the most accurate to least accurate instrument. This large range is explained by the large deviation from two part B instruments with particularly excessive deviations. The majority of weighting factors were within a more reasonable range of three. The final choice of sensitivity coefficient was based on the observation of results from five instruments selected as representative of typical instruments and observing uncertainty value estimates.

- A revised estimate of the actual helix errors a, b, c…..can be calculated using

$$a = \frac{\sum a_i/\left(1 + ks_i^2\right)}{\sum 1/\left(1 + ks_i^2\right)} \tag{5.4}$$

Where the estimated variance of a is given by

$$s_a^2 = \frac{\sum s_i^2/\left(1 + ks_i^2\right)}{\sum 1/\left(1 + ks_i^2\right)} \tag{5.5}$$

This is repeated for the remaining flanks b. c etc.

- The new estimates of the slope errors for a, b, c etc are used in an iteration procedure that converges to a stable estimate of errors.

In all cases the change in value between weighted and un-weighted mean was less than 0.5μm.

5.4 Estimation of individual instrument uncertainties.

The comparator method of estimating measurement uncertainties was used to evaluate individual instrument uncertainty. The method used for helix (lead) measurement is described below:

- Estimate the standard deviation (s_i) and mean error (x_i) from the differences between the weighted reference data and the individual measured errors.
- Estimate the standard deviation of the reference data *(s)*.
- Calculate the instrument uncertainty U_{95} using the following method:

$$U_{95} = \sqrt{\left[(2 \cdot s)^2 + \left(2 \cdot s_i\right)^2 + (0.7 \cdot x_i)^2\right]} \qquad (5.6)$$

This method follows the standard comparator method with one notable difference, namely the inclusion of an error term added quadratically within the expression. In a normal estimation procedure the error or mean bias of an instrument when compared to the reference values is either corrected or added linearly to the quadratic expression. However the bias was determined with a finite series of measurement and does not include reproducibility errors that would account for a change in bias over a longer period of time. Thus the actual bias calculated is simply a sample bias for the process. If the bias is used as an estimate of the range of biases that exist, it can be considered as an additional distribution, see (section 4.9).

The 0.7 coefficient applied to the bias value was selected as an 'engineering estimate' of the likely range of biases expected from the measurement process to give a 95% confidence interval. With experience from subsequent work, this coefficient should not have been applied but, the resulting estimate of uncertainty still appears to be valid after examining the values that this method returns.

5.5 Instruments surveyed

The survey covered 28 organisations and 46 inspection instruments of varying types and conditions. A summary of the lead and profile instruments and the pitch measuring instruments is given in Tables 5.5 and 5.6, respectively.

Table 5.5 Range of evaluated lead and profile measuring instruments.

Instrument	Type	Capacity, diameter [mm]	Part A Number	Part B Number
Maag PH60	BD	600		5
David Brown 18T	BD	450	1	4
Frenco SH450	BD	450	1	
Goulder 3I	BD	-		1
Höfler EFRS 630	BD	630	1	1
Klingelnberg PFS600	BD	600		1
Fellows Profile machine	BD	-		1
Maag SP60	IVH	600	1	1
Maag PH100	IVH	1000		1
Maag SP130	IVH	1300	1	
Maag SP160	IVH	1600	1	
Goulder IL600	IVH	600		1
Klingelnberg PFSU600	IVH	600		1
Klingelnberg PFSU1200	IVH	1200	1	
Höfler EFRS630	SVM	630		1
Gleason GMS430	CNC	430	2	3
Fette PKM300	CNC	300	1	
M & M 3000QC	CNC	300	1	
Zeiss ZMC 550	CMM	550	1	
Zeiss UPMC850	CMM	850	2	
Höfler EMZ401	CMM	400	1	
Maag SP65	CNC	650	1	
		Total:	16	21

(Instrument type code: BD- base disc instrument, IVM-infinitely variable mechanism machine, SVM- step variable mechanism machine, CNC- dedicated CNC gear checking machine & CMM- coordinate measuring machines with gear software)

Table 5.6 Range of evaluated pitch measuring instruments.

Machine	Type	Capacity Diameter [mm]	Part A Number	Part B Number
Gleason GMS430	CNC	430	2	1
Zeiss UPMC 850	CMM	850	2	
Zeiss ZMC550	CMM	550	1	
Höfler EVTM	Portable	-	1	1
M & M 3000QC	CNC	300	1	
Fette PKM300	CNC	300	1	
Maag ES401	Portable	999 teeth	2	1
Matrix circular division tester	Mech	-	1	
HöflerUP400/A	Portable	-		1
HöflerKP400	Portable	-		1
Goulder	Portable	-		1
		Total	11	6

(Instrument type code: CNC-dedicated CNC gear measuring instrument, CMM-coordinate measuring machine, Portable-portable machine mounted on a rotary table, Mech- mechanical indexing machine with sine bar indexing system)

5.6 Survey results

A summary of the results from the survey [Frazer,1991 and 1992] are presented in Tables A1 to A12 in Appendix A for both group A and B instruments. Note that the results are coded to maintain company confidentiality.

The definition of the helix (lead) slope error sign is different to normal ISO definition It is positive if the slope error tends to a right helix, and negative if it tends to a left helix error. This convention allows the identification of any significant trends in the instrument such as simple alignment errors. A discussion of the results is included in the next section.

There is a greater quantity of data for lead measurement performance which requires more stringent instrument alignment for accurate measurement and thus instrument performance focuses on lead/helix results.

5.7 Discussion of results

5.7.1 Instrument condition

Part A instruments

Each company participating in the survey received a confidential report with results and recommendations for improving measurement capability.

The condition of the machine and its environment is more important than the type of instrument used. Part A instruments included some older mechanical instruments which were well maintained and had a similar performance to more modern CNC instruments. The following points were noted:

- Many of the newer CNC instruments were checked infrequently and consequently had significant alignment errors, but due to the degradation in alignment of the axis between centres or excessive runout of centres.

- The driving dogs or couplings used to drive the gear on a rotary table often introduce large errors when measuring lead/helix. Differences in lead error slope of between 2 to 3μm over 100mm were not untypical. These errors were caused by poor design or insufficient care taken when attaching the coupling to the gear.

- Often when a particular lead master was close to the capacity limit of an instrument then typically larger errors would be measured. This was verified with the second lead master.

- The majority of instruments were situated in inspection rooms, some of which had temperature control, whereas others rely on normal shop floor heating systems. In general instruments were isolated from the production environment.

- It was noted that although many of the instruments were relatively new, the basic checks described in 5.2.3 revealed 40% of the instruments were adjusted to minimise the alignment errors before artefact measurements were taken.

Part B Instruments

Because all gear measuring machines are affected by Abbe offset issues, the fundamental accuracy of the instrument depends on mechanical alignment or effective error mapping. Given that these errors should be small on accurate machines the lack of understanding of the importance of these issues throughout the industry was surprising. Some of the common faults found on group B instruments are summarised in Table 5.7.

Table 5.7 Common faults found in Part B gear measuring instruments

Parameter	Measured errors	Comments
Alignment between centres	Min 0-1μm/100mm Max 16μm/100mm	Maximum recommended VDI/VDE 2512 pt2 guideline is 2μm/100mm
Centre runout	Mean : Top 2.4μm/bottom 5.0μm Max. 25μm	Recommended maximum error is 2.5μm. runout effects lead, profile and pitch measurement
Probe magnification	25% of machines indicate an error of 20% or greater	The 30μm feeler represents a typical; error measured on high quality gears.
Base disc clearance on centres	38% of mechanical instruments had >5.0μm clearance	Excessive clearance causes runout or size errors on the base disc cause lead and profile measuring errors
Base disc runout on mechanical instruments	Mean 4.0μm TIR Max 25.0μm TIR	Most operators said 5-7.5μm was acceptable. 5.0μm is OK for DIN 3961 grade 8 gears. Lower values needed for high accuracy gears.
Damage to machine centres	50% of instruments tested show excessive damage to centres that will compromise measurement performance	Simple maintenance programmes will address this issue
Maintenance and calibration	70% of instruments are routinely serviced and 'calibrated' but less than 5% could demonstrate traceability to national standards	80% of companies involved in the survey were ISO 9000 accredited.
Environment	15% of part B instruments were housed in a room separated from the workshop	Dirt and thermal effects will reduce the accuracy and reliability of the instrument.

5.7.2 Capability of UK industry

Lead capability

The measurement uncertainty values for lead/helix measurement are shown in figure 5.5. The mean value was ±4.6μm. These are typical of tolerance values specified for an ISO 1328 Grade 5 gear. Examination of the results in figure 5.5 reveals that the 100mm diameter lead master measurement uncertainty for instrument A03 and A05 data is significantly larger than other instruments. In both cases the instruments were correctly aligned so the results are a true reflection on their performance. Instrument A03 could measure the 100mm diameter lead master but it is a mechanical instrument and was operating at its minimum size limit and examination of the 200mm diameter lead results show better performance. Instrument A05 is a dedicated gear measuring instrument but although it was relatively new, it had an unusual arrangement and the design was discontinued.

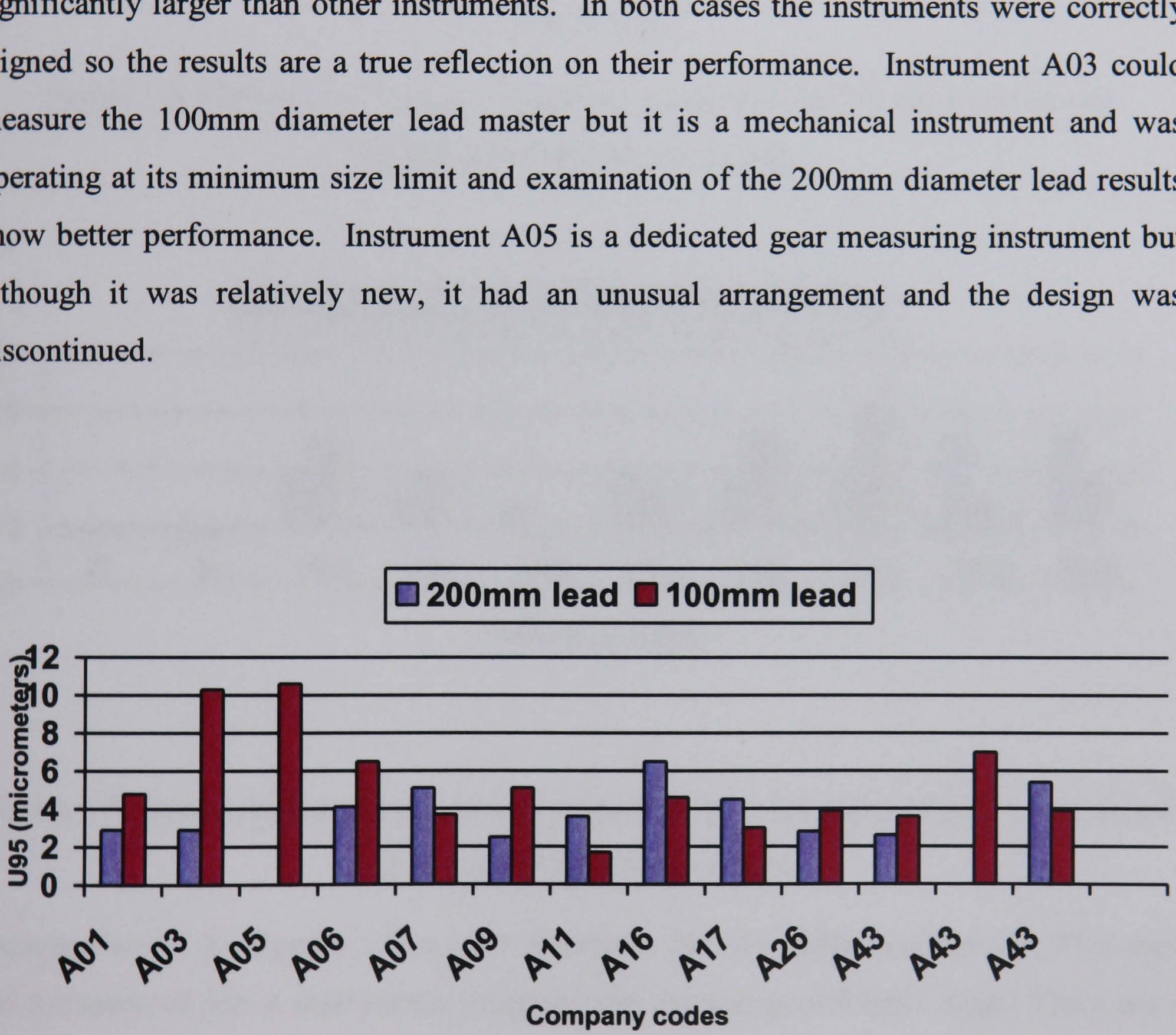

Figure 5.5 Estimated lead measurement uncertainty U_{95} for part A instruments

The difference between the weighted mean of the 200mm lead artefact results and PTB data available for the tests PTB 1982 1992 and 2000 is shown in figures 5.6 and 5.7 for the 100mm diameter lead artefact.

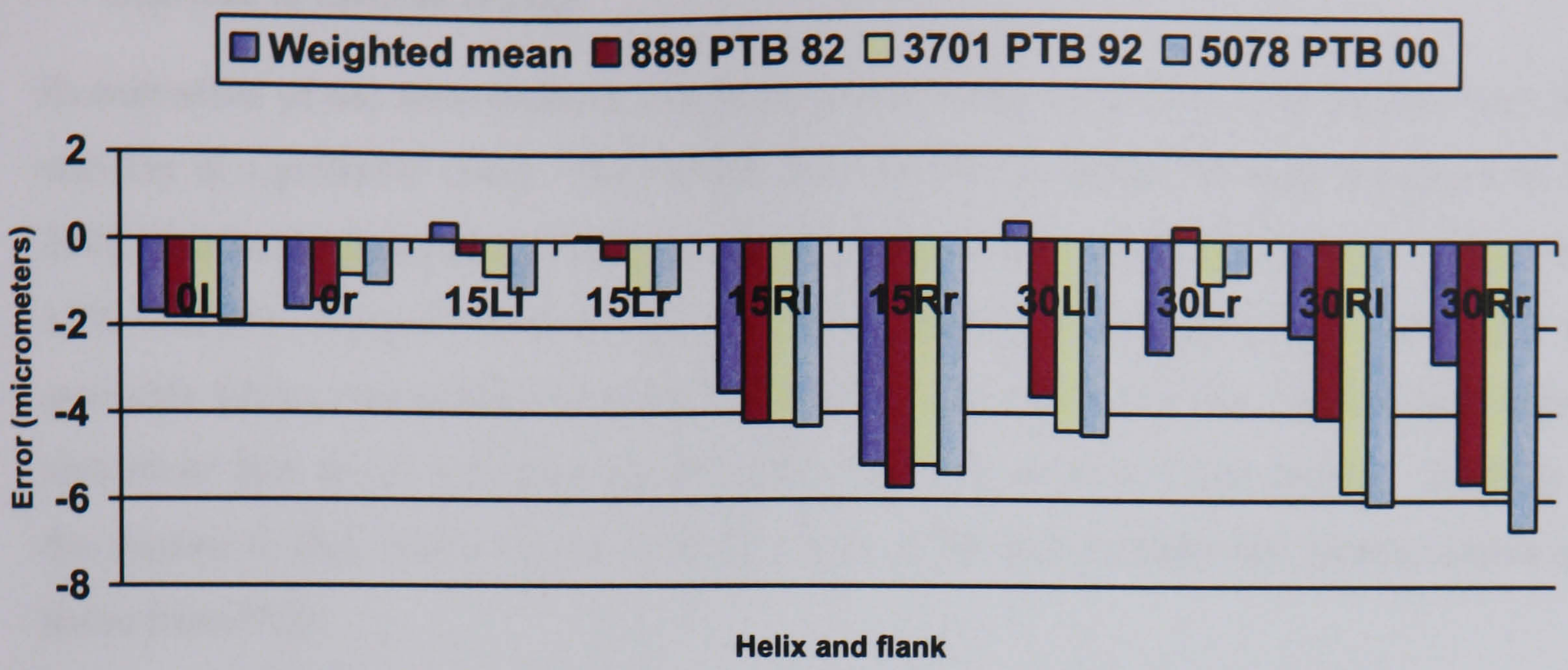

Figure 5.6 200mm lead artefact comparison between mean of part A results and subsequent PTB calibration data.

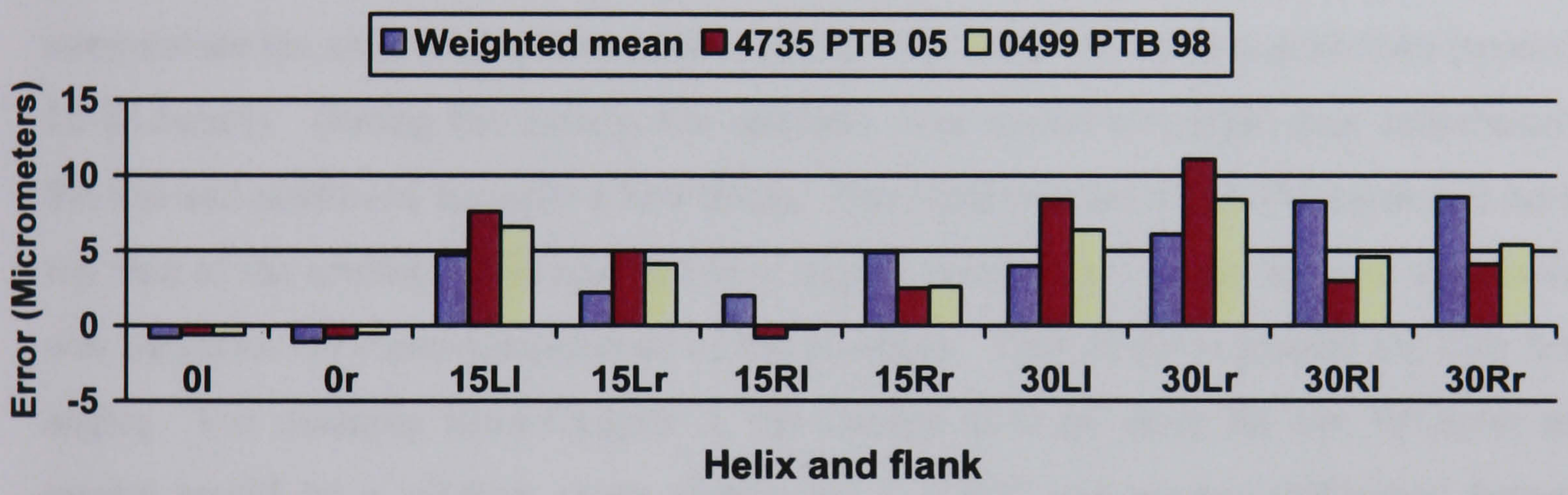

Figure 5.7 100mm diameter lead artefact comparison between mean of part A results and subsequent PTB calibration data.

Examination of the figures 5.6 and 5.7 illustrates that the difference between PTB data and the mean of part A instruments progressively increasing with helix angle. There are a number of possible reasons for this:

- Differences in the calculation procedure for lead error slope.
- The stability of the artefact over the 8 year interval since it was calibrated by PTB
- Bias in the PTB calibration process.
- Bias in the instrument setting procedure in the UK due to a lack of traceability.

- Bias due to thermal effects.

Examination of the measurement results from the 200mm diameter lead master show that stability is a probable issue. The results from the 1982 calibration data compared to the 2000 data have changed by 2μm over the 100mm face width while the results between 1992 and 200 changed less than 1μm. Although data for the 100mm lead master was not available during the initial work the calibration data values for the 100mm lead master also show that this is changing significantly with time over a 5 year period. Stability of the artefact is thus one of the most likely cause of the bias between the survey results and those from PTB.

An alternative explanation is that temperature during the survey was not monitored correctly. The 100mm and 200mm diameter lead artefacts require a significant soak time to thermally stabilise them in a new environment. Work completed in the NGML [Brentnall] has shown that although the surface temperature may have reached room temperature the core temperature takes significantly longer to reach equilibrium (typically 12-24 hours). During the survey, the artefacts were stored overnight then introduced to the site and stabilised for only a few hours. The limit was set at ±2.0°C measured on the top face of the artefact. It is reasonable to expect that in many cases the core temperature was less than the room temperature of the machine. This effect is greater for high helix angles. For example from Chapter 3, the change in slope error for the 30° helix lead master would be a +0.6μm slope change for a -1.0°C temperature difference between artefact and instrument temperature. A 1 to 2μm difference in results is thus not surprising. One of the key findings of the survey was the realisation of the importance of temperature on helix and profile measurement.

Profile capability

Profile results show a similar trend. Figure 5.8 shows the variation in slope error result for left and right flanks. The mean for the Part A instruments was approximately 1.7μm less than the 1992 PTB data obtained after the survey work was published. The PTB data has proven reliable within the stated measurement uncertainty, as shown in Appendix B, Table B.4, with the difference between data being less than 0.5μm. This is supported by the work reported in Chapter 6.

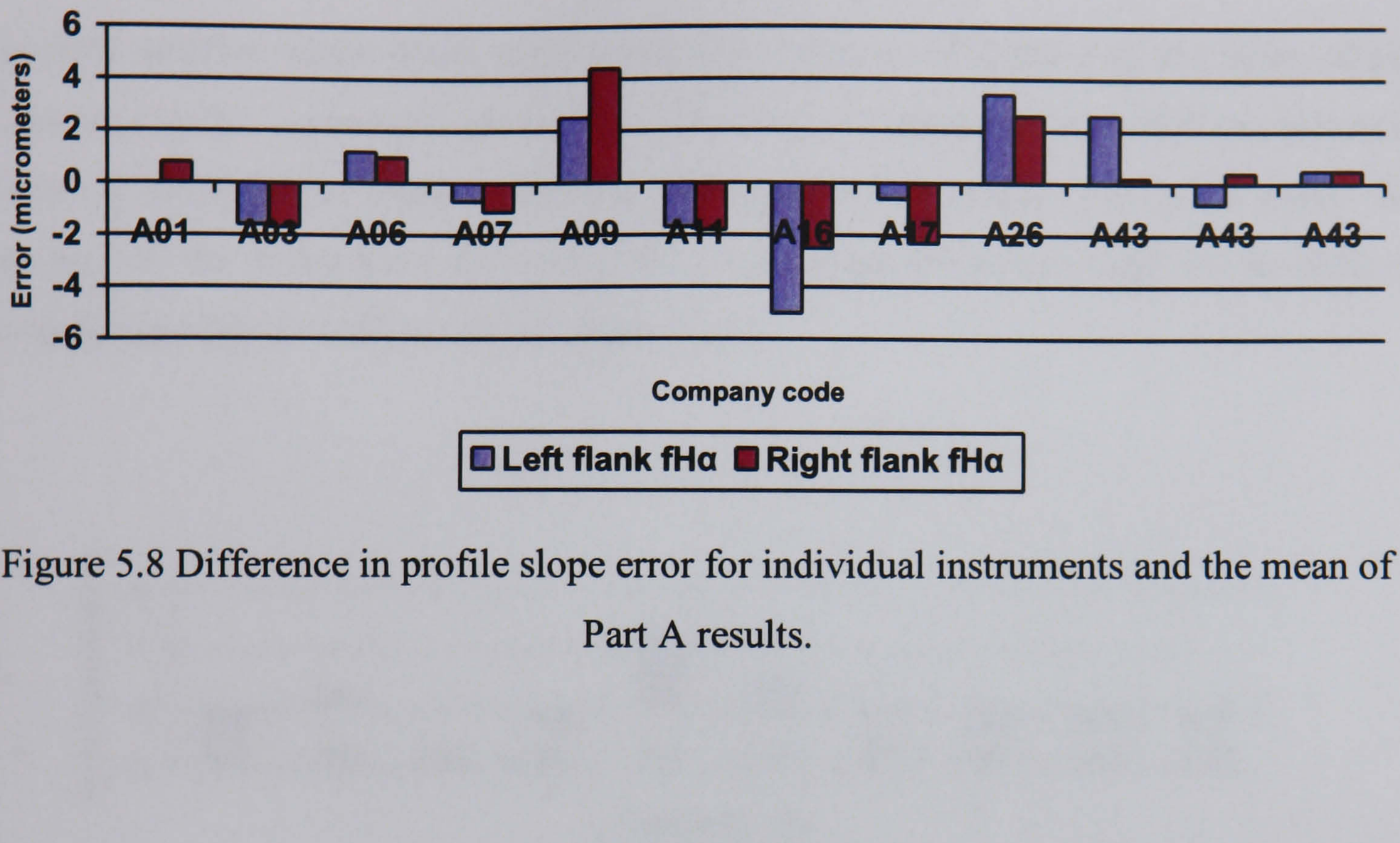

Figure 5.8 Difference in profile slope error for individual instruments and the mean of Part A results.

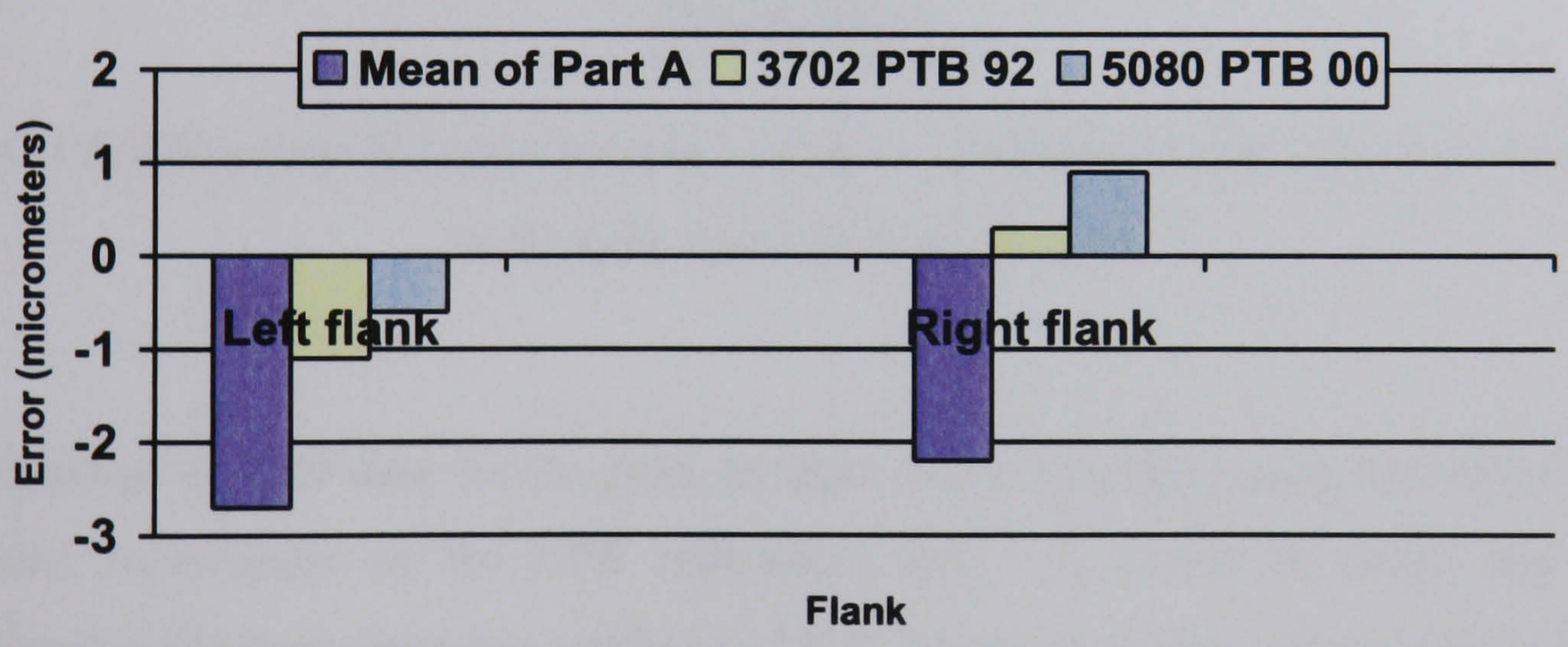

Figure 5.9 Difference between the mean of Part A instruments and PTB calibration data for the 200mm profile artefact.

The negative bias could also be due to the influence of a temperature error in the same way as it affects lead measurement. The procedure followed was to first use pitch and profile artefacts during the visit primarily because they were the smallest and therefore more likely to be thermally stable. The 200mm profile artefact has a 38mm length of roll, which from yields a -0.5µm slope error for every -1 °C the artefact is below the instrument temperature (see Chapter 3). Differences of 1.7µm are thus possible for this

artefact. Regretfully only one profile artefact was available for these tests so no reliable reasons can be given for this bias in results.

Pitch capability

The pitch artefact results show good correlation between PTB data and the mean of part A instruments for cumulative pitch error. The bias of 0.4μm between PTB and the mean of Part A instruments is well within the measurement uncertainty U_{95} of ±1.2μm. The majority of the companies surveyed who could measure pitch could do so with an acceptable accuracy, as illustrated in figure 5.10.

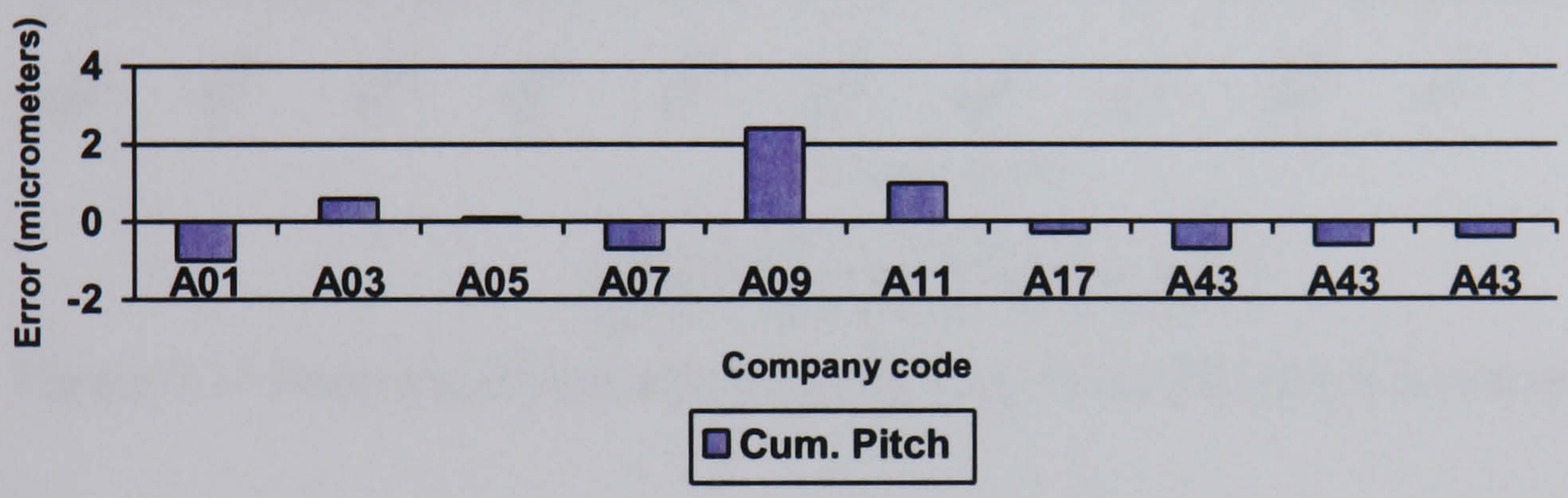

Figure 5.10 Differences between the mean of Part A instruments and individual results for maximum cumulative pitch (Fp)

A comparison of PTB data for the pitch artefact shows that the results are stable within the stated uncertainty on the PTB calibration data. It should be noted that mean temperature differences between artefact and instrument have only second order effect on pitch measurement results.

5.7.3 Industrial capability

Lead capability

The results from the 100mm and 200mm diameter lead artefacts show that the mean of Part B instruments, where machine operators used their own practice, was 11.5μm/100mm face width for gears up to 30° helix angle. This is shown graphically in figure 5.11 and in Appendix A Tables A4 and A7.

The accuracy of the final inspection equipment must reflect the quality and accuracy with which gears can be manufactured in the UK so significant improvements were clearly identified. The results imply that without significant outlay in new equipment but following simple calibration routines and robust product measurement practice, significant improvements in measurement capability are achievable.

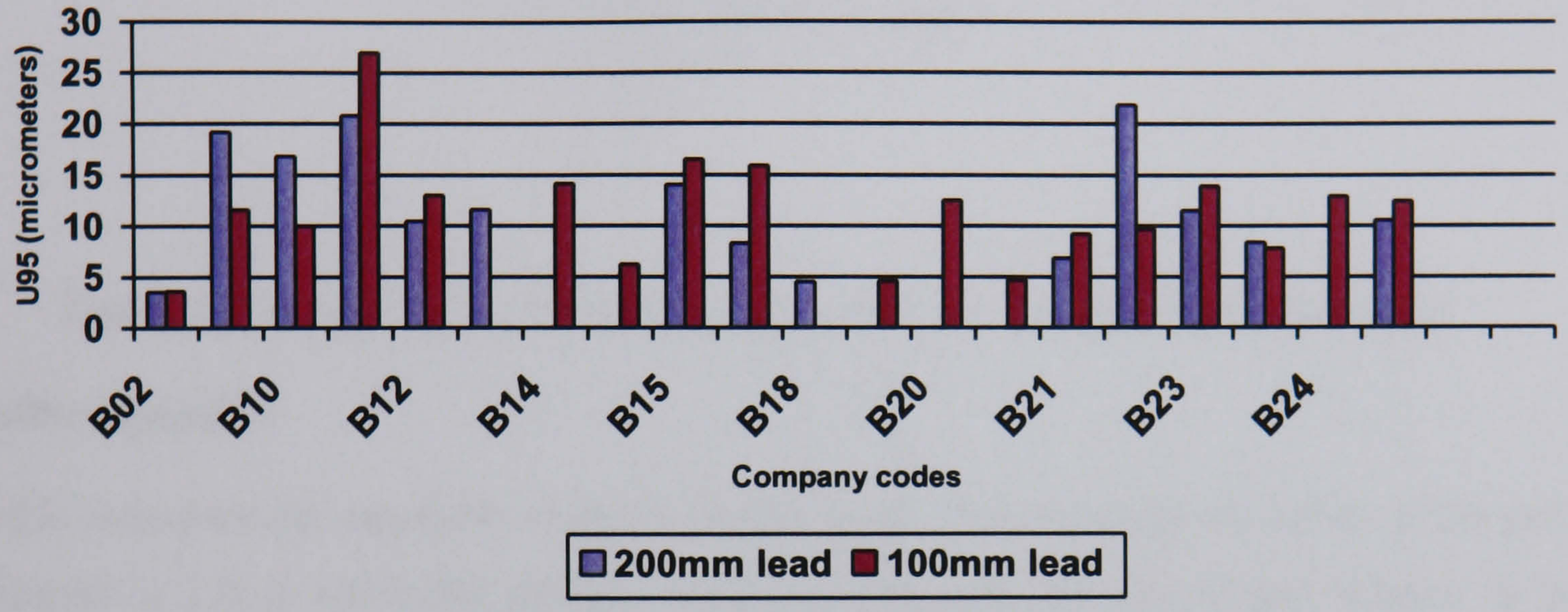

Figure 5.11 Estimate of lead measurement uncertainty for part B instruments

The main differences between the part A and part B results were attributed to:

- Poor measuring technique
- Insufficient or in some cases no-existent calibration routines
- Lack of routine servicing
- Poor environmental conditions
- A lack of traceable calibration on master gears

All these issues are easy to address. The effect of measuring instrument was not an issue although most of the instruments in Part A were relatively new. A comparison of two instruments of the same type is shown in figure 5.12 and shows a significant difference between achievable performance and actual performance. The factor of two difference is clearly evident between the two instruments.

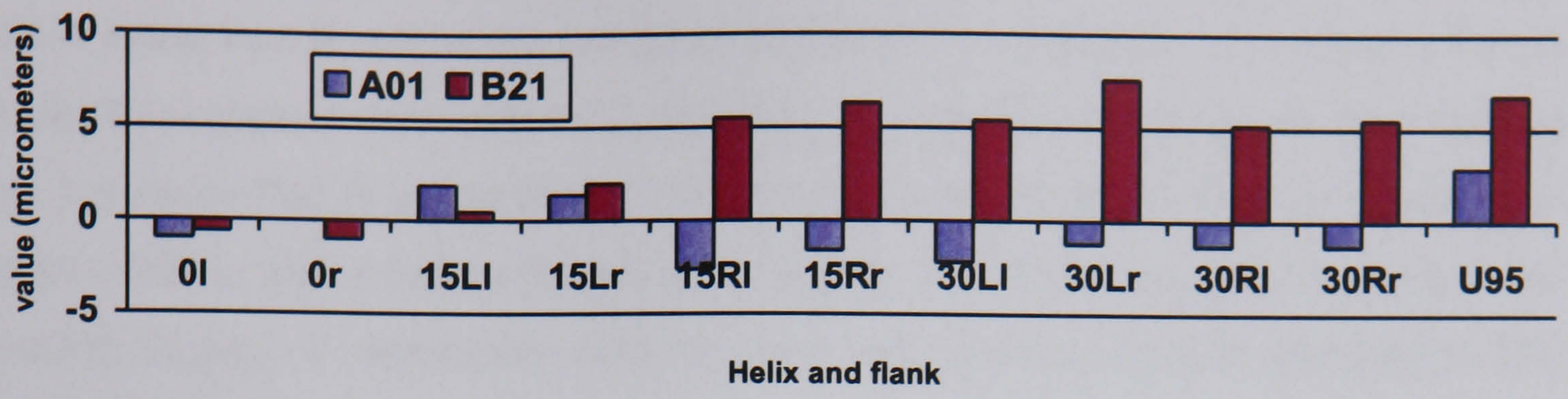

Figure 5.12 Comparison of lead measurement from two identical instruments.

Profile capability

Profile measurement capability shows a similar trend. The standard deviation of the part A results is 2.2μm while the standard deviation of results for part B was 4.4μm. It is interesting to note that the difference between the mean results of Part A and Part B companies was no greater than 0.3μm, inferring that the stability or temperature issue applies equally to part A and part B.

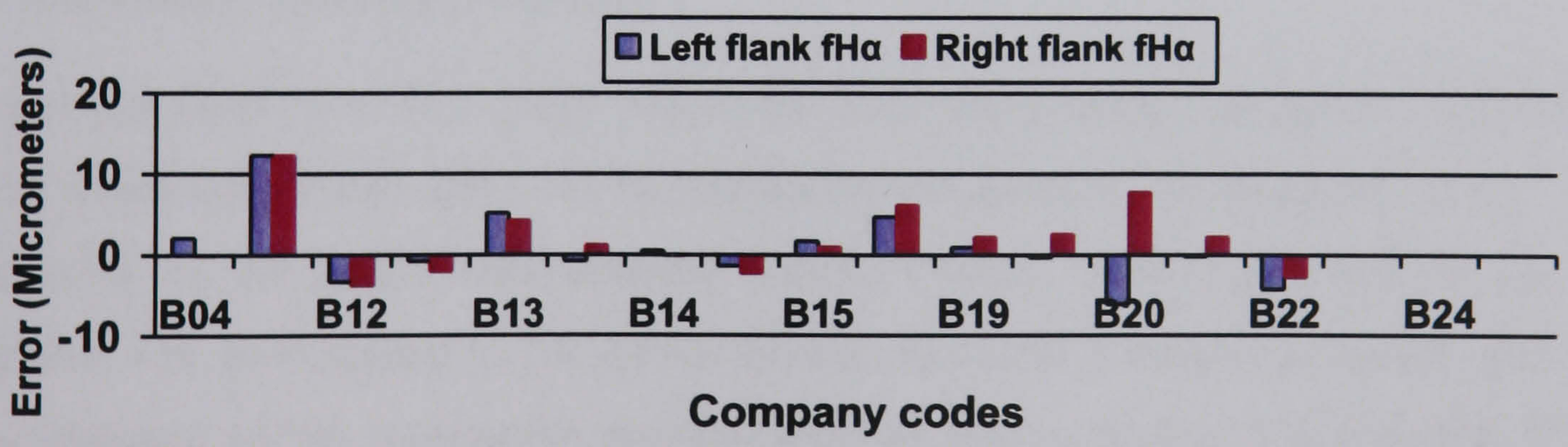

Figure 5.13 Comparison of Part B profile results with the mean of Part A results.

Pitch capability

Results for pitch measurement, see figure 5.15, were similar to the profile measurement, however fewer Part B companies had pitch measurement capability. The mean of Part A and Part B companies were within 0.1μm but with a standard deviation of 1.0μm for Part A and 2.6μm for Part B instruments. The fact that fewer companies had the capability to measure pitch is also of interest because it implies that some companies cannot a full inspection of gears in accordance with accuracy standard requirements specified in ISO 1328, Part 1 and Part 2.

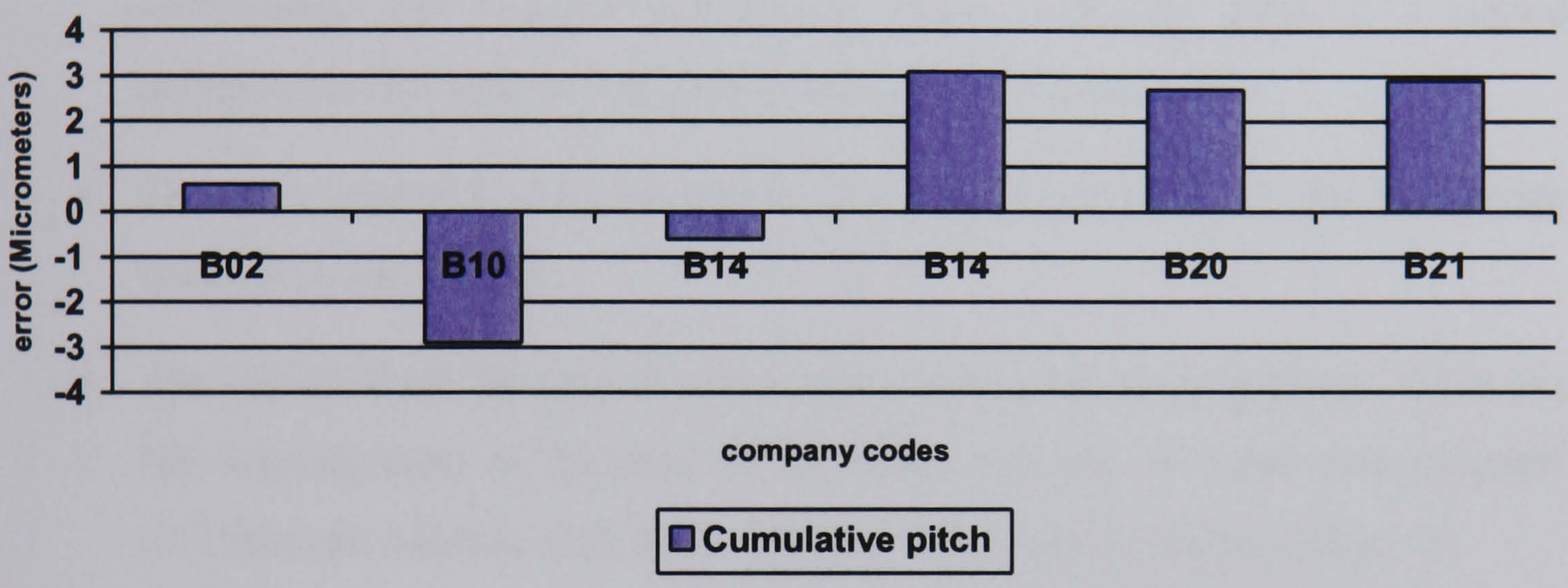

Figure 5.15 Difference between Part B results and mean of Part A.

5.7.4 Uncertainty estimation method

A visual examination of the results shows that the measurement uncertainty estimation process yields results that appear to be reasonable compared to the measured errors. An examination of the confidential detailed reports [Frazer, 1989] submitted to the 28 companies who participated in the survey reveals that only 5 results lie outside the U_{95} limits estimated by the comparator process, adopted from a total of 1960 readings (The results presented in the tables for part A are the mean of a number of measurements). This is much smaller number than would be predicted if the U_{95} are valid which would expect to produce 98 results outside these confidence limits. It is reasonable to conclude that simple comparator method of estimating measurement uncertainty is valid, although pessimistic, based on the results obtained. The method of applying a proportion of the bias as representative of the range of probable biases from a process appears to be reasonable although it is not possible to justify this statistically.

5.8 Summary

- The results from Part A of the survey showed that the mean measurement uncertainty U_{95} for Helix or Lead measurement was ±4.6µm per 100mm face width, for helix angles up to and including 30°. Referring to the VDI guideline this suggested that even instruments in good condition are only suitable for ISO 1328 grade 8 gears. This uncertainty value surprised gear manufacturers who assumed they were better than this, however the results were subsequently confirmed by the experience of the USA survey [Smith].
- There was no quantifiable difference in performance between modern CNC instruments and manual instruments tested although there is a significant difference in the ease of use and reliability of the instruments.
- The most important criterion was the instrument condition and the environment in which it as maintained.
- The results from the part B tests show clearly that the capability of the average UK manufacturer at the time of the study for lead or helix measurement was ±11.5µm per 100mm face width for helix angles up to and including 30°.
- The difference between best capability and average capability is a factor of two. The difference in capability was due to
    - Poor measuring technique
    - Insufficient or non-existent calibration routines
    - A lack of routine servicing
    - Poor environmental conditions
    - Lack of traceability for master gears and artefacts
- The problems associated with poor results can easily be overcome with relatively little investment.
- The comparator method of estimating measurement uncertainty appears to be satisfactory but pessimistic when verified by examining individual measurement reports submitted to the participating companies.

The following recommendations should be adopted:

- Guidance documents in the form of a code of practice should be prepared in order to provide sound practical advice on gear measurement procedures and calibration methods [Frazer, 1993 and 1994, BGA].

- Regular training courses and seminars should be introduced to provide continuous training for inspectors and those who supervise them to ensure sound decisions are made when manufacturing gears.

Chapter 6

AN INTERNATIONAL COMPARISON OF INVOLUTE PROFILE, HELIX AND PITCH MEASUREMENT

This chapter presents the results from an international comparison of gear measurement capability with the 200mm and 100mm gear artefact set from the NGML. These are the first international comparison for helix and profile measurement published by NMIs to date. It also reports the comparison results from a pitch measurement project arranged by the USA. Results show good compatibility between NMIs within their claimed measurement uncertainty.

6.1 Introduction

The previous chapter looked in detail at the capability of UK gear manufacturers, comparing the results to the weighted mean and to data obtained from the National Measurement Institutes (NMIs) of PTB, Germany and NGML in the UK. This chapter focuses on the validity of the data supplied by the NMIs themselves.

The compatibility of gear measurement between trading nations is important if costly disputes due to differences in results are to be avoided. The gear industry operates in a global market and measuring and manufacturing machines from the major suppliers are traded globally, so any differences should be small. However, calibration data used to calibrate and often compensate industrial metrology equipment results is supplied by NMIs. Thus NMI compatibility is of paramount importance for ensuring free and open trade. The potential measurement differences are of course more critical for high accuracy gears, master gears and involute spline gauges, where tolerances of 2 to 5μm are common. This is a market in which the UK is very competitive and has many world leading manufacturers.

The above issues prompted NGML to arrange the first international comparison [Bicker,2003] of gear measurement capability that involved a comparison with both the

- 200mm diameter profile and helix artefacts and
- 100mm diameter profile and helix artefacts

A further comparison of adjacent pitch, cumulative pitch and radial runout with a master gear was arranged by AGMA (American Gear Manufacturers Association) in the USA which was a natural development from a USA gear manufacturers study of measurement capability.

International comparisons are not new. They form the basis of an agreement for the mutual recognition of national standards and of calibration certificates issued by NMIs agreed by CIPM (Comité International des Poids et Mesures). These are named 'key comparisons' and are initiated by Consultative Committees to CIPM to test principal measurement methods for realising measurands in a particular field. The key comparison determines the deviation of an individual measurement result from a KCRV (Key Comparison Reference Value) and the uncertainty of this deviation.

The work reported in this chapter was not regulated or arranged by CIPM, however there is no reason that it can not be adopted as such in the future. Each of the comparisons is described in the following sections and several issues that arose as a result of the work are discussed.

6.2 200mm diameter profile and helix comparison

The assessment of measurement uncertainty of the shop floor inspection process requires the use of calibrated gears and gear like artefacts. Thus the capability of NMI's for calibrating gears and artefacts with low measurement uncertainty underpins any improvements in manufacturing capability. For example, most NMI's measure the helix on gears with an uncertainty of 1 to 2μm, depending on the helix and diameter. This is unacceptably high for verifying shop floor instruments used for measuring parameters with tolerances of 5 to 10μm. Any reduction in uncertainty will improve the confidence of measurements from gear manufacturers thus making them more competitive.

Some work from this section has been published in [Frazer, 1999 and 2003] and summarises the results from the first international comparison of helix and profile

measurement capability for NMIs. The objective of the work was to establish the compatibility of gear measurement with the final goal of reducing measurement uncertainty.

The comparison used two gear artefacts, namely a 200mm diameter helix artefact, with helix angles of 0° and 15°, 30°, 45° left and right hand, and a 200 mm diameter profile artefact with two calibrated flanks. They were selected for the comparison because they are similar to industrial artefacts calibrated by the NMI's and thus may be measured with their standard measurement procedures.

The gear measurands are recognised to be of great importance and were in the CMC lists of EUROMET (European Collaboration in Measurement Standards) and COOMET (Euro-Asian Cooperation of National Metrology Institutes) since its inception. The comparison serves as a mutual acceptance for the measurands between the involved nations and will thus promote trade. The measurements confirm the qualifications of the countries involved. and it is therefore recommended that the results become accepted as a key comparison. The four participating Institutions, equipment used and environmental conditions are in Table 6.1.

Table 6.1 Participating Organisations, Equipment and Environment

Country	Institution	Equipment	Environment
Germany	Physikalisch-Technische Bundesanstalt (PTB)	Zeiss UPMC 850 CMM	± 0.2°C
USA	National Institute of Standards and Technology (NIST)	Leitz PMM CMM	± 0.1°C
USA	BWXT Y-12, L.L.C	Leitz PMM CMM	± 0.1°C
UK	National Gear Metrology Laboratory (NGML)	Hofler EMZ 632 CNC gear measuring machine	± 1.0°C

Figure 6.1 shows the helix gear artefact and Table 6.2 contains the basic gear geometry and evaluation range. Each of the 14 calibrated flanks was evaluated in accordance with the parameters specified in ISO 1328-1. The helix parameters are: total error (F_{β}), slope

error ($f_{H\beta}$), which is evaluated by the method of least squares and form error ($f_{f\beta}$) as defined in Chapter 1. The artefact helix errors represent typical errors measured on gear measuring instruments and lie within the range 0.5 to 20μm. This differs from many artefacts that have small flank deviations. Smaller deviations are generally easier to measure and evaluate, but these are more representative of real gears made in industry.

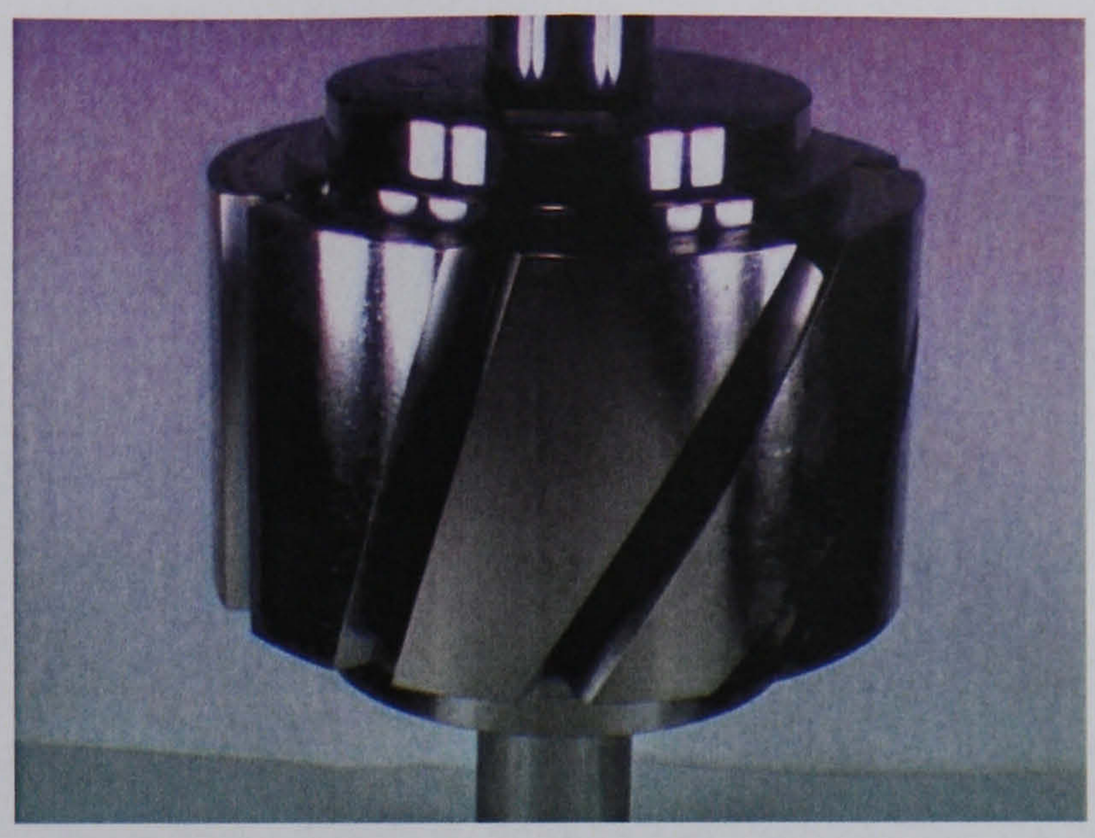

Figure 6.1 The 200mm diameter Helix artefact from NGML

Table 6.2 200mm helix artefact basic gear geometry and evaluation range

Parameter	Helix angle (β)			
	0°	15° LH & RH	30° LH & RH	45° LH & RH
Teeth (z)	25	25	25	25
Normal module (m_n)	8.000 mm	7.72741 mm	6.92820 mm	5.65685 mm
Normal pressure angle (α_n)	20°0'0"	19°22'12"	17°29'43"	14°25'58"
Diameter (d)	200.0 mm	200.0 mm	200.0 mm	200.0 mm
Evaluation length (L_β)	100.0 mm	100.0 mm	100.0 mm	100.0 mm
Face width (b)	127.0 mm	127.0 mm	127.0 mm	127.0 mm

Figure 6.2 shows the profile artefact and Table 6.3 contains the basic gear geometry and evaluation ranges. The two measured flanks were evaluated in accordance with the parameters specified in ISO1328-1. The profile parameters are total error (F_α), slope error ($f_{H\alpha}$) which is evaluated by the method of least squares and form error ($f_{f\alpha}$). The artefact profile errors lie within the range 0.5 to 3.0μm, similar to those of high accuracy power transmission gears, but are not as challenging as the helix artefact deviations.

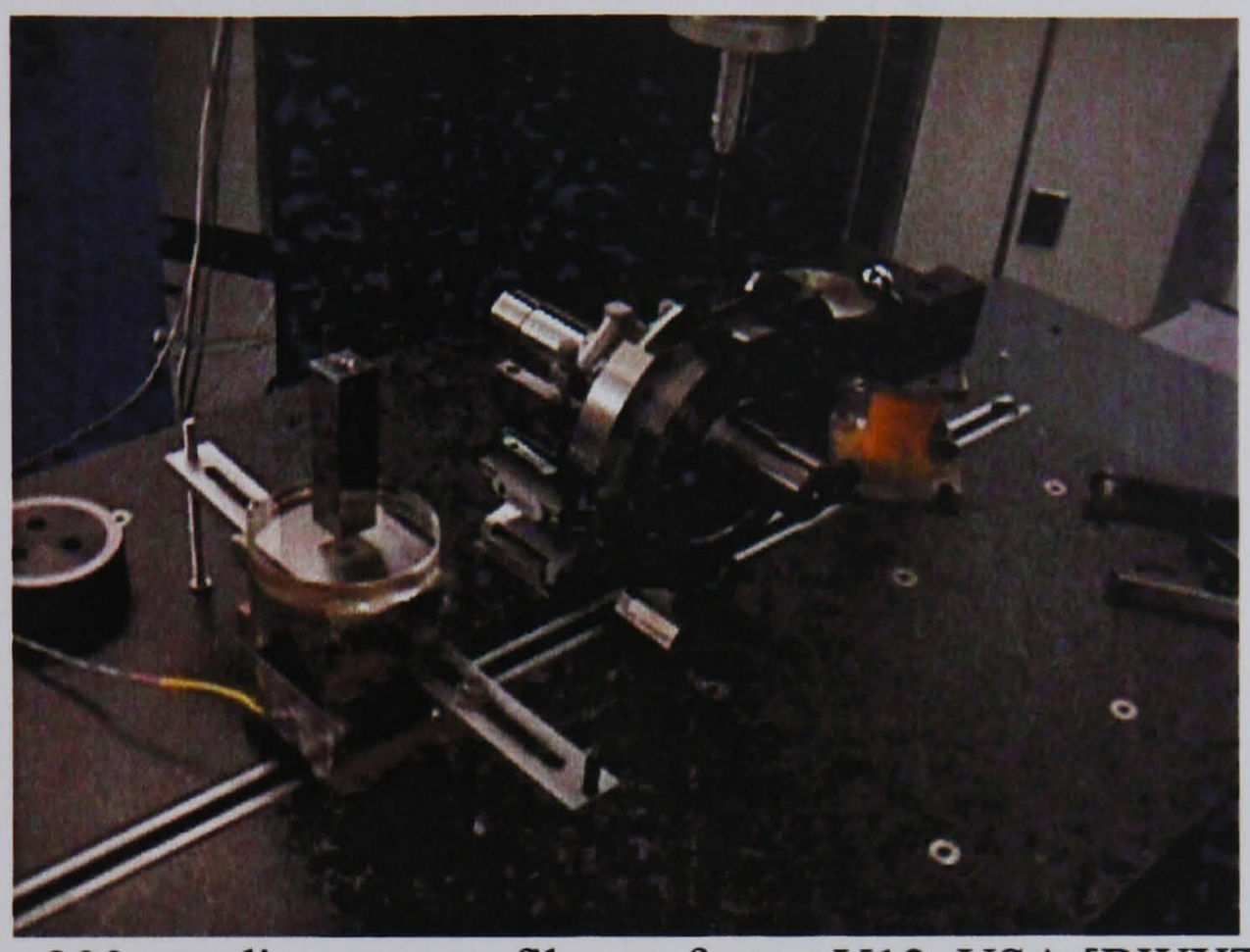

Figure 6.2 The 200mm diameter profile artefact at Y12, USA [BWXT Y-12 L.L.C]

Table 6.3 200mm profile artefact basic gear geometry and evaluation range

Parameter	
Teeth (z)	25
Normal module (m_n)	8.000 mm
Normal pressure angle (α_n)	20°0'0"
Diameter (d)	200.000 mm
Helix angle (β)	0°
Evaluation length (L_α)	38.0 mm
Face width (b)	5.0 mm

Results

The results from the comparison are presented in Appendix B, Tables B.1 to B.6 and illustrated in graphical form in figures 6.3 to 6.8. They show the difference between the individual laboratory results and the unweighted mean of the 5 sets of results with error bands representing the measurement uncertainty (U_{95}) of the data from an individual laboratory. Only differences are presented so the artefacts may be used for future comparisons and because some flanks have significant deviations that reduce the resolution of the graphical representation of the results.

The results from PTB calibrations performed in 1992 and 2000 have equal weighting in this analysis. The two sets of PTB data were included to verify the stability of the artefacts over the comparison period.

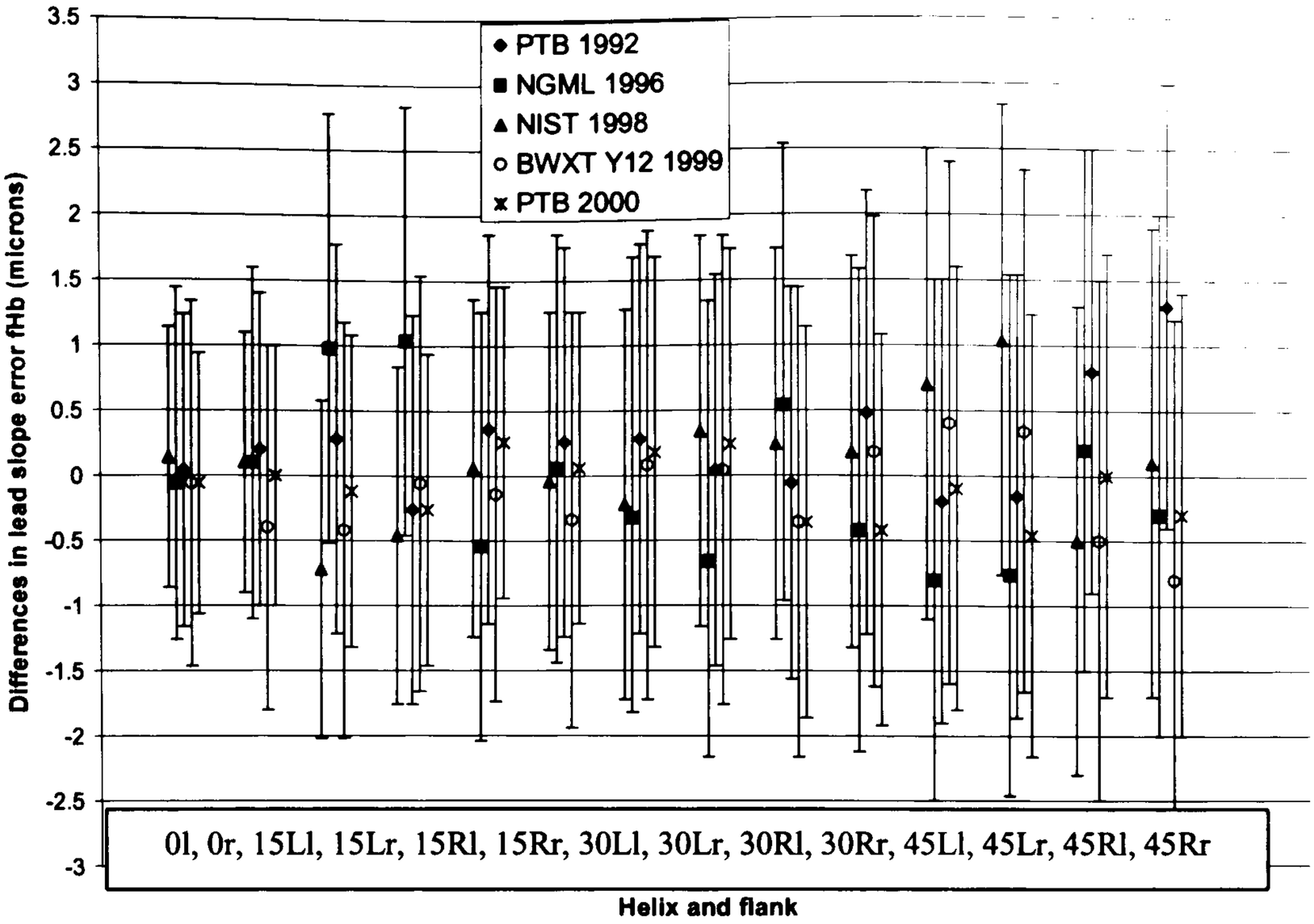

Figure 6.3 200mm Helix artefact. Differences between the individual laboratory results for helix slope error ($f_{H\beta}$) and the laboratory measurement uncertainty (U_{95}) μm.

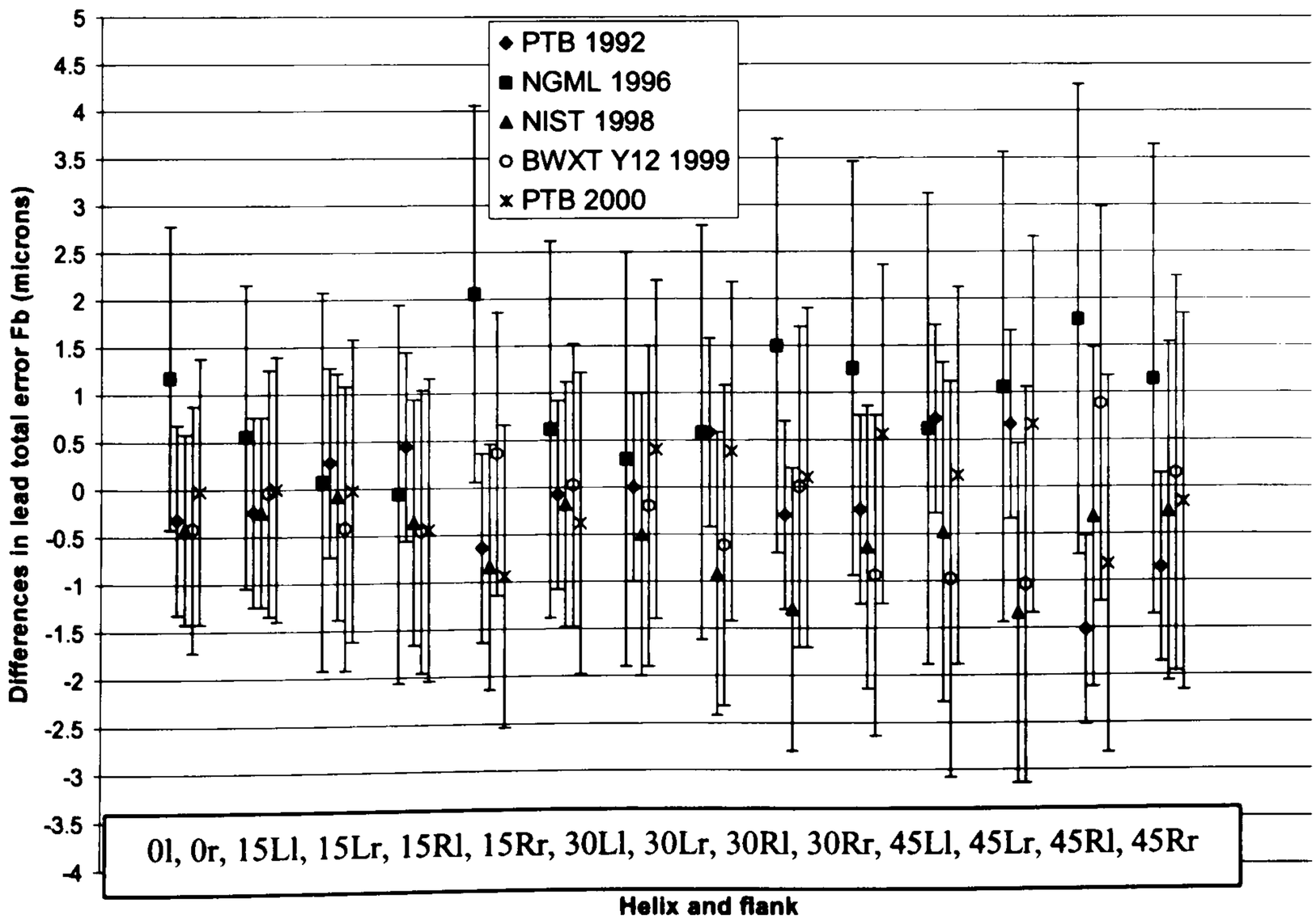

Figure 6.4 200mm Helix artefact. Differences between the individual laboratory results for helix total error (F_{β}) and the measurement uncertainty (U_{95}) [μm].

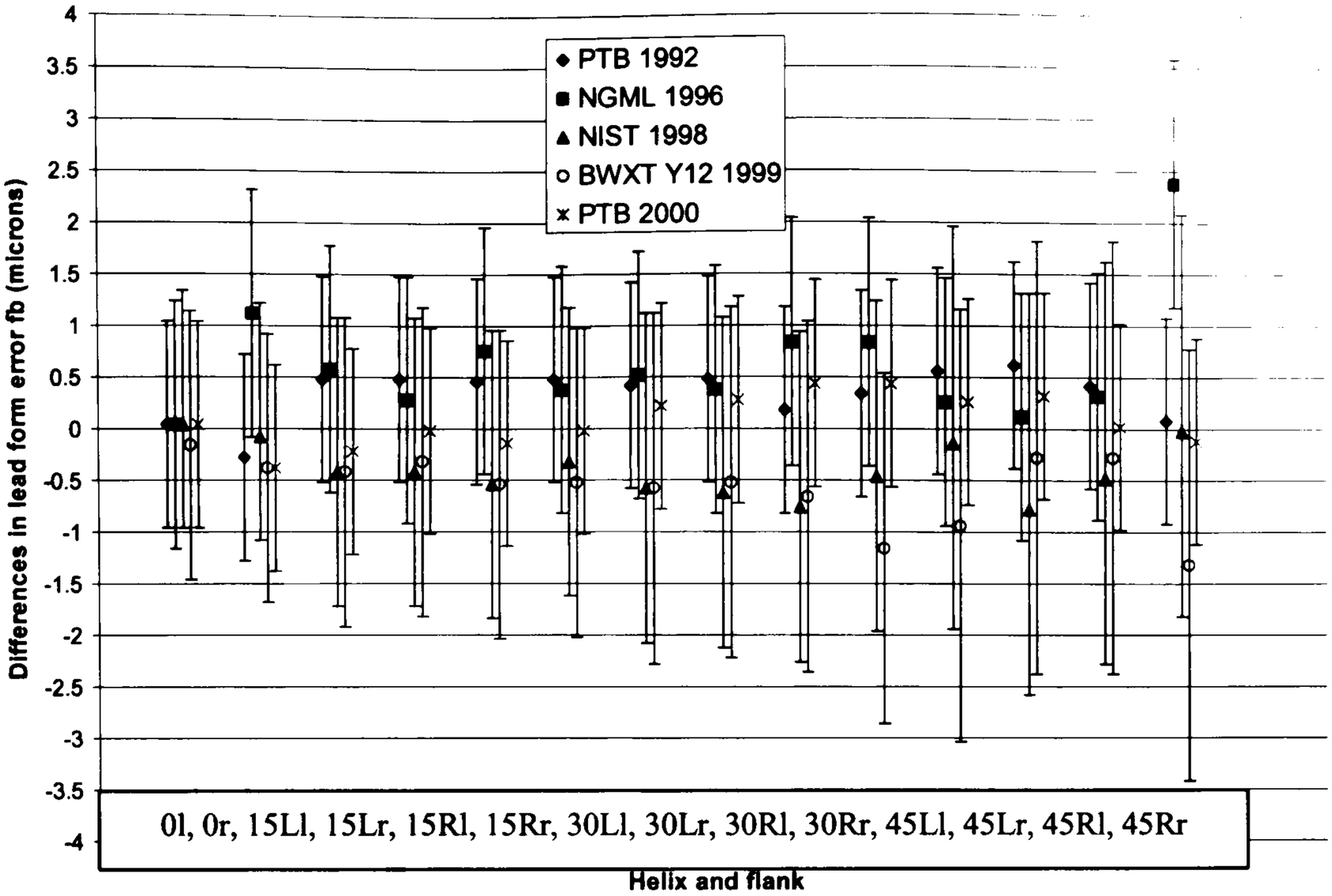

Figure 6.5 200mm Helix artefact. Differences between the individual laboratory results for helix form error ($f_{\beta f}$) and the measurement uncertainty (U_{95}) [μm].

Traceability Issues

PTB, NIST and BWXT Y-12 [Cox, 1998] are national laboratories that derive the evaluated gear parameters directly to length and angle standards. The NGML obtain traceability from gear artefacts calibrated by PTB, under a EUROMET agreement. The resulting correlations of measurement uncertainties have been ignored from this comparison and the laboratory results have been assumed to be independent of PTB. This is valid because the data was not compensated for the bias between PTB and NGML.

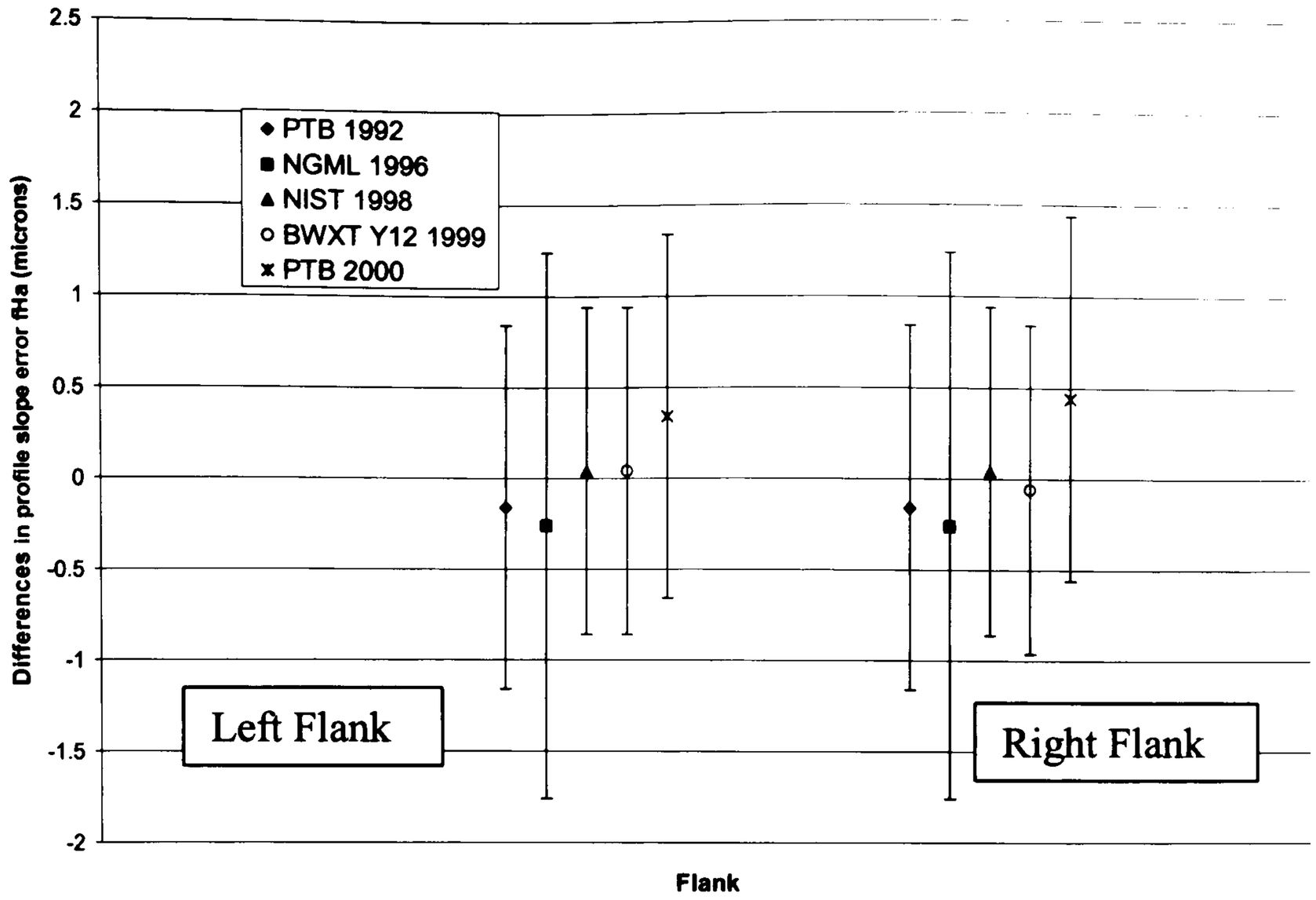

Figure 6.6 200mm profile artefact. Differences between the unweighted mean and laboratory results for profile slope error ($f_{H\alpha}$) with (U_{95}) error bands in μm.

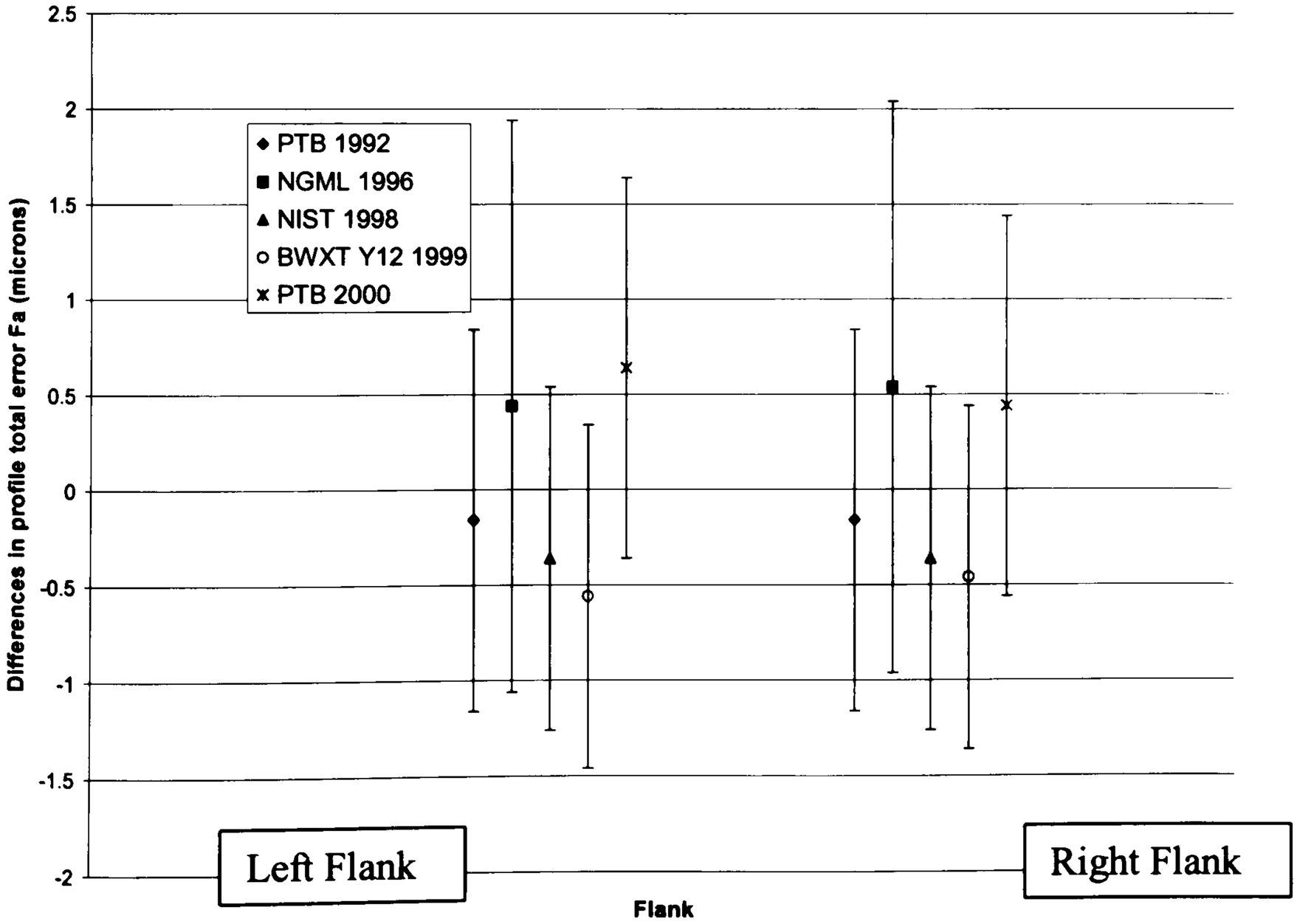

Figure 6.7 200mm profile artefact. Differences between the unweighted mean and laboratory results for profile total error (F_{α}) with (U_{95}), error bands in μm

.

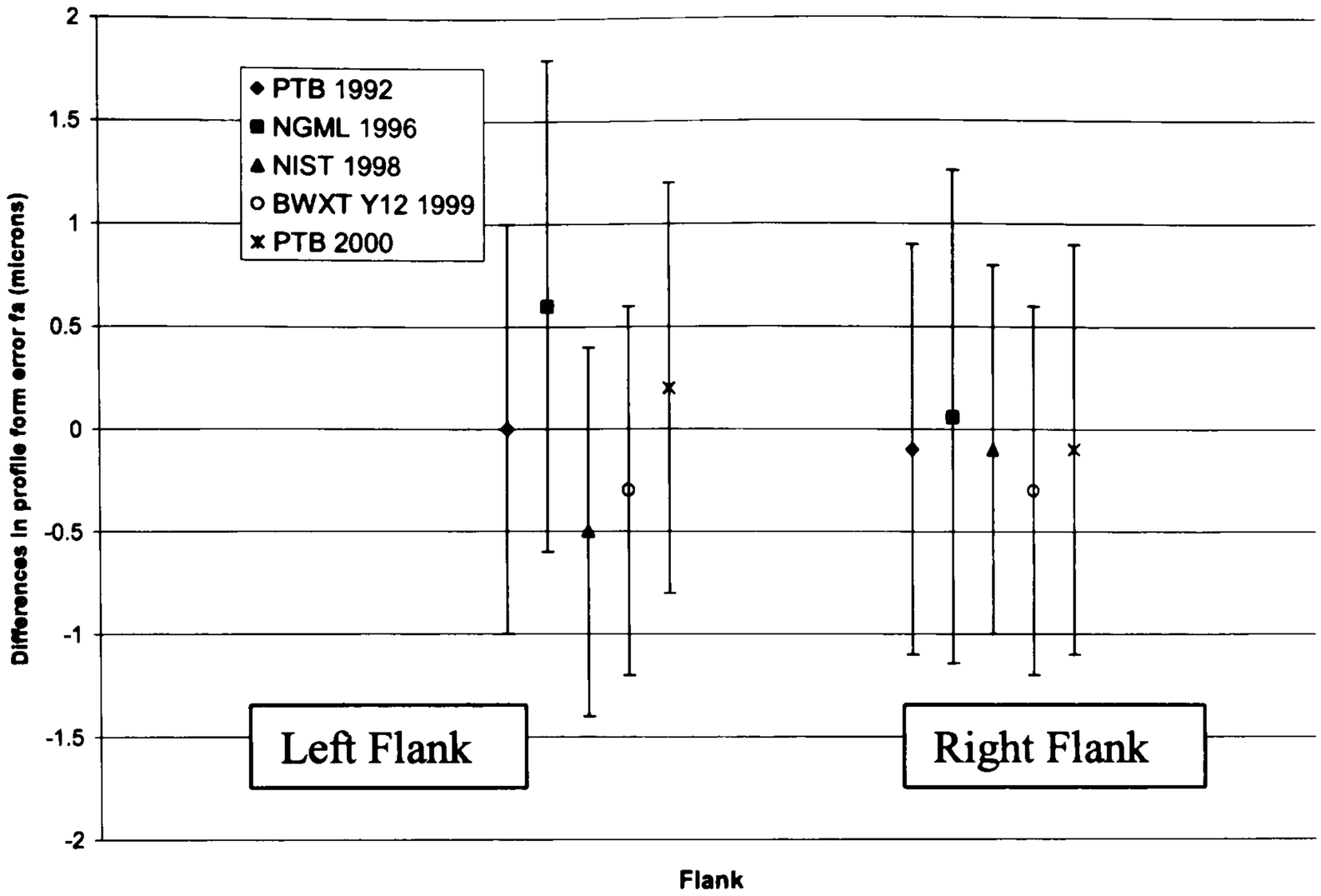

Figure 6.8 200mm profile artefact. Differences between the unweighted mean and laboratory results for profile form error ($f_{f\alpha}$) with (U_{95}) error bands in µm.

Discussion of results

Helix results

An examination of the 200mm diameter helix results illustrated in figures 6.3 to 6.5 shows that with the exception of one value of form error on the 45° right helix right flank, the difference between the unweighted mean and an individual laboratory result lies within the measurement uncertainty of an individual laboratory. This demonstrates the validity of the uncertainty estimates provided by the laboratory. The 0° helix results on the artefact shows particularly good correlation of results with differences within 0.4µm.

The 45° results represent the largest helix angle that is likely to be measured on a gear measuring machine for cylindrical gear applications. It provides the most difficult measurement challenge. Compatibility of the 45° helix results provide confidence with the measurement strategy and equipment used in the NMIs.

Profile results

An examination of the profile measurement results in figures 6.6 to 6.8 shows that the differences between the unweighted mean and an individual laboratory result lies within the measurement uncertainty of an individual laboratory. The range of values is 0.64μm.

6.3 100mm diameter profile and helix comparison

The 200mm diameter lead and profile comparison yielded excellent compatibility between the four calibration facilities involved with the survey. Differences between NGML and PTB have always been small when comparing measurement data to establish traceability to PTB under the EUROMET agreement with these 200mm diameter artefacts. However this was not the case with the 100mm diameter artefacts and thus was one reason for instigating the international comparisons to investigate these differences. The results of this comparison are presented in the following sections.

Artefacts and gear geometry

Figure 6.9 shows the helix gear artefact and Table 6.4 provides the basic gear geometry and evaluation ranges. Each of the ten calibrated flanks was evaluated in accordance with the parameters specified in ISO 1328-1. The helix parameters are: total error (F_{β}), slope error ($f_{H\beta}$) evaluated by the method of least squares and form error ($f_{f\beta}$). The artefact helix errors represent typical errors measured on gear measuring instruments and lie within the range 0.5 to 12μm.

Figure 6.9 100mm diameter 3.1 lead artefact at Y12 USA[BWXT Y-12, L.L.C]

Table 6.4 100mm diameter lead/helix artefact basic gear geometry and evaluation range

Parameter	Helix angle (β)		
	0°	15° LH & RH	30° LH & RH
Teeth (z)	20	20	20
Normal module (m_n)	5.00000 mm	4.82963 mm	4.33013 mm
Normal pressure angle (α_n)	20°0'0"	19°22'12"	17°29'43"
Diameter (d)	100.0 mm	100.0 mm	100.0 mm
Evaluation length (L_β)	100.0 mm	100.0 mm	100.0 mm
Face width (b)	125.0 mm	125.0 mm	125.0 mm

Figure 6.10 shows the profile artefact and Table 6.5 contains the basic gear geometry and evaluation ranges. Both measured flanks were evaluated in accordance with the parameters specified in ISO1328-1. The profile parameters are total error (F_α), slope error ($f_{H\alpha}$) evaluated by the method of least squares and form error ($f_{f\alpha}$). The artefact profile errors lie within the range 1.5 to 3.0μm but unlike the 200mm profile artefact the form error is large and has a significant concave form on one flank.

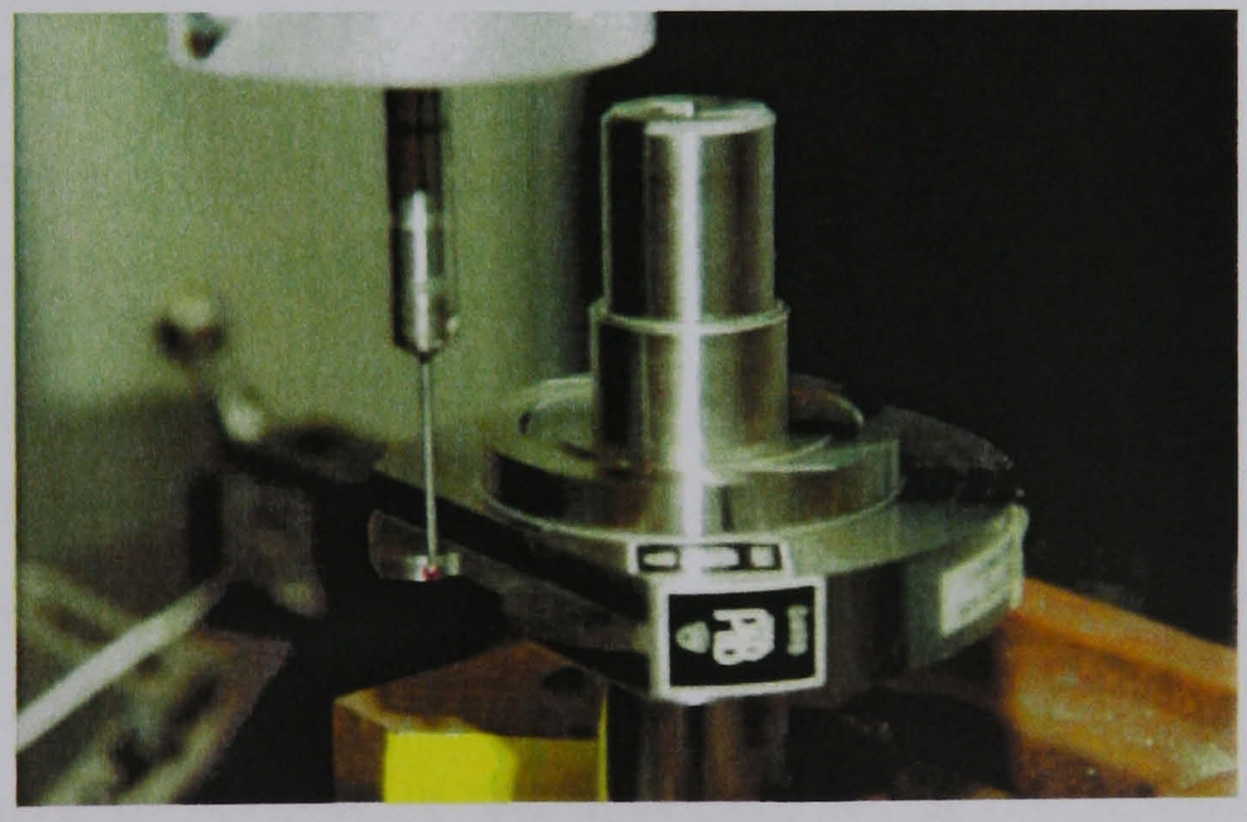

Figure 6.10 100mm diameter 3.1mm profile artefact at Y12, USA [BWXT Y-12, L.L.C]

Table 6.5 100mm diameter profile artefact basic gear geometry and evaluation range

Parameter	
Teeth (z)	20
Normal module (m_n)	5.000 mm
Normal pressure angle (α_n)	20°0'0"
Diameter (d)	100.000 mm
Helix angle (β)	0°
Evaluation length (L_α)	26.0 mm
Face width (b)	5.0 mm

Discussion of results

Helix results

The helix results are presented in Appendix B Tables B7 to B9 and shown graphically in figures 6.11 to 6.13. They show good correlation for all helices with maximum differences in slope error of 0.8μm for spur and 15° helix angles. This is well within the measurement uncertainty for the individual laboratories (shown as error bands on each result). Similarly, good correlation was achieved for the total helix (F_β) and helix form error ($f_{f\beta}$) parameters. (However it should be noted that these parameters are maximum parameters and do not include information on the position where the error occurs, and as such they are not robust indicators of measurement performance).

The 30° helix angles revealed an interesting result. Examination of the comparison of PTB data for 1998 and 2005 shows significant changes in the data. This suggests the artefact is not stable because the results for the 200mm artefact were stable over a similar time interval. It can be concluded that instrument or traceability issues are unlikely to be an issue. The most likely cause of this difference is that the artefacts were sent to the USA by air freight and the artefact was subject to sub-zero temperatures and tool steel used to manufacture the artefacts is susceptible to dimensional instability. An examination of the results in Table 5.14 for the 30° helix show very good compatibility between PTB, Y12 and NGML if the first set of PTB results are excluded from the comparison. It can be concluded that although these artefacts are over 20 years old they may not be stable so, accordingly, calibration intervals should be reduced from 5 years to 3 years in the first instance, with subsequent reviews to ensure that calibration data is reliable.

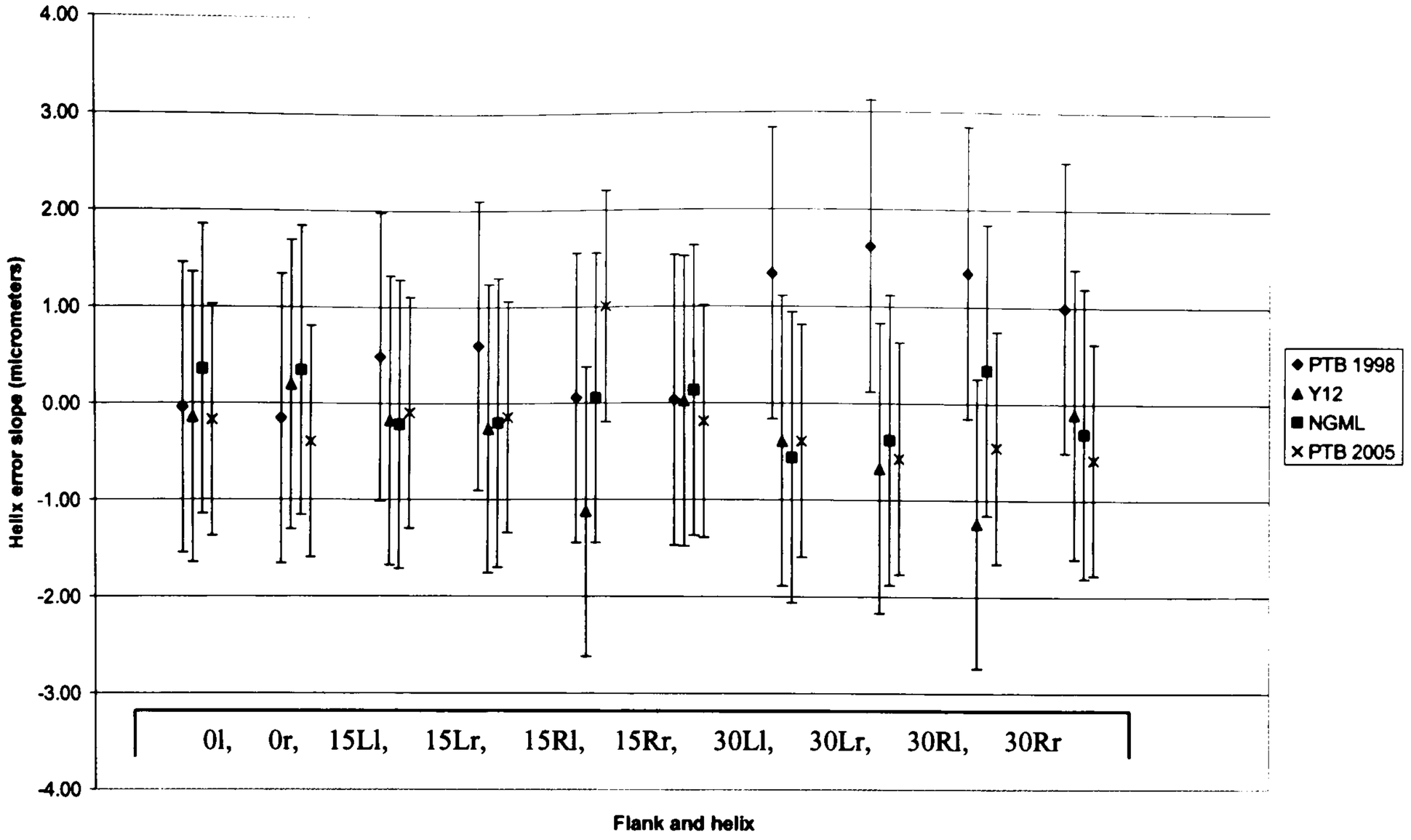

Figure 6.11 100mm helix artefact. Differences between the unweighted mean and individual laboratory results for helix slope error ($f_{H\beta}$) and the individual laboratory measurement uncertainty (U_{95}) shown as an error band in μm

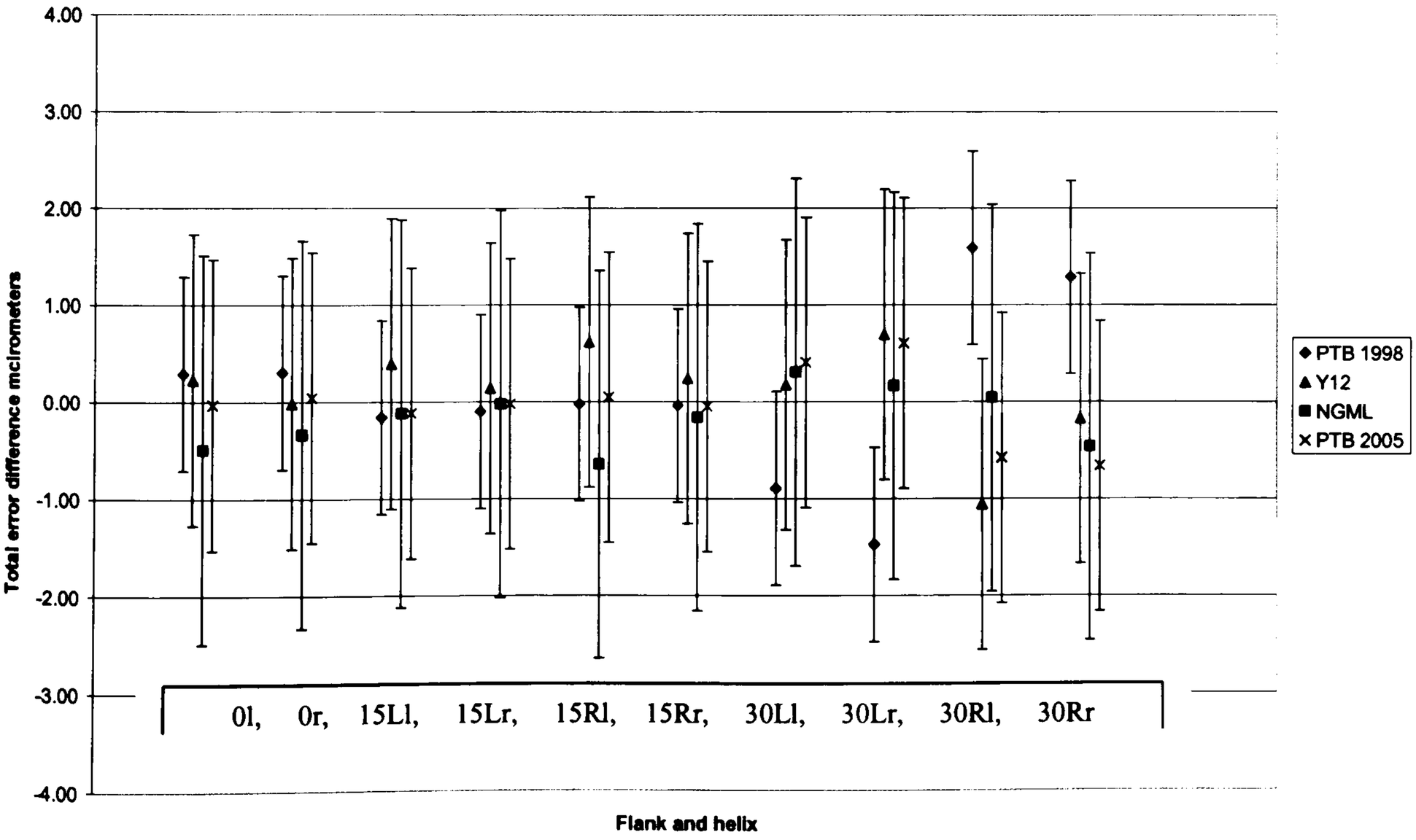

Figure 6.12 100mm helix artefact Differences between the unweighted mean and individual laboratory results for helix total error (F_{β}) and the individual laboratory measurement uncertainty (U_{95}) shown as an error band in μm.

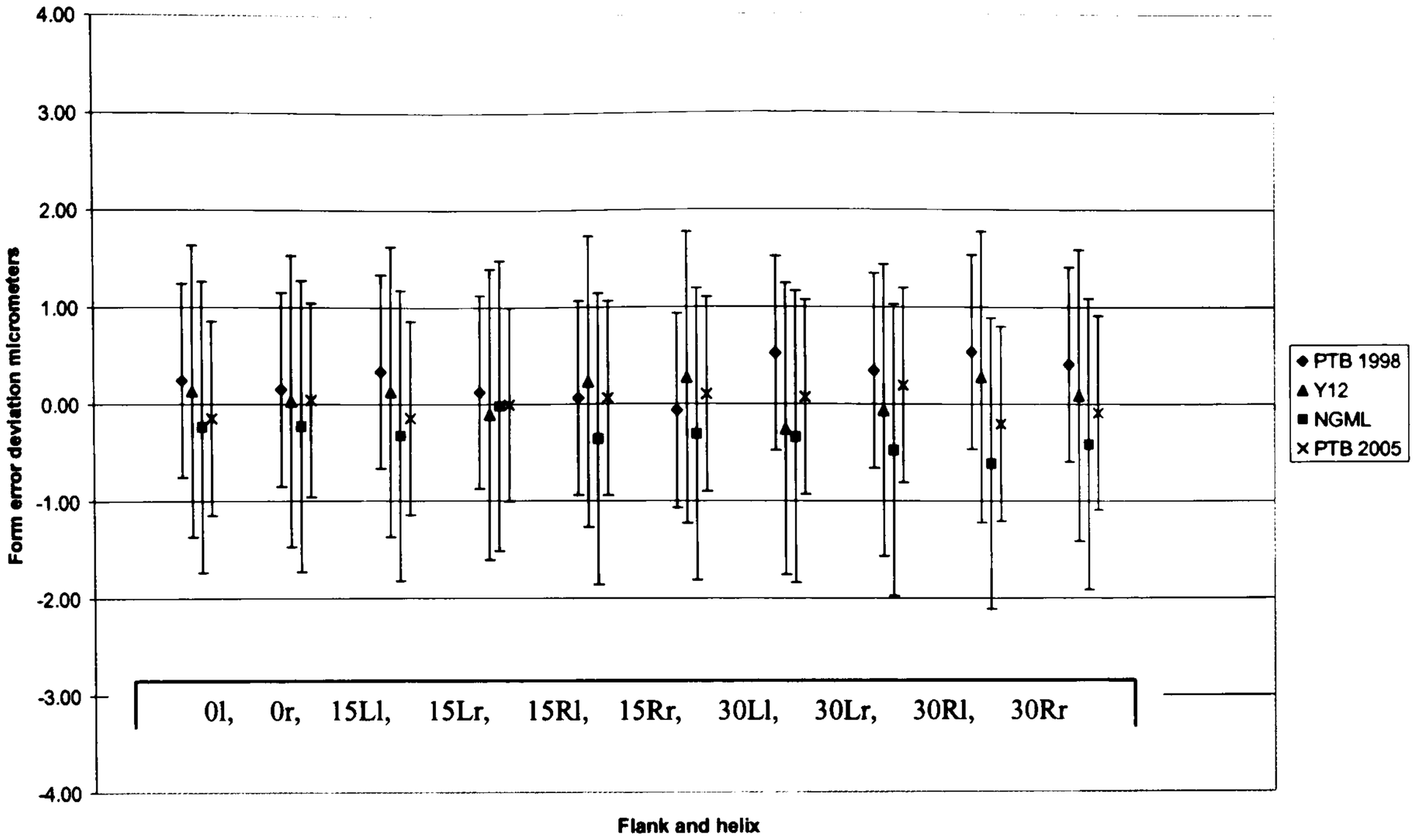

Figure 6.13 100mm helix artefact. Differences between the unweighted mean and individual laboratory results for helix form error ($f_{\beta f}$) and the individual laboratory measurement uncertainty (U_{95}) shown as an error band in μm.

Profile results

The results from the profile comparison are presented in Appendix B Tables B.10 to B.12 and illustrated graphically in figures 6.14 to 6.16. They show the results are compatible within the estimated measurement uncertainty for the individual laboratories. Examination of the results shows that the differences between results for form and total error parameters are within 0.6μm while the slope error parameters show a greater difference of 1.2μm on the right flank. This confirms that form and total error parameters are independent of the position that the maximum error occurs, which is consistent with other form parameters such as roundness. However after further consideration it was concluded that the shape of the right flank involute deviation may be sensitive to the different measurement methods employed by the laboratories. This issue is investigated in the following section.

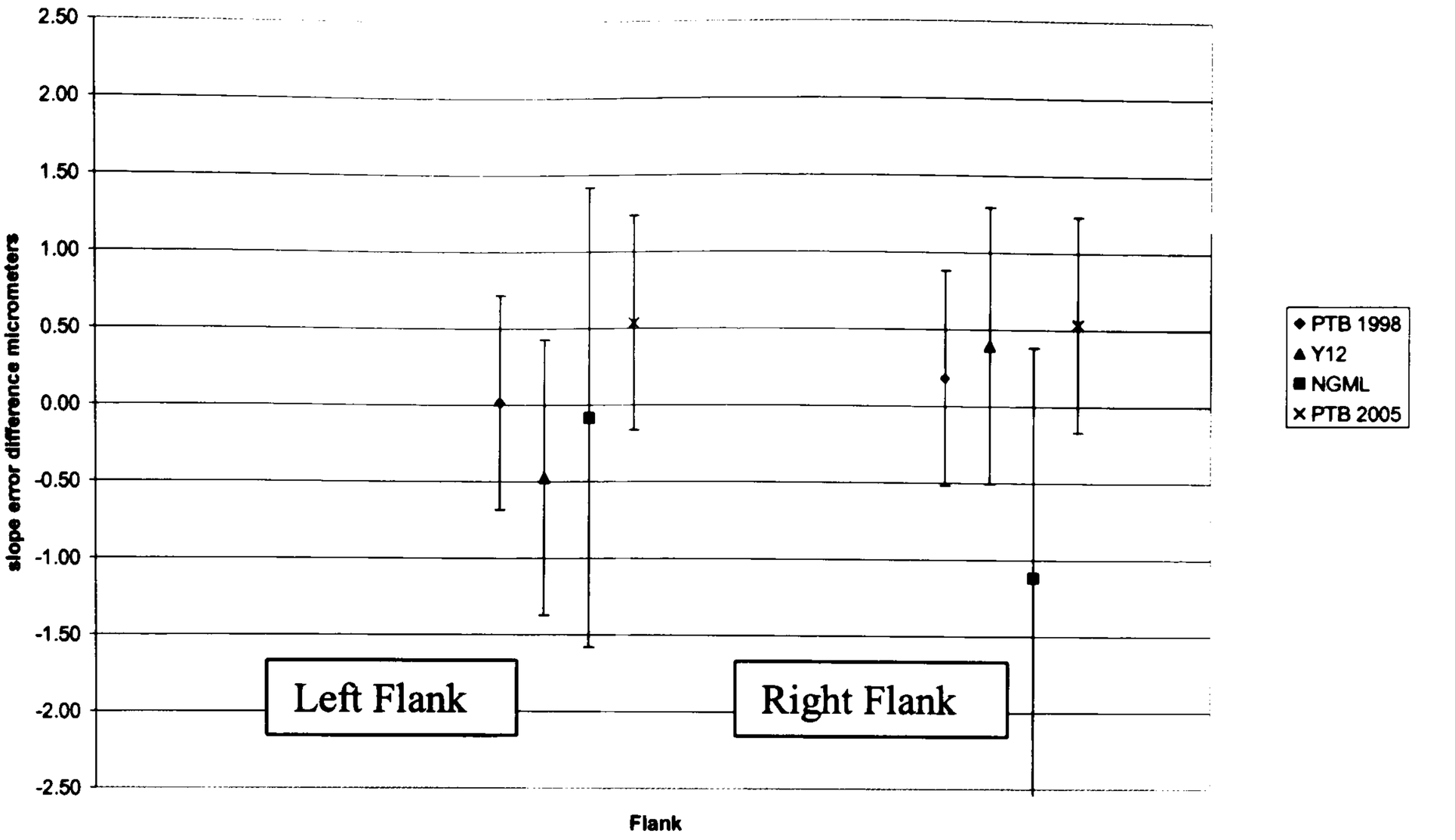

Figure 6.14 100mm profile master deviations between the unweighted mean profile error slope ($f_{H\alpha}$) and the individual laboratory result in [μm].

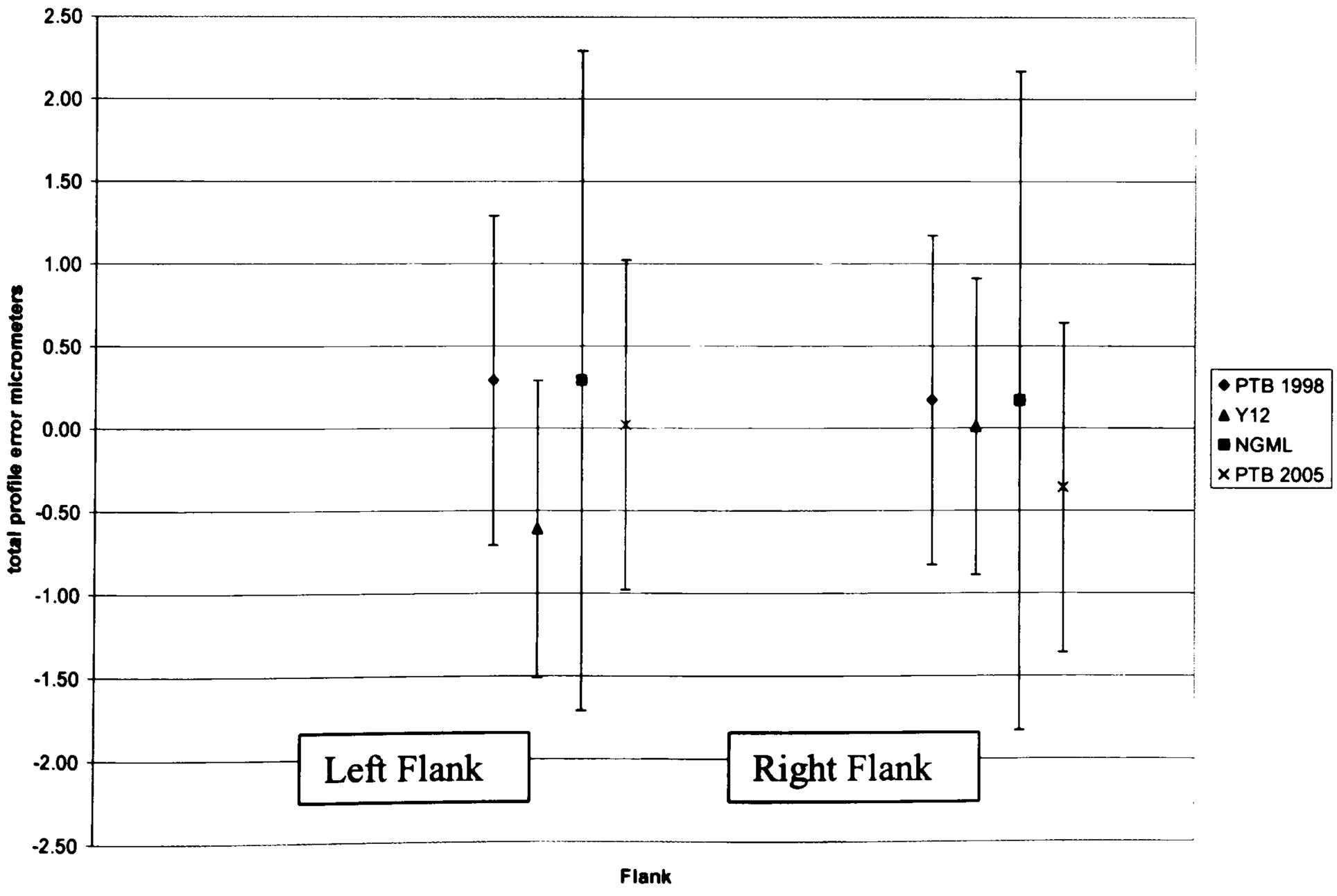

Figure 6.15 100mm profile master deviations between the unweighted Total profile error slope (F_{α}) and the individual laboratory result in [μm].

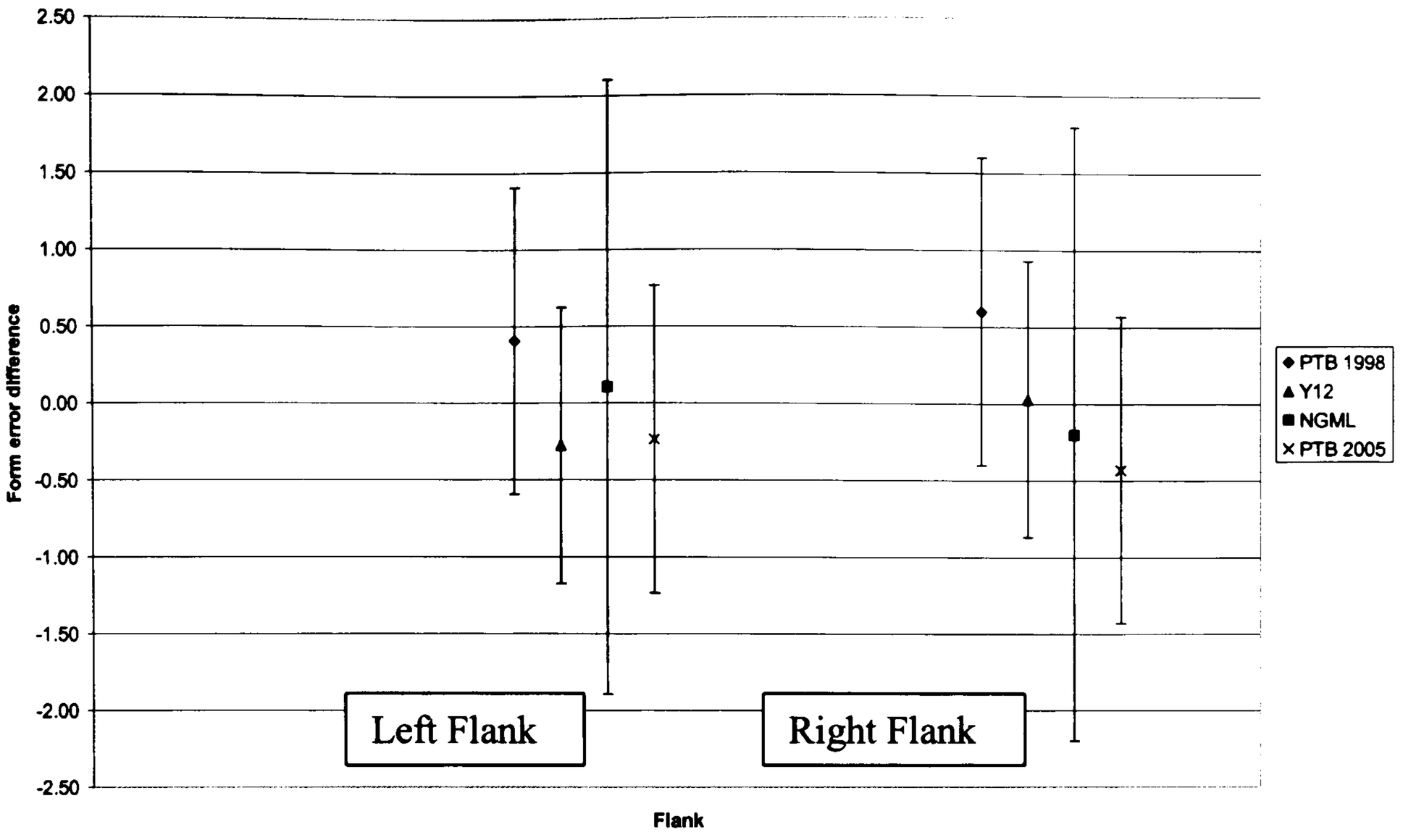

Figure 6.16 100mm profile master deviations between the unweighted profile form error slope ($f_{f\alpha}$) and the individual laboratory result in [μm].

The influence of data point position on the 100mm profile master

Figure 6.14 shows that the differences between NGML and PTB and Y12 are within the claimed measurement uncertainty for the NMIs but there is clearly closer similarity between the Y12 and PTB results than with the NGML results. This bias of the NGML results is not evident when examining the 200mm profile artefact results, and is one of the main reasons for initiating the 100mm comparison exercise.

NGML uses a different measurement strategy compared to PTB and Y12 who use CMMs for gear measurement. Data points on the NGML instruments are taken at equal spaces along the profile length of roll, while Y12 and PTB have data which is equally spaced along a radial distance across the profile. This difference does not change the measurement results on profiles with low form errors but with significant form errors, such as those on the 100mm profile artefact shown in figure 6.17, there may be difference in the evaluated least squares fit slope result.

A simulation of the effect is shown in figure 6.18. The PTB profile error trace was digitised manually taking 21 points between the defined evaluation lines. The slope of

the 'least squares fit line' was 2.35μm for points spaced equally along a length of roll, as measured by NGML, but for points spaced at equal radial distance the error is evaluated as 3.16μm. (The effect of change in data density can be seen with close examination of the PTB measurement curve form error). This difference will change with form error shape and data density but nevertheless offers an explanation for the difference between NGML and PTB/Y12 results. The 200mm profile errors show that it is not so susceptible to data spacing affects. Column A measurement points (in figure 6.17) are space linearly along a length of roll, similarly to NGMLs Klingelnberg P65 while Column B points (figure 6.17) are spaced evenly in the radial direction, measured in accordance with Y12 and PTBs measurement procedure.

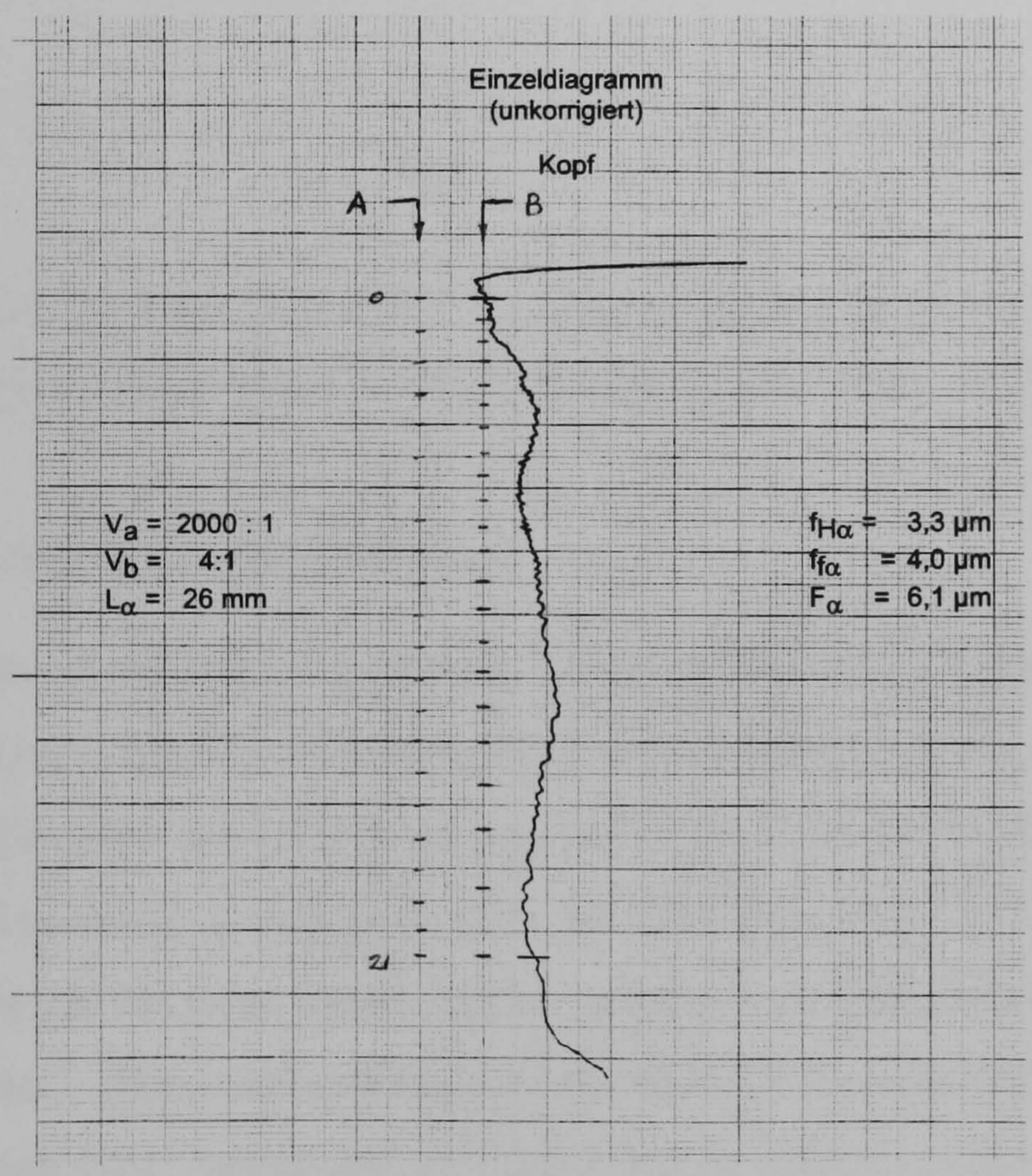

Figure 6.17 Copy of the profile error trace from the PTB calibration certificate number 0498 PTB 98 showing the 100mm profile master left flank profile error.

Figure 6.18 Effective profile shape difference due to differences in data sampling strategy (equally spaced along a length of roll or equally spaced in the radial direction).

6.4 Pitch and runout comparison

Pitch measurement is generally considered to be one of the easiest parameters to measure but as this comparison exercise shows the differences in results can be significant but the reasons for the differences are difficult to quantify. The (AGMA) Calibration Committee initiated this international comparison after its Chairman, Mr. R.E. Smith, reported significant differences between radial runout results from different measurement and evaluation processes. This was corroborated by M & M [Lawson, 2002] who reported differences on measuring instruments of 1.0μm due to analysis procedures on a single instrument alone. Radial runout is the variation in radial position of a ball sat in a tooth space caused by varying tooth thickness, pitch eccentricity and form errors of the gear flank. It is either measured directly by 'floating' a ball into a tooth space and measuring its position or indirectly by measuring pitch errors on left and right flanks and calculating the effect of the measured pitch (position) errors would have on the radial position of a ball of the appropriate size to contact both flanks.

Initially the work involved only organisations in the USA but was quickly extended to include PTB in Germany and NGML in the UK after these organisations expressed an

interest in the project. The artefact selected by AGMA was a 24 tooth master gear with two datum axes as illustrated in figure 6.19. The two datum axes are arranged to produce concentric pitch errors with low deviations and an eccentric datum surface that produced cumulative pitch deviations in the region of 70µm.

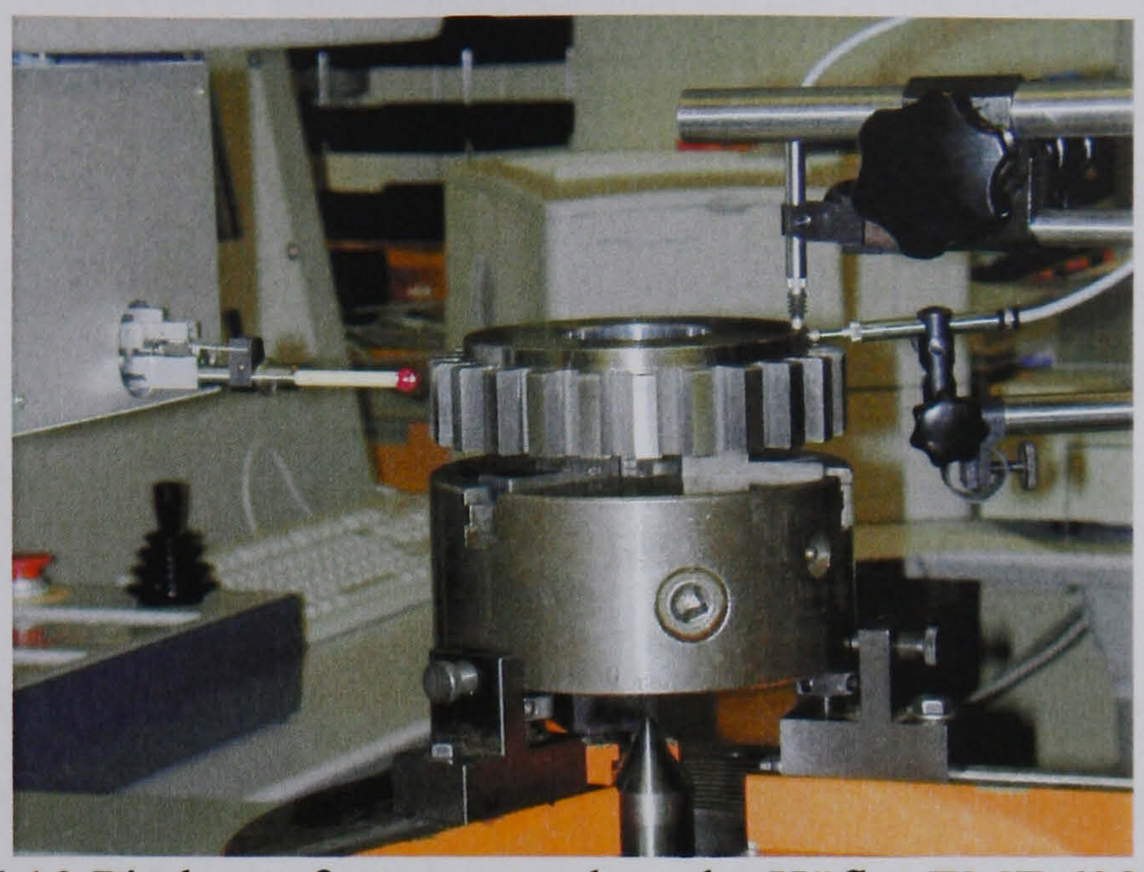

Figure 6.19 Pitch artefact mounted on the Höfler EMZ 632 at NGML.

The parameters evaluated in the comparison included individual adjacent pitch (f_p), cumulative pitch (F_p) and radial runout errors for all teeth on left and right flanks. The runout parameter (F_r) was considered the most likely parameter to cause problems in the comparison because of the sensitive nature of this parameter due to both instrument errors and form errors on the artefact. These parameters are fully defined in ISO1328 and are discussed in Chapter 1.

The evaluation of pitch errors is defined in the gear accuracy standard ISO1328-1 as the largest measured adjacent pitch error from all the pitch error data. Most instruments thus only tabulate this largest value and it is common practice to simply compare the magnitude of these values. However this ignores the position (pitch number) where the error occurs. Data supplied by PTB and Y12 includes a table with the individual errors for each pitch and these have been compared also and plotted for comparison purposes.

Excellent correlation between measuring instruments is usually obtained when comparing the maximum errors. Pitch errors on a good quality master gear tend to be similar or, in the case of cumulative pitch, vary in a sinusoidal manner. When random errors in the measurement process (caused by instrument repeatability and differences in measurement position on artefacts) are applied to these pitch errors the likelihood of the largest errors being similar is increased. A comparison of individual pitch errors provides the most

accurate method of determining pitch measurement capability and also reveals differences in pitch definition between instruments.

Pitch calibration methods

In the comparison procedure that follows, two methods are used for pitch measurement. The method used by Y12 [Cox, 1999] and NGML is a simple measurement of pitch, either using a rotary table as an angle reference as used by NGML, or using a calibrated CMM (Y12, Oakridge). NGML index the gear artefact on the rotary table to change the phase of the measured errors and use the mean results to define the calibrated pitch errors. This method requires a calibrated pitch artefact to establish instrument performance prior to calibrating the workpiece on the instrument.

The second method employed by PTB is an absolute pitch calibration method that requires simply a calibrated probe to define traceability. The method involves measuring the 24 pitches 24 times with the artefact indexed by one pitch at each repeat measurement. The resulting error matrix can be solved to separate the pitch errors in the artefact and pitch errors on the instrument with redundancy that enables us to quantify the uncertainty of the measurement process [Estler, Mark]. This process offers the lowest measurement uncertainty and is adopted by PTB if specifically requested by the customer.

Measurement details

The geometry of the pitch artefact is defined in Table 6.6. The radial runout of the tooth space was not measured directly but calculated from the pitch measurement results measured at 148.879mm diameter. This diameter was selected because it is the theoretical position at which a 8.000mm diameter ball should sit between the tooth flanks. There is often a difference between results from calculating tooth space position and measuring it directly due to flank form errors.

Table 6.6 24 tooth pitch artefact basic gear geometry and measurement diameters.

Parameter	
Teeth (z)	24
Normal module (m_n)	6.500 mm
Normal pressure angle (α_n)	20°0'0"
Diameter (d), pitch measurement	156.000 mm
Diameter for runout measurement	148.879 mm
Helix angle (β)	0°
Face width (b)	31.9 mm

The calibrated flanks were measured relative to two datum surfaces. One datum was concentric with the teeth and the second datum eccentric to the teeth. Figure 6.20 illustrates the definition of pitch number 1 used for the comparison. Different instruments use different definition for pitch 1 and may use a different definition for positive and negative pitch errors [Wilson, 2003].

At NGML, the artefact was measured 5 times with the mean results presented for comparison purposes [Wilson, 2003]. A potential problem with taking mean data in this way is rounding errors. The effect of rounding errors may be assessed by performing a closing error calculation to verify that the sum of all adjacent pitch errors is zero. This was verified for the NGML data with maximum closing error of 0.02μmm, which is acceptable.

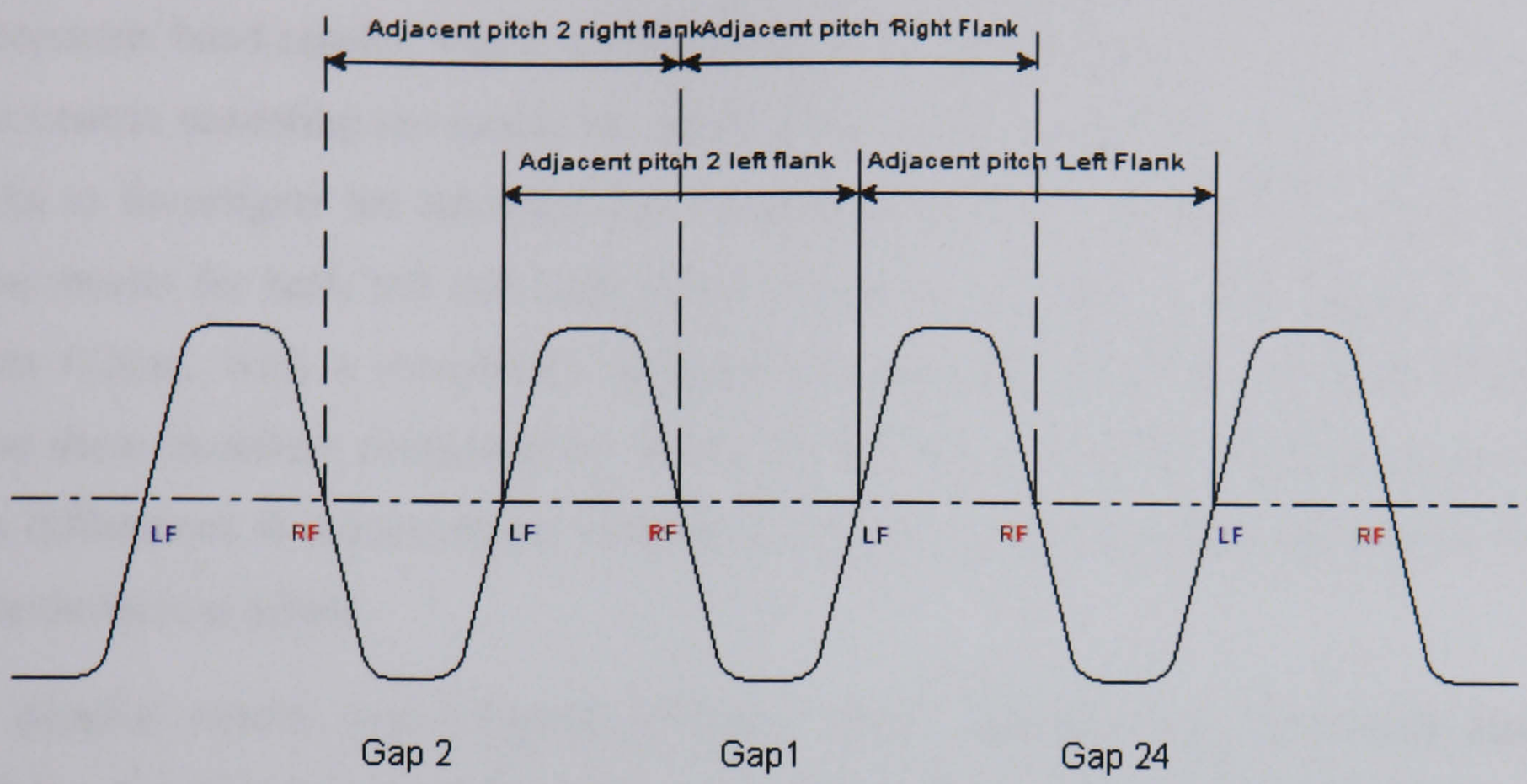

Figure 6.20 definition of pitch number 1 on Klingelnberg P65 Gear Measuring Centre[Wilson, 2003].

Discussion of results

A summary of comparison of measurement parameters is given in Table 6.7. It shows good compatibility of pitch results that are all well within the stated measurement uncertainty for the individual laboratories for adjacent pitch and cumulative pitch. The variation of radial runout also appears to be within the stated measurement uncertainty but there is a more significant bias between NGML results and those from Y12 and PTB. Because the radial runout errors are measured at a different diameter (148.879mm) to those used for the pitch comparison (156.000mm) it is not possible to determine if this is due to the basic pitch readings or an algorithm problem in evaluating radial runout from pitch errors.

As previously noted, differences between the maximum evaluated parameters from the individual NMIs is small (see Table 6.7).

Figures 6.21 and 6.22 show the comparison of the eccentric adjacent pitch error data supplied by AGMA to the participating laboratories. Compatibility between PTB and NGML is good with a maximum difference of 0.4μm while differences in results from individual results Y12 vary by up to 1.0μm from NGML. All results are within the claimed measurement uncertainty

The results in figure 6.23 & 6.24 for the concentric datum, by comparison, yield differences within 1.0μm, which is still within the measurement uncertainty differences, but is greater than the eccentric band. In general, the variation in results was greater than the eccentric band results, which is particularly surprising because the errors measured on the eccentric mounting are nearly ten times those of the concentric band. As part of the checks to investigate the anomaly, the concentric band was re-measured by the author. These results for both left and right flanks are shown in figures 6.23 and 6.24 and are within 0.2μm, with a completely different measurement setup and probe calibration. These show excellent compatibility within the NGML and suggest that there may have been differences in measurement position or changes in the artefact responsible for the larger deviations noted.

The detailed results were reported [Wilson, 2003] and show the maximum standard deviation for the tests was 0.34μm for cumulative pitch and 0.15μm for adjacent pitch, based on 5 tests with the artefact indexed by 90° between each measurement and the datum axes re-measured.

Table 6.7 Pitch and runout results comparison and measurement uncertainty[μm]

Datum/flank	Parameter	Y12	PTB	NGML
Concentric/left	fp	1.203 (±0.57)	1.268 (±0.5)	1.46 (±1.5)
Concentric/left	Fp	2.308 (±0.57)	2.303 (±0.5)	2.22 (±2.0)
Concentric/right	fp	1.679 (±0.57)	1.050 (±0.5)	1.18 (±1.5)
Concentric/right	Fp	2.261 (±0.57)	2.170 (±0.5)	2.08 (±2.0)
Concentric	Fr	7.378 (±0.57)	6.07 (±1.5)	8.02 (±2.5)
Eccentric/left	fp	10.625 (±0.57)	10.665 (±0.5)	10.88 (±1.5)
Eccentric/left	Fp	73.969 (±0.57)	72.741 (±0.5)	75.68 (±2.0)
Eccentric/right	fp	10.753 (±0.57)	10.074 (±0.5)	9.86 (±1.5)
Eccentric/right	Fp	72.660 (±0.57)	73.154 (±0.5)	73.16 (±2.0)
Eccentric	Fr	72.718(±0.57)	72.718 (±1.5)	73.30 (±2.5)

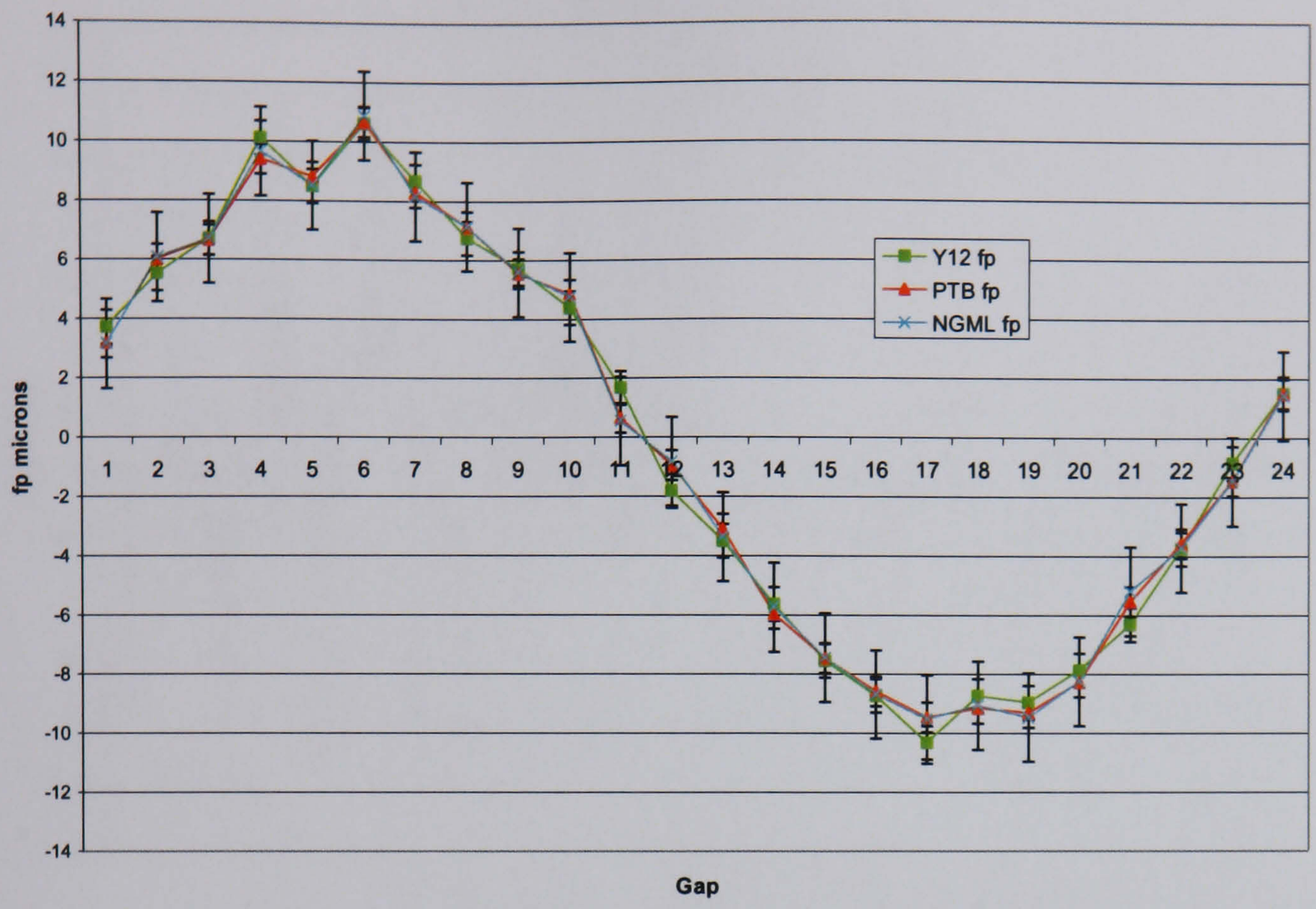

Figure 6.21 Pitch artefact comparison of individual left flank adjacent pitch results for the eccentric datum axes.

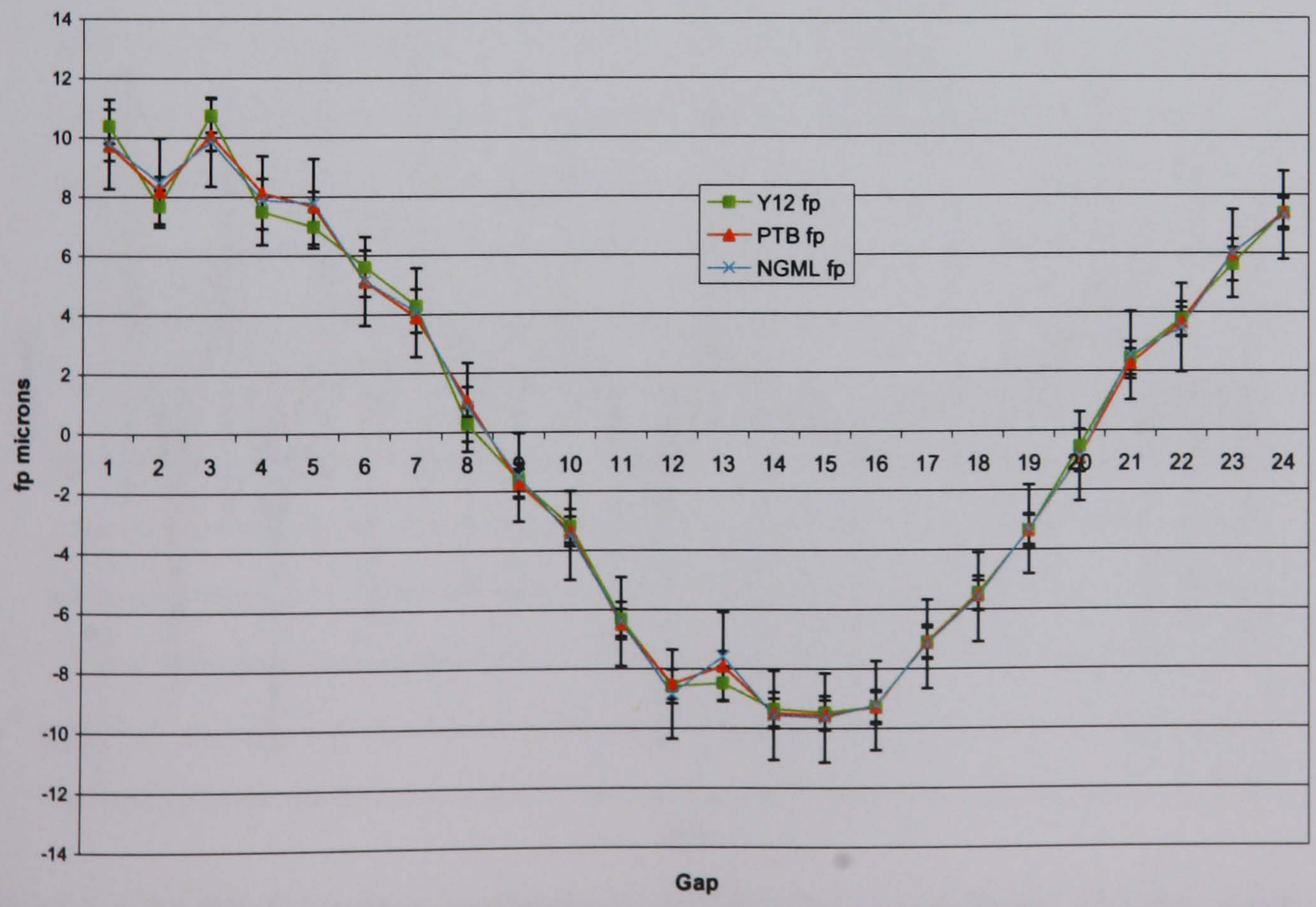

Figure 6.22 Pitch artefact comparison of individual right flank adjacent pitch results for the eccentric datum axes.

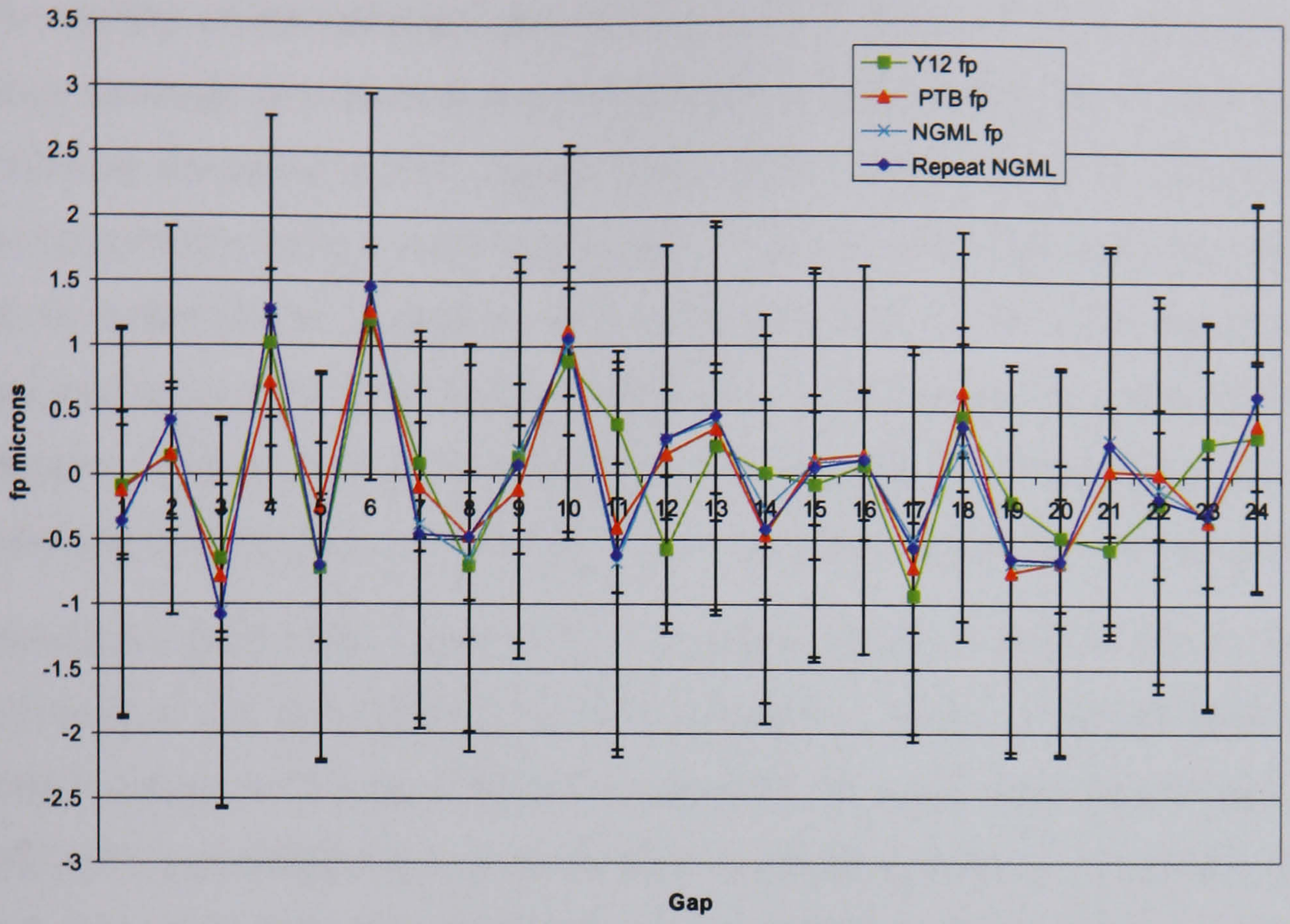

Figure 6.23 Pitch artefact comparison of individual left flank adjacent pitch results for the concentric datum axes.

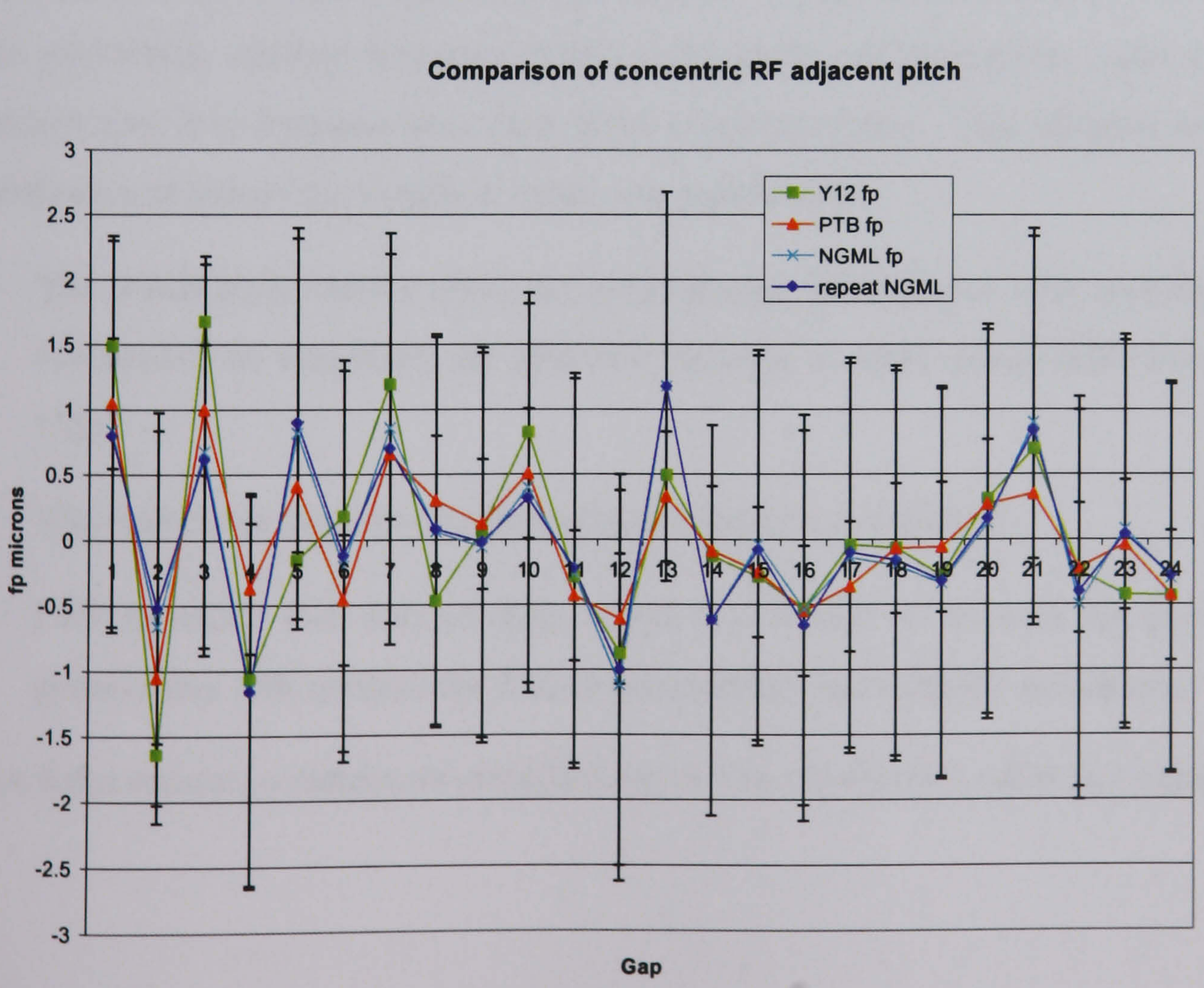

Figure 6.24 Pitch artefact comparison of individual right flank adjacent pitch results for the concentric datum aces

6.5 Determining reference data for the comparisons

The quality of the reference data is key to the validity of any comparative assessment. Many methods have been developed for establishing robust data for comparing KCRVs. These are discussed in NPL reports [Cox, 1999], and all determine the mean (KCRV) of the comparison using a weighting system. The classical approach is to use the reciprocal of the measurement uncertainty as a weighted mean, but as discussed in Chapter 5, this can lead to specific data having an excessive influence on the mean of the comparison exercise. This is considered acceptable if the estimate of the measurement uncertainty is valid and appropriate for the test result, however this cannot always be guaranteed.

Alternative approaches include using simulated data derived from the mean and standard deviation of the data values from the comparison. Data can be generated using Monte-Carlo methods with large numbers of trials and the mean value determined with the 0.025 and 0.975 percentiles set to give the 95% confidence interval. Of course there is always an assumption that the distributions are normal and this may not always be true. Dimensional metrology often suffers from a dearth of data and it is not possible to determine if the distributions are truly 'normal'. Other methods put even less reliance on the probability density functions (pdfs) and use the robust median value which has the benefit that it is immune from bias from extreme results. The decision to ignore these methods and use an un-weighted mean was justified by:

- The uncertainty values from the participating laboratories were similar (factor of 2 difference) so weighting the data was unlikely to make much difference to the mean value.
- The maximum number of submissions is small (maximum 5)
- PTB provided two sets of data, which is difficult to account for in any statistical process that will assume the data is independent and without correlation.

For these reasons a simple un-weighted mean was chosen as a reference value.

6.6 Summary

- The compatibility of NMI helix error measurement in involute gears was established using a 200mm artefact with helix angles varying between 0° and 45°. The results show that differences in the laboratory results lie within the claimed measurement uncertainty with a 95% confidence interval for helix errors on all results except one form error parameter.

- The compatibility of NMI profile error measurement in involute gears was established with a 200mm profile artefact. Again, the results show that differences lie well within the claimed measurement uncertainty with a 95% confidence interval.

- Compatibility between dedicated gear measuring machines and CMMs with gear software has been demonstrated, within the claimed measurement uncertainty.

- The 100mm lead master comparison shows that gear artefacts over 20 years old may suffer from instability and it is recommended that re-calibration intervals should be no greater than 3 years. The results were compatible within the NMIs claimed measurement uncertainty.

- The 100mm profile master shows excellent compatibility for all parameters except profile error slope. The different measurement strategies of CMMs and dedicated measuring instruments can bring about a significant difference in results when form errors are significant. The accuracy standard ISO 1328 should be amended to define the data density, filter parameters and data spacing to ensure compatibility of measurement evaluation.

- Traceability issues for helix and profile measurement should not affect trading between the participating nations.

- The pitch master comparison arranged by the AGMA shows compatibility within the NMIs claimed measurement uncertainty. Differences between individual pitch errors are larger than the difference between the maximum error measured by each NMI. This demonstrates the importance of tabulating pitch data for comparison purposes. It should be noted however that the position and sign of the error is not normally important but the magnitude of the error is often important.

- The measurement uncertainties from NMI's must be reduced further if the needs of the gear industry are to be addressed as discussed in section 6.1.

Chapter 7

CLASSICAL UNCERTAINTY EVALUATION METHODS

This chapter applies the conventional uncertainty estimation procedure commonly known as 'the uncertainty budget method' and applies it to gear measurement. Example measurement uncertainties are developed and the benefits and limitations of the method demonstrated. It quantifies the law of propagation of measurement uncertainty and its implications to industrial measurement uncertainty.

7.1 Background

The application of the traditional approach to uncertainty assessment defined in standards [VIM, 1995 and UKAS, M3003] is commonly termed the preparation of an 'uncertainty budget'. The research into industrial gear measurement capability discussed in Chapter 5 included a simple uncertainty budget to estimate measurement uncertainty using the comparator method to establish traceability. It is an appropriate method for any dimensional measurement process but is limited in its scope of application. Chapter 6 compared results from NMIs and demonstrated that the estimate of measurement uncertainty was valid by proving that differences between pairs of measurement results were within the uncertainty defined by a 95% confidence interval. Furthermore, the methods included in ISO 18653 are, essentially, the comparator method with the addition of a procedure to include uncorrected bias in the measurement process determined by the calibration procedure. Thus, the investigation of the validity of the comparator method and its further extension for measuring un-calibrated workpieces is important. The following sections describe the process of constructing an uncertainty budget (or estimate).

7.1.1 General procedure

All methods of estimating measurement uncertainty follow the same procedure:

- Express the relationship between the measurand (measurement result) and the input quantities which influence the measurement result. This is a mathematical model of the measurement process and includes measurement and calibration procedures, and corrections that influence the measurand.

- Quantify the magnitude of the likely range of input quantities (by testing using methods as close to the normal measurement process as possible) and define the appropriate probability distribution function (pdf), eg normal, rectangular and triangular distributions etc, for each input quantity. In gear measurement procedures, the rectangular and normal distributions are the most commonly used although occasionally a triangular distribution may be appropriate if two rectangular distributions are convoluted.

- Determine the standard uncertainty for the chosen distribution (ie. one standard deviation for the defined pdf).

- Define the sensitivity coefficients that quantify the change in input quantity with change in the measurand. These are in the form of partial derivatives in a mathematical model (for example the coefficient of linear expansion relating the change in linear length due to a change in temperature).

- Combine the uncertainty and sensitivity coefficients into a model to estimate the overall 'Standard Uncertainty' for the total measurement process.

- Calculate an expanded uncertainty with the required confidence interval (which is usually 95% for most measurement processes) to define the process measurement uncertainty.

Chapter 2 included a discussion of sources of error and uncertainty in the gear measurement process. These should be quantified when constructing the uncertainty budget and set to zero if negligible, included directly if significant, or grouped together with other input quantities if they are small or cannot be determined independently as appropriate. Some [Adams] recommend ignoring values less than 10% of the largest uncertainty, but it may be better to include them and show that they are negligible in order to demonstrate that they have a negligible influence.

7.1.2 Guidelines

The following points discuss some of underlying principles that apply when attempting to estimate measurement uncertainty:

- The model estimates the uncertainty of a result from a 'measurement process'. Measuring instruments do not have an uncertainty unless they are used to perform a specific task, such as the measurement of calibrated artefacts to establish traceability or the measurement of un-calibrated workpieces. The measurement process includes checks on the instrument performance including establishing traceability (law of propagation of uncertainties).

- It is usual to estimate measurement uncertainty with a 95% confidence interval, i.e. there is 95% chance the actual error lies within the limits stated. There is a 5% chance it is outside these limits. Machine tool makers tend to use a 99% confidence interval [Holmes, 2004] but this is problematic and potentially error prone when low numbers of data samples are used to verify the distribution assumptions.

- The process of gear measurement involves many sources of uncertainty and it is important not to duplicate them in the analysis. This may be avoided and simplified by combining many sources of uncertainty together by simply measuring typical workpieces using standard processes. This provides data on the reproducibility of the measurement process and will automatically include most thermal and mounting errors, alignment and operator sources of uncertainties with a single source of uncertainty.

- The same method used to measure workpieces is be used to calibrate an instrument. This means employing the same measurement methods and auxiliary equipment under the same environmental conditions. Thus, it provides accurate data to quantify the uncertainty of the measurement value.

- It is common to consider two uncertainty distributions i.e. the normal (Gaussian) distribution and the rectangular distribution. The general rule is that unless sufficient measurement data is available to produce a normal distribution, a rectangular distribution is used. This is a slightly pessimistic assumption in some cases but where data is limited no other option can be recommended.

- The 'bias' or 'error' in a measurement process, estimated by measuring a calibrated workpiece can significantly affect the uncertainty statement values. The methodology adopted in ISO 18653 is to add any uncorrected bias values linearly to the uncertainty statement. In the uncertainty budgets discussed in this chapter, bias is within limits defined by rectangular distribution and included in the budget. However if bias is corrected, the residual uncertainty of the bias correction remains in the budget.

- Geometric differences between calibrated artefacts used to establish traceability and workpieces can still cause difficulties when assessing workpiece measurement uncertainty. ISO 18653 addresses the measurement of calibrated workpieces only and does not address uncalibrated workpieces. ISO/TR 10064-5 'Cylindrical Gears – Code of Inspection Practice – Part 5. Recommendations Relative to Evaluation of Gear Measuring Instruments' makes some recommendations for uncalibrated workpieces. The benefits and limitations of the methods are discussed in this chapter.

- There are a number of uncertainty sources that are either 2nd order or have no effect on the process uncertainty. They are included in the budget to show they have been considered and set to zero.

7.1.3 Uncertainty budget layout

The uncertainty budget is conveniently prepared in a table format [UKAS M3003] with the following headings:

Uncertainty Source	Units	Value	Distribution	Divisor	Ci	n	Ui

Where:

Uncertainty Source: is the input quantity or source of uncertainty x_i

Units: are units of the uncertainty contribution.

Value: magnitude of the uncertainty x_i

Distribution: type of distribution, r-rectangular, n-normal, t-triangular.

Divisor: the divisor to convert the 95% confidence interval to one standard uncertainty. ($\sqrt{3}$ for rectangular distribution, 2 for a normal distribution with a 95% confidence interval).

Ci: the sensitivity coefficient or partial derivative linking the change in measurand for a given change in input quantity, e.g., coefficient of linear expansion for thermal effects, geometry effects, etc.

n: the number of repeat measurements made. If the mean of a number (n) of readings is taken as part of the standard measurement procedure the contribution x_i is divided by $\sqrt{n}$.

Ui: the standard uncertainty for a particular contribution (discussed in chapter 3).

The combined standard uncertainty for the process is estimated from the root of the sum of U_i^2

The 'process measurement uncertainty' is the expanded uncertainty which is calculated from the combined standard uncertainty multiplied by a coverage factor (K=2) to give a confidence interval of approximately 95% assuming a large number of tests are performed. In most processes, this gives sufficient confidence but sometimes it is necessary to use the 'Students-t' distribution for the appropriate number of degrees of freedom. The effective number of degrees of freedom estimated by the Welch-Slaterthwaite equation discussed in Chapter 4.

7.2 Example uncertainty budget

An example uncertainty budget for measuring involute profile error has been prepared for a simple mechanical base disc instrument shown in figure 7.1. The comparator method is used to establish traceability with a traceably calibrated profile master to determine the bias of the instrument. This involves the measurement of the calibrated master, verifying the bias is within acceptable predefined limits with uncertainty contributions for the calibration certificate, temperature effects and then measuring an un-calibrated workpiece with a number of uncertainty contributions including repeatability effects, mounting errors, thermal errors and system discrimination errors.

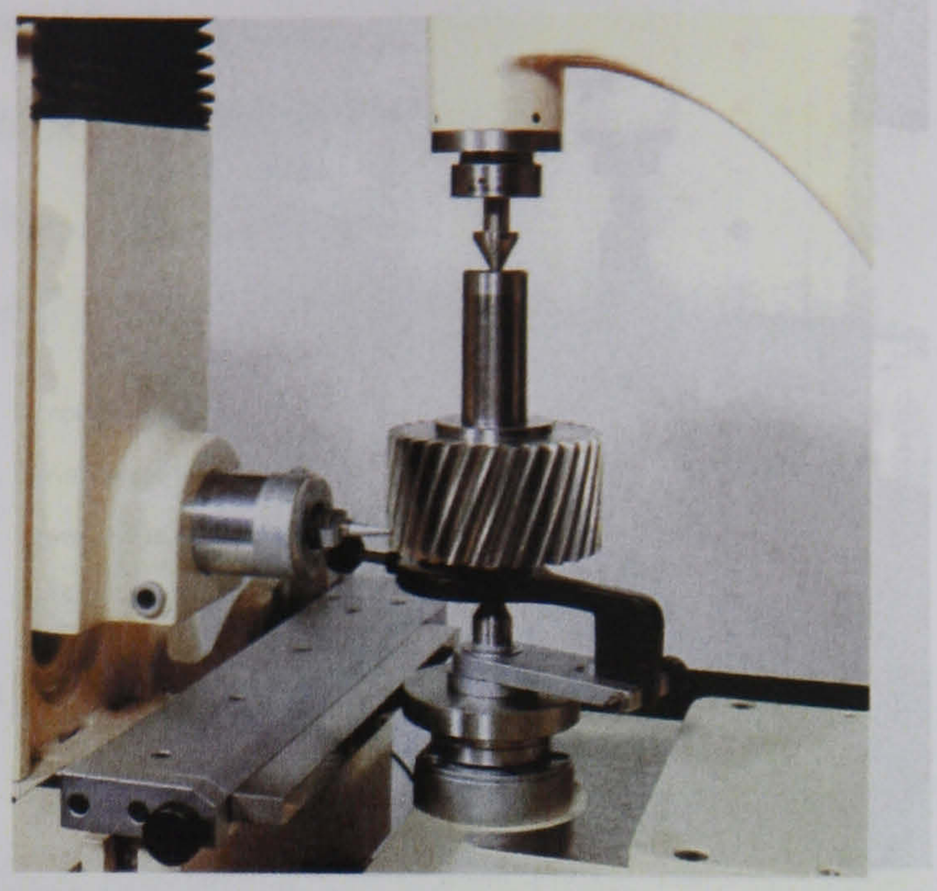

Figure 7.1 Frenco SH450 base disc instrument used for involute profile measurement and the subject of the example uncertainty budget.

The example estimate has been prepared for the measurement of an un-calibrated workpiece of identical geometry to that of a calibrated workpiece, used in the USA, for Fellows type profile masters. The measurement process is as follows:

- The calibrated gear artefact was measured 5 times and the mean result used to estimate the bias of the instrument relative to the calibration data. The 5 measurements include indexing the artefact by 90° on the instrument centres and averaging the result to minimise centre runout effects.
- The resulting bias between the mean measurement result and the calibration data value remains uncorrected but it is within the defined acceptance limits.
- The temperature difference between instrument and artefact are within defined limits. The effects of temperature difference are not corrected.
- Runout of the uncalibrated workpiece in measured and verified that it is within acceptable limits, but not compensated.
- A single measurement from the workpiece is used.
- There is no correction for base disc runout, but it is measured to verify that it is within defined limits.
- There is no correction for base disc size errors, but again it is measured to verify that it is within defined limits.

The geometry of the artefact and the identical workpiece is summarised in Table 7.1 and the uncertainty budget shown in Table 7.2a. The calibration data uncertainty for the artefact is ±1.5μm. The table shows the overall uncertainty of the process to measure an uncalibrated gear of identical geometry is ±2.5μm.

Table 7.1 Workpiece geometry and material properties.

Parameter	**Value**
Overall length between centres [mm]	300.0
Length between radial datum surfaces [mm]	200.0
Base diameter [mm]	100.0
Base helix angle [°]	0.0
Profile length of roll [mm]	26.0
Coefficient of linear expansion [m/m/°C]	11.6x10E-6

Table 7.2a Example uncertainty budget for profile error slope

	Uncertainty Source	Units	Value	Dist	Divisor	Ci	n	Ui
	Calibrated artefact uncertainties							
1	Artefact	µm	1.5	n	2	1	1	0.75
2	Repeatability of artefact measurement	µm	0.2	n	1	1	1	0.2
3	Uncorrected differences between data	µm	0.5	r	1.732	1	1	0.288684
4	Drift of the reference artefact	µm	0	n	1.732	1	1	0
5	Difference in artefact Temp. and 20C	Deg C	1	r	1.732	3.02E-01	1	0.174134
6	Uncertainty in artefact CTE	Na	1.16E-06	r	1.732	26000	1	0.017413
	Workpiece uncertainties							
7	Test piece runout	µm	1.5	r	1.732	0.2627797	1	0.227581
8	test piece runout detection	µm	0.2	n	2	0.2627797	1	0.026278
9	test piece runout	µm	1.5	r	1.732	0.2627797	1	0.227581
10	test piece runout detection	µm	0.2	n	2	0.2627797	1	0.026278
11	Spindle alignment	µm	0.4	r	1.732	0	1	0
12	Spindle alignment detection	µm	0.2	n	2	0	1	0
13	Alignment between centres	µm	0.5	r	1.732	0.1	1	0.028868
14	Alignment between centres detection	µm	0.5	n	2	0.1	1	0.025
15	Base disc size	µm	3.354102	r	1.732	0.2766862	1	0.535816
16	Base disc runout	µm	2.061553	r	1.732	0.2627797	1	0.31278
17	test piece form error uncertainty	µm	0.5	r	1.732	1	1	0.288684
18	Difference in temp. between artefact & 20C	deg C	1	r	1.732	3.02E-01	1	0.174134
19	Uncertainty in workpiece CTE	na	1.16E-06	r	1.732	26000	1	0.017413
20	Repeatability of workpiece measurement	µm	0.4	n	1	1	1	0.4
21	Probing compression	µm	0	r	1	1	1	0
22	Drift of the workpiece	µm	0	r	1	1	1	0
23	Elasticity of the workpiece	µm	0	r	1	1	1	0
	Discrimination/resolution							
24	System discrimination	µm	0.25	n	2	1	1	0.125
25	Report resolution	µm	0.05	r	1.732	1	1	0.028868
	Instrument geometry uncertainties							
26	Zero degree setting & uncertainty	µm	2	r	1.732	0	1	0
27	X-axis combined uncorrected slide errors	µm	0		1	0	1	0
28	X-axis uncertainty	µm	0		1	0	1	0
29	Y-axis combined uncorrected slide errors	µm	0	r	1.732	0	1	0
30	Y-axis uncertainty	µm	0	n	2	0	1	0
31	Z-axis combined uncorrected slide errors	µm	0.4	r	1.732	0	1	0
32	Z-axis uncertainty	µm	0.5	n	2	0	1	0
33	R-axis uncorrected position errors	µm /m	3.6	r	1.732	0	5	0
34	R-axis uncertainty	µm /m	3.6	r	1.732	0	5	0
	Combined Standard Uncertainty							1.224027
	Expanded Uncertainty k=2 (rounded up)							**2.5**

An explanation of the elements in Table 7.2a follows:

1. The uncertainty of artefact data from the calibration certificate is assumed to have a normal distribution and is defined for a 95% confidence interval with a

divisor of 2 to calculate the standard uncertainty. The sensitivity coefficient is defined as 1, because its influence on the measurand uncertainty is 1:1.

2. The repeatability of measurements on the calibrated artefact to establish traceability and quantify the bias has a standard deviation. In this case the mean from a series of tests is used determine the bias, the standard deviation is divided by $\sqrt{n}$. Repeatability is defined by a single standard deviation so the divisor is set to 1.

3. Any differences between calibration data and measured data must either be corrected or lie within specified limits and added as an uncertainty source. If the bias was corrected, this term would be zero in the uncertainty assessment but the uncertainty of the correction (element 3) would remain. The rectangular distribution represents the maximum allowable difference between calibration data and measured data, and can be determined from reproducibility data. The divisor to give 1 standard deviation is $\sqrt{3}$ for rectangular distribution.

4. Drift in the reference artefact is assumed to be zero in this case. Most artefacts are stable, but re-calibration by an accredited calibration laboratory will verify this. The recommendation in ISO 18653 is to use 'workpiece like artefacts may lead to more unstable materials used as calibration artefacts. In these circumstances, a more frequent calibration interval is required to keep calibration data valid. Alternatively, it should be included in the uncertainty statement on the calibration certificate similar to the way uncertainty of gauge block stability is added to a budget prepared for gauge block calibration.

5. The temperature effect with a reference artefact is always present. If the difference between 20°C and actual temperature is compensated, the uncertainty of the correction process must be added. The sensitivity coefficient 0.301 is calculated from the coefficient of linear expansion for the material multiplied by the profile length of roll [LOR] yielding a coefficient of *[11.6.10^{-6}.26.0mm[LOR].temperature difference]*. Figure 3.5 illustrates that profile is simply length measurement.

6. The uncertainty due to temperature must be included in the budget. This should also include the uncertainty of the material coefficient of linear

expansion, which may be as large as 20% depending on the actual material composition [Cubis, 2001]. The sensitivity coefficient c_i is given by $11.6.10^{-6}\,\Delta t x 1000.26.0[LOR]=2600$.

7. - 10. The mounting uncertainty for each datum surface is separate because the sensitivity coefficient depends on the artefact profile and datum surface geometry. In addition, the measurement uncertainty of the test method is separate. If the mounting error effects were compensated, terms 7 and 9 are set to zero. The uncertainty of the compensation method would however remain. The sensitivity coefficients in 7-10 are identical and are a combination of both the effect the runout has on profile measurement, if it was in the same axial section as the profile measurement, and a second correction to compensate for the fact that this is not usually the case. (The correction based on the geometry of the workpiece, and position of the datum surface). c_i=*0.5[convert from TIR].Sin(angle of roll).* Note: TIR is total indicator reading.

11. - 12. Alignment of the rotary table is an uncertainty source if the workpiece attaches to it without the tailstock centre. The c_i is set to 1 if the calibrated artefact is mounted on the table or set to 0 if the workpiece is between centres, as shown in this example.

13. - 14. Tailstock alignment is set to 0 if not used or if this is included in the work piece repeatability (this depends on how the workpiece repeatability information is gathered).

15. - 16. Base disc size is always an issue. The x_i value should include the uncertainty of the measurement process and thermal effects. The effect of base disc size is included in the sensitivity coefficient and is a geometry calculation involving base radius and length of roll, $c_i=LOR/(d_b)$. The base-disc runout *ci* also consists of geometry effects, and in this case it is $Sin(LOR/r_b)$. The value represents a reasonable estimate of the maximum expected error with the c_i as elements 7-10.

17. Form error effects are always present and their influence depends on the filters applied to the data including probe radius, mechanical damping, hysteresis and (and the data point spacing on a CNC instrument). The value for *ci* is a best

estimate but work reported in Chapter 8 may indicate that this value is pessimistic.

18. The temperature effects of the reference artefacts are always present. If the difference between 20°C and measured temperature is correctly compensated, then the resulting uncertainty of the correction process must be added. The sensitivity coefficient 0.301 is calculated from the coefficient of linear expansion for the material multiplied by the profile length of roll[LOR] *[$11.6.10^{-6}$x26.0mm[LOR].temperature difference]*.

19. See element 5. The temperature uncertainty effect is identical to the reference artefact.

20. Simple repeatability is defined as a series of repeat measurements taken by the same operator at the same time under the same conditions. This includes mounting error uncertainties, thermal affects and alignment uncertainties if these tests are performed over a long period of time and we can eliminate many sources of uncertainty in the budget. See the simplified budget in Table 6.2b that extends this element and renames it 'reproducibility'.

21. Probing compression is usually set to zero for ferrous materials. The actual probe force compression is not negligible (0.1 to 0.2μm), but is constant throughout the measurement of profile and thus does not influence the measurement result.

22. Workpiece drift value is set to 0 because the drift in the workpiece is small when compared to geometrical tolerance values. This may become an issue if gears are measured in their soft condition and they are subsequently heat treated, with a resulting change/distortion in geometry caused by internal changes in structure.

23. Workpiece deflection is zero, in this case, but it can be a problem with more flexible materials or with long or thin steel components that are located in a chuck.

24. If the discrimination is greater than the standard deviation for repeat tests, use the discrimination value in 2 & 20. A rectangular distribution is used because the best estimate is the limits that are likely to occur. In older manual

instruments the discrimination is defined by the probe and plotter performance. In CNC instruments the probe or encoder performance may define the discrimination.

25. Report resolution. If the results are rounded when reporting to the customer the resolution is ±1/2 the lowest bit. Again this is a rectangular distribution.

26. Helix angle setting on a manual instrument has no effect on the profile measurement results but is included in the budget to remind the user this is the case.

27. - 34. These are geometrical guideway error effects and set to 0 if covered effectively with a calibrated artefact. If a suitable artefact is not available it requires a simple model of the measurement process and gear geometry to generate the effects that the parametric guideway errors have on gear measurement process.

The Ui column in Table 7.2a is a list of the uncertainty sources. There are 34 sources of uncertainty considered in this estimate but many of the elements are set to zero (elements 4, 11, 12, 21, 22, 23, and 26 to 34 inclusive) because they are not required in this example. They remain in the budget because they demonstrate that they have been considered but are not appropriate for this particular measurement task. If for example, the workpiece geometry is significantly different to the calibrated artefact, the guideway geometry elements 26 to 34 may have to be included or if the workpiece was excessively flexible compared to the calibrated artefact (element 23) would be used. The root mean square of these terms in Table 7.2a is 1.25μm and is called the process 'standard uncertainty'. To present the results with the conventional 95% confidence interval a coverage factor of two was used, yielding a U_{95} of ±2.5μm. The uncertainty budget is complex in terms of the number of elements it includes but the process of constructing it is relatively simple. Possibly the most important feature of this method is that it allows the user to assess the importance of each element contributing to the overall uncertainty estimate. Thus informed decisions can be made to consider how to improve the measurement process and reduce the overall uncertainty

A simple method of estimating measurement uncertainty using reproducibility data is presented in Table 7.2b (the reproducibility method is the basis of the ISO 18653 method developed in ISO/TR10064-5). Although the full method of assessing measurement uncertainty is relatively simple, it is very time consuming to apply and in many industrial and laboratory environments not appropriate. The simplified method replaces many of the individual sources of uncertainty with a single term of workpiece process reproducibility (element 12 in Table 7.2b). The reproducibility is determined by measuring a typical workpiece many times over an extended period of time so that mounting, alignment, temperature, repeatability and operator influences are included in the variation in measurement results obtained on the designated workpiece.

An examination of Table 7.2b shows that temperature has been included as an additional separate element. This is because the reproducibility test workpiece was stored in the laboratory environment and thus did not represent the condition of an individual workpiece that is stabilised for a short period of time before calibration.

The result from the simplified budget is an uncertainty value that agrees with the more detailed analysis and requires only 9 elements in the total budget. This is the method that is recommended for industrial and commercial calibration laboratories.

Further uncertainty budgets for other parameter measured in gears were prepared and are included in Appendix C.

Table 7.2b Example profile error slope measurement uncertainty budget using the simplified reproducibility method.

	Uncertainty Source	Units	Value	Dist	Divisor	Ci	n	Ui
	Calibrated artefact uncertainties							
1	Artefact	µm	1.5	n	2	1	1	0.75
2	Repeatability of artefact measurement	µm	0.2	n	1	1	1	0.2
3	Uncorrected differences between data	µm	0.5	r	1.732	1	1	0.288684
4	Drift of the reference artefact	µm	0	n	1.732	1	1	0
5	Difference in artefact Temp. and 20C	deg C	1	r	1.732	3.02E-01	1	0.174134
6	Uncertainty in artefact CTE	na	1.16E-06	r	1.732	26000	1	0.017413
	Workpiece uncertainties							
7	Base disc size	µm	3.354102	r	1.732	0.276686	1	0.535816
8	Base disc runout	µm	0	r	1.732	0.26278	1	0
9	test piece form error uncertainty	µm	0.5	r	1.732	1	1	0.288684
10	Difference in temp. between artefact & 20C	deg C	1	r	1.732	3.02E-01	1	0.174134
11	Uncertainty in workpiece CTE	na	1.16E-06	r	1.732	26000	1	0.017413
12	Reproducibility of workpiece measurement	µm	0.8	n	1	1	1	0.8
13	Probing compression	µm	0	r	1	1	1	0
14	Drift of the workpiece	µm	0	r	1	1	1	0
15	Elasticity of the workpiece	µm	0	r	1	1	1	0
	Discrimination/resolution							
16	System discrimination	µm	0.25	n	2	1	1	0.125
17	Report resolution	µm	0.05	r	1.732	1	1	0.028868
	Instrument geometry uncertainties							
18	Zero degree setting &uncertainty	µm	2	r	1.732	0	1	0
19	X-axis combined uncorrected slide errors	µm	0		1	0	1	0
20	X-axis uncertainty	µm	0		1	0	1	0
21	Y-axis combined uncorrected slide errors	µm	0	r	1.732	0	1	0
22	Y-axis uncertainty	µm	0	n	2	0	1	0
23	Z-axis combined uncorrected slide errors	µm	0.4	r	1.732	0	1	0
24	Z-axis uncertainty	µm	0.5	n	2	0	1	0
25	R-axis uncorrected position errors	µm /m	3.6	r	1.732	0	5	0
26	R-axis uncertainty	µm/m	3.6	r	1.732	0	5	0
	Combined Standard Uncertainty							1.222287
	Expanded Uncertainty k=2 (rounded up)							**2.5**

7.3 Application of simple comparator models

The procedure described in section 7.1.3 is complex and although it yields reasonable uncertainty estimates, it is more suitable for calibration laboratory environment than the industrial shop floor. The simplified comparator methods described in the standards and codes of practice [ISO 18653 and BGA, 1994] are robust and methods of estimating uncertainty using calibrated gears or gear artefacts. The methods provide an estimate of the uncertainty of measuring the calibrated artefact but a simple modification to the procedures allows us to extend it to include un-calibrated workpieces, provided conditions of geometrical similarity are satisfied. The two procedures are discussed in the following sections and examples are investigated.

7.3.1 ISO 18653 procedures for industrial instruments

ISO 18653:2003, 'Gears- Evaluation of instruments for the measurement of individual gears' procedures, were developed from the guidance in [ISO14253-1], [Adams, 2002] and [BGA, 1994] and involves the use of calibrated gear artefacts. The evaluation of measurement uncertainty uses equation 7.1. This is a reliable procedure but it ignores some potentially significant sources of uncertainty.

$$U_{95} = \sqrt{(2.u_m)^2 + (2.u_n)^2} + |E| \qquad (7.1)$$

Where u_m standard uncertainty of measurements on the instrument

u_n standard uncertainty for the calibration data on the artefact

E bias (difference) between reference data and measured data values.

The above formula assumes a coverage factor of two and defines the 95% confidence interval for the process, irrespective of the actual number of degrees of freedom for the system.

The standard states that a minimum of 10 tests are required to define u_m, (an upper limit of 30 is also recommended in ISO/TR 10064-5), and recommends these are taken over a long period of time, representing different operators, environmental conditions different machine alignments, thus including a number of sources of measurement uncertainty. This is good practice but it is time consuming if the

procedures are to be used for testing compliance with specification for a new measuring instrument. It also recommends the gear artefact is removed from the instrument between measurements, which is good practice, but again is time consuming for acceptance testing the instrument.

There are many sources of uncertainty that are not included in the estimate of the measurement process capability but these contributions are generally small compared to the likely variation in a shop floor instrument under normal operating conditions (small in this context is defined as less than 10% of the largest uncertainty). What is not clear and hence is investigated in section 7.3.3 is when the full uncertainty budget method should be invoked and when the simplified method from the standard is acceptable.

One final part of the standard that requires investigation is how it addresses uncorrected bias or deviation between reference data and measured data in the measurement process. Most uncertainty evaluation processes assume that biases detected by the calibration process will be corrected. The method of adding the magnitude of the bias directly was discussed in Chapter 4 but this must be considered as a pessimistic interpretation of uncertainty, and does comply with the ethos prevailing in GUM, that realistic uncertainty models are constructed rather than safe models that err on the side of caution.

7.3.2 BGA Code of practice DUCOP 05/1

The method for estimating uncertainty in the BGA code was developed in 1992-1993 as part of work funded by the UK Department of Trade and Industry National Measurement System programme of work. It therefore predates the ISO document by ten years and has been used with approximately 50 different measuring instruments during this time by the NGML. Reasonable uncertainty estimates were obtained producing no instances where an individual result is outside the 95% confidence interval using the simple BGA formula is shown in (7.2) [Frazer, 2002].

$$U_{95} = \sqrt{(k.u_m)^2 + (2.u_n)^2 + |E|^2} \qquad (7.2)$$

Where:

u_m standard uncertainty of measurements on the instrument

u_n standard uncertainty for the calibration data on the artefact

E bias (difference) between reference data and measured data

k coverage factor chosen from Student's t-distribution for 95% confidence interval.

The coverage factor $k=2$ is chosen for a confidence interval for the appropriate number of degrees of freedom but is often used for practical applications.

The BGA process differs from the ISO method because it involves measuring the calibrated artefact only 5 times. However by indexing the artefact on the rotary table by 90 degree intervals for each test, the effect of runout of the rotary table and the axis between centres is included in the variation in measurement results. The deliberate indexing implies that the data is not truly random and the resulting standard deviation is likely to be larger than that obtained by random measurements. This is balanced to some extent by the use of the coverage factor $k=2$ that will tend to underestimate the uncertainty.

7.3.3 Comparison of BGA and ISO 18653 methods

The following example determines the lead slope error on a CNC gear measuring instrument. Data was obtained from a master gear measured on the Klingelnberg P65 CNC Gear Measuring Centre at NGML and was gathered strictly in accordance with the procedures described in ISO 18653 and BGA Code DUCOP 05/1. Calibration data is from previous work by the NGML. The gear geometry is summarised in Table 7.3 and measurement data is presented in Tables 7.4 and 7.5 for both methods.

Table 7.3 Gear Geometry

Parameter	
Teeth (z)	30
Normal module (m_n)	5.000 mm
Normal pressure angle (α_n)	20°0'0"
Diameter (d)	173.2051 mm
Helix angle (β)	30°Right helix
Evaluation length (L_α)	20.98 mm
Evaluation Length (L_β)	24.00mm
Face width (b)	30.0 mm

BGA Code 05/1 method

The results from measuring 5 positions at 90 degree intervals is given in Table 7.4 and shows the mean and standard deviation for the 5 results and the calibration certificate values and measurement uncertainty.

Table 7.4 Measurement results from the BGA method and the calibration data values with the associated uncertainty U_{95} [μm]

Results							Mean	SD	Calibration	
									data	U_{95}
Profile Tooth 1, RF	$f_{H\alpha}$	3.2	3.1	3.1	3.0	3.1	3.10	0.09	2.8	1.5
	F_{α}	3.9	3.9	3.8	3.7	3.9	3.84	0.09	-	2.0
	$f_{f\alpha}$	1.7	1.9	1.8	2.0	1.9	1.86	0.11	-	2.0
Lead Tooth 1 RF	$f_{H\beta}$	-0.3	-0.4	-0.4	-0.4	-0.4	-0.38	0.04	-0.6	1.5
	F_{β}	2.7	2.7	2.6	2.7	2.7	2.68	0.04	-	2.0
	$f_{f\beta}$	2.5	2.5	2.4	2.5	2.4	2.46	0.05	-	2.0

Using 7.2 to calculate the measurement uncertainty from the BGA method, for the slope parameters yields

$$f_{H\alpha}\ (U_{95}) = \pm 1.55\mu m$$

$$f_{H\beta}\ (U_{95}) = \pm 1.52\mu m$$

Defining the coverage factor k=2.78 for 4 degrees of freedom and a 95% confidence interval yields uncertainty values of

$$f_{H\alpha}\ (U_{95}) = \pm 1.57\mu m$$

$$f_{H\beta}\ (U_{95}) = \pm 1.52\mu m$$

The BGA method does not account for the number of tests completed to establish the bias. It would be considered normal practice to divide the standard deviation by the $\sqrt{n}$ to obtain the standard error of the mean. This ensures that the process yields a value that reflects the process capability for a single measurement.

ISO 18653 method

The results from the implementation of the ISO procedure are in Table 7.5. The ten results were at random positions in accordance with ISO procedure and with the gear removed from the machine and replaced each time before re-measurement.

Table 7.5 Measurement results from the ISO method and calibration data values with the associated uncertainty U_{95} [μm]

Results												X	SD	Cal. data	
														x	U_{95}
Profile	$f_{H\alpha}$	3.1	3.1	3.1	3.3	3.2	3.3	3.2	3.2	3.1	3.2	3.20	0.11	2.8	1.5
Tooth 1, RF	F_{α}	3.9	3.9	4.0	4.0	4.0	4.1	3.9	4.0	4.0	4.0	3.98	0.06	-	2.0
	$f_{f\alpha}$	1.8	1.9	1.8	1.8	1.9	2.0	1.8	2.2	2.1	1.9	1.92	0.13	-	2.0
Lead	$f_{H\beta}$	-0.5	-0.5	-0.4	-0.6	-0.5	-0.6	-0.5	-0.5	-0.5	-0.5	-0.51	0.06	-0.6	1.5
Tooth 1	F_{β}	2.8	2.7	2.7	2.8	2.7	2.8	2.7	2.8	2.8	2.8	2.76	0.05	-	2.0
RF	$f_{f\beta}$	2.5	2.4	2.5	2.4	2.4	2.3	2.4	2.5	2.4	2.5	2.45	0.05	-	2.0

From 7.1 the calculated measurement uncertainty from the ISO method yields:

$$f_{H\alpha}\ (U_{95}) = \pm 1.91 \mu m$$

$$f_{H\beta}\ (U_{95}) = \pm 1.59 \mu m$$

Review of the two methods

Similar results are obtained from the two methods and they appear to produce realistic uncertainty estimates; if the individual results are examined, they show all are well within the uncertainty statement. The BGA method uses fewer data points but is more suitable for performing acceptance tests on an instrument because reliable data can be generated quickly. The ISO method has the benefit of not requiring a rotary table, the data can be acquired over longer period and so it also includes reproducibility influences.

The most significant difference is in the use of uncorrected bias data. The assumption with the ISO method is that the measured bias is the 'actual system bias' and not simply an 'example bias' that will change, depending on test conditions, appears to be over pessimistic. Furthermore, the assumption that the bias may be equal in

magnitude but have an opposite sign also seems to be pessimistic. GUM, Appendix E [VIM,1995] states that the procedures should produce 'realistic uncertainty estimates', and not 'safe estimates' is contravened by the methodology in ISO 18653.

Alternative analysis of ISO 18653 method

The simplest amendment to the formula from ISO 18653 shown in (7.1) is suggested below in 7.3

$$U_{95} = E \pm \sqrt{(2.u_m)^2 + (2.u_n)^2} \qquad (7.3)$$

This maintains the same elements but presents them in a more realistic manner. It also reminds the users of the results that the uncertainty estimate applies to the measurement on the calibrated artefact only. Re-evaluation of the 'profile error slope' uncertainty with this revised value yields the uncertainty result, which is arguably more realistic:

$f_{H\alpha}\ (U_{95}) = +0.4 \pm 1.51 \mu m$

A further interpretation follows the A2LA (American Association of Laboratory Accreditation) practice, namely to ignore the bias unless the difference between reference data and measured results is within the claimed reference data uncertainty [Adams]. This would yield the uncertainty of

$f_{H\alpha}\ (U_{95}) = \pm 1.51 \mu m.$

This may be reasonable, but it implies that the calibration process has an insignificant contribution to the total process measurement uncertainty, a fact which is known not to be true. Also it does not use the bias data at any stage of the process, which appears to be fundamentally wrong when analysing the data.

Although each method has some limitations, even the lowest estimate of uncertainty appears to provide a realistic result when the measured data in Tables 7.4 and 7.5 are considered. Further investigation is required to assess the sensitivity of the methods to different bias and uncertainty conditions.

7.3.4 Uncertainty budget method

For comparison purposes, the uncertainty budget method described in Section 7.2 has been applied to the profile measurement example and to a lead measurement example

as shown in Tables 7.6 and 7.7. It is from the Klingelnberg P65 CNC Gear Measurement Centre and uses data from the ISO 18653 analysis method for the repeatability uncertainty contribution. The uncertainty is for the establishment of bias or error in the instrument from calibration data and uses the comparator method. The terms for measuring uncalibrated work-pieces, ie lines 7 to 21 inclusive, are set to 0 for this example. The overall uncertainty from the uncertainty budget method is

$f_{H\alpha}(U_{95}) = \pm 1.58\mu m.$

$f_{H\beta}(U_{95}) = \pm 1.52\mu m.$

This includes residual thermal uncertainties, discrimination and resolution of the measurement system. This is probably the most realistic uncertainty for the process and following classical measurement uncertainty methods and it lies close to the BGA method with the coverage factor defined by the degrees of freedom of the process. The results are consistent with both the BGA and ISO methods of evaluating measurement uncertainty.

Table 7.6 Example profile error slope measurement uncertainty [µm]

	Uncertainty Source	Units	Value	Dist	Divisor	Ci	n	Ui
	Calibrated artefact uncertainties							
1	Artefact	µm	1.5	n	2	1	1	0.75
2	Repeatability of artefact measurement	µm	0.11	n	1	1	10	0.035
3	Uncorrected differences between data	µm	0.4	r	1.732	1	1	0.230
4	Drift of the reference artefact	mu	0	n	1.732	1	1	0
5	Difference in artefact Temp. and 20C	deg C	0.3	r	1.732	0.3016	1	0.052
6	Uncertainty in artefact CTE	na	1.16E-06	r	1.732	7800	1	0.005
	Workpiece uncertainties							
7	Test piece runout	µm	0	r	1.732	0.49	1	0
8	test piece runout detection	µm	0	n	1	0.49	1	0
9	test piece runout	µm	0	r	1.732	0.49	1	0
10	test piece runout detection	µm	0	n	1	0.49	1	0
11	Spindle alignment	µm	0	r	1.732	0	1	0
12	Spindle alignment detection	µm	0	n	1	0	1	0
13	Alignment between centres	µm	0	r	1.732	0	1	0
14	Alignment between centres detection	µm	0	n	1	0	1	0
15	test piece form error uncertainty	µm	0	r	1.732	1	1	0
15	Difference in temp. between artefact & 20C	deg C	0	r	1.732	0.30	1	0
17	Uncertainty in workpiece CTE	na	0	r	1.732	0	1	0
18	Repeatability of workpiece measurement	µm	0	n	1	1	1	0
19	Probing compression	µm	0	r	1	1	1	0
20	Drift of the workpiece	µm	0	r	1	1	1	0
21	Elasticity of the workpiece	µm	0	r	1	1	1	0
	Discrimination/resolution							
22	System discrimination	µm	0.05	n	2	1	1	0.025
23	Report resolution	µm	0.05	r	1.732	1	1	0.029

Combined Standard Uncertainty	0.7882
Expanded Uncertainty k=2	**1.58**

Table 7.7 Example lead error uncertainty budget for a master gear

	Uncertainty Source	Units	Value	Dist	Divisor	Ci	n	Ui
	Calibrated artefact uncertainties							
1	Artefact	µm	1.5	n	2	1	1	0.75
2	Repeatability of artefact measurement	µm	0.04	n	1	1	10	0.013
3	Uncorrected differences between data	µm	0.2	r	1.732	1	1	0.12
4	Drift of the reference artefact	mu	0	n	1.732	1	1	0
5	Difference in artefact Temp. and 20C	deg C	0.3	r	1.732	3.95E-01	1	0.07
6	Uncertainty in artefact CTE	na	1.16E-06	r	1.732	10219.28	1	0.006
	Workpiece uncertainties							
7	Test piece runout	µm	0	r	1.732	0.16	1	0
8	test piece runout detection	µm	0	n	2	0.16	1	0
9	test piece runout	µm	0	r	1.732	0.16	1	0
10	test piece runout detection	µm	0	n	2	0.16	1	0
11	Spindle alignment	µm	0	r	1.732	0	1	0
12	Spindle alignment detection	µm	0	n	2	0	1	0
13	Alignment between centres	µm	0	r	1.732	0.256	1	0
14	Alignment between centres detection	µm	0	n	2	0.256	1	0
15	test piece form error uncertainty	µm	0	r	1.732	1	1	0
16	Difference in temp. between artefact & 20C	deg C	0	r	1.732	3.95E-01	1	0
17	Uncertainty in CTE	na	0.00E+00	r	1.732	0	1	0
18	Repeatability of workpiece measurement	µm	0	n	1	1	1	0
19	Probing compression	µm	0	r	1	1	1	0
20	Drift of the workpiece	µm	0	r	1	1	1	0
21	Elasticity of the workpiece	µm	0	r	1	1	1	0
	Discrimination/resolution							
22	System discrimination	µm	0.05	n	2	1	1	0.025
23	Report resolution	µm	0.05	r	1.732	1	1	0.028

Combined Standard Uncertainty	0.76
Expanded Uncertainty k=2	**1.52**

7.4 Comparison of traditional methods

The previous sections demonstrated that the simplified comparator methods ignore important uncertainty contributions and therefore underestimate measurement uncertainty. The primary reason for this is that the uncertainty of the calibration data dominates the evaluation so reducing the influence of instrument repeatability in the overall uncertainty estimate. This section investigates when differences between the uncertainty budget method, as described in tables 7.6 and 7.7, and BGA or ISO comparator methods become negligible for practical applications.

The test conditions are summarised below:

- CNC gear measuring instrument with a rotary table
- Mounting between centres, no mounting error correction
- Ambient temperature variation ± 2ºC
- Form errors effects are 0.1µm
- No drift in the artefact
- 10 tests assumed

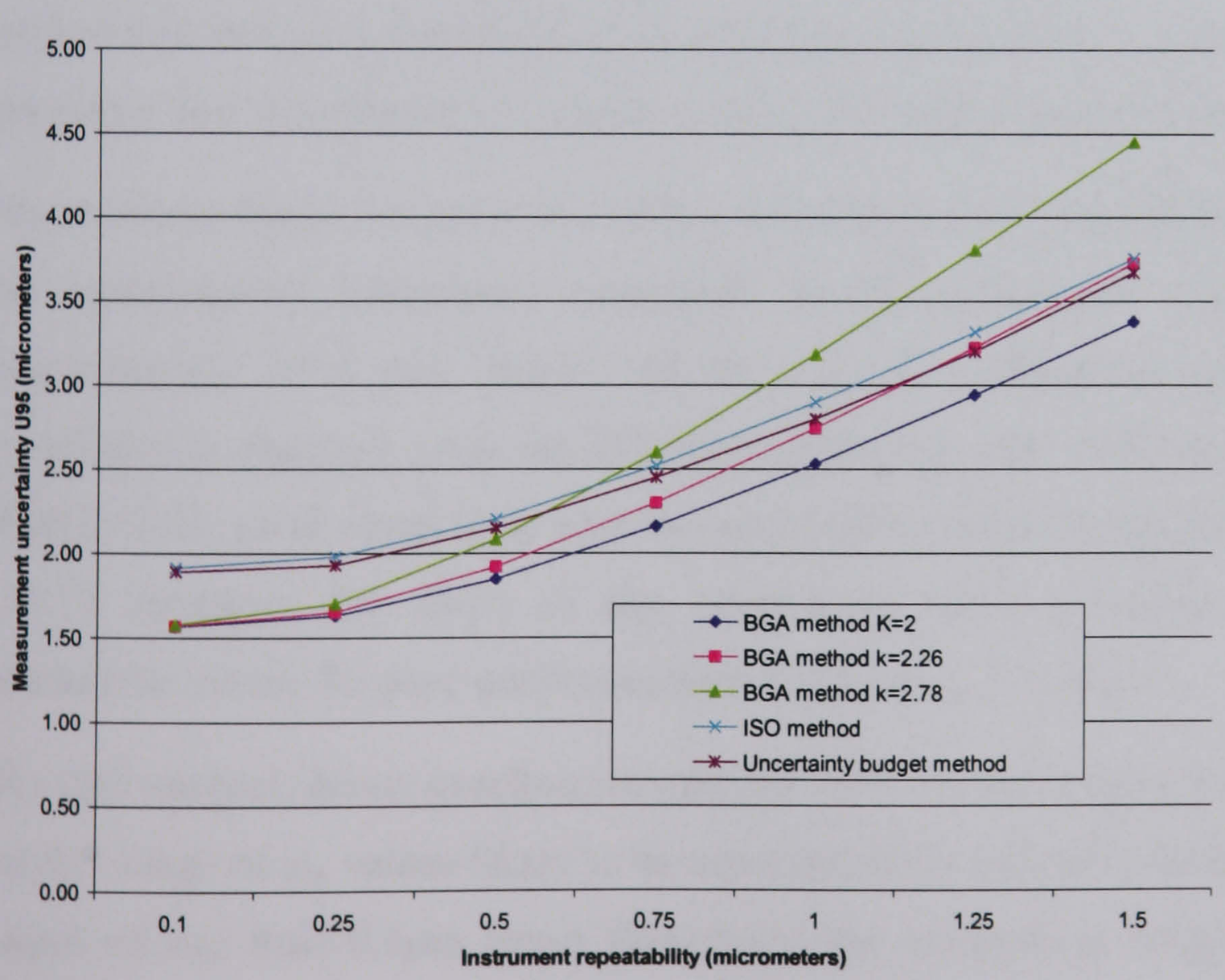

Figure 7.2 Comparison of the evaluation methods with instrument repeatability u_m.(bias 0.4µm, U_{cal} ±1.5µm)

Figure 7.2 shows a comparison of results for uncertainty estimates for the conditions previously defined and a bias between the mean of the instrument measurement results and calibration certificate value of 0.4μm calibration data uncertainty of U_{cal} equal to 1.5μm. For the purposes of the comparison, the uncertainty budget method is the reference model.

The range of instrument repeatability values varies between 0.1 and 1.5μm. The 0.1μm value is typical of a new instrument in a stable environment [Harrison, 2004]. It is expected that most instruments in industry to be repeatable having standard deviations within 0.5 to 1.0μm. Repeatability errors greater than 1.0μm, usually indicates either poor servicing, damage to the centres or poor environmental conditions [Wilson, 2005].

The results for the BGA method in figure 7.2 include three options (k=2.0, k=2.26, k=2.78). The coverage factors represent the range that could be reasonably attributed to the random repeatability errors. k=2 is the default value and assumes that the sample to establish the distribution is large. k=2.26 is the Students-t distribution coverage factor for 9 degrees of freedom, and is consistent with the ISO 18653 method that defines a minimum of 10 readings while k=2.78 is consistent with BGA procedure that recommends 5 measurements at 90 degree intervals in the rotary table.

The results in figure 7.2 show the BGA method with K=2 consistently underestimates the measurement uncertainty compared to the uncertainty budget method by approximately 25% and should not be used for industrial instruments. Better correlation is obtained using the ISO method for this case with low bias conditions. With k=2.26, good correlation with the uncertainty budget method is achieved while k=2.78 increases the slope of the uncertainty curve resulting in significantly pessimistic values for poor quality instruments (with $u_m > 0.8\mu m$).

The ISO method shows excellent correlation with the uncertainty budget method for the full range of u_m values likely to be encountered in industrial instruments with U_{95} values of less than 0.1μm larger throughout the comparison range. However, with larger bias values the uncertainty estimate will be proportionally larger because of the linear addition of bias to the uncertainty sum.

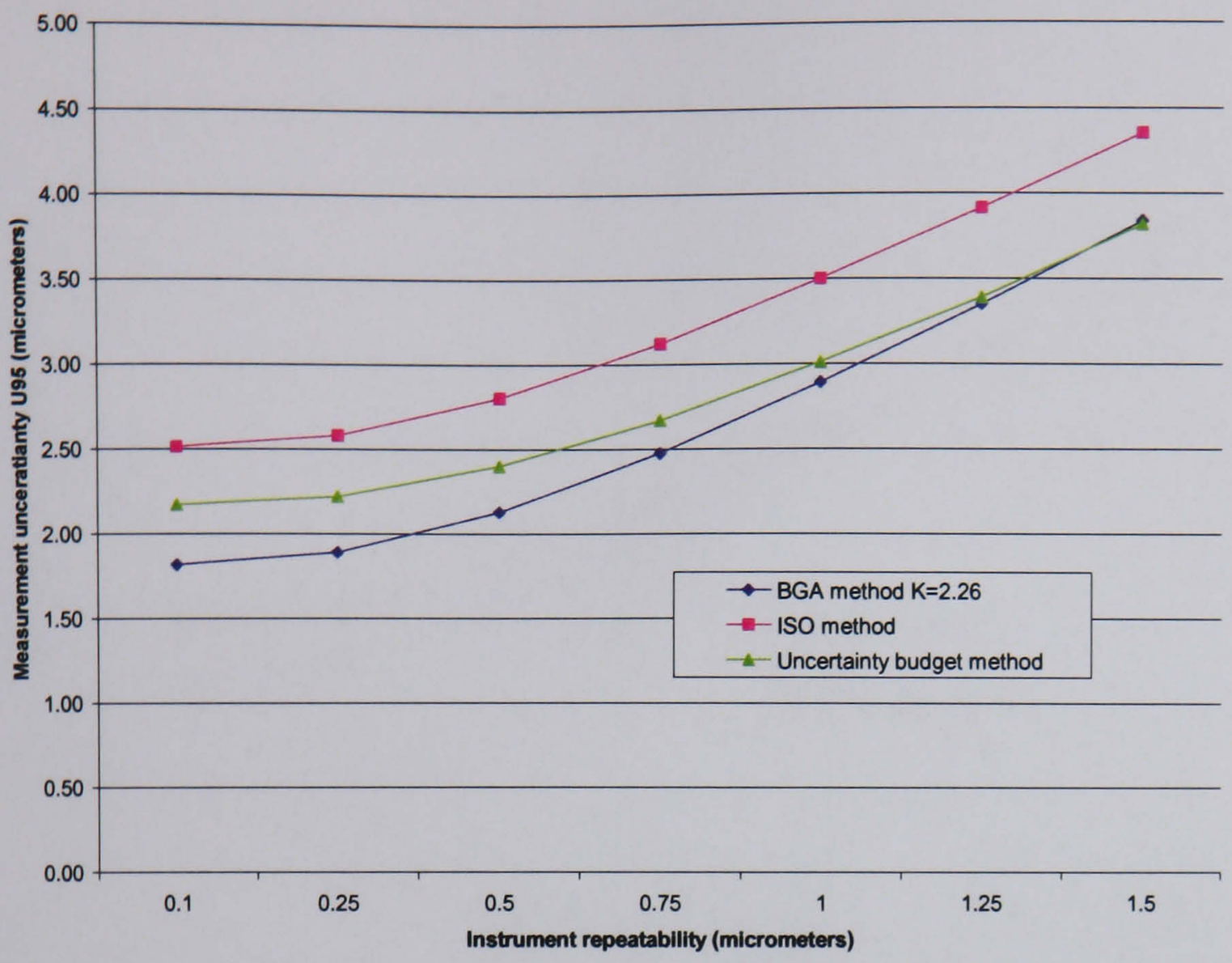

Figure 7.3 Comparison of the evaluation methods with instrument repeatability u_m.

(1μm bias, U_{cal} ±1.5μm)

Figure 7.3 shows a comparison with 1μm bias. The obvious difference is that the ISO method overestimates the uncertainty budget method by approximately 0.3μm throughout the range of evaluated uncertainties which represents between 8 and 14% error in the estimate of measurement uncertainty. The 1μm bias is common in industrial instruments so the excessive estimate of uncertainty is not acceptable.

The BGA method consistently underestimates the uncertainty until u_m=1.4μm, which is equally unacceptable. The only positive point to note is that the results reported in section 7.3.2 show that while the results are lower than the reference methods, test results show that the values returned by the method are valid.

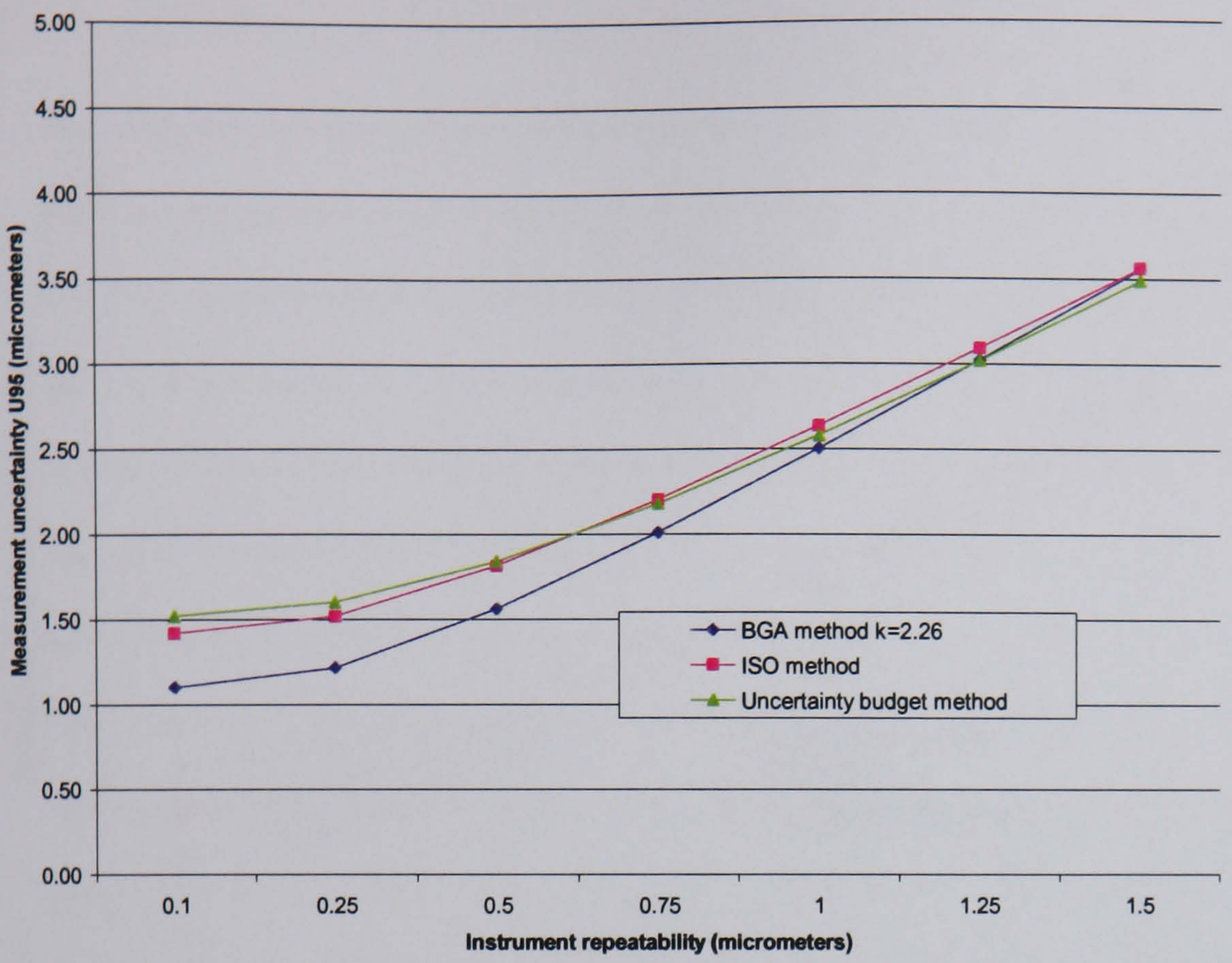

Figure 7.4 Comparison of the evaluation methods with instrument repeatability u_m. ($0.5\mu m$ bias , $U_{cal} \pm 1.0\mu m$).

Figure 7.4 shows good correlation between the uncertainty budget method and ISO method illustrated in figure 7.2 when a low bias between calibration data values and instrument values prevail. The BGA method significantly underestimates uncertainty when repeatability errors are less than $0.6\mu m$ producing errors in U_{95} estimates of greater than 15%.

Under conditions with low bias and calibration data uncertainty significant differences exist between the uncertainty budget method and the BGA method in highly repeatable instruments. This is primarily because the additional sources of uncertainty included in the uncertainty budget method become more significant and have a greater influence on the overall uncertainty estimates. With instruments whose repeatability is less than $0.6\mu m$, the ISO and BGA methods give significant underestimates of measurement uncertainty (ie. >13%).

Figure 7.5 illustrates a significant underestimate in measurement uncertainty with highly repeatable and accurate instruments using both the BGA or ISO methods when very low uncertainty calibration data is available. In practice calibration data with less than $0.7\mu m$ uncertainty is not likely within the next 10 years but this should be accounted for with the revision of the BGA and ISO documents.

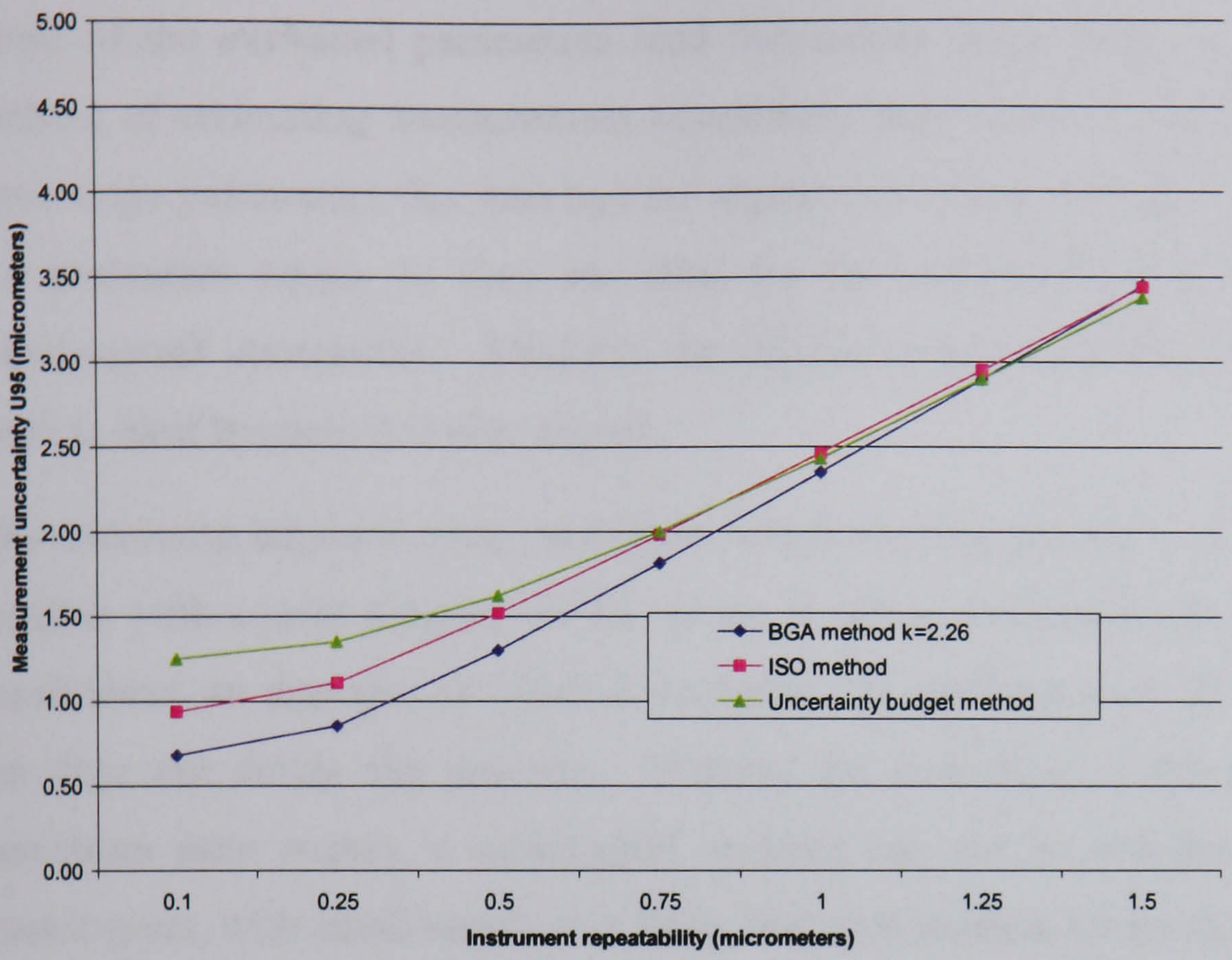

Figure 7.5 Comparison of the evaluation methods with instrument repeatability u_m.

($0.5\mu m$ bias, U_{cal} $\pm 0.5\mu m$).

The following comments on the validity of the 3 main methods can be made:

- All the methods provide values that are verified by practical measurement (in section 7.3) for the example results in figures 7.2 to 7.5.
- Although the BGA method returns consistently lower values than the other methods there is no evidence to suggest that the values are wrong. Examination of calibration certificates issued by the NGML show that if a correctly maintained measuring instrument is tested, the bias is no greater than the calibration data measurement uncertainty. This implies that the BGA method is valid.
- The uncertainty budget values are the result of applying standard procedures and are the reference method. As calibration data uncertainty is reduced and industrial instrument performance improved, there will be a need to adopt the uncertainty budget method more frequently in the future.
- If we are overestimating measurement uncertainty applying standard methods, then either, the calibration data, which is the dominant source of uncertainty, is too great, or there are other errors in the analysis.

7.5 Limitations of the comparator methods

Some of the evaluated parameters lend themselves more readily to the comparator method of estimating measurement uncertainty than others. The profile and helix error slope parameters ($f_{H\alpha}$ and $f_{H\beta}$) are signed (±) values and use all the data within the evaluation range, so they are ideal for the comparator method of estimating measurement uncertainty. Similarly the adjacent pitch error on an individual tooth pitch is ideal because it is also signed.

The maximum adjacent pitch parameter, which is often printed on a gear result sheet together with a print diagram of the errors, is not so convenient for evaluation. The result sheet, an example of which is in figure 7.6, tabulates only the maximum error but does not define the position. Without the definition of the position that the maximum error occurs, a meaningful analysis can not be completed. In accurate master gears, with small errors, it is likely that with random errors in the measurement process that very good agreement in the value of the maximum error will occur between different measuring processes. Comparing maximum errors can thus lead to an optimistic estimate of measurement uncertainty.

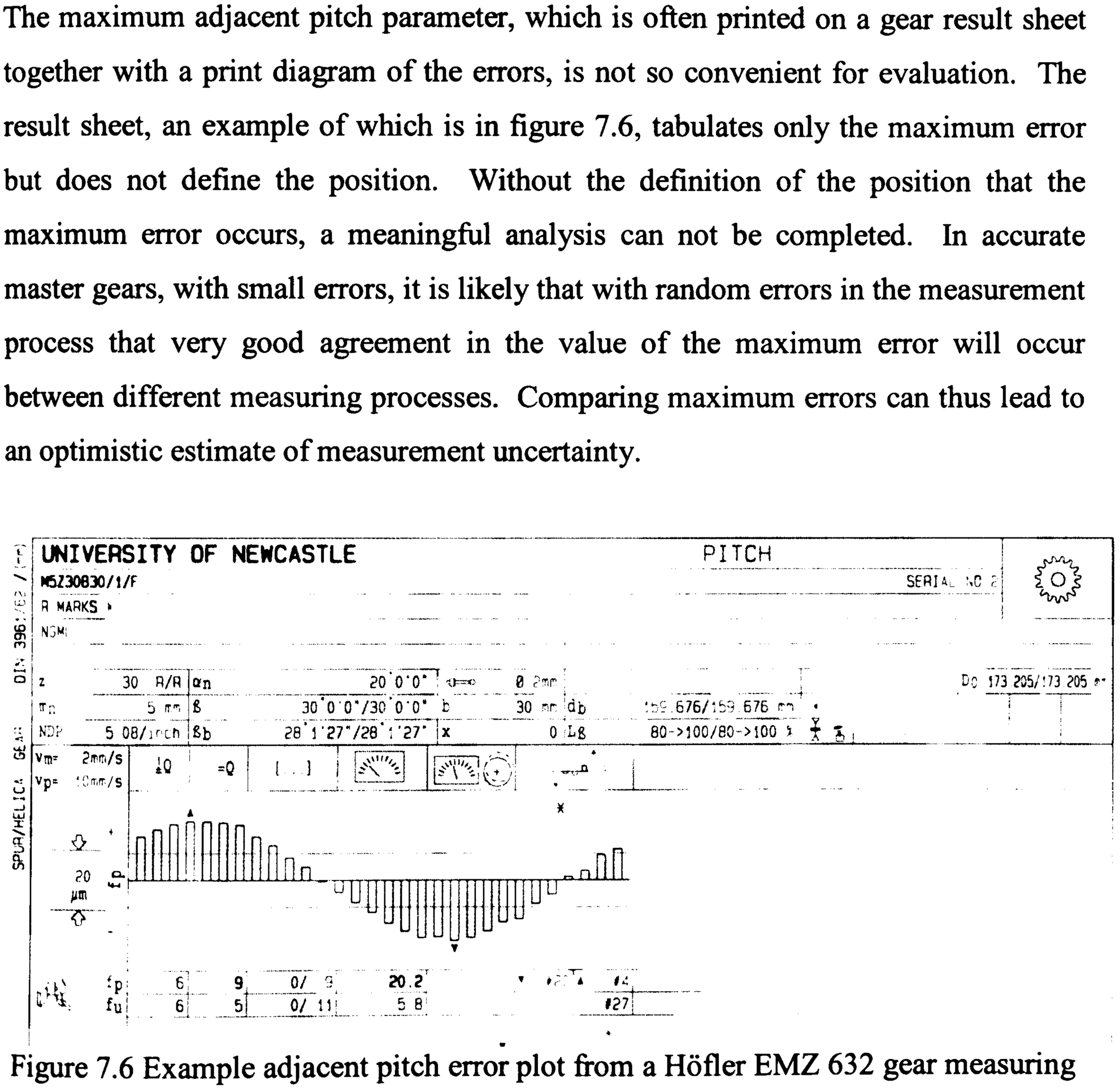

Figure 7.6 Example adjacent pitch error plot from a Höfler EMZ 632 gear measuring machine tabulating the maximum right flank adjacent pitch error of 20.2µm.

This effect is shown in Table 7.10, which is a comparison of adjacent pitch results reported in Chapter 6 from PTB in Germany, NGML and Oakridge Metrology Centre

(Y12). The maximum difference between PTB and NGML is 0.215µm. (the maximum difference from the Y12 data is 0.893µm, which suggests a significant bias between NGML and Y12 is evident)

Table 7.10 Comparison of maximum adjacent pitch results [µm]

NMI	Concentric data		Eccentric data	
	Left flank	Right flank	Left flank	Right flank
PTB	1.268	1.050	10.665	10.074
NGML	1.46	1.18	10.88	9.86
Difference	-0.192	-0.13	-0.215	0.214
Y12	1.203	1.679	10.625	10.753

Table 7.11 shows a comparison of all individual adjacent pitch errors from the 3 NMIs. The maximum difference between a PTB pitch error and an NGML pitch error is 0.85µm, which is significantly higher than the 0.215µm when comparing maximum adjacent pitch errors. A similar problem arises with the maximum cumulative pitch error parameter F_p. Note that the pitch position is not recorded on most instruments when reporting the maximum pitch value.

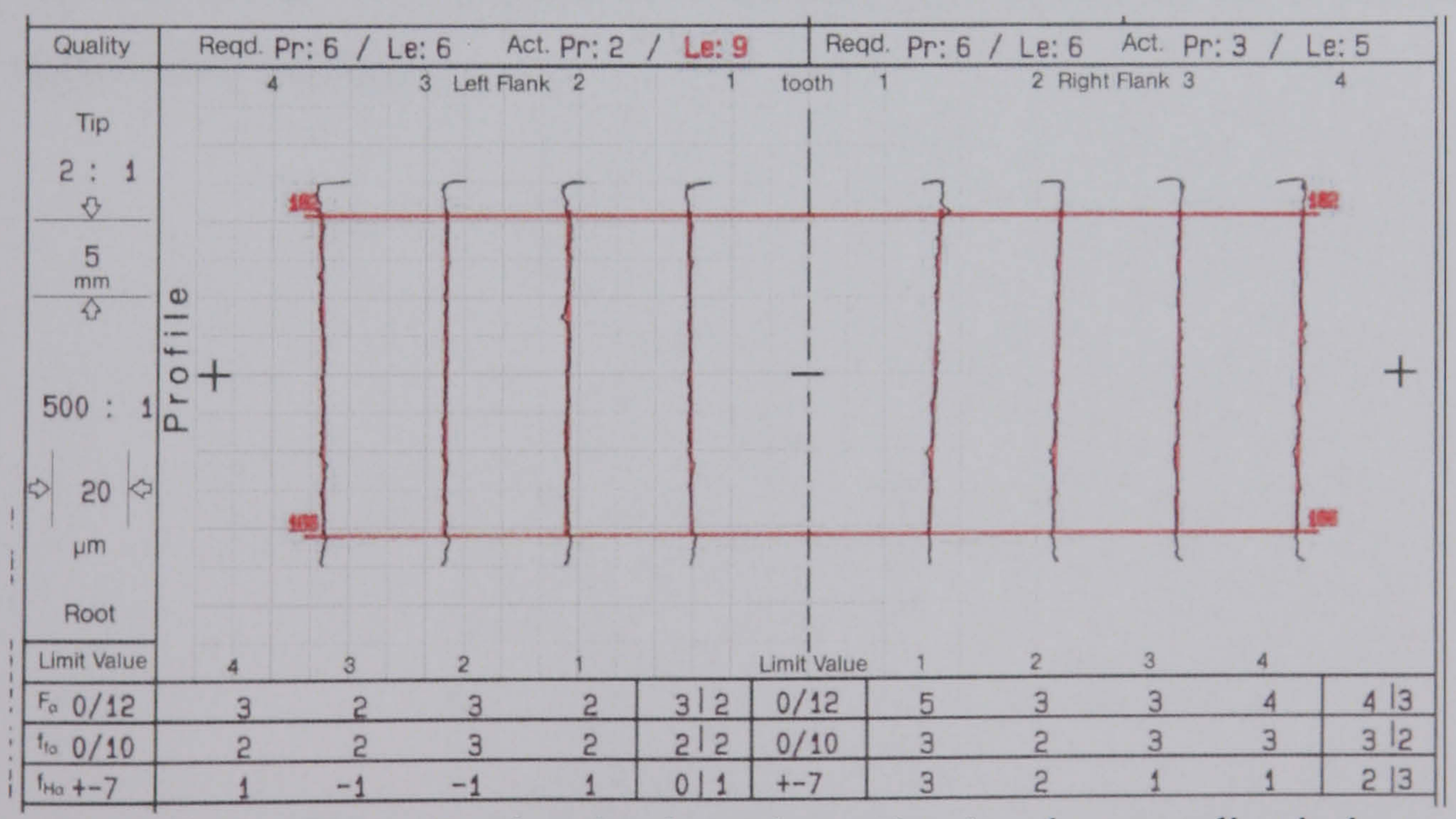

Figure 7.7 Example profile errors showing how the evaluation does not discriminate the positions at which maximum total and form deviations occur.

Form and total error parameters evaluated from profile (see Figure 7.7), and helix errors are also prone to misinterpretation when applying the comparator method of evaluating measurement uncertainty. The software evaluates maximum deviations

within the evaluation range and the instrument prints the maximum error. The tendency is for the uncertainty analysis to again be optimistic, particularly with high accuracy gears. Some of these issues can be avoided if master gears or gear artefacts with larger errors are used for evaluating uncertainty. As a general guide, the errors in the calibrated artefact should be similar to the errors in the product gears measured by the instrument.

A further limitation of the comparator method of assessing measurement uncertainty using conventional statistical methods is the apparent sub-zero errors effect. A profile error of 1.1 with a U_{95} of ±2.0μm implies that the actual error lies between –0.9μm and 3.1μm with a 95% confidence interval. In practice the error must be > 0 so any negative results are simply an artefact of the evaluation process. This type of anomaly is common in dimensional measurement and arises because evaluated parameters do not make robust measurands. Simply defining the position of the two measurement points that define the maximum error will not avoid this problem.

Alternative analysis methods such as the Monte Carlo Simulation method of evaluating measurement uncertainty [Cox, 2001] may provide a more robust method of evaluating uncertainty in these instances. These methods are researched as part of the work reported in Chapter 8.

Table 7.11 Comparison of individual pitch errors with maximum adjacent pitch error [Wilson, 2003]

Gap	Concentric										Eccentric									
	Left Flank					Right Flank					Left Flank					Right Flank				
	Y12 fp	PTB fp	NGML fp	PTB diff	Y12 diff	Y12 fp	PTB fp	NGML fp	PTB diff.	Y12 diff	Y12 fp	PTB fp	NGML fp	PTB diff	Y12 diff	Y12 fp	PTB fp	NGML fp	PTB diff	Y12 diff
1	-0.086	-0.12	-0.38	-0.26	-0.294	1.488	1.05	0.84	-0.21	-0.648	3.722	3.19	3.16	-0.03	-0.562	10.383	9.73	9.78	0.05	-0.603
2	0.142	0.16	0.42	0.26	0.278	-1.638	-1.05	-0.66	0.39	0.978	5.527	6.01	6.08	0.07	0.553	7.666	8.18	8.48	0.3	0.814
3	-0.645	-0.78	-1.06	-0.28	-0.415	1.679	1	0.68	-0.32	-0.999	6.711	6.66	6.7	0.04	-0.011	10.753	10.07	9.86	-0.21	-0.893
4	1.019	0.72	1.28	0.56	0.261	-1.065	-0.37	-1.14	-0.77	-0.075	10.116	9.4	9.66	0.26	-0.456	7.485	8.12	7.88	-0.24	0.395
5	-0.719	-0.25	-0.72	-0.47	-0.001	-0.156	0.41	0.82	0.41	0.976	8.495	8.81	8.52	-0.29	0.025	6.969	7.67	7.78	0.11	0.811
6	1.203	1.27	1.46	0.19	0.257	0.181	-0.46	-0.2	0.26	-0.381	10.625	10.67	10.88	0.21	0.255	5.618	5.13	5.14	0.01	-0.478
7	0.089	-0.09	-0.38	-0.29	-0.469	1.197	0.66	0.86	0.2	-0.337	8.677	8.29	8.16	-0.13	-0.517	4.289	3.9	4.08	0.18	-0.209
8	-0.702	-0.47	-0.64	-0.17	0.062	-0.472	0.3	0.06	-0.24	0.532	6.759	7.14	7.14	0	0.381	0.282	1.06	0.86	-0.2	0.578
9	0.143	-0.11	0.2	0.31	0.057	0.068	0.12	-0.06	-0.18	-0.128	5.732	5.56	5.6	0.04	-0.132	-1.607	-1.73	-1.52	0.21	0.087
10	0.883	1.12	1	-0.12	0.117	0.829	0.51	0.4	-0.11	-0.429	4.391	4.85	4.76	-0.09	0.369	-3.172	-3.35	-3.48	-0.13	-0.308
11	0.393	-0.41	-0.68	-0.27	-1.073	-0.287	-0.43	-0.26	0.17	0.027	1.688	0.66	0.56	-0.1	-1.128	-6.312	-6.48	-6.4	0.08	-0.088
12	-0.577	0.16	0.28	0.12	0.857	-0.877	-0.61	-1.12	-0.51	-0.243	-1.811	-0.94	-0.82	0.12	0.991	-8.582	-8.51	-8.84	-0.33	-0.258
13	0.223	0.36	0.42	0.06	0.197	0.495	0.33	1.18	0.85	0.685	-3.497	-3.09	-3.36	-0.27	0.137	-8.476	-7.9	-7.58	0.32	0.896
14	0.018	-0.46	-0.26	0.2	-0.278	-0.129	-0.09	-0.62	-0.53	-0.491	-5.62	-5.97	-5.74	0.23	-0.12	-9.351	-9.49	-9.56	-0.07	-0.209
15	-0.074	0.12	0.1	-0.02	0.174	-0.288	-0.25	-0.04	0.21	0.248	-7.545	-7.45	-7.44	0.01	0.105	-9.471	-9.55	-9.64	-0.09	-0.169
16	0.076	0.16	0.12	-0.04	0.044	-0.533	-0.55	-0.54	0.01	-0.007	-8.723	-8.58	-8.68	-0.1	0.043	-9.271	-9.27	-9.22	0.05	0.051
17	-0.929	-0.71	-0.5	0.21	0.429	-0.043	-0.36	-0.14	0.22	-0.097	-10.316	-9.45	-9.52	-0.07	0.796	-7.092	-7.11	-7.16	-0.05	-0.068
18	0.455	0.65	0.22	-0.43	-0.235	-0.065	-0.07	-0.2	-0.13	-0.135	-8.732	-9.15	-9.06	0.09	-0.328	-5.447	-5.53	-5.58	-0.05	-0.133
19	-0.204	-0.75	-0.68	0.07	-0.476	-0.282	-0.06	-0.34	-0.28	-0.058	-8.954	-9.31	-9.46	-0.15	-0.506	-3.356	-3.34	-3.32	0.02	0.036
20	-0.478	-0.67	-0.68	-0.01	-0.202	0.312	0.27	0.12	-0.15	-0.192	-7.864	-8.27	-8.24	0.03	-0.376	-0.528	-0.89	-0.86	0.03	-0.332
21	-0.571	0.04	0.28	0.24	0.851	0.697	0.35	0.9	0.55	0.203	-6.312	-5.53	-5.18	0.35	1.132	2.44	2.26	2.54	0.28	0.1
22	-0.216	0.02	-0.1	-0.12	0.116	-0.248	-0.22	-0.5	-0.28	-0.252	-3.749	-3.57	-3.72	-0.15	0.029	3.777	3.67	3.48	-0.19	-0.297
23	0.255	-0.35	-0.32	0.03	-0.575	-0.426	-0.04	0.08	0.12	0.506	-0.845	-1.44	-1.46	-0.02	-0.615	5.633	5.98	6	0.02	0.367
24	0.305	0.4	0.6	0.2	0.295	-0.435	-0.43	-0.3	0.13	0.135	1.525	1.51	1.44	-0.07	-0.085	7.371	7.38	7.3	-0.08	-0.071
Max error				0.56	-1.073				0.85	-0.999			10.88	0.35	1.132			9.86	-0.33	0.896

7.6 Reducing measurement uncertainty

The objective of work programmes in the UK National Gear Metrology Laboratory is to reduce measurement uncertainty on the shop floor. Simply reducing uncertainty on artefacts at the NMI is laudable and necessary but can only have limited impact. This is demonstrated by the analysis presented in Table 7.12.

Table 7.12 Effect of reducing NMI measurement uncertainty, using the ISO 18653 model to estimate measurement uncertainty.

Source of Uncertainty	Uncertainty Values (U_{95}) Micrometers			
Calibration Artefact	**1.0**	**0.5**	**0.25**	**0.5**
Artefact reproducibility	1.0	1.0	1.0	0.8
Workpiece effects	1.0	1.0	1.0	0.8
Root sum of squares	1.73	1.50	1.44	1.24
Bias	1.0	1.0	1.0	1.0
Total U_{95}	**2.73**	**2.50**	**2.44**	**2.24**

The analysis shows a simple estimate of measurement uncertainty following the method defined is ISO 18653 and ISO/TR10064/5. The sources of uncertainty are:

- Uncertainty of data from the calibration laboratory.
- The repeatability or possibly reproducibility of using that calibrated artefact to determine the bias.
- The uncertainty of measurement of measuring an uncalibrated workpiece, including repeatability, form errors, mounting errors etc. (The three uncertainty sources are combined as the root mean square, in accordance with standard procedures).
- The bias value from the calibrated artefact, which is added linearly to the measurement uncertainty in accordance with ISO 18653.

The table shows that reducing calibration data from the NMI from 1.0 to 0.5μm reduces overall measurement uncertainty by 0.23μm. A reduction in 0.5μm uncertainty from the NMI is a very difficult and expensive technical challenge with only a small impact on shop floor instrument measurement uncertainty. The effect of

further reducing NMI uncertainty to 0.25μm has even less impact, even if it were technically possible to achieve it.

The last two columns in Table 7.12 show the benefit of reducing NMI uncertainty combined with a very modest reduction in measurement uncertainty. Clearly if improvements in shop floor measurement uncertainty are needed the emphasis on any programme of work has to be concentrated on shop floor measurement practices, using calibrated artefacts that are similar in geometry to workpieces and minimising bias in results from good calibration practices.

7.7 Summary

- The measurement uncertainty budget method is considered the reference method for estimating measurement uncertainty.
- The application of this method may be simplified with the use of reproducibility data account for a number of individual uncertainty sources.
- The uncertainty budget method is more appropriate for calibration laboratory environments where it provides clear information on the significance of uncertainty sources.
- The comparator methods adopted by ISO and the BGA codes have small differences in their uncertainty estimates but are reasonable for shop floor applications with differences of less than 10% between the methods. The tests completed show that when bias is within the calibration data uncertainty, the ISO method provides closer results to the uncertainty budget method and is thus the preferred method.
- The ISO method should be revised however to return more realistic values where bias is a significant contribution.
- Errors in uncertainty evaluation become more significant on higher performance instruments where the calibration data uncertainty becomes dominant. Guidance on when this should be applied is required in the ISO Standard.

- No comparator methods based around comparison of evaluated parameters can be considered reliable for form or total error parameter uncertainty assessment. Comparison should be by measurement data points.

- The analysis of reducing shop floor uncertainty shows that reducing artefact calibration uncertainty has only limited value unless it is matched with improvements in shop floor performance.

Chapter 8

ALTERNATIVE EVALUATION METHODS

This chapter introduces alternative methods of evaluating flank profile and helix measurements that avoid the use of evaluated parameters. It is implemented as part of the comparator method of estimating uncertainty for profile measurement and is further developed as part of a Monte Carlo Simulation to model the measurement process. The benefits and limitations of this approach are also discussed.

8.1 Background

The limitations of parameter based measurement uncertainty evaluations was discussed with respect to pitch measurement in Chapter 7. It concluded that the use of maximum evaluated parameters such as adjacent pitch or cumulative pitch was suspect because the position that the maximum errors occur are not considered by this type of analysis. The same issue affects other areas of measurement such as roundness (form) measurement, but in these fields it is usual to report only the measurement data results, at defined positions, rather than use the evaluated roundness parameter [Taylor-Hobson, 1999]. While this procedure is widely used, it is not favoured by users of roundness measurement equipment because it is difficult to verify the performance of an instrument without comparing actual data values manually.

The use of data point comparison methods applied to involute profile measurement is investigated by a number of methods. Initial work to develop this approach was undertaken by the National Institute of Advanced Industrial Science and Technology [Kondo, 2002], using a novel ball artefact as a surrogate involute artefact. NGML were involved with a comparison exercise arranged by AIST, Japan and the results from this work are discussed in the next section. The use of involute artefacts is then investigated

and the performance of the Klingelnberg P65 is quantified by analysis of individual measurement data points. The method is then applied to involute artefact calibration with a comparison of involute data errors with PTB, Germany. Finally the evaluation of data points is extended by the use a Monte Carlo Simulation of the process to estimate gear measurement uncertainty.

8.2 Japan Double Ball Artefact (DBA)

The replacement of an involute with a circular arc is not new [AGMA 931] but the use of a precision calibration sphere, as shown in figure 8.1, is a unique method of evaluating involute gear measuring instruments. This technique was developed in Japan [Kondo] and implemented as a solution for establishing traceability to National Standards throughout Japan [Takatsuji]. The method is not without its problems and in the opinion of the author, is not suitable for shop floor instruments. The DBA measurement is highly sensitive to some geometric errors that are negligible when measuring an involute profile and in some cases may result in erroneous interpretation of the causes of measured errors. However there some benefits in using this type of artefact and analysis method.

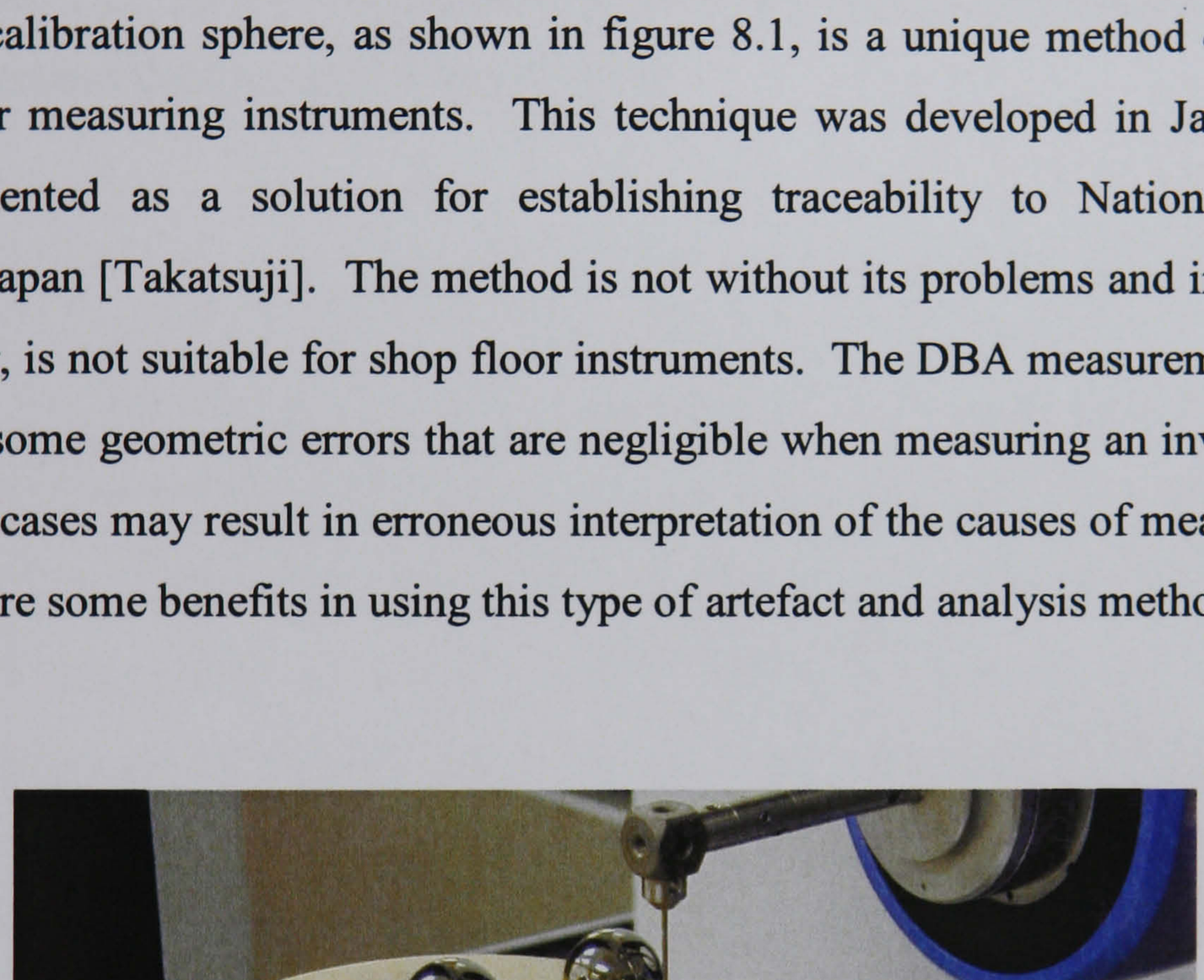

Figure 8.1 Japanese Double Ball Artefact (DBA) on the Klingelnberg P65 in the NGML.

The DBA is required to be manually set up on a fixture mounted on the rotary table, see figure 8.1, because automatic datum axis measurement and correction routines are not

available for this arrangement of datum surfaces. The radial datum is the centre of the inner ball and the 'Zerodur' flat defines the axial datum. The probe shown in figure 8.1 scans the surface of the surrogate involute (ball) by measuring the ball as an involute profile. Deviations between the sphere surface and the involute form are recorded as deviations in the measurement profile. The method of calculating the deviations is described in an ISO Technical Report ISO/TR 10064-5, and requires detailed knowledge of the mounting errors of the artefact and the actual probe radius. The deviations between the sphere and the involute are large, of the order 80μm and are shown in figure 8.2. Errors in probe size, artefact runout and probe datum affect the resulting deviations, and these are described in detail in ISO TR 10064-5.

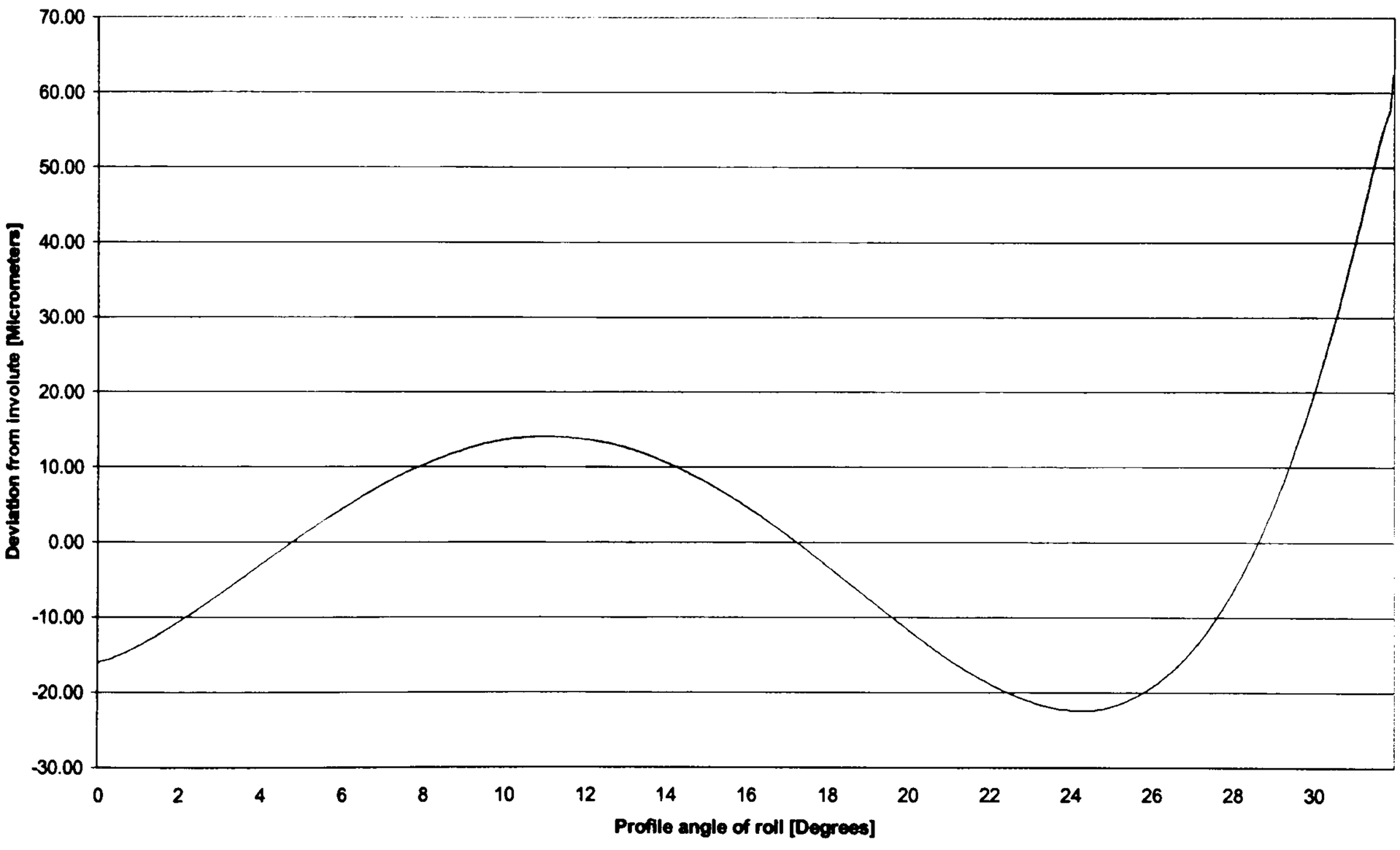

Figure 8.2 Deviation between sphere and involute form (measured as a left flank)

A perfect involute yields a horizontal straight line with zero deviations. The large deviations on a DBA mean that true deviations from the theoretical shape need to be evaluated and subsequent errors analysed on a point by point basis so the evaluation by traditional profile parameters is not used. An example evaluation of deviations between the theoretical involute deviation (computed from the calibration ball size and position) and actual measured deviation was provided by the Japanese NIM and is presented in figure 8.3. The profile data from the Klingelnberg P65, 480 points per trace length, was

extracted from the instrument using existing software functions and the mean and standard deviation for each data point for 5 tests was analysed.

The results analysis are shown in figure 8.3 [Kubo]. The blue error curve shows the deviation between NGML measured data and the calculated theoretical curve (shown in black). Key features of the NGML results are :

- as roll angle increases to around 18° the error falls to -2.5 micrometers (shown in blue). This apparent error could be caused by probe magnification errors, change in effective probe radius or, as suggested by the NIM analysis data tabulated below the graph, an eccentricity or mounting error.
- If the results are corrected for the calculated eccentricity the deviation between corrected profile and theoretical profile is significantly reduced and is shown in red, with a deviation below 0.5μm.
- The results in figure 8.3 (blue trace) also show a form error or undulation over the surface which is probably caused by the guideway ball bearings. The benefit of the sphere as a surrogate involute artefact is that its form errors are of the order of 10nm thus enabling the detection and evaluation of high frequency deviations in guideways.

The mean deviation between an involute and a sphere yield large form errors as shown in figure 8.2 and the standard deviation of each (the mean of 5 tests on each data point) is shown in figure 8.4. The data point resolution is 0.1μm and this yields the somewhat unusual pattern in the standard deviation results in figure 8.4.

The results presented in figure 8.4 show that as the deviation from involute increases the standard deviation also increases except over the mid section where there is a significant increase as the deviation trend changes from negative to positive. This could be a hysteresis affect but it is more likely that it is an artefact from working with data which is less than the resolution of the reported results. Further investigation is thus recommended.

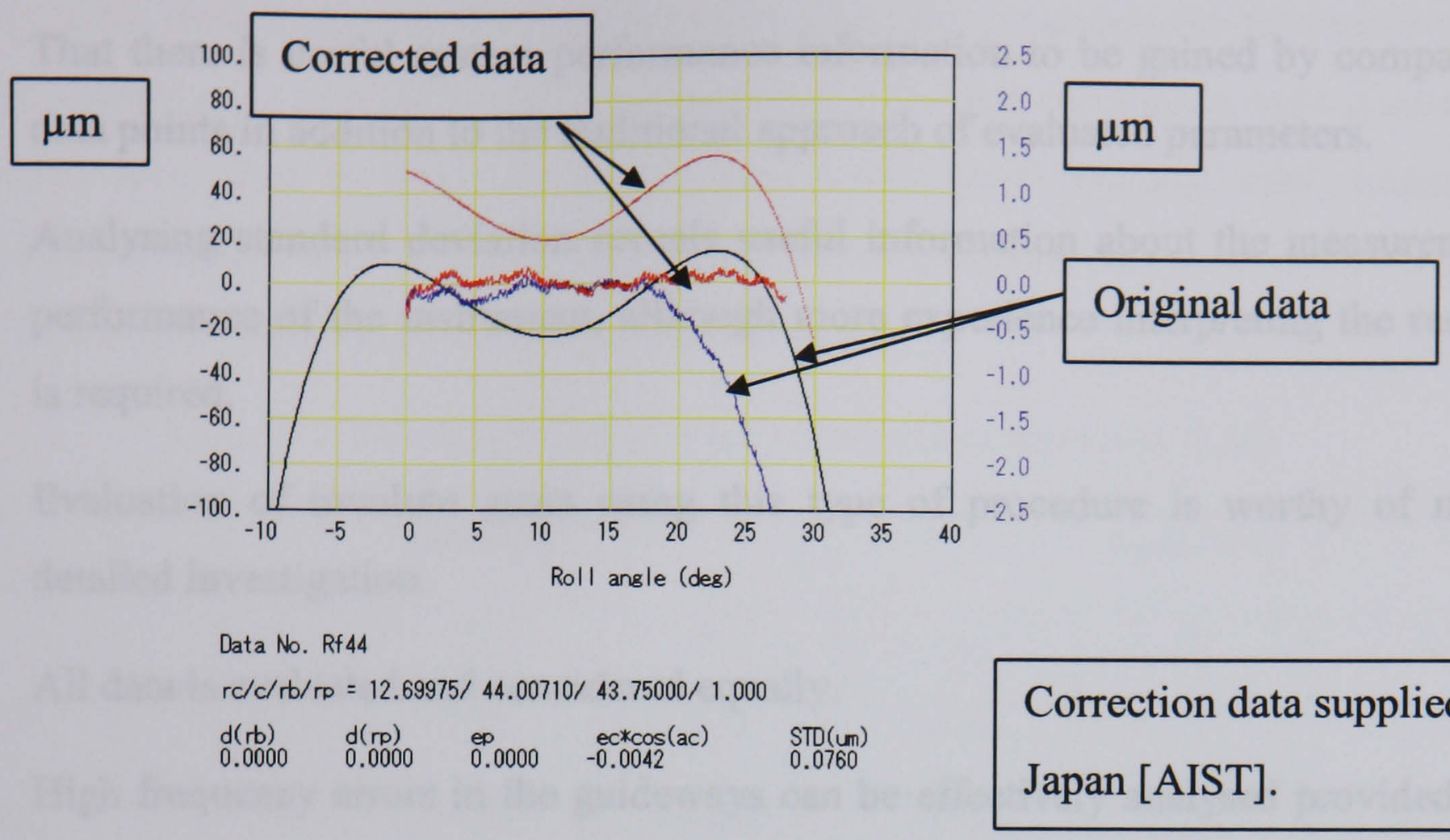

Correction data supplied by Japan [AIST].

Figure 8.3 Example DBA analysis prepared by AIST, Japan showing measured deviations from the theoretical shape.

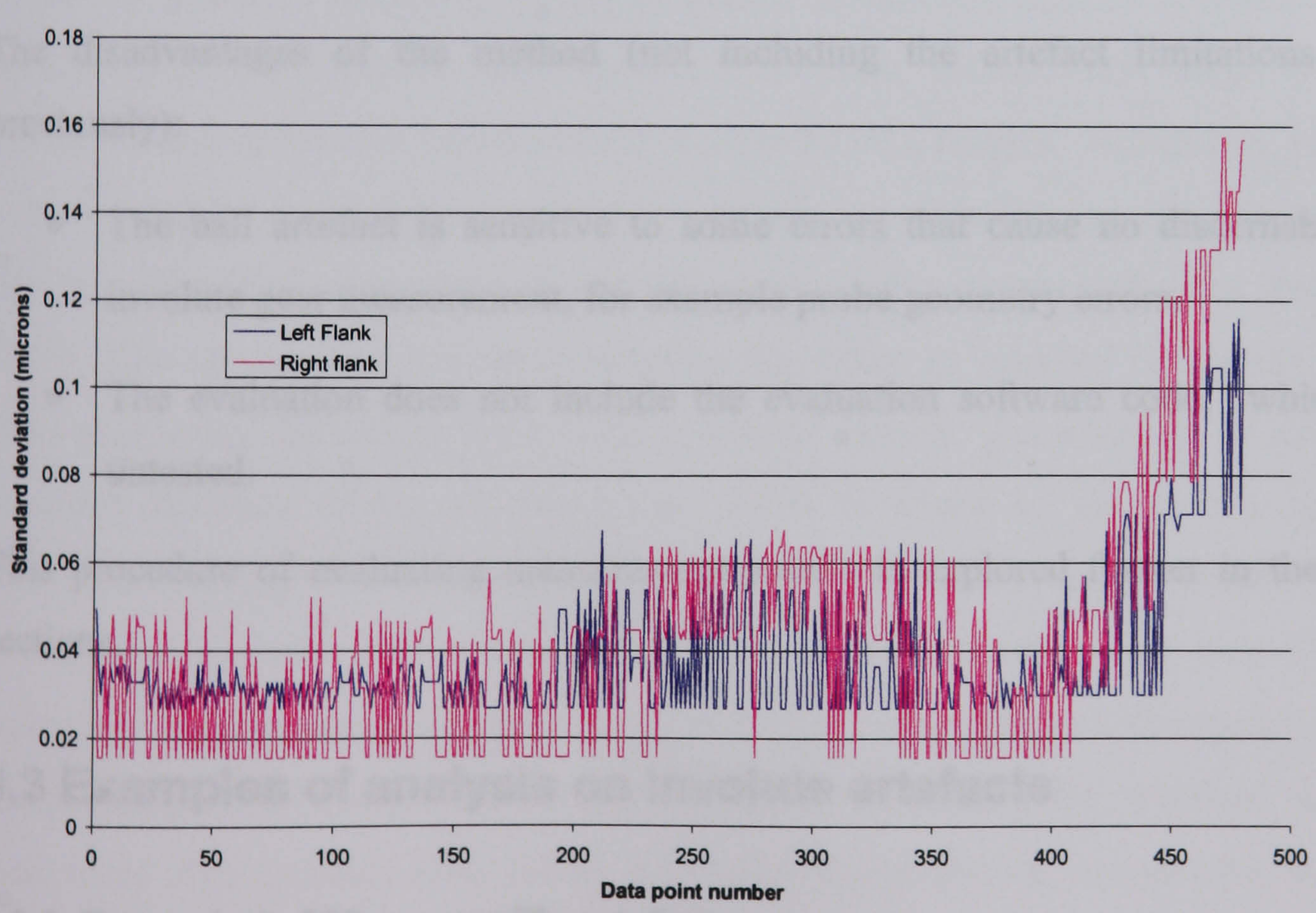

Figure 8.4 Standard deviation of the 480 data points for left and right flank of the Japanese DBA.

We may conclude from these initial tests

- That there is useful system performance information to be gained by comparing data points in addition to the traditional approach of evaluated parameters.
- Analysing standard deviation reveals useful information about the measurement performance of the instrument, although more experience interpreting the results is required.
- Evaluation of involute gears using this type of procedure is worthy of more detailed investigation.
- All data is evaluated and considered equally.
- High frequency errors in the guideways can be effectively analysed provided the artefact has appropriately small form errors, similar to the artefact tested.
- The evaluation process by its nature includes the position of errors.
- The surrogate artefact can yield useful information about the probe performance provided that other sources of error can be eliminated.

The disadvantages of the method (not including the artefact limitations discussed previously):

- The ball artefact is sensitive to some errors that cause no discernable error in involute gear measurement, for example probe geometry errors.
- The evaluation does not include the evaluation software code, which remains untested.

This procedure of evaluating measurement results is explored further in the following sections.

8.3 Examples of analysis on involute artefacts

8.3.1 Example 1: 200mm profile artefact

The 200mm profile artefact was selected for the initial investigation because good compatibility between PTB and NGML has been achieved over 8 years.

The Klingelnberg P65 gathers 480 measurement points during a profile traverse from root to tip. Five measurements were taken using standard measurement procedures that involve indexing the artefact by 90° after each test. The test conditions were typical for calibration conditions to minimise uncertainty: runout correction was used, alignment between axis centres was less than 1μm TIR, and temperature varied between 20.05 to 20.07°C measured with an NPL calibrated thermistor.

Table 8.1 200mm profile artefact parameter comparison (μm)

Results	Left flank			Right Flank		
	$f_{H\alpha}$	F_{α}	$f_{f\alpha}$	$f_{H\alpha}$	F_{α}	$f_{f\alpha}$
NGML	+0.02	2.78	2.78	+1.24	2.78	2.58
(SD)	(0.13)	(0.08)	(0.08)	(0.05)	(0.04)	(0.04)
PTB	-0.6	3.8	3.4	+0.9	3.6	3.0
[U_{95}]	[±1.0]	[±1.4]	[±1.0]	[±1.0]	[±1.4]	[±1.0]

Table 8.1 shows a summary of the evaluated parameters usually analysed for profile measurement performance showing the PTB data, NGML and data and Standard Deviation and deviations between PTB and the NGML results. Acceptable compatibility between results is demonstrated and no significant variations except that the standard deviation for flank slope error $f_{H\alpha}$ is noticeably higher on the left flank than the right flank. The cause of the difference between the values of standard deviations is not clear from examining the results table or the graphical results. Examination of the plot of the standard deviation of the individual data points in figure 8.5 shows that the left flank deviations are significantly higher on values near the end of active profile (points 430 onwards). The left flank data was analysed without the third test (run 3) and some reduction in the standard deviation at the end of active profile near data point 480, but the trend remains the same. Thus the benefit of evaluating the standard deviation of individual measurement data points has been clearly shown because the cause of the increase in standard deviation on the 200mm left flank profile errors are identified near the end of active profile. Appropriate steps can be taken to identify the cause of this error, probably from either a contaminant on the artefact or the instrument guideway.

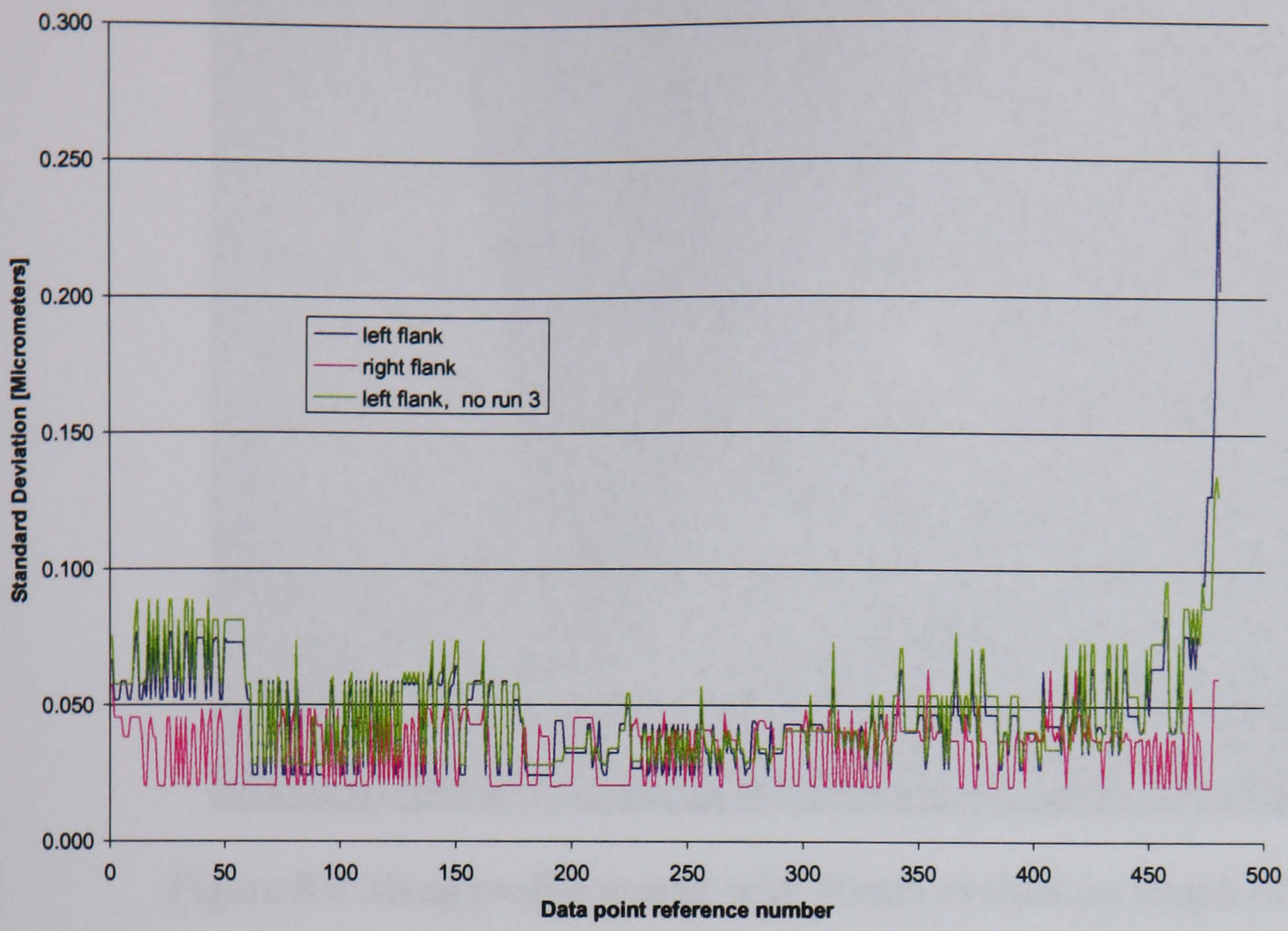

Figure 8.5 Standard deviation of profile measurement data points measured on the 200mm profile artefact.

8.3.2 Example 2: Maag profile master

The Maag SP200 lead and profile measuring instruments use a single base disc and lever system to generate the correct involute curve and helix. They have a capacity of 2m diameter and represented the limit of development of the base disc method of measuring involute gears. The instrument is calibrated using involute artefacts of the form shown in figure 8.6. The artefact has a traditional involute form but because the instrument is large it has a 90mm length of roll, nearly 2.5 times greater than any artefacts used in the NGML. Figure 8.7 shows example involute measurement results which illustrate the relatively straight involute form and also the waviness of the form error.

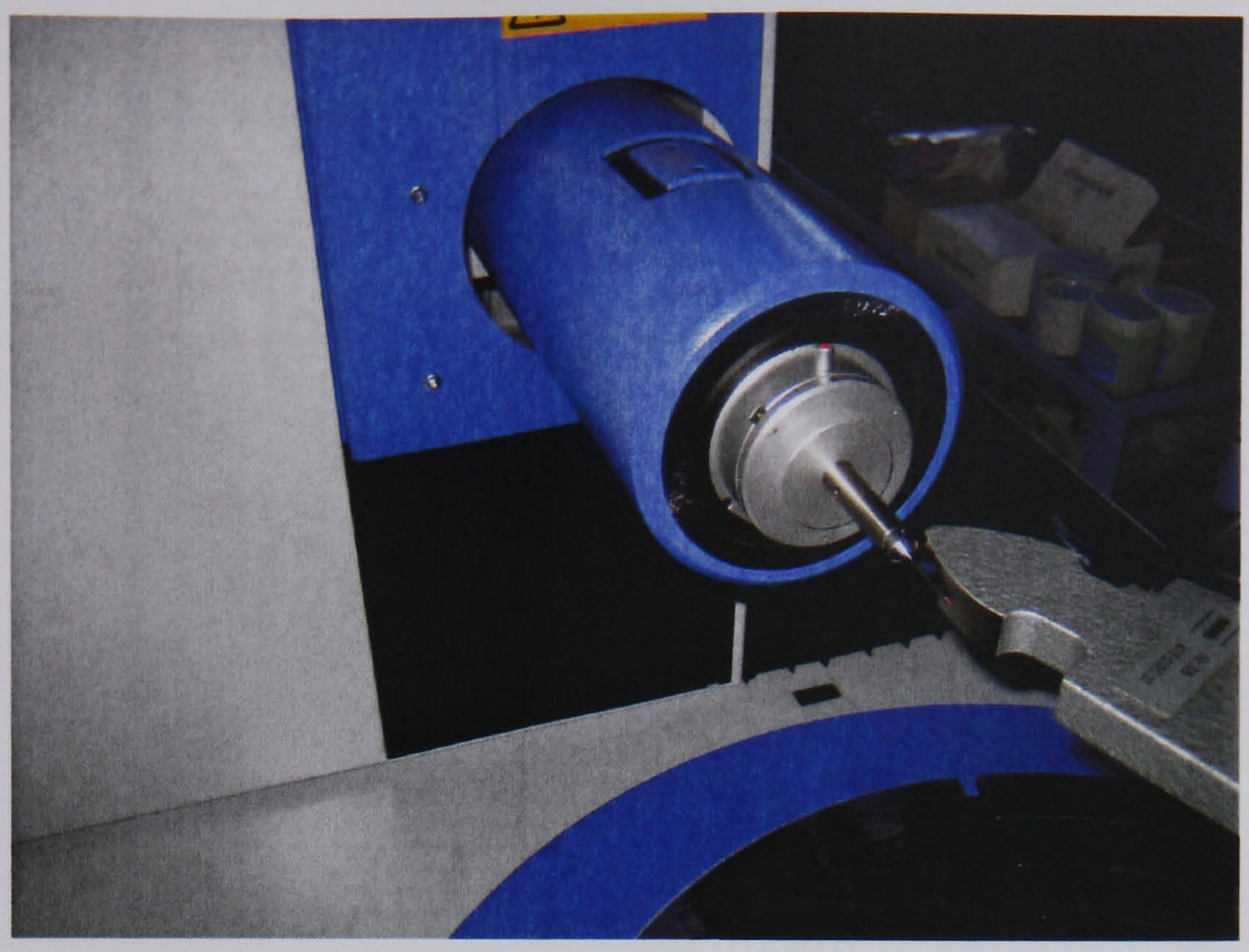

Figure 8.6 Maag profile master with 90mm evaluation length of roll

The results from the evaluation of profile measurement parameters are shown in Table 8.2 and show typical standard deviations for measuring involute masters, consistent with the smaller 200mm profile master shown in Table 8.1.

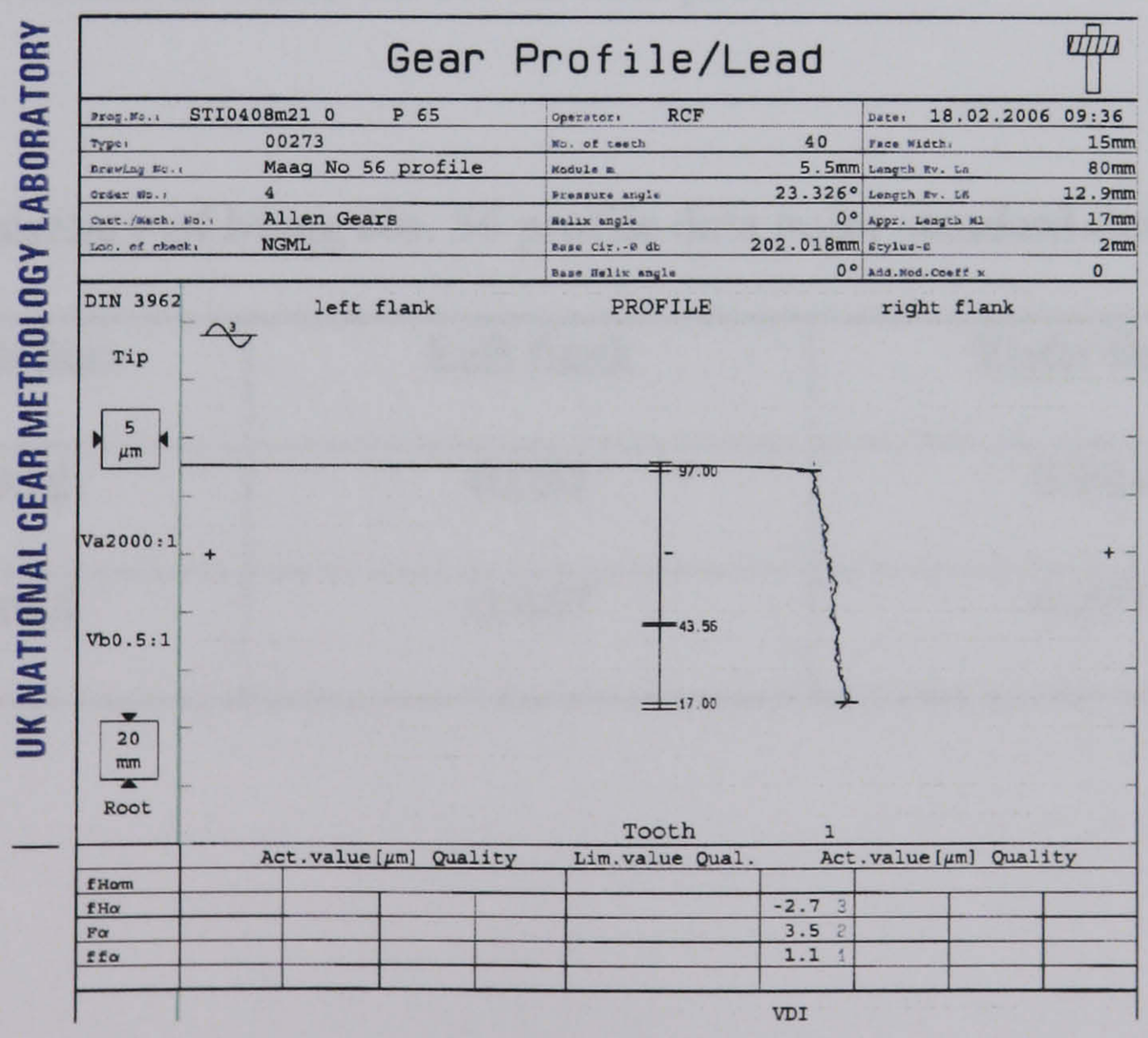

Figure 8.7a Maag profile master graphical results (right flank).

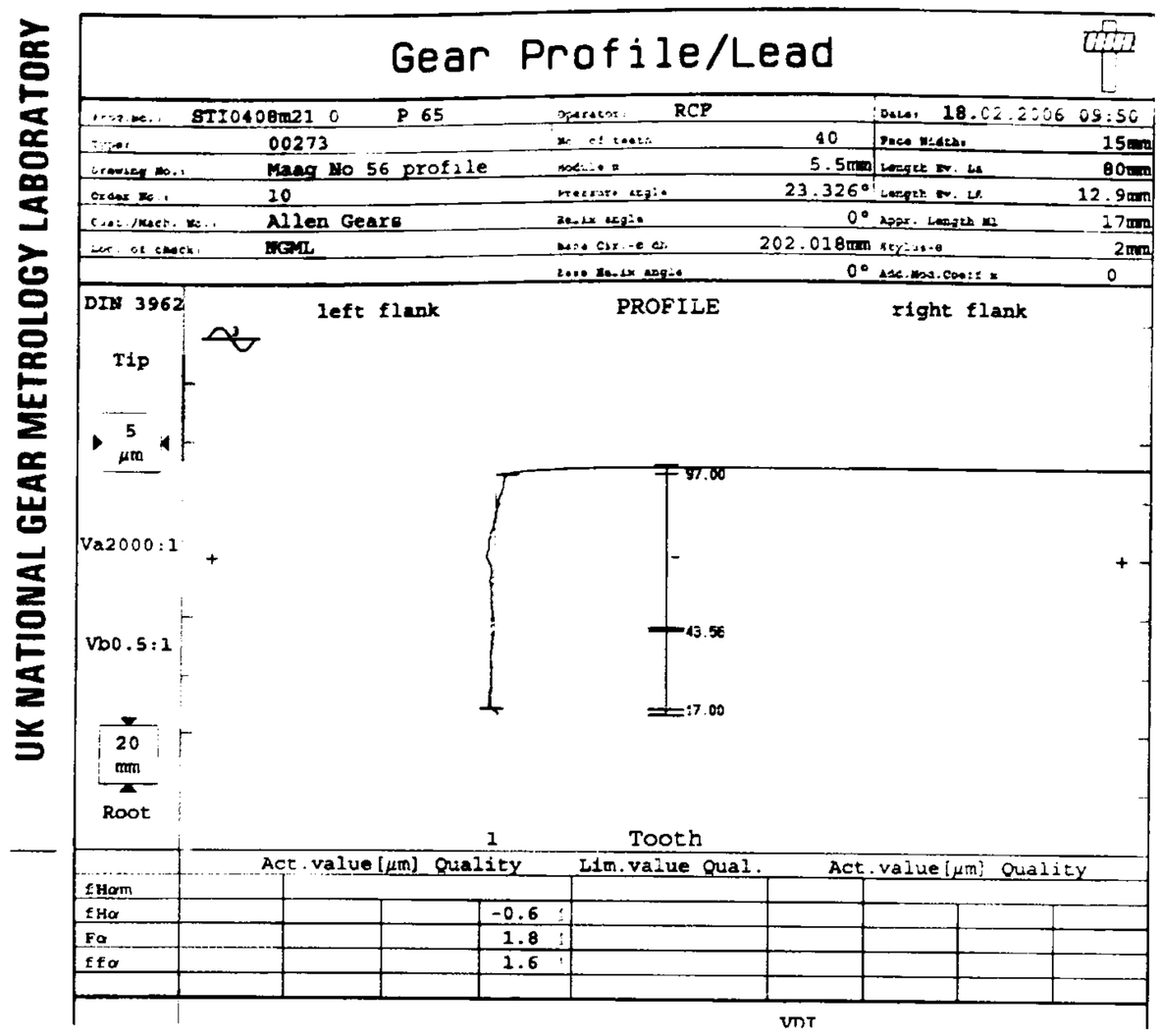

Figure 8.7b Maag profile master graphical results (left flank).

Evaluating the measurement point data in the same way as the 200mm master, ie for 5 repeat tests indexed at 90 degree intervals on the rotary table results in standard deviations shown graphically in figure 8.8 for the artefact mounted in the normal orientation and figure 8.9 when mounted inverted. The mean of the standard deviation of the results is summarised in Table 8.2 for all data points.

Table 8.2 Summary of Maag No. 56 profile data point standard deviation [µm].

Orientation	Left flank	Right flank
Normal	0.052	0.064
Inverted	0.047	0.037

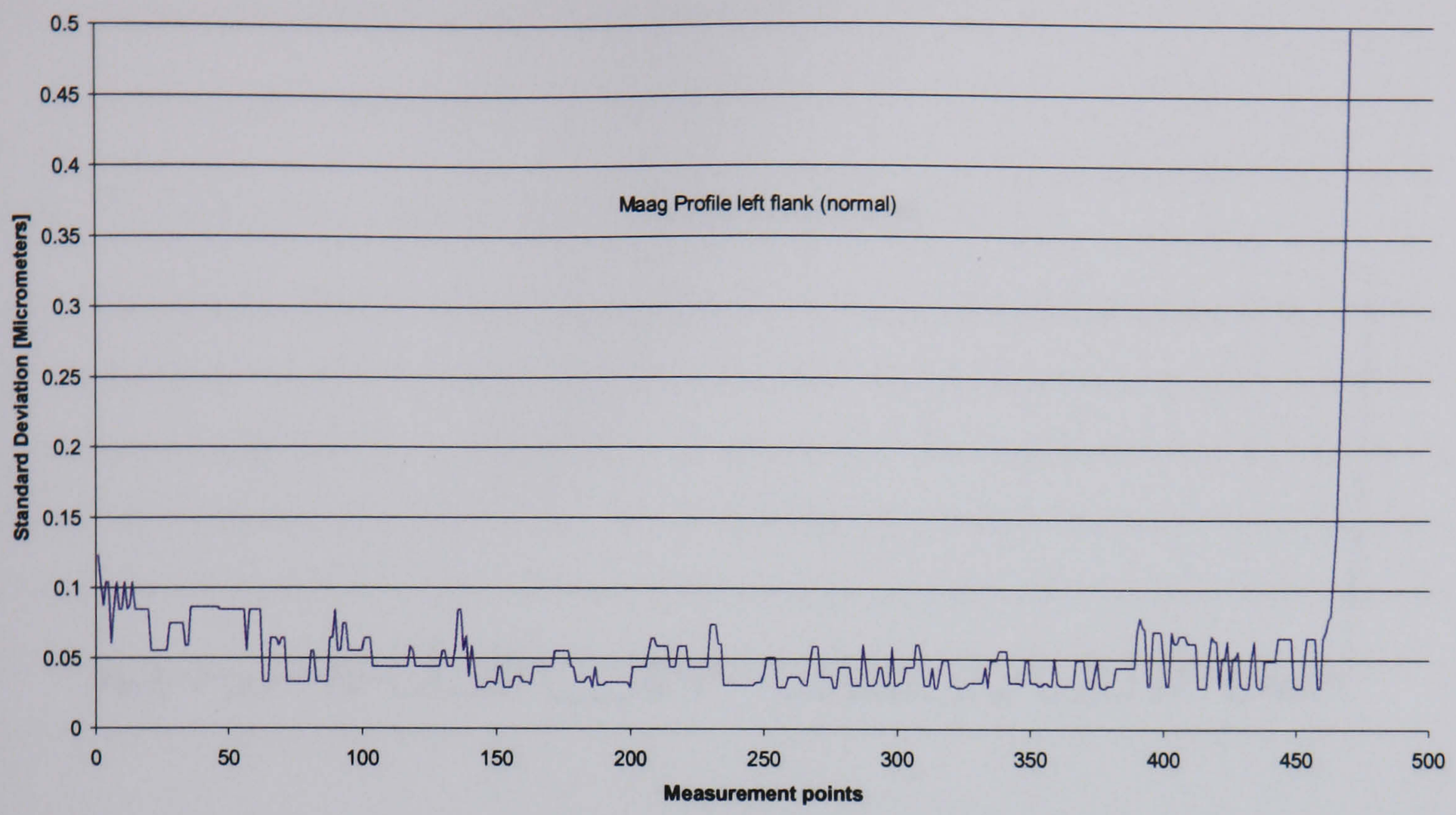

Figure 8.8a Maag profile master No. 56, left flank standard deviation of measurement data points from 5 tests using standard NGML procedure (normal orientation).

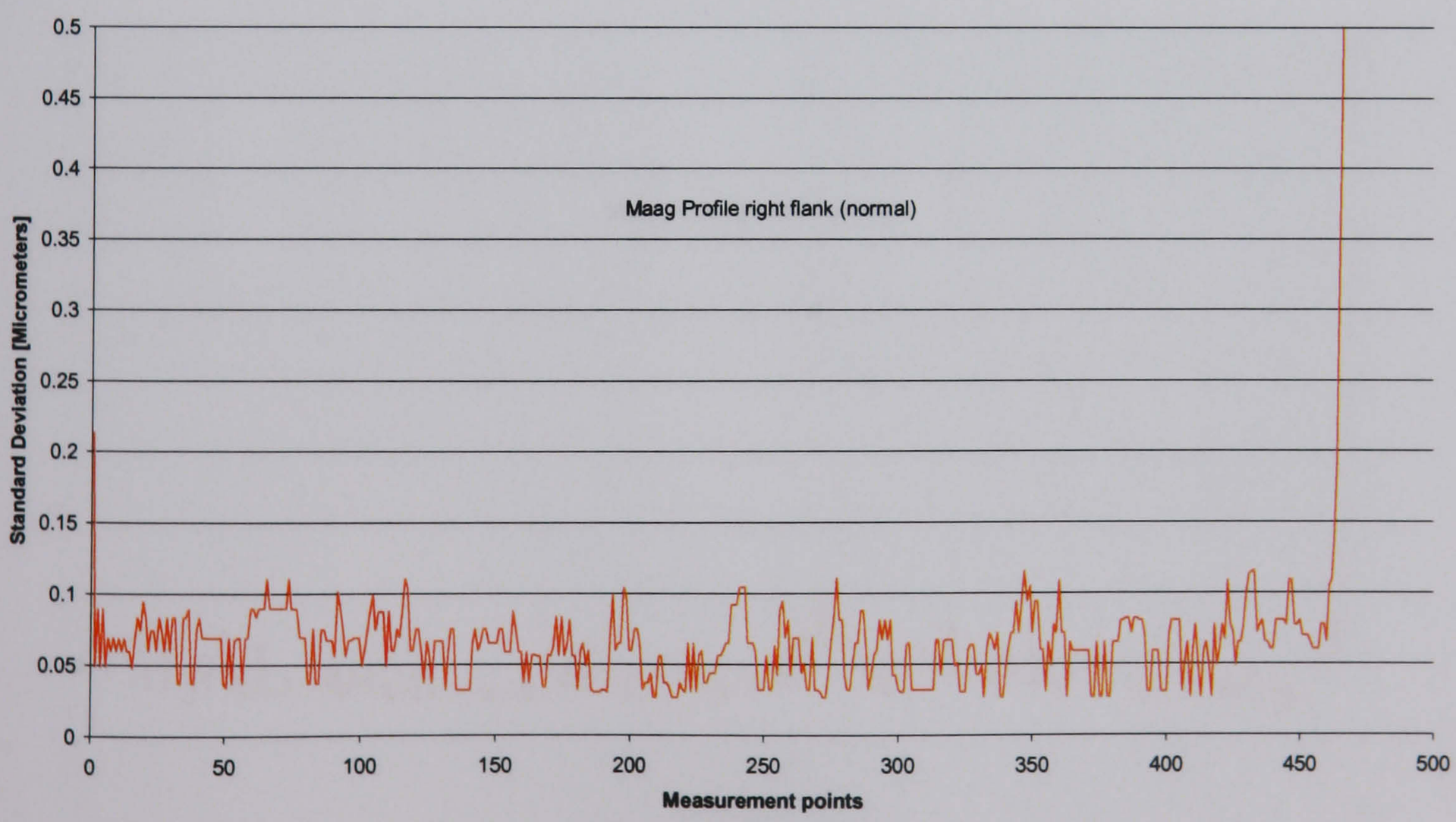

Figure 8.8b Maag profile master No. 56, right flank standard deviation of measurement data points from 5 tests using standard NGML procedure (normal orientation).

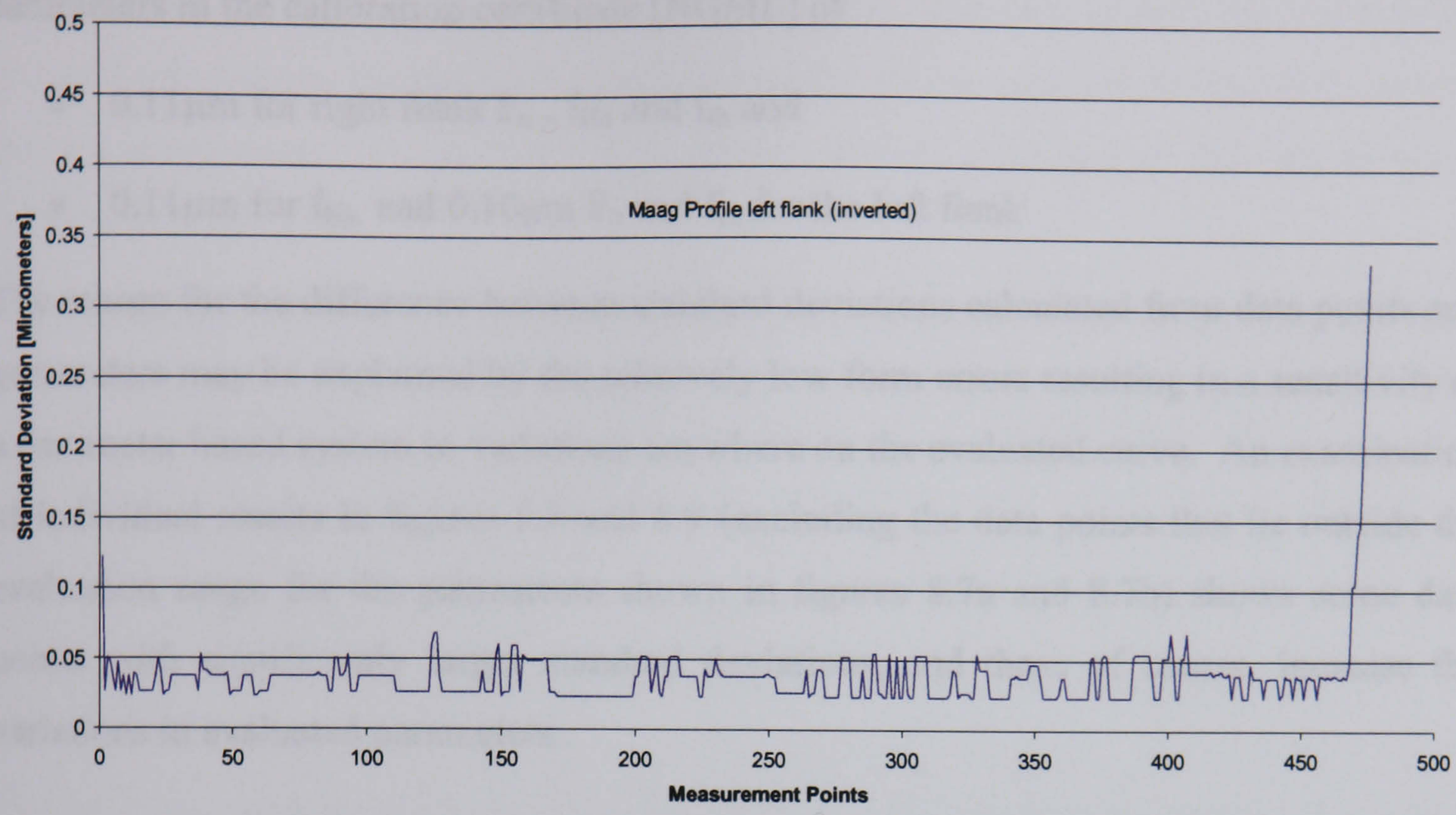

Figure 8.9a Maag profile master No. 56, left flank standard deviation of measurement data points from 5 tests using standard NGML procedure (inverted orientation).

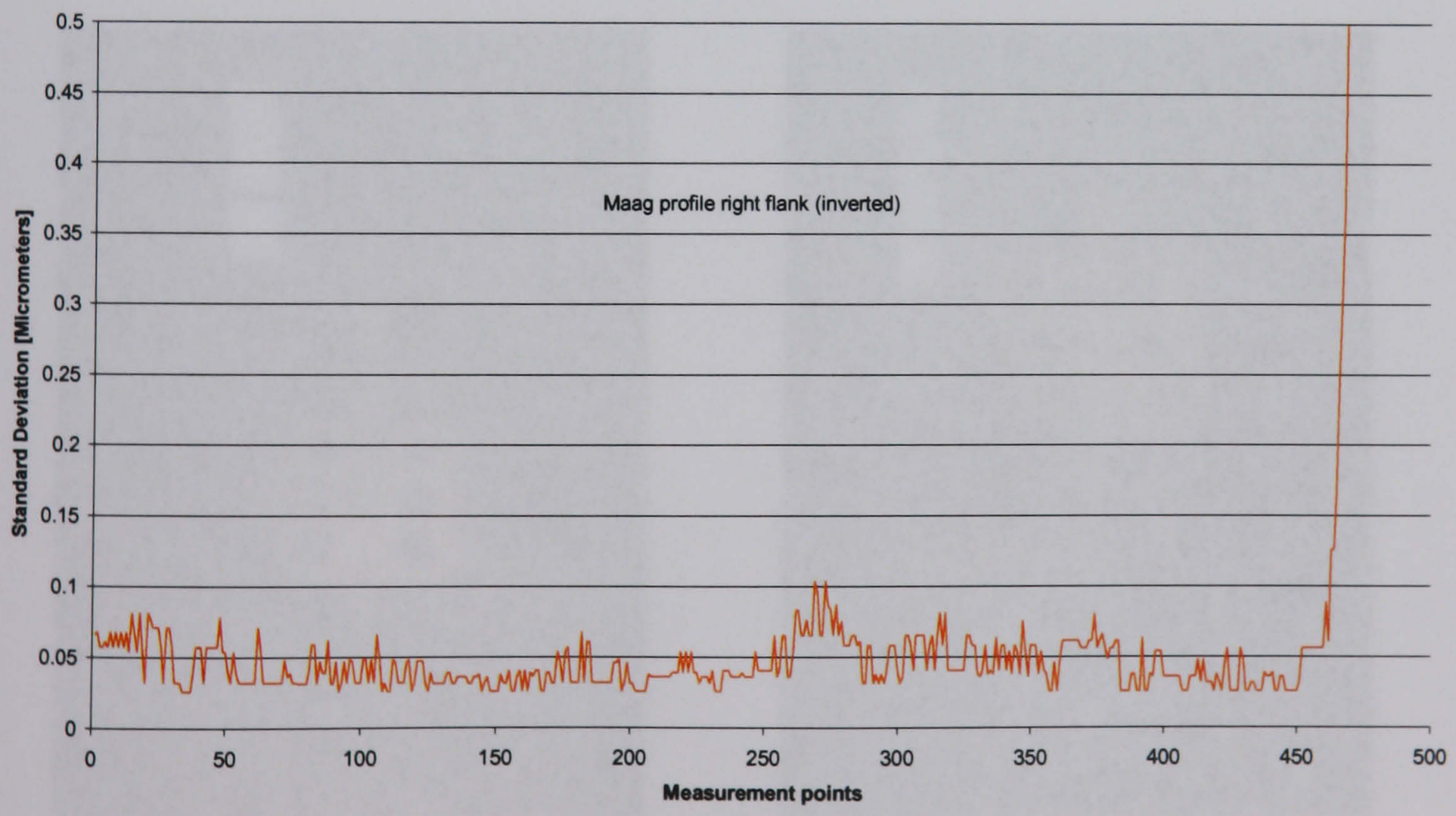

Figure 8.9b Maag profile master No. 56, right flank standard deviation of measurement data points from 5 tests using standard NGML procedure (inverted orientation).

The results in Table 8.2 can be compared to standard deviation for the evaluated parameters in the calibration certificate [NGML] of

- 0.11μm for right flank F_α , $f_{H\alpha}$ and $f_{f\alpha}$ and
- 0.11μm for $f_{H\alpha}$ and 0.10μm F_α and $f_{f\alpha}$ for the left flank

The reason for the difference between standard deviations calculated from data points and parameters may be explained by the relatively low form errors resulting in a sensitivity of a parameter based system to variations anywhere on the evaluated curve. An examination of individual results in figures 8.8 and 8.9 (excluding the data points that lie outside the evaluation range for the parameters shown in figures 8.7a and 8.7b) shows some data points with significantly larger standard deviations, and these of course, increase the variations in evaluated parameters.

8.3.3 Example 3: Maag helix artefact

The analysis was extended to the the helix artefact shown in figure 8.10, also designed for the Maag SP200. The artefact has two calibrated flanks representing a left and right hand helix and a face width of 155mm.

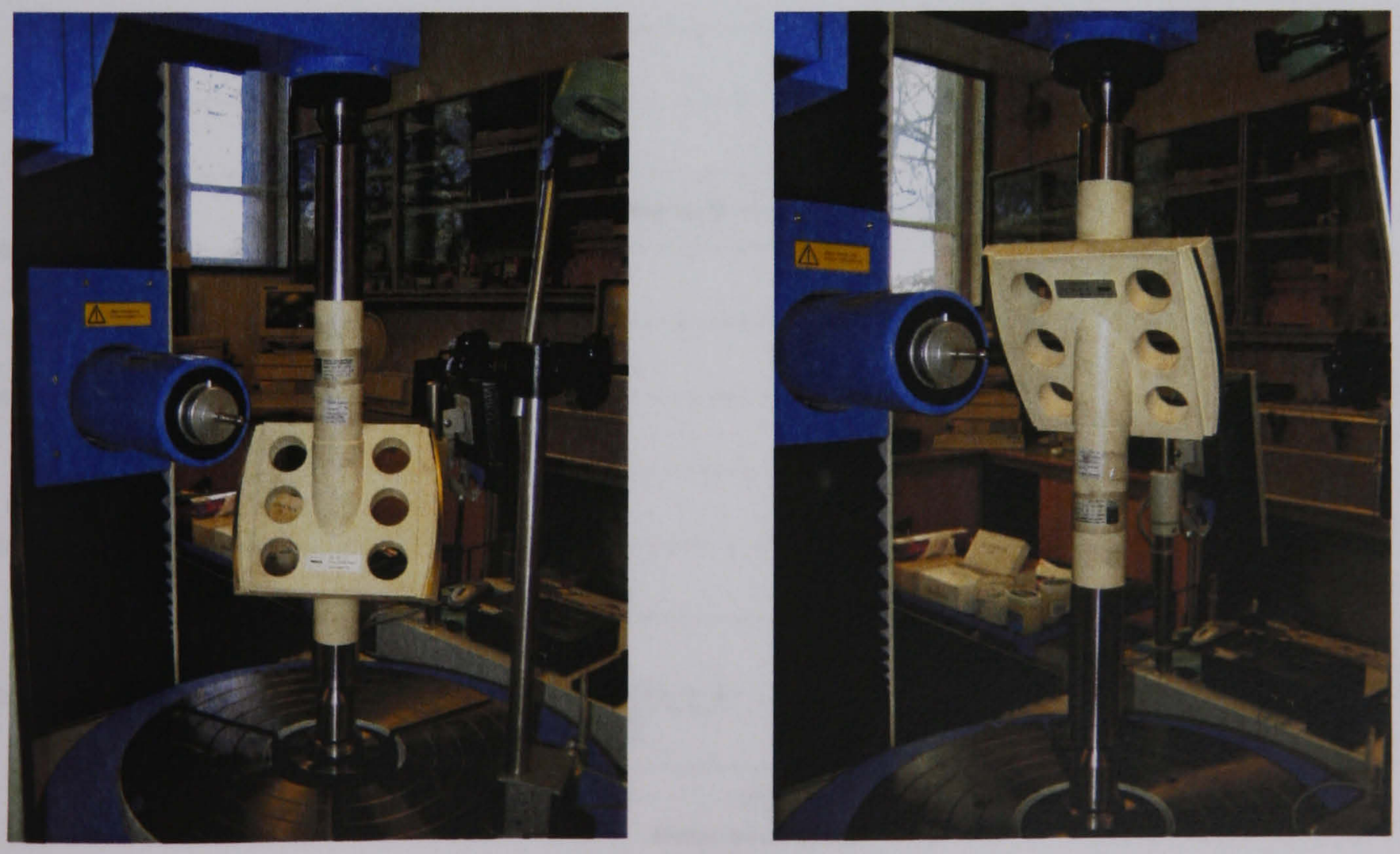

Figure 8.10 Maag No 58 helix master measured normal (left) and inverted (right) on the Klingelnberg P65 at NGML.

Figures 8.11 and 8.12 show the variation in standard deviation of the mean helix measurement data points for the left and right helix, mounted in both the normal and inverted orientation. Figure 8.13a and b shows the measurement error traces illustrating the low form errors. A summary of the mean standard deviation of the data points is presented in Table 8.3.

Table 8.3 Summary of Maag No. 58 helix data point standard deviation [μm].

Orientation	Left hand helix	Right hand helix
Normal	0.051	0.047
Inverted	0.047	0.080

The 0.080μm mean standard deviation for the right helix reported in Table 8.3 appears to be due to the larger standard deviation of the right flank at either end of the helix while the mid region has a standard deviation of around 0.040μm, as shown in figure 8.12 (RH flank). Additional work is recommended to investigate these effects further because at present there is no explanation for these differences.

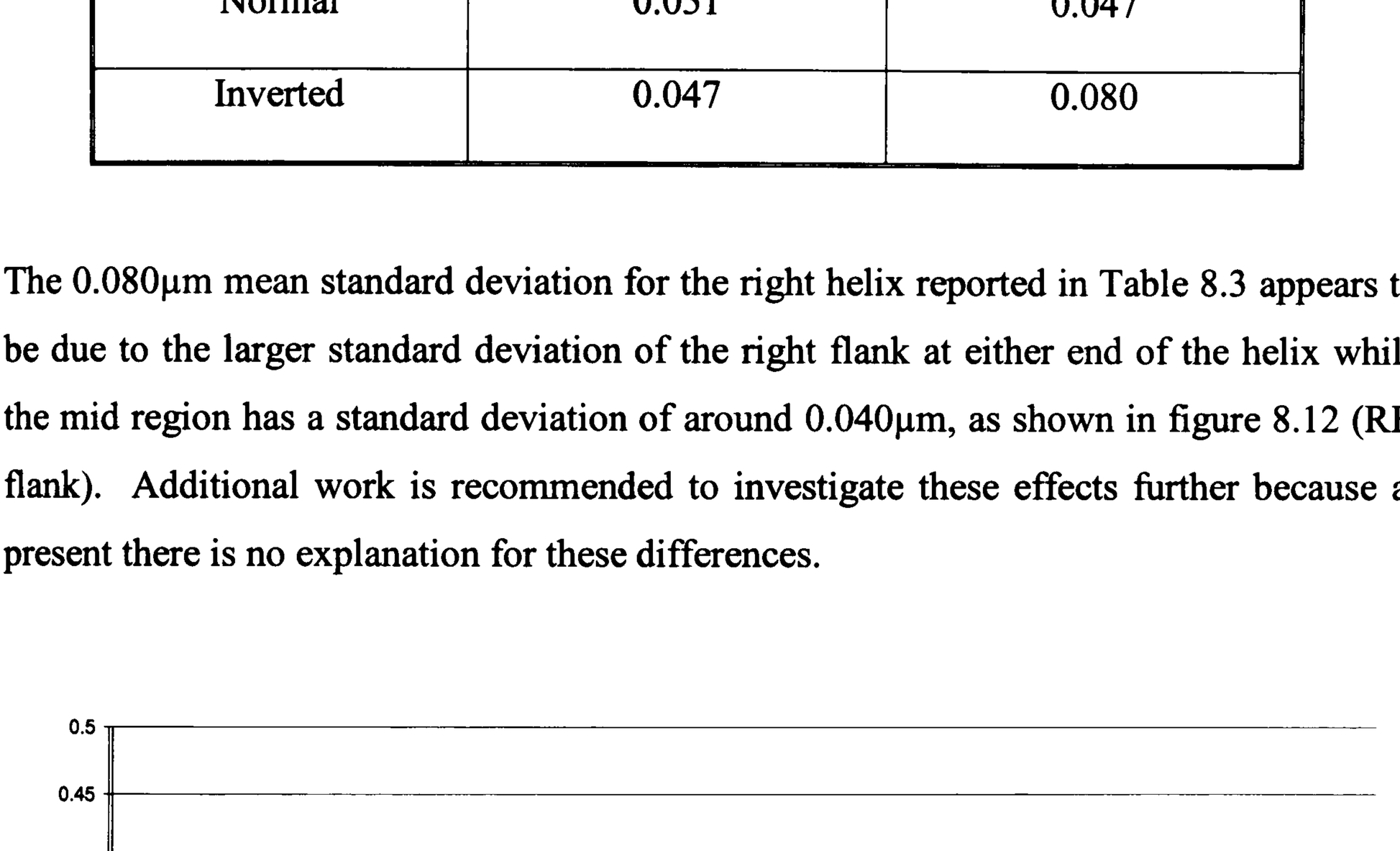

Figure 8.11a Maag 58 helix Master, left flank standard deviation of measurement points from 5 tests using the standard NGML procedure (normal orientation).

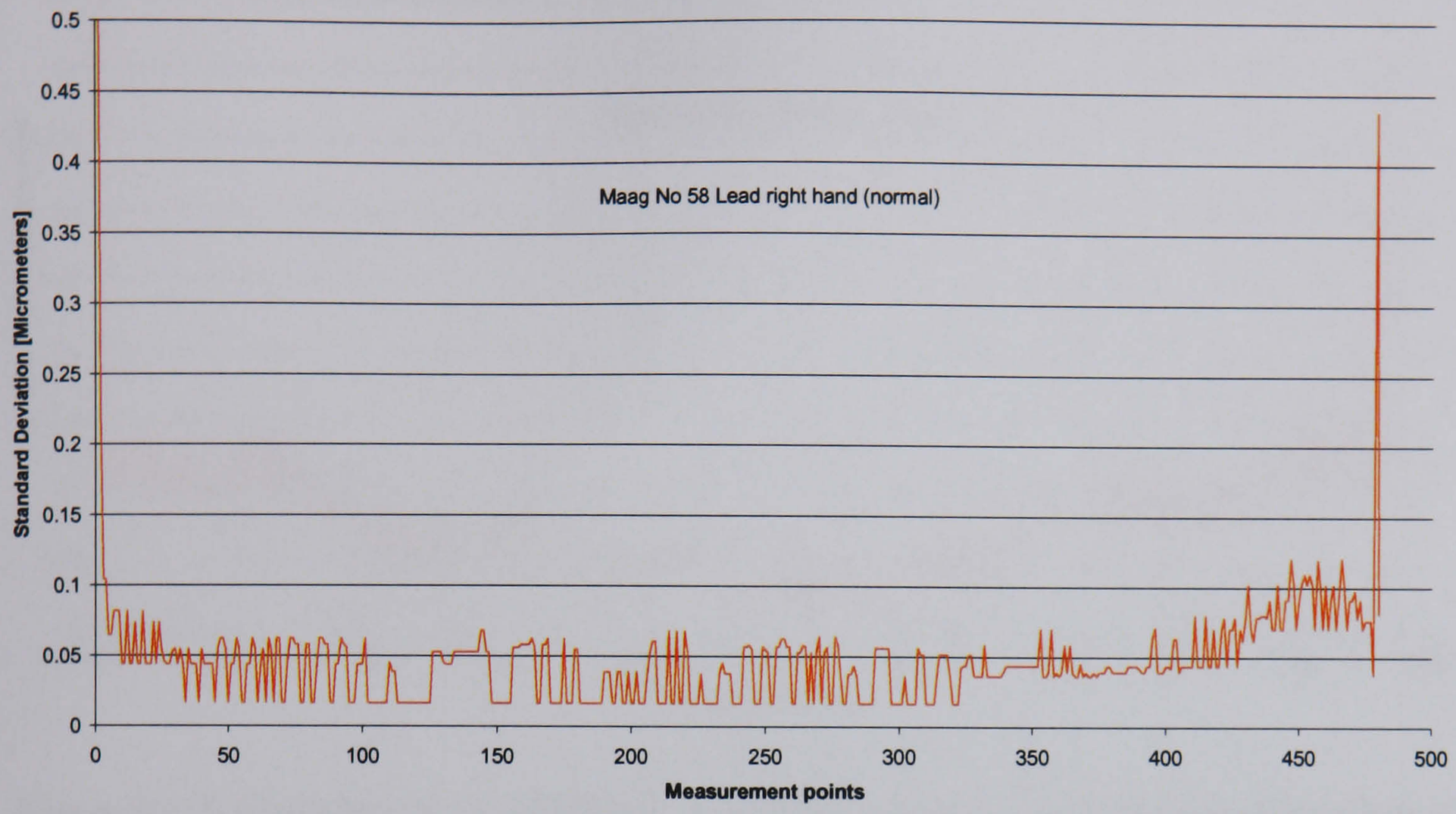

Figure 8.11b Maag 58 helix Master, right flank standard deviation of measurement points from 5 tests using the standard NGML procedure (normal orientation).

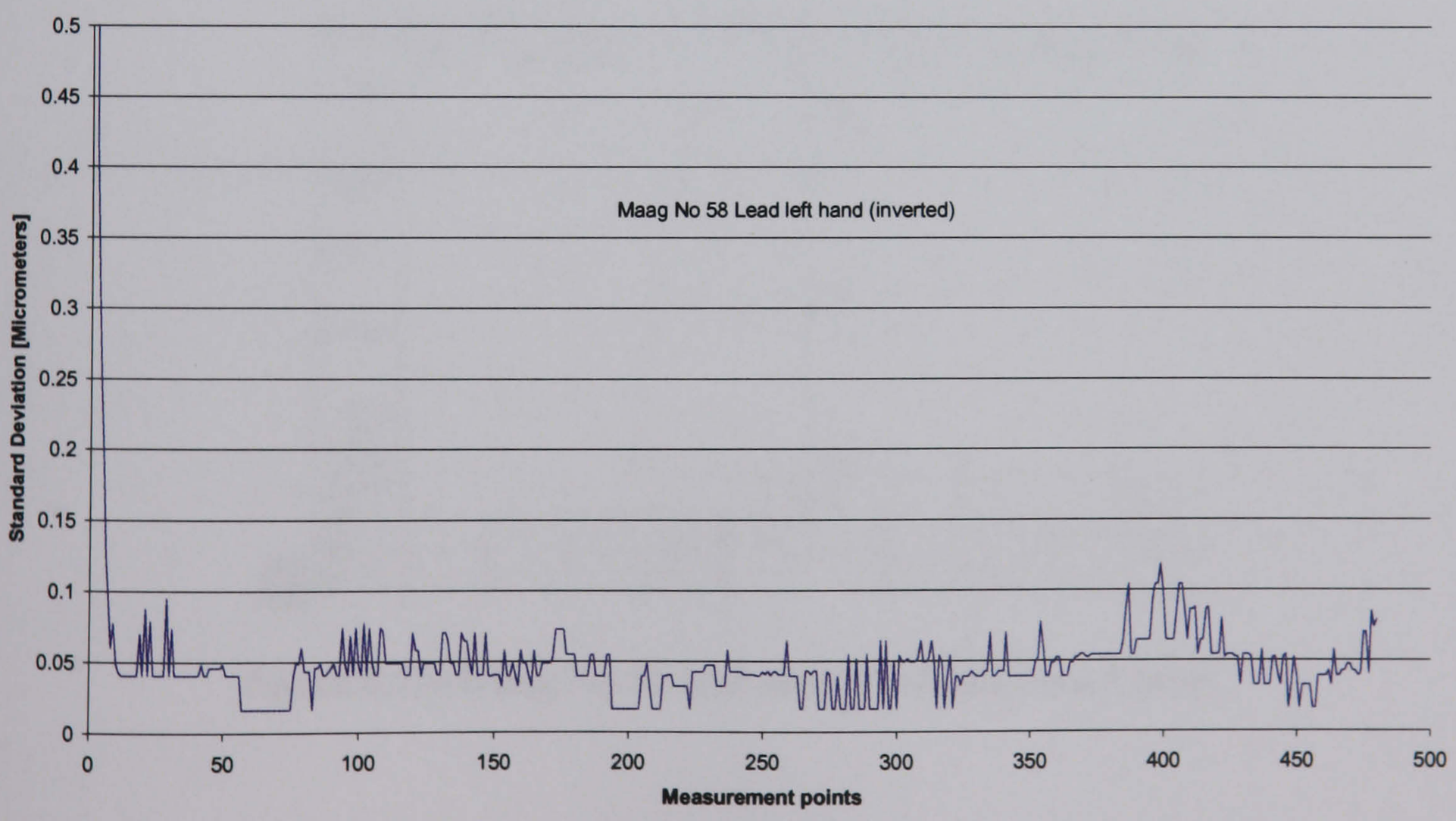

Figure 8.12a Maag No 58 Lead Master, left flank standard deviation of measurement points from 5 tests using the standard NGML procedure (inverted orientation).

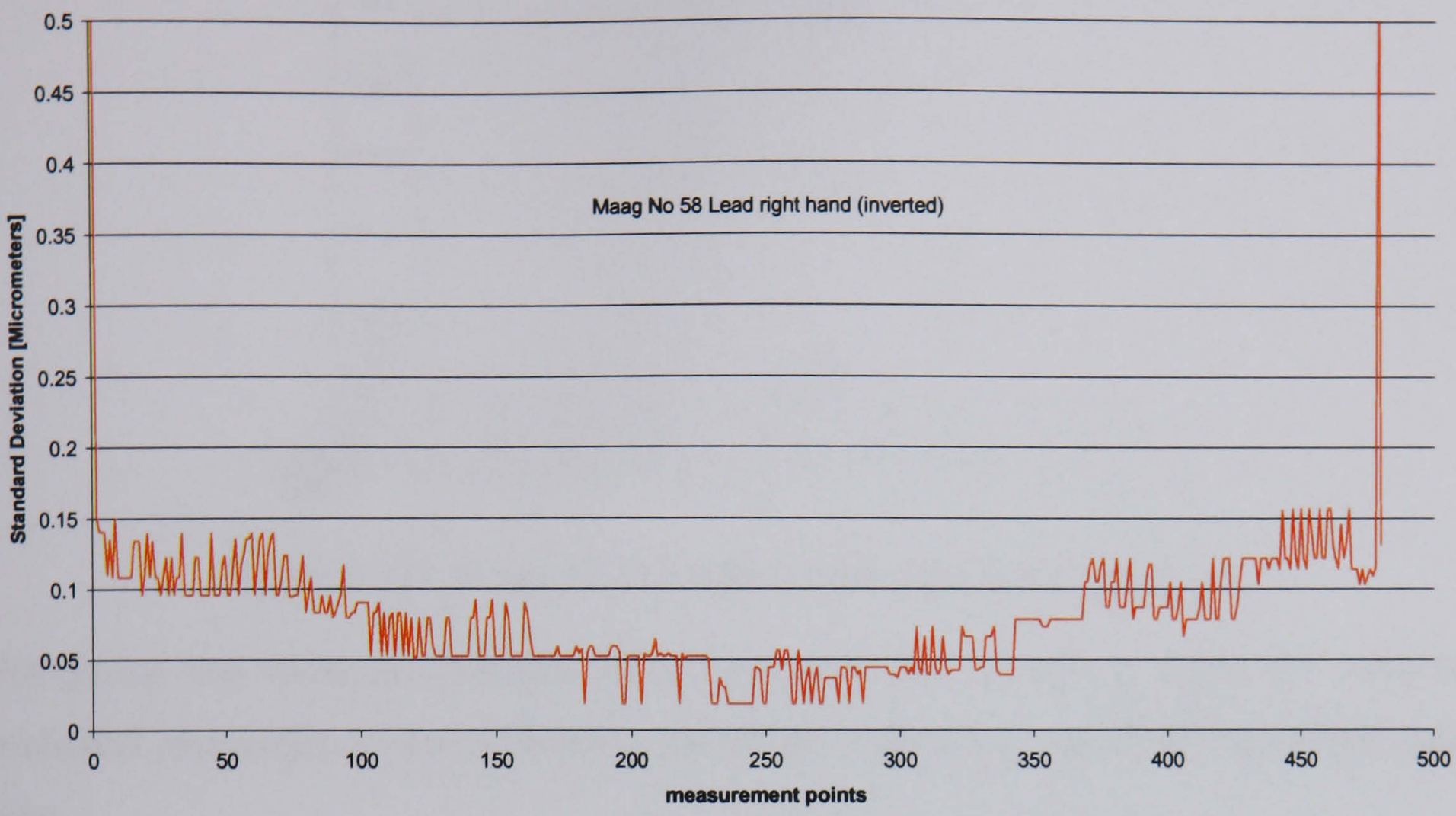

Figure 8.12b Maag No 58 Lead Master, right flank standard deviation of measurement points from 5 tests using the standard NGML procedure (inverted orientation).

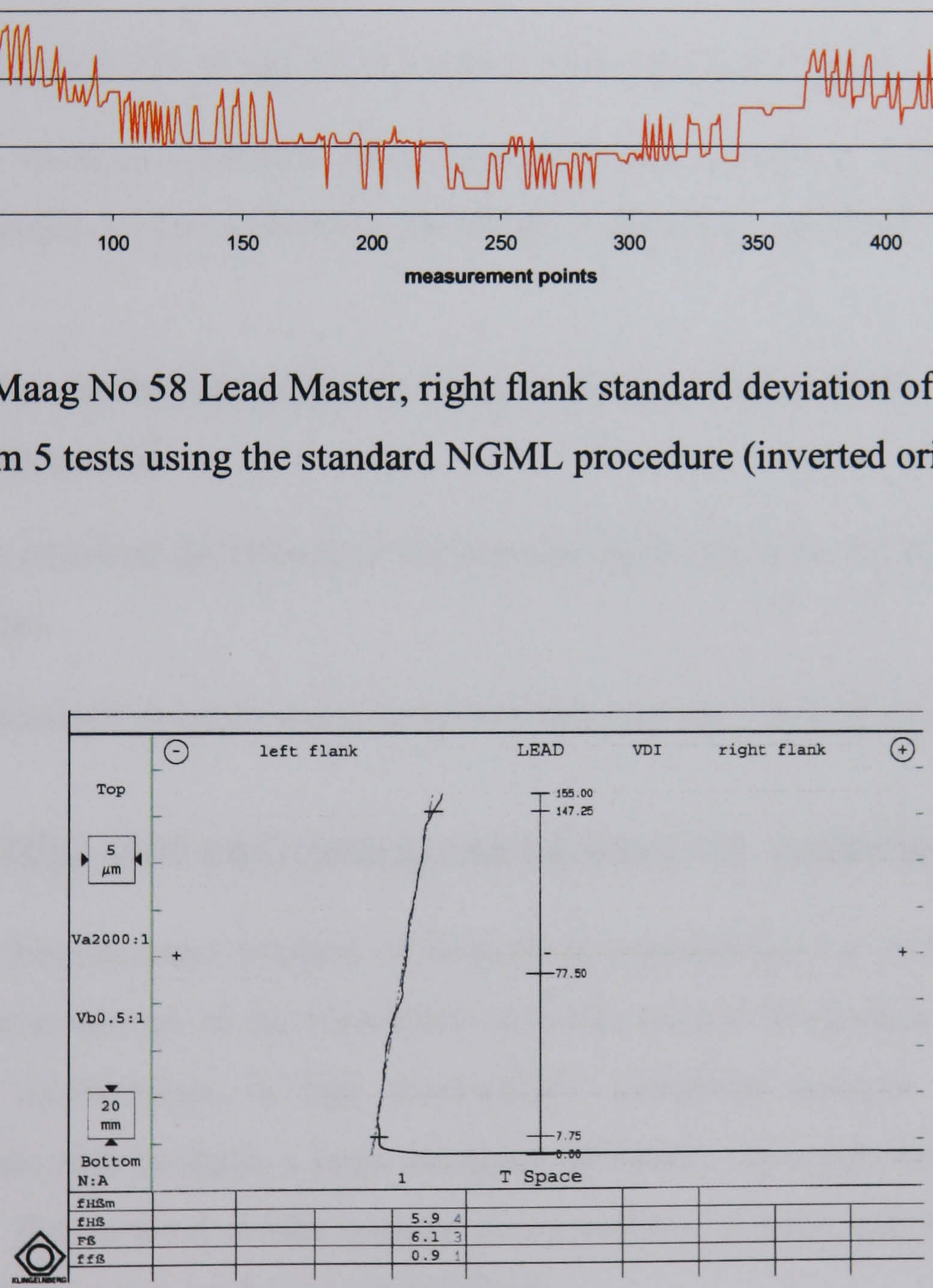

Figure 8.13a Maag No.56 lead master left helix error trace

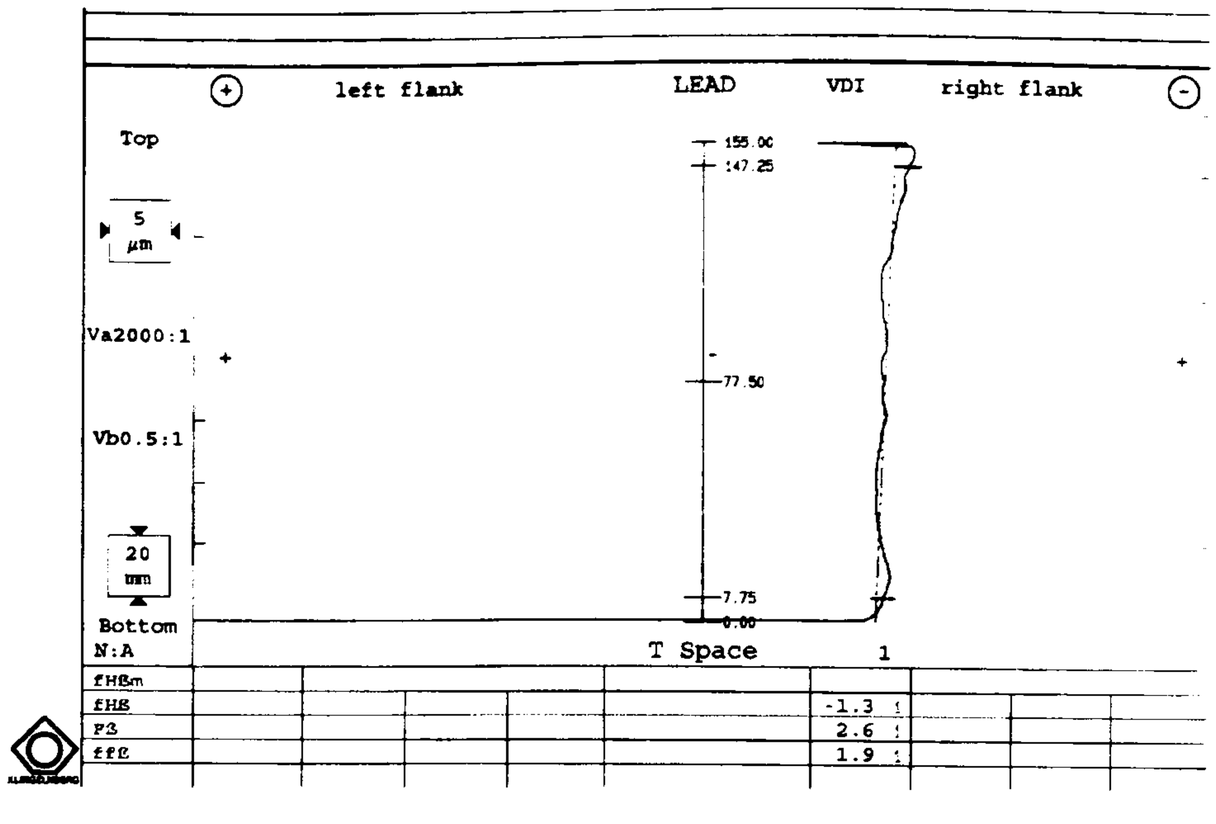

Figure 8.13b Maag No.56 Lead master right helix error trace

Comparing the standard deviation from measured data points in Table 8.3 with the evaluated parameters in the calibration certificate worksheets [0250/00272, NGML] that give:

- right helix standard deviations of 0.10µm for $f_{H\beta}$, 0.08µm for F_β and 0.02µm for $f_{f\beta}$ parameters and
- left helix standard deviations of 0.13µm for $f_{H\beta}$, 0.10µm for F_β and 0.05µm for $f_{f\beta}$ parameters

shows that the standard deviations are consistent between the two evaluation methods.

8.4 Traceability and estimating measurement uncertainty

The data point measurement method of evaluating repeatability by evaluating standard deviation has been shown to be consistent with the results from evaluating parameter repeatability. Furthermore, it has successfully identified specific regions in the measurement data that produce a large standard deviation, although the causes of these are no clearer. The method would become more useful if it were extended to include a comparison with traceable calibration data values.

8.4.1 Traceability

PTB, Germany provide the primary standards for gear measurement in the UK by calibrating the evaluated parameters from measurements on gear artefacts. Two of these masters, the 200mm profile master, calibrated in 2000 by PTB, and the 100mm profile master, calibrated in 2005 by PTB with the Zeiss CMM facility. PTB agreed to

collaborate with NGML and provide calibration data [Härtig, 2006] in the form of data points for these artefacts for comparison purposes with NGML. PTB also kindly provided estimates of measurement uncertainty for the data points.

A criticism of this approach is that the evaluation algorithms are not included in the assessment process. This shortcoming was addressed in a project completed by PTB [Härtig, 2006] in collaboration with German industry to develop a method of validating involute gear evaluation software with an estimated uncertainty of ±0.1μm for normal error magnitudes. Thus, an uncertainty model can be developed using a comparator approach for estimating measurement uncertainty from comparison of individual data points that includes evaluation uncertainty as a separate independent variable.

However, there are differences in the measurement method and data density between the two facilities. The PTB measure profile errors with points spaced equally in the radial direction whereas the NGML use points spaced equally in the base tangent plane. Thus, selecting suitable data points for comparison is likely to be a potential problem. A number of solutions were considered using curve fitting techniques for generating data at the required positions (including Fourier analysis, spline fits or polynomial fits) but these methods introduce residual errors of around 0.1 to 0.2μm from the actual recorded form data. A visual examination of the measurement point data from PTB showed that indicated form errors of less than 0.010μm would result if measurement point positions from the PTB and NGML were within 0.050mm. Thus a limited comparison of a single data point at approximately 1mm intervals of length of roll was selected for the comparison. This is less than would be required if the method was adopted for establishing traceability within the NGML but is acceptable for developing the evaluation method and proving the validity of the uncertainty assessment.

The 100mm profile master has been used predominantly for this analysis because the data supplied by PTB was obtained directly from the measurement process. The 200mm master was calibrated over six years ago and PTB has since discarded the measurement data. The reference data for the comparison was obtained from digitised graphical data thus less confidence can placed in this analysis and we would expect larger deviations between PTB and NGML data. Information from the NGML is included in Appendix D but the PTB data shall remain confidential in the spirit of the informal agreement between the two organisations.

8.4.2 NGML measurement results

100mm profile master results

An example set of measurement results is shown in figure 8.14. This shows the significant form errors in the right flank profile which caused differences in parameter evaluation between PTB and NGML.

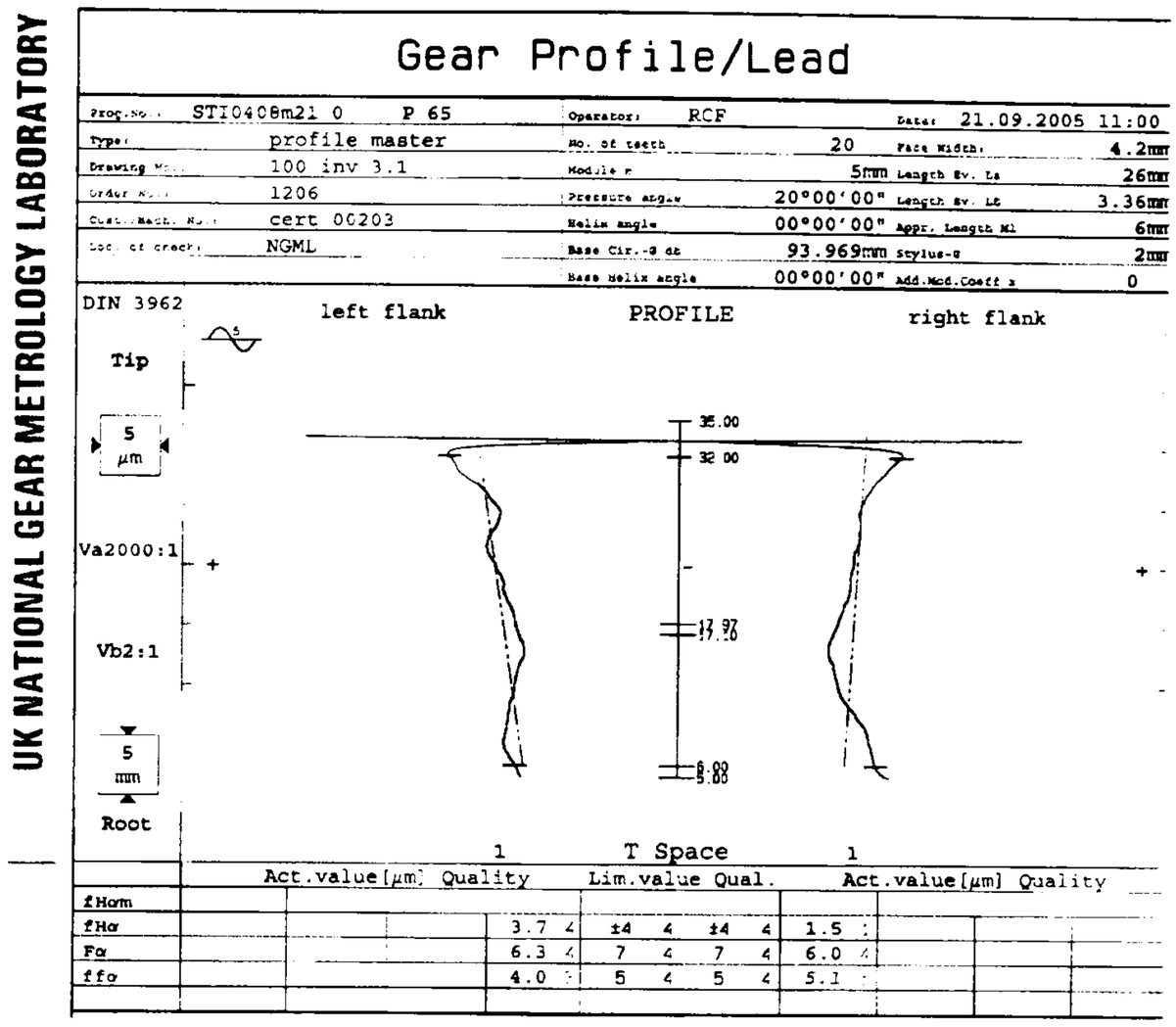

Figure 8.14 100mm profile master error data measured on the Klingelnberg P65 at NGML.

Table 8.4 contains a comparison between the PTB and NGML parameters and shows the standard deviation and measurement uncertainty of the evaluated parameters from both set of results. The results show good agreement within the measurement uncertainty stated by the PTB, provided the right flank slope parameter ($f_{H\alpha}$) value is ignored.

Table 8.4 100mm profile artefact mean of parameters and PTB reference data (µm)

Results	Left flank			Right Flank		
	$f_{H\alpha}$	F_α	$f_{f\alpha}$	$f_{H\alpha}$	F_α	$f_{f\alpha}$
NGML (SD)	+3.78 (0.08)	6.30 (0.06)	4.00 (0.00)	+1.52 (0.11)	6.01 (0.04)	5.12 (0.04)
PTB [U_{95}]	+3.92 [±0.7]	5.73 [±1.0]	3.56 [±1.0]	+3.15 [±0.7]	5.57 [±1.0]	4.87 [±1.0]

The Klingelnberg P65 at NGML measures 480 data points over the defined measurement range. These data points were imported to an Excel spreadsheet and evaluated for mean and standard deviation from 5 tests following the standard laboratory calibration procedures. The standard deviation of the measured data points illustrated in figures 8.15a and b show consistent low standard deviations for all data points. The mean values of standard deviation are 0.049μm and 0.050μm for the left and right flank respectively. Care was taken to ensure the measurement range was limited to the involute surface and the probe did not traverse over the edge of the flank.

Figures 8.16a and 8.16b shows the comparison between PTB and NGML data points at the selected points over approximately 28mm length of roll, with the PTB data selected as the reference values. The estimated measurement uncertainty for each data point from PTB is ±1.0μm and the maximum deviation for the left flank is 0.38μm and for the right flank is 0.46μm. Both of which are well within the stated measurement uncertainty.

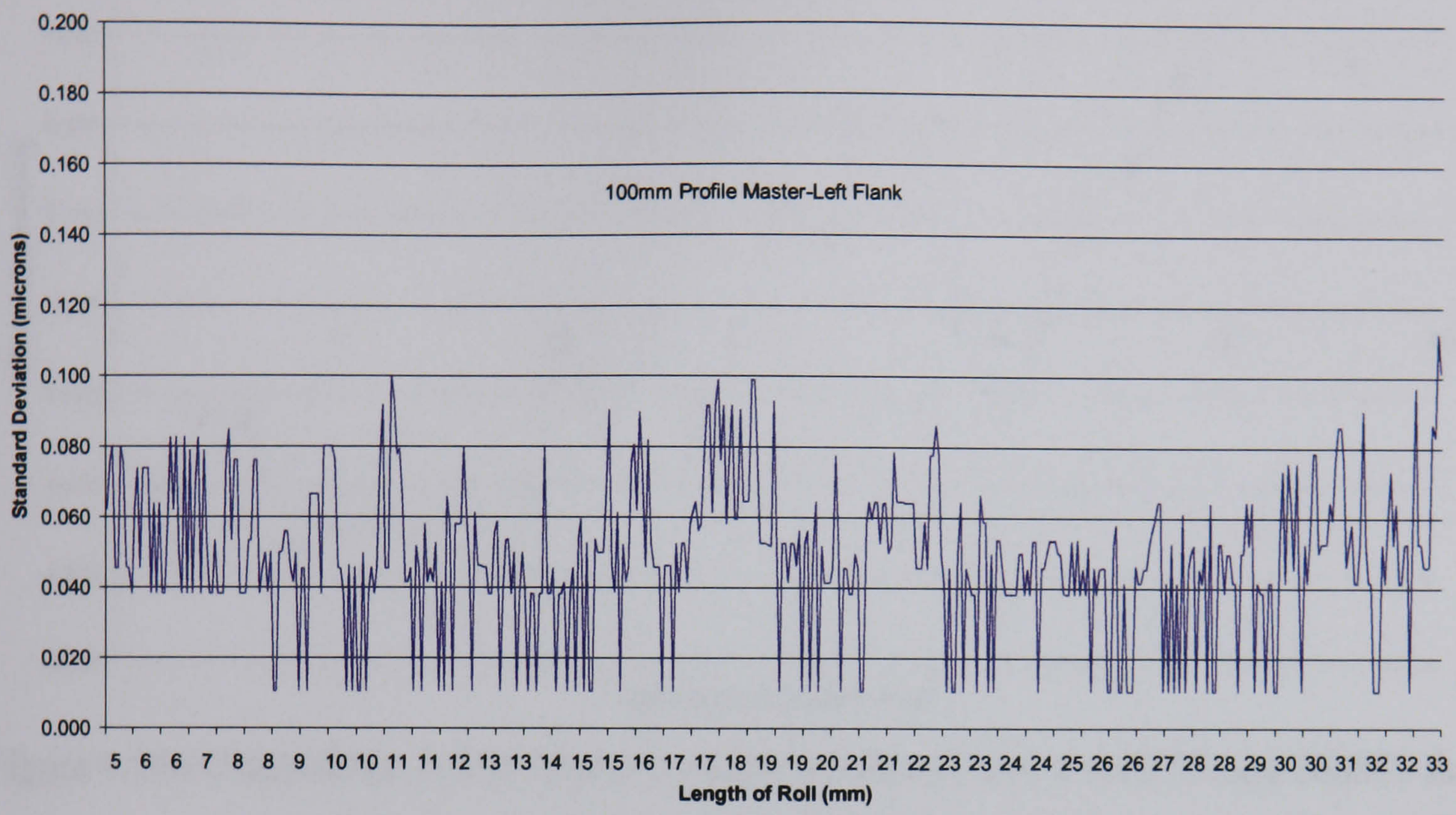

Figure 8.15a Standard deviation of left flank measurement points from the 100mm Profile Master (measured on a Klingelnberg P65 at NGML).

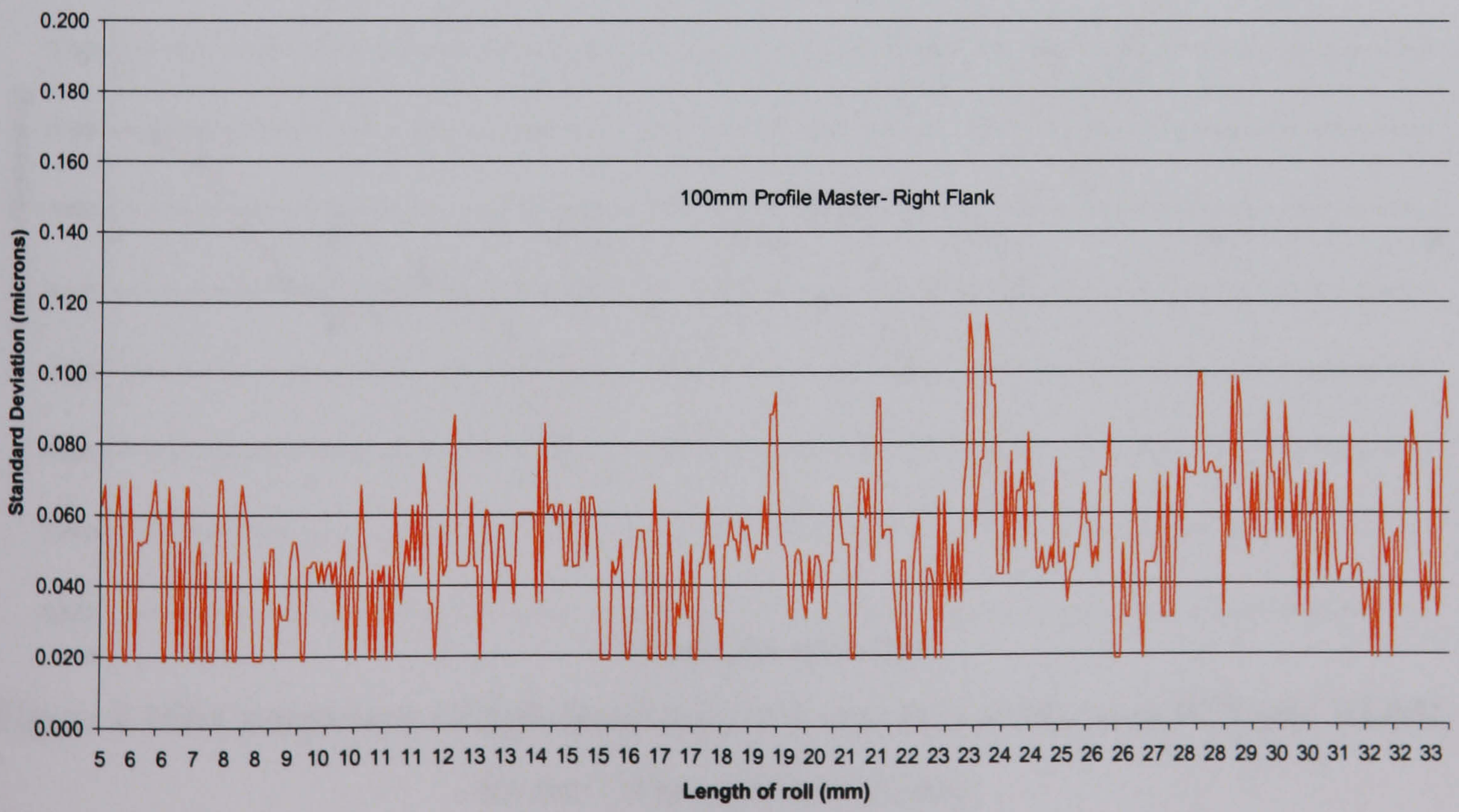

Figure 8.15b Standard deviation of right flank measurement points from the 100mm Profile Master (measured on a Klingelnberg P65 at NGML).

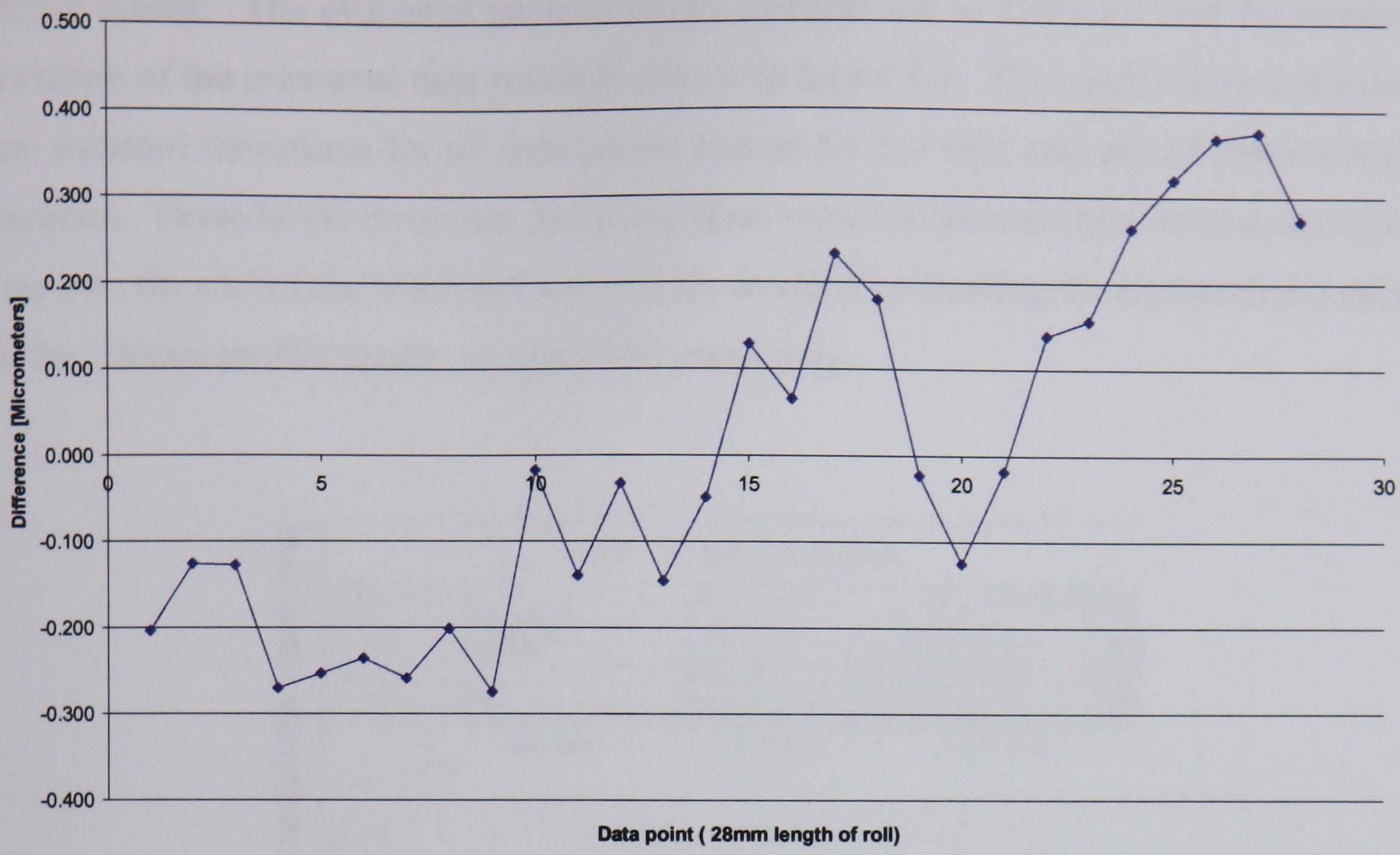

Figure 8.16a Comparison of left flank measurement data points from PTB and NGML for the 100mm profile master.

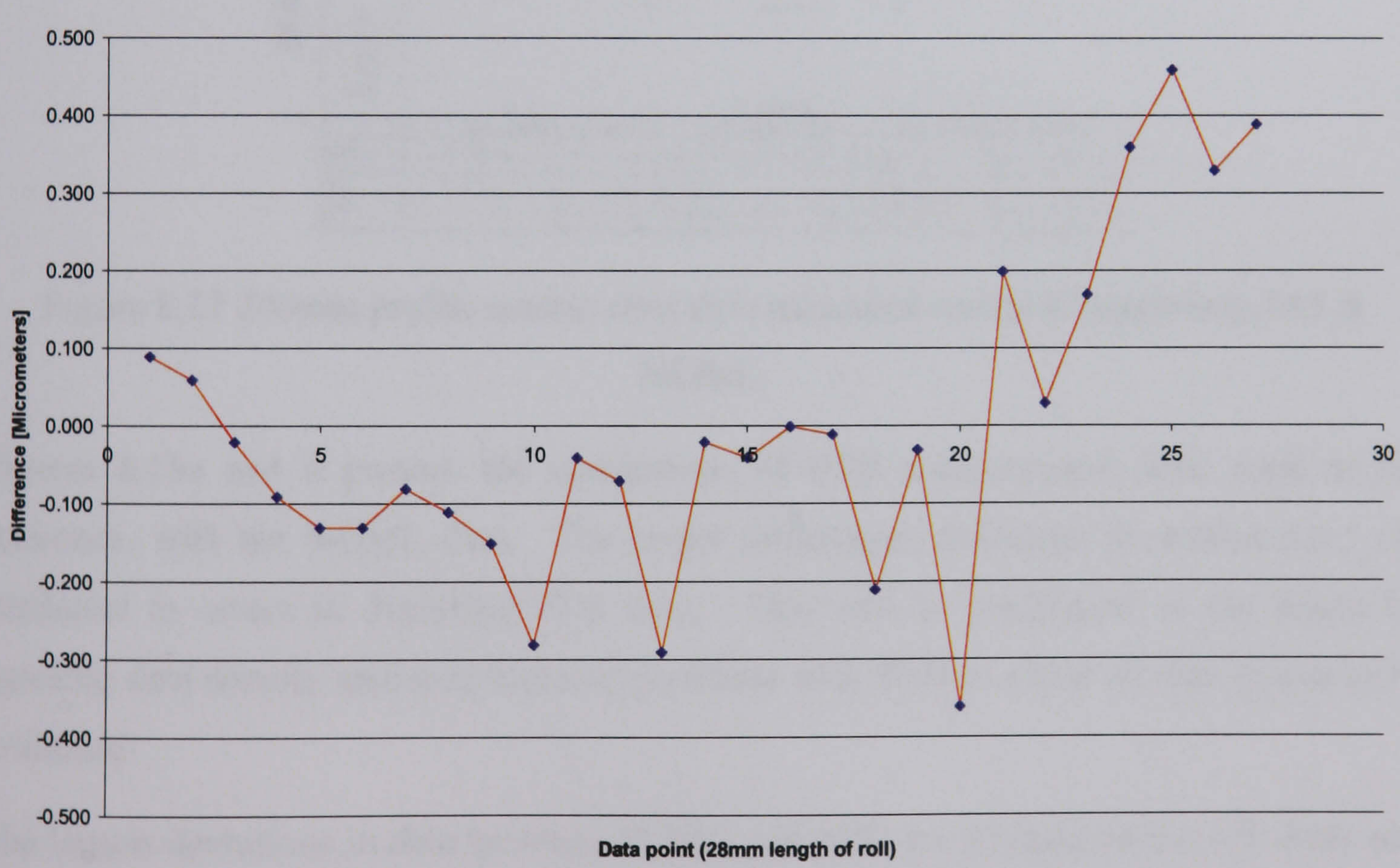

Figure 8.16b Comparison of right flank measurement data points from PTB and NGML for the 100mm profile master.

200mm profile master results

A sample set of measurement results is shown in figure 8.17 obtained from the Klingelnberg P65 at NGML using the same measurement strategy as for the 100mm

profile master. The evaluated parameters are summarised in Table 8.1 and the standard deviation of the measured data points is shown in figure 8.5. The results show consistent low standard deviations for all data points except for the start and end of measurement traverses. These larger errors are due to the form errors at the end of traverse as the stylus runs over the end of the involute flank and are avoided by limiting the measurement range on the 100mm profile master, as described previously.

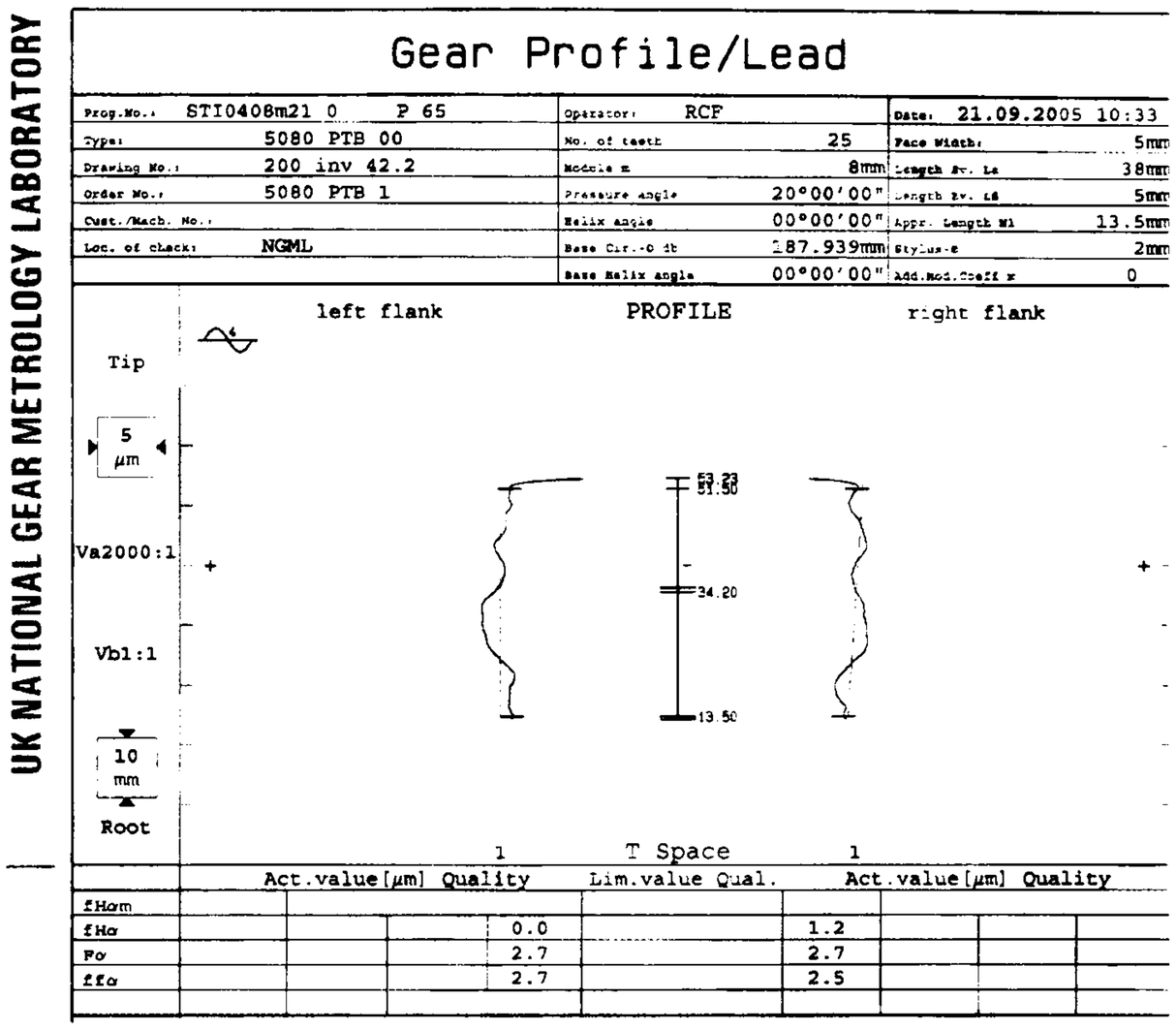

Figure 8.17 200mm profile master error data measured on the Klingelnberg P65 at NGML.

Figures 8.18a and b present the comparison of PTB measurement data, used as the reference, with the NGML data. The larger differences discussed in section 8.6.1 are attributed to errors in digitising PTB data. This will be confirmed in the future by agreeing data density and measurement positions with PTB to allow all data points to be evaluated.

The largest deviations in data between NGML and PTB are 0.99µm on the left flank and 0.94µm on the right flank. Both of these occur near the start of active profile below the start of evaluation range normally selected for comparison of evaluated parameters. These deviations are just within the PTB uncertainty (U_{95}) of ±1.0µm.

An evaluation of measurement uncertainty from both the 200mm and 100mm profile artefacts follows in the next section.

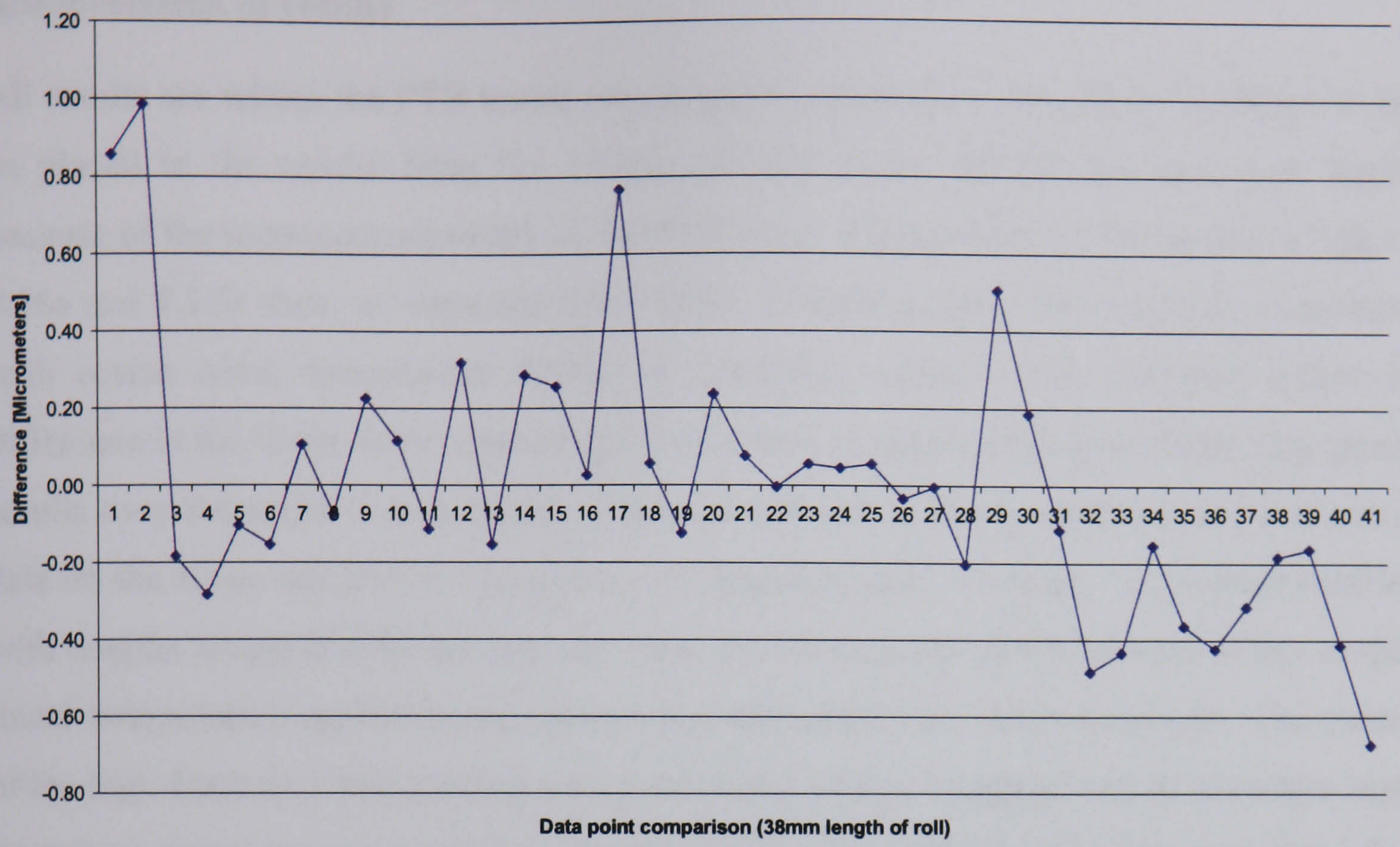

Figure 8.18a Comparison of left flank measurement data points from PTB and NGML for the 200mm profile master.

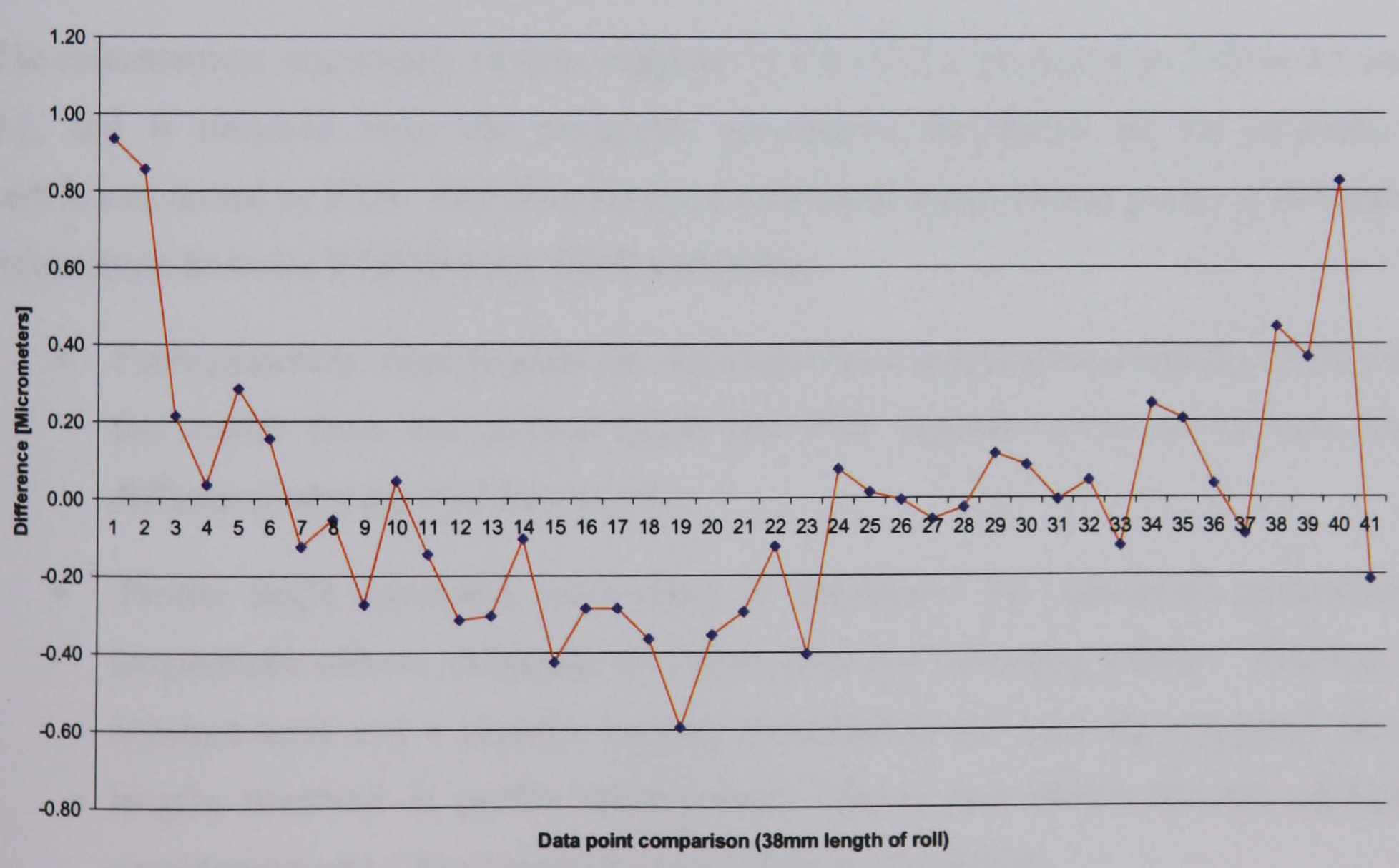

Figure 8.18b Comparison of right flank measurement data points from PTB and NGML for the 200mm profile master.

Interpretation of results

All results are within the PTB stated measurement uncertainty but greater confidence can be placed in the results from the 100mm profile master for the left and right flanks because of the increased reliability of the PTB data. Examination of the results in figures 8.16a and 8.16b show an apparent trend in the deviation curve that would be consistent with cosine error, temperature effects or guideway errors. One potential source of difference is the linear error map on the P65 which is constructed from Koba step gauge results over the entire X-axis travel. These results are at 40mm intervals and correction data on the Koba step has an uncertainty of approximately ±0.4μm. Traversing profiles with lengths within this 40mm step may thus introduce slope errors because of the simple linear interpolation applied to measurement points within the 40mm intervals. The nature of the high frequency ball passing errors and linear motor 'cogging' which introduce high frequency errors are not correctly compensated by the method. It is thus recommended these effects are further investigated and smaller calibration intervals are defined.

8.4.3 Evaluation of measurement uncertainty

The measurement uncertainty of data supplied by the PTB is presented in Tables 8.1 and 8.2, and is obtained from the parameter uncertainty statements on the calibration certificates issued by PTB. The uncertainty of individual measurement points is different. Information from the PTB [Härtig, 2006] states that:

- Form parameter uncertainties are dominated by the probe head and the quality of the master form and surface finish and PTB estimate a U_{95} of ±1.0μm (the difference between two data points).

- Profile angle parameter uncertainty is dominated by instrument guideways, temperature effects, definition of datum axes and clamping affects. This has a constant term and a linearly varying contribution but over the relatively short lengths involved in profile measurement (26mm and 38mm for the artefacts considered here) a fixed term U_{95} of ±1.0μm is appropriate.

- Total error parameter is a combination of both these affects so they are combined together to give :

$$U_{95} = \pm\sqrt{\left(1.0^2 + 1.0^2\right)} = \pm 1.4\mu m \qquad (8.1)$$

The form error parameter should be used for assessing data point uncertainty in the first instance, since it is actually the difference between two data points and is independent of slope uncertainty. The uncertainty of one data point is 0.71μm, thus

$$U_{form} = \pm\sqrt{\left(0.707^2 + 0.707^2\right)} = \pm 1.0\mu m \tag{8.2}$$

Table 8.5 is an extract from the 100mm profile master data supplied by PTB [Härtig, 2006]. It shows errors varying by less than 0.2μm over a 0.3mm interval suggesting that the uncertainty contribution from the master gear is overestimated, probably because of the filtering characteristic from a (relatively) large diameter probe scanning a relatively rough ground surface with R_a less than 0.3μm. The effect is that the uncertainty by the comparator method is dominated by the calibration data uncertainty contribution, similarly to the parameter method discussed in Chapter 4.

Table 8.5 Extract from 100mm profile master right flank results showing change in error value with measurement position from PTB data.

Length of Roll (mm)	Error (μm)
20.0194	1.48669
20.1346	1.57702
20.2521	1.54735
20.3678	1.61768
20.4823	1.638
20.5957	1.65832
20.7114	1.72865
20.8232	1.68897
20.9368	1.70929
21.0473	1.7196
21.16	1.65992

NGML uncertainty estimate by the comparator method

The sources of uncertainty that have been included in the NGML uncertainty estimate are:

- Repeatability
- Temperature (proportional to predicted temperature difference and distance from the datum to the measured value, measured as a length of roll)

- Artefact form (caused by differences in measurement position between the PTB data and NGML data.
- PTB uncertainty (either as form value quoted by PTB or as 0.707 of it, assuming 2 values contribute as a root sum of squares)
- Bias or error.

All except the last term, bias, is added quadratically in accordance with the standard procedures discussed in Chapter 7. The bias is either added linearly, in accordance with ISO 18653 or quadratically by assuming that the error term represents a distribution of possible errors that vary within defined limits. The calculation of form and total error uncertainty by data point comparison is presented in figures 8.19a and 8.19b for the 100mm profile master and figures 8.20a and 8.20b for the 200mm profile master.

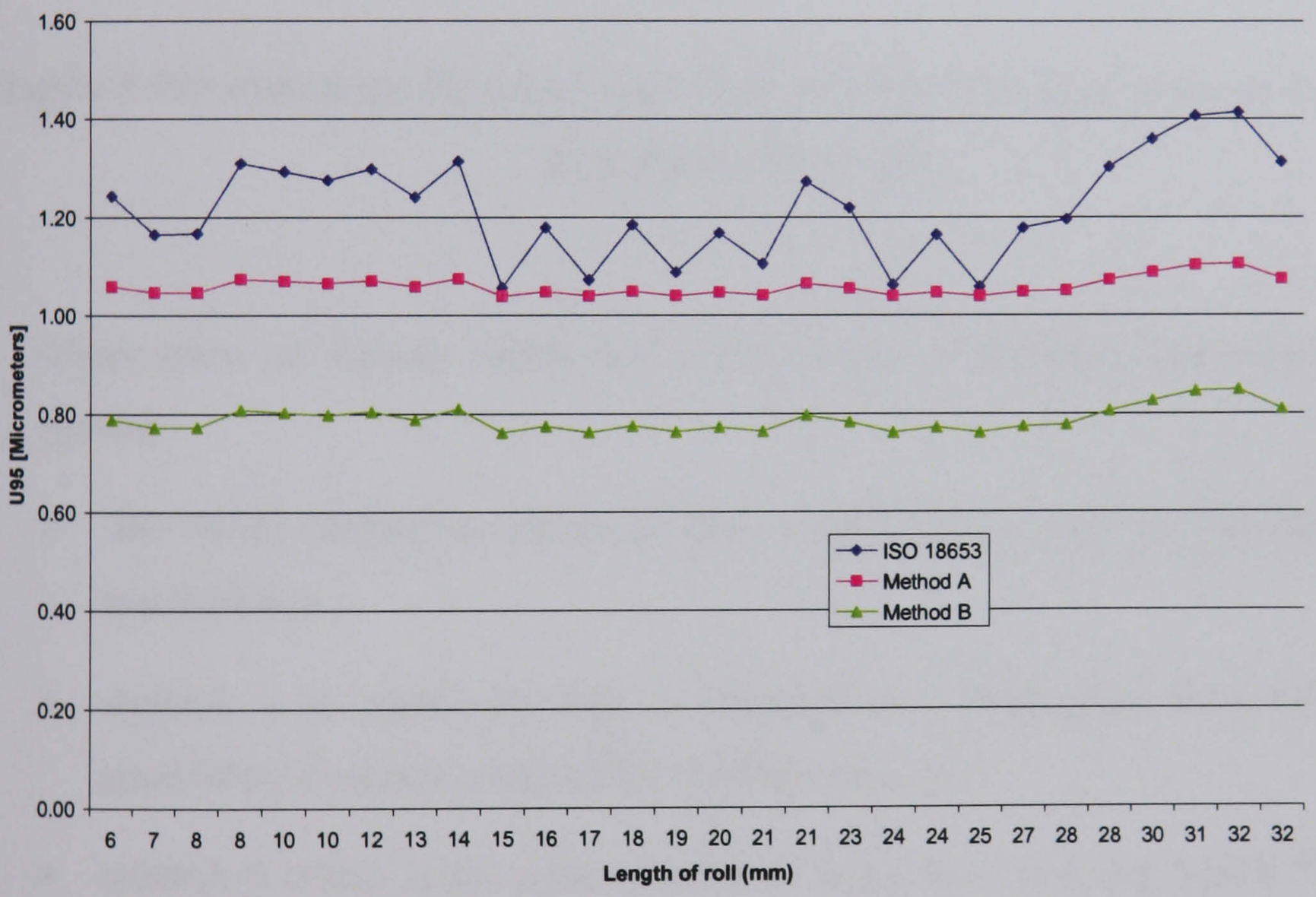

Figure 8.19a 100mm profile master left flank estimate of measurement uncertainty for comparison data points.

Figure 8.19b 100mm profile master right flank estimate of measurement uncertainty for comparison data points.

Observation of figures 8.19a and 8.19b shows 3 different uncertainty estimate options:

- ISO 18653 method in which the bias is added linearly to the combined random uncertainties,
- method A in which the bias is included as a rectangular distribution in the uncertainty evaluation and added quadratically ; and
- method B which is the same as method A but the uncertainty from PTB data is assumed to be (0.707μm).

The results show that the ISO method returns the largest uncertainty and is most susceptible to variations in bias or error. All three methods return values that are similar to those obtained from parameter based methods and all uncertainty values are large compared to the bias or error between the measurement processes.

This trend is supported by the results from the 200mm profile master, illustrated in figures 8.20a and b, but the uncertainties are larger due to the increased bias between data, as previously discussed. The apparent peak in uncertainty around 28mm length of

roll on the left flank is due to a combination of larger bias and the effect of temperature as the length of roll increases.

Figure 8.20a 200mm profile master left flank estimate of measurement uncertainty for comparison data points

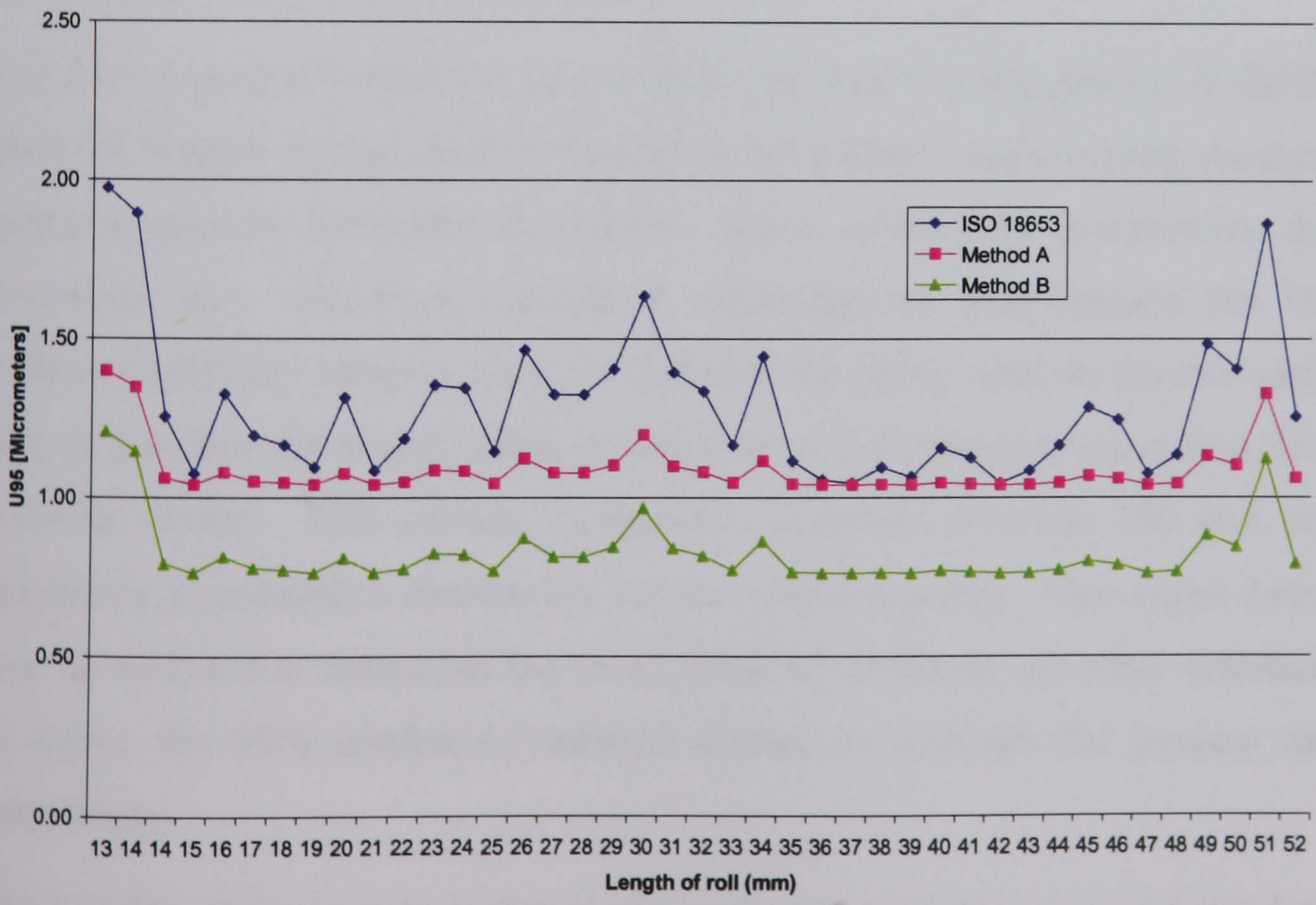

Figure 8.20b 200mm profile master right flank estimate of measurement uncertainty for comparison data points

The results from this analysis show:

- the uncertainty from the PTB is conservative.
- All the 3 methods thus appear to return results verified by these tests.
- The most conservative method appears to be the ISO 18653 method that is not consistent with the GUM recommendation that uncertainty estimates are realistic, and not conservative.
- The data point method of evaluating gear measurement uncertainty has been validated.

8.5 Application of the Monte Carlo Simulation method

8.5.1 Background

The Monte Carlo Simulation (MCS) method is a procedure that uses random numbers to simulate processes that have outcomes which are dependant on one or more random events. It is used in a variety of different applications, as discussed in Chapter 4, including measurement uncertainty where it is used in flow, electrical, substance quantity and dimensional measurement processes.

Software is used to model the measurement process and the process is developed in an identical manner to that used to formulate uncertainty models using mainstream GUM methods (namely formulate the model, define uncertainty distributions and standard deviations etc). However, instead of combining the distributions, the Monte Carlo method repeatedly samples from the distributions using random number generators and then determines the output value by combining the input data quantities in accordance with the model. This process is repeated anywhere between 200 and 10000 times, generating a probability distribution for the output quantity. The output distribution can then be analysed to determine the mean, standard deviation and other statistical measures to define the 95% confidence interval needed to estimate the process measurement uncertainty.

The benefits of the process is that it can be used to estimate mean and standard deviation of more complicated models with squared or cubed terms or where other constraints exist such as the difficulty in differentiating the expression to determine the sensitivity

coefficients. The methods have been applied in many applications for assessing measurement uncertainty and NPL [Cox, 2001] consider it the reference method to estimate measurement uncertainty and use it to validate mainstream GUM methods. Furthermore, the method is key to the VCMM (Virtual Coordinate Measuring Machine) method of assessing the uncertainty of complex measurements on a CMM.

The MCS method has been applied to gear measurement to assess the uncertainty of the Least Squares (LS) fit line parameter for profile error data given an uncertainty estimate for individual data points. An important point to this work is an assessment of the effect that form deviations have on the uncertainty of the LS fit model, in which the deviations are squared and thus weighted to produce a potentially biased solution. The effect of random errors on data with significant form deviations is unknown. The method has also been applied to PTB data to assess the LS fit parameter uncertainty and used to assess residual bias between, PTB and NGML data. The model was used to provide a definitive comparison of profile slope data and to eliminate the anomaly between profile slope data between PTB and NGML with the 100mm diameter profile master. It was also applied to data for the 200mm diameter profile master.

The MCS model was constructed using MATLAB (Mathworks) software because this has been previously used and recommended by NPL [Harris, 2002] and the quality of the random number generators, which are key for a valid application of the method, are considered suitable for this type of application.

8.5.2 MCS model

Appendix E provides a listing of the MATLAB code prepared for the model and also describes the function of each line of the code. The code was developed from a simple demonstrator example kindly supplied by NPL [Harris, 2006]. The structure of the model is described below:

- Measurement data (from PTB, NGML and differences between NGML) is defined. The NGML data is the mean obtained from measurements using the standard measurement procedure (5 tests at 90° intervals on the rotary table). The data for the exercise is at approximately 1mm intervals as described in section 7.4 resulting in 32 data points for the 100mm artefact and 44 data points for the 200mm artefact.

- A random data value is generated from the assigned normal distribution with a standard deviation of 0.35μm and added to the mean data point value. This is repeated for each of the data points to produce a unique set of data values.
- The 'regression' function fits a least squares line to the generated data values and the result is stored.
- The process is repeated for the defined number of simulated measurements.
- The resulting results for the simulated measurements are analysed and the mean, standard deviation, maximum, minimum and 2.5% and 97.5% quartiles are printed.
- A graph showing the mean and simulated profile point data and the resulting output (LS line value) pdf is plotted.

Number of trials

The number of trials required to define a reliable output pdf and statistical parameters was determined. The results are included in Appendix E and a summary is presented in Table 8.6.

An examination of Table 8.6 shows:

- The mean value is constant within 0.015μm for all trial numbers.
- The standard deviation is constant to within 0.005μm with >1000 trials.
- The trend is for the range to increase with trial number.
- The 2.5 and 97.5% quartiles are constant within 0.02μm with >100 trials.
- A comparison of the 95% range defined by the quartiles and 3.92xSD (for a 95% confidence interval) shows differences of less than 0.005μm with >1000 trials.

Table 8.6 Effect of number of trials on output pdf statistics

Trials (No.)	Mean	Standard Deviation (x3.92)	Minimum	Maximum	Range	Percentile		Range 95%
						2.5%	97.5%	
500	2.3897	0.2164 (0.8483)	1.6820	3.0090	1.3270	1.9876	2.7965	0.8089
1000	2.3782	0.2258 (0.8852)	1.4702	3.1000	1.6298	1.9412	2.8229	0.8817
2000	2.3902	0.2248 (0.8812)	1.6218	3.1429	1.5211	1.9432	2.8105	0.8673
5000	2.3929	0.2193 (0.8596)	1.6636	3.2021	1.5385	1.9627	2.8387	0.8760
10000	2.3947	0.2258 (0.8851)	1.6269	3.2481	1.6212	1.9549	2.8361	0.8812
20000	2.3931	0.2241 (0.8785)	1.4702	3.2481	1.7780	1.9536	2.8343	0.8807
30000	2.3938	0.2245 (0.8800)	1.4424	3.2660	1.8237	1.9528	2.8333	0.8805
50000	2.3932	0.2248 (0.8812)	1.4424	3.3373	1.8950	1.9525	2.8371	0.8846

It was concluded that 2000 trials give a reasonable result. Other methods of determining the pdf parameters such as skewness to determine symmetry, kurtosis to determine how outlier prone the resulting distribution, or the Jarque-Bera test for verifying normal distribution are not relevant to this analysis because the input pdfs are simple normal distributions.

8.5.3 100mm diameter profile master results

Figures 8.21a and 8.21b show the results from the MCS with the PTB data. The large dot for each series of points in the figures represents the mean data value extracted from data supplied by PTB. The results from the simulation are represented by the smaller dots scattered about the mean. The simulated results are generated from a random number

generator with a Gaussian pdf defined with a standard deviation of 0.35μm. The 0.35μm was derived the estimated data point uncertainty of 0.707μm assumed as the individual data point uncertainty from the PTB form data uncertainty statements. The figures also clearly show the difference in form error that causes the significant variation in profile slope data between PTB and NGML.

The data from each of the trials is fitted to a LS line. The resulting distribution of LS results from the 2000 trials is shown in figures 8.22a and 8.22b. A visual examination shows a near Gaussian distribution for both the left and right flank simulations with the right flank (the flank with the largest form deviation) yielding a slightly higher standard deviation of 0.2230μm compared to 0.2180μm to the left flank and the resulting right flank range of 1.6570μm compared to the left flank of 1.3421μm. For practical purposes there is no difference between the standard deviation of these results. Similar results were obtained from the NGML data presented in Appendix E. The NGML MCS data produced a standard deviation and range of 0.2224μm and 1.3944μm for the right flank and 0.2115μm and 1.5640μm for the left flank. Thus the effect of form deviations on the LS fit is noticeable but not considered significant for practical applications.

A comparison of NGML and PTB data has been completed to assess the form of differences between PTB and NGML. By considering differences in this way the option to compensate measuring instruments for deviations between national measurement institutions (NMIs) and thus apply true compensations for bias in data has been investigated. The results from this work are summarised in figures 8.23a and b for the left and right flank respectively, showing the bias between the NGML and the PTB data (with PTB providing the reference data). The standard deviation used for the MCS was 0.5μm (from a root of sum of squares combination of 0.35μm standard deviation from each source). The difference between the mean slopes for the left flank was 0.5746μm and the right flank 0.3537μm. (This is shown in the resulting output distribution summary shown in figures 8.24a and b). The resulting differences show low form errors and a clear bias in the slope from data at approximately 1mm intervals along the length of roll. This is an interesting result for the Klingelnberg P65 that uses rolling element bearing where we would expect to see some high frequency components in the error trace. One potential cause of this slope bias is that the Kobastep gauge used for the axis position error compensation has correction intervals of 40.0mm with an uncertainty of ±0.4μm, as discussed in section 8.4.2.

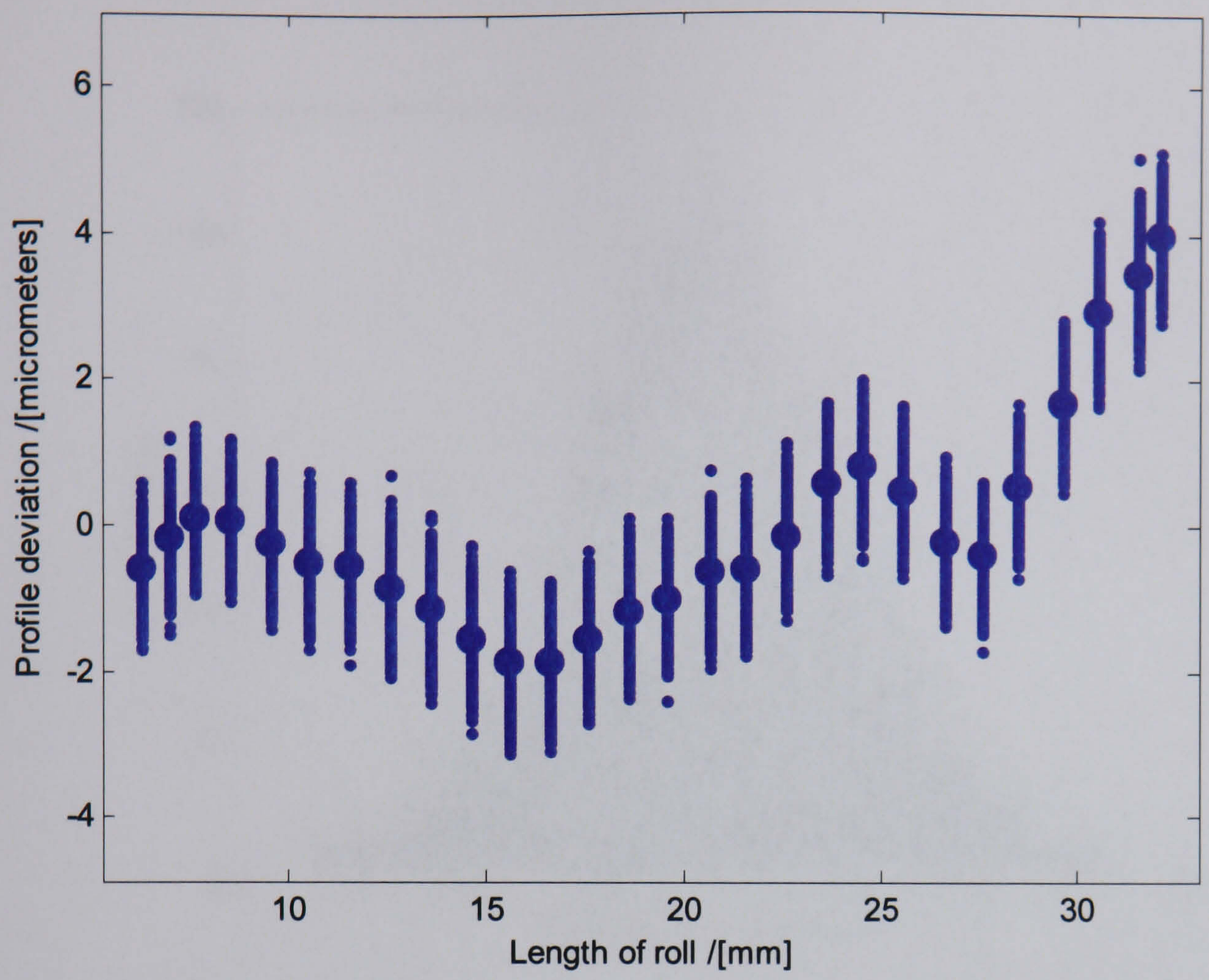

Figure 8.21a MCS run with 100mm profile master PTB left flank data (2000 trials)

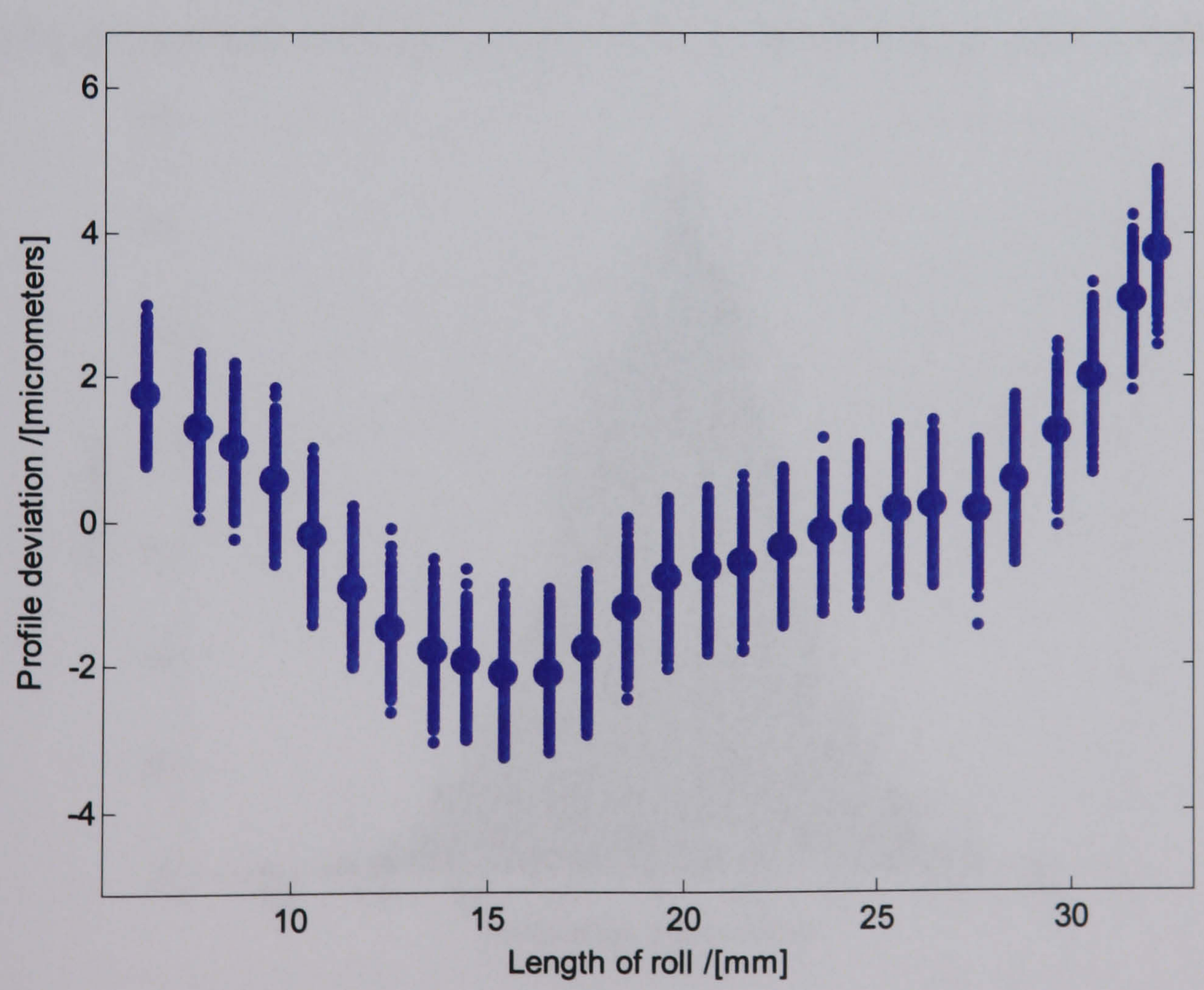

Figure 8.21b MCS run with 100mm profile master PTB right flank data (2000 trials)

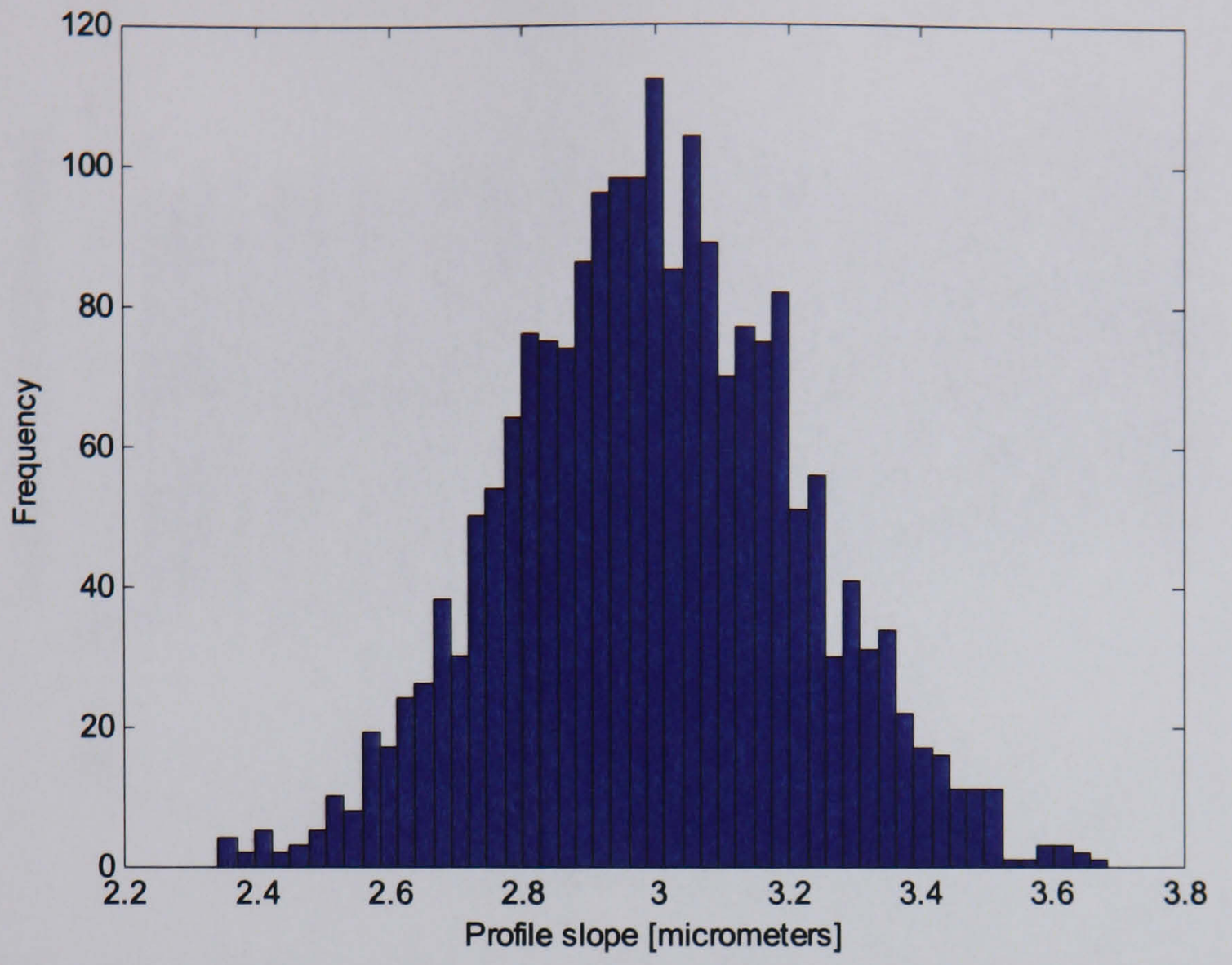

Mean	Min	Max	SD	Range	2.5%	97.5%
2.9985	2.3430	3.6851	0.2180	1.3421	2.5766	3.4289

Figure 8.22a Summary of LS fit line MCS of PTB 100mm profile master left flank data.

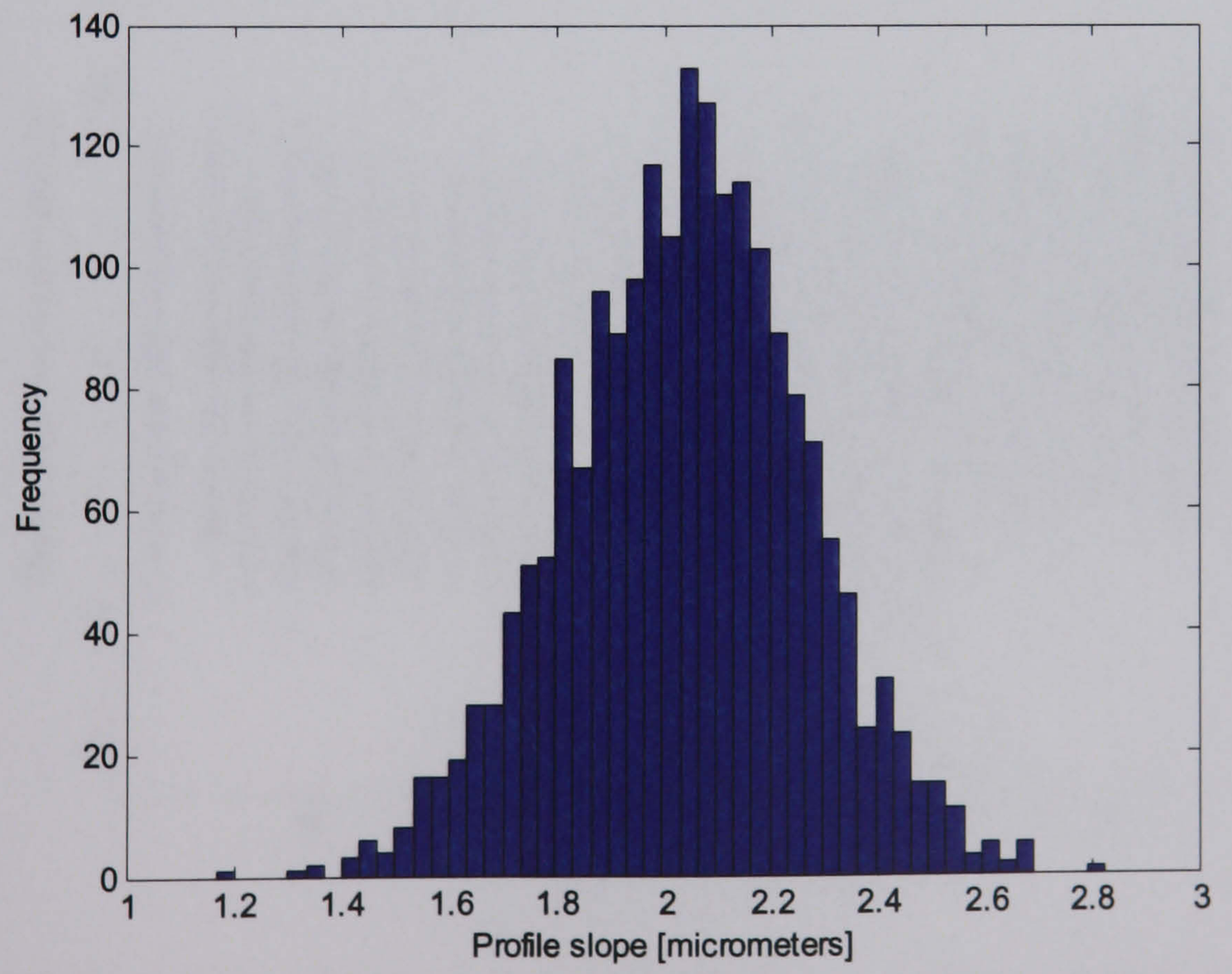

Mean	Min	Max	SD	Range	2.5%	97.5%
2.0365	1.1662	2.8232	0.2230	1.6570	1.5850	2.4731

Figure 8.22b Summary of LS fit line MCS of PTB 100mm profile master right flank data.

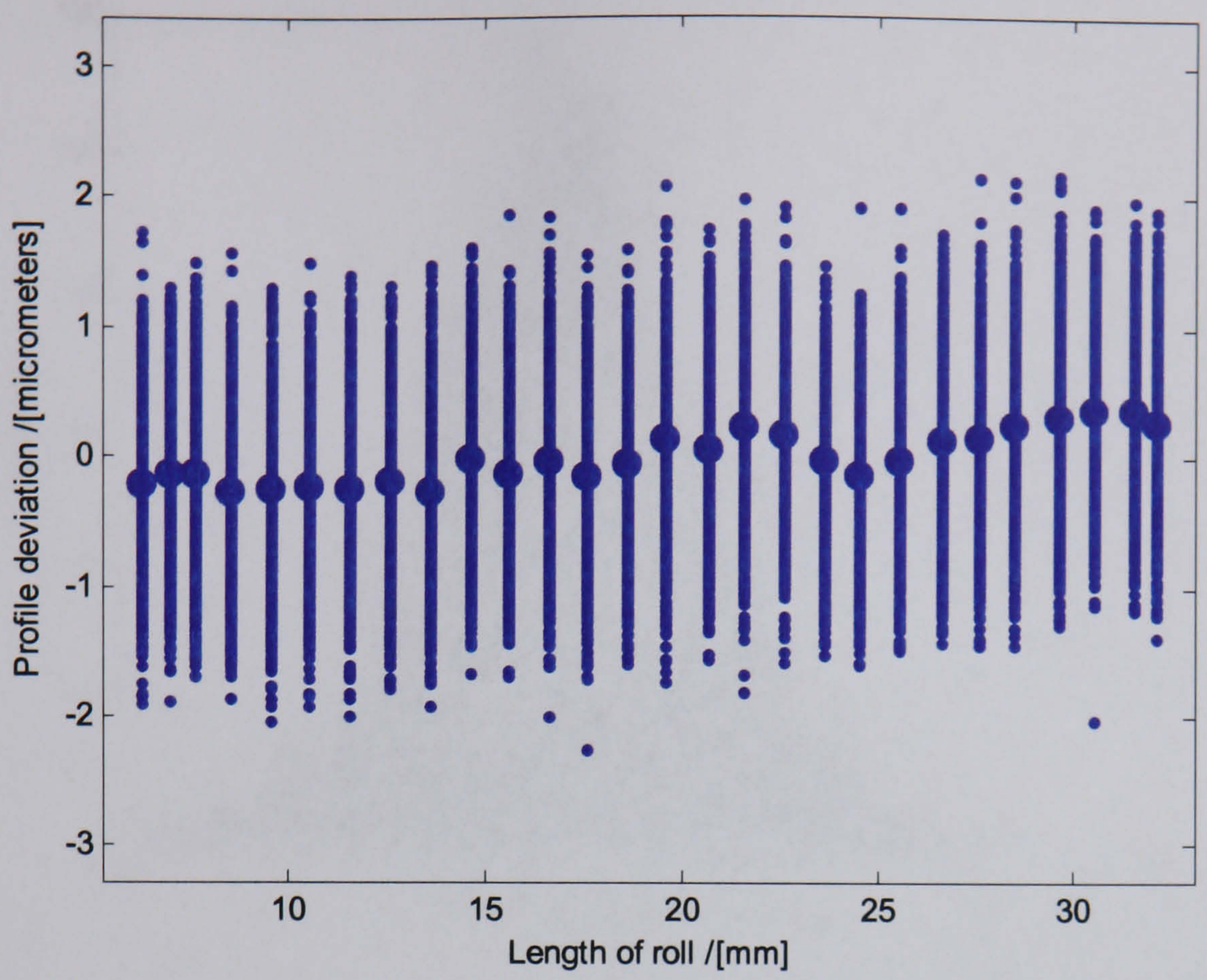

Figure 8.23a MCS of the difference between NGML and PTB for 100mm profile master left flank data

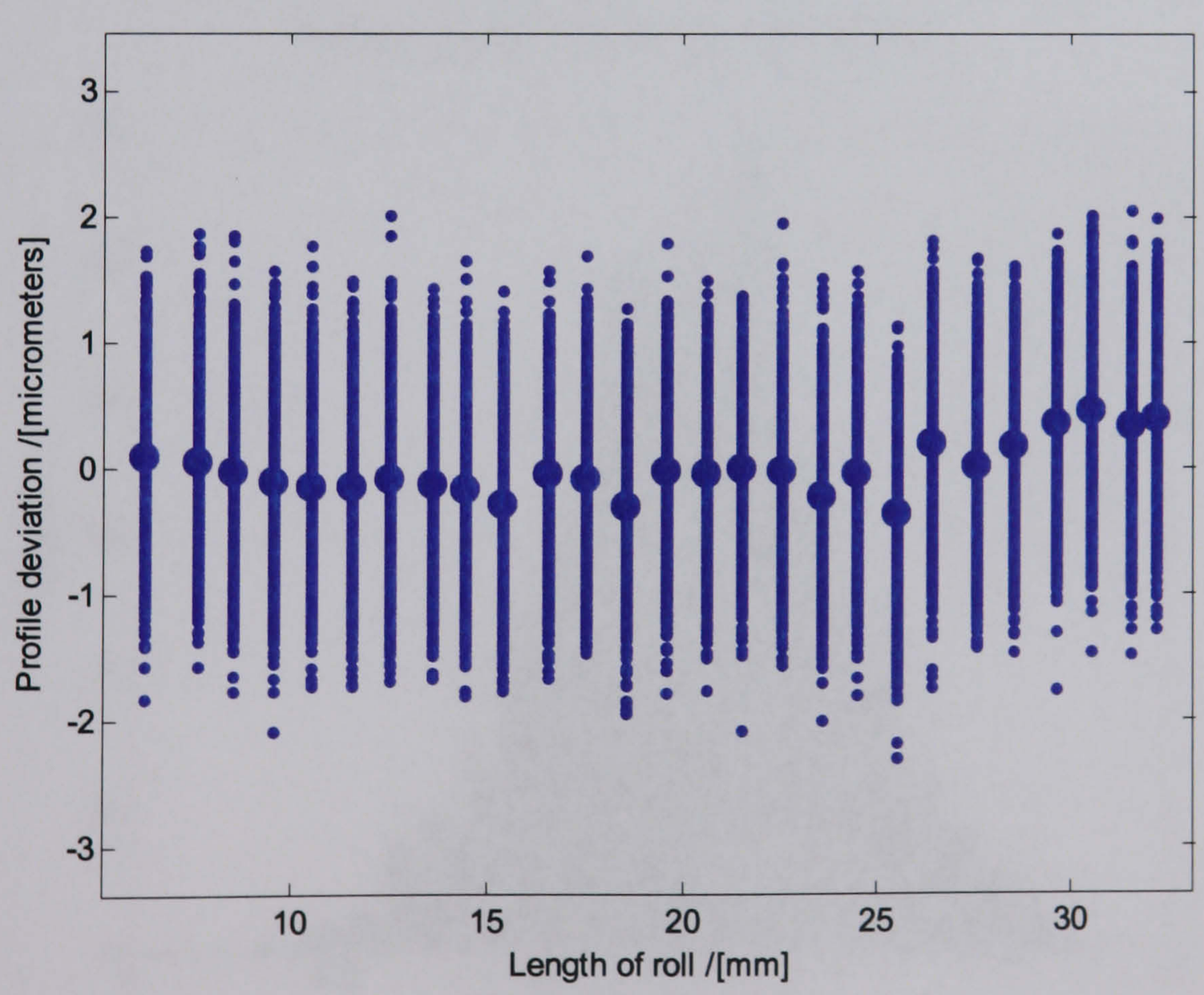

Figure 8.23b MCS of the difference between NGML and PTB for 100mm profile master right flank data

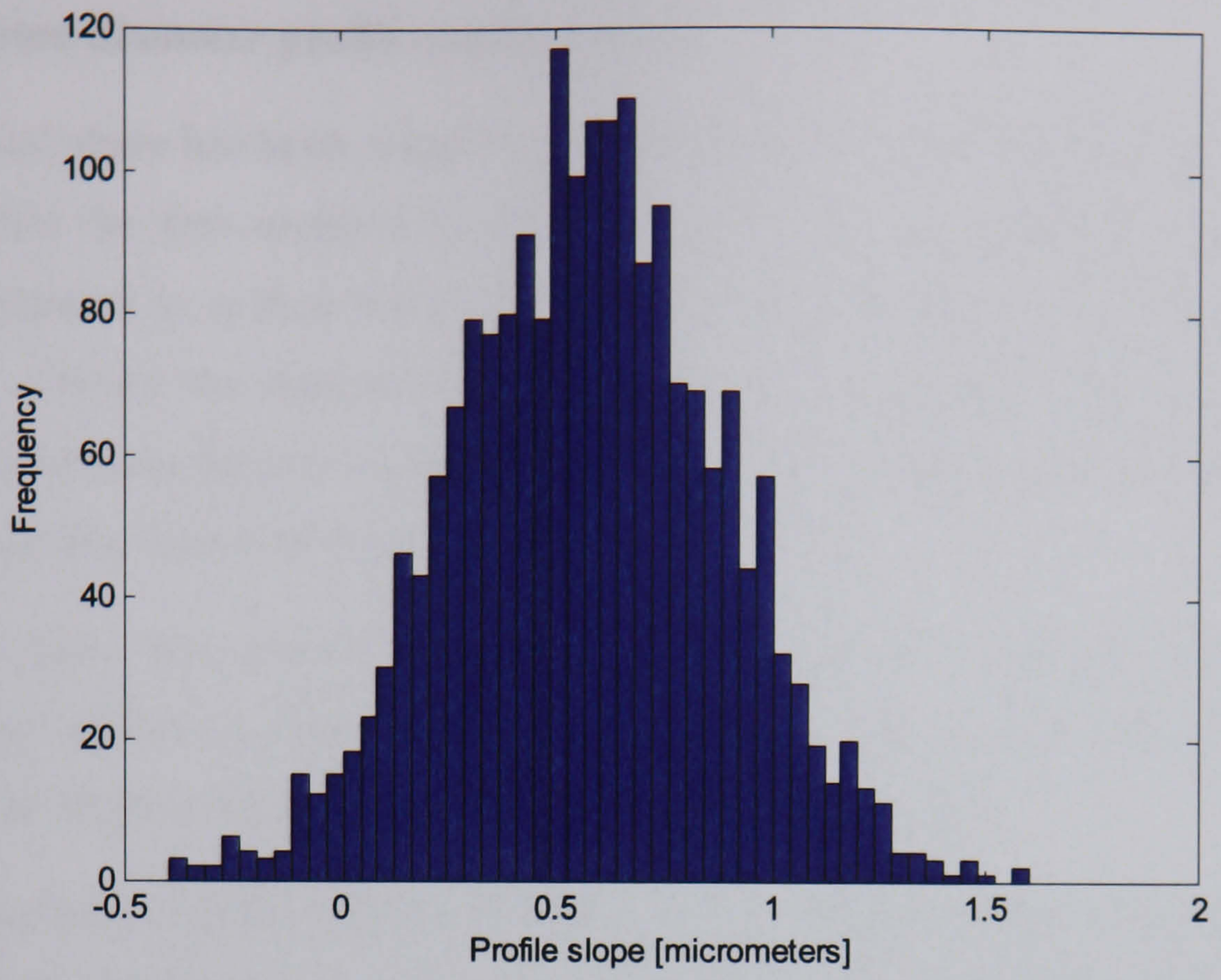

Mean	Min	Max	SD	Range	2.5%	97.5%
0.5746	-0.3915	1.6032	0.3075	1.9947	-0.0344	1.1893

Figure 8.24a Summary of LS fit line MCS of the differences between NGML and PTB 100mm profile master left flank data.

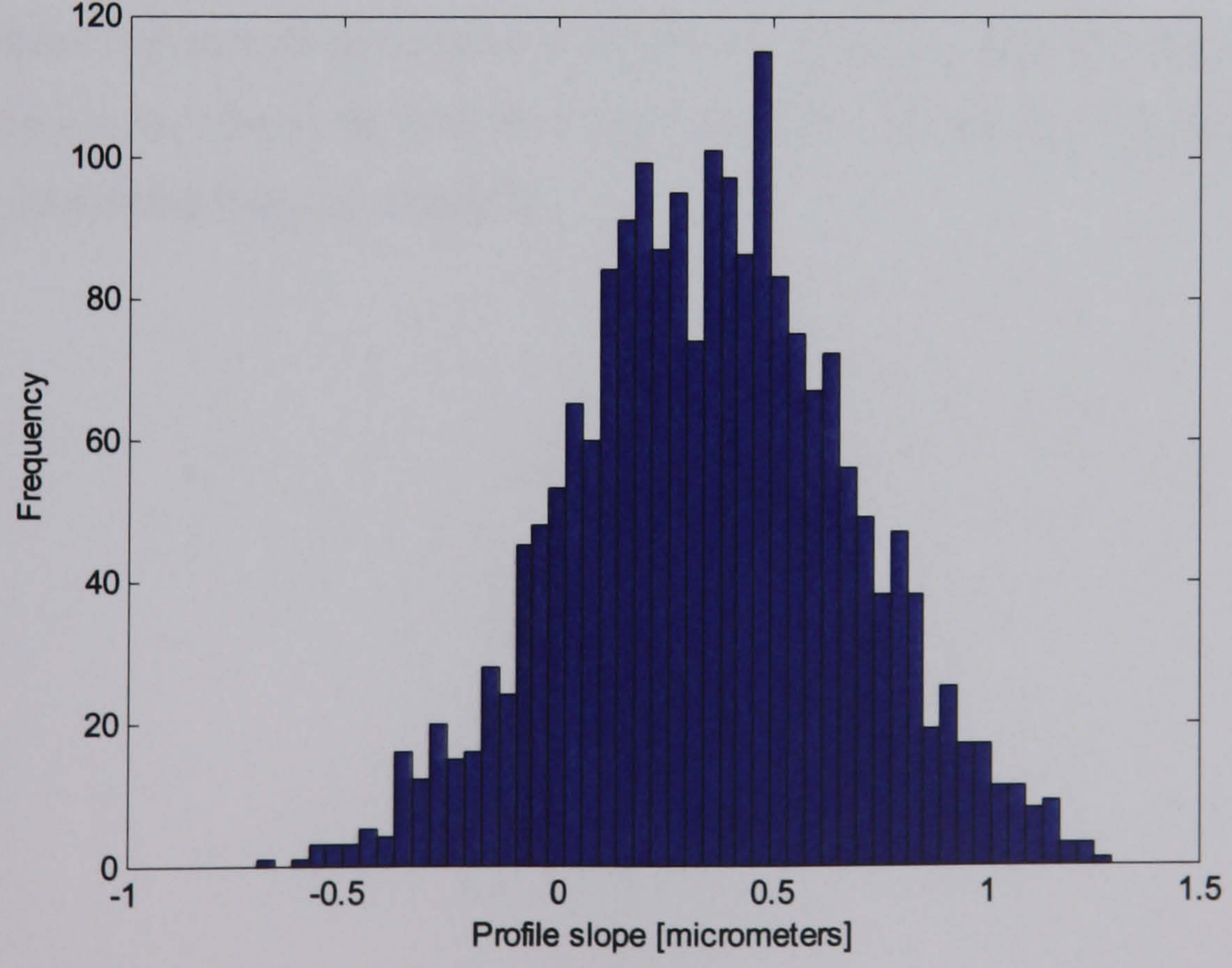

Mean	Min	Max	SD	Range	2.5%	97.5%
0.3537	-0.6988	1.2930	0.3253	1.9918	-0.2953	1.0066

Figure 8.24b Summary of LS fit line MCS of the differences between NGML and PTB 100mm profile master right flank data.

8.5.4 200mm diameter profile master results

An identical study has been completed on the 200mm diameter profile master. It will be recalled that the data supplied by PTB for this work was digitised data and that data points compared in section 8.4 at the start of active profile show significant deviations. This has affected the analysis but does not indicate errors on the Klingelnberg P65 guideways because there is an overlap in the guideway range used to measure the 100mm diameter profile master and the 200mm diameter master.

The data from this analysis is presented in Appendix E and the summary of the comparison shown in figures 8.25a and 8.25b for the left and right flanks and the resulting LS slope analysis is shown in Figures 8.26a and 8.26b.

The comparison of mean slope data shows similar standard deviations for the two flanks of 0.2591μm and 0.2553μm for the left and right flank respectively, and differences in bias between PTB and NGML of -0.5975μm and +0.0484μm for left and right respectively. The MCS for the right flank from the NGML data is shown in figure 8.27a and for the PTB data in figure 8.27b. A visual examination of this data shows that the most likely explanation would be errors in digitising the data from PTB.

The significant differences between data at the start of active profile will have influenced this analysis but the results are still consistent with the uncertainty of the Kobastep gauge correction data measurement uncertainty.

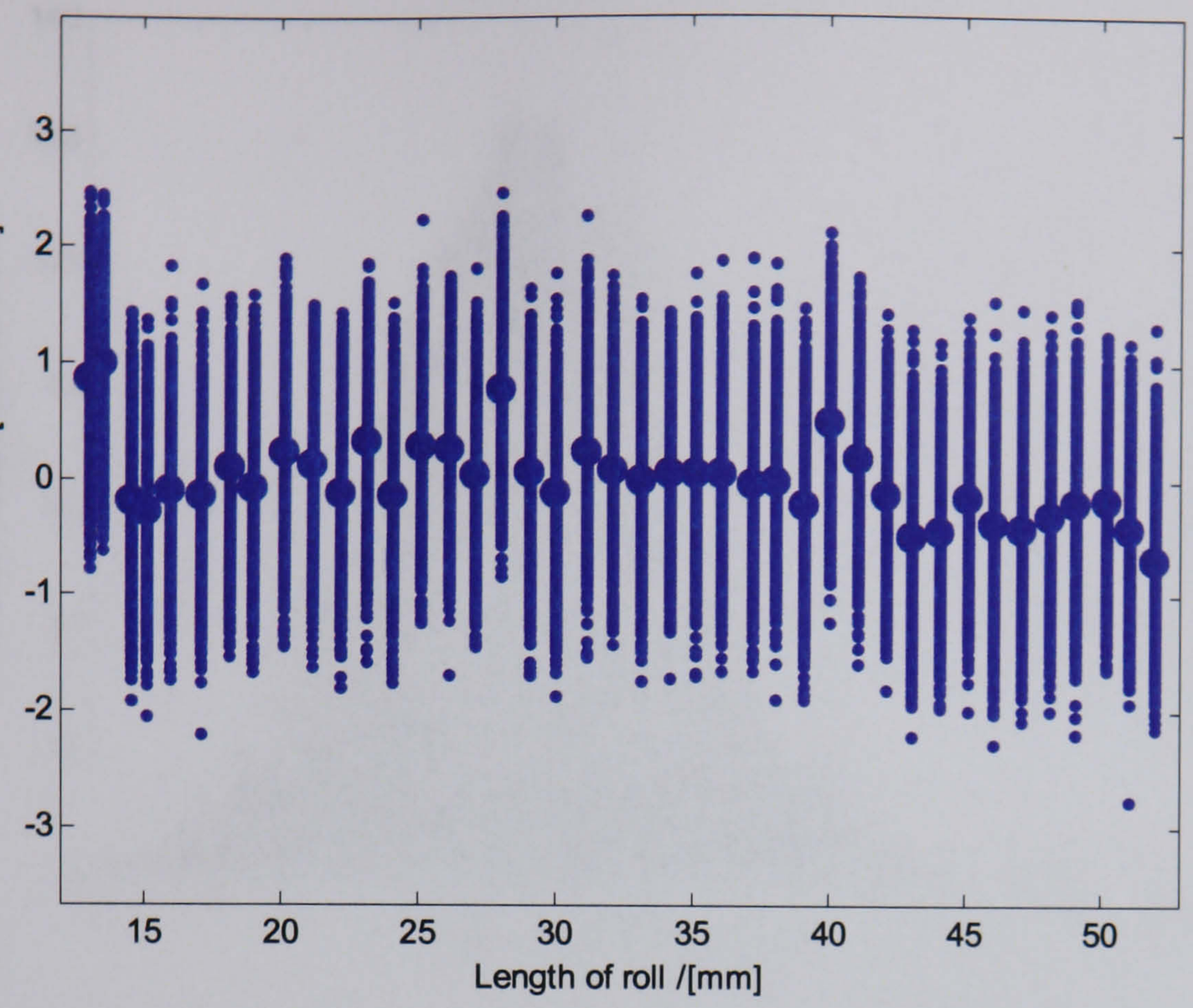

Figure 8.25a MCS of the difference between NGML and PTB for 200mm profile master left flank.

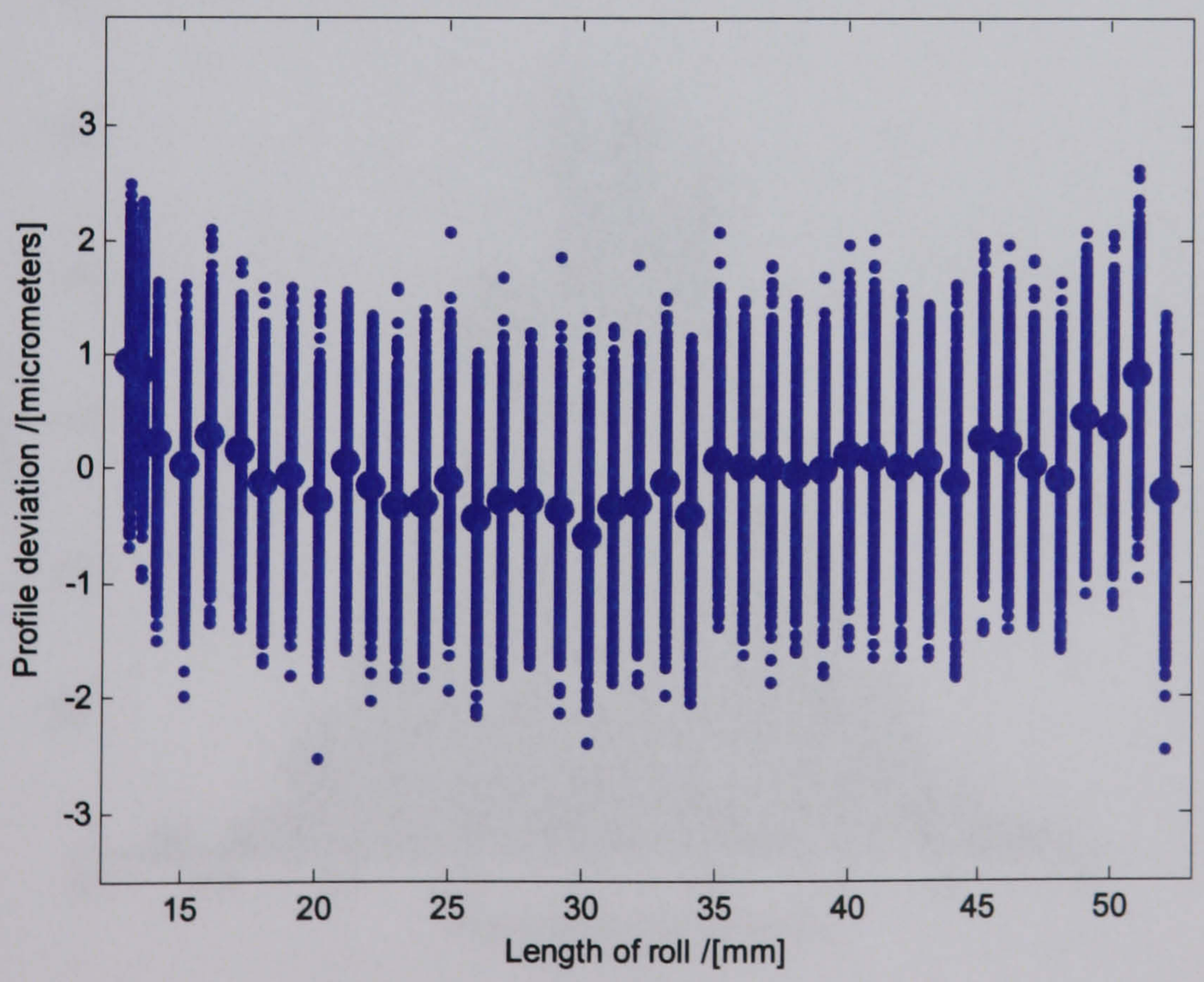

Figure 8.25b MCS of the difference between NGML and PTB for 200mm profile master right flank.

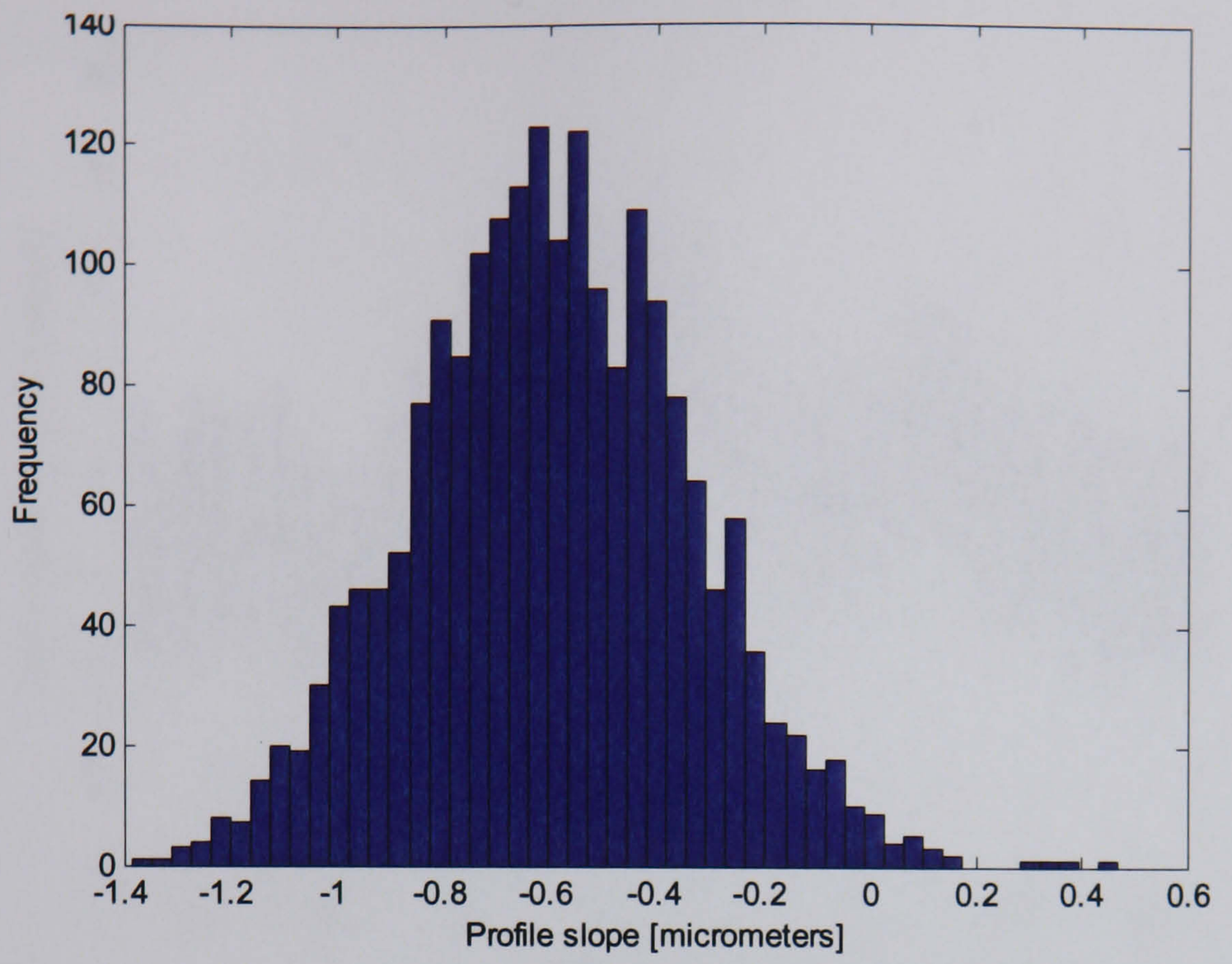

Mean	Min	Max	SD	Range	2.5%	97.5%
-0.5979	-1.3849	0.4706	0.2591	1.8555	-1.1035	-0.0778

Figure 8.26a Summary of LS fit line MCS of the differences between NGML and PTB 200mm profile master left flank.

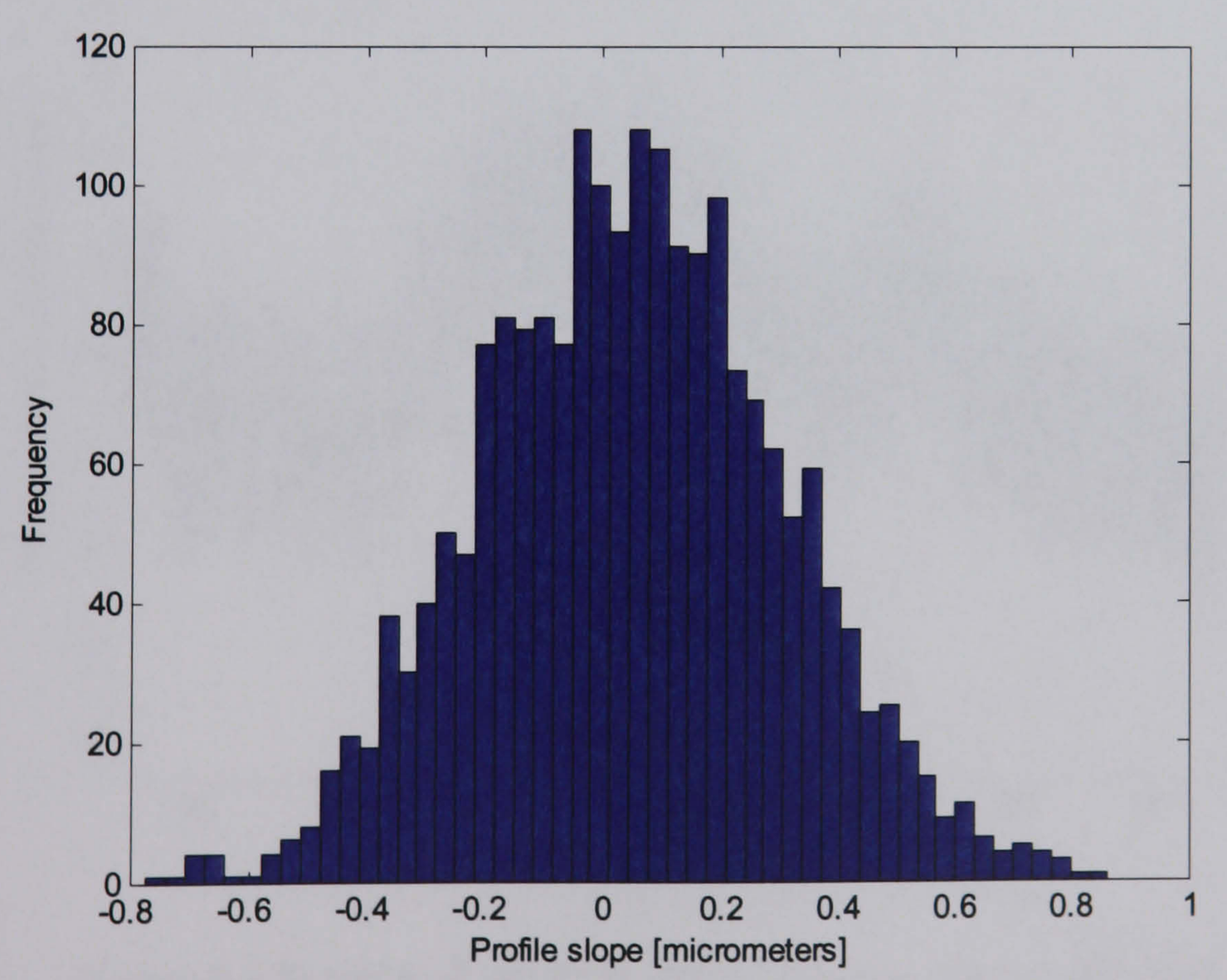

Mean	Min	Max	SD	Range	2.5%	97.5%
0.0484	-0.7732	0.8627	0.2553	1.6359	-0.4397	0.5471

Figure 8.26b Summary of LS fit line MCS of the differences between NGML and PTB 200mm profile master right flank data.

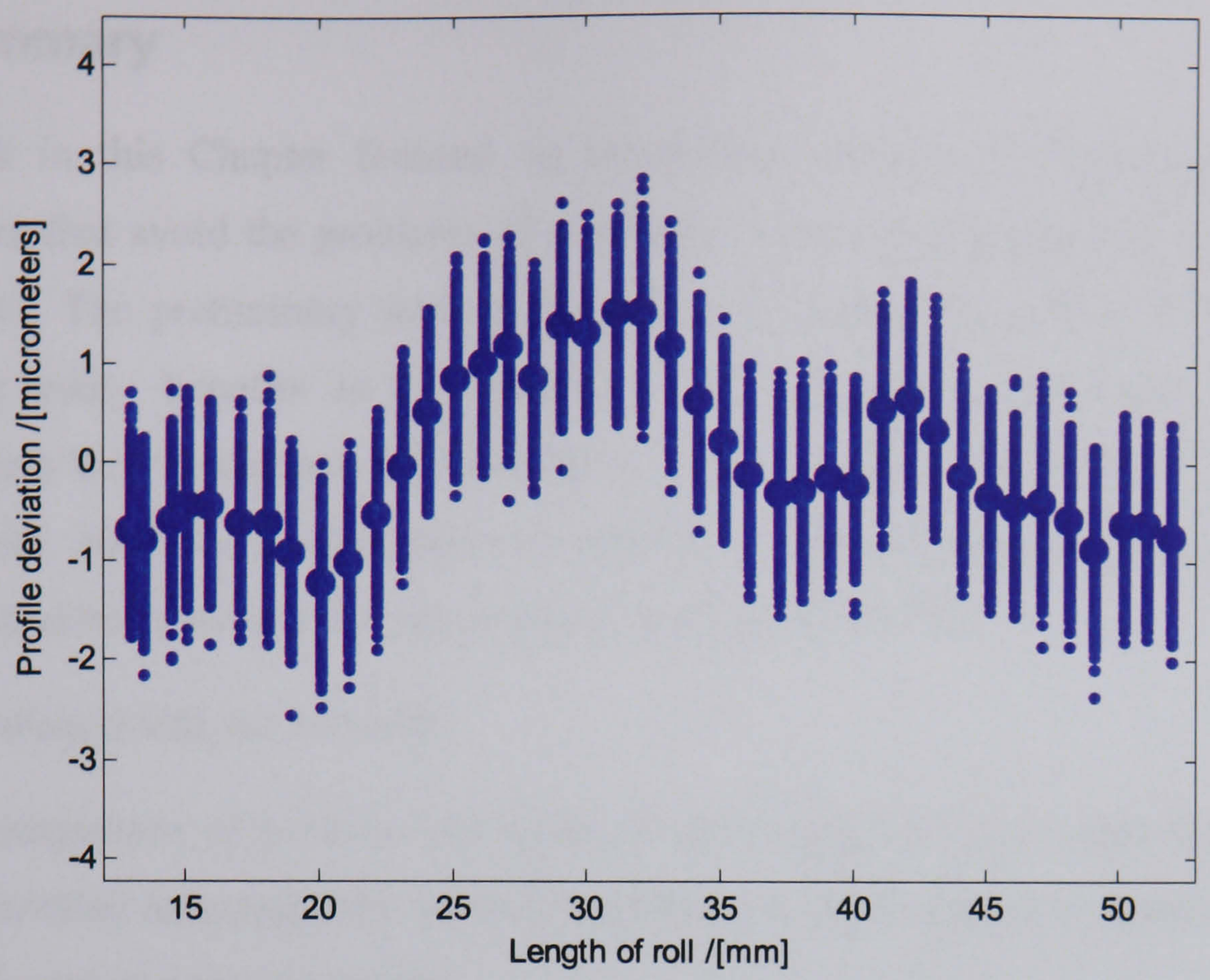

Figure 8.27a MCS of the NGML 200mm profile master left flank

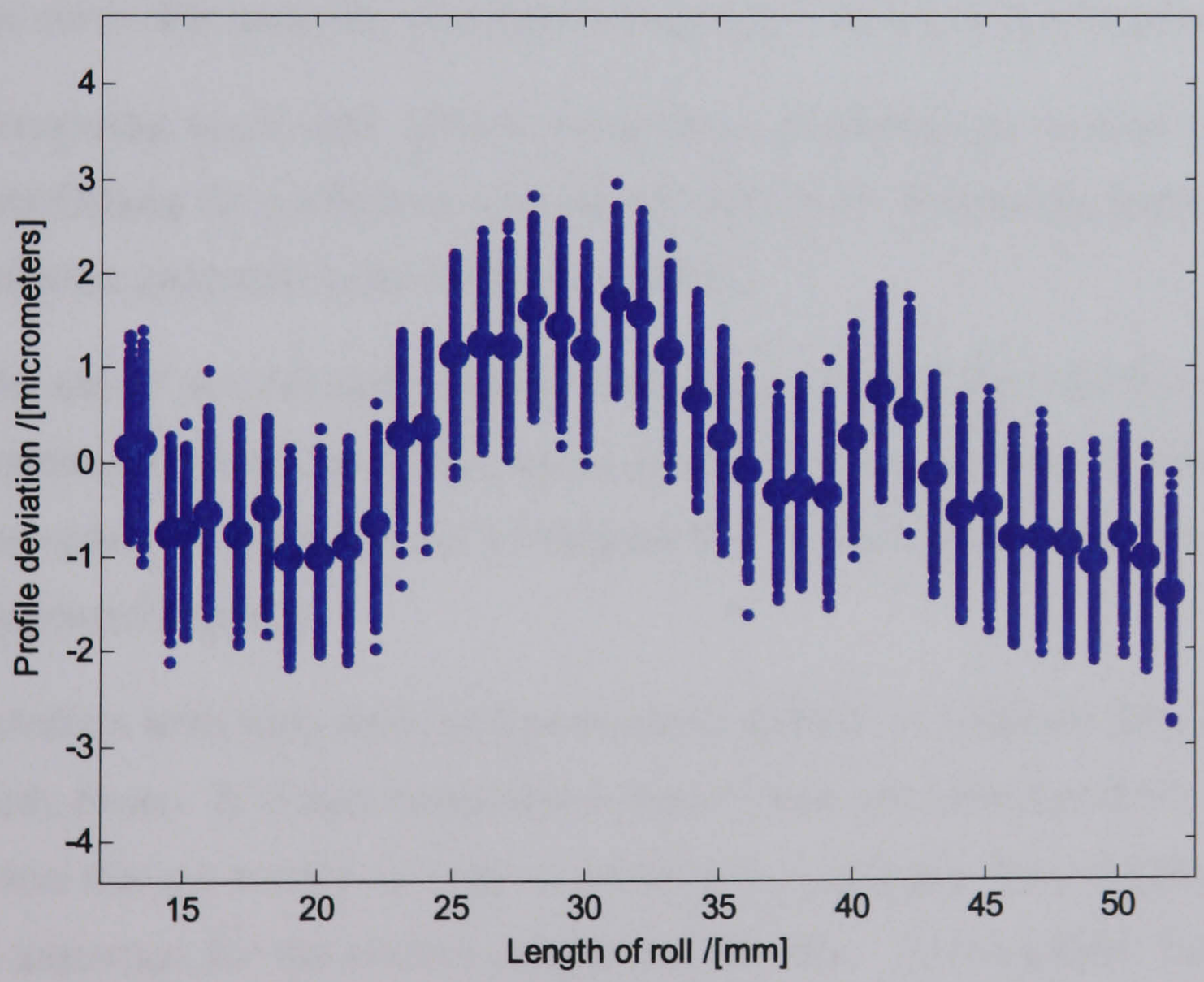

Figure 8.27b MCS of the PTB 200mm profile master left flank

8.6 Summary

The work in this Chapter focused on identifying methods of improving uncertainty assessment that avoid the problems of parameter comparison researched and reported in Chapter 6. The preliminary work completed with collaboration from PTB shows that there are many benefits in implementing the data point comparison method that demonstrate the importance of developing better mapping procedures for measuring instruments. However the procedures require more rigorous testing and research with the higher data density before they are implemented by the NGML.

The following points can be made:

- Comparison of point by point data is an acceptable way to establish traceability provided independently validated software is used when the instrument is used in its normal operating mode.
- Analysing point by point data allows additional information about the nature of the errors that cause the variation in parameters during normal instrument usage.
- Comparing point data allows verification of individual sources of error, thus establishing the performance of the instrument for measuring gears which are of different geometry to the calibrated artefact.
- The use of non-involute artefacts such as the Japan DBA can be used to assess instrument performance. But errors generated by the difference between involute and spherical geometry can be important if the cause of measured errors is to be diagnosed correctly.
- Artefacts with form error can prove more difficult to calibrate than those without form errors. It is thus important to ensure that gear artefacts have realistic form errors that are similar to those in workpieces inspected. Data density and spacing is important for the correct comparison of data. The standards that specify the parameters should also specify the data density and define the spacing is constant along the profile length of roll.
- The use of the MCS to predict the LS fit slope measurement uncertainty has been validated. The method allows accurate comparison of individual data and shows that the uncertainty values used by NGML are pessimistically large. Uncertainty

estimates should be revised after valid measurement point data is obtained from PTB.

- The use of the Kobastep gauge (a proprietary step gauge that has the measurement faces on the neutral axis of its section) for error mapping position errors in linear axes has been validated by this process. However, reducing the data spacing is of prime importance for the future improvements in performance. Higher data density will allow for the accurate interpretation of instrument guide form errors, and provide an acceptable way to error map an instrument.

Chapter 9

DISCUSSION AND CONCLUSIONS

Gears are important items in any modern mechanical transmission system. They maximise a systems operational efficiency by reducing running costs, minimising plant manufacturing costs and thus minimising environmental impact. Furthermore, in a modern global economy, the need to reduce costs to ensure the UK remains competitive, demands both higher accuracy and reduction in scrap and wastage rates. Underpinning these requirements is a need to maximise power density by improving the design and manufacturing accuracy of the gear system. Modern manufacturing and measuring equipment can ensure both the quality and accuracy of gear products, but it is available to all in a worldwide marketplace. Thus, if the UK is to remain competitive in its most effective markets, namely high precision, relatively low volume applications, the way in which measurement technology is applied and used on a daily basis is crucial to maintaining its competitive advantage.

Quantifying the accuracy of measurement results from gear measuring machines is thus of paramount importance if reliable control of manufacturing processes decisions are to be made and the benefits of investment in modern equipment are to be realised. The measuring equipment needs to be carefully maintained, used in a skilful manner with appropriate interpretation of results and carefully calibrated to quantify the validity of measurement results.

The wide ranging work reported in this thesis has been undertaken over an extensive period of time with the opportunity to review its wide implementation from National Measurement Institutes through to the shop floor measuring equipment. The purpose of the work was to improve the application and understanding of the limitations of

measurement uncertainty methods applicable to shop floor inspection facilities, calibration laboratories and NMIs. The unique work completed in this study includes:

- The first survey of UK gear measurement uncertainty.
- The establishment of uncertainty budgets that apply the classical GUM methods to the gear measurement process.
- The first international comparison of gear measurement capability.
- The application of the MCS method to involute profile measurement uncertainty and a preliminary international comparison of the method.
- The establishment of reference gear artefacts in the UK with the most reliable calibration data.

In any complex measurement process there are numerous sources of measurement uncertainty. This is particularly the case for analytical gear measurement which is a dynamic scanning process simultaneously combining both form and length measurement. A systematic review of measurement sources was completed using ISO TS 14253-2 for guidance and all the significant uncertainty sources have been considered and the relationships have been quantified for all helix, profile and pitch measurement parameters. Although the processes used to measure gears are complex with many sources of uncertainty, the relationship of the uncertainty sources to the measurands are a simple combination of workpiece and instrument geometry. The fundamental problem is the number of potential uncertainty sources coupled to the difficulty in reducing the overall uncertainty with so many potential significant sources. These relationships were defined in Chapter 3 but with so many uncertainty sources it is important to verify that each may be considered as independent so that co-variances may be ignored. The work has concluded that the uncertainty sources may be treated as independent and thus comprehensive uncertainty budgets were developed for all the gear parameters in Chapter 7 and Appendix C.

There is also a tendency within the dimensional metrology field to treat gear measurement as a special case. Traditionally this was because the earlier mechanical gear measuring machines (described in Chapter 3) were radically different to other measuring processes. Nowadays this is not the case. General CMMs use high precision or mapped guideways to measure general 3-dimensional components. Many of the latest CMMs use

scanning type probes and differ from gear measuring machines only by their lack of rotary table and slightly different guideway geometry. The work undertaken for gear measuring machines is directly applicable to CMMs and gear instrument calibration may be considered as a task specific calibration process that can be applied to any general measurement task.

Development of the Virtual CMM (VCMM) for general CMM measurement uncertainty estimation has taken many years to perfect because of its complexity. Developing robust methods of modelling a CMM is difficult but even more problematic are methods of reliably establishing calibration data. The VCMM has not been implemented on a dedicated gear measuring machine because, to date, it has not included a rotary table. But without this limitation, there are serious concerns about the validity of this approach because a) it requires test methods that are significantly different to those used to measure gears and b) the stability of these instruments in shop floor and calibration laboratory environments fall short of the requirements for an NMI. Thus, traditional artefact based evaluation methods that are consistent with 'task specific calibration' are likely to remain the preferred method of establishing traceability in calibration laboratories and manufactures inspection facilities for the foreseeable future.

Alternative mathematical models were discussed in Chapter 4. Most of these have been applied in some form or other during this research programme with the exception of robust statistical methods and Bayesian methods which were not tested. The robust methods were demonstrated to be effective methods of estimating uncertainty but more work is required to justify their application when mainstream GUM methods are readily applied using existing software and coding. However, Bayesian methods are worthy of more study and offer the opportunity to use data from routine testing on instrument performance in order to reduce uncertainty. Furthermore, the more tests that are completed, provided they are representative of the measurement process, the more appropriate the resulting uncertainty estimate. They encourage users to verify instrument performance because there are tangible benefits in doing so. It is thus recommended that a research project into this method is initiated.

The results from a survey of industrial gear measurement performance was presented in Chapter 5. This was the first industrial survey of its type and although it was completed several years ago, it remains the most comprehensive survey to date. The re-evaluation and interpretation of these results was required to quantify differences in artefact

calibration data over a significant period of time and assess the methodology employed by the author during the survey. The initial analysis of the survey findings estimated measurement uncertainty from the helix master results because they required most stringent instrument alignment requirements and there was more data to analyse. The results showed that good quality calibrated instruments in an industrial environment achieved a mean of ±4.6μm/100mm facewidth while typical instruments used on a daily basis only achieved ±11.5μm/100mm. The differences between the two were attributed to poor procedures, non-existent or poor calibration routines, lack of traceability and poor environment. The results from this work prompted the publication of the BGA codes of practice for gear measurement, instrument calibration and measurement result interpretation codes.

The subsequent re-calibration of these artefacts by NMIs at PTB in Germany and Y12 in the USA provided further useful information about the initial analysis. Of particular importance was the re-analysis of the results with respect to data supplied by PTB, Germany. There were significant differences between the reference data derived from the weighted mean and the PTB data. The method used to determine the reference data is similar to those from the 'key comparison reference values'. The differences are due in part to the temperature effects that were not correctly controlled during the initial survey. There was an expectancy that the artefacts would be stable after a four hour soak but subsequent work reported in Chapter 6 shows that this is not sufficient for the large artefacts. Furthermore, most of the survey work was completed in the winter period and the average artefact temperature after transporting to site will be less than the temperature of the measuring instruments. The results from the 100mm diameter lead artefact were more difficult to interpret. The results from the PTB calibration data supports work at the NGML that indicate the artefact is not stable, although it is over 25 years old. The importance of regular calibration intervals and international comparisons at NMI level has thus been demonstrated.

The importance of shop floor measurement methods is quantified further in Chapter 7. Table 7.12 illustrated that significant improvements in shop floor measurement capability is only achievable if improvements in NMI measurement performance are matched with similar improvements in shop floor capability. It is a direct result of the 'law of propagation of uncertainty'. Thus the approach of the NGML of matching work

programmes to improve NGMLs services with programmes that enhance industrial gear measurement capability is validated.

The work reported in this thesis has researched many uncertainty models and applied them to a range of installations from NMIs to shop floor instruments. They have all been based on the comparator method for assessing measurement uncertainty using either mainstream GUM or the MCS methods researched in Chapter 8. A common conclusion drawn by all models and methods is that the measurement uncertainty from the NMIs is often the largest source of uncertainty. The results from the first international comparison, arranged by the author, are reported in Chapter 6 which used the 100mm and 200mm diameter profile and helix artefacts to compare measurement performance of NMIs. All results apart from the right flank 100mm diameter profile master slope error and the 200mm flank form error were within the stated measurement uncertainty for an individual laboratory (the difference in 100mm diameter profile results were attributed to sampling strategy and can thus be ignored at present). This suggests that the uncertainty of data from the National Laboratory is pessimistic. The research on assessing data point uncertainty evaluation methods in Chapter 8 also reached the same conclusion. The most likely explanation for this is that form error uncertainty in artefacts is over estimated. Table 8.5 illustrates this with an extract from PTB data for the 100mm profile artefact. Over a 1mm length, form errors on this relatively poorly finished artefact is less than 0.2μm and data point position uncertainty would yield errors of less than 0.1μm deviations. The suggested reason for this is the filtering effect of a spherical stylus but it may be due to damping and hysteresis in the probe system. There is evidence to suggest that the probe system on the Klingelnberg P65 at NGML detects runout better than ±0.2μm compared to a mechanical indicator (Mikrokator) [Lewis, 2005] but calibrating the system with an uncertainty of ±0.1μm will be very difficult without removing it from the instrument frame. However if these results can be validated, the form measurement uncertainty can be reduced and this will significantly reduce measurement uncertainty for all gear parameters.

The influence of pessimistic NMI measurement uncertainty has further implications. Manufacturers of measuring equipment have no incentive to develop the instrument capability if the uncertainty of calibration data prevents them from proving the performance of the instrument. Furthermore the influence of calibration data measurement uncertainty when included in an uncertainty model shows that encouraging

best practice, investing in state of the art equipment in an industrial environment will deliver little improvement in uncertainty without reductions in measurement uncertainty from the NMI. The reduction in calibration uncertainty using realistic models is thus an important requirement for and NMI and should continue.

The 100mm diameter profile artefact comparison also demonstrated the importance of defining the measurand more carefully. The right flank profile form error indicated that data density should be defined as being equi-spaced along a length of roll in the base tangent plane and not, equi-spaced on a radial section (as many CMMs apply). It is important to note that PTB have adopted this measurement strategy. Form errors can influence the profile slope error generated by differing point spacing. Differences of 1.6μm between PTB data and NGML data were later reduced to 0.6μm when data was gathered at equal intervals. An important recommendation from this work is that standards define the minimum measurement data density and its spacing in appropriate ISO standards.

The methods defined in the ISO, DIN, VDI and BGA standards and associated codes of practice are correctly based around the comparator method. They are all simplified methods of assessing measurement uncertainty to establish the traceability of the instrument with calibrated artefacts. Uncalibrated workpieces are not considered except in ISO TR 10064-5. The research into the application of these methods is reported in Chapter 7. Although some documents have been available for many years, a systematic review has not been completed because there has been no reference method for comparison. The uncertainty budget method, which is compliant with mainstream GUM was developed and applied to gear measurement processes in Chapter 7. It is an accepted method that is realistic for the gear measurement process because most of the uncertainty contributions are either normal or rectangular distributions with no significant non-linear effects that define the shape of the output distribution. Uncertainty budgets have been developed for the main measurement parameters and are presented in Appendix C. Simplified sample uncertainty estimates were made for an industrial measurement process and shown to be equally valid for estimating uncertainty as the more detailed procedure. It is thus recommended that the simplified method is adopted by calibration laboratories for estimating uncertainty using methods that are compliant with the requirements of ISO 17025. While the uncertainty budget method is obviously more accurate, it takes much time and effort to prepare and Accredited Calibration Laboratories find the

implementation of these methods time consuming and difficult. For industrial shop floor situations, the methods outlined in the ISO 18653 and BGA DUCOP05 are simpler to apply but these documents make no reference to when they should be applied and when they are not appropriate. The relevant documents should be revised to make this distinction more clearly.

The work reported in Chapter 7 concluded that the method defined in ISO 18653 was not compliant with mainstream GUM because it included the error or bias as a straight addition to the uncertainty budget. However, the method developed by the author in the BGA codes was clearly demonstrated to underestimate the uncertainty when compared to the uncertainty budget method. The main reasons for this are that although all elements are included in a manner consistent with GUM there are some significant uncertainty sources (temperature and mounting effects) that are not included in the BGA method. Thus it is recommended that the BGA methods of calculating uncertainty are no longer used and the documents are withdrawn. There is a caveat to this statement. The BGA method has been applied to literally hundreds of machines (and thus thousands of measurements) in the UK and there are no instances where results lie outside the 95% confidence intervals estimated by the process.

The ISO 18653 method is not without its limitations. If the bias is greater than half of the calibration data uncertainty, the resulting overall uncertainty will be excessively large compared to the uncertainty budget method. It is thus recommended that this is defined within the document in the next revision. The addition of bias linearly to the combined random uncertainty estimate should be carefully reconsidered. All evidence show that this is not consistent with the requirement in GUM that estimates are 'realistic' rather than 'safe'. However the methodology recommended in the ISO standard of gathering data over a period of time to estimate uncertainty includes environmental effects and thus will generate a reliable estimate of the process uncertainty This procedure is consistent with the test method used to apply the simplified uncertainty budget method in Chapter 7.

Only the ISO TR 10064-5 document defines how to extend the methods to include the measurement of uncalibrated workpieces and this is similar to the simplified uncertainty budget method, and is thus recommended. The remaining issue with uncalibrated workpieces is the strategy for accommodating the difference in geometry between the calibrated artefact and the uncalibrated workpiece. A potentially significant uncertainty is caused by differences in guideway errors when measuring the workpiece. The models for

this are relatively simple, based on the geometry of the workpiece and the instrument and measurement strategy. But reliable methods of measuring the error contributions are more difficult to realise. Simple robust methods of gathering this data are required that produce a fine grid of points to map the guideway form errors. The remaining issue is how to use this information for mapping purposes.

The problem of using evaluated parameters was researched with a pitch master from the USA as part of an international pitch measurement comparison. The work concluded that form and maximum parameters are unreliable unless the position of the errors is correctly reported. There is a tendency for differences between maximum errors to be smaller than differences between actual errors at defined positions. This may contribute to the explanation of the apparent over estimation of measurement uncertainty by the NMIs. The answer to this problem may lie with an alternative measurement strategy researched in this programme but initiated by work in Japan using the Double Ball Artefact (DBA). The DBA method of defining performance with comparison of data points has been researched with the DBA and extended to a number of involute artefacts, as discussed in Chapter 8. This has resulted in a new proposed method for establishing gear measurement uncertainty. Comparison using data points has traditionally been avoided because the calibration method ignores potential errors in the parameter evaluation software. Work at PTB to verify evaluation software independently from artefacts enables them to certify the code and thus allow alternative methods to establish traceability. The data point analysis method was tested on two artefacts calibrated by PTB who also provided reference data. Although issues with data point density were still a problem, this preliminary study indicates it is a powerful and valid method of establishing measurement uncertainty.

The method was further extended to include a Monte Carlo Simulation (MCS) of the measurement process to validate the uncertainty estimate of LS fit slope parameters. The MCS identified that different standard deviation for a given form errors results in the LS parameter but this is small for most practical applications. It further suggested that some reduction in LS fit parameters may be possible after evaluating the process with the MCS method. Thus the data point comparison method, coupled to a MCS is a recommended process for further research and development with an overall objective of improving traceability and reducing measurement uncertainty.

Throughout this study, work has been undertaken using traditional profile, pitch and helix artefacts. The 100mm and 200mm diameter artefacts that were designed for mechanical gear measuring instruments in the 1980's, have proved the most valuable tool for assessing measurement uncertainty and diagnosing errors and trends in instruments. The gear artefacts are probably the most valuable in world because they have such an extensive calibration history. But the needs of CNC instruments are changing artefact requirements and workpiece like artefacts are likely to become more common in future years to minimise the geometry differences between workpieces and calibration items. This will place greater importance on matching measurement and calibration strategy to avoid differences caused by gear form errors. It will also mean that specialised artefacts similar to the Japanese DBA will not be used for routine verification of instruments, in the UK at least.

An area of work that has not been addressed by this study but is of fundamental importance is to review the measurements, measurement strategy and interpretation and use of measurement data. Measurement of helix profile and pitch errors have been conducted because they are easily controlled and adjusted in the manufacturing process. The influence on gear performance is less easy to quantify. Gears are surfaces, not single planes and with the capability of modern CNC measuring instruments it is feasible to measure many more sections and thus predict load distributions and performance more easily than ever before. FE models exist that can accept error data in this format and process it to predict with much greater accuracy the resulting stresses as discussed in Chapter 2, where it was shown the importance of improving the design of gear tooth relief. It is thus recommended that the benefits of mapping both the active flank and the root area that dictates the maximum bending stress are researched to fully realise the investment companies make in new measuring and manufacturing equipment.

9.1 Conclusions

The research hypothesis that directed this work was:

Is it possible to develop a systematic and quantifiable measurement uncertainty procedure applicable to the gear measurement process?

The answer to this question as a result of this programme of work is a definite *yes*, but there is a tendency to over estimate gear measurement uncertainty using conventional

measurement uncertainty assessment methods. This is not necessarily a bad thing if an industrial metrologist interprets the results from a calibration process as directly applicable to product gear measurement uncertainty (without considering the additional sources of measurement uncertainty).

The following conclusions can made from this work programme:

- The ISO 18653 method of evaluating measurement uncertainty can be applied to industrial instruments, provided that the bias is less than 50% of the calibration data uncertainty, without excessively overestimating of measurement uncertainty. The procedure of using a sample size of 10 is preferred with data gathered over a longer period of time so that environmental effects are included. However the procedure is not appropriate for estimating the uncertainty of uncalibrated workpieces, where the uncertainty budget method is more appropriate for including the workpiece influences.

- The use of evaluated parameters for establishing traceability is recommended for industrial measuring instruments but the calibration artefacts should have similar deviations to those of workpieces measured. It is recommended that all pitch errors are tabulated rather than simply stating the largest error, as required by the accuracy standards ISO 1328.

- The uncertainty budget method of assessing uncertainty, consistent with mainstream GUM procedures is used to assess uncertainty when the ISO 18653 method is not valid (calibration laboratories and high quality industrial measurement facilities). It recommended that this uses reproducibility test data over an extensive period of time in the simplified form of uncertainty budget for ease of application.

- ISO 1328-1 and 2 should be revised to include definitions of data point density and define the base tangent measurement plane. Furthermore it should include robust algorithms for evaluating how to interpret measurement data with deliberate departures from involute form.

- The BGA method of evaluating measurement uncertainty is discontinued.

- The international compatibility of gear measurement has been established and quantified with 5 gear artefacts. The results show compatibility within the

laboratory stated measurement uncertainty. The evidence to date is that the uncertainty estimate appears to be pessimistic and this has implication on shop floor capability and the development of future measuring systems. Over estimating measurement uncertainty is not beneficial to anyone.

- The initial test results on the use of data point calibration methods indicate it provides a robust and accurate method for evaluating uncertainty and provides additional information on the measurement system performance. This method is not yet fully developed and understood but avoids many problems associated with evaluated parameters.

- Probe calibration methods should be developed further to validate the performance of the probe system independently of the instrument, with a target uncertainty of ±0.2μm in the first instance.

- Error mapping and artefact calibration methods should also be developed further to enable mapping of geometrical slide errors with an uncertainty of ±0.2μm.

- The MCS method should be extended and applied to calibration data supplied by NMIs to verify capability using the MCS method to analyse the results.

- Workpiece like artefacts need to be developed and applied to industrial calibration needs.

- A plan of continued reduction in uncertainty is required to improve support to UK industry and ensure their continued competitiveness provided this is matched with improvements in shop floor capability through enhanced knowledge transfer.

9.2 Recommendations for further work

The following recommendations are made for future work programmes:

- Apply the data point comparison method to a series of calibrated artefacts and use the MCS method to assess the compatibility of the results and estimate measurement uncertainty.

- Develop new probe calibration methods with reduced uncertainty.

- Develop new error mapping artefacts for linear axes and a measurement strategy with data point intervals of 1mm or less.
- Repeat the survey of UK measurement capability with workpiece like artefacts to minimise the gap between NMIs and shop floor capability.
- Continue the programme of work to reduce NMI measurement uncertainty.
- Develop a programme of work to improve shop floor measurement capability by knowledge transfer. Initiate a programme of research on the application of Bayesian statistical methods to gear measurement uncertainty.
- Research different measurement parameters and strategies to provide better data for design verification purposes and ensure that stress analysis standards reflect the benefits of this.

References

Adams, T.M., A2LA Guide for the estimation of the uncertainty of dimensional calibration and testing results, A2LA, July 2002.

Anon., Traceability of co-ordinate measurements according to the method of the virtual measuring machine, Proposed guideline as August 1997, Proc. Workshop on traceability of co-ordinate measuring machines, PTB, 9 & 10 Oct 1997.

ANSI/AGMA 2014-A98, 1998, *Measuring instrument calibration, gear pitch and runout measurement.*

ANSI/AGMA 2015-A02, 2002, *Accuracy classification system- Tangential measurements for cylindrical gears.*

ANSI/AGMA 2016-A05, 2005, *Evaluation of double flank testers for radial composite measurement of gears* .

ANSI/AGMA 931-A02, 2002, *Calibration of gear measuring instruments and their application to the inspection of gears.*

ANSI/AGMA 935-A05, 2005, *Recommendations relative to the evaluation of radial composite gear double flank testers.*

ASME PTC 19.1-1998 Test uncertainty, instruments and apparatus, Performance test codes, 1998, The American Society of Mechanical Engineers.

Bailey, D, Lawson, E, Smith R E , Detection of hidden runout, Proc. American Gear Manufacturers Association, Fall Tech Meeting, 1995.

Basil, M, Jamieson, A W, Uncertainty of complex systems by Monte Carlo Simulation. Proc. North Sea Flow Measurement Workshop, Gleneagles, October 1998.

Beyer, W., 1999, Traceable strategies for the calibration of involute spline gauges , Technical Paper. American Gear Manufacturers Association (AGMA), 99FTM2 Alexandria, Virginia, ISBN, 1-5589-740-1.

Beyer, W., 1996, Traceable calibration of master gears at PTB, Technical Paper. American gear Manufacturers Association (AGMA), 96FTM4 Alexandria, Virginia, ISBN, 1-5589-671-5.

BGA *Code of Practice for gear Measurement : DUCOP.01 The Specification of Gear Geometry & Associated Tolerances for Involute Gears, iss 1 BGA, July 1994.*

BGA *Code of Practice for Gear Measurement : DUCOP.02 The Specification of Gear Blanks for Involute Gears , iss. 1, BGA, July 1994.*

BGA *Code of Practice for Gear Measurement : DUCOP.03 Involute gear Measurement, iss. 1, BGA, July 1994.*

BGA *Code of Practice for Gear Measurement : DUCOP.04 Checking the repeatability of gear measuring machines, iss.1, BGA, July 1994.*

BGA *Code of practice for Gear measurement : DUCOP.05.1 Verifying the accuracy of gear measuring machines, part 1, iss. 1, BGA, July 1994.*

BGA *Code of practice for Gear Measurement : DUCOP.05.2 Verifying the accuracy of gear measuring machines Part 2, iss.1 BGA, July 1994.*

BGA *Code of Practice for Gear Measurement : DUCOP.06 Interpretation of results, iss. 1 BGA, July 1994.*

Brentnall, J, Heat transfer analysis of master gears and artefacts, Stage 4 project report, Dept. MMMEng., University of Newcastle upon Tyne, 2000.

Bicker, R, Frazer, R C, Wehmeyer, D, Verifying position errors in CNC gear measuring instruments using a laser interferometer with dynamic data capture software. Proc. Laser Metrology and Machine Performance, LAMDAMAP 01, Birmingham, July 2001.

Bicker, R, Cox, B, Frazer R C, Harary, H, Härtig, F, An international comparison of involute gear profile and helix measurement, J. Metrologia, Vol. 41 pp-12-16, 2003.

BS ISO TR 13989-1 :2000, *Calculation of scuffing load capacity of cylindrical, bevel and hypoid gears- Part 1: Flash temperature method.*

BS ISO 5725-2: 1994, *Accuracy (trueness and precision) of measurement methods and results, Part2- Basic methods for the determination of repeatability and reproducibilty of a standard measurement method.*

BS ISO 18653:2003 *Gears-Evaluation of instruments for the measurement of individual gears BSI.*

BS EN ISO 14253-1:1999 *Geometrical Product Specifications (GPS) Inspection by measurement of workpieces and measuring equipment- Part 1: Decision rules for proving confirmation or non-conformance with specifications.*

BS EN ISO 14253-2:1999 *Geometrical Product Specifications (GPS) Inspection by measurement of workpieces and measuring equipment- Part 2 Guide to the estimation of uncertainty in GPS measurement, in calibration of measuring equipment and in product verification.*

Cox, M.G, Dainton M.P. and Harris, P.M., Uncertainty and statistical modelling national physical laboratory software support for metrology best practice guide No.6, March 2001.

Cox, M.G., Forbes, A.B., Harris, P.M., User guide for CMM uncertainty evaluation, NPL report for DTI, March 2002.

Cox. M.G. A discussion of approaches for determining a reference in the analysis of key comparison data, NPL report CISE 42/99, October 1999.

Cox, M.G., Forbes, A.B., Peggs, G N, CMM verification and grading, NPL report CLM 1 for DTI, September 1997.

Cox, M.G. , Dainton, M.P, Harris, P.M, testing functions for linear regression, NPL report CMSC08/00 to NMSPU, DTI, October 2000.

Cox, M G, Forbes, A B, Harris, P M, Bayesian estimation methods in metrology, NPL report, www.npl.co.uk, 2004.

Cox, B.L., Rasnick, B., Adkins, B., Walker, E., Calibration of Master gears on co-ordinate measuring machines. Technical Paper. American Gear Manufacturers Association (AGMA), 98FTM6. 1998.

Cox, B.L. Measurement uncertainty for pitch and runout artefacts, Technical Paper. American Gear Manufacturers Association (AGMA), 99FTM3 Alexandria, Virginia, ISBN, 1-5589-740-1.1999.

Cox, B.L. An update on the national centre for gear metrology, SME 2001.

Cross, N, private email correspondence from NPL, UK, March 2002.

Cubis, J, private correspondence relating to uncertainty of coefficient of linear expansion, UKAS, 2001.

Cubis, J, private correspondence, Oct. 2002.

Dama, R. Uncertainties in error compensation of co-ordinate measuring machines, PhD Thesis, Penn State University, May 1998.

Dietrich, C.F., Uncertainty, calibration and probability, Adam Hilger 1991, ISBN 0-7503-0060-4.

Doiron, T, Stoup, J., Uncertainty and dimensional calibrations J. Res. National Institute of Standards and Technology, Vol 102, No. 6, 647, 1997.

Duncan, R, Techniques for determining the uncertainty of measurement: use of expert opinion, Draft ISO/TS 15530-2, ISO/TC 213/WG 10 N 496, Sept. 2002.

EA-4/02, Expression of the uncertainty of measurement in calibration, European Co-operation for Accreditation, 1999.

Eberhardt, KR, Phillips, S D, Parry, B, Guidelines for expressing the uncertainty of measurement results containing uncorrected bias, J. Res. Natl. Inst. Stand. Technol. Vol. 102, pp577-585, 1997.

Estler, W T, Uncertainty analysis for angle calibrations using circle closure, J. Res. Natl. Inst. Stand. Technol., Vol 103, pp141-151, 1998.

Frazer, R C, Survey of UK industrial gear measurement capability, Final report for Department of Trade and Industry, National Measurement System Policy Unit. 1990.

Frazer, R C, Pennell, J A The accuracy and calibration of gear measuring machines, Pt. 1: Accuracy Survey of Gear Measuring Machines in Industry , Proc. ImechE seminar Aerospace Quality Assurance, Bristol Nov. 1991

Frazer, R C, Pennell, J A, The accuracy and calibration of gear measuring machines Pt. 2: Calibration Procedures and Measuring Techniques for Accurate Gear Measurement. Proc ImechE Seminar Aerospace Quality Assurance Bristol Nov 1991

Frazer, R C, Do we measure gears accurately enough? Proc. 5th (BGA) Annual British Gear Association Technical Congress, Sheffield, 1992.

Frazer, R C, An introduction to the codes of practice for gear measurement. Proc. 6th BGA Annual Technical Congress, Sheffield, 1993.

Frazer, R C, Hofmann, D A, Pennell, J A, Codes of practice for gear measurement, Proc. 1994 International Gearing Conference, Newcastle Upon Tyne, UK, Sept 1994.

Frazer, R C, Hu, J, The differences between 3-Axis and 4-Axis gear measuring machines. Proc. British Gear Association Seminar, Huddersfield, October 1996.

Frazer, R C, Hu, J, Methods of testing calibration equipment in the UK's National Gear Metrology Laboratory. Proc. Laser Metrology and Machine Performance, LAMDAMAP 97, Huddersfield, July 1997, pp 231-242. ISBN: 1-85312-536-9.

Frazer, R C, Hu, J, Verifying the accuracy of involute gear measuring machines. Proc. Laser Metrology and Machine Performance, LAMDAMAP 97, Huddersfield, July 1997, pp 293-302. ISBN: 1-85312-536-9.

Frazer, R C, Hofmann, D A, International gear metrology round robin. Proc. Laser Metrology and Machine Performance, LAMDAMAP 99, Newcastle upon Tyne, July 1999, pp205-214 ISBN 1-853212 661-6.

Frazer, R C, Gear specification, gear measurement and gear accuracy standards. Proc. ImechE Seminar Gear Technology - Gaining a Competitive Edge, September 1999, pp47-63. ISBN 1 86058 280 X.

Frazer, R C, Report for BSI and BGA on MCE5 on ISO TC60 WG2 meeting, Frankfurt, Sept. 2002.

Frazer, R C , Confidential measurement result from a form grinding machine measured at NGML, 2005.

Franke, M., Trapet, E., The ball cube method for CMM interim checks, Proc. Workshop on traceability of co-ordinate measuring machines, PTB, 9 & 10 Oct 1997.

Frenco, private correspondence with Mr R Frost, regarding measurement strategy, 1992.

Goch, G, Gear Metrology, Annals of the CIRP Vol. 52/2/2003.

Haddad, C D, Pennell J A, A PC based program for three dimensional elastic analysis of load distribution in wide faced gears, Proc 3rd World Congress on gearing and power transmission, pp201-211, Paris, 1992.

Hampel, F R, Ronchetti, E M, Rousseeuw, P J, Stahel, W A, Robust statistics. The approach based on influence functions. New York: John Wiley and Sons. 1986.

Harris, P M, Software support for metrology workshop, NPL, March 2002.

Harris, P M, Example MCS Matlab code for linear regression analysis from workshop training material, NPL, August 2006.

Harrison, P, private correspondence regarding M&M instrument repeatability at Rolls Royce, Derby, 2004.

Härtig, F., How to work with the online virtual CMM, Proc. Workshop on traceability of co-ordinate measuring machines, PTB, 9 & 10 Oct 1997.

Härtig, F., Waldele, F., Traceability of gears- New ideas, Recent developments Technical Paper. American gear Manufacturers Association (AGMA), 01FTM5, 2001.

Härtig, F, Lotze, W, 3D gear measurement by CMM, Proc. Laser metrology and machine performance, Birmingham UK, pp333-344, ISBN:1-85312-890-2.

Härtig, F, 100mm and 200mm profile master data supplied in data point format from PTB in accordance with requirements defined by NGML via email. March 2006.

Hofmann, D A, Maillardet, P, Norman, M E, A new tool for designing quiet, low vibration main propulsion gears, Proc. INEC 96, Warship design What is so different?, Institute of Marine Engineers. April 1996.

Holmes, C, email correspondence with Holroyd Ltd relating to coverage factor used in machine tool specification compared to a measuring instrument relating to FDIS-ISO 18653. 2004

Huber, P J, Robust statistics, New York, John Wiley and Sons, 1981.

ISO 6336-1: 1996 *Calculation of load capacity for spur and helical gears- Part 1 Basic Principles, introduction and general influence factors.*

ISO 6336-2: 1996 *Calculation of load capacity for spur and helical gears- Part 2 Calculation of surface durability (pitting).*

ISO 6336-3: 1996 *Calculation of load capacity for spur and helical gears- Part 3 Calculation of tooth bending strength.*

ISO TR 5168: 1998, *Measurement of fluid flow- Evaluation of uncertainties.*

ISO 10360-1:2001, *Geometrical Product Specifications (GPS)- Acceptance and reverification tests for co-ordinate measuring machines (CMM): part 1: Vocabulary.*

ISO 10360-2:2001, *Geometrical Product Specifications (GPS)- Acceptance and reverification tests for co-ordinate measuring machines (CMM): part 2: CMMS used for measuring linear dimensions.*

ISO 10360-3:2001, *Geometrical Product Specifications (GPS)- Acceptance and reverification tests for co-ordinate measuring machines (CMM): part 3: CMMS with the axis of a rotary table as the fourth axis.*

ISO 10360-4:2001, *Geometrical Product Specifications (GPS)- Acceptance and reverification tests for co-ordinate measuring machines (CMM): part 4: CMMs used in scanning measuring mode.*

ISO 15530-5 (draft) Techniques for determining the uncertainty of measurement: the use of statistical measurement history, ISO/TC 213/WG 10 N 495, 2002.

Kirk, R., Scoles, C A, Gear metrology, Macdonald Technical and Scientific, London, UK, 1969.

Klingelnberg, P65 CNC Gear Measuring Centre, specification material, Anon.

Kondo, K., Mizutani, H., Measurement uncertainty of tooth profile by master balls, International conference on gears, 2002, Vol. 2, VDI-Brerichte 1665, p797-810.

Kohler, H K, The measurement and mechanism of dynamic loading of spur gears, PhD Thesis, Sheffield University, 1959.

Kohler, H K, Gear measurement course notes, Design Unit, University of Newcastle, 1989.

Kubo, A, analysis of DBA measurement results submitted by the NGML as part of a comparison and evaluation exercise, unpublished, by email. 2005.

Lacey & Danziger, The Year 1000 P118, Abacus 1999 ISBN 0 349 11306 8.

Lawson, E, Laskin, I, Smith, R E, Effect of radial runout on element measurements, Proc. American Gear Manufacturers Association Fall Tech Meeting, 1993.

Lawson, E, Laskin, I, Separation of runout from elemental inspection data, Proc. American Gear Manufacturers Association Fall Tech Meeting, 1995.

Lawson, E, private correspondence, 2002.

Lotze, W., Härtig, F., 2001, 3D gear measurement by CMM. Proc. Laser measurement and machine tool performance, Birmingham pp333-344, ISBN1-85312-890-2.

Lewis, J, Implementation of traceable pitch calibration by the error separation method, unpublished work, NGML, Design Unit, University Newcastle upon Tyne. 2005.

Levasier, L. CMM stability evaluation by periodic measurement of a simple 1D artefact, Proc. Workshop on traceability of co-ordinate measuring machines, PTB, 9 & 10 Oct 1997.

Ling, P H K, Munro, R G, A new method of measuring involute profile deviations of gear teeth, Proc. IMechE, Pt. C., J of Mechanical Engineering Science, Vol. 210, 1996.

Maillio, C M, Improving the performance of gear measuring instruments, MSc thesis, Newcastle University,1998.

Mancasola, P, private correspondence Klingelnberg GmbH, 2003.

Mandel, J, The statistical analysis of experimental data, Dover Publications Inc 1964, ISBN 0-486-64666-1.

Mark, W D, Method for precision calibration of rotary scale errors and precision determination of gear tooth index errors, J. Mechanical Systems and Signal Processing, Vol. 12, pp723-752, 1998.

Morrish, L, Munro, R G, Palmer, D, An experimental method to measure tooth stiffness throughout and beyond the path of contact, Proc. IMechE, Pt. C, J Mech Eng. Sci., vol 215, 2001.

Munro, R G, The dynamic behaviour of spur gears, PhD Thesis, Cambridge University, 1962.

Munro, R G, Gear measurement course notes, Design Unit, University of Newcastle, 1989.

Munro, R G, The use of optical gratings in gear metrology, Proc. Lamdamap 97, West Yorkshire, UK, 1997.

Myers, E J, Private correspondence on ISO 6336 safety factor definition, 2001.

NGML, UKAS calibration certificate no. 0250/00272, NGML, Design Unit, University of Newcastle upon Tyne, 2005.

NGML, UKAS calibration certificate no. 0250/00273, NGML, Design Unit, University of Newcastle upon Tyne, 2005.

NIST. Bayesian metrology: overview. National Institute Standards and Technology, Statistical Engineering Division. www.itl.nist.gov/div898/basyesian. August 2001.

Onakereru, M O, Measurement uncertainty in gear metrology, MSc Thesis, University of Newcastle upon Tyne, 2003.

Pommer, A. Gear ROLLSCAN for high speed gear measurement. A revolutionary new method for a complete topographical inspection of gears, International Conference on Gears, Vol.2 VDI-Berichte 1665, pp785-796.

PTB. 200mm (2.2) diameter lead master calibration certificate no. 889PTB82. 1982.

PTB. 200mm (2.2) diameter lead master calibration certificate no. 3701PTB92. 1992.

PTB. 200mm (2.2) diameter lead master calibration certificate no. 5078PTB00. 2000.

PTB. 100mm (3.1) diameter lead master calibration certificate no. 0499PTB98. 1998.

PTB. 100mm (3.1) diameter lead master calibration certificate no. 4735PTB05. 2005.

PTB. 200mm (42.2) diameter profile master calibration certificate no. 3702PTB92. 1992.

PTB. 200mm (42.2) diameter profile master calibration certificate no. 5080PTB00. 2000.

Robert, C P, Cassella, G, Monte carlo statistical methods, Springer-Verlag, New York, 1999.

Rolt, F.H Gauges and Fine Measurements Vol. II, Macmillan & Co. 1929.

Schellekens, P.H.J, Debressine, F.L.M., Brouns, D.S.G., Ageneric model for predicting thermo-mechanic errors of multi-axis machines, Proc. Workshop on traceability of co-ordinate measuring machines, PTB, 9 & 10 Oct 1997.

Schwenke, H, Wäldele, F, Siebert, B R L, Kunzmann, H, Assessment of uncertainities in dimensional metrology by monte carlo simulation, proposal for a modular and visual software. *Annals CIRP*, 49 pp395-398, 2000.

Smith, R E, AGMA involute round robin results presented at AGMA (American Gear Manufacturers Association) FTM, USA. 1997.

Takatsuji, T, Kondo, K, Kubo, A, Haertig, F, Osawa, S, Naoi, K, Kurosawa, T, Komori, M, Performance assessment of involute gear measurement by CMM using a double-ball artefact. Proc. SPIE. Vol. SPIE-5879, pp. 247-253. 2005

Taylor B.N. & Kuyatt, C.E., NIST Technical Note 1297, Guidelines for evaluating and expressing the uncertainty of NIST measurement results, September 1994, National Institute of Standards and Technology.

Timms, C, Recent developments in gear metrology, Proc. Engineering dimensional metrology, Vol. 2 pp349-358, NPL, UK, 1953.

Tomlinson, A.G., Tomilnson's gear measuring machine, Engineer, Vol 116, p104, 1923.

Trapet, E., Introduction to traceability with the virtual CMM, Proc. Workshop on traceability of co-ordinate measuring machines, PTB, 9 & 10 Oct 1997.

UKAS, M3003 The expression of Uncertainty and Confidence in Measurement, United Kingdom Accreditation Service, 1997.

VDI/VDE 2607 *Computer-aided evaluation of profile and helix measurements on cylindrical gears with involute profile, Verein Deutscher Ingenieure, Feburary 2000.*

VDI/VDE 2612 part 1, *Testing of involute cylindrical gears, profile measurement, Verein Deutscher Ingenieure, Nov. 1978.*

VDI/VDE 2612 draft, *Testing of involute cylindrical gears, profile measurement, Verein Deutscher Ingenieure, July 1988.*

VDI/VDE 2612 part 2, *Testing of involute cylindrical gears, tooth trace testing, Verein Deutscher Ingenieure, September 1980.*

VDI/VDE 2613, *Pitch testing on gears, spur gears (cylindrical gears), wormwheels and bevel gears, Verein Deutscher Ingenieure, Dec. 1983.*

VDI/VDE 2617 part 1, *Accuracy of co-ordinate measuring machines: characteristics and their checking generalities, Verein Deutscher Ingenieure, April. 1986.*

VDI/VDE 2617 part 2.1, *Accuracy of co-ordinate measuring machines: characteristics parameters and their checking, measurement task specific measurement uncertainty, length measurement uncertainty, Verein Deutscher Ingenieure, Dec.. 1986.*

VDI/VDE 2617 part 2.2 draft, *Accuracy of co-ordinate measuring machines: parameters and their reverification,form measurement, Verein Deutscher Ingenieure, June 1999.*

VDI/VDE 2617 part 3, *Accuracy of co-ordinate measuring machines: characteristics parameters and their checking, components of measurement deviation of the machine, Verein Deutscher Ingenieure, May. 1989.*

VDI/VDE 2617 part 4, *Accuracy of co-ordinate measuring machines: characteristics parameters and their checking, rotary tables on co-ordinate measuring machines, Verein Deutscher Ingenieure, Sept. 1989.*

Vocabulary of Metrology (VIM), *BSI PD6461 PT3 Part 3 Guide to the expression of uncertainty in measurement,1995.*

Vocabulary of Metrology (VIM) *BSI PD6461 PT1 Part 1 Basic and general terms(international),1995.*

WECC Doc. 19, Guidelines for the expression of the uncertainty of measurement in calibrations, Western European Calibration Cooperation,1990.

Weise, K, Wöger, W, Comparison of two measurement results using Bayesian theory of measurement uncertainty, Meas. Sci. Techno., pp879-882, 1994.

Wilson, S J, Pitch measurement results and analysis report, unpublished, Design Unit, University of Newcastle upon Tyne, 2003.

Wilson, S J, Frazer, R C, Review of UKAS on-site instrument calibration certificate results, unpublished, Design Unit, University of Newcastle upon Tyne, 2005.

Appendix A

Survey of gear measurement capability

This appendix contains Tables A1 to A12 that report the results from the artefact measurements for the survey of gear measurement capability completed in 1989-1990.

Table A1 200mm diameter lead master mean lead error slope $f_{H\beta}$ over 100mm face (normal plane) part A instruments.

Code	Lead error slope ($f_{H\beta}$) over 100mm face (normal plane)										
	0l	0r	15Ll	15Lr	15Rl	15Rr	30Ll	30Lr	30Rl	30Rr	Error
A01	-2.8	-2.1	2.3	1.5	-6.1	-6.8	-1.8	-3.8	-3.5	-4.1	0
A03			1.8	2.0	-3.6	-5.4	-1.4	-4.0	-0.4	-1.7	0
A06	-1.4	-0.8	-2.4	1.7	0.8	-2.7	1.8	-3.1	1.2	-1.1	1.5
A07	-2.6	-2.0	-1..3	-1.9	-4.1	-6.6	2.7	-2.2	-8.5	-7.7	0
A09	-1.9	-1.9	1.2	0.5	-4.1	-5.3	2.6	-1	-3.6	-4.4	0
A11	-3.0	-2.1	3.0	3.0	-4.9	-4.9	-1.2	-5.1	-2.2	-2.0	0
A16	-0.3	0	-2.7	-3.2	2.5	-1.9	-1.7	-3.6	1.9	0.4	1.7
A17	-4.1	-5.8	-4.3	-5.8	-5.4	-5.6	-1.9	-5.9	-2.6	-2.2	0
A26	0.5	0.2	4.0	3.2	-0.8	-3.6	-0.6	-2.8	0.3	0.0	0
A43	-0.9	-0.7	0.1	0.9	-2.5	-3.4	-0.1	0.8	0.2	-0.6	0
A43	-0.7	-0.1	1.4	-0.8	-4.7	-6.8					0
A43	-1.6	-2.1	2.9	1.0	-4.7	-6.1	5.5	-0.6	-6.0	-6.2	0
Mean	-1.8	-1.6	0.3	0.1	-3.5	-5.2	0.0	-2.6	-2.3	-2.9	
SD	1.2	1.5	2.9	2.7	2.1	1.2	2.6	2.2	2.8	2.3	
Weighted mean	-1.7	-1.6	0.4	0.1	-3.5	-5.2	0.4	-2.6	-2.2	-2.8	
889 PTB 82	-1.8	-1.4	-0.3	-0.4	-4.2	-5.7	-3.6	0.3	-4.1	-5.6	
3701 PTB 92	-1.8	-0.8	-0.8	-1.2	-4.2	-5.2	-4.4	-1.0	-5.8	-5.8	
5078 PTB 00	-1.9	-1.0	-1.2	-1.2	-4.3	-5.4	-4.5	-0.8	-6.1	-6.7	

Table A2 200mm diameter lead master mean lead error slope $f_{H\beta}$ over 100mm face (normal plane) part B instruments

Code	Lead error slope ($f_{H\beta}$) over 100mm face (normal plane)										
	0l	0r	15Ll	15Lr	15Rl	15Rr	30Ll	30Lr	30Rl	30Rr	Error
B02	-1.8	-1.4	0.3	0.4	-4.1	-5.5	-3.1	-0.3	-3.6	-4.9	0
B04	-5.7	-4.8	-6.7	-8.9	0.5	4.2	-6.9		10.6	13.3	-1
B10	-1.2	-1.8	-8.5	-9.1	-6.7	-4.1	-7.1	-5.5	11.6	10.9	1.
B12	-0.6	-1.6	3.9	4.2	11.5	5.1	31.3	12			1
B12	-0.9	4.0	-0.5	-2.4	1.6	4.6	4.6	-2.3	5.2	10.8	1.8
B13	2.7	4.6	7.1	-3.7	0.8	-2.1	7.7	-5.2	-12.1	-4.3	2
B15	-0.1	-0.3	16.4	12.7	3.5	1.6	14.9	14.5	-2.3	-2.2	0
B15	-6.0	-2.2	-1.0	0.6	-8.7	-7.7	5.4	4.2	-5.6	-5.2	3.3
B18	0.2	0.0	-1.3	-2.2	-2.3	-2.8	-0.2	-3.0	0.9	-1.6	3.3
B19	8.0	6.4									-7.0
B21	-2.4	-2.6	0.9	2.1	2.0	1.1	5.8	5.0	3.0	2.7	0
B22	-16.0	-9.8	13.3	15.4	7.1	6.8	15.8	13.9	-1.2	0	-16.0
B23	2.8	1.5	2.8	0.5	-4.5	4.6	10.0	3.2	14.5	9.0	0
B24	-3.0	-4.3	-4.6	-4.8	-1.0	-4.8	-7.4	-10.2	2.0	-4.6	-1.0
B25	-8.1	-4.6	0	0.2	-1.0	1.5	1.1	-3.7	8.0	4.8	0
Mean	-2.1	-1.1	1.6	0.4	-0.1	0.2	5.5	1.7	2.3	2.3	

Table A3 200mm diameter lead master mean lead error slope $f_{H\beta}$ over 100mm face (normal plane) difference between individual results part A instruments and. part A instrument weighted mean.

Code	Lead error slope ($f_{H\beta}$) over 100mm face (normal plane)										
	0l	0r	15Ll	15Lr	15Rl	15Rr	30Ll	30Lr	30Rl	30Rr	U95
A01	-1.0	-0.5-	1.9	1.4	-2.6	-1.6	-2.2	-1.2	-1.3	-1.3	2.9
A03			1.4	1.9	-0.1	-0.2	-1.8	-1.4	1.8	1.1	2.9
A06	-1.1	-0.7	-4.3	0.1	2.8	1.1	-0.7	-2.1	1.9	0.2	4.1
A07	-0.8	-0.4	-1.7	-2.0	-0.6	-1.4	2.3	0.4	-6.3	-4.9	5.1
A09	-0.1	-0.3	0.8	0.4	-0.6	-0.1	2.2	1.6	-1.4	-1.6	2.5
A11	-1.2	-0.5	2.6	2.9	-1.4	0.3	-1.6	-2.5	0.0	0.8	3.6
A16	-0.2	-0.1	-4.8	-5.0	4.3	1.6	-3.8	-2.7	2.4	1.5	6.5
A17	-2.3	-4.2	-4.7	-5.9	-1.9	-0.4	-2.3	-3.3	-0.4	0.6	4.5
A26	2.3	1.8	3.6	3.1	2.7	1.6	0.2	-0.2	2.5	2.8	2.8
A43	0.9	0.9	-0.3	0.8	1.0	1.8	-0.5	3.4	2.4	2.2	2.6
A43	1.1	1.5	1	-0.9	-1.2	-1.6					
A43	0.2	-0.5	2.5	0.9	-1.2	-0.9	5.1	2.0	-3.8	-3.4	5.4
Mean measurement uncertainty											3.5

Table A4 200mm diameter lead master mean lead error slope $f_{H\beta}$ over 100mm face (normal plane) difference between part B instruments and weighted mean of part A instruments

Code	Lead error slope ($f_{H\beta}$) over 100mm face (normal plane)										
	0l	0r	15Ll	15Lr	15Rl	15Rr	30Ll	30Lr	30Rl	30Rr	U95
B02	0.7	0.2	0.5	0.2	-0.9	0.6	2.2	1.8	-2	-1.4	3.5
B04	-2.9	-2.2	-6.1	-8.0	5.0	10.4	-6.3		13.8	17.1	19.2
B10	-0.4	-1.2	-9.9	-10.2	-4.2	-0.1	-8.5	-3.9	12.8	12.7	16.8
B12	-0.6	-1.8	1.7	2.3	13.2	8.5	29.1	12.8			20.8
B12	-1.1	3.6	-2.9	-4.5	3.1	7.8	2.2	-1.7	5.4	11.6	10.4
B13	4.5	6.2	6.7	-3.8	4.3	3.1	7.3	-2.6	-9.9	-1.5	11.6
B15	1.7	1.3	16	12.6	7.0	6.8	14.5	17.1	-0.1	0.6	14.0
B15	-7.5	-3.9	-4.7	-2.8	-8.5	-5.8	1.7	3.5	-6.7	-5.7	8.3
B18	-1.3	-1.7	-5	-5.6	-2.1	-0.9	-3.9	-3.7	-0.2	-2.1	4.5
B19	16.8	15.3									-
B21	-0.6	-1.0	0.5	2.0	5.5	6.3	5.4	7.6	5.2	5.5	6.8
B22	1.8	7.8	28.9	31.3	26.6	28.0	31.4	32.5	17.0	18.8	21.9
B23	4.6	3.1	2.4	0.4	-1.0	9.8	9.6	5.8	16.7	11.8	11.5
B24	-0.2	-1.7	-4.0	-3.9	3.5	1.4	-6.8	-6.6	5.2	-0.8	8.4
B25	-6.3	-3.0	-0.4	0.1	2.5	6.7	0.7	-1.1	10.2	7.6	10.5
Mean measurement uncertainty											10.8

Table A5 100mm diameter lead master mean lead error slope $f_{H\beta}$ over 100mm face (normal plane) part A instruments.

Code	Lead error slope ($f_{H\beta}$) over 100mm face (normal plane)										
	0l	0r	15Ll	15Lr	15Rl	15Rr	30Ll	30Lr	30Rl	30Rr	Error
A01	-0.6	-0.2	3.9	1.7	3.9	6.7	0.4	2.6	10.9	11.9	0
A03	-0.1	0.1	1.7	-1.7	4.7	7.7	-2.2	-0.9	16	15.5	0
A05	-3.0	-3.0	0.9	-1.0	8	2.0	-8.0	-2.0	13.0	7.0	-2.0
A06	2.1	0.9	6.5	0.8	4.0	10.8	0.6	3.5	6.0	4.9	1.5
A07	-2.2	-1.7	4.7	2.6	-0.2	3.0	6.5	9.1	6.6	6.6	0
A09	-2.1	-2.1	5.6	3.3	-1.7	2.2	5.4	7.5	2.8	4.4	-2.0
A11	0.2	-0.2	5.6	1.9	2.8	6.5	4.3	5.6	8.4	10.4	0
A16	1.6	1.0	6.8	3.9	3.5	5.9	6.5	10.5	6.0	5.2	1.7
A17	-2.4	-3.9	1.9	0.3	3.4	2.4	2.7	4.9	5.4	8.5	0.
A26	-0.7	-1.5	2.0	2.2	0.8	4.7	5.1	5.2	11.8	11.9	0
A43	-1.3	-1.6	4.3	3.9	0.9	4.3	5.1	5.2	11.8	11.9	0
A43	-1.1	-1.0	6.9	3.5	-1.1	3.1	9.8	13.5	7.9	5.5	0
A43	-0.5	-0.5	7.8	3.8	0.4	5.5	7.4	9.4	6.6	7.6	0
Mean	-0.7	-1.0	4.6	2.0	2.3	5.1	3.4	5.7	8.8	8.6	
SD											
Weighted mean	-0.8	-1.1	4.7	2.2	2.0	4.9	4.0	6.1	8.3	8.6	
0499 PTB 98	-0.6	-0.5	6.6	4.1	-0.2	2.6	6.4	8.4	4.6	5.4	
4735 PTB 05	-0.6	-0.8	7.6	5.0	-0.8	2.5	8.4	11.1	3.0	4.1	

Table A6 100mm diameter lead master mean lead error slope $f_{H\beta}$ over 100mm face (normal plane) part B instruments

Code	Lead error slope ($f_{H\beta}$) over 100mm face (normal plane)										
	0l	0r	15Ll	15Lr	15Rl	15Rr	30Ll	30Lr	30Rl	30Rr	Error
B02	-1.8	-1.1	5.5	4.1	-0.4	3.4	4.4	6.2	4.8	5.6	-1
B04	-1.5	-2.1	2.8	-0.8	5.7	8.7	-.3	1.7	16.5	21.5	-1
B10	-1.0	-0.2	-3.6	-4.6	-0.6	1.5	-5.1	-4.4	10.2	10.5	1
B12	6.4	1.6	9.9	1.8	14.0	15.6		-27.0	11.1	13.4	1.8
B12	2.4	2.0	6.7	4.9	10.5	5.6	6.1	-8.1	18.2	13.0	2
B14	2.5	1.8	0.0	-4.8	-4.2	-11.6	10.0	8.8	3.8	4.8	4
B14	-1.2	-0.9	7	3.8	2.8	1.1	5.5	6.3	3.4	2.0	0
B15	-2.2	-4.1	9.4	10.6	-9.1	-3.9	15.6	9.7	8.5	-4.2	0
B15			-2.0	-1.8	5.0	2.4	7.7	-1.4	-8.7	-5.5	3.3
B18	1.0	0.5	7.2	8.2	8.3	5.9	5.7	12.8	13.2	14.0	3.3
B19	12.5	14.0									-7
B20	-6.4	-4.8	-8.5	-4.0	5.1	7.0					1.5
B20	0.0	0.0	9.7	6.3	3.9	7.7	6.2	11.0	8.2	8.9	-2
B21	-0.9	-1.8	2.1	-0.3	1.5	7.3	0.1	-1.5	9.2	18.4	0
B22	-10.5	-18	-1.5	-4.5	-0.2	-5.1	-3.9	-6.5	2.6	2.2	-16
B23	-1.3	-2.5	-0.3	2.9	8.5	7.7	-2.5	7.8	25.8	15.9	0
B24	-1.3	-1.3	2.3	4.6	3.8	6.1	-3.9	-2.8	8.9	7.4	-1.0
B24	-1.5	-2.5	5.3	4.5	0.6	-2.1	12.0	6.0	-0.8	-6.2	0
B25	7.6	9.2	11.3	8.5	-0.4	3.4	4.4	6.2	4.8	5.6	-1
Mean	-2.1	-1.1	1.6	0.4	-0.1	0.2	5.5	1.7	2.3	2.3	

Table A7 100mm diameter lead master mean lead error slope $f_{H\beta}$ over 100mm face (normal plane) difference between part A instruments weighted mean and individual instrument results.

Code	Lead error slope ($f_{H\beta}$) over 100mm face (normal plane)										
	0l	0r	15Ll	15Lr	15Rl	15Rr	30Ll	30Lr	30Rl	30Rr	U95
A01	0.2	0.9	-0.8	-0.5	1.9	1.8	-3.6	-3.6	2.6	3.4	4.8
A03	0.7	1.2	-3.0	.-3.9	2.7	2.8	-6.2	-7.1	7.7	7.0	10.3
A05	-0.2	0.1	-1.8	-1.2	8.0	-0.9	-10.0	-6.2	6.7	0.5	10.6
A06	1.4	0.5	0.3	-2.9	0.5	4.4	-4.9	-4.2	-3.8	-5.2	6.5
A07	-1.4	-0.6	0.0	0.4	-2.2	-1.9	2.5	2.9	-1.7	-2.0	3.7
A09	0.7	1.0	2.9	3.1	-1.7	-0.7	3.4	3.3	-3.5	-2.2	5.1
A11	1.0	0.9	0.9	-0.3	0.8	1.6	0.3	-0.6	0.1	1.9	1.7
A16	0.7	0.4	0.5	0.00	-0.2	-0.7	0.8	2.6	-4.0	-5.1	4.6
A17	-1.6	-2.8	-2.8	-1.9	1.4	-2.5	-1.3	-1.3	-2.9	-0.1	3.0
A26	0.1	-0.4	-2.7	0.0	-1.2	-0.2	1.1	-1.0	3.5	3.4	3.9
A43	-0.5	-0.5	-0.4	1.7	-1.1	-0.6	1.1	-1.0	3.5	3.4	3.6
A43	-0.3	0.1	2.2	1.3	-3.1	-1.8	5.8	7.3	-0.4	-3.1	7.0
A43	0.3	0.6	3.1	1.6	-1.6	0.6	3.4	3.2	-1.7	-1.0	3.9
Mean measurement uncertainty											5.3

Table A8 100mm diameter lead master mean lead error slope $f_{H\beta}$ over 100mm face (normal plane) difference between weighted mean of part A instruments and part B instruments

Code	Lead error slope ($f_{H\beta}$) over 100mm face (normal plane)										
	0l	0r	15Ll	15Lr	15Rl	15Rr	30Ll	30Lr	30Rl	30Rr	U95
B02	-0.1	1.0	1.8	2.9	-1.4	-0.5	1.4	1.1	-2.5	-2.0	3.6
B04	0.3	-0.1	-0.9	-2.0	4.7	4.8	-3.3	-3.5	9.2	13.9	11.6
B10	-1.2	-0.1	-9.3	-7.8	-3.6	-4.4	-10.1	-11.5	0.9	0.9	10.0
B12	5.4	0.9	3.4	-2.2	10.2	8.9		-34.9	1.0	3.0	27.0
B12	1.2	1.1	0.0	0.7	6.5	-1.3	0.1	-16.2	7.8	2.4	13.0
B14	-0.7	-1.1	-8.7	-10.9	-10.2	-20.5	2.0	-1.3	-8.5	-7.8	14.1
B14	-0.4	0.2	2.3	1.6	0.8	-3.8	1.5	0.2	-4.9	-6.6	6.2
B15	-1.4	-3.0	4.74	8.4	-11.1	-8.8	11.6	3.6	0.2	-12.7	16.5
B15			-10.0	-7.3	-0.3	-5.8	0.4	-10.8	-20.3	-17.4	15.9
B18											
B19	-1.5	-1.7	-0.8	2.7	3.0	-2.3	-1.6	3.4	1.6	2.1	4.6
B20	-7.2	-5.2	-14.7	-7.7	1.6	0.6					12.5
B20	2.8	3.1	7.0	6.1	3.9	4.8	4.2	6.9	1.9	2.3	4.7
B21	-0.1	-0.7	-2.6	-2.5	-0.5	2.4	-3.9	-7.6	0.9	9.8	9.2
B22	6.3	-0.9	9.8	9.3	13.8	6.0	8.1	3.4	10.3	9.6	9.7
B23	-0.5	-1.4	-5.0	0.7	6.5	2.8	-6.5	1.7	17.5	7.3	13.9
B24	0.5	0.8	-1.4	3.4	2.8	2.2	-6.9	-7.9	1.6	-0.2	7.8
B24	-0.7	-1.4	0.6	2.3	-1.4	-7.0	8.0	-0.1	-9.1	-14.8	12.9
B25	8.4	10.3	6.6	6.3	-3.4	-7.7	9.0	7.4	-1.0	0.9	12.4
Mean measurement uncertainty											10.8
Mean	-2.1	-1.1	1.6	0.4	-0.1	0.2	5.5	1.7	2.3	2.3	

Table A9 200mm diameter profile master part a profile slope error results

Code	Mean measured errors		Deviation between mean of A companies and individual errors	
	Left flank $f_{H\alpha}$	Right flank $f_{H\alpha}$	Left flank $f_{H\alpha}$	Right flank $f_{H\alpha}$
A01	-2.7	-1.4	0.0	0.8
A03	-4.3	-3.9	-1.6	-1.7
A06	-1.5	-1.2	1.2	1.0
A07	-3.4	-3.3	-0.7	-1.1
A09	-0.2	2.2	2.5	4.4
A11	-4.4	-4.0	-1.7	-1.8
A16	-7.7	-4.7	-5.0	-2.5
A17	-3.3	-4.5	-0.6	-2.3
A26	0.7	0.4	3.4	2.6
A43	-0.1	-2.0	2.6	0.2
A43	-3.5	-1.8	-0.8	0.4
A43	-2.2	-1.7	0.5	0.5
Mean	-2.7	-2.2	-	-
Standard deviation	2.3	2.1	-	-
3702 PTB 92	-1.1	0.3		
5080 PTB 00	-0.6	0.9		

Table A10 200mm diameter profile master part B profile slope error results

Code	Mean measured errors		Deviation between mean of A companies and individual errors	
	Left flank $f_{H\alpha}$	Right flank $f_{H\alpha}$	Left flank $f_{H\alpha}$	Right flank $f_{H\alpha}$
B04	-0.8	-2.1	2.1	-0.1
B10	9.6	10.1	12.3	12.3
B12	-6.0	-6.0	-3.3	-3.8
B12	-3.5	-4.1	-0.8	-2.1
B13	2.5	2.1	5.2	4.3
B14	-3.5	-1.0	-0.8	1.2
B14	-2.2	-2.3	0.5	-0.1
B15	-4.1	-4.5	-1.4	-2.3
B15	-1.0	-1.2	1.7	1.0
B18	2.0	4.0	4.7	6.2
B19	-1.8	0.0	0.9	2.2
B20	-3.0	-4.8	-0.3	2.6
B20	-8.8	-10.0	-6.1	7.8
B21	-2.9	0.0	-0.2	2.2
B22	-7.0	-5.0	-4.3	-2.8
B24	-7.8	-6.7	-3.1	-5.5
B24	-0.2	1.2	2.5	3.4
B25	-6.0	-3.0	-3.3	-0.8
Mean	-2.5	-1.9	-	-
SD	4.3	4.5	-	-
3702 PTB 92	-1.1	0.3		
5080 PTB 00	-0.6	0.9		

Table A11 200mm diameter radial flank cumulative results and difference between average and individual results.

Code	Cumulative pitch Fp	Difference between mean part A
A01	5.2	-1.0
A03	6.8	0.6
A05	6.3	0.1
A07	5.5	-0.7
A09	8.6	2.4
A11	7.2	1.0
A17	5.9	-0.3
A43	5.5	-0.7
A43	5.6	-0.6
A43	5.8	-0.4
Mean	6.2	-
SD	1.0	-
2667 PTB 93	5.8	-
4411 PTB 01	4.6	-

Table A12 200mm diameter oblique flank cumulative results for part b companies and difference between average and individual results.

Code	Cumulative pitch Fp	Difference between mean of Part A
B02	6.8	0.6
B10	3.3	-2.9
B14	5.6	-0.6
B14	9.3	3.1
B20	3.5	2.7
B21	9.1	2.9
Mean	6.3	-
SD	2.6	-
2667 PTB 93	5.8	-
4411 PTB 01	4.6	-

Appendix B

An international comparison of involute profile, helix and pitch measurement-

Measurement result tables

This appendix contains the results from the first international comparisons of gear measurement arranged by the National Gear Metrology Laboratory. The measurement results are presented as deviations from the unweighted mean from the participating National Measurement Institutes.

The Tables are:

B1 200mm diameter helix artefact, helix slope error ($f_{H\beta}$)

B2 200mm diameter helix artefact, helix total error (F_{β})

B3 200mm diameter helix artefact, helix form error ($f_{\beta f}$)

B4 200mm diameter profile artefact, profile slope error ($f_{H\alpha}$)

B5 200mm diameter profile artefact, profile total error (F_{α})

B6 200mm diameter profile artefact, profile form error ($f_{f\alpha}$)

B7 100mm diameter helix artefact, helix slope error ($f_{H\beta}$)

B8 100mm diameter helix artefact, helix total error (F_{β})

B9 100mm diameter helix artefact, helix form error ($f_{\beta f}$)

B10 100mm diameter profile artefact, profile slope error ($f_{H\alpha}$)

B11 100mm diameter profile artefact, profile total error (F_{α})

B12 100mm diameter profile artefact, profile form error ($f_{f\alpha}$)

B13 48A pitch artefact

Table B1 200mm helix artefact. Differences between the unweighted mean and individual laboratory results for helix slope error ($f_{H\beta}$) and the individual laboratory measurement uncertainty ($\pm U_{95}$) in µm.

Helix/ Flank	PTB 1992	NGML 1996	NIST 1998	BWXT Y-12 1999	PTB 2000
0l	0.04 (±1.2)	-0.06 (±1.5)	0.14 (±1.0)	-0.06 (±1.3)	-0.06 (±1.0)
0r	0.20 (±1.2)	0.10 (±1.5)	0.10 (±1.0)	-0.40 (±1.3)	0.00 (±1.0)
-15l	0.28 (±1.5)	0.98 (±1.8)	-0.72 (±1.3)	-0.42 (±1.5)	-0.12 (±1.2)
-15r	-0.26 (±1.5)	1.04 (±1.8)	-0.46 (±1.3)	-0.06 (±1.5)	-0.26 (±1.2)
15l	0.36 (±1.5)	-0.54 (±1.8)	0.06 (±1.3)	-0.14 (±1.5)	0.26 (±1.2)
15r	0.26 (±1.5)	0.06 (±1.8)	-0.04 (±1.3)	-0.34 (±1.5)	0.06 (±1.2)
-30l	0.28 (±1.5)	-0.32 (±2.0)	-0.22 (±1.5)	0.08 (±1.7)	0.18 (±1.5)
-30r	0.04 (±1.5)	-0.66 (±2.0)	0.34 (±1.5)	0.04 (±1.7)	0.24 (±1.5)
30l	-0.06 (±1.5)	0.54 (±2.0)	0.24 (±1.5)	-0.36 (±1.7)	-0.36 (±1.5)
30r	0.48 (±1.5)	-0.42 (±2.0)	0.18 (±1.5)	0.18 (±1.7)	-0.42 (±1.5)
-45l	-0.20 (±1.7)	-0.80 (±2.3)	0.70 (±1.8)	0.40 (±2.1)	-0.10 (±1.7)
-45r	-0.16 (±1.7)	-0.76 (±2.3)	1.04 (±1.8)	0.34 (±2.1)	-0.46 (±1.7)
45l	0.80 (±1.7)	0.20 (±2.3)	-0.50 (±1.8)	-0.50 (±2.1)	0.00 (±1.7)
45r	1.30 (±1.7)	-0.30 (±2.3)	0.10 (±1.8)	-0.80 (±2.1)	-0.30 (±1.7)

Table B2 200mm helix artefact. Differences between the unweighted mean and individual laboratory results for helix total error (F_β) and the individual laboratory measurement uncertainty ($\pm U_{95}$) in μm.

Helix/ Flank	PTB 1992	NGML 1996	NIST 1998	BWXT Y-12 1999	PTB 2000
0l	-0.32 (±1.0)	1.18 (±1.6)	-0.42 (±1.0)	-0.42 (±1.3)	-0.02 (±1.4)
0r	-0.24 (±1.0)	0.56 (±1.6)	-0.24 (±1.0)	-0.04 (±1.3)	-.004 (±1.4)
-15l	0.28 (±1.0)	0.08 (±2.0)	-0.08 (±1.3)	-0.42 (±1.5)	-0.02 (±1.6)
-15r	0.44 (±1.0)	-0.06 (±2.0)	-0.36 (±1.3)	-0.4 6 (±1.5)	-0.44 (±1.6)
15l	-0.64 (±1.0)	2.06 (±2.0)	-0.84 (±1.3)	0.36 (±1.5)	-0.94 (±1.6)
15r	-0.08 (±1.0)	0.62 (±2.0)	-0.18 (±1.3)	0.02 (±1.5)	-0.38 (±1.6)
-30l	0.00 (±1.0)	0.30 (±2.2)	-0.50 (±1.5)	-0.20 (±1.7)	0.40 (±1.8)
-30r	0.58 (±1.0)	0.58 (±2.2)	-0.92 (±1.5)	-0.62 (±1.7)	0.38 (±1.8)
30l	-0.30 (±1.0)	1.50 (±2.2)	-1.30 (±1.5)	0.00 (±1.7)	0.10 (±1.8)
30r	-0.24 (±1.0)	1.26 (±2.2)	-0.64 (±1.5)	-0.94 (±1.7)	0.56 (±1.8)
-45l	0.72 (±1.0)	0.62 (±2.5)	-0.48 (±1.8)	-0.98 (±2.1)	0.12 (±2.0)
-45r	0.66 (±1.0)	1.06 (±2.5)	-1.34 (±1.8)	-1.04 (±2.1)	0.66 (±2.0)
45l	-1.52 (±1.0)	1.78 (±2.5)	-0.32 (±1.8)	0.88 (±2.1)	-0.82 (±2.0)
45r	-0.86 (±1.0)	1.14 (±2.5)	-0.26 (±1.8)	0.14 (±2.1)	-0.16 (±2.0)

Table B3 200mm helix artefact. Differences between the unweighted mean and individual laboratory results for helix form error ($f_{\beta f}$) and the individual laboratory measurement uncertainty ($\pm U_{95}$) in µm.

Helix/ Flank	PTB 1992	NGML 1996	NIST 1998	BWXT Y-12 1999	PTB 2000
0l	0.04 (±1.0)	0.04 (±1.2)	0.04 (±1.0)	-0.16 (±1.3)	0.04 (±1.0)
0r	-0.28 (±1.0)	1.12 (±1.2)	-0.08 (±1.0)	-0.38 (±1.3)	-0.38 (±1.0)
-15l	0.48 (±1.0)	0.58 (±1.2)	-0.42 (±1.3)	-0.42 (±1.5)	-0.22 (±1.0)
-15r	0.48 (±1.0)	0.28 (±1.2)	-0.42 (±1.3)	-0.32 (±1.5)	-0.02 (±1.0)
15l	0.46 (±1.0)	0.76 (±1.2)	-0.54 (±1.3)	-0.54 (±1.5)	-0.14 (±1.0)
15r	0.48 (±1.0)	0.38 (±1.2)	-0.32 (±1.3)	-0.52 (±1.5)	-0.02 (±1.0)
-30l	0.42 (±1.0)	0.52 (±1.2)	-0.58 (±1.5)	-0.58 (±1.7)	0.22 (±1.0)
-30r	0.48 (±1.0)	0.38 (±1.2)	-0.62 (±1.5)	-0.52 (±1.7)	0.28 (±1.0)
30l	0.18 (±1.0)	0.84 (±1.2)	-0.76 (±1.5)	-0.66 (±1.7)	0.44 (±1.0)
30r	0.34 (±1.0)	0.84 (±1.2)	-0.46 (±1.5)	-1.16 (±1.7)	0.44 (±1.0)
-45l	0.56 (±1.0)	0.26 (±1.2)	-0.14 (±1.8)	-0.94 (±2.1)	0.26 (±1.0)
-45r	0.62 (±1.0)	0.12 (±1.2)	-0.78 (±1.8)	-0.28 (±2.1)	0.32 (±1.0)
45l	0.42 (±1.0)	0.32 (±1.2)	-0.48 (±1.8)	-0.28 (±2.1)	0.02 (±1.0)
45r	0.08 (±1.0)	2.38 (±1.2)	-0.02 (±1.8)	-1.32 (±2.1)	-0.12 (±1.0)

Table B4 200mm profile artefact. Differences between the unweighted mean and individual laboratory results for profile slope error ($f_{H\alpha}$) and the individual laboratory measurement uncertainty ($\pm U_{95}$) in μm.

Flank	PTB 1992	NGML 1996	NIST 1998	BWXT Y-12 1999	PTB 2000
L	-0.16 (±1.0)	-0.26 (±1.5)	0.04 (±0.9)	0.04 (±0.9)	0.34 (±1.0)
R	-0.16(±1.0)	-0.26 (±1.5)	0.04 (±0.9)	-0.06 (±0.9)	0.44 (±1.0)

Table B5 200mm profile artefact. Differences between the unweighted mean and individual laboratory results for profile total error (F_{α}) and the individual laboratory measurement uncertainty ($\pm U_{95}$) in μm.

Flank	PTB 1992	NGML 1996	NIST 1998	BWXT Y-12 1999	PTB 2000
L	-0.16 (±1.0)	0.44 (±1.6)	-0.36 (±0.9)	-0.56 (±0.9)	0.64 (±1.0)
R	-0.16 (±1.0)	0.54 (±1.6)	-0.36 (±0.9)	-0.46 (±0.9)	0.44 (±1.0)

Table B6 200mm profile artefact. Differences between the unweighted mean and individual laboratory results for profile form error ($f_{f\alpha}$) and the individual laboratory measurement uncertainty ($\pm U_{95}$) in μm.

Flank	PTB 1992	NGML 1996	NIST 1998	BWXT Y-12 1999	PTB 2000
L	0.00 (±1.0)	0.60 (±1.2)	-0.50 (±0.9)	-0.30 (±0.9)	0.20 (±1.0)
R	-0.10 (±1.0)	0.06 (±1.2)	-0.10 (±0.9)	-0.30 (±0.9)	-0.10 (±1.0)

Table B7 100mm helix artefact. Differences between the unweighted mean and individual laboratory results for helix slope error ($f_{H\beta}$) and the individual laboratory measurement uncertainty ($\pm U_{95}$) in μm

Helix/ Flank	PTB 1998	BWXT Y-12 2002	NGML 2005	PTB 2005
0l	-0.04 (±1.0)	-0.14 (±1.3)	0.36 (±1.5)	-0.17 (±1.0)
0r	-0.15 (±1.0)	0.20 (±1.3)	0.35 (±1.5)	-0.39 (±1.0)
-15l	0.48 (±1.2)	-0.18 (±1.5)	-0.22 (±1.6)	-0.10 (±1.2)
-15r	0.6 (±1.2)	-0.26 (±1.5)	-0.20 (±1.6)	-0.14 (±1.2)
15l	0.06 (±1.2)	-1.12 (±1.5)	0.06 (±1.6)	1.01 (±1.2)
15r	0.03 (±1.2)	0.02 (±1.5)	0.13 (±1.6)	-0.19 (±1.2)
-30l	1.34 (±1.3)	-0.39 (±1.7)	-0.56 (±1.6)	-0.39 (±1.3)
-30r	1.62 (±1.3)	-0.67 (±1.7)	-0.38 (±1.6)	-0.57 (±1.3)
30l	1.35 (±1.3)	-1.24 (±1.7)	0.35 (±1.6)	-0.45 (±1.3)
30r	0.99 (±1.3)	-0.11 (±1.7)	-0.31 (±1.6)	-0.58 (±1.3)

Table B8 100mm helix artefact. Differences between the unweighted mean and individual laboratory results for helix total error (F_β) and the individual laboratory measurement uncertainty ($\pm U_{95}$) in μm.

Helix/ Flank	PTB 1998	BWXT Y-12 2002	NGML 2005	PTB 2005
0l	0.29 (±1.0)	0.23 (±1.3)	-0.49 (±2.0)	-0.03 (±1.4)
0r	0.31 (±1.0)	-0.01 (±1.3)	-0.34 (±2.0)	-0.04 (±1.4)
-15l	-0.16 (±1.0)	0.39 (±1.5)	-0.12 (±2.0)	-0.12 (±1.5)
-15r	-0.10 (±1.0)	0.14 (±1.5)	-0.02 (±2.0)	-0.02 (±1.5)
15l	-0.02 (±1.0)	0.62 (±1.5)	-0.64 (±2.0)	0.05 (±1.5)
15r	-0.04 (±1.0)	0.24 (±1.5)	-0.16(±2.0)	-0.38 (±1.5)
-30l	-0.89(±1.0)	0.18 (±1.7)	0.31 (±2.0)	0.41 (±1.6)
-30r	-1.47 (±1.0)	0.70 (±1.7)	0.17 (±2.0)	0.61 (±1.6)
30l	1.59 (±1.0)	-1.06 (±1.7)	0.04 (±2.0)	-0.58 (±1.6)
30r	1.29 (±1.0)	-0.17 (±1.7)	-0.46 (±2.0)	-0.66 (±1.6)

Table B9 100mm helix artefact. Differences between the unweighted mean and individual laboratory results for helix form error ($f_{\beta f}$) and the individual laboratory measurement uncertainty ($\pm U_{95}$) in μm.

Helix/ Flank	PTB 1998	BWXT Y-12 2002	NGML 2005	PTB 2005
0l	0.25 (±1.0)	0.14 (±1.3)	-0.24 (±1.5)	-0.15 (±1.0)
0r	0.15 (±1.0)	0.03 (±1.3)	-0.23 (±1.5)	0.04 (±1.0)
-15l	0.34 (±1.0)	0.13 (±1.5)	-0.32 (±1.5)	-0.14 (±1.0)
-15r	0.13 (±1.0)	-0.11 (±1.5)	-0.02 (±1.5)	-0.00 (±1.0)
15l	0.06 (±1.0)	0.23 (±1.5)	-0..36 (±1.5)	0.06 (±1.0)
15r	-0.07 (±1.0)	0.27 (±1.5)	-0.31 (±1.5)	0.10 (±1.0)
-30l	0.52 (±1.0)	-0.26 (±1.7)	-0.34 (±1.5)	0.07 (±1.0)
-30r	0.35 (±1.0)	-0.07 (±1.7)	-0.48 (±1.5)	0.19 (±1.0)
30l	0.54 (±1.0)	0.28 (±1.7)	-0.61 (±1.5)	-0.20 (±1.0)
30r	0.41 (±1.0)	0.09 (±1.7)	-041 (±1.5)	-0.09 (±1.0)

Table B10 100mm profile artefact. Differences between the unweighted mean and individual laboratory results for profile slope error ($f_{H\alpha}$) and the individual laboratory measurement uncertainty ($\pm U_{95}$) in µm.

Flank	PTB 1998	BWXT Y-12 2002	NGML 2005	PTB 2005
L	-0. 02 (±1.0)	-0.47 (±1.5)	-0.08 (±0.9)	0.54 (±1.0)
R	0.19 (±1.0)	-0.40 (±1.5)	-1.12 (±0.9)	0.54 (±1.0)

Table B11 100mm profile artefact. Differences between the unweighted mean and individual laboratory results for profile total error (F_{α}) and the individual laboratory measurement uncertainty ($\pm U_{95}$) in µm.

Flank	PTB 1998	BWXT Y-12 2002	NGML 2005	PTB 2005
L	0.29 (±1.0)	-0.61(±1.6)	0.29 (±0.9)	0.02 (±1.0)
R	0.17 (±1.0)	0.01 (±1.6)	0.17 (±0.9)	-0.36 (±1.0)

Table B12 100mm profile artefact. Differences between the unweighted mean and individual laboratory results for profile form error ($f_{f\alpha}$) and the individual laboratory measurement uncertainty ($\pm U_{95}$) in µm.

Flank	PTB 1998	BWXT Y-12 2002	NGML 2005	PTB 2005
L	0.41 (±1.0)	-0.28 (±1.2)	0.11 (±0.9)	-0.24 (±1.0)
R	0.60 (±1.0)	-0.03 (±1.2)	-0.2 (±0.9)	-0.43 (±1.0)

Table B13 48A pitch artefact pitch and runout results comparison and measurement uncertainty [μm]

Datum/flank	Parameter	Y12	PTB	NGML
Concentric/left	fp	1.203 (±0.57)	1.268 (±0.5)	1.46 (±1.5)
Concentric/left	Fp	2.308 (±0.57)	2.303 (±0.5)	2.22 (±2.0)
Concentric/right	fp	1.679 (±0.57)	1.050 (±0.5)	1.18 (±1.5)
Concentric/right	Fp	2.261 (±0.57)	2.170 (±0.5)	2.08 (±2.0)
Concentric	Fr	7.378 (±0.57)	6.07 (±1.5)	8.02 (±2.5)
Eccentric/left	fp	10.625 (±0.57)	10.665 (±0.5)	10.88 (±1.5)
Eccentric/left	Fp	73.969 (±0.57)	72.741 (±0.5)	75.68 (±2.0)
Eccentric/right	fp	10.753 (±0.57)	10.074 (±0.5)	9.86 (±1.5)
Eccentric/right	Fp	72.660 (±0.57)	73.154 (±0.5)	73.16 (±2.0)
Eccentric	Fr	72.718(±0.57)	72.718 (±1.5)	73.30 (±2.5)

Appendix C

Further uncertainty budgets

The following uncertainty budgets are from the National Gear Metrology Laboratory for parameters listed in the UKAS schedule of accreditation. Each budget is presented in the same format used in Chapter 6. They cover the following parameters:

- Helix total error, form, and slope parameters (spur and helical gears)
- Profile total error, form and slope parameters (spur and helical gears)
- Adjacent pitch error
- Cumulative pitch error
- Radial runout error
- Tooth thickness

In each case the uncertainty is estimated using the comparator method. This ignores the limitations of evaluating form and total error parameters without including the position of the maximum evaluated form error.

Each budget uses calibrated artefacts with the lowest calibration data uncertainty available to the laboratory. Furthermore, it assumes that the workpiece is similar in geometry to the calibrated artefact so that additional sources of uncertainty to account for using different parts of the instrument measuring volume are not needed.

Each uncertainty budget table is followed by a table that explains the key elements in each contribution.

Table C1a Uncertainty Budget : Lead Measurement (slope error)

Instrument : Klingelnberg P65

Artefact Parameters:	**Reference**	**Test Item**
face width	125	
overall length	250	250
Length between datum surfaces	200	200
Base helix angle	0	0
Profile length of roll		
Lead evaluation length	64	64
reference diameter	50	50
module		
pressure angle		
teeth		

	Uncertainty Source	**Units**	**Value**	**Dist**	**Divisor**	**Ci**	**n**	**Ui**
	Calibrated artefact uncertainties							
1	Artefact	mu	0.80	n	2.00	1.00	1.00	0.40
2	Repeatability of artefact measurement	mu	0.10	n	1.00	1.00	5.00	0.04
3	Uncorrected differences between data	mu	0.30	r	1.73	1.00	1.00	0.17
4	Drift of the reference artefact	mu	0.00	n	1.73	1.00	1.00	0.00
5	Difference in artefact Temp. and 20C	deg C	0.30	r	1.73	0.00	1.00	0.00
6	Uncertainty in artefact CTE	na	0.00	r	1.73	0.00	1.00	0.00
	Workpiece uncertainties							
7	Test piece runout	mu	0.00	r	1.73	0.32	1.00	0.00
8	test piece runout detection	mu	0.20	n	1.00	0.32	1.00	0.06
9	test piece runout	mu	0.00	r	1.73	0.32	1.00	0.00
10	test piece runout detection	mu	0.20	n	1.00	0.32	1.00	0.06
11	Spindle alignment	mu	0.40	r	1.73	0.00	1.00	0.00
12	Spindle alignment detection	mu	0.20	n	1.00	0.00	1.00	0.00
13	Alignment between centres	mu	0.40	r	1.73	0.26	1.00	0.06
14	Alignment between centres detection	mu	0.20	n	1.00	0.26	1.00	0.05
15	test piece form error uncertainty	mu	0.10	r	1.73	1.00	1.00	0.06
16	Difference in temp. between artefact & 20C	deg C	0.30	r	1.73	0.00	1.00	0.00
17	Uncertainty in workpiece CTE	na	0.00	r	1.73	0.00	1.00	0.00
18	Repeatability of workpiece measurement	mu	0.20	n	1.00	1.00	5.00	0.09
19	Probing compression	mu	0.00	r	1.00	1.00	1.00	0.00
20	Drift of the workpiece	mu	0.00	r	1.00	1.00	1.00	0.00
21	Elasticity of the workpiece	mu	0.00	r	1.00	1.00	1.00	0.00
	Discrimination/resolution							
22	System discrimination	mu	0.05	n	2.00	1.00	1.00	0.03
23	Report resolution	mu	0.05	r	1.73	1.00	1.00	0.03
	Instrument geometry uncertainties							
24	X-axis combined uncorrected slide errors		0.00		1.00	0.00	1.00	0.00
25	X-axis uncertainty		0.00		1.00	0.00	1.00	0.00
26	Y-axis combined uncorrected slide errors	mu/m	0.00	r	1.73	0.06	1.00	0.00
27	Y-axis uncertainty	mu/m	0.00	n	2.00	0.06	1.00	0.00
28	Z-axis combined uncorrected slide errors	mu	0.40	r	1.73	0.00	1.00	0.00
29	Z-axis uncertainty	mu	0.50	n	2.00	0.00	1.00	0.00
30	R-axis uncorrected position errors	mu/m	3.60	r	1.73	0.00	5.00	0.00
31	R-axis uncertainty	mu/m	3.60	r	1.73	0.00	5.00	0.00
	Combined Standard Uncertainty							0.47
	Expanded Uncertainty k=2							**0.94**

Table C1b description of contributions to Lead error slope uncertainty for a spur gear. [μm]

line	Uncertainty source	Sensitivity coefficient
1	Artefact calibration data uncertainty	Set to 1 because it is a direct affect on measurand
2	Repeatability of calibration process on instrument, assuming a normal distribution	Direct affect on measurand. Mean of 5 tests at 90° intervals determines bias, divide by √5
3	Bias between calibration data and measured data, uncorrected. Rectangular distribution used because we have set this as a maximum limit	Direct affect on measurand.
4	Estimated change in the reference artefact if not included in the calibration data	Direct affect on measurand
5	Affect of temperature difference from 20°	C_i is the coefficient of linear expansion is zero for a spur gear
6	Uncertainty of expansion coefficient	C_i is the temperature difference*facewidth*tan(base helix) which is zero for a spur gear
7	Test piece runout maximum permitted value. Limit is a rectangular distribution. Set to zero if runout is compensated	C_i is a geometry factor that is proportional to the affect runout has on gear tooth alignment.
8	Uncertainty of test piece runout detection. Includes form errors in the reference surface	C_i is a geometry factor that is proportional to the affect runout has on gear tooth alignment.
9	As 7. But a different entry to allow for axial runout measurement affect or radial runout measurement.	C_i is a geometry factor that is proportional to the affect runout has on gear tooth alignment.
10	As 8	As 8
11	Spindle alignment with z-axis.	Direct affect if workpiece mounted on the spindle, set to zero if the workpiece is mounted between centres.
12	Spindle alignment detection uncertainty	Set to zero if 11 is zero.
13	Alignment between centres allowable maximum error (TIR)	C_i is geometry ratio of face evaluation length/length between centres.
14	Alignment between centres detection	Set to zero if centres not used
15	Estimate of affects of form errors on the evaluated parameter	Direct affect on measurand
16	Affect of temperature difference from 20°	C_i is the coefficient of linear expansion is zero for a spur gear
17	Uncertainty of expansion coefficient	C_i is the temperature difference*facewidth*tan(base helix)
18	Repeatability of workpiece measurement	Direct affect on measurand, if 5 measurement used, divide by √5
19	Probe compression affects normally set to zero	Direct affect on measurand.
20	Stability affects of workpiece if relevant	
21	Elasticity of workpiece during datum definition and lead measurement	Direct affect
22	System discrimination	
23	Report resolution	
24-31	Additional slide and instrument geometry errors are not considered in this model.	

Table C2a Uncertainty Budget : Lead Measurement (slope error)

Instrument : Klingelnberg P65

Artefact Parameters:	**Reference**	**Test Item**
face width	125	
overall length	250	250
Length between datum surfaces	200	200
Base helix angle	30	30
Profile length of roll		
Lead evaluation length	64	64
reference diameter	50	50
module		
pressure angle		
teeth		

	Uncertainty Source	**Units**	**Value**	**Dist**	**Divisor**	**Ci**	**n**	**Ui**
	Calibrated artefact uncertainties							
1	Artefact	mu	1.00	n	2.00	1.00	1.00	0.50
2	Repeatability of artefact measurement	mu	0.10	n	1.00	1.00	5.00	0.04
3	Uncorrected differences between data	mu	0.40	r	1.73	1.00	1.00	0.23
4	Drift of the reference artefact	mu	0.00	n	1.73	1.00	1.00	0.00
5	Difference in artefact Temp. and 20C	deg C	0.30	r	1.73	0.43	1.00	0.07
6	Uncertainty in artefact CTE	na	0.00	r	1.73	11085.13	1.00	0.01
	Workpiece uncertainties							
7	Test piece runout	mu	0.00	r	1.73	0.32	1.00	0.00
8	test piece runout detection	mu	0.20	n	1.00	0.32	1.00	0.06
9	test piece runout	mu	0.00	r	1.73	0.32	1.00	0.00
10	test piece runout detection	mu	0.20	n	1.00	0.32	1.00	0.06
11	Spindle alignment	mu	0.40	r	1.73	0.00	1.00	0.00
12	Spindle alignment detection	mu	0.20	n	1.00	0.00	1.00	0.00
13	Alignment between centres	mu	0.40	r	1.73	0.26	1.00	0.06
14	Alignment between centres detection	mu	0.20	n	1.00	0.26	1.00	0.05
15	test piece form error uncertainty	mu	0.10	r	1.73	1.00	1.00	0.06
16	Difference in temp. between artefact & 20C	deg C	0.30	r	1.73	0.43	1.00	0.07
17	Uncertainty in CTE	na	0.00	r	1.73	11085.13	1.00	0.01
18	Repeatability of workpiece measurement	mu	0.20	n	1.00	1.00	5.00	0.09
19	Probing compression	mu	0.00	r	1.00	1.00	1.00	0.00
20	Drift of the workpiece	mu	0.00	r	1.00	1.00	1.00	0.00
21	Elasticity of the workpiece	mu	0.00	r	1.00	1.00	1.00	0.00
	Discrimination/resolution							
22	System discrimination	mu	0.05	n	2.00	1.00	1.00	0.03
23	Report resolution	mu	0.05	r	1.73	1.00	1.00	0.03
	Instrument geometry uncertainties							
24	X-axis combined uncorrected slide errors		0.00		1.00	0.00	1.00	0.00
25	X-axis uncertainty		0.00		1.00	0.00	1.00	0.00
26	Y-axis combined uncorrected slide errors	mu/m	0.00	r	1.73	0.06	1.00	0.00
27	Y-axis uncertainty	mu/m	0.00	n	2.00	0.06	1.00	0.00
28	Z-axis combined uncorrected slide errors	mu	0.53	r	1.73	0.00	1.00	0.00
29	Z-axis uncertainty	mu	0.56	n	2.00	0.00	1.00	0.00
30	R-axis uncorrected position errors	mu/m	3.60	r	1.73	0.00	5.00	0.00
31	R-axis uncertainty	mu/m	3.60	r	1.73	0.00	5.00	0.00
	Combined Standard Uncertainty							0.59
	Expanded Uncertainty k=2							**1.17**

Table C2b description of contributions to Lead error slope uncertainty for a helical gear. [μm]

line	Uncertainty source	Sensitivity coefficient
1	Artefact calibration data uncertainty	Set to 1 because it is a direct affect on measurand
2	Repeatability of calibration process on instrument, assuming a normal distribution	Direct affect on measurand. Mean of 5 tests at 90° intervals determines bias, divide by √5
3	Bias between calibration data and measured data, uncorrected. Rectangular distribution used because we have set this as a maximum limit	Direct affect on measurand.
4	Estimated change in the reference artefact if not included in the calibration data	Direct affect on measurand
5	Affect of temperature difference from 20°	C_i is the coefficient of linear expansion *facewidth*tan(base helix)
6	Uncertainty of expansion coefficient	C_i is the temperature difference*facewidth*tan(base helix)
7	Test piece runout maximum permitted value. Limit is a rectangular distribution. Set to zero if runout is compensated	C_i is a geometry factor that is proportional to the affect runout has on gear tooth alignment.
8	Uncertainty of test piece runout detection. Includes form errors in the reference surface	C_i is a geometry factor that is proportional to the affect runout has on gear tooth alignment.
9	As 7. But a different entry to allow for axial runout measurement affect or radial runout measurement.	C_i is a geometry factor that is proportional to the affect runout has on gear tooth alignment.
10	As 8	As 8
11	Spindle alignment with z-axis.	Direct affect if workpiece mounted on the spindle, set to zero if the workpiece is mounted between centres.
12	Spindle alignment detection uncertainty	Set to zero if 11 is zero.
13	Alignment between centres allowable maximum error (TIR)	C_i is geometry ratio of face evaluation length/length between centres.
14	Alignment between centres detection	Set to zero if centres not used
15	Estimate of affects of form errors on the evaluated parameter	Direct affect on measurand
16	Affect of temperature difference from 20°	C_i is the coefficient of linear expansion is zero for a spur gear
17	Uncertainty of expansion coefficient	C_i is the temperature difference*facewidth*tan(base helix)
18	Repeatability of workpiece measurement	Direct affect on measurand, if 5 measurement used, divide by √5
19	Probe compression affects normally set to zero	Direct affect on measurand.
20	Stability affects of workpiece if relevant	
21	Elasticity of workpiece during datum definition and lead measurement	Direct affect
22	System discrimination	
23	Report resolution	
24-31	Additional slide and instrument geometry errors are not considered in this model.	

Table C3a Uncertainty Budget : Lead Measurement (Total error)

Instrument : Klingelnberg P65

Artefact Parameters:	**Reference**	**Test Item**
face width	125	
overall length	250	250
Length between datum surfaces	200	200
Base helix angle	0	0
Profile length of roll		
Lead evaluation length	64	64
reference diameter	50	50
module		
pressure angle		
teeth		

	Uncertainty Source	**Units**	**Value**	**Dist**	**Divisor**	**Ci**	**n**	**Ui**
	Calibrated artefact uncertainties							
1	Artefact	mu	1.10	n	2.00	1.00	1.00	0.55
2	Repeatability of artefact measurement	mu	0.10	n	1.00	1.00	5.00	0.04
3	Uncorrected differences between data	mu	0.30	r	1.73	1.00	1.00	0.17
4	Drift of the reference artefact	mu	0.00	n	1.73	1.00	1.00	0.00
5	Difference in artefact Temp. and 20C	deg C	0.30	r	1.73	0.00	1.00	0.00
6	Uncertainty in artefact CTE	na	0.00	r	1.73	0.00	1.00	0.00
	Workpiece uncertainties							
7	Test piece runout	mu	0.00	r	1.73	0.32	1.00	0.00
8	test piece runout detection	mu	0.20	n	1.00	0.32	1.00	0.06
9	test piece runout	mu	0.00	r	1.73	0.32	1.00	0.00
10	test piece runout detection	mu	0.20	n	1.00	0.32	1.00	0.06
11	Spindle alignment	mu	0.40	r	1.73	0.00	1.00	0.00
12	Spindle alignment detection	mu	0.20	n	1.00	0.00	1.00	0.00
13	Alignment between centres	mu	0.40	r	1.73	0.26	1.00	0.06
14	Alignment between centres detection	mu	0.20	n	1.00	0.26	1.00	0.05
15	test piece form error uncertainty	mu	0.10	r	1.73	1.00	1.00	0.06
16	Difference in temp. between artefact & 20C	deg C	0.30	r	1.73	0.00	1.00	0.00
17	Uncertainty in workpiece CTE	na	0.00	r	1.73	0.00	1.00	0.00
18	Repeatability of workpiece measurement	mu	0.20	n	1.00	1.00	5.00	0.09
19	Probing compression	mu	0.00	r	1.00	1.00	1.00	0.00
20	Drift of the workpiece	mu	0.00	r	1.00	1.00	1.00	0.00
21	Elasticity of the workpiece	mu	0.00	r	1.00	1.00	1.00	0.00
	Discrimination/resolution							
22	System discrimination	mu	0.05	n	2.00	1.00	1.00	0.03
23	Report resolution	mu	0.05	r	1.73	1.00	1.00	0.03
	Instrument geometry uncertainties							
24	X-axis combined uncorrected slide errors		0.00		1.00	0.00	1.00	0.00
25	X-axis uncertainty		0.00		1.00	0.00	1.00	0.00
26	Y-axis combined uncorrected slide errors	mu/m	0.00	r	1.73	0.06	1.00	0.00
27	Y-axis uncertainty	mu/m	0.00	n	2.00	0.06	1.00	0.00
28	Z-axis combined uncorrected slide errors	mu	0.40	r	1.73	0.00	1.00	0.00
29	Z-axis uncertainty	mu	0.50	n	2.00	0.00	1.00	0.00
30	R-axis uncorrected position errors	mu/m	3.60	r	1.73	0.00	5.00	0.00
31	R-axis uncertainty	mu/m	3.60	r	1.73	0.00	5.00	0.00
	Combined Standard Uncertainty							0.60
	Expanded Uncertainty k=2							**1.20**

Table C3b description of contributions to Lead total error uncertainty for a spur gear. [μm]

line	Uncertainty source	Sensitivity coefficient
1	Artefact calibration data uncertainty	Set to 1 because it is a direct affect on measurand
2	Repeatability of calibration process on instrument, assuming a normal distribution	Direct affect on measurand. Mean of 5 tests at 90° intervals determines bias, divide by √5
3	Bias between calibration data and measured data, uncorrected. Rectangular distribution used because we have set this as a maximum limit	Direct affect on measurand.
4	Estimated change in the reference artefact if not included in the calibration data	Direct affect on measurand
5	Affect of temperature difference from 20°	C_i is the coefficient of linear expansion is zero for a spur gear
6	Uncertainty of expansion coefficient	C_i is the temperature difference*facewidth*tan(base helix). This is zero in a spur gear
7	Test piece runout maximum permitted value. Limit is a rectangular distribution. Set to zero if runout is compensated	C_i is a geometry factor that is proportional to the affect runout has on gear tooth alignment.
8	Uncertainty of test piece runout detection. Includes form errors in the reference surface	C_i is a geometry factor that is proportional to the affect runout has on gear tooth alignment.
9	As 7. But a different entry to allow for axial runout measurement affect or radial runout measurement.	C_i is a geometry factor that is proportional to the affect runout has on gear tooth alignment.
10	As 8	As 8
11	Spindle alignment with z-axis.	Direct affect if workpiece mounted on the spindle, set to zero if the workpiece is mounted between centres.
12	Spindle alignment detection uncertainty	Set to zero if 11 is zero.
13	Alignment between centres allowable maximum error (TIR)	C_i is geometry ratio of face evaluation length/length between centres.
14	Alignment between centres detection	Set to zero if centres not used
15	Estimate of affects of form errors on the evaluated parameter	Direct affect on measurand
16	Affect of temperature difference from 20°	C_i is the coefficient of linear expansion is zero for a spur gear
17	Uncertainty of expansion coefficient	C_i is the temperature difference*facewidth*tan(base helix)
18	Repeatability of workpiece measurement	Direct affect on measurand, if 5 measurement used, divide by √5
19	Probe compression affects normally set to zero	Direct affect on measurand.
20	Stability affects of workpiece if relevant	
21	Elasticity of workpiece during datum definition and lead measurement	Direct affect
22	System discrimination	
23	Report resolution	
24-31	Additional slide and instrument geometry errors are not considered in this model.	

Table C4a Uncertainty Budget : Lead Measurement (total error)

Instrument : Klingelnberg P65

Artefact Parameters:	**Reference**	**Test Item**
face width	125	
overall length	250	250
Length between datum surfaces	200	200
Base helix angle	30	30
Profile length of roll		
Lead evaluation length	64	64
reference diameter	50	50
module		
pressure angle		
teeth		

	Uncertainty Source	**Units**	**Value**	**Dist**	**Divisor**	**Ci**	**n**	**Ui**
	Calibrated artefact uncertainties							
1	Artefact	mu	1.40	n	2.00	1.00	1.00	0.70
2	Repeatability of artefact measurement	mu	0.10	n	1.00	1.00	5.00	0.04
3	Uncorrected differences between data	mu	0.40	r	1.73	1.00	1.00	0.23
4	Drift of the reference artefact	mu	0.00	n	1.73	1.00	1.00	0.00
5	Difference in artefact Temp. and 20C	deg C	0.30	r	1.73	0.43	1.00	0.07
6	Uncertainty in artefact CTE	na	0.00	r	1.73	11085.13	1.00	0.01
	Workpiece uncertainties							
7	Test piece runout	mu	0.00	r	1.73	0.32	1.00	0.00
8	test piece runout detection	mu	0.20	n	1.00	0.32	1.00	0.06
9	test piece runout	mu	0.00	r	1.73	0.32	1.00	0.00
10	test piece runout detection	mu	0.20	n	1.00	0.32	1.00	0.06
11	Spindle alignment	mu	0.40	r	1.73	0.00	1.00	0.00
12	Spindle alignment detection	mu	0.20	n	1.00	0.00	1.00	0.00
13	Alignment between centres	mu	0.40	r	1.73	0.26	1.00	0.06
14	Alignment between centres detection	mu	0.20	n	1.00	0.26	1.00	0.05
15	test piece form error uncertainty	mu	0.10	r	1.73	1.00	1.00	0.06
16	Difference in temp. between artefact & 20C	deg C	0.30	r	1.73	0.43	1.00	0.07
17	Uncertainty in CTE	na	0.00	r	1.73	11085.13	1.00	0.01
18	Repeatability of workpiece measurement	mu	0.20	n	1.00	1.00	5.00	0.09
19	Probing compression	mu	0.00	r	1.00	1.00	1.00	0.00
20	Drift of the workpiece	mu	0.00	r	1.00	1.00	1.00	0.00
21	Elasticity of the workpiece	mu	0.00	r	1.00	1.00	1.00	0.00
	Discrimination/resolution							
22	System discrimination	mu	0.05	n	2.00	1.00	1.00	0.03
23	Report resolution	mu	0.05	r	1.73	1.00	1.00	0.03
	Instrument geometry uncertainties							
24	X-axis combined uncorrected slide errors		0.00		1.00	0.00	1.00	0.00
25	X-axis uncertainty		0.00		1.00	0.00	1.00	0.00
26	Y-axis combined uncorrected slide errors	mu/m	0.00	r	1.73	0.06	1.00	0.00
27	Y-axis uncertainty	mu/m	0.00	n	2.00	0.06	1.00	0.00
28	Z-axis combined uncorrected slide errors	mu	0.53	r	1.73	0.00	1.00	0.00
29	Z-axis uncertainty	mu	0.56	n	2.00	0.00	1.00	0.00
30	R-axis uncorrected position errors	mu/m	3.60	r	1.73	0.00	5.00	0.00
31	R-axis uncertainty	mu/m	3.60	r	1.73	0.00	5.00	0.00
	Combined Standard Uncertainty							0.76
	Expanded Uncertainty k=2							**1.53**

Table C4a description of contributions to Lead error slope uncertainty for a helical gear. [μm]

line	Uncertainty source	Sensitivity coefficient
1	Artefact calibration data uncertainty	Set to 1 because it is a direct affect on measurand
2	Repeatability of calibration process on instrument, assuming a normal distribution	Direct affect on measurand. Mean of 5 tests at 90° intervals determines bias, divide by √5
3	Bias between calibration data and measured data, uncorrected. Rectangular distribution used because we have set this as a maximum limit	Direct affect on measurand.
4	Estimated change in the reference artefact if not included in the calibration data	Direct affect on measurand
5	Affect of temperature difference from 20°	C_i is the coefficient of linear expansion *facewidth*tan(base helix)
6	Uncertainty of expansion coefficient	C_i is the temperature difference*facewidth*tan(base helix)
7	Test piece runout maximum permitted value. Limit is a rectangular distribution. Set to zero if runout is compensated	C_i is a geometry factor that is proportional to the affect runout has on gear tooth alignment.
8	Uncertainty of test piece runout detection. Includes form errors in the reference surface	C_i is a geometry factor that is proportional to the affect runout has on gear tooth alignment.
9	As 7. But a different entry to allow for axial runout measurement affect or radial runout measurement.	C_i is a geometry factor that is proportional to the affect runout has on gear tooth alignment.
10	As 8	As 8
11	Spindle alignment with z-axis.	Direct affect if workpiece mounted on the spindle, set to zero if the workpiece is mounted between centres.
12	Spindle alignment detection uncertainty	Set to zero if 11 is zero.
13	Alignment between centres allowable maximum error (TIR)	C_i is geometry ratio of face evaluation length/length between centres.
14	Alignment between centres detection	Set to zero if centres not used
15	Estimate of affects of form errors on the evaluated parameter	Direct affect on measurand
16	Affect of temperature difference from 20°	C_i is the coefficient of linear expansion is zero for a spur gear
17	Uncertainty of expansion coefficient	C_i is the temperature difference*facewidth*tan(base helix)
18	Repeatability of workpiece measurement	Direct affect on measurand, if 5 measurement used, divide by √5
19	Probe compression affects normally set to zero	Direct affect on measurand.
20	Stability affects of workpiece if relevant	
21	Elasticity of workpiece during datum definition and lead measurement	Direct affect
22	System discrimination	
23	Report resolution	
24-31	Additional slide and instrument geometry errors are not considered in this model.	

Table C5a Uncertainty Budget : Lead Measurement (Form error)

Instrument : Klingelnberg P65

Artefact Parameters:	**Reference**	**Test Item**
face width	125.00	
overall length	250.00	250.00
Length between datum surfaces	200.00	200.00
Base helix angle	0.00	0.00
Profile length of roll		
Lead evaluation length	64.00	64.00
reference diameter	50.00	50.00
module		
pressure angle		
teeth		

	Uncertainty Source	**Units**	**Value**	**Dist**	**Divisor**	**Ci**	**n**	**Ui**
	Calibrated artefact uncertainties							
1	Artefact	mu	1.00	n	2.00	1.00	1.00	0.50
2	Repeatability of artefact measurement	mu	0.10	n	1.00	1.00	5.00	0.04
3	Uncorrected differences between data	mu	0.40	r	1.73	1.00	1.00	0.23
4	Drift of the reference artefact	mu	0.00	n	1.73	1.00	1.00	0.00
5	Difference in artefact Temp. and 20C	deg C	0.30	r	1.73	0.00	1.00	0.00
6	Uncertainty in artefact CTE	na	0.00	r	1.73	0.00	1.00	0.00
	Workpiece uncertainties							
7	Test piece runout	mu	0.00	r	1.73	0.32	1.00	0.00
8	test piece runout detection	mu	0.20	n	1.00	0.32	1.00	0.06
9	test piece runout	mu	0.00	r	1.73	0.32	1.00	0.00
10	test piece runout detection	mu	0.20	n	1.00	0.32	1.00	0.06
11	Spindle alignment	mu	0.40	r	1.73	0.00	1.00	0.00
12	Spindle alignment detection	mu	0.20	n	1.00	0.00	1.00	0.00
13	Alignment between centres	mu	0.40	r	1.73	0.26	1.00	0.06
14	Alignment between centres detection	mu	0.20	n	1.00	0.26	1.00	0.05
15	test piece form error uncertainty	mu	0.10	r	1.73	1.00	1.00	0.06
16	Difference in temp. between artefact & test	deg C	0.30	r	1.73	0.00	1.00	0.00
17	Difference in CTE between artefact & test	na	0.00	r	1.73	0.00	1.00	0.00
18	Repeatability of workpiece measurement	mu	0.20	n	1.00	1.00	5.00	0.09
19	Probing compression	mu	0.00	r	1.00	1.00	1.00	0.00
20	Drift of the workpiece	mu	0.00	r	1.00	1.00	1.00	0.00
21	Elasticity of the workpiece	mu	0.00	r	1.00	1.00	1.00	0.00
	Discrimination/resolution							
22	System discrimination	mu	0.05	n	2.00	1.00	1.00	0.03
23	Report resolution	mu	0.05	r	1.73	1.00	1.00	0.03
	Instrument geometry uncertainties							
24	X-axis combined uncorrected slide errors		0.00		1.00	0.00	1.00	0.00
25	X-axis uncertainty		0.00		1.00	0.00	1.00	0.00
26	Y-axis combined uncorrected slide errors	mu/m	0.00	r	1.73	0.06	1.00	0.00
27	Y-axis uncertainty	mu/m	0.00	n	2.00	0.06	1.00	0.00
28	Z-axis combined uncorrected slide errors	mu	0.40	r	1.73	0.00	1.00	0.00
29	Z-axis uncertainty	mu	0.50	n	2.00	0.00	1.00	0.00
30	R-axis uncorrected position errors	mu/m	3.60	r	1.73	0.00	5.00	0.00
31	R-axis uncertainty	mu/m	3.60	r	1.73	0.00	5.00	0.00
	Combined Standard Uncertainty							0.58
	Expanded Uncertainty k=2							**1.15**

Table C5b description of contributions to Lead error slope uncertainty for a helical gear. [μm]

line	Uncertainty source	Sensitivity coefficient
1	Artefact calibration data uncertainty	Set to 1 because it is a direct affect on measurand
2	Repeatability of calibration process on instrument, assuming a normal distribution	Direct affect on measurand. Mean of 5 tests at 90° intervals determines bias, divide by √5
3	Bias between calibration data and measured data, uncorrected. Rectangular distribution used because we have set this as a maximum limit	Direct affect on measurand.
4	Estimated change in the reference artefact if not included in the calibration data	Direct affect on measurand
5	Affect of temperature difference from 20°	C_i is the coefficient of linear expansion *facewidth*tan(base helix)
6	Uncertainty of expansion coefficient	C_i is the temperature difference*facewidth*tan(base helix)
7	Test piece runout maximum permitted value. Limit is a rectangular distribution. Set to zero if runout is compensated	C_i is a geometry factor that is proportional to the affect runout has on gear tooth alignment.
8	Uncertainty of test piece runout detection. Includes form errors in the reference surface	C_i is a geometry factor that is proportional to the affect runout has on gear tooth alignment.
9	As 7. But a different entry to allow for axial runout measurement affect or radial runout measurement.	C_i is a geometry factor that is proportional to the affect runout has on gear tooth alignment.
10	As 8	As 8
11	Spindle alignment with z-axis.	Direct affect if workpiece mounted on the spindle, set to zero if the workpiece is mounted between centres.
12	Spindle alignment detection uncertainty	Set to zero if 11 is zero.
13	Alignment between centres allowable maximum error (TIR)	C_i is geometry ratio of face evaluation length/length between centres.
14	Alignment between centres detection	Set to zero if centres not used
15	Estimate of affects of form errors on the evaluated parameter	Direct affect on measurand
16	Affect of temperature difference from 20°	C_i is the coefficient of linear expansion is zero for a spur gear
17	Uncertainty of expansion coefficient	C_i is the temperature difference*facewidth*tan(base helix)
18	Repeatability of workpiece measurement	Direct affect on measurand, if 5 measurement used, divide by √5
19	Probe compression affects normally set to zero	Direct affect on measurand.
20	Stability affects of workpiece if relevant	
21	Elasticity of workpiece during datum definition and lead measurement	Direct affect
22	System discrimination	
23	Report resolution	
24-31	Additional slide and instrument geometry errors are not considered in this model.	

Table C6a Uncertainty Budget : Lead Measurement (slope error)

Instrument : Klingelnberg P65

Artefact Parameters:	**Reference**	**Test Item**
face width	125	
overall length	250	250
Length between datum surfaces	200	200
Base helix angle	30	30
Profile length of roll		
Lead evaluation length	64	64
reference diameter	50	50
module		
pressure angle		
teeth		

	Uncertainty Source	**Units**	**Value**	**Dist**	**Divisor**	**Ci**	**n**	**Ui**
	Calibrated artefact uncertainties							
1	Artefact	mu	1.00	n	2.00	1.00	1.00	0.50
2	Repeatability of artefact measurement	mu	0.10	n	1.00	1.00	5.00	0.04
3	Uncorrected differences between data	mu	0.40	r	1.73	1.00	1.00	0.23
4	Drift of the reference artefact	mu	0.00	n	1.73	1.00	1.00	0.00
5	Difference in artefact Temp. and 20C	deg C	0.30	r	1.73	0.43	1.00	0.07
6	Uncertainty in artefact CTE	na	0.00	r	1.73	11085.13	1.00	0.01
	Workpiece uncertainties							
7	Test piece runout	mu	0.00	r	1.73	0.32	1.00	0.00
8	test piece runout detection	mu	0.20	n	1.00	0.32	1.00	0.06
9	test piece runout	mu	0.00	r	1.73	0.32	1.00	0.00
10	test piece runout detection	mu	0.20	n	1.00	0.32	1.00	0.06
11	Spindle alignment	mu	0.40	r	1.73	0.00	1.00	0.00
12	Spindle alignment detection	mu	0.20	n	1.00	0.00	1.00	0.00
13	Alignment between centres	mu	0.40	r	1.73	0.26	1.00	0.06
14	Alignment between centres detection	mu	0.20	n	1.00	0.26	1.00	0.05
15	test piece form error uncertainty	mu	0.10	r	1.73	1.00	1.00	0.06
16	Difference in temp. between artefact & 20C	deg C	0.30	r	1.73	0.43	1.00	0.07
17	Uncertainty in CTE	na	0.00	r	1.73	11085.13	1.00	0.01
18	Repeatability of workpiece measurement	mu	0.20	n	1.00	1.00	5.00	0.09
19	Probing compression	mu	0.00	r	1.00	1.00	1.00	0.00
20	Drift of the workpiece	mu	0.00	r	1.00	1.00	1.00	0.00
21	Elasticity of the workpiece	mu	0.00	r	1.00	1.00	1.00	0.00
	Discrimination/resolution							
22	System discrimination	mu	0.05	n	2.00	1.00	1.00	0.03
23	Report resolution	mu	0.05	r	1.73	1.00	1.00	0.03
	Instrument geometry uncertainties							
24	X-axis combined uncorrected slide errors		0.00		1.00	0.00	1.00	0.00
25	X-axis uncertainty		0.00		1.00	0.00	1.00	0.00
26	Y-axis combined uncorrected slide errors	mu/m	0.00	r	1.73	0.06	1.00	0.00
27	Y-axis uncertainty	mu/m	0.00	n	2.00	0.06	1.00	0.00
28	Z-axis combined uncorrected slide errors	mu	0.53	r	1.73	0.00	1.00	0.00
29	Z-axis uncertainty	mu	0.56	n	2.00	0.00	1.00	0.00
30	R-axis uncorrected position errors	mu/m	3.60	r	1.73	0.00	5.00	0.00
31	R-axis uncertainty	mu/m	3.60	r	1.73	0.00	5.00	0.00
	Combined Standard Uncertainty							0.59
	Expanded Uncertainty k=2							**1.17**

Table C6b description of contributions to Lead error slope uncertainty for a helical gear. [μm]

line	Uncertainty source	Sensitivity coefficient
1	Artefact calibration data uncertainty	Set to 1 because it is a direct affect on measurand
2	Repeatability of calibration process on instrument, assuming a normal distribution	Direct affect on measurand. Mean of 5 tests at 90° intervals determines bias, divide by √5
3	Bias between calibration data and measured data, uncorrected. Rectangular distribution used because we have set this as a maximum limit	Direct affect on measurand.
4	Estimated change in the reference artefact if not included in the calibration data	Direct affect on measurand
5	Affect of temperature difference from 20°	C_i is the coefficient of linear expansion *facewidth*tan(base helix)
6	Uncertainty of expansion coefficient	C_i is the temperature difference*facewidth*tan(base helix)
7	Test piece runout maximum permitted value. Limit is a rectangular distribution. Set to zero if runout is compensated	C_i is a geometry factor that is proportional to the affect runout has on gear tooth alignment.
8	Uncertainty of test piece runout detection. Includes form errors in the reference surface	C_i is a geometry factor that is proportional to the affect runout has on gear tooth alignment.
9	As 7. But a different entry to allow for axial runout measurement affect or radial runout measurement.	C_i is a geometry factor that is proportional to the affect runout has on gear tooth alignment.
10	As 8	As 8
11	Spindle alignment with z-axis.	Direct affect if workpiece mounted on the spindle, set to zero if the workpiece is mounted between centres.
12	Spindle alignment detection uncertainty	Set to zero if 11 is zero.
13	Alignment between centres allowable maximum error (TIR)	C_i is geometry ratio of face evaluation length/length between centres.
14	Alignment between centres detection	Set to zero if centres not used
15	Estimate of affects of form errors on the evaluated parameter	Direct affect on measurand
16	Affect of temperature difference from 20°	C_i is the coefficient of linear expansion is zero for a spur gear
17	Uncertainty of expansion coefficient	C_i is the temperature difference*facewidth*tan(base helix)
18	Repeatability of workpiece measurement	Direct affect on measurand, if 5 measurement used, divide by √5
19	Probe compression affects normally set to zero	Direct affect on measurand.
20	Stability affects of workpiece if relevant	
21	Elasticity of workpiece during datum definition and lead measurement	Direct affect
22	System discrimination	
23	Report resolution	
24-31	Additional slide and instrument geometry errors are not considered in this model.	

Table C7a Uncertainty Budget : Profile Measurement (slope error)

Instrument : Klingelnberg P65

Artefact Parameters:	**Reference**	**Test Item**
face width	8	
overall length	300	300
Length between datum surfaces	200	200
Base helix angle	0	0
Profile length of roll	26	26
Lead evaluation length	8	8
reference diameter	100	100
module		
pressure angle		
teeth		

	Uncertainty Source	**Units**	**Value**	**Dist**	**Divisor**	**Ci**	**n**	**Ui**
	Calibrated artefact uncertainties							
1	Artefact	mu	0.70	n	2.00	1.00	1.00	0.35
2	Repeatability of artefact measurement	mu	0.10	n	1.00	1.00	5.00	0.04
3	Uncorrected differences between data	mu	0.50	r	1.73	1.00	1.00	0.29
4	Drift of the reference artefact	mu	0.00	n	1.73	1.00	1.00	0.00
5	Difference in artefact Temp. and 20C	deg C	0.30	r	1.73	0.30	1.00	0.05
6	Uncertainty in artefact CTE	na	0.00	r	1.73	7800.00	1.00	0.01
	Workpiece uncertainties							
7	Test piece runout	mu	0.00	r	1.73	0.50	1.00	0.00
8	test piece runout detection	mu	0.20	n	1.00	0.50	1.00	0.10
9	test piece runout	mu	0.00	r	1.73	0.50	1.00	0.00
10	test piece runout detection	mu	0.20	n	1.00	0.50	1.00	0.10
11	Spindle alignment	mu	0.40	r	1.73	0.00	1.00	0.00
12	Spindle alignment detection	mu	0.20	n	1.00	0.00	1.00	0.00
13	Alignment between centres	mu	0.40	r	1.73	0.00	1.00	0.00
14	Alignment between centres detection	mu	0.20	n	1.00	0.00	1.00	0.00
15	test piece form error uncertainty	mu	0.10	r	1.73	1.00	1.00	0.06
15	Difference in temp. between artefact & 20C	deg C	0.20	r	1.73	0.30	1.00	0.03
17	Uncertainty in workpiece CTE	na	0.00	r	1.73	5200.00	1.00	0.00
18	Repeatability of workpiece measurement	mu	0.15	n	1.00	1.00	5.00	0.07
19	Probing compression	mu	0.00	r	1.00	1.00	1.00	0.00
20	Drift of the workpiece	mu	0.00	r	1.00	1.00	1.00	0.00
21	Elasticity of the workpiece	mu	0.00	r	1.00	1.00	1.00	0.00
	Discrimination/resolution							
22	System discrimination	mu	0.05	n	2.00	1.00	1.00	0.03
23	Report resolution	mu	0.05	r	1.73	1.00	1.00	0.03
	Instrument geometry uncertainties							
24	X-axis combined uncorrected slide errors		0.00		1.00	0.00	1.00	0.00
25	X-axis uncertainty		0.00		1.00	0.00	1.00	0.00
26	Y-axis combined uncorrected slide errors	mu/m	0.00	r	1.73	0.00	1.00	0.00
27	Y-axis uncertainty	mu/m	0.00	n	2.00	0.00	1.00	0.00
28	Z-axis combined uncorrected slide errors	mu	0.40	r	1.73	0.00	1.00	0.00
29	Z-axis uncertainty	mu	0.50	n	2.00	0.00	1.00	0.00
30	R-axis uncorrected position errors	mu/m	3.60	r	1.73	0.00	5.00	0.00
31	R-axis uncertainty	mu/m	3.60	r	1.73	0.00	5.00	0.00
	Combined Standard Uncertainty							0.49
	Expanded Uncertainty k=2							**0.98**

Table C7b description of contributions to profile error slope uncertainty for a spur gear. [μm]

line	Uncertainty source	Sensitivity coefficient
1	Artefact calibration data uncertainty	Set to 1 because it is a direct affect on measurand
2	Repeatability of calibration process on instrument, assuming a normal distribution	Direct affect on measurand. Mean of 5 tests at 90° intervals determines bias, divide by √5
3	Bias between calibration data and measured data, uncorrected. Rectangular distribution used because we have set this as a maximum limit	Direct affect on measurand.
4	Estimated change in the reference artefact if not included in the calibration data	Direct affect on measurand
5	Affect of temperature difference from 20°	C_i is the coefficient of linear expansion *length of roll[mm]
6	Uncertainty of expansion coefficient	C_i is the temperature difference*length of roll[mm]
7	Test piece runout maximum permitted value. Limit is a rectangular distribution. Set to zero if runout is compensated	C_i is a geometry factor that is proportional to the affect runout has on profile given by sin(angle of roll/base radius)
8	Uncertainty of test piece runout detection. Includes form errors in the reference surface	C_i is a geometry factor that is proportional to the affect runout has on profile given by sin(angle of roll/base radius).
9	As 7. But a different entry to allow for axial runout measurement affect or radial runout measurement.	C_i is a geometry factor that is proportional to the affect runout has on profile given by sin(angle of roll/base radius)
10	As 8	As 8
11	Spindle alignment with z-axis in the measurement plane	Direct affect if workpiece mounted on the spindle given by error over profile length of roll*tan(βb) or set to zero if the workpiece is mounted between centres.
12	Spindle alignment detection uncertainty	Set to zero if 11 is zero.
13	Alignment between centres allowable maximum error (TIR)	C_i is geometry ratio of error over profile length of roll*tan(βb)
14	Alignment between centres detection	Set to zero if centres not used
15	Estimate of affects of form errors on the evaluated parameter	Direct affect on measurand
16	Affect of temperature difference from 20°	C_i is the coefficient of linear expansion *profile length of roll[mm]
17	Uncertainty of expansion coefficient	C_i is the temperature difference*profile length of roll[mm]
18	Repeatability of workpiece measurement	Direct affect on measurand, if 5 measurement used, divide by √5
19	Probe compression affects normally set to zero	Direct affect on measurand.
20	Stability affects of workpiece if relevant	
21	Elasticity of workpiece during datum definition and lead measurement	Direct affect
22	System discrimination	
23	Report resolution	
24-31	Additional slide and instrument geometry errors are not considered in this model.	

Table C8a Uncertainty Budget : Profile Measurement (Total error)

Instrument : Klingelnberg P65

Artefact Parameters:	**Reference**	**Test Item**
face width	8	8
overall length	300	300
Length between datum surfaces	200	200
Base helix angle	0	0
Profile length of roll	26	26
Lead evaluation length	8	8
reference diameter	200	200
module		
pressure angle		
teeth		

	Uncertainty Source	**Units**	**Value**	**Dist**	**Divisor**	**Ci**	**n**	**Ui**
	Calibrated artefact uncertainties							
1	Artefact	mu	1.00	n	2.00	1.00	1.00	0.50
2	Repeatability of artefact measurement	mu	0.10	n	1.00	1.00	5.00	0.04
3	Uncorrected differences between data	mu	0.40	r	1.73	1.00	1.00	0.23
4	Drift of the reference artefact	mu	0.00	n	1.73	1.00	1.00	0.00
5	Difference in artefact Temp. and 20C	deg C	0.30	r	1.73	0.30	1.00	0.05
6	Uncertainty in artefact CTE	na	0.00	r	1.73	7800.00	1.00	0.01
	Workpiece uncertainties							
7	Test piece runout	mu	0.00	r	1.73	0.26	1.00	0.00
8	test piece runout detection	mu	0.20	n	1.00	0.26	1.00	0.05
9	test piece runout	mu	0.00	r	1.73	0.26	1.00	0.00
10	test piece runout detection	mu	0.20	n	1.00	0.26	1.00	0.05
11	Spindle alignment	mu	0.40	r	1.73	0.00	1.00	0.00
12	Spindle alignment detection	mu	0.20	n	1.00	0.00	1.00	0.00
13	Alignment between centres	mu	0.40	r	1.73	0.00	1.00	0.00
14	Alignment between centres detection	mu	0.20	n	1.00	0.00	1.00	0.00
15	test piece form error uncertainty	mu	0.10	r	1.73	1.00	1.00	0.06
15	Difference in temp. between artefact & 20C	deg C	0.30	r	1.73	0.30	1.00	0.05
17	Uncertainty in workpiece CTE	na	0.00	r	1.73	7800.00	1.00	0.01
18	Repeatability of workpiece measurement	mu	0.15	n	1.00	1.00	5.00	0.07
19	Probing compression	mu	0.00	r	1.00	1.00	1.00	0.00
20	Drift of the workpiece	mu	0.00	r	1.00	1.00	1.00	0.00
21	Elasticity of the workpiece	mu	0.00	r	1.00	1.00	1.00	0.00
	Discrimination/resolution							
22	System discrimination	mu	0.05	n	2.00	1.00	1.00	0.03
23	Report resolution	mu	0.05	r	1.73	1.00	1.00	0.03
	Instrument geometry uncertainties							
24	X-axis combined uncorrected slide errors		0.00		1.00	0.00	1.00	0.00
25	X-axis uncertainty		0.00		1.00	0.00	1.00	0.00
26	Y-axis combined uncorrected slide errors	mu/m	0.00	r	1.73	0.00	1.00	0.00
27	Y-axis uncertainty	mu/m	0.00	n	2.00	0.00	1.00	0.00
28	Z-axis combined uncorrected slide errors	mu	0.40	r	1.73	0.00	1.00	0.00
29	Z-axis uncertainty	mu	0.50	n	2.00	0.00	1.00	0.00
30	R-axis uncorrected position errors	mu/m	3.60	r	1.73	0.00	5.00	0.00
31	R-axis uncertainty	mu/m	3.60	r	1.73	0.00	5.00	0.00
	Combined Standard Uncertainty							0.57
	Expanded Uncertainty k=2							**1.14**

Table C8b description of contributions to total profile error uncertainty for a helical gear. [μm]

line	Uncertainty source	Sensitivity coefficient
1	Artefact calibration data uncertainty	Set to 1 because it is a direct affect on measurand
2	Repeatability of calibration process on instrument, assuming a normal distribution	Direct affect on measurand. Mean of 5 tests at 90° intervals determines bias, divide by √5
3	Bias between calibration data and measured data, uncorrected. Rectangular distribution used because we have set this as a maximum limit	Direct affect on measurand.
4	Estimated change in the reference artefact if not included in the calibration data	Direct affect on measurand
5	Affect of temperature difference from 20°	C_i is the coefficient of linear expansion *length of roll[mm]
6	Uncertainty of expansion coefficient	C_i is the temperature difference*length of roll[mm]
7	Test piece runout maximum permitted value. Limit is a rectangular distribution. Set to zero if runout is compensated	C_i is a geometry factor that is proportional to the affect runout has on profile given by sin(angle of roll/base radius)
8	Uncertainty of test piece runout detection. Includes form errors in the reference surface	C_i is a geometry factor that is proportional to the affect runout has on profile given by sin(angle of roll/base radius).
9	As 7. But a different entry to allow for axial runout measurement affect or radial runout measurement.	C_i is a geometry factor that is proportional to the affect runout has on profile given by sin(angle of roll/base radius)
10	As 8	As 8
11	Spindle alignment with z-axis.	Direct affect if workpiece mounted on the spindle given by error over profile length of roll*tan(βb) or set to zero if the workpiece is mounted between centres.
12	Spindle alignment detection uncertainty	Set to zero if 11 is zero.
13	Alignment between centres allowable maximum error (TIR)	C_i is geometry ratio of error over profile length of roll*tan(βb)
14	Alignment between centres detection	Set to zero if centres not used
15	Estimate of affects of form errors on the evaluated parameter	Direct affect on measurand
16	Affect of temperature difference from 20°	C_i is the coefficient of linear expansion *profile length of roll[mm]
17	Uncertainty of expansion coefficient	C_i is the temperature difference*profile length of roll[mm]
18	Repeatability of workpiece measurement	Direct affect on measurand, if 5 measurement used, divide by √5
19	Probe compression affects normally set to zero	Direct affect on measurand.
20	Stability affects of workpiece if relevant	
21	Elasticity of workpiece during datum definition and lead measurement	Direct affect
22	System discrimination	
23	Report resolution	
24-31	Additional slide and instrument geometry errors are not considered in this model.	

Table C9a Uncertainty Budget : Profile Measurement (form error)

Instrument : Klingelnberg P65

Artefact Parameters:	**Reference**	**Test Item**
face width	8	8
overall length	300	300
Length between datum surfaces	200	200
Base helix angle	0	0
Profile length of roll	26	26
Lead evaluation length	8	8
reference diameter	200	200
module		
pressure angle		
teeth		

	Uncertainty Source	**Units**	**Value**	**Dist**	**Divisor**	**Ci**	**n**	**Ui**
	Calibrated artefact uncertainties							
1	Artefact	mu	1.00	n	2.00	1.00	1.00	0.50
2	Repeatability of artefact measurement	mu	0.10	n	1.00	1.00	5.00	0.04
3	Uncorrected differences between data	mu	0.40	r	1.73	1.00	1.00	0.23
4	Drift of the reference artefact	mu	0.00	n	1.73	1.00	1.00	0.00
5	Difference in artefact Temp. and 20C	deg C	0.30	r	1.73	0.30	1.00	0.05
6	Uncertainty in artefact CTE	na	0.00	r	1.73	7800.00	1.00	0.01
	Workpiece uncertainties							
7	Test piece runout	mu	0.00	r	1.73	0.26	1.00	0.00
8	test piece runout detection	mu	0.20	n	1.00	0.26	1.00	0.05
9	test piece runout	mu	0.00	r	1.73	0.26	1.00	0.00
10	test piece runout detection	mu	0.20	n	1.00	0.26	1.00	0.05
11	Spindle alignment	mu	0.40	r	1.73	0.00	1.00	0.00
12	Spindle alignment detection	mu	0.20	n	1.00	0.00	1.00	0.00
13	Alignment between centres	mu	0.40	r	1.73	0.00	1.00	0.00
14	Alignment between centres detection	mu	0.20	n	1.00	0.00	1.00	0.00
15	test piece form error uncertainty	mu	0.10	r	1.73	1.00	1.00	0.06
15	Difference in temp. between artefact & 20C	deg C	0.30	r	1.73	0.30	1.00	0.05
17	Uncertainty in workpiece CTE	na	0.00	r	1.73	7800.00	1.00	0.01
18	Repeatability of workpiece measurement	mu	0.15	n	1.00	1.00	5.00	0.07
19	Probing compression	mu	0.00	r	1.00	1.00	1.00	0.00
20	Drift of the workpiece	mu	0.00	r	1.00	1.00	1.00	0.00
21	Elasticity of the workpiece	mu	0.00	r	1.00	1.00	1.00	0.00
	Discrimination/resolution							
22	System discrimination	mu	0.05	n	2.00	1.00	1.00	0.03
23	Report resolution	mu	0.05	r	1.73	1.00	1.00	0.03
	Instrument geometry uncertainties							
24	X-axis combined uncorrected slide errors		0.00		1.00	0.00	1.00	0.00
25	X-axis uncertainty		0.00		1.00	0.00	1.00	0.00
26	Y-axis combined uncorrected slide errors	mu/m	0.00	r	1.73	0.00	1.00	0.00
27	Y-axis uncertainty	mu/m	0.00	n	2.00	0.00	1.00	0.00
28	Z-axis combined uncorrected slide errors	mu	0.40	r	1.73	0.00	1.00	0.00
29	Z-axis uncertainty	mu	0.50	n	2.00	0.00	1.00	0.00
30	R-axis uncorrected position errors	mu/m	3.60	r	1.73	0.00	5.00	0.00
31	R-axis uncertainty	mu/m	3.60	r	1.73	0.00	5.00	0.00
	Combined Standard Uncertainty							0.57
	Expanded Uncertainty k=2							**1.14**

Table C9b description of contributions to profile form error uncertainty for a helical gear. [μm]

line	Uncertainty source	Sensitivity coefficient
1	Artefact calibration data uncertainty	Set to 1 because it is a direct affect on measurand
2	Repeatability of calibration process on instrument, assuming a normal distribution	Direct affect on measurand. Mean of 5 tests at 90° intervals determines bias, divide by √5
3	Bias between calibration data and measured data, uncorrected. Rectangular distribution used because we have set this as a maximum limit	Direct affect on measurand.
4	Estimated change in the reference artefact if not included in the calibration data	Direct affect on measurand
5	Affect of temperature difference from 20°	C_i is the coefficient of linear expansion *length of roll[mm]
6	Uncertainty of expansion coefficient	C_i is the temperature difference*length of roll[mm]
7	Test piece runout maximum permitted value. Limit is a rectangular distribution. Set to zero if runout is compensated	C_i is a geometry factor that is proportional to the affect runout has on profile given by sin(angle of roll/base radius)
8	Uncertainty of test piece runout detection. Includes form errors in the reference surface	C_i is a geometry factor that is proportional to the affect runout has on profile given by sin(angle of roll/base radius).
9	As 7. But a different entry to allow for axial runout measurement affect or radial runout measurement.	C_i is a geometry factor that is proportional to the affect runout has on profile given by sin(angle of roll/base radius)
10	As 8	As 8
11	Spindle alignment with z-axis.	Direct affect if workpiece mounted on the spindle given by error over profile length of roll*tan(βb) or set to zero if the workpiece is mounted between centres.
12	Spindle alignment detection uncertainty	Set to zero if 11 is zero.
13	Alignment between centres allowable maximum error (TIR)	C_i is geometry ratio of error over profile length of roll*tan(βb)
14	Alignment between centres detection	Set to zero if centres not used
15	Estimate of affects of form errors on the evaluated parameter	Direct affect on measurand
16	Affect of temperature difference from 20°	C_i is the coefficient of linear expansion *profile length of roll[mm]
17	Uncertainty of expansion coefficient	C_i is the temperature difference*profile length of roll[mm]
18	Repeatability of workpiece measurement	Direct affect on measurand, if 5 measurement used, divide by √5
19	Probe compression affects normally set to zero	Direct affect on measurand.
20	Stability affects of workpiece if relevant	
21	Elasticity of workpiece during datum definition and lead measurement	Direct affect
22	System discrimination	
23	Report resolution	
24-31	Additional slide and instrument geometry errors are not considered in this model.	

Table C10a Uncertainty Budget : Adjacent Pitch Measurement

Instrument : Klingelnberg P65

Artefact Parameters:	**Reference**	**Test Item**
face width	8	
overall length	250	
Length between datum surfaces	210	
helix angle	0	
Profile length of roll		
Lead evaluation length		
reference diameter	190	190
module		
pressure angle	20	
teeth	30	48

	Uncertainty Source	**Units**	**Value**	**Dist**	**Divisor**	**Ci**	**n**	**Ui**
	Calibrated artefact uncertainties							
1	Artefact	mu	0.80	n	2.00	1.00	1.00	0.40
2	Repeatability of artefact measurement	mu	0.10	n	1.00	1.00	5.00	0.04
3	Uncorrected differences between data	mu	0.30	r	1.73	1.00	1.00	0.17
4	Drift of the reference artefact	mu	0.00	n	1.73	1.00	1.00	0.00
5	Difference in artefact Temp. and 20C	deg C	0.30	r	1.73	0.00	1.00	0.00
6	Uncertainty in artefact CTE	na	0.00	r	1.73	0.00	1.00	0.00
	Workpiece uncertainties							
7	Test piece runout	mu	0.00	r	1.73	0.13	1.00	0.00
8	Test piece runout detection	mu	0.20	n	1.00	0.13	1.00	0.03
9	Test piece runout	mu	0.00	r	1.73	0.13	1.00	0.00
10	Test piece runout detection	mu	0.20	n	1.00	0.13	1.00	0.03
11	Spindle alignment	mu	0.40	r	1.73	0.00	1.00	0.00
12	Spindle alignment detection	mu	0.20	n	2.00	0.00	1.00	0.00
13	Alignment between centres	mu	0.40	r	1.73	0.01	1.00	0.00
14	Alignment between centres detection	mu	0.20	n	2.00	0.01	1.00	0.00
15	test piece form error uncertainty	mu	0.10	r	1.73	1.00	1.00	0.06
16	Difference in workpiece temp. and 20C	deg C	0.30	r	1.73	0.00	1.00	0.00
17	Uncertainty in CTE	na	0.00	r	1.73	0.00	1.00	0.00
18	Repeatability of test piece measurement	mu	0.10	n	1.00	1.00	5.00	0.04
19	Probing compression	mu	0.00	r	1.00	1.00	1.00	0.00
20	Drift of the workpiece	mu	0.00	r	1.00	1.00	1.00	0.00
21	Elasticity of the workpiece	mu	0.00	r	1.00	1.00	1.00	0.00
	Discrimination/resolution							
22	System discrimination	mu	0.05	r	1.73	1.00	1.00	0.03
23	Result resolution	mu	0.05	r	1.73	1.00	1.00	0.03
	Instrument geometry uncertainties							
24	R-axis uncorrected position errors	mu/m	0.00	r	1.73	0.10	1.00	0.00
25	R-axis uncertainty	mu/m	0.00	r	1.73	0.10	1.00	0.00

Combined Standard Uncertainty	0.45
Expanded Uncertainty k=2	**0.90**

Table C10b description of contributions to adjacent pitch uncertainty [μm]

line	Uncertainty source	Sensitivity coefficient
1	Artefact calibration data uncertainty	Set to 1 because it is a direct affect on measurand
2	Repeatability of calibration process on instrument, assuming a normal distribution	Direct affect on measurand. Mean of 5 tests at 90° intervals determines bias.
3	Bias between calibration data and measured data, uncorrected. Rectangular distribution used because we have set this as a maximum limit	Direct affect on measurand.
4	Estimated change in the reference artefact if not included in the calibration data	Direct affect on measurand
5	Affect of temperature difference from 20°	C_i is zero (it has no first order affects)
6	Uncertainty of expansion coefficient	C_i is zero (it has no first order affects)
7	Test piece runout maximum permitted value. Limit is a rectangular distribution. Set to zero if runout is compensated	C_i is the maximum affect of runout over the indexing angle of 1 pitch given by sin(2*PI/Z)
8	Uncertainty of test piece runout detection. Includes form errors in the reference surface	C_i is the maximum affect of runout over the indexing angle of 1 pitch given by sin(2*PI/Z)
9	As 7. But a different entry to allow for axial runout measurement affect or radial runout measurement.	C_i is the maximum affect of runout over the indexing angle of 1 pitch given by sin(2*PI/Z)
10	As 8	As 8
11	Spindle alignment with z-axis.	Direct affect if workpiece mounted on the spindle, set to zero if the workpiece is mounted between centres.
12	Spindle alignment detection uncertainty	Set to zero if 11 is zero.
13	Alignment between centres allowable maximum error (TIR)	C_i is geometry ratio of profile length of roll/length between centres plus a factor to account for the residual error in the driver and indexing accuracy for repeat tests. Set to zero if not used
14	Alignment between centres detection	Set to zero if centres not used, otherwise as above
15	Estimate of affects of form errors on the evaluated parameter	Direct affect on measurand
16	Affect of temperature difference from 20°	C_i is zero (it has no first order affects)
17	Uncertainty of expansion coefficient	C_i is zero (it has no first order affects)
18	Repeatability of workpiece measurement	Direct affect on measurand, if 5 measurement used, divide by $\sqrt{5}$
19	Probe compression affects normally set to zero	Direct affect on measurand.
20	Stability affects of workpiece if relevant	
21	Elasticity of workpiece during datum definition and lead measurement	Direct affect
22	System discrimination	
23	Report resolution	
24-31	Additional slide and instrument geometry errors are not considered in this model.	

Table C11a Uncertainty Budget : Cumulative Pitch Measurement

Instrument : Klingelnberg P65

Artefact Parameters:	**Reference**	**Test Item**
face width	8	
overall length	250	
Length between datum surfaces	210	
helix angle	0	
Profile length of roll		
Lead evaluation length		
reference diameter	190	190
module		
pressure angle	20	20
teeth	30	48

	Uncertainty Source	**Units**	**Value**	**Dist**	**Divisor**	**Ci**	**n**	**Ui**
	Calibrated artefact uncertainties							
1	Artefact	mu	1.20	n	2.00	1.00	1.00	0.60
2	Repeatability of artefact measurement	mu	0.10	n	1.00	1.00	5.00	0.04
3	Uncorrected differences between data	mu	0.50	r	1.73	1.00	1.00	0.29
4	Drift of the reference artefact	mu	0.00	n	1.73	1.00	1.00	0.00
5	Difference in artefact Temp. and 20C	deg C	0.30	r	1.73	0.00	1.00	0.00
6	Uncertainty in artefact CTE	na	0.00	r	1.73	0.00	1.00	0.00
	Workpiece uncertainties							
7	Test piece runout	mu	0.00	r	1.73	0.00	1.00	0.00
8	Test piece runout detection	mu	0.20	n	2.00	1.06	1.00	0.11
9	Test piece runout	mu	0.00	r	1.73	0.00	1.00	0.00
10	Test piece runout detection	mu	0.20	n	2.00	1.06	1.00	0.11
11	Spindle alignment	mu	0.40	r	1.73	0.00	1.00	0.00
12	Spindle alignment detection	mu	0.20	n	2.00	0.00	1.00	0.00
13	Alignment between centres	mu	0.40	r	1.73	0.10	1.00	0.02
14	Alignment between centres detection	mu	0.20	n	2.00	0.10	1.00	0.01
15	test piece form error uncertainty	mu	0.10	r	1.73	1.00	1.00	0.06
16	Difference in workpiece temp. and 20C	deg C	0.20	r	1.73	0.00	1.00	0.00
17	Uncertainty in CTE	na	0.00	r	1.73	0.00	1.00	0.00
18	Repeatability of test piece measurement	mu	0.10	n	1.00	1.00	5.00	0.04
19	Probing compression	mu	0.00	r	1.00	1.00	1.00	0.00
20	Drift of the workpiece	mu	0.00	r	1.00	1.00	1.00	0.00
21	Elasticity of the workpiece	mu	0.00	r	1.00	1.00	1.00	0.00
	Discrimination/resolution							
22	System discrimination	mu	0.05	r	1.73	1.00	1.00	0.03
23	Result resolution	mu	0.05	r	1.73	1.00	1.00	0.03
	Instrument geometry uncertainties							
24	R-axis uncorrected position errors	mu/m	0.00	r	1.73	0.10	1.00	0.00
25	R-axis uncertainty	mu/m	0.00	r	1.73	0.10	1.00	0.00
	Combined Standard Uncertainty							0.69
	Expanded Uncertainty k=2							**1.38**

Table C11b description of contributions to cumulative pitch uncertainty [μm]

line	Uncertainty source	Sensitivity coefficient
1	Artefact calibration data uncertainty	Set to 1 because it is a direct affect on measurand
2	Repeatability of calibration process on instrument, assuming a normal distribution	Direct affect on measurand. Mean of 5 tests at 90° intervals determines bias.
3	Bias between calibration data and measured data, uncorrected. Rectangular distribution used because we have set this as a maximum limit	Direct affect on measurand.
4	Estimated change in the reference artefact if not included in the calibration data	Direct affect on measurand
5	Affect of temperature difference from 20°	C_i is zero (it has no first order affects)
6	Uncertainty of expansion coefficient	C_i is zero (it has no first order affects)
7	Test piece runout maximum permitted value. Limit is a rectangular distribution. Set to zero if runout is compensated	C_i is the maximum affect of runout over the indexing angle of 1 pitch given by sin(2*PI/Z)
8	Uncertainty of test piece runout detection. Includes form errors in the reference surface	C_i is the maximum affect of runout over the indexing angle of 1 pitch given by sin(PI)
9	As 7. But a different entry to allow for axial runout measurement affect or radial runout measurement.	C_i is the maximum affect of runout over the indexing angle of 1 pitch given by sin(PI/)
10	As 8	As 8
11	Spindle alignment with z-axis.	Direct affect if workpiece mounted on the spindle, set to zero if the workpiece is mounted between centres.
12	Spindle alignment detection uncertainty	Set to zero if 11 is zero.
13	Alignment between centres allowable maximum error (TIR)	C_i is geometry ratio of profile length of roll/length between centres plus a factor to account for the residual error in the driver and indexing accuracy for repeat tests. Set to zero if not used
14	Alignment between centres detection	Set to zero if centres not used, otherwise as above
15	Estimate of affects of form errors on the evaluated parameter	Direct affect on measurand
16	Affect of temperature difference from 20°	C_i is zero (it has no first order affects)
17	Uncertainty of expansion coefficient	C_i is zero (it has no first order affects)
18	Repeatability of workpiece measurement	Direct affect on measurand, if 5 measurement used, divide by $\sqrt{5}$
19	Probe compression affects normally set to zero	Direct affect on measurand.
20	Stability affects of workpiece if relevant	
21	Elasticity of workpiece during datum definition and lead measurement	Direct affect
22	System discrimination	
23	Report resolution	
24-31	Additional slide and instrument geometry errors are not considered in this model.	

Table C12a Uncertainty Budget : Radial runout Measurement, individual result

Instrument : Klingelnberg P65
Method: assume the results from 2 cumulative pitch results contribute to the radial runot error.

Artefact Parameters:	**Reference**	**Test Item**
face width	8	
overall length	250	
Length between datum surfaces	210	
helix angle	0	
Profile length of roll		
Lead evaluation length		
reference diameter	190	190
module		
pressure angle	20	20
teeth	30	48

	Uncertainty Source	**Units**	**Value**	**Dist**	**Divisor**	**Ci**	**n**	**Ui**
	Calibrated artefact uncertainties							
1	Artefact	mu	1.50	n	2.00	1.00	1.00	0.75
2	Repeatability of artefact measurement	mu	0.25	n	1.00	1.00	5.00	0.11
3	Uncorrected differences between data	mu	2.30	r	1.73	1.00	1.00	1.33
4	Drift of the reference artefact	mu	0.00	n	1.73	1.00	1.00	0.00
5	Difference in artefact Temp. and 20C	deg C	0.30	r	1.73	0.00	1.00	0.00
6	Uncertainty in artefact CTE	na	0.00	r	1.73	0.00	1.00	0.00
	Workpiece uncertainties							
7	Test piece runout	mu	0.00	r	1.73	0.00	1.00	0.00
8	Test piece runout detection	mu	0.20	n	2.00	1.00	1.00	0.10
9	Test piece runout	mu	0.00	r	1.73	0.00	1.00	0.00
10	Test piece runout detection	mu	0.20	n	2.00	1.00	1.00	0.10
11	Spindle alignment	mu	0.40	r	1.73	0.00	1.00	0.00
12	Spindle alignment detection	mu	0.20	n	2.00	0.00	1.00	0.00
13	Alignment between centres	mu	0.40	r	1.73	0.10	1.00	0.02
14	Alignment between centres detection	mu	0.20	n	2.00	0.10	1.00	0.01
15	test piece form error uncertainty	mu	0.10	r	1.73	1.00	1.00	0.06
16	Difference in workpiece temp. and 20C	deg C	0.30	r	1.73	0.00	1.00	0.00
17	Uncertainty in CTE	na	0.00	r	1.73	0.00	1.00	0.00
18	Repeatability of test piece measurement	mu	0.25	n	1.00	1.00	5.00	0.11
19	Probing compression	mu	0.00	r	1.00	1.00	1.00	0.00
20	Drift of the workpiece	mu	0.00	r	1.00	1.00	1.00	0.00
21	Elasticity of the workpiece	mu	0.00	r	1.00	1.00	1.00	0.00
	Discrimination/resolution							
22	System discrimination	mu	0.05	r	1.73	1.00	1.00	0.03
23	Result resolution	mu	0.05	r	1.73	1.00	1.00	0.03
	Instrument geometry uncertainties							
24	R-axis uncorrected position errors	mu/m	0.00	r	1.73	0.10	1.00	0.00
25	R-axis uncertainty	mu/m	0.00	r	1.73	0.10	1.00	0.00
	Combined Standard Uncertainty							1.54
	Expanded Uncertainty k=2							**3.08**

Table C12b description of contributions to radial runout uncertainty [μm]

line	Uncertainty source	Sensitivity coefficient
1	Artefact calibration data uncertainty	Set to 1 because it is a direct affect on measurand
2	Repeatability of calibration process on instrument, assuming a normal distribution	Direct affect on measurand. Mean of 5 tests at 90° intervals determines bias.
3	Bias between calibration data and measured data, uncorrected. Rectangular distribution used because we have set this as a maximum limit	Direct affect on measurand.
4	Estimated change in the reference artefact if not included in the calibration data	Direct affect on measurand
5	Affect of temperature difference from 20°	C_i is zero (it has no first order affects)
6	Uncertainty of expansion coefficient	C_i is zero (it has no first order affects)
7	Test piece runout maximum permitted value. Limit is a rectangular distribution. Set to zero if runout is compensated	C_i is 1 if runout of workpiece is not corrected or set to zero if it is
8	Uncertainty of test piece runout detection. Includes form errors in the reference surface	C_i is 1 if runout of workpiece is not corrected or set to zero if it is
9	As 7. But a different entry to allow for axial runout measurement affect or radial runout measurement.	C_i is 1 if runout of workpiece is not corrected or set to zero if it is
10	As 8	As 8
11	Spindle alignment with z-axis.	Direct affect if workpiece mounted on the spindle, set to zero if the workpiece is mounted between centres.
12	Spindle alignment detection uncertainty	Set to zero if 11 is zero.
13	Alignment between centres allowable maximum error (TIR)	C_i is geometry ratio of face evaluation length/length between centres.
14	Alignment between centres detection	Set to zero
15	Estimate of affects of form errors on the evaluated parameter	Direct affect on measurand
16	Affect of temperature difference from 20°	C_i is zero (it has no first order affects)
17	Uncertainty of expansion coefficient	C_i is zero (it has no first order affects)
18	Repeatability of workpiece measurement	Direct affect on measurand, if 5 measurement used, divide by $\sqrt{5}$
19	Probe compression affects normally set to zero	Direct affect on measurand.
20	Stability affects of workpiece if relevant	
21	Elasticity of workpiece during datum definition and lead measurement	Direct affect
22	System discrimination	
23	Report resolution	
24& 25	Additional slide and instrument geometry errors are not considered in this model.	

Table C13a Uncertainty Budget : dimension between pins or balls measurement uncertainty

Instrument : Pins and Gauge blocks

Artefact Parameters:	**Reference**	**Test Item**
face width	30	30
overall length	300	300
Length between datum surfaces	250	250
Base helix angle	30	30
Profile length of roll		
Lead evaluation length	100	100
reference diameter	60	55
module	5	5
pressure angle	20	20
teeth	30	30
Pin size		5
dimension over pins		60

	Uncertainty Source	**Units**	**Value**	**Dist**	**Divisor**	**Ci**	**n**	**Ui**
	Calibrated artefact uncertainties							
1	Gauge blocks	mu	0.35	n	2.00	1.00	1.00	0.17
2	Repeatability of artefact measurement	mu	0.10	n	1.00	1.00	5.00	0.04
3	Uncorrected differences during re-check	mu	0.00	r	1.73	1.00	1.00	0.00
4	Drift of the reference artefact	mu	0.00	n	1.73	1.00	1.00	0.00
5	Difference in artefact Temp. and 20C	deg C	0.20	r	1.73	0.70	1.00	0.08
6	Uncertainty in artefact CTE	na	0.00	r	1.73	12000.00	1.00	0.01
	Workpiece uncertainties							
7	Uncertainty of size of 1 pin	mu	0.50	n	2.00	1.96	1.00	0.49
8	Uncertainty of size of 1 pin	mu	0.50	n	2.00	1.96	1.00	0.49
9	Uncertainty of pin temperature	deg C	0.20	r	1.73	0.16	1.00	0.02
10	Uncertainty of pin CTE	na	0.00	r	1.73	32959.96	1.00	0.02
11	test piece form error uncertainty	mu	0.20	r	1.73	2.92	1.00	0.34
12	Difference in temp. between workpiece & 20C	deg C	0.20	r	1.73	1.87	1.00	0.22
13	Uncertainty in CTE	na	0.00	r	1.73	11000.00	1.00	0.01
14	Repeatability of workpiece measurement	mu	0.10	n	1.00	1.00	5.00	0.04
15	Probing compression	mu	0.20	r	1.73	1.00	1.00	0.12
16	Drift of the workpiece	mu	0.00	r	1.00	1.00	1.00	0.00
17	Elasticity of the workpiece	mu	0.00	r	1.00	1.00	1.00	0.00
	Discrimination/resolution							
18	System discrimination	mu	0.10	n	2.00	1.00	1.00	0.05
19	Report resolution	mu	0.05	r	1.73	1.00	1.00	0.03
	Combined Standard Uncertainty							0.65
	Expanded Uncertainty k=2							**1.35**

Table C13b description of contributions to dimension between balls uncertainty [μm]

line	Uncertainty source	Sensitivity coefficient
1	Gauge block calibration data uncertainty	Set to 1 because it is a direct affect on measurand
2	Repeatability of calibration process on instrument, assuming a normal distribution	Direct affect on measurand. Mean of 5 tests at 90° intervals determines bias.
3	Uncorrected differences between initial value and checked value after measurement	Direct affect on measurand.
4	Estimated change in the reference artefact if not included in the calibration data	Direct affect on measurand
5	Affect of temperature difference from 20°	C_i is the coefficient of linear expansion *distance between pins
6	Uncertainty of expansion coefficient	C_i is the temperature difference*distance between pins
7	Uncertainty of pin size	C_i has 2 components: a direct size error for the free end of the pin and an affect depending on the tan(contacting pressure angle of the pin)
8	Uncertainty of pin size	C_i has 2 components: a direct size error for the free end of the pin and an affect depending on the tan(contacting pressure angle of the pin)
9	Uncertainty of pin temperature	C_i has 2 components of error as above. The overall C_i is multiplied by $\sqrt{2}$ to account for the 2 pins
10	Uncertainty of pin CTE	C_i is temperature difference*geometry effect above
11	Test piece form error uncertainty	C_i is geometry effect based on 1/sin(contact pressure angle) for the 4 contact points of the pins.
12	Affect of temperature difference from 20°	C_i is the coefficient of linear expansion is zero for a spur gear
13	Uncertainty of expansion coefficient	C_i is the temperature difference*artefact length
14	Repeatability of workpiece measurement	Direct affect on measurand, if 5 measurement used, divide by $\sqrt{5}$
15	Probe compression affects normally set to zero	Direct affect on measurand.
16	Stability affects of workpiece if relevant	Direct affect
171	Elasticity of workpiece during datum definition and lead measurement	Direct affect
18	System discrimination	Direct affect
19	Report resolution	Direct affect

Table C14a Uncertainty Budget : dimension over pins or balls measurement uncertainty

Instrument : Vertical comparator with gauge block slave plattern

Artefact Parameters:	**Reference**	**Test Item**
face width	30	30
overall length	300	300
Length between datum surfaces	250	250
Base helix angle	30	30
Profile length of roll		
Lead evaluation length	100	100
reference diameter	60	55
module	5	5
pressure angle	20	20
teeth	30	30
Pin size		5
dimension over pins		60

	Uncertainty Source	**Units**	**Value**	**Dist**	**Divisor**	**Ci**	**n**	**Ui**
	Calibrated artefact uncertainties							
1	Gauge blocks	mu	0.347563	n	2	1	1	0.174
2	Repeatability of artefact measurement	mu	0.1	n	1	1	5	0.045
3	Uncorrected differences during re-check	mu	0.2	r	1.732	1	1	0.115
4	Drift of the reference artefact	mu	0	n	1.732	1	1	0.000
5	Difference in artefact Temp. and 20C	deg C	0.2	r	1.732	0.696	1	0.080
6	Uncertainty in artefact CTE	na	1.16E-06	r	1.732	12000	1	0.008
	Workpiece uncertainties							
7	Uncertainty of size of 1 pin	mu	0.5	n	2	1.961902	1	0.490
8	Uncertainty of size of 1 pin	mu	0.5	n	2	1.961902	1	0.490
9	Uncertainty of pin temperature	deg C	0.2	r	1.732	1.911678	1	0.221
10	Uncertainty of pin CTE	na	1.16E-06	r	1.732	32959.96	1	0.022
11	test piece form error uncertainty	mu	0.2	r	1.732	2.923804	1	0.338
12	Difference in temp. between workpiece & 20C	deg C	0.2	r	1.732	0.638	1	0.074
13	Uncertainty in CTE	na	1.16E-06	r	1.732	11000	1	0.007
14	Repeatability of workpiece measurement	mu	0.1	n	1	1	5	0.045
15	Probing compression	mu	0.2	r	1.73	1	1	0.116
16	Drift of the workpiece	mu	0	r	1	1	1	0.000
17	Elasticity of the workpiece	mu	0	r	1	1	1	0.000
	Discrimination/resolution							
18	System discrimination	mu	0.1	n	2	1	1	0.050
19	Report resolution	mu	0.05	r	1.732	1	1	0.029
	Instrument geometry uncertainties							
20	plattern flatness	mu	0.2	r	1.732	1	1	0.115
	Combined Standard Uncertainty							0.667
	Expanded Uncertainty k=2							**1.334**

Table C14b description of contributions to dimension over pins uncertainty [μm]

line	Uncertainty source	Sensitivity coefficient
1	Gauge block calibration data uncertainty	Set to 1 because it is a direct affect on measurand
2	Repeatability of calibration process on instrument, assuming a normal distribution	Direct affect on measurand. Mean of 5 tests at 90° intervals determines bias.
3	Uncorrected differences between initial value and checked value after measurement	Direct affect on measurand.
4	Estimated change in the reference artefact if not included in the calibration data	Direct affect on measurand
5	Affect of temperature difference from 20°	C_i is the coefficient of linear expansion *distance between pins
6	Uncertainty of expansion coefficient	C_i is the temperature difference*distance between pins
7	Uncertainty of pin size	C_i has 2 components: a direct size error for the free end of the pin and an affect depending on the tan(contacting pressure angle of the pin)
8	Uncertainty of pin size	C_i has 2 components: a direct size error for the free end of the pin and an affect depending on the tan(contacting pressure angle of the pin)
9	Uncertainty of pin temperature	C_i has 2 components of error as above. The overall C_i is multiplied by $\sqrt{2}$ to account for the 2 pins
10	Uncertainty of pin CTE	C_i is temperature difference*geometry effect above
11	Test piece form error uncertainty	C_i is geometry effect based on 1/sin(contact pressure angle) for the 4 contact points of the pins.
12	Affect of temperature difference from 20°	C_i is the coefficient of linear expansion is zero for a spur gear
13	Uncertainty of expansion coefficient	C_i is the temperature difference*artefact length
14	Repeatability of workpiece measurement	Direct affect on measurand, if 5 measurement used, divide by $\sqrt{5}$
15	Probe compression affects normally set to zero	Direct affect on measurand.
16	Stability affects of workpiece if relevant	Direct affect
171	Elasticity of workpiece during datum definition and lead measurement	Direct affect
18	System discrimination	Direct affect
19	Report resolution	Direct affect
20	Plattern flatness	Direct affect

Table C15a Uncertainty Budget : Radial tooth space error

Instrument : Klingelnberg P65

Artefact Parameters:	**Reference**	**Test Item**
face width	8	
overall length	250	
Length between datum surfaces	210	
helix angle	0	
Profile length of roll		
Lead evaluation length		
reference diameter	190	190
module		
pressure angle	20	20
teeth	30	48

	Uncertainty Source	**Units**	**Value**	**Dist**	**Divisor**	**Ci**	**n**	**Ui**
	Calibrated artefact uncertainties							
1	Artefact	mu	0.50	n	2.00	1.00	1.00	0.25
2	Repeatability of artefact measurement	mu	0.10	n	1.00	1.00	5.00	0.04
3	Uncorrected differences between data	mu	0.30	r	1.73	1.00	1.00	0.17
4	Drift of the reference artefact	mu	0.00	n	1.73	1.00	1.00	0.00
5	Difference in artefact Temp. and 20C	deg C	0.30	r	1.73	0.00	1.00	0.00
6	Uncertainty in artefact CTE	na	0.00	r	1.73	0.00	1.00	0.00
	Workpiece uncertainties							
7	Test piece runout	mu	0.00	r	1.73	0.13	1.00	0.00
8	Test piece runout detection	mu	0.20	n	2.00	0.13	1.00	0.01
9	Test piece runout	mu	0.00	r	1.73	0.13	1.00	0.00
10	Test piece runout detection	mu	0.20	n	2.00	0.13	1.00	0.01
11	Spindle alignment	mu	0.40	r	1.73	0.00	1.00	0.00
12	Spindle alignment detection	mu	0.20	n	2.00	0.00	1.00	0.00
13	Alignment between centres	mu	0.40	r	1.73	0.01	1.00	0.00
14	Alignment between centres detection	mu	0.20	n	2.00	0.01	1.00	0.00
15	test piece form error uncertainty	mu	0.10	r	1.73	1.00	1.00	0.06
16	Difference in workpiece temp. and 20C	deg C	0.20	r	1.73	0.00	1.00	0.00
17	Uncertainty in CTE	na	0.00	r	1.73	0.00	1.00	0.00
18	Repeatability of test piece measurement	mu	0.10	n	1.00	1.00	5.00	0.04
19	Probing compression	mu	0.00	r	1.00	1.00	1.00	0.00
20	Drift of the workpiece	mu	0.00	r	1.00	1.00	1.00	0.00
21	Elasticity of the workpiece	mu	0.00	r	1.00	1.00	1.00	0.00
	Discrimination/resolution							
22	System discrimination	mu	0.05	r	1.73	1.00	1.00	0.03
23	Result resolution	mu	0.05	r	1.73	1.00	1.00	0.03
	Instrument geometry uncertainties							
24	R-axis uncorrected position errors	mu/m	0.00	r	1.73	0.10	1.00	0.00
25	R-axis uncertainty	mu/m	0.00	r	1.73	0.10	1.00	0.00
	Combined Standard Uncertainty							0.32
	Expanded Uncertainty k=2							**0.64**

Table C15b description of contributions to radial tooth space uncertainty [μm]

line	Uncertainty source	Sensitivity coefficient
1	Artefact calibration data uncertainty	Set to 1 because it is a direct affect on measurand
2	Repeatability of calibration process on instrument, assuming a normal distribution	Direct affect on measurand. Mean of 5 tests at 90° intervals determines bias.
3	Bias between calibration data and measured data, uncorrected. Rectangular distribution used because we have set this as a maximum limit	Direct affect on measurand.
4	Estimated change in the reference artefact if not included in the calibration data	Direct affect on measurand
5	Affect of temperature difference from 20°	C_i is the coefficient of linear expansion *spacewidth*tan(pressure angle)
6	Uncertainty of expansion coefficient	C_i is the temperature difference *spacewidth*tan(pressure angle)
7	Test piece runout maximum permitted value. Limit is a rectangular distribution. Set to zero if runout is compensated	C_i is a geometry factor that is proportional to the affect runout has on gear tooth alignment.
8	Uncertainty of test piece runout detection. Includes form errors in the reference surface	C_i is a geometry factor that is proportional to the affect runout has on gear tooth alignment.
9	As 7. But a different entry to allow for axial runout measurement affect or radial runout measurement.	C_i is a geometry factor that is proportional to the affect runout has on gear tooth alignment.
10	As 8	As 8
11	Spindle alignment with z-axis.	Direct affect if workpiece mounted on the spindle, set to zero if the workpiece is mounted between centres.
12	Spindle alignment detection uncertainty	Set to zero if 11 is zero.
13	Alignment between centres allowable maximum error (TIR)	C_i is geometry ratio of face evaluation length/length between centres.
14	Alignment between centres detection	Set to zero if centres not used
15	Estimate of affects of form errors on the evaluated parameter	Direct affect on measurand
16	Affect of temperature difference from 20°	C_i is the coefficient of linear expansion *spacewidth*tan(pressure angle)
17	Uncertainty of expansion coefficient	C_i is the temperature difference *spacewidth*tan(pressure angle)
18	Repeatability of workpiece measurement	Direct affect on measurand, if 5 measurement used, divide by $\sqrt{5}$
19	Probe compression affects normally set to zero	Direct affect on measurand.
20	Stability affects of workpiece if relevant	
21	Elasticity of workpiece during datum definition and lead measurement	Direct affect
22	System discrimination	Direct affect
23	Report resolution	Direct affect
24-31	Additional slide and instrument geometry errors are not considered in this model.	

Table C16a Uncertainty Budget : Normal circular tooth thickness measurement uncertainty

Instrument : Klingelnberg P65
Process measures average tooth thickness

Artefact Parameters:	**Reference**	**Test Item**
face width	30	30
overall length	300	300
Length between datum surfaces	250	250
Base helix angle	30	30
Profile length of roll		
Lead evaluation length	100	100
reference diameter	170	170
module	5	5
pressure angle	20	20
teeth	30	30

	Uncertainty Source	**Units**	**Value**	**Dist**	**Divisor**	**Ci**	**n**	**Ui**
	Calibrated artefact uncertainties							
1	Artefact	mu	1.50	n	2.00	1.00	1.00	0.75
2	Repeatability of artefact measurement	mu	0.10	n	1.00	1.00	5.00	0.04
3	Uncorrected differences between data	mu	0.00	r	1.73	1.00	1.00	0.00
4	Drift of the reference artefact	mu	0.00	n	1.73	1.00	1.00	0.00
5	Difference in artefact Temp. and 20C	deg C	0.20	r	1.73	0.72	1.00	0.08
6	Uncertainty in artefact CTE	na	0.00	r	1.73	12374.99	1.00	0.01
	Workpiece uncertainties							
7	Test piece runout	mu	0.00	r	1.73	1.00	1.00	0.00
8	test piece runout detection	mu	0.20	n	2.00	1.00	1.00	0.10
9	test piece runout	mu	0.00	r	1.73	1.00	1.00	0.00
10	test piece runout detection	mu	0.20	n	2.00	1.00	1.00	0.10
11	Spindle alignment	mu	0.40	r	1.73	0.00	1.00	0.00
12	Spindle alignment detection	mu	0.20	n	2.00	0.00	1.00	0.00
13	Alignment between centres	mu	0.40	r	1.73	1.00	1.00	0.23
14	Alignment between centres detection	mu	0.20	n	2.00	1.00	1.00	0.10
15	test piece form error uncertainty	mu	0.40	r	1.73	1.00	1.00	0.23
16	Difference in temp. between artefact & 20C	deg C	0.20	r	1.73	0.72	1.00	0.08
17	Uncertainty in CTE	na	0.00	r	1.73	12374.99	1.00	0.01
18	Repeatability of workpiece measurement	mu	0.10	n	1.00	1.00	5.00	0.04
19	Probing compression and form error	mu	0.50	r	1.73	1.00	1.00	0.29
20	Drift of the workpiece	mu	0.00	r	1.00	1.00	1.00	0.00
21	Elasticity of the workpiece	mu	0.00	r	1.00	1.00	1.00	0.00
	Discrimination/resolution							
22	System discrimination	mu	0.05	n	2.00	1.00	1.00	0.03
23	Report resolution	mu	0.50	r	1.73	1.00	1.00	0.29
	Instrument geometry uncertainties							
24	X-axis combined uncorrected slide errors		0.00		1.00	0.00	1.00	0.00
25	X-axis uncertainty		0.00		1.00	0.00	1.00	0.00
26	Y-axis combined uncorrected slide errors	mu/m	0.00	r	1.73	0.10	1.00	0.00
27	Y-axis uncertainty	mu/m	0.00	n	2.00	0.10	1.00	0.00
28	Z-axis combined uncorrected slide errors	mu	0.53	r	1.73	0.00	1.00	0.00
29	Z-axis uncertainty	mu	0.56	n	2.00	0.00	1.00	0.00
30	R-axis uncorrected position errors	mu/m	3.60	r	1.73	0.00	5.00	0.00
31	R-axis uncertainty	mu/m	3.60	r	1.73	0.00	5.00	0.00
	Combined Standard Uncertainty							0.94
	Expanded Uncertainty k=2							**1.88**

Table C16b description of contributions to radial tooth space uncertainty [μm]

line	Uncertainty source	Sensitivity coefficient
1	Artefact calibration data uncertainty	Set to 1 because it is a direct affect on measurand
2	Repeatability of calibration process on instrument, assuming a normal distribution	Direct affect on measurand. Mean of 5 tests at 90° intervals determines bias.
3	Bias between calibration data and measured data, uncorrected. Rectangular distribution used because we have set this as a maximum limit	Direct affect on measurand.
4	Estimated change in the reference artefact if not included in the calibration data	Direct affect on measurand
5	Affect of temperature difference from 20°	C_i is the coefficient of linear expansion *tooth thickness*tan(pressure angle)
6	Uncertainty of expansion coefficient	C_i is the temperature difference *too thickness*tan(pressure angle)
7	Test piece runout maximum permitted value. Limit is a rectangular distribution. Set to zero if runout is compensated	C_i is a geometry factor that is proportional to the affect runout has on gear tooth alignment.
8	Uncertainty of test piece runout detection. Includes form errors in the reference surface	C_i is a geometry factor that is proportional to the affect runout has on gear tooth alignment.
9	As 7. But a different entry to allow for axial runout measurement affect or radial runout measurement.	C_i is a geometry factor that is proportional to the affect runout has on gear tooth alignment.
10	As 8	As 8
11	Spindle alignment with z-axis.	Direct affect if workpiece mounted on the spindle, set to zero if the workpiece is mounted between centres.
12	Spindle alignment detection uncertainty	Set to zero if 11 is zero.
13	Alignment between centres allowable maximum error (TIR)	C_i is geometry ratio of face evaluation length/length between centres.
14	Alignment between centres detection	Set to zero if centres not used
15	Estimate of affects of form errors on the evaluated parameter	Direct affect on measurand
16	Affect of temperature difference from 20°	C_i is the coefficient of linear expansion *tooth thickness*tan(pressure angle)
17	Uncertainty of expansion coefficient	C_i is the temperature difference *tooth thickness*tan(pressure angle)
18	Repeatability of workpiece measurement	Direct affect on measurand, if 5 measurement used, divide by $\sqrt{5}$
19	Probe compression affects normally set to zero	Direct affect on measurand.
20	Stability affects of workpiece if relevant	
21	Elasticity of workpiece during datum definition and lead measurement	Direct affect
22	System discrimination	Direct affect
23	Report resolution	Direct affect
24-31	Additional slide and instrument geometry errors are not considered in this model.	

Appendix D

Summary of profile comparison data

This Appendix contains the data from the National Gear Metrology Laboratory (NGML) for the point by point comparison performed with PTB and discussed in Chapter 7.

Results from PTB were compared to data at discrete points at approximately 1mm intervals.

Two artefacts examined were the 100mm and 200mm diameter profile masters. Examination of the example results in tables D1 for the 100mm diameter profile master show the standard deviation of individual measurement points and provide insight of measured form errors on the gear artefacts, which are generally smaller than would normally be expected for a ground finish artefact. The 100mm diameter artefact was measured with and without an additional filter applied to the data. If a filter is called within the high level Klingelnberg P65, only filtered data can be recorded. Thus the data with and without is from different tests on the 100mm diameter artefact. The filter was set to Standard Klingelnberg No.4.

D1

Table D1 Summary of results: 100mm diameter profile master

Details: ı Left Flank normal
No filter

	Data from P65					P65 Data (deviation from mean value)						Standard
Position	**Run 1**	**Run 2**	**Run 3**	**Run 4**	**Run 5**	**Run 1**	**Run 2**	**Run 3**	**Run 4**	**Run 5**	**Mean**	**Deviation**
5.001	-15.4	-16.3	-16.4	-18.3	-16.3	1.394	1.300	1.220	1.308	1.315	1.307	0.062
5.060	-15.4	-16.2	-16.3	-18.3	-16.4	1.394	1.400	1.320	1.308	1.215	1.327	0.075
5.119	-15.4	-16.3	-16.4	-18.4	-16.4	1.394	1.300	1.220	1.208	1.215	1.267	0.080
5.178	-15.5	-16.3	-16.4	-18.4	-16.4	1.294	1.300	1.220	1.208	1.215	1.247	0.045
5.237	-15.5	-16.3	-16.4	-18.4	-16.4	1.294	1.300	1.220	1.208	1.215	1.247	0.045
5.296	-15.5	-16.4	-16.5	-18.5	-16.5	1.294	1.200	1.120	1.108	1.115	1.167	0.080
5.355	-15.6	-16.4	-16.5	-18.5	-16.6	1.194	1.200	1.120	1.108	1.015	1.127	0.075
5.414	-15.7	-16.5	-16.6	-18.5	-16.6	1.094	1.100	1.020	1.108	1.015	1.067	0.046
5.473	-15.7	-16.5	-16.6	-18.6	-16.6	1.094	1.100	1.020	1.008	1.015	1.047	0.045
5.531	-15.7	-16.6	-16.6	-18.6	-16.6	1.094	1.000	1.020	1.008	1.015	1.027	0.038
5.590	-15.7	-16.6	-16.7	-18.6	-16.6	1.094	1.000	0.920	1.008	1.015	1.007	0.062
5.649	-15.8	-16.6	-16.8	-18.7	-16.7	0.994	1.000	0.820	0.908	0.915	0.927	0.074
5.708	-15.8	-16.6	-16.7	-18.7	-16.7	0.994	1.000	0.920	0.908	0.915	0.947	0.045
5.767	-15.8	-16.7	-16.8	-18.7	-16.8	0.994	0.900	0.820	0.908	0.815	0.887	0.074
5.826	-15.8	-16.7	-16.8	-18.7	-16.8	0.994	0.900	0.820	0.908	0.815	0.887	0.074
5.885	-15.8	-16.7	-16.8	-18.7	-16.8	0.994	0.900	0.820	0.908	0.815	0.887	0.074
5.944	-15.9	-16.8	-16.8	-18.8	-16.8	0.894	0.800	0.820	0.808	0.815	0.827	0.038
6.003	-15.9	-16.8	-16.8	-18.8	-16.9	0.894	0.800	0.820	0.808	0.715	0.807	0.064
6.062	-16	-16.9	-16.9	-18.9	-16.9	0.794	0.700	0.720	0.708	0.715	0.727	0.038
6.121	-16	-16.9	-16.9	-18.9	-17	0.794	0.700	0.720	0.708	0.615	0.707	0.064
6.180	-16	-16.9	-16.9	-18.9	-16.9	0.794	0.700	0.720	0.708	0.715	0.727	0.038
6.239	-16	-16.9	-16.9	-18.9	-16.9	0.794	0.700	0.720	0.708	0.715	0.727	0.038
6.298	-16	-16.9	-17	-18.9	-16.9	0.794	0.700	0.620	0.708	0.715	0.707	0.062
6.357	-16	-17	-17	-18.9	-17	0.794	0.600	0.620	0.708	0.615	0.667	0.083
6.416	-16.1	-17	-17.1	-19	-17	0.694	0.600	0.520	0.608	0.615	0.607	0.062
6.474	-16.1	-17.1	-17.1	-19	-17.1	0.694	0.500	0.520	0.608	0.515	0.567	0.083
6.533	-16.2	-17.1	-17.1	-19	-17.1	0.594	0.500	0.520	0.608	0.515	0.547	0.050
6.592	-16.2	-17.1	-17.1	-19.1	-17.1	0.594	0.500	0.520	0.508	0.515	0.527	0.038
6.651	-16.2	-17.2	-17.2	-19.1	-17.2	0.594	0.400	0.420	0.508	0.415	0.467	0.083
6.710	-16.3	-17.2	-17.2	-19.2	-17.2	0.494	0.400	0.420	0.408	0.415	0.427	0.038
6.769	-16.3	-17.3	-17.3	-19.2	-17.2	0.494	0.300	0.320	0.408	0.415	0.387	0.079
6.828	-16.4	-17.3	-17.3	-19.3	-17.3	0.394	0.300	0.320	0.308	0.315	0.327	0.038
6.887	-16.4	-17.4	-17.3	-19.3	-17.3	0.394	0.200	0.320	0.308	0.315	0.307	0.070
6.946	-16.4	-17.4	-17.4	-19.4	-17.4	0.394	0.200	0.220	0.208	0.215	0.247	0.082
7.005	-16.5	-17.4	-17.4	-19.4	-17.4	0.294	0.200	0.220	0.208	0.215	0.227	0.038
7.064	-16.5	-17.5	-17.5	-19.4	-17.4	0.294	0.100	0.120	0.208	0.215	0.187	0.079
7.123	-16.6	-17.5	-17.5	-19.5	-17.4	0.194	0.100	0.120	0.108	0.215	0.147	0.053
7.182	-16.6	-17.5	-17.5	-19.5	-17.5	0.194	0.100	0.120	0.108	0.115	0.127	0.038
7.241	-16.6	-17.5	-17.5	-19.5	-17.5	0.194	0.100	0.120	0.108	0.115	0.127	0.038
7.300	-16.7	-17.6	-17.6	-19.6	-17.5	0.094	0.000	0.020	0.008	0.115	0.047	0.053
7.359	-16.7	-17.6	-17.6	-19.6	-17.6	0.094	0.000	0.020	0.008	0.015	0.027	0.038
7.418	-16.7	-17.6	-17.6	-19.6	-17.6	0.094	0.000	0.020	0.008	0.015	0.027	0.038
7.476	-16.7	-17.6	-17.6	-19.6	-17.6	0.094	0.000	0.020	0.008	0.015	0.027	0.038
7.535	-16.7	-17.6	-17.7	-19.7	-17.6	0.094	0.000	-0.080	-0.092	0.015	-0.013	0.076
7.594	-16.7	-17.7	-17.7	-19.7	-17.6	0.094	-0.100	-0.080	-0.092	0.015	-0.033	0.085
7.653	-16.8	-17.7	-17.7	-19.7	-17.6	-0.006	-0.100	-0.080	-0.092	0.015	-0.053	0.053
7.712	-16.7	-17.6	-17.7	-19.7	-17.6	0.094	0.000	-0.080	-0.092	0.015	-0.013	0.076
7.771	-16.7	-17.6	-17.7	-19.7	-17.6	0.094	0.000	-0.080	-0.092	0.015	-0.013	0.076
7.830	-16.8	-17.7	-17.7	-19.7	-17.7	-0.006	-0.100	-0.080	-0.092	-0.085	-0.073	0.038
7.889	-16.8	-17.7	-17.7	-19.7	-17.7	-0.006	-0.100	-0.080	-0.092	-0.085	-0.073	0.038
7.948	-16.8	-17.7	-17.7	-19.7	-17.7	-0.006	-0.100	-0.080	-0.092	-0.085	-0.073	0.038
8.007	-16.8	-17.7	-17.7	-19.7	-17.6	-0.006	-0.100	-0.080	-0.092	0.015	-0.053	0.053
8.066	-16.8	-17.7	-17.7	-19.7	-17.6	-0.006	-0.100	-0.080	-0.092	0.015	-0.053	0.053
8.125	-16.7	-17.6	-17.7	-19.7	-17.6	0.094	0.000	-0.080	-0.092	0.015	-0.013	0.076
8.184	-16.7	-17.6	-17.7	-19.7	-17.6	0.094	0.000	-0.080	-0.092	0.015	-0.013	0.076
8.243	-16.7	-17.6	-17.6	-19.6	-17.6	0.094	0.000	0.020	0.008	0.015	0.027	0.038
8.302	-16.7	-17.5	-17.6	-19.6	-17.6	0.094	0.100	0.020	0.008	0.015	0.047	0.045
8.361	-16.7	-17.6	-17.6	-19.5	-17.6	0.094	0.000	0.020	0.108	0.015	0.047	0.050
8.420	-16.7	-17.5	-17.6	-19.5	-17.5	0.094	0.100	0.020	0.108	0.115	0.087	0.039
8.478	-16.7	-17.5	-17.5	-19.5	-17.4	0.094	0.100	0.120	0.108	0.215	0.127	0.050
8.537	-16.7	-17.5	-17.5	-19.5	-17.5	0.094	0.100	0.120	0.108	0.115	0.107	0.011
8.596	-16.7	-17.5	-17.5	-19.5	-17.5	0.094	0.100	0.120	0.108	0.115	0.107	0.011
8.655	-16.7	-17.5	-17.5	-19.5	-17.4	0.094	0.100	0.120	0.108	0.215	0.127	0.050
8.714	-16.7	-17.5	-17.5	-19.5	-17.4	0.094	0.100	0.120	0.108	0.215	0.127	0.050
8.773	-16.7	-17.4	-17.5	-19.5	-17.4	0.094	0.200	0.120	0.108	0.215	0.147	0.056
8.832	-16.7	-17.4	-17.5	-19.5	-17.4	0.094	0.200	0.120	0.108	0.215	0.147	0.056

8.891	-16.6	-17.4	-17.4	-19.5	-17.4	0.194	0.200	0.220	0.108	0.215	0.187	0.046
8.950	-16.6	-17.3	-17.4	-19.4	-17.4	0.194	0.300	0.220	0.208	0.215	0.227	0.042
9.009	-16.5	-17.3	-17.4	-19.4	-17.3	0.294	0.300	0.220	0.208	0.315	0.267	0.050
9.068	-16.5	-17.3	-17.3	-19.3	-17.3	0.294	0.300	0.320	0.308	0.315	0.307	0.011
9.127	-16.4	-17.2	-17.3	-19.3	-17.3	0.394	0.400	0.320	0.308	0.315	0.347	0.045
9.186	-16.4	-17.2	-17.3	-19.3	-17.3	0.394	0.400	0.320	0.308	0.315	0.347	0.045
9.245	-16.4	-17.2	-17.2	-19.2	-17.2	0.394	0.400	0.420	0.408	0.415	0.407	0.011
9.304	-16.3	-17.2	-17.2	-19.3	-17.2	0.494	0.400	0.420	0.308	0.415	0.407	0.067
9.363	-16.3	-17.2	-17.2	-19.3	-17.2	0.494	0.400	0.420	0.308	0.415	0.407	0.067
9.421	-16.3	-17.2	-17.2	-19.3	-17.2	0.494	0.400	0.420	0.308	0.415	0.407	0.067
9.480	-16.3	-17.2	-17.2	-19.3	-17.2	0.494	0.400	0.420	0.308	0.415	0.407	0.067
9.539	-16.3	-17.2	-17.2	-19.2	-17.2	0.494	0.400	0.420	0.408	0.415	0.427	0.038
9.598	-16.2	-17.1	-17.2	-19.2	-17.2	0.594	0.500	0.420	0.408	0.415	0.467	0.080
9.657	-16.2	-17.1	-17.2	-19.2	-17.2	0.594	0.500	0.420	0.408	0.415	0.467	0.080
9.716	-16.2	-17.1	-17.2	-19.2	-17.2	0.594	0.500	0.420	0.408	0.415	0.467	0.080
9.775	-16.2	-17.1	-17.2	-19.2	-17.2	0.594	0.500	0.420	0.408	0.415	0.467	0.080
9.834	-16.2	-17.1	-17.2	-19.2	-17.1	0.594	0.500	0.420	0.408	0.515	0.487	0.076
9.893	-16.2	-17	-17.1	-19.1	-17.1	0.594	0.600	0.520	0.508	0.515	0.547	0.045
9.952	-16.2	-17	-17.1	-19.1	-17.1	0.594	0.600	0.520	0.508	0.515	0.547	0.045
10.011	-16.2	-17.1	-17.1	-19.1	-17.1	0.594	0.500	0.520	0.508	0.515	0.527	0.038
10.070	-16.3	-17.1	-17.1	-19.1	-17.1	0.494	0.500	0.520	0.508	0.515	0.507	0.011
10.129	-16.3	-17.1	-17.1	-19	-17.1	0.494	0.500	0.520	0.608	0.515	0.527	0.046
10.188	-16.3	-17.1	-17.1	-19.1	-17.1	0.494	0.500	0.520	0.508	0.515	0.507	0.011
10.247	-16.2	-17	-17.1	-19	-17.1	0.594	0.600	0.520	0.608	0.515	0.567	0.046
10.306	-16.2	-17	-17	-19	-17	0.594	0.600	0.620	0.608	0.615	0.607	0.011
10.365	-16.2	-17	-17	-19	-17	0.594	0.600	0.620	0.608	0.615	0.607	0.011
10.423	-16.1	-16.9	-17	-19	-16.9	0.694	0.700	0.620	0.608	0.715	0.667	0.050
10.482	-16.1	-16.9	-16.9	-18.9	-16.9	0.694	0.700	0.720	0.708	0.715	0.707	0.011
10.541	-16	-16.9	-16.9	-18.9	-16.9	0.794	0.700	0.720	0.708	0.715	0.727	0.038
10.600	-16	-16.8	-16.9	-18.8	-16.9	0.794	0.800	0.720	0.808	0.715	0.767	0.046
10.659	-15.9	-16.8	-16.8	-18.8	-16.8	0.894	0.800	0.820	0.808	0.815	0.827	0.038
10.718	-15.9	-16.7	-16.8	-18.8	-16.8	0.894	0.900	0.820	0.808	0.815	0.847	0.045
10.777	-15.9	-16.7	-16.9	-18.8	-16.8	0.894	0.900	0.720	0.808	0.815	0.827	0.074
10.836	-15.9	-16.7	-16.9	-18.9	-16.8	0.894	0.900	0.720	0.708	0.815	0.807	0.092
10.895	-16	-16.8	-16.9	-18.9	-16.9	0.794	0.800	0.720	0.708	0.715	0.747	0.045
10.954	-16	-16.8	-16.9	-18.9	-16.9	0.794	0.800	0.720	0.708	0.715	0.747	0.045
11.013	-16	-16.8	-17	-19	-17	0.794	0.800	0.620	0.608	0.615	0.687	0.100
11.072	-16	-16.8	-16.9	-19	-17	0.794	0.800	0.720	0.608	0.615	0.707	0.093
11.131	-16	-16.8	-16.9	-19	-16.9	0.794	0.800	0.720	0.608	0.715	0.727	0.078
11.190	-16.1	-16.8	-16.9	-19	-17	0.694	0.800	0.720	0.608	0.615	0.687	0.079
11.249	-16.1	-16.8	-16.9	-18.9	-17	0.694	0.800	0.720	0.708	0.615	0.707	0.066
11.308	-16.1	-16.8	-16.9	-18.9	-16.9	0.694	0.800	0.720	0.708	0.715	0.727	0.042
11.367	-16.1	-16.8	-16.9	-18.9	-16.9	0.694	0.800	0.720	0.708	0.715	0.727	0.042
11.425	-16	-16.8	-16.9	-18.9	-16.9	0.794	0.800	0.720	0.708	0.715	0.747	0.045
11.484	-16	-16.8	-16.8	-18.8	-16.8	0.794	0.800	0.820	0.808	0.815	0.807	0.011
11.543	-16	-16.8	-16.8	-18.9	-16.9	0.794	0.800	0.820	0.708	0.715	0.767	0.052
11.602	-16	-16.8	-16.9	-18.9	-16.9	0.794	0.800	0.720	0.708	0.715	0.747	0.045
11.661	-16.1	-16.9	-16.9	-18.9	-16.9	0.694	0.700	0.720	0.708	0.715	0.707	0.011
11.720	-16.1	-16.8	-16.8	-18.8	-16.9	0.694	0.800	0.820	0.808	0.715	0.767	0.058
11.779	-16	-16.8	-16.8	-18.8	-16.9	0.794	0.800	0.820	0.808	0.715	0.787	0.041
11.838	-16	-16.8	-16.9	-18.9	-16.9	0.794	0.800	0.720	0.708	0.715	0.747	0.045
11.897	-16	-16.7	-16.8	-18.8	-16.8	0.794	0.900	0.820	0.808	0.815	0.827	0.042
11.956	-16	-16.7	-16.7	-18.7	-16.7	0.794	0.900	0.920	0.908	0.915	0.887	0.053
12.015	-15.9	-16.7	-16.7	-18.7	-16.7	0.894	0.900	0.920	0.908	0.915	0.907	0.011
12.074	-15.9	-16.6	-16.7	-18.7	-16.7	0.894	1.000	0.920	0.908	0.915	0.927	0.042
12.133	-15.8	-16.6	-16.6	-18.6	-16.6	0.994	1.000	1.020	1.008	1.015	1.007	0.011
12.192	-15.8	-16.5	-16.6	-18.6	-16.7	0.994	1.100	1.020	1.008	0.915	1.007	0.066
12.251	-15.9	-16.6	-16.6	-18.7	-16.7	0.894	1.000	1.020	0.908	0.915	0.947	0.058
12.310	-15.8	-16.6	-16.6	-18.6	-16.6	0.994	1.000	1.020	1.008	1.015	1.007	0.011
12.369	-15.9	-16.6	-16.6	-18.6	-16.7	0.894	1.000	1.020	1.008	0.915	0.967	0.058
12.427	-15.9	-16.6	-16.6	-18.7	-16.7	0.894	1.000	1.020	0.908	0.915	0.947	0.058
12.486	-15.9	-16.6	-16.6	-18.6	-16.7	0.894	1.000	1.020	1.008	0.915	0.967	0.058
12.545	-15.9	-16.6	-16.5	-18.6	-16.6	0.894	1.000	1.120	1.008	1.015	1.007	0.080
12.604	-15.8	-16.5	-16.5	-18.6	-16.5	0.994	1.100	1.120	1.008	1.115	1.067	0.061
12.663	-15.7	-16.5	-16.5	-18.6	-16.5	1.094	1.100	1.120	1.008	1.115	1.087	0.046
12.722	-15.7	-16.5	-16.5	-18.5	-16.5	1.094	1.100	1.120	1.108	1.115	1.107	0.011
12.781	-15.8	-16.6	-16.5	-18.5	-16.6	0.994	1.000	1.120	1.108	1.015	1.047	0.061
12.840	-15.8	-16.6	-16.6	-18.5	-16.6	0.994	1.000	1.020	1.108	1.015	1.027	0.046
12.899	-15.8	-16.6	-16.6	-18.5	-16.6	0.994	1.000	1.020	1.108	1.015	1.027	0.046
12.958	-15.7	-16.5	-16.6	-18.5	-16.6	1.094	1.100	1.020	1.108	1.015	1.067	0.046
13.017	-15.7	-16.5	-16.6	-18.5	-16.6	1.094	1.100	1.020	1.108	1.015	1.067	0.046
13.076	-15.6	-16.5	-16.5	-18.5	-16.5	1.194	1.100	1.120	1.108	1.115	1.127	0.038
13.135	-15.5	-16.4	-16.4	-18.4	-16.4	1.294	1.200	1.220	1.208	1.215	1.227	0.038
13.194	-15.5	-16.4	-16.3	-18.4	-16.4	1.294	1.200	1.320	1.208	1.215	1.247	0.055
13.253	-15.5	-16.4	-16.3	-18.4	-16.3	1.294	1.200	1.320	1.208	1.315	1.267	0.059

13.312	-15.6	-16.4	-16.4	-18.4	-16.4	1.194	1.200	1.220	1.208	1.215	1.207	0.011
13.370	-15.5	-16.4	-16.4	-18.4	-16.4	1.294	1.200	1.220	1.208	1.215	1.227	0.038
13.429	-15.5	-16.4	-16.4	-18.4	-16.3	1.294	1.200	1.220	1.208	1.315	1.247	0.053
13.488	-15.5	-16.4	-16.4	-18.3	-16.3	1.294	1.200	1.220	1.308	1.315	1.267	0.054
13.547	-15.4	-16.3	-16.3	-18.3	-16.3	1.394	1.300	1.320	1.308	1.315	1.327	0.038
13.606	-15.4	-16.3	-16.2	-18.2	-16.2	1.394	1.300	1.420	1.408	1.415	1.387	0.050
13.665	-15.4	-16.2	-16.2	-18.2	-16.2	1.394	1.400	1.420	1.408	1.415	1.407	0.011
13.724	-15.4	-16.3	-16.3	-18.3	-16.3	1.394	1.300	1.320	1.308	1.315	1.327	0.038
13.783	-15.4	-16.3	-16.3	-18.2	-16.3	1.394	1.300	1.320	1.408	1.315	1.347	0.050
13.842	-15.4	-16.2	-16.3	-18.2	-16.2	1.394	1.400	1.320	1.408	1.415	1.387	0.039
13.901	-15.4	-16.2	-16.2	-18.2	-16.2	1.394	1.400	1.420	1.408	1.415	1.407	0.011
13.960	-15.3	-16.2	-16.2	-18.2	-16.2	1.494	1.400	1.420	1.408	1.415	1.427	0.038
14.019	-15.3	-16.2	-16.2	-18.2	-16.2	1.494	1.400	1.420	1.408	1.415	1.427	0.038
14.078	-15.3	-16.1	-16.1	-18.1	-16.1	1.494	1.500	1.520	1.508	1.515	1.507	0.011
14.137	-15.3	-16.2	-16.2	-18.2	-16.2	1.494	1.400	1.420	1.408	1.415	1.427	0.038
14.196	-15.3	-16.2	-16.2	-18.2	-16.2	1.494	1.400	1.420	1.408	1.415	1.427	0.038
14.255	-15.2	-16.1	-16.2	-18.2	-16.2	1.594	1.500	1.420	1.408	1.415	1.467	0.080
14.314	-15.2	-16.1	-16.1	-18.1	-16.1	1.594	1.500	1.520	1.508	1.515	1.527	0.038
14.372	-15.2	-16.1	-16.1	-18.1	-16.1	1.594	1.500	1.520	1.508	1.515	1.527	0.038
14.431	-15.3	-16.1	-16.2	-18.2	-16.2	1.494	1.500	1.420	1.408	1.415	1.447	0.045
14.490	-15.3	-16.1	-16.1	-18.1	-16.1	1.494	1.500	1.520	1.508	1.515	1.507	0.011
14.549	-15.2	-16.1	-16.1	-18.1	-16.1	1.594	1.500	1.520	1.508	1.515	1.527	0.038
14.608	-15.2	-16.1	-16.1	-18.1	-16.1	1.594	1.500	1.520	1.508	1.515	1.527	0.038
14.667	-15.3	-16.1	-16.1	-18.1	-16.2	1.494	1.500	1.520	1.508	1.415	1.487	0.041
14.726	-15.3	-16.1	-16.1	-18.1	-16.1	1.494	1.500	1.520	1.508	1.515	1.507	0.011
14.785	-15.1	-16	-16	-18	-16	1.694	1.600	1.620	1.608	1.615	1.627	0.038
14.844	-15.1	-15.9	-15.9	-18	-15.9	1.694	1.700	1.720	1.608	1.715	1.687	0.046
14.903	-15.2	-16	-16	-18	-16	1.594	1.600	1.620	1.608	1.615	1.607	0.011
14.962	-15.1	-16	-16	-17.9	-15.9	1.694	1.600	1.620	1.708	1.715	1.667	0.054
15.021	-15.1	-15.9	-15.9	-17.8	-15.8	1.694	1.700	1.720	1.808	1.815	1.747	0.059
15.080	-15	-15.8	-15.8	-17.8	-15.8	1.794	1.800	1.820	1.808	1.815	1.807	0.011
15.139	-15.1	-15.8	-15.8	-17.8	-15.8	1.694	1.800	1.820	1.808	1.815	1.787	0.053
15.198	-15	-15.8	-15.8	-17.8	-15.8	1.794	1.800	1.820	1.808	1.815	1.807	0.011
15.257	-14.9	-15.7	-15.7	-17.7	-15.7	1.894	1.900	1.920	1.908	1.915	1.907	0.011
15.316	-14.8	-15.7	-15.7	-17.6	-15.6	1.994	1.900	1.920	2.008	2.015	1.967	0.054
15.374	-14.8	-15.7	-15.6	-17.6	-15.6	1.994	1.900	2.020	2.008	2.015	1.987	0.050
15.433	-14.8	-15.7	-15.6	-17.6	-15.6	1.994	1.900	2.020	2.008	2.015	1.987	0.050
15.492	-14.8	-15.7	-15.6	-17.6	-15.6	1.994	1.900	2.020	2.008	2.015	1.987	0.050
15.551	-14.9	-15.7	-15.6	-17.6	-15.6	1.894	1.900	2.020	2.008	2.015	1.967	0.064
15.610	-14.9	-15.7	-15.6	-17.5	-15.6	1.894	1.900	2.020	2.108	2.015	1.987	0.090
15.669	-14.8	-15.6	-15.6	-17.5	-15.6	1.994	2.000	2.020	2.108	2.015	2.027	0.046
15.728	-14.7	-15.5	-15.6	-17.5	-15.5	2.094	2.100	2.020	2.108	2.115	2.087	0.039
15.787	-14.8	-15.6	-15.5	-17.5	-15.6	1.994	2.000	2.120	2.108	2.015	2.047	0.061
15.846	-14.8	-15.6	-15.6	-17.6	-15.6	1.994	2.000	2.020	2.008	2.015	2.007	0.011
15.905	-14.8	-15.6	-15.5	-17.6	-15.6	1.994	2.000	2.120	2.008	2.015	2.027	0.052
15.964	-14.7	-15.4	-15.5	-17.5	-15.5	2.094	2.200	2.120	2.108	2.115	2.127	0.042
16.023	-14.6	-15.4	-15.5	-17.4	-15.5	2.194	2.200	2.120	2.208	2.115	2.167	0.046
16.082	-14.7	-15.4	-15.6	-17.5	-15.6	2.094	2.200	2.020	2.108	2.015	2.087	0.076
16.141	-14.7	-15.5	-15.7	-17.5	-15.6	2.094	2.100	1.920	2.108	2.015	2.047	0.081
16.200	-14.7	-15.6	-15.7	-17.6	-15.6	2.094	2.000	1.920	2.008	2.015	2.007	0.062
16.259	-14.7	-15.5	-15.7	-17.6	-15.7	2.094	2.100	1.920	2.008	1.915	2.007	0.090
16.317	-14.8	-15.6	-15.7	-17.7	-15.8	1.994	2.000	1.920	1.908	1.815	1.927	0.075
16.376	-14.9	-15.7	-15.8	-17.7	-15.8	1.894	1.900	1.820	1.908	1.815	1.867	0.046
16.435	-14.9	-15.7	-15.8	-17.7	-15.9	1.894	1.900	1.820	1.908	1.715	1.847	0.082
16.494	-15	-15.7	-15.8	-17.7	-15.8	1.794	1.900	1.820	1.908	1.815	1.847	0.053
16.553	-14.9	-15.7	-15.8	-17.7	-15.8	1.894	1.900	1.820	1.908	1.815	1.867	0.046
16.612	-14.9	-15.7	-15.8	-17.7	-15.8	1.894	1.900	1.820	1.908	1.815	1.867	0.046
16.671	-14.9	-15.7	-15.8	-17.7	-15.8	1.894	1.900	1.820	1.908	1.815	1.867	0.046
16.730	-15	-15.8	-15.8	-17.8	-15.8	1.794	1.800	1.820	1.808	1.815	1.807	0.011
16.789	-15	-15.8	-15.8	-17.7	-15.8	1.794	1.800	1.820	1.908	1.815	1.827	0.046
16.848	-15	-15.8	-15.8	-17.7	-15.8	1.794	1.800	1.820	1.908	1.815	1.827	0.046
16.907	-15	-15.8	-15.8	-17.7	-15.8	1.794	1.800	1.820	1.908	1.815	1.827	0.046
16.966	-15.1	-15.9	-15.9	-17.9	-15.9	1.694	1.700	1.720	1.708	1.715	1.707	0.011
17.025	-15.2	-15.9	-16	-17.9	-16	1.594	1.700	1.620	1.708	1.615	1.647	0.053
17.084	-15.1	-15.9	-16	-17.9	-15.9	1.694	1.700	1.620	1.708	1.715	1.687	0.039
17.143	-15.2	-15.9	-15.9	-17.9	-15.9	1.594	1.700	1.720	1.708	1.715	1.687	0.053
17.202	-15.2	-15.9	-15.9	-17.9	-15.9	1.594	1.700	1.720	1.708	1.715	1.687	0.053
17.261	-15.2	-15.9	-16	-18	-16	1.594	1.700	1.620	1.608	1.615	1.627	0.042
17.319	-15.3	-16	-16	-18	-16.1	1.494	1.600	1.620	1.608	1.515	1.567	0.058
17.378	-15.3	-16.1	-16	-18	-16.1	1.494	1.500	1.620	1.608	1.515	1.547	0.061
17.437	-15.2	-16	-15.9	-17.9	-15.9	1.594	1.600	1.720	1.708	1.715	1.667	0.064
17.496	-15.2	-15.9	-16	-17.9	-15.9	1.594	1.700	1.620	1.708	1.715	1.667	0.056
17.555	-15.3	-16	-16	-18	-16.1	1.494	1.600	1.620	1.608	1.515	1.567	0.058
17.614	-15.4	-16.1	-16.1	-18	-16.1	1.394	1.500	1.520	1.608	1.515	1.507	0.076
17.673	-15.4	-16.1	-16	-18	-16.1	1.394	1.500	1.620	1.608	1.515	1.527	0.092

17.732	-15.4	-16.1	-16	-18	-16.1	1.394	1.500	1.620	1.608	1.515	1.527	0.092
17.791	-15.4	-16.2	-16.1	-18.1	-16.2	1.394	1.400	1.520	1.508	1.415	1.447	0.061
17.850	-15.6	-16.3	-16.2	-18.2	-16.3	1.194	1.300	1.420	1.408	1.315	1.327	0.092
17.909	-15.6	-16.3	-16.2	-18.2	-16.2	1.194	1.300	1.420	1.408	1.415	1.347	0.099
17.968	-15.5	-16.2	-16.2	-18.1	-16.2	1.294	1.400	1.420	1.508	1.415	1.407	0.076
18.027	-15.5	-16.2	-16.1	-18.1	-16.2	1.294	1.400	1.520	1.508	1.415	1.427	0.092
18.086	-15.5	-16.2	-16.2	-18.2	-16.3	1.294	1.400	1.420	1.408	1.315	1.367	0.058
18.145	-15.6	-16.3	-16.3	-18.2	-16.3	1.194	1.300	1.320	1.408	1.315	1.307	0.076
18.204	-15.6	-16.3	-16.2	-18.2	-16.3	1.194	1.300	1.420	1.408	1.315	1.327	0.092
18.262	-15.5	-16.3	-16.3	-18.2	-16.2	1.294	1.300	1.320	1.408	1.415	1.347	0.059
18.321	-15.6	-16.4	-16.4	-18.3	-16.3	1.194	1.200	1.220	1.308	1.315	1.247	0.059
18.380	-15.7	-16.4	-16.4	-18.3	-16.3	1.094	1.200	1.220	1.308	1.315	1.227	0.091
18.439	-15.6	-16.4	-16.3	-18.3	-16.3	1.194	1.200	1.320	1.308	1.315	1.267	0.064
18.498	-15.6	-16.4	-16.3	-18.3	-16.3	1.194	1.200	1.320	1.308	1.315	1.267	0.064
18.557	-15.7	-16.5	-16.4	-18.4	-16.4	1.094	1.100	1.220	1.208	1.215	1.167	0.064
18.616	-15.8	-16.5	-16.4	-18.4	-16.4	0.994	1.100	1.220	1.208	1.215	1.147	0.099
18.675	-15.7	-16.4	-16.3	-18.3	-16.3	1.094	1.200	1.320	1.308	1.315	1.247	0.099
18.734	-15.7	-16.4	-16.3	-18.4	-16.4	1.094	1.200	1.320	1.208	1.215	1.207	0.080
18.793	-15.7	-16.4	-16.4	-18.4	-16.4	1.094	1.200	1.220	1.208	1.215	1.187	0.053
18.852	-15.7	-16.4	-16.4	-18.4	-16.4	1.094	1.200	1.220	1.208	1.215	1.187	0.053
18.911	-15.7	-16.4	-16.4	-18.4	-16.4	1.094	1.200	1.220	1.208	1.215	1.187	0.053
18.970	-15.6	-16.4	-16.3	-18.4	-16.4	1.194	1.200	1.320	1.208	1.215	1.227	0.052
19.029	-15.5	-16.3	-16.3	-18.4	-16.4	1.294	1.300	1.320	1.208	1.215	1.267	0.052
19.088	-15.5	-16.3	-16.4	-18.5	-16.5	1.294	1.300	1.220	1.108	1.115	1.207	0.093
19.147	-15.7	-16.5	-16.5	-18.6	-16.6	1.094	1.100	1.120	1.008	1.015	1.067	0.052
19.206	-15.8	-16.6	-16.6	-18.6	-16.6	0.994	1.000	1.020	1.008	1.015	1.007	0.011
19.264	-15.9	-16.6	-16.6	-18.6	-16.6	0.894	1.000	1.020	1.008	1.015	0.987	0.053
19.323	-15.9	-16.6	-16.6	-18.6	-16.6	0.894	1.000	1.020	1.008	1.015	0.987	0.053
19.382	-15.9	-16.6	-16.7	-18.7	-16.7	0.894	1.000	0.920	0.908	0.915	0.927	0.042
19.441	-16	-16.7	-16.7	-18.7	-16.7	0.794	0.900	0.920	0.908	0.915	0.887	0.053
19.500	-16	-16.7	-16.8	-18.7	-16.8	0.794	0.900	0.820	0.908	0.815	0.847	0.053
19.559	-16	-16.8	-16.8	-18.7	-16.8	0.794	0.800	0.820	0.908	0.815	0.827	0.046
19.618	-16	-16.7	-16.8	-18.7	-16.7	0.794	0.900	0.820	0.908	0.915	0.867	0.056
19.677	-15.9	-16.7	-16.7	-18.7	-16.7	0.894	0.900	0.920	0.908	0.915	0.907	0.011
19.736	-16	-16.7	-16.8	-18.7	-16.8	0.794	0.900	0.820	0.908	0.815	0.847	0.053
19.795	-16.1	-16.8	-16.9	-18.8	-16.8	0.694	0.800	0.720	0.808	0.815	0.767	0.056
19.854	-16.1	-16.9	-16.9	-18.9	-16.9	0.694	0.700	0.720	0.708	0.715	0.707	0.011
19.913	-16.1	-16.9	-16.9	-18.9	-16.8	0.694	0.700	0.720	0.708	0.815	0.727	0.050
19.972	-16.1	-16.9	-16.8	-18.8	-16.8	0.694	0.700	0.820	0.808	0.815	0.767	0.064
20.031	-16.1	-16.9	-16.9	-18.9	-16.9	0.694	0.700	0.720	0.708	0.715	0.707	0.011
20.090	-16.1	-16.9	-16.9	-19	-17	0.694	0.700	0.720	0.608	0.615	0.667	0.052
20.149	-16.2	-17	-17	-19	-17.1	0.594	0.600	0.620	0.608	0.515	0.587	0.041
20.208	-16.2	-17	-17	-19	-17.1	0.594	0.600	0.620	0.608	0.515	0.587	0.041
20.266	-16.2	-17	-17	-19	-17.1	0.594	0.600	0.620	0.608	0.515	0.587	0.041
20.325	-16.2	-17	-17.1	-19.1	-17.1	0.594	0.600	0.520	0.508	0.515	0.547	0.045
20.384	-16.2	-17.1	-17.1	-19.2	-17.2	0.594	0.500	0.520	0.408	0.415	0.487	0.078
20.443	-16.3	-17.1	-17.1	-19.2	-17.2	0.494	0.500	0.520	0.408	0.415	0.467	0.052
20.502	-16.3	-17.1	-17.1	-19.1	-17.1	0.494	0.500	0.520	0.508	0.515	0.507	0.011
20.561	-16.3	-17.1	-17.1	-19.2	-17.1	0.494	0.500	0.520	0.408	0.515	0.487	0.046
20.620	-16.3	-17.1	-17.2	-19.2	-17.2	0.494	0.500	0.420	0.408	0.415	0.447	0.045
20.679	-16.3	-17.2	-17.2	-19.2	-17.2	0.494	0.400	0.420	0.408	0.415	0.427	0.038
20.738	-16.3	-17.2	-17.2	-19.2	-17.2	0.494	0.400	0.420	0.408	0.415	0.427	0.038
20.797	-16.4	-17.2	-17.3	-19.3	-17.2	0.394	0.400	0.320	0.308	0.415	0.367	0.050
20.856	-16.4	-17.2	-17.2	-19.3	-17.2	0.394	0.400	0.420	0.308	0.415	0.387	0.046
20.915	-16.4	-17.2	-17.2	-19.2	-17.2	0.394	0.400	0.420	0.408	0.415	0.407	0.011
20.974	-16.4	-17.2	-17.2	-19.2	-17.2	0.394	0.400	0.420	0.408	0.415	0.407	0.011
21.033	-16.5	-17.2	-17.2	-19.3	-17.3	0.294	0.400	0.420	0.308	0.315	0.347	0.058
21.092	-16.5	-17.3	-17.2	-19.2	-17.2	0.294	0.300	0.420	0.408	0.415	0.367	0.064
21.151	-16.4	-17.2	-17.2	-19.1	-17.1	0.394	0.400	0.420	0.508	0.515	0.447	0.059
21.209	-16.4	-17.2	-17.1	-19.1	-17.1	0.394	0.400	0.520	0.508	0.515	0.467	0.064
21.268	-16.4	-17.2	-17.1	-19.1	-17.1	0.394	0.400	0.520	0.508	0.515	0.467	0.064
21.327	-16.4	-17.1	-17.1	-19.1	-17.1	0.394	0.500	0.520	0.508	0.515	0.487	0.053
21.386	-16.3	-17.1	-17	-19.1	-17	0.494	0.500	0.620	0.508	0.615	0.547	0.064
21.445	-16.4	-17.2	-17.1	-19.2	-17.1	0.394	0.400	0.520	0.408	0.515	0.447	0.064
21.504	-16.5	-17.4	-17.3	-19.3	-17.3	0.294	0.200	0.320	0.308	0.315	0.287	0.050
21.563	-16.6	-17.4	-17.3	-19.4	-17.4	0.194	0.200	0.320	0.208	0.215	0.227	0.052
21.622	-16.7	-17.4	-17.4	-19.4	-17.3	0.094	0.200	0.220	0.208	0.315	0.207	0.079
21.681	-16.7	-17.5	-17.4	-19.4	-17.4	0.094	0.100	0.220	0.208	0.215	0.167	0.064
21.740	-16.7	-17.5	-17.4	-19.4	-17.4	0.094	0.100	0.220	0.208	0.215	0.167	0.064
21.799	-16.8	-17.6	-17.5	-19.5	-17.5	-0.006	0.000	0.120	0.108	0.115	0.067	0.064
21.858	-16.8	-17.6	-17.5	-19.6	-17.5	-0.006	0.000	0.120	0.008	0.115	0.047	0.064
21.917	-16.8	-17.6	-17.5	-19.6	-17.5	-0.006	0.000	0.120	0.008	0.115	0.047	0.064
21.976	-16.8	-17.6	-17.5	-19.6	-17.5	-0.006	0.000	0.120	0.008	0.115	0.047	0.064
22.035	-16.8	-17.6	-17.5	-19.6	-17.5	-0.006	0.000	0.120	0.008	0.115	0.047	0.064
22.094	-16.8	-17.6	-17.6	-19.7	-17.6	-0.006	0.000	0.020	-0.092	0.015	-0.013	0.046

22.153	-16.9	-17.7	-17.7	-19.8	-17.7	-0.106	-0.100	-0.080	-0.192	-0.085	-0.113	0.046
22.211	-16.9	-17.7	-17.7	-19.8	-17.7	-0.106	-0.100	-0.080	-0.192	-0.085	-0.113	0.046
22.270	-16.9	-17.8	-17.7	-19.8	-17.7	-0.106	-0.200	-0.080	-0.192	-0.085	-0.133	0.059
22.329	-16.9	-17.7	-17.8	-19.8	-17.8	-0.106	-0.100	-0.180	-0.192	-0.185	-0.153	0.045
22.388	-16.9	-17.7	-17.8	-19.9	-17.8	-0.106	-0.100	-0.180	-0.292	-0.185	-0.173	0.078
22.447	-17	-17.8	-17.9	-20	-17.9	-0.206	-0.200	-0.280	-0.392	-0.285	-0.273	0.078
22.506	-17.1	-17.9	-18	-20.1	-17.9	-0.306	-0.300	-0.380	-0.492	-0.285	-0.353	0.086
22.565	-17.1	-17.9	-18	-20.1	-18	-0.306	-0.300	-0.380	-0.492	-0.385	-0.373	0.078
22.624	-17.1	-17.9	-18	-20	-17.9	-0.306	-0.300	-0.380	-0.392	-0.285	-0.333	0.050
22.683	-17.1	-17.8	-17.9	-19.9	-17.9	-0.306	-0.200	-0.280	-0.292	-0.285	-0.273	0.042
22.742	-17.1	-17.9	-17.9	-19.9	-17.9	-0.306	-0.300	-0.280	-0.292	-0.285	-0.293	0.011
22.801	-17.1	-17.9	-17.9	-20	-17.9	-0.306	-0.300	-0.280	-0.392	-0.285	-0.313	0.046
22.860	-17.2	-18	-18	-20	-18	-0.406	-0.400	-0.380	-0.392	-0.385	-0.393	0.011
22.919	-17.2	-18	-18	-20	-18	-0.406	-0.400	-0.380	-0.392	-0.385	-0.393	0.011
22.978	-17.2	-18	-18	-20	-17.9	-0.406	-0.400	-0.380	-0.392	-0.285	-0.373	0.050
23.037	-17.2	-18	-17.9	-19.9	-17.9	-0.406	-0.400	-0.280	-0.292	-0.285	-0.333	0.064
23.096	-17.2	-18	-18	-20	-18	-0.406	-0.400	-0.380	-0.392	-0.385	-0.393	0.011
23.155	-17.2	-18	-18	-20.1	-18	-0.406	-0.400	-0.380	-0.492	-0.385	-0.413	0.046
23.213	-17.3	-18	-18.1	-20.1	-18.1	-0.506	-0.400	-0.480	-0.492	-0.485	-0.473	0.042
23.272	-17.2	-18.1	-18.1	-20.1	-18.1	-0.406	-0.500	-0.480	-0.492	-0.485	-0.473	0.038
23.331	-17.2	-18.1	-18.1	-20.1	-18.1	-0.406	-0.500	-0.480	-0.492	-0.485	-0.473	0.038
23.390	-17.3	-18.1	-18.1	-20.1	-18.1	-0.506	-0.500	-0.480	-0.492	-0.485	-0.493	0.011
23.449	-17.3	-18.2	-18.2	-20.3	-18.2	-0.506	-0.600	-0.580	-0.692	-0.585	-0.593	0.067
23.508	-17.4	-18.3	-18.2	-20.3	-18.2	-0.606	-0.700	-0.580	-0.692	-0.585	-0.633	0.059
23.567	-17.4	-18.3	-18.2	-20.3	-18.2	-0.606	-0.700	-0.580	-0.692	-0.585	-0.633	0.059
23.626	-17.5	-18.3	-18.3	-20.3	-18.3	-0.706	-0.700	-0.680	-0.692	-0.685	-0.693	0.011
23.685	-17.5	-18.3	-18.4	-20.4	-18.3	-0.706	-0.700	-0.780	-0.792	-0.685	-0.733	0.050
23.744	-17.6	-18.4	-18.4	-20.4	-18.4	-0.806	-0.800	-0.780	-0.792	-0.785	-0.793	0.011
23.803	-17.6	-18.5	-18.5	-20.4	-18.4	-0.806	-0.900	-0.880	-0.792	-0.785	-0.833	0.054
23.862	-17.6	-18.5	-18.5	-20.4	-18.4	-0.806	-0.900	-0.880	-0.792	-0.785	-0.833	0.054
23.921	-17.6	-18.4	-18.5	-20.4	-18.5	-0.806	-0.800	-0.880	-0.792	-0.885	-0.833	0.046
23.980	-17.6	-18.5	-18.5	-20.5	-18.5	-0.806	-0.900	-0.880	-0.892	-0.885	-0.873	0.038
24.039	-17.6	-18.5	-18.5	-20.5	-18.5	-0.806	-0.900	-0.880	-0.892	-0.885	-0.873	0.038
24.098	-17.6	-18.5	-18.5	-20.5	-18.5	-0.806	-0.900	-0.880	-0.892	-0.885	-0.873	0.038
24.156	-17.6	-18.5	-18.5	-20.5	-18.5	-0.806	-0.900	-0.880	-0.892	-0.885	-0.873	0.038
24.215	-17.6	-18.5	-18.5	-20.5	-18.5	-0.806	-0.900	-0.880	-0.892	-0.885	-0.873	0.038
24.274	-17.6	-18.5	-18.5	-20.4	-18.5	-0.806	-0.900	-0.880	-0.792	-0.885	-0.853	0.050
24.333	-17.6	-18.5	-18.4	-20.4	-18.4	-0.806	-0.900	-0.780	-0.792	-0.785	-0.813	0.050
24.392	-17.5	-18.4	-18.4	-20.4	-18.4	-0.706	-0.800	-0.780	-0.792	-0.785	-0.773	0.038
24.451	-17.5	-18.3	-18.4	-20.4	-18.4	-0.706	-0.700	-0.780	-0.792	-0.785	-0.753	0.045
24.510	-17.4	-18.3	-18.3	-20.3	-18.3	-0.606	-0.700	-0.680	-0.692	-0.685	-0.673	0.038
24.569	-17.4	-18.3	-18.3	-20.3	-18.2	-0.606	-0.700	-0.680	-0.692	-0.585	-0.653	0.053
24.628	-17.4	-18.3	-18.3	-20.3	-18.2	-0.606	-0.700	-0.680	-0.692	-0.585	-0.653	0.053
24.687	-17.5	-18.3	-18.3	-20.3	-18.3	-0.706	-0.700	-0.680	-0.692	-0.685	-0.693	0.011
24.746	-17.5	-18.3	-18.4	-20.3	-18.4	-0.706	-0.700	-0.780	-0.692	-0.785	-0.733	0.046
24.805	-17.5	-18.3	-18.3	-20.4	-18.3	-0.706	-0.700	-0.680	-0.792	-0.685	-0.713	0.046
24.864	-17.5	-18.4	-18.3	-20.3	-18.3	-0.706	-0.800	-0.680	-0.692	-0.685	-0.713	0.050
24.923	-17.5	-18.4	-18.4	-20.3	-18.3	-0.706	-0.800	-0.780	-0.692	-0.685	-0.733	0.054
24.982	-17.5	-18.4	-18.4	-20.4	-18.3	-0.706	-0.800	-0.780	-0.792	-0.685	-0.753	0.053
25.041	-17.5	-18.4	-18.4	-20.3	-18.3	-0.706	-0.800	-0.780	-0.692	-0.685	-0.733	0.054
25.100	-17.5	-18.4	-18.4	-20.3	-18.4	-0.706	-0.800	-0.780	-0.692	-0.785	-0.753	0.050
25.158	-17.5	-18.3	-18.4	-20.4	-18.3	-0.706	-0.700	-0.780	-0.792	-0.685	-0.733	0.050
25.217	-17.5	-18.3	-18.4	-20.3	-18.3	-0.706	-0.700	-0.780	-0.692	-0.685	-0.713	0.039
25.276	-17.4	-18.3	-18.3	-20.3	-18.3	-0.606	-0.700	-0.680	-0.692	-0.685	-0.673	0.038
25.335	-17.4	-18.3	-18.3	-20.3	-18.3	-0.606	-0.700	-0.680	-0.692	-0.685	-0.673	0.038
25.394	-17.4	-18.3	-18.3	-20.3	-18.2	-0.606	-0.700	-0.680	-0.692	-0.585	-0.653	0.053
25.453	-17.3	-18.2	-18.2	-20.2	-18.2	-0.506	-0.600	-0.580	-0.592	-0.585	-0.573	0.038
25.512	-17.3	-18.2	-18.2	-20.1	-18.1	-0.506	-0.600	-0.580	-0.492	-0.485	-0.533	0.054
25.571	-17.2	-18.1	-18.1	-20.1	-18.1	-0.406	-0.500	-0.480	-0.492	-0.485	-0.473	0.038
25.630	-17.2	-18	-18.1	-20.1	-18.1	-0.406	-0.400	-0.480	-0.492	-0.485	-0.453	0.045
25.689	-17.1	-18	-18	-20	-18	-0.306	-0.400	-0.380	-0.392	-0.385	-0.373	0.038
25.748	-17.1	-17.9	-17.9	-20	-18	-0.306	-0.300	-0.280	-0.392	-0.385	-0.333	0.052
25.807	-17.1	-17.9	-17.9	-19.9	-17.9	-0.306	-0.300	-0.280	-0.292	-0.285	-0.293	0.011
25.866	-17	-17.8	-17.9	-19.8	-17.9	-0.206	-0.200	-0.280	-0.192	-0.285	-0.233	0.046
25.925	-16.9	-17.8	-17.8	-19.8	-17.8	-0.106	-0.200	-0.180	-0.192	-0.185	-0.173	0.038
25.984	-16.9	-17.7	-17.8	-19.8	-17.8	-0.106	-0.100	-0.180	-0.192	-0.185	-0.153	0.045
26.043	-16.9	-17.7	-17.8	-19.7	-17.8	-0.106	-0.100	-0.180	-0.092	-0.185	-0.133	0.046
26.102	-16.9	-17.7	-17.8	-19.7	-17.8	-0.106	-0.100	-0.180	-0.092	-0.185	-0.133	0.046
26.160	-16.9	-17.7	-17.7	-19.7	-17.7	-0.106	-0.100	-0.080	-0.092	-0.085	-0.093	0.011
26.219	-16.9	-17.7	-17.7	-19.7	-17.7	-0.106	-0.100	-0.080	-0.092	-0.085	-0.093	0.011
26.278	-16.9	-17.7	-17.6	-19.7	-17.7	-0.106	-0.100	0.020	-0.092	-0.085	-0.073	0.052
26.337	-16.9	-17.6	-17.6	-19.6	-17.7	-0.106	0.000	0.020	0.008	-0.085	-0.033	0.058
26.396	-16.8	-17.6	-17.6	-19.6	-17.6	-0.006	0.000	0.020	0.008	0.015	0.007	0.011
26.455	-16.8	-17.6	-17.6	-19.6	-17.6	-0.006	0.000	0.020	0.008	0.015	0.007	0.011
26.514	-16.8	-17.6	-17.6	-19.6	-17.7	-0.006	0.000	0.020	0.008	-0.085	-0.013	0.041

26.573	-16.8	-17.6	-17.6	-19.6	-17.6	-0.006	0.000	0.020	0.008	0.015	0.007	0.011
26.632	-16.7	-17.5	-17.5	-19.5	-17.5	0.094	0.100	0.120	0.108	0.115	0.107	0.011
26.691	-16.7	-17.5	-17.5	-19.5	-17.5	0.094	0.100	0.120	0.108	0.115	0.107	0.011
26.750	-16.7	-17.5	-17.5	-19.4	-17.5	0.094	0.100	0.120	0.208	0.115	0.127	0.046
26.809	-16.6	-17.4	-17.4	-19.4	-17.5	0.194	0.200	0.220	0.208	0.115	0.187	0.041
26.868	-16.6	-17.4	-17.4	-19.4	-17.5	0.194	0.200	0.220	0.208	0.115	0.187	0.041
26.927	-16.5	-17.3	-17.4	-19.4	-17.4	0.294	0.300	0.220	0.208	0.215	0.247	0.045
26.986	-16.5	-17.3	-17.4	-19.4	-17.4	0.294	0.300	0.220	0.208	0.215	0.247	0.045
27.045	-16.6	-17.3	-17.4	-19.3	-17.4	0.194	0.300	0.220	0.308	0.215	0.247	0.053
27.103	-16.6	-17.3	-17.4	-19.3	-17.3	0.194	0.300	0.220	0.308	0.315	0.267	0.056
27.162	-16.6	-17.4	-17.4	-19.3	-17.3	0.194	0.200	0.220	0.308	0.315	0.247	0.059
27.221	-16.6	-17.4	-17.3	-19.3	-17.3	0.194	0.200	0.320	0.308	0.315	0.267	0.064
27.280	-16.6	-17.4	-17.3	-19.3	-17.3	0.194	0.200	0.320	0.308	0.315	0.267	0.064
27.339	-16.6	-17.4	-17.4	-19.4	-17.4	0.194	0.200	0.220	0.208	0.215	0.207	0.011
27.398	-16.6	-17.3	-17.4	-19.4	-17.4	0.194	0.300	0.220	0.208	0.215	0.227	0.042
27.457	-16.6	-17.4	-17.4	-19.4	-17.4	0.194	0.200	0.220	0.208	0.215	0.207	0.011
27.516	-16.7	-17.4	-17.4	-19.4	-17.4	0.094	0.200	0.220	0.208	0.215	0.187	0.053
27.575	-16.7	-17.5	-17.5	-19.5	-17.5	0.094	0.100	0.120	0.108	0.115	0.107	0.011
27.634	-16.7	-17.5	-17.5	-19.5	-17.6	0.094	0.100	0.120	0.108	0.015	0.087	0.041
27.693	-16.7	-17.5	-17.5	-19.5	-17.5	0.094	0.100	0.120	0.108	0.115	0.107	0.011
27.752	-16.8	-17.6	-17.5	-19.5	-17.6	-0.006	0.000	0.120	0.108	0.015	0.047	0.061
27.811	-16.9	-17.7	-17.7	-19.7	-17.7	-0.106	-0.100	-0.080	-0.092	-0.085	-0.093	0.011
27.870	-17	-17.8	-17.9	-19.9	-17.9	-0.206	-0.200	-0.280	-0.292	-0.285	-0.253	0.045
27.929	-17.1	-18	-17.9	-19.9	-17.9	-0.306	-0.400	-0.280	-0.292	-0.285	-0.313	0.050
27.988	-17.2	-18	-17.9	-20	-18	-0.406	-0.400	-0.280	-0.392	-0.385	-0.373	0.052
28.047	-17.3	-18.1	-18.1	-20.1	-18.1	-0.506	-0.500	-0.480	-0.492	-0.485	-0.493	0.011
28.105	-17.3	-18.1	-18.2	-20.2	-18.2	-0.506	-0.500	-0.580	-0.592	-0.585	-0.553	0.045
28.164	-17.4	-18.2	-18.2	-20.2	-18.3	-0.606	-0.600	-0.580	-0.592	-0.685	-0.613	0.041
28.223	-17.5	-18.3	-18.2	-20.3	-18.3	-0.706	-0.700	-0.580	-0.692	-0.685	-0.673	0.052
28.282	-17.6	-18.4	-18.4	-20.4	-18.4	-0.806	-0.800	-0.780	-0.792	-0.785	-0.793	0.011
28.341	-17.7	-18.5	-18.4	-20.5	-18.4	-0.906	-0.900	-0.780	-0.892	-0.785	-0.853	0.064
28.400	-17.7	-18.5	-18.5	-20.5	-18.5	-0.906	-0.900	-0.880	-0.892	-0.885	-0.893	0.011
28.459	-17.7	-18.5	-18.5	-20.5	-18.5	-0.906	-0.900	-0.880	-0.892	-0.885	-0.893	0.011
28.518	-17.8	-18.5	-18.5	-20.5	-18.5	-1.006	-0.900	-0.880	-0.892	-0.885	-0.913	0.053
28.577	-17.9	-18.6	-18.6	-20.6	-18.6	-1.106	-1.000	-0.980	-0.992	-0.985	-1.013	0.053
28.636	-17.8	-18.6	-18.7	-20.6	-18.6	-1.006	-1.000	-1.080	-0.992	-0.985	-1.013	0.039
28.695	-17.8	-18.6	-18.7	-20.7	-18.6	-1.006	-1.000	-1.080	-1.092	-0.985	-1.033	0.050
28.754	-17.8	-18.6	-18.7	-20.7	-18.6	-1.006	-1.000	-1.080	-1.092	-0.985	-1.033	0.050
28.813	-17.9	-18.6	-18.7	-20.7	-18.7	-1.106	-1.000	-1.080	-1.092	-1.085	-1.073	0.042
28.872	-18	-18.7	-18.8	-20.8	-18.8	-1.206	-1.100	-1.180	-1.192	-1.185	-1.173	0.042
28.931	-18	-18.8	-18.8	-20.8	-18.8	-1.206	-1.200	-1.180	-1.192	-1.185	-1.193	0.011
28.990	-18	-18.9	-18.8	-20.8	-18.8	-1.206	-1.300	-1.180	-1.192	-1.185	-1.213	0.050
29.049	-18.1	-19	-18.9	-20.9	-18.9	-1.306	-1.400	-1.280	-1.292	-1.285	-1.313	0.050
29.107	-18.3	-19.1	-19	-21	-19	-1.506	-1.500	-1.380	-1.392	-1.385	-1.433	0.064
29.166	-18.3	-19.1	-19	-21.1	-19.1	-1.506	-1.500	-1.380	-1.492	-1.485	-1.473	0.052
29.225	-18.4	-19.2	-19.1	-21.1	-19.1	-1.606	-1.600	-1.480	-1.492	-1.485	-1.533	0.064
29.284	-18.4	-19.2	-19.2	-21.2	-19.2	-1.606	-1.600	-1.580	-1.592	-1.585	-1.593	0.011
29.343	-18.5	-19.2	-19.3	-21.3	-19.3	-1.706	-1.600	-1.680	-1.692	-1.685	-1.673	0.042
29.402	-18.6	-19.4	-19.5	-21.4	-19.4	-1.806	-1.800	-1.880	-1.792	-1.785	-1.813	0.039
29.461	-18.7	-19.5	-19.6	-21.5	-19.5	-1.906	-1.900	-1.980	-1.892	-1.885	-1.913	0.039
29.520	-18.8	-19.6	-19.6	-21.6	-19.6	-2.006	-2.000	-1.980	-1.992	-1.985	-1.993	0.011
29.579	-18.9	-19.6	-19.7	-21.7	-19.7	-2.106	-2.000	-2.080	-2.092	-2.085	-2.073	0.042
29.638	-19	-19.7	-19.8	-21.8	-19.8	-2.206	-2.100	-2.180	-2.192	-2.185	-2.173	0.042
29.697	-19.1	-19.9	-19.9	-21.9	-19.9	-2.306	-2.300	-2.280	-2.292	-2.285	-2.293	0.011
29.756	-19.2	-20	-20	-22	-20	-2.406	-2.400	-2.380	-2.392	-2.385	-2.393	0.011
29.815	-19.4	-20.1	-20.1	-22.1	-20.1	-2.606	-2.500	-2.480	-2.492	-2.485	-2.513	0.053
29.874	-19.5	-20.1	-20.2	-22.2	-20.2	-2.706	-2.500	-2.580	-2.592	-2.585	-2.593	0.073
29.933	-19.5	-20.2	-20.3	-22.3	-20.3	-2.706	-2.600	-2.680	-2.692	-2.685	-2.673	0.042
29.992	-19.6	-20.3	-20.5	-22.4	-20.5	-2.806	-2.700	-2.880	-2.792	-2.885	-2.813	0.076
30.050	-19.7	-20.4	-20.6	-22.5	-20.5	-2.906	-2.800	-2.980	-2.892	-2.885	-2.893	0.064
30.109	-19.7	-20.5	-20.6	-22.6	-20.6	-2.906	-2.900	-2.980	-2.992	-2.985	-2.953	0.045
30.168	-19.8	-20.5	-20.7	-22.6	-20.7	-3.006	-2.900	-3.080	-2.992	-3.085	-3.013	0.076
30.227	-19.9	-20.6	-20.7	-22.7	-20.7	-3.106	-3.000	-3.080	-3.092	-3.085	-3.073	0.042
30.286	-20	-20.8	-20.8	-22.8	-20.8	-3.206	-3.200	-3.180	-3.192	-3.185	-3.193	0.011
30.345	-20.1	-20.8	-20.9	-22.8	-20.9	-3.306	-3.200	-3.280	-3.192	-3.285	-3.253	0.053
30.404	-20.1	-20.8	-20.9	-22.9	-20.9	-3.306	-3.200	-3.280	-3.292	-3.285	-3.273	0.042
30.463	-20.2	-20.9	-21	-22.9	-20.9	-3.406	-3.300	-3.380	-3.292	-3.285	-3.333	0.056
30.522	-20.3	-21	-21	-23	-20.9	-3.506	-3.400	-3.380	-3.392	-3.285	-3.393	0.079
30.581	-20.4	-21.1	-21.1	-23.1	-21	-3.606	-3.500	-3.480	-3.492	-3.385	-3.493	0.079
30.640	-20.4	-21.2	-21.2	-23.2	-21.1	-3.606	-3.600	-3.580	-3.592	-3.485	-3.573	0.050
30.699	-20.5	-21.2	-21.2	-23.2	-21.2	-3.706	-3.600	-3.580	-3.592	-3.585	-3.613	0.053
30.758	-20.5	-21.2	-21.2	-23.2	-21.2	-3.706	-3.600	-3.580	-3.592	-3.585	-3.613	0.053
30.817	-20.6	-21.3	-21.3	-23.3	-21.3	-3.806	-3.700	-3.680	-3.692	-3.685	-3.713	0.053
30.876	-20.6	-21.4	-21.3	-23.3	-21.3	-3.806	-3.800	-3.680	-3.692	-3.685	-3.733	0.064
30.935	-20.6	-21.4	-21.4	-23.3	-21.3	-3.806	-3.800	-3.780	-3.692	-3.685	-3.753	0.059

30.994	-20.7	-21.4	-21.4	-23.3	-21.4	-3.906	-3.800	-3.780	-3.692	-3.785	-3.793	0.076
31.052	-20.7	-21.4	-21.4	-23.3	-21.5	-3.906	-3.800	-3.780	-3.692	-3.885	-3.813	0.086
31.111	-20.7	-21.4	-21.4	-23.3	-21.5	-3.906	-3.800	-3.780	-3.692	-3.885	-3.813	0.086
31.170	-20.7	-21.4	-21.4	-23.3	-21.4	-3.906	-3.800	-3.780	-3.692	-3.785	-3.793	0.076
31.229	-20.6	-21.4	-21.4	-23.3	-21.4	-3.806	-3.800	-3.780	-3.692	-3.785	-3.773	0.046
31.288	-20.7	-21.4	-21.4	-23.4	-21.4	-3.906	-3.800	-3.780	-3.792	-3.785	-3.813	0.053
31.347	-20.7	-21.4	-21.4	-23.4	-21.5	-3.906	-3.800	-3.780	-3.792	-3.885	-3.833	0.058
31.406	-20.7	-21.4	-21.5	-23.5	-21.5	-3.906	-3.800	-3.880	-3.892	-3.885	-3.873	0.042
31.465	-20.7	-21.4	-21.5	-23.5	-21.5	-3.906	-3.800	-3.880	-3.892	-3.885	-3.873	0.042
31.524	-20.8	-21.5	-21.5	-23.5	-21.5	-4.006	-3.900	-3.880	-3.892	-3.885	-3.913	0.053
31.583	-20.9	-21.6	-21.6	-23.5	-21.5	-4.106	-4.000	-3.980	-3.892	-3.885	-3.973	0.091
31.642	-20.9	-21.6	-21.6	-23.6	-21.6	-4.106	-4.000	-3.980	-3.992	-3.985	-4.013	0.053
31.701	-20.9	-21.6	-21.7	-23.7	-21.7	-4.106	-4.000	-4.080	-4.092	-4.085	-4.073	0.042
31.760	-21	-21.7	-21.8	-23.8	-21.8	-4.206	-4.100	-4.180	-4.192	-4.185	-4.173	0.042
31.819	-21	-21.8	-21.8	-23.8	-21.8	-4.206	-4.200	-4.180	-4.192	-4.185	-4.193	0.011
31.878	-21	-21.8	-21.8	-23.8	-21.8	-4.206	-4.200	-4.180	-4.192	-4.185	-4.193	0.011
31.937	-21	-21.8	-21.8	-23.8	-21.8	-4.206	-4.200	-4.180	-4.192	-4.185	-4.193	0.011
31.996	-21.1	-21.8	-21.9	-23.8	-21.9	-4.306	-4.200	-4.280	-4.192	-4.285	-4.253	0.053
32.054	-21.1	-21.8	-21.9	-23.9	-21.9	-4.306	-4.200	-4.280	-4.292	-4.285	-4.273	0.042
32.113	-21.2	-21.9	-21.9	-23.9	-22	-4.406	-4.300	-4.280	-4.292	-4.385	-4.333	0.058
32.172	-21.3	-21.9	-22	-24	-22	-4.506	-4.300	-4.380	-4.392	-4.385	-4.393	0.073
32.231	-21.3	-22	-22.1	-24	-22.1	-4.506	-4.400	-4.480	-4.392	-4.485	-4.453	0.053
32.290	-21.3	-22	-22.2	-24.1	-22.1	-4.506	-4.400	-4.580	-4.492	-4.485	-4.493	0.064
32.349	-21.4	-22.2	-22.2	-24.2	-22.3	-4.606	-4.600	-4.580	-4.592	-4.685	-4.613	0.041
32.408	-21.6	-22.3	-22.4	-24.4	-22.4	-4.806	-4.700	-4.780	-4.792	-4.785	-4.773	0.042
32.467	-21.7	-22.4	-22.5	-24.4	-22.5	-4.906	-4.800	-4.880	-4.792	-4.885	-4.853	0.053
32.526	-21.8	-22.5	-22.5	-24.5	-22.5	-5.006	-4.900	-4.880	-4.892	-4.885	-4.913	0.053
32.585	-21.8	-22.6	-22.6	-24.6	-22.6	-5.006	-5.000	-4.980	-4.992	-4.985	-4.993	0.011
32.644	-21.7	-22.5	-22.4	-24.4	-22.5	-4.906	-4.900	-4.780	-4.792	-4.885	-4.853	0.061
32.703	-21.7	-22.3	-22.3	-24.3	-22.3	-4.906	-4.700	-4.680	-4.692	-4.685	-4.733	0.097
32.762	-21.3	-22	-22	-24	-22	-4.506	-4.400	-4.380	-4.392	-4.385	-4.413	0.053
32.821	-20.8	-21.5	-21.6	-23.5	-21.6	-4.006	-3.900	-3.980	-3.892	-3.985	-3.953	0.053
32.880	-20.1	-20.9	-20.9	-22.8	-20.9	-3.306	-3.300	-3.280	-3.192	-3.285	-3.273	0.046
32.939	-19.1	-19.9	-20	-21.9	-20	-2.306	-2.300	-2.380	-2.292	-2.385	-2.333	0.046
32.997	-17.9	-18.7	-18.7	-20.6	-18.7	-1.106	-1.100	-1.080	-0.992	-1.085	-1.073	0.046
33.056	-16.2	-17.1	-17.1	-18.9	-17.1	0.594	0.500	0.520	0.708	0.515	0.567	0.087
33.115	-14.2	-15.1	-15.1	-16.9	-15	2.594	2.500	2.520	2.708	2.615	2.587	0.083
33.174	-12.1	-13	-13.1	-14.9	-12.8	4.694	4.600	4.520	4.708	4.815	4.667	0.113
33.233	-13.6	-14.5	-14.5	-16.3	-14.3	3.194	3.100	3.120	3.308	3.315	3.207	0.102
Average	**-16.79417**	**-17.59958**	**-17.61958**	**-19.60792**	**-17.61521**						**Mean**	**0.049**

Appendix E
Monte Carlo Simulation

This appendix contains the Matlab programme listing used for the Monte Carlo Simulation (MCS) and the output results used to determine the optimum number of MCS trials. The results from the this process were summarised in Table 8.6 which showed quite clearly that using greater than 1000 trials produces robust estimates of the mean and standard deviation of the measurement process.

Figures E1 to E6 summarise the results and resulting distributions for 500, 1000, 2000, 10000, 20000, 300000 trials.

The Matlab program listing follows the figures is annotated for clarity.

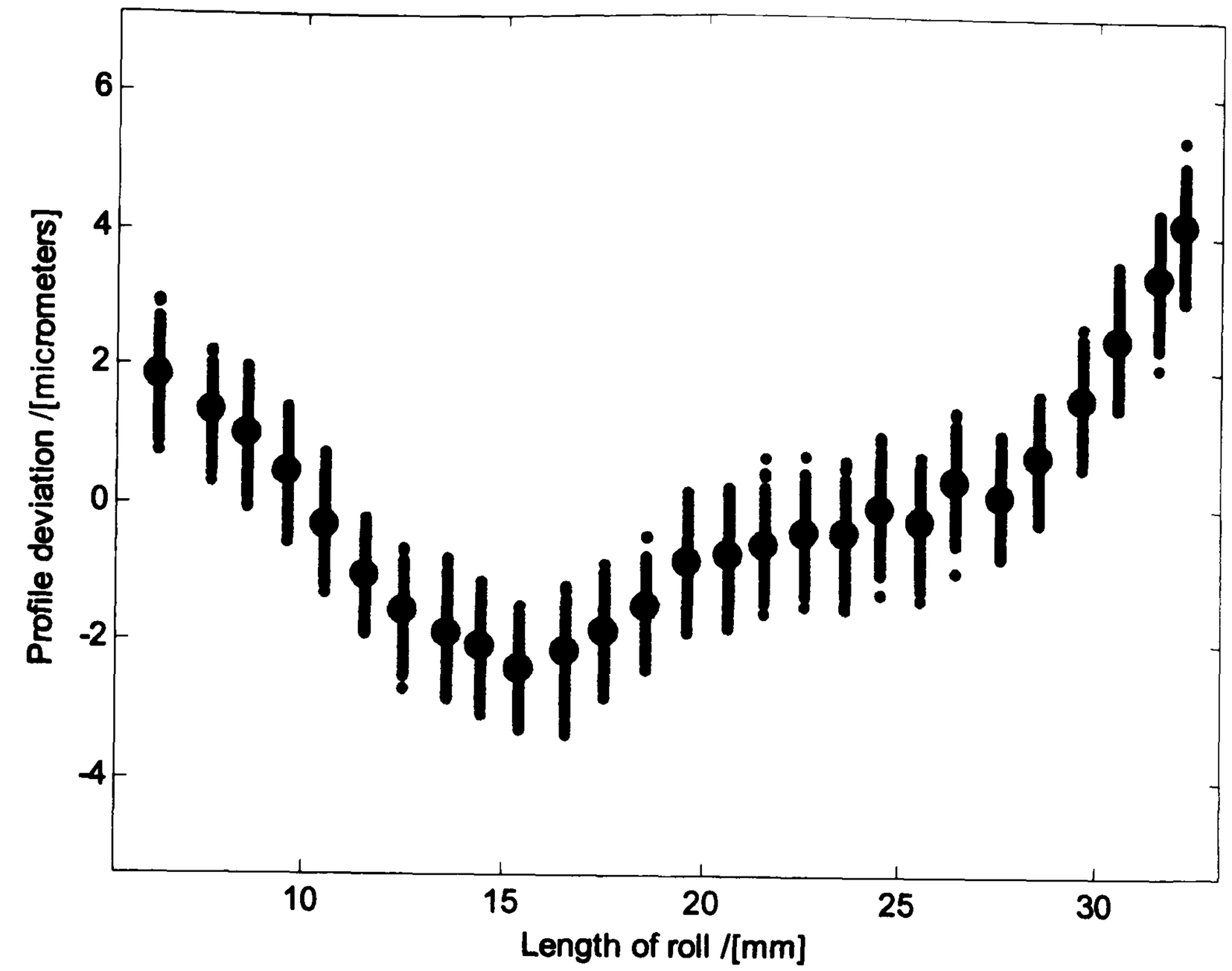

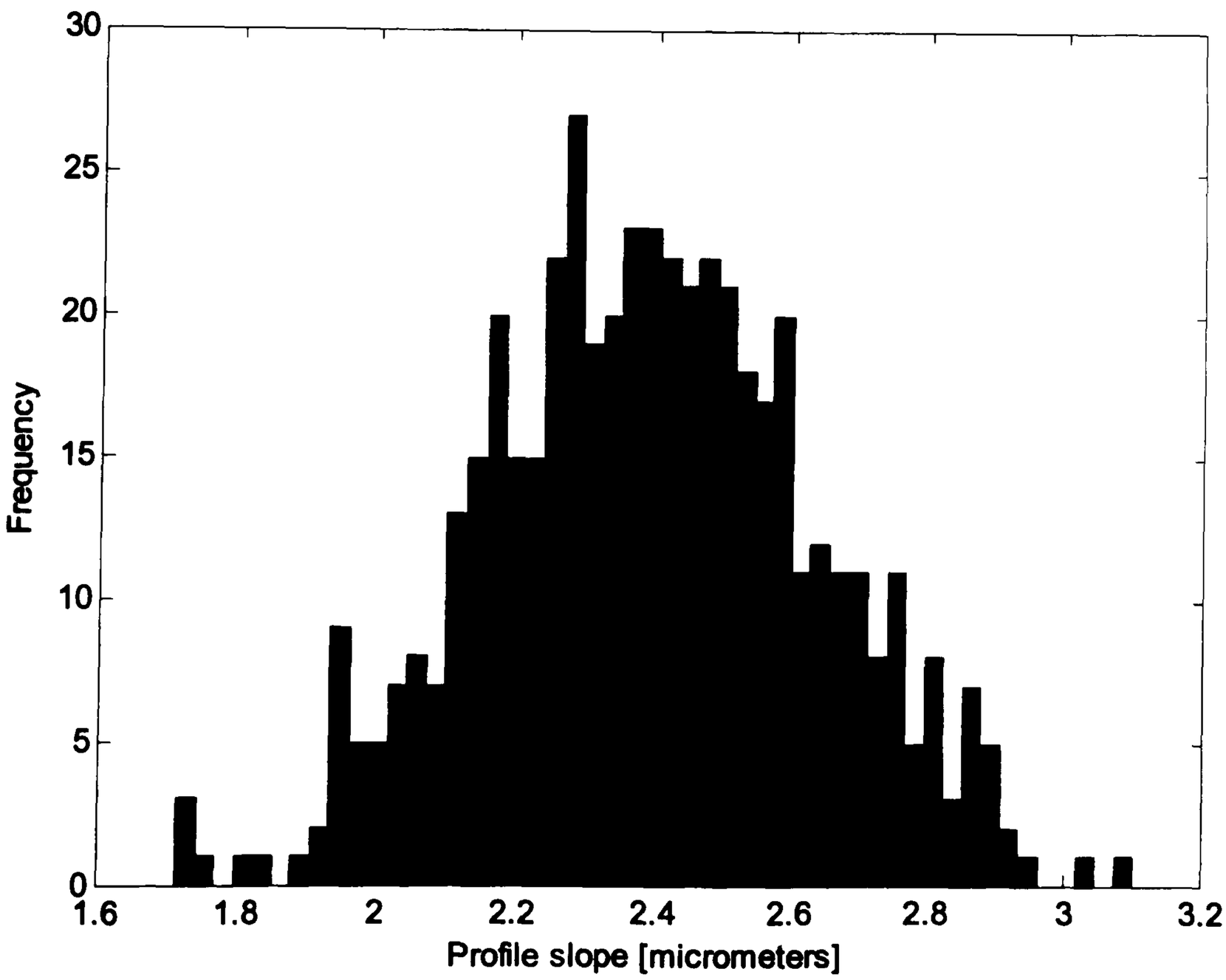

Mean	Min	Max	SD	Range	2.5%	97.5%
2.3963	1.7130	3.0999	0.2401	1.3869	1.9382	2.8707

Figure E1Number of trials, M = 500

(100mm profile master NGML RF data deviations-unfiltered)

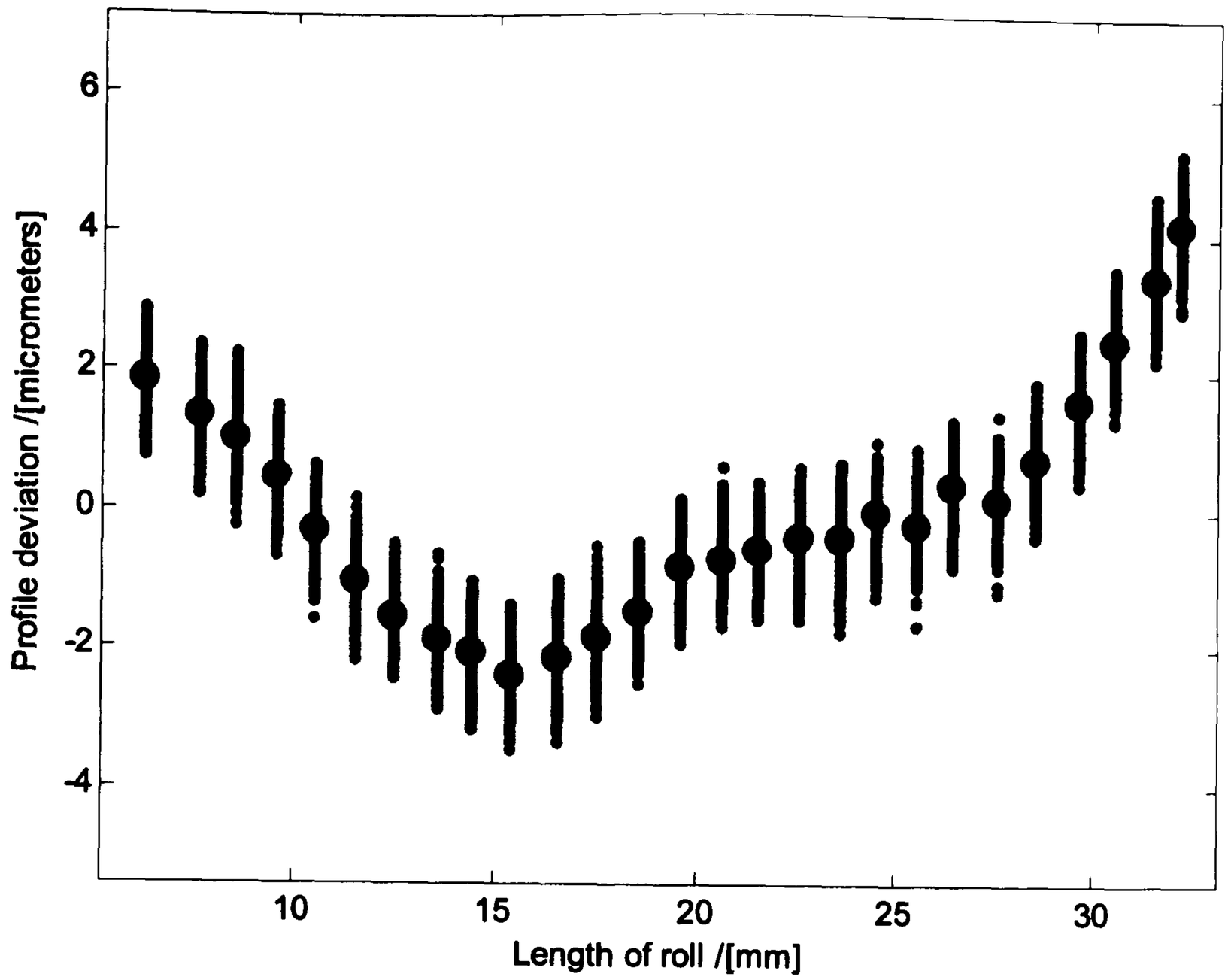

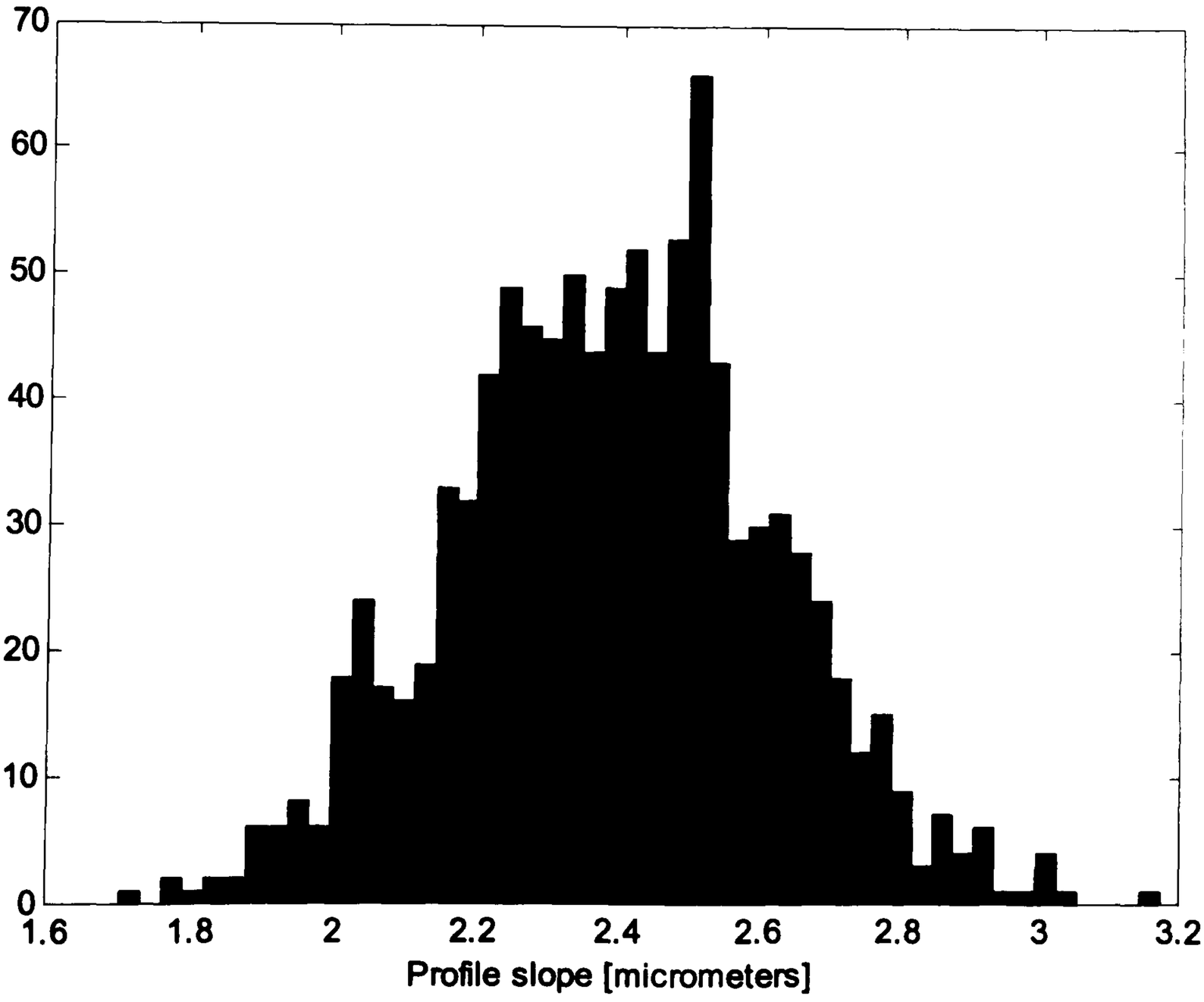

Mean	Min	Max	SD	Range	2.5%	97.5%
2.3929	1.7002	3.1730	0.2249	1.4728	1.9474	2.8503

Figure E2 Number of trials, M = 1000

(100mm profile master NGML RF data deviations-unfiltered)

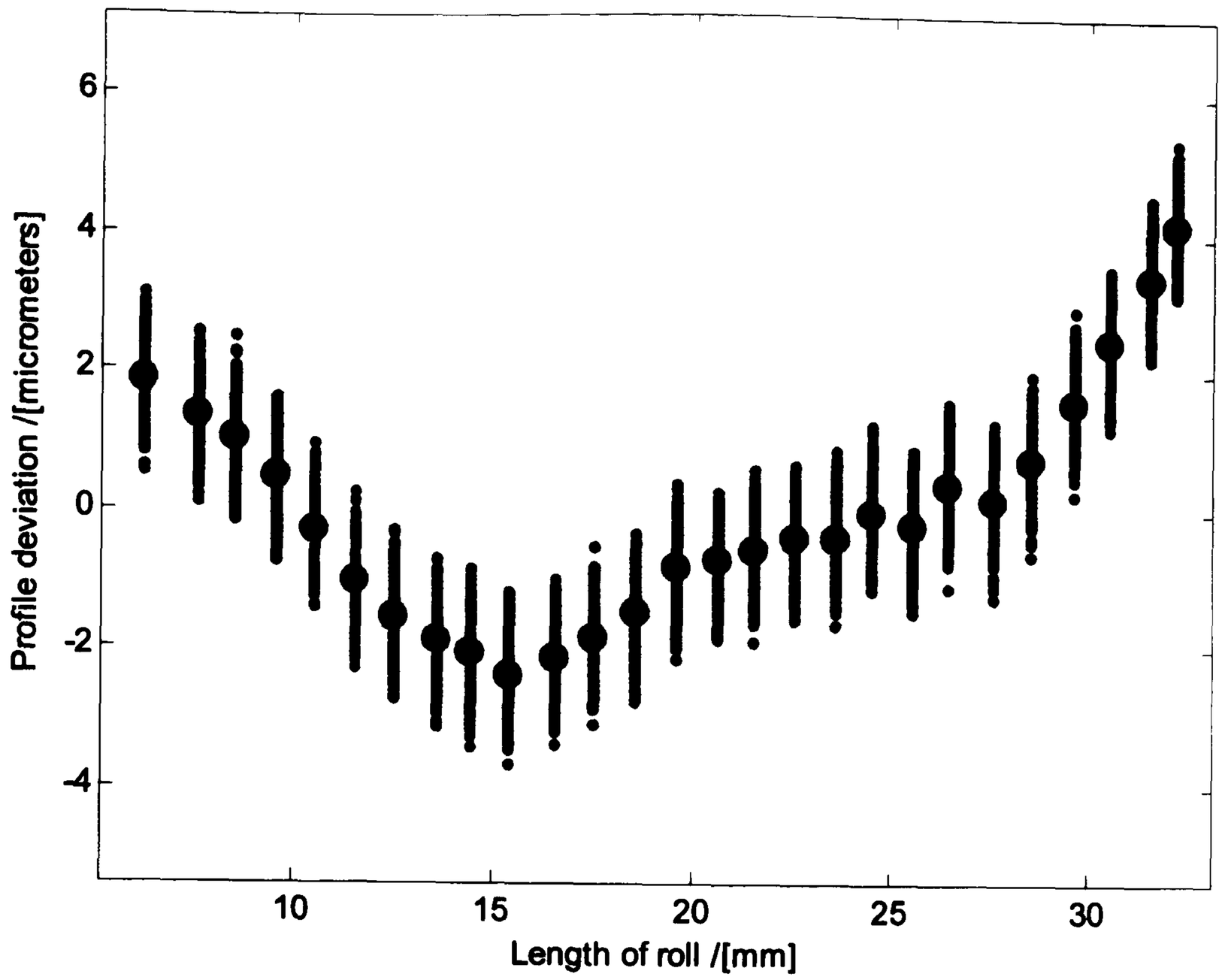

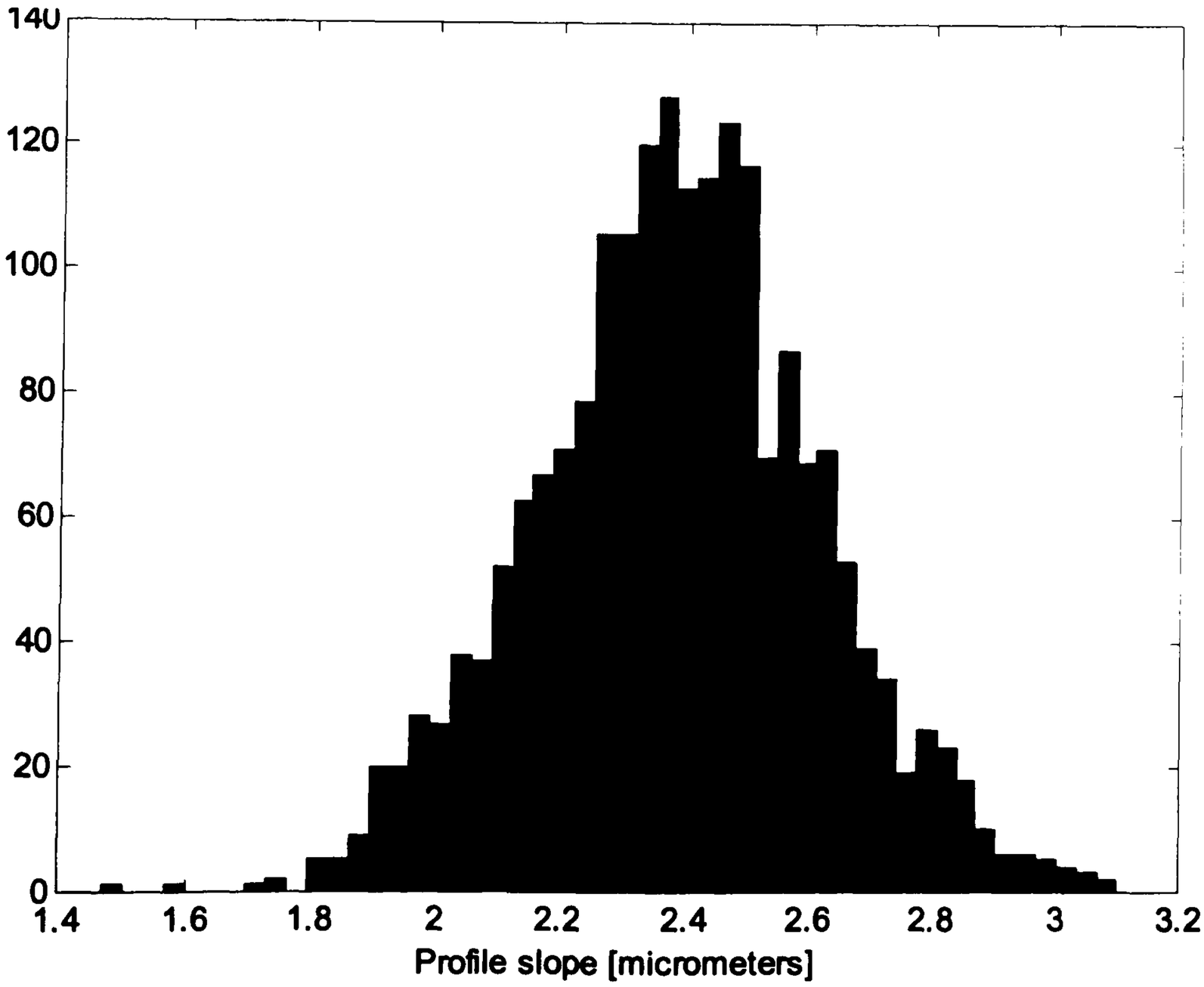

Mean	Min	Max	SD	Range	2.5%	97.5%
2.3874	1.4702	3.1000	0.2270	1.6298	1.9336	2.8493

Figure E3 Number of trials, M = 2000

(100mm profile master NGML RF data deviations-unfiltered)

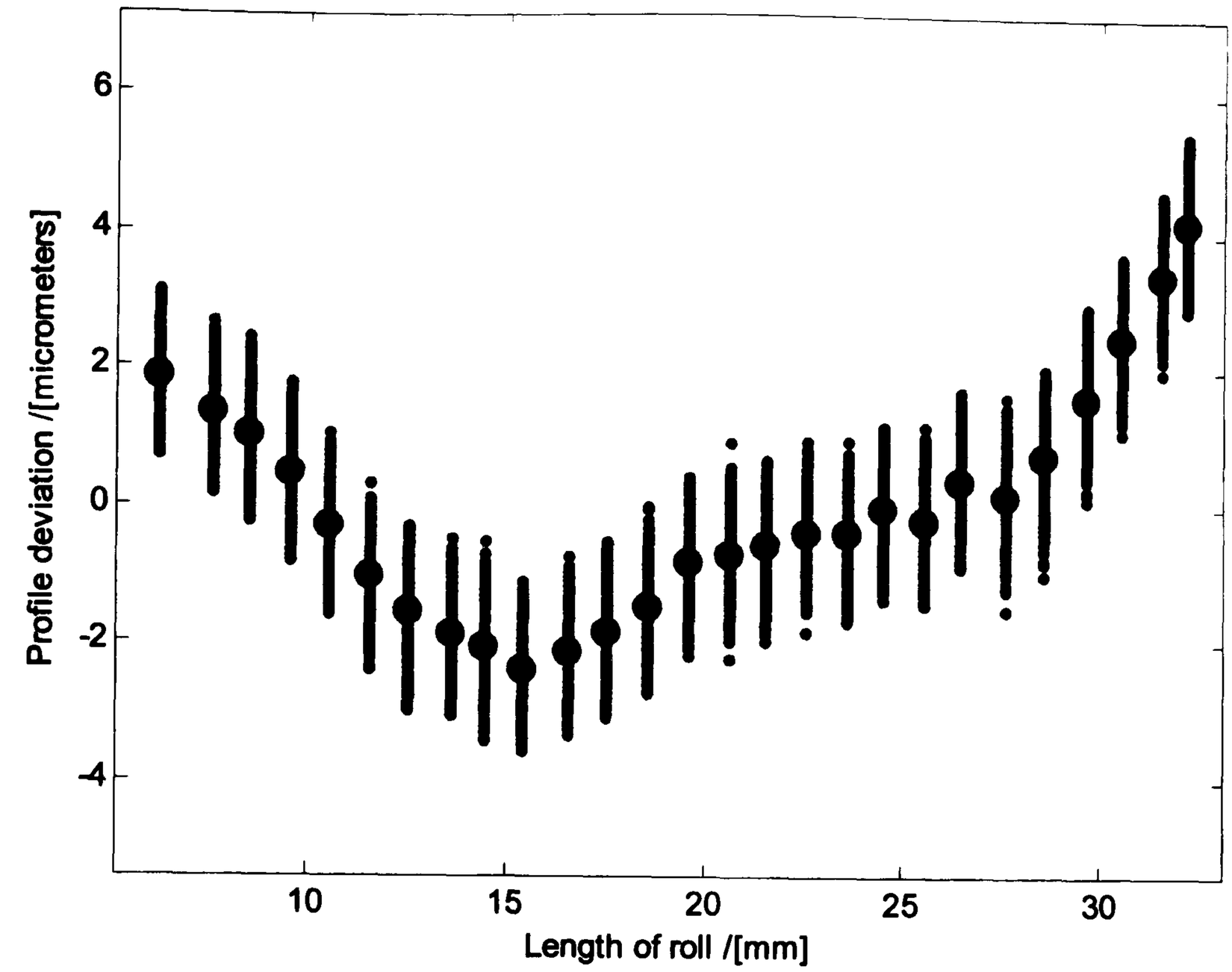

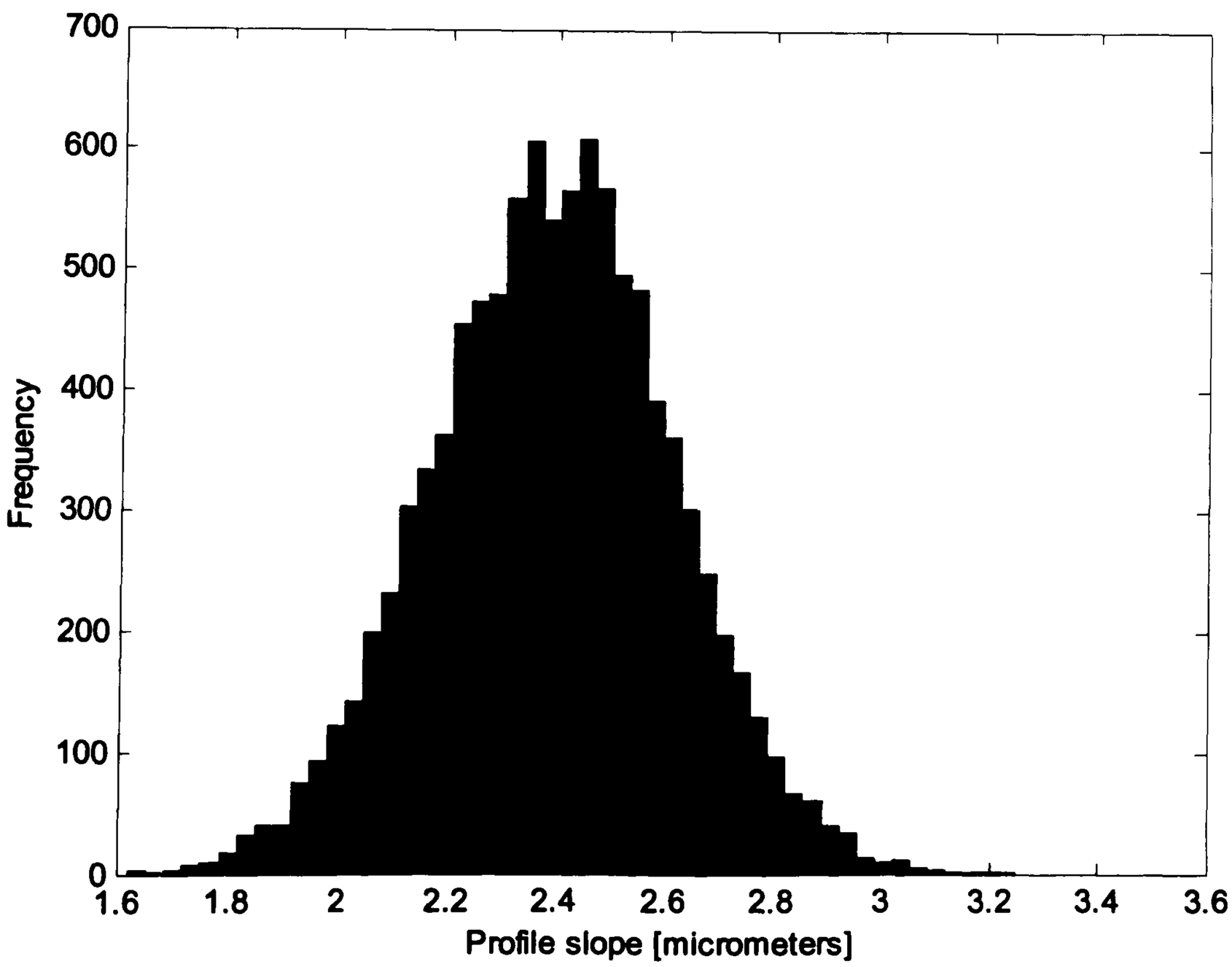

Mean	Min	Max	SD	Range	2.5%	97.5%
2.3920	1.6218	3.2481	0.2211	1.6263	1.9547	2.8251

Figure E4Number of trials, M = 10000

(100mm profile master NGML RF data deviations-unfiltered)

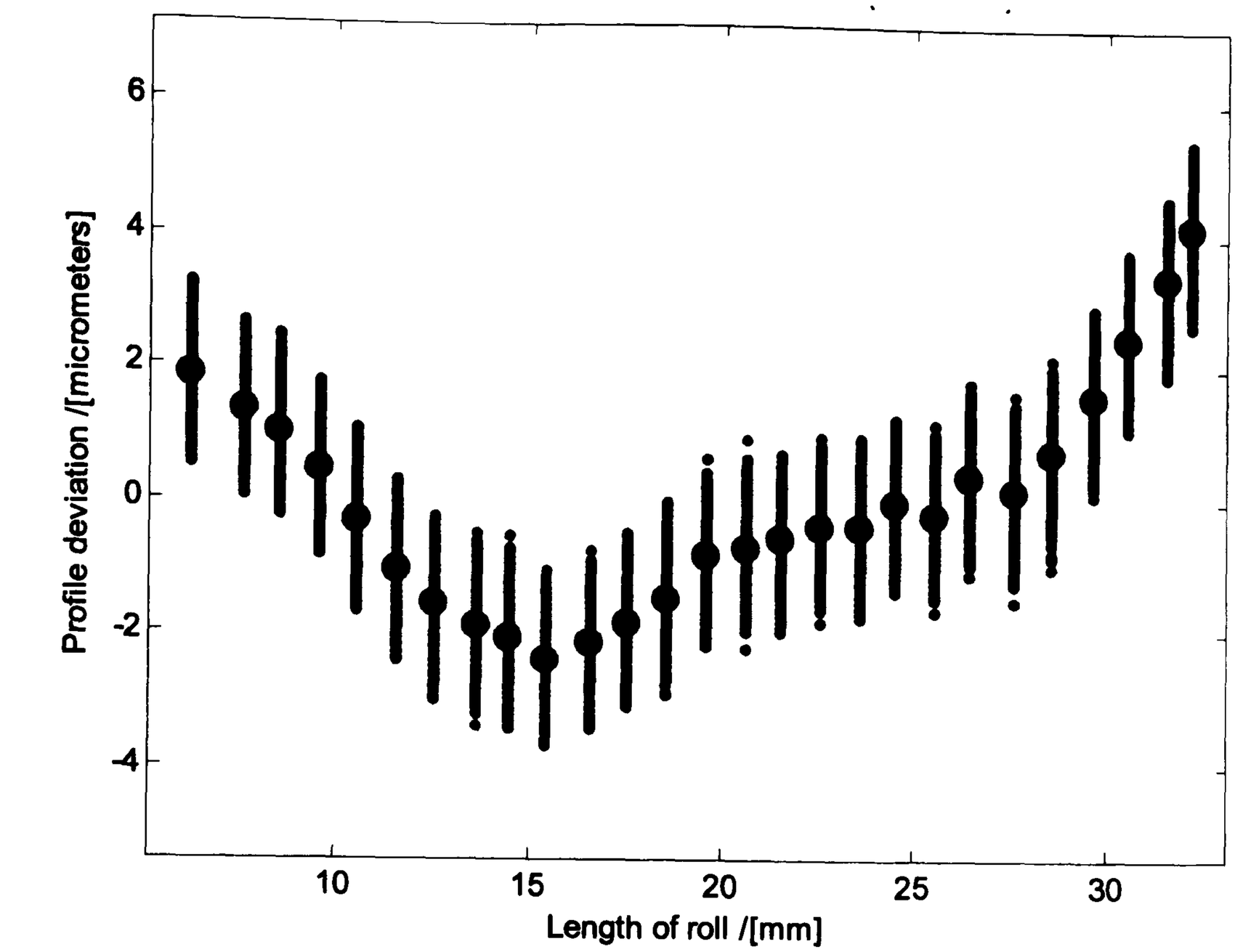

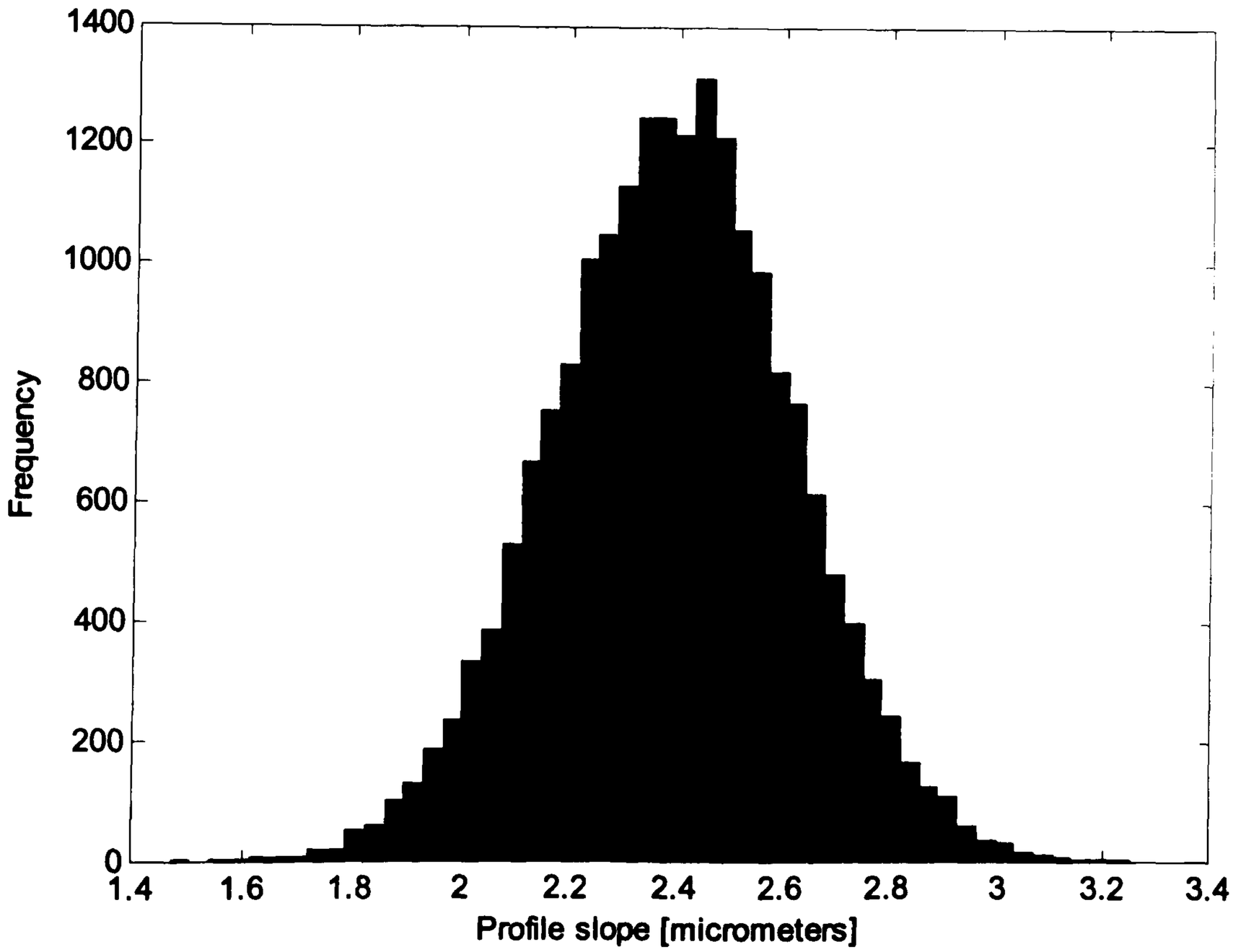

Mean	Min	Max	SD	Range	2.5%	97.5%
2.3931	1.4702	3.2481	0.2241	1.7780	1.9536	2.8343

Figure E5 Number of trials, M = 20000

(100mm profile master NGML RF data deviations-unfiltered)

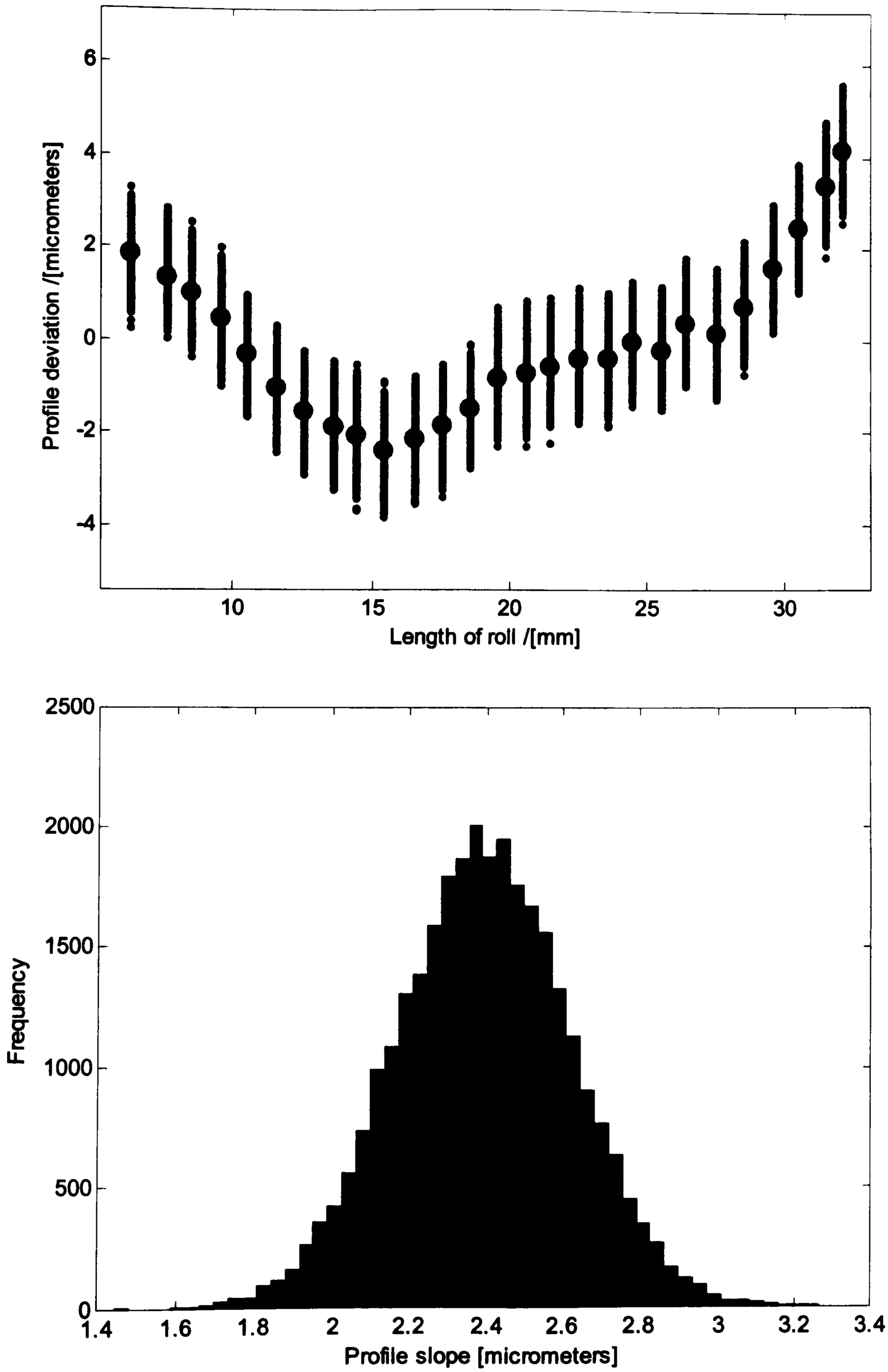

Mean	Min	Max	SD	Range	2.5%	97.5%
2.3938	1.4424	3.2660	0.2245	1.8237	1.9528	2.8333

Figure E6 Number of trials, M = 30000

(100mm profile master NGML RF data deviations-unfiltered)

Matlab program listing

```
% ------------------------------------------------------------------------
---
% MCS slope parameter uncertainty
%
% Rob Frazer
% NGML
% Design Unit
%
% Developed :
%
% Software reference: Peter Harris, NPL SSfM Constrained slope example
% 16-8-2006
% ------------------------------------------------------------------------
---
% data source:
% ------------------------------------------------------------------------
---
% Nominal data points:
% x- length of roll [mm]
%------------------------------------------------------------------------
---
%
%100mm profile master LF-PTB NGML data points
%----------------------------------------
%  x = [6.2576 6.9695 7.6162 8.4900 9.5359 10.4715 11.5392 12.5148 ...
%       13.5938 14.5910 15.5279 16.5522 17.5159 18.5564 19.5445 20.5957
...
%       21.4889 22.5584 23.5744 24.4558 25.4932 26.5741 27.5288 28.4541
...
%        29.5852 30.5248 31.5115 32.0997]';
%------------------------------------------------------------------------
---
%100mm profile master RF-PTB NGML data points
%----------------------------------------
  x = [6.2552 7.6092 8.4913 9.5305 10.4702 11.5389 12.5143 13.5904 ...
       14.4272 15.3730 16.5496 17.5106 18.5512 19.5395 20.5913 21.4837
...
       22.5521 23.5734 24.4524 25.4882 26.3911 27.5248 28.5285 29.5833
...
       30.5183 31.5044 32.1688]';
%------------------------------------------------------------------------
---
%
%200mm profile master LF-PTB NGML data points
%----------------------------------------
%  x = [13.000 13.500 14.503 15.045 15.962 17.006 18.047 18.966 20.051
...
%       21.135 22.136 23.051 24.052 25.051 26.090 27.053 28.012 29.014
...
%       30.015 31.098 32.016 33.060 34.103 35.106 36.066 37.109 38.027
...
%       39.069 40.027 41.028 42.077 43.031 44.075 45.034 46.036 47.079
...
%       48.079 49.039 50.165 51.000 51.960]';
%------------------------------------------------------------------------
---
%
```

```
%200 profile master RF-PTB NGML data points
%-----------------------------------------
%  x = [13.005 13.500 14.077 15.109 16.017 17.130 18.038 19.029 20.060
...
%      21.133 22.041 23.031 24.021 25.011 26.084 27.033 28.065 29.137
...
%      30.169 31.159 32.108 33.098 34.047 35.079 36.110 37.142 38.008
...
%      39.081 40.071 41.020 42.010 43.083 44.073 45.104 46.053 47.003
...
%      48.117 49.024 50.015 51.046 52.037]';
%
%
%-------------------------------------------------------------------
---
% yref- mean error value from measured data [micometers]+ is plus metal
%-------------------------------------------------------------------
---
%name = ('100mm PTB LF data deviation values')
%-----------------------------------------
%yref = [-0.579 -0.177 0.104 0.087 -0.230 -0.528 -0.565 -0.852 -1.159
...
%     -1.556 -1.883 -1.880 -1.578 -1.175 -1.022 -0.609 -0.576 -0.137 ...
%     0.600 0.822 0.495 -0.202 -0.399 0.573 1.697 2.969 3.482 4.004]';
%
%name = ('100mm NGML LF data deviation (unfiltered)')
%-----------------------------------
%yref = [-0.783 -0.303 -0.023 -0.183 -0.483 -0.763 -0.823 -1.053 -1.433
...
%     -1.573 -2.023 -1.913 -1.723 -1.223 -0.893 -0.543 -0.343 0.317 ...
%     0.577 0.697 0.477 -0.063 -0.243 0.837 2.017 3.337 3.857 4.277]';
%
%name = ('100mm LF Difference between NGML-PTB data (NGML unfiltered)')
%-------------------------------------------
% yref = [-0.204 -0.126 -0.128 -0.270 -0.253 -0.236 -0.259 -0.201 -0.275
...
%     -0.017 -0.140 -0.033 -0.146 -0.049 0.129 0.066 0.233 0.180 ...
%     -0.023 -0.125 -0.018 0.139 0.156 0.263 0.320 0.368 0.375 0.273]';
%
%-------------------------------------------------------------------
---
%
%name = ('100mm PTB RF data deviations')
%-----------------------------
% yref = [1.763 1.293 1.033 0.563 -0.177 -0.907 -1.467 -1.777 -1.917 ...
%      -2.107 -2.087 -1.757 -1.197 -0.787 -0.647 -0.567 -0.357 -0.157 ...
%      0.023 0.173 0.213 0.143 0.583 1.253 2.013 3.083 3.783]';
%
name = ('100mm NGML RF data deviations (unfiltered)')
%-------------------------------------------
 yref = [1.851 1.351 1.011 0.471 -0.309 -1.039 -1.549 -1.889 -2.069 ...
     -2.389 -2.129 -1.829 -1.489 -0.809 -0.689 -0.569 -0.369 -0.369 ...
     -0.009 -0.189 0.411 0.171 0.751 1.611 2.471 3.411 4.171]';
%
%  name = ('100mm RF Difference between NGML-PTB data')
%-------------------------------------------
% yref = [0.089 0.059 -0.021 -0.091 -0.131 -0.131 -0.081 -0.111 -0.151
...
%      -0.281 -0.041 -0.071 -0.291 -0.021 -0.041 -0.001 -0.011 -0.211 ...
%      -0.031 -0.361 0.199 0.029 0.169 0.359 0.459 0.329 0.389]';
%
```

```
%  name = ('200mm PTB LF data deviations')
%-----------------------------------------
% yref = [0.16 0.21 -0.76 -0.72 -0.54 -0.75 -0.49 -0.99 -0.99 -0.90 ...
%     -0.65 0.28 0.37 1.13 1.26 1.21 1.61 1.44 1.19 1.74 1.58 1.16 ...
%     0.66 0.25 -0.08 -0.33 -0.28 -0.36 0.27 0.73 0.53 -0.14 -0.55 ...
%     -0.47 -0.80 -0.80 -0.87 -1.04 -0.78 -1.03 -1.41]';
%-------------------------------------------------------------------
---
%
%  name = ('200mm NGML LF data deviations')
%-----------------------------------------
% yref = [-0.70 -0.78 -0.58 -0.44 -0.44 -0.60 -0.60 -0.92 -1.22 -1.02
...
%     -0.54 -0.04 0.52 0.84 1.00 1.18 0.84 1.38 1.31 1.50 1.50 1.16 ...
%     0.60 0.20 -0.14 -0.30 -0.28 -0.16 -0.24 0.54 0.64 0.34 -0.12 ...
%     -0.32 -0.44 -0.38 -0.56 -0.86 -0.62 -0.62 -0.74]';
%
%  name = ('200mm LF difference between NGML-PTB data')
%-----------------------------------------------------
% yref = [0.86 0.99 -0.18 -0.28 -0.10 -0.15 0.11 -0.07 0.23 0.12 -0.11
...
%    0.32 -0.15 0.29 0.26 0.03 0.77 0.06 -0.12 0.24 0.08 0.00 0.06 ...
%    0.05 0.06 -0.03 0.00 -0.20 0.51 0.19 -0.11 -0.48 -0.43 -0.15 ...
%    -0.36 -0.42 -0.31 -0.18 -0.16 -0.41 -0.67]';
%
% name = ('200mm RF PTB data deviations')
%----------------------------------------
% yref = [0.18 -0.16 -0.80 -0.80 -0.97 -1.44 -1.82 -1.70 -1.67 -1.29 ...
%     -0.54 -0.21 0.38 0.84 0.66 0.74 0.70 0.56 0.27 0.55 0.55 0.50 ...
%     -0.18 0.11 -0.06 -0.10 -0.11 0.14 0.64 0.97 0.96 0.91 0.62 0.87
...
%     0.65 0.10 -0.49 -0.12 -0.04 0.75 -0.09]';
%
% name = ('200mm RF NGML data deviations')
%----------------------------------------
% yref = [-0.76 -1.02 -1.02 -0.84 -1.26 -1.60 -1.70 -1.65 -1.40 -1.34
...
%     -0.40 0.10 0.68 0.94 1.08 1.02 0.98 0.92 0.86 0.90 0.84 0.62 ...
%     0.22 0.03 -0.08 -0.10 -0.06 0.16 0.52 0.88 0.96 0.86 0.74 0.62 ...
%     0.44 0.06 -0.40 -0.57 -0.41 -0.08 0.12]';
%
% name = ('200mm RF difference between NGML and PTB data')
%-------------------------------------------------------
% yref = [0.94 0.86 0.22 0.04 0.29 0.16 -0.12 -0.05 -0.27 0.05 -0.14 ...
%     -0.31 -0.30 -0.10 -0.42 -0.28 -0.28 -0.36 -0.59 -0.35 -0.29 ...
%     -0.12 -0.40 0.08 0.02 0.00 -0.05 -0.02 0.12 0.09 0.00 0.05 ...
%     -0.12 0.25 0.21 0.04 -0.09 0.45 0.37 0.83 -0.21]';
%
%
%-------------------------------------------------------------------
---
% Add reference values to figure 1.
  figure(1)
  hold off
% reset default figure values
  plot(x, yref, 'o', 'LineWidth', 3)
% the 'o' defines the point as a circle
%  figure(gcf)
%
% Standard deviation of yref in [micrometers]
  uy = 0.35;
```

```
%
% Number of Monte Carlo trials
  M = 30000
%  disp(M);
%
% Array to hold gradient values
  slope = zeros(1,M);
%
% Loop over Monte Carlo trials
  for k = 1 : M
%
%   Generate synthesised data set with randn-normal distribution
    e = uy*randn(size(yref));
    y = yref + e;
%
%   Fit straight line
    A = [ones(size(x))  x];
    b = regress(y,A);
%   disp (b);
%   note b(1) is first element and is the intersect, (2) is the slope
    slope(k) = b(2);
%
%
%
%   Augment plot with
    hold on
    plot(x, y, '.')
  end
%
% Labels for plot
  axis([min(x)-1  max(x)+1  min(yref)-3.0  max(yref)+3.0])
  xlabel('Length of roll /[mm]')
  ylabel('Profile deviation /[micrometers]')
  title(name);
%
% Histogram of slope error values.
  figure(2)
  hist((slope*(max(x)-min(x))), 50)
  xlabel('Profile slope [micrometers]')
  ylabel('Frequency')
  title(name);

   m = mean(slope)*(max(x)-min(x));
   m0 = min(slope)*(max(x)-min(x));
   m1 = max(slope)*(max(x)-min(x));
   mu = std(slope)*(max(x)-min(x));
   mr = m1-m0;
   m25 = prctile(slope,2.5)*(max(x)-min(x));
   m975 = prctile(slope,97.5)*(max(x)-min(x));

   disp('   Mean      Min       Max       SD       Range       2.5%     97.5%
');
   fprintf('%8.4f %8.4f %8.4f %8.4f %8.4f %8.4f %8.4f\n',m, m0, m1, mu,
mr, m25, m975);
%
% End.
```